FOSSILS AND STRATA

An international monograph series of palaeontology and stratigraphy

Number 72 • December 2025

Ichnology of the Ediacaran–Cambrian Chapel Island Formation of Newfoundland, Canada: unraveling bioturbation at the onset of the Cambrian Explosion

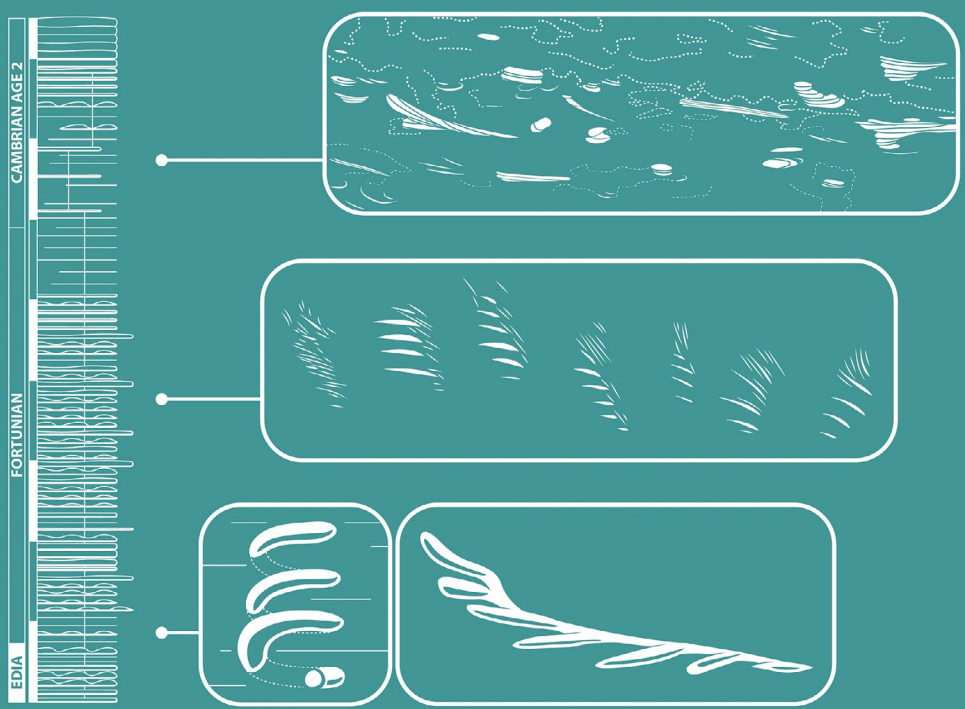

Romain Gougeon, M. Gabriela Mángano, Luis A. Buatois, Guy M. Narbonne, Brittany A. Laing and Maximiliano Paz

Scandinavian University Press

Fossils and Strata is an international series of monographs and memoirs in palaeontology and stratigraphy, published in cooperation between the Scandinavian countries. It is issued in ***Numbers*** with individual pagination.

Fossils and Strata forms part of the same structured publishing programme as the international journal ***Lethaia***, however, is an outlet for more comprehensive systematic and regional monographs.

Many regional or systematic descriptions and revisions contain a nucleus of results which are of immediate and general interest to international palaeontology and stratigraphy. It is expected that authors of such papers will to some extent duplicate their publication in the form of an article for a journal, in the first place ***Lethaia***.

Fossils and Strata is owned by the Lethaia Foundation, Copenhagen, Denmark, and published by Scandinavian University Press.

Editor-in-Chief: Hans Arne Nakrem, Prof. Dr. sci., Natural History Museum, University of Oslo, Norway

Contact: Hans Arne Nakrem, Natural History Museum, PO Box 1172 Blindern, NO-0318 Oslo, Norway, h.a.nakrem@nhm.uio.no. Please visit the series' website for author and submission guidelines.

Website: https://www.scup.com/series/fas

ISSN print: 0300-9491
ISSN online: 2637-6032

This book was first published December 2025 by Scandinavian University Press.
eISBN 978-82-94-16712-8 published on 12.12.2025
ISBN 978-82-94-16711-1 published on 23.12.2025

ISBN printed edition (print on demand): 978-82-94-16711-1
ISBN electronic PDF edition: 978-82-94-16712-8
DOI: 10.18261/9788294167128-2025

Enquiries about this publication may be directed to:

post@scup.com
www.scup.com

Cover picture: Stratigraphic column of the Chapel Island Formation and trace fossils evidencing the appearance of bed-penetrative burrows (*Gyrolithes scintillus* and *Treptichnus pedum*, bottom diagrams), of arthropod trackways (cf. *Allocotichnus dyeri*, middle diagram), and of mixgrounds overprinted by mid-tier burrows (*Teichichnus rectus*, upper diagram). Drawings of trace fossils are based on material found in the succession.

Ichnology of the Ediacaran–Cambrian Chapel Island Formation of Newfoundland, Canada: unraveling bioturbation at the onset of the Cambrian Explosion

by

Romain Gougeon, M. Gabriela Mángano, Luis A. Buatois, Guy M. Narbonne, Brittany A. Laing and Maximiliano Paz

Financial support for the publication of this issue of Fossils and Strata was provided by the Lethaia Foundation

Contents

Ichnology of the Ediacaran–Cambrian Chapel Island Formation of Newfoundland, Canada: unraveling bioturbation at the onset of the Cambrian Explosion

ROMAIN GOUGEON, M. GABRIELA MÁNGANO, LUIS A. BUATOIS, GUY M. NARBONNE, BRITTANY A. LAING & MAXIMILIANO PAZ

FOSSILS AND STRATA

THE LETHAIA FOUNDATION

Gougeon, R., Mángano, M.G., Buatois, L.A., Narbonne, G.M., Laing, B.A. & Paz, M. 2025. Ichnology of the Ediacaran–Cambrian Chapel Island Formation of Newfoundland, Canada: unravelling bioturbation at the onset of the Cambrian Explosion. *Fossils and Strata,* No. 72, 1–215. https://doi.org/10.18261/9788294167128-2025.

The Chapel Island Formation is a 1000+ m-thick, mainly siliciclastic succession that is well exposed in coastal cliffs of Burin Peninsula, southeastern Newfoundland, eastern Canada. This unit contains an outstanding record of late Ediacaran–early Cambrian trace fossils with some intervals rich in small shelly fossils, and in 1992 the Fortune Head section was ratified as Global Stratotype Section and Point for the Cambrian System. This contribution represents the first study integrating sedimentologic and ichnologic information for the whole formation and the first systematic monographic work, involving documentation of the trace fossils in classic sections at Fortune Head, Grand Bank Head, and Little Dantzic Cove, as well as in less-explored sections at Fortune North, Lewin's Cove, and Point May. More than 1700 m of strata were logged, and fourteen sedimentary facies composing five facies associations were described and interpreted to be deposited in: (1) mud-flat, mixed-flat, sand-flat, and tide-dominated or -influenced embayments (Facies Association A); (2) middle and lower shoreface (Facies Association B); (3) offshore transition, upper offshore, and lower offshore (Facies Association C); (4) shelf (*stricto sensu*) (Facies Association D); and (5) carbonate subtidal and intertidal environments (Facies Association E). An extensive trace-fossil dataset was gathered and provides records of bioturbation intensity (1596 data points on vertical bioturbation, 1481 data points on bedding plane bioturbation) and of trace-fossil metrics (3162 data points on burrow width, 1473 data points on burrow depth). A comprehensive revision of the trace-fossil composition (3508 trace fossil specimens recorded) allowed the description of twenty-eight ichnogenera and fifty-two ichnospecies, which consist of cf. *Allocotichnus dyeri*, *Archaeonassa fossulata*, *Arenicolites* aff. *A. carbonarius*, *Arenicolites* isp., *Bergaueria perata*, *B.* cf. *B. radiata*, *Circulichnis ligusticus*, *C. montanus*, *Cochlichnus anguineus*, *C. luguanensis*, *Conichnus conicus*, *Cruziana problematica*, *Curvolithus multiplex*, *C. simplex*, *Curvolithus* isp., *Dendroidichnites* aff. *D. irregulare*, *Didymaulichnus miettensis*, *Dimorphichnus* isp. A, *Dimorphichnus* isp. B, cf. *Dimorphichnus* isp., ?*Diplocraterion* isp., *Gordia marina*, *Gyrolithes gyratus*, *G. scintillus*, *Halopoa imbricata*, *Helminthoidichnites tenuis*, *Helminthopsis abeli*, *H. hieroglyphica*, *H. tenuis*, *Monomorphichnus bilinearis*, *M. lineatus*, *M. needleiunm*, *Monomorphichnus* isp., *Palaeophycus annulatus*, *P. tubularis*, *Palaeophycus* isp., *Psammichnites gigas circularis*, *P.* cf. *P. saltensis*, *Rosselia erecta*, *Rosselia* isp., *Rusophycus avalonensis*, *Rusophycus dabardae* isp. nov., *Rusophycus* isp., *Saerichnites kutscheri* comb. nov., *Teichichnus rectus*, *Torrowangea rosei*, *Treptichnus bifurcus*, *T. coronatum*, *T. pedum*, *T. pollardi*, *Trichichnus linearis*, and *Trichichnus* isp. The trace-fossil distribution and other ichnologic information allow the identification of three palaeoecologic events in the succession: (1) an Ediacaran matground ecology, dominated by simple horizontal trails associated with microbially stabilized surfaces and limited vertical bioturbation; (2) a Fortunian matground/firmground ecology, with evidence of penetrative shallow-tier bioturbation and a burst in trace-fossil diversity; and (3) a late Fortunian/Cambrian Age 2 mixground ecology, with high bioturbation intensities and the development of a shallow mixed layer and deeper transition layer with a structure similar to that of modern seafloors. Overall, this study reinforces the status of the current Cambrian Global Stratotype Section and Point and advocates for the need of comprehensive and multi-disciplinary approaches to fully decipher the scale, tempo, and loci of the early evolution of animal life on Earth.
❐ Trace fossils; bioturbation; ichnotaxonomy; sedimentology; Ediacaran–Cambrian; animal evolution.

Romain Gougeon [gougeon.romain@gmail.com], Department of Geological Sciences, University of Saskatchewan, Saskatoon, SK, S7N 5E2, Canada and Geo-Ocean, University of Brest, CNRS, Ifremer, UMR 6538, Plouzané, F-29280, France; M. Gabriela Mángano [gabriela.mangano@usask.ca], Department of Geological Sciences, University of Saskatchewan, Saskatoon, SK, S7N 5E2, Canada; Luis A. Buatois [luis.buatois@usask.ca],

Department of Geological Sciences, University of Saskatchewan, Saskatoon, SK, S7N 5E2, Canada; Guy M. Narbonne [narbonne@queensu.ca], Department of Geological Sciences and Geological Engineering, Queen's University, Kingston, ON, K7L 3N6, Canada; Brittany A. Laing [brittany.a.laing@gmail.com], Department of Geological Sciences, University of Saskatchewan, Saskatoon, SK, S7N 5E2, Canada and Saskatchewan Geological Survey, Geoscience Information & Modelling Group, Ministry of Energy and Resources, 11th Floor, 1945 Hamilton Street, Regina, SK, S4P 2C7, Canada; Maximiliano Paz [mpaz@oberlin.edu], Department of Geological Sciences, University of Saskatchewan, Saskatoon, SK, S7N 5E2, Canada and Oberlin College, Department of Geosciences, 52 W Lorain St., 44074, Oberlin, Ohio, USA. *Manuscript received on 14/06/2023; manuscript accepted on 29/05/2024.*

Introduction

The transition from the Ediacaran (635–538 Ma) to the Cambrian (538–487 Ma) was a landmark moment in the history of life. Prior to the Ediacaran, prokaryotes and simple eukaryotes represented the life on ocean bottoms, whereas cyanobacterial phytoplankton abounded in the water column (Knoll & Novak 2017; Butterfield 2018). Then, the appearance of the Ediacara Biota (575–538 Ma), with macroscopic organisms of unique body plans that included stem-group bilaterians, represented a macroevolutionary breakthrough (Narbonne 2005; Xiao & Laflamme 2009; Dunn & Liu 2019). Body fossil assemblages of the Cambrian Explosion are commonly recorded from *ca.* 520 Ma onward and contain annelids, arthropods, brachiopods, echinoderms, hemichordates, molluscs, and priapulids, among others (Valentine 1995; Erwin & Valentine 2013; Mángano & Buatois 2014, 2021; Briggs 2015; Erwin 2020). However, an interval of *ca.* 20 Ma exists between the end of the Ediacara Biota and lagerstätten of the Cambrian Explosion. In this interval, trace fossils are notably abundant (Jensen 1997; Mángano & Buatois 2014, 2020) alongside small shelly fossils (Sepkoski & Knoll 1983; Devaere *et al.* 2021; Topper *et al.* 2022). Some of the trace fossils depict complex infaunal behaviours that demonstrate the presence of a coelom acting as a hydrostatic skeleton, an unequivocal attestation of triploblastic animal life (Clark 1964; Valentine 1994; Erwin 1999).

From 1972 to 1992, a Working Group of the Subcommission on Cambrian Stratigraphy actively visited sections spanning the Precambrian–Cambrian boundary interval in Africa, North America, Asia, Australia, and Europe, with the aim of defining a type section for the Cambrian (Cowie 1989, 1992). After considerable discussion, the Cambrian Global Stratotype Section and Point was placed at the first appearance datum of the complex trace fossil *Treptichnus pedum* (Seilacher) in the Chapel Island Formation at Fortune Head, Burin Peninsula, southeastern Newfoundland, eastern Canada (Brasier *et al.* 1994a). This unit is a 1000+ m-thick succession mostly composed of siliciclastic sedimentary rocks and subdivided into five informal members based on lithology (Bengtson & Fletcher 1983; Myrow 1987). This remarkable succession was also selected for its ease of access, its extensive stratal continuity without major breaks, and its monofacial sedimentology across the Ediacaran–Cambrian boundary interval (Brasier & Cowie 1989). Trace fossils are pristine and abundant, demonstrating a general increase in diversity as well as major changes in seafloor colonisation through late Ediacaran to Cambrian Age 2 (Crimes & Anderson 1985; Narbonne *et al.* 1987; Narbonne & Myrow 1988; McIlroy & Logan 1999; Gehling *et al.* 2001; Droser *et al.* 2002; Buatois *et al.* 2014; Herringshaw *et al.* 2017; Gougeon *et al.* 2018a, 2023, 2025a; Laing *et al.* 2018, 2019). Crimes & Anderson (1985) provided the first and only taxonomic treatment of trace fossils, describing twenty-one ichnogenera in the Chapel Island Formation. However, over the last four decades, ichnotaxonomy benefitted greatly from continuous methodologic and conceptual improvements. Notably, ichnotaxobases provide a way to standardize trace-fossil descriptions, which results in the identification of taxonomically redundant junior synonyms (Bromley 1990, 1996; Bertling *et al.* 2006, 2022; Buatois & Mángano 2011; Rindsberg 2018). For instance, Crimes & Anderson (1985) described *Neonereites uniserialis* Seilacher and *Taphrhelminthopsis circularis* Crimes, Legg, Marcos & Arboleya in the Chapel Island Formation, two ichnospecies nowadays considered junior synonyms of *Nereites missouriensis* (Weller) and *Psammichnites gigas circularis* (Crimes, Legg, Marcos & Arboleya), respectively, based on re-evaluations of type materials (Uchman 1995; Mángano *et al.* 2022). These approaches are necessary to fully decipher the scale of the Cambrian Explosion, as taxonomic decisions have major influences on macroevolutionary trends (e.g. Buatois *et al.* 2016a, 2025a; Muñoz *et al.* 2019; Mángano *et al.* 2022).

In this study, the Cambrian type section at Fortune Head was revisited alongside other sections hosting records of the Chapel Island Formation at Fortune North, Grand Bank Head, Lewin's Cove, Little Dantzic Cove, and Point May. The aims of this paper

are fourfold: (1) to provide new datasets on ichnology and sedimentology from the Chapel Island Formation; (2) to review in detail the trace-fossil taxonomy of the succession; (3) to describe and interpret sedimentary facies; and (4) to articulate sedimentologic and ichnologic datasets to further our understanding of secular changes in bioturbation across the Ediacaran–Cambrian boundary interval.

Geologic setting

Previous ichnologic and geologic work

Previous work before the mid-eighties was well summarized by Myrow (1987) and covers the first exploration of Fortune Bay by Dale (1927), the erection of the Chapel Island Formation by Widmer (1950) and Hutchinson (1962), and the renewed interest in the seventies in relation to the first geologic mapping of Burin Peninsula (O'Brien *et al.* 1976, 1977). However, emphasis was mostly placed on stratigraphical and sedimentological aspects, and much has been published since then due to the importance of this formation.

Trace fossils of the Chapel Island Formation were first mentioned succinctly in a short paper by Bengtson & Fletcher (1981) that was prepared for the Second International Symposium on the Cambrian System (Taylor 1981). Bengtson & Fletcher (1983) later provided more details and recorded *Harlaniella* Sokolov (at the time thought to be a trace fossil) in Member 1, and *Astropolithon* Dawson (= *Astropolichnus* Crimes & Anderson), *Monomorphichnus* Crimes and *Neonereites* Seilacher within Member 2. Crimes & Anderson (1985) provided the first descriptions of trace fossils from both Chapel Island and Random formations. They described twenty-one ichnogenera and thirty ichnospecies in the Chapel Island Formation, which led them to evaluate ichnodiversity changes through time at member scale. Although Bengtson & Fletcher (1983) and Crimes & Anderson (1985) mostly focussed on sections at Grand Bank Head and Little Dantzic Cove, Narbonne *et al.* (1987) raised attention on the quality of the Fortune Head section. These authors reviewed the stratigraphical definition of members of the Chapel Island Formation (following Myrow 1987) and defined an ichnostratigraphical scheme depicting increased trace-fossil diversity and complexity from upper Ediacaran to lower Cambrian strata (following Crimes 1987). The publication by Narbonne *et al.* (1987) has been widely cited and was instrumental in the definition of the Cambrian Global Stratotype Section and Point at Fortune Head (Brasier *et al.* 1994a). As a complement, Landing *et al.* (1988) published a field guide for the Precambrian–Cambrian Boundary Working Group Meeting that took place in August 1987 in St John's (Newfoundland, Canada). The field guide provides detailed sedimentological logs with notes on the stratigraphical appearance of trace fossils, as well as detailed maps. In addition to the field guide, Narbonne & Myrow (1988) contributed with a paper focussing on trace-fossil biozonation in the Chapel Island Formation.

Following work focussed on more specific aspects of Chapel Island Formation trace fossils. McIlroy & Logan (1999) revisited the unit as part of a study comparing ichnofabric development in Newfoundland and in other successions in North Wales and Finnmark. Gehling *et al.* (2001) recorded *Treptichnus pedum* 4.41 m below the Global Stratotype Section and Point at Fortune Head, which was explained by confidence intervals related to first appearance datum. Droser *et al.* (2002) focussed on Member 2 at Fortune Head and argued that the earliest Cambrian was dominated by firmground conditions typified by sharp-walled, passively filled burrows. Buatois *et al.* (2014) noted that an Ediacaran-style ecology characterised by simple horizontal grazing trails associated with microbial mats persisted within the Fortunian at Fortune Head, and Ediacaran body fossils were absent despite favorable taphonomic conditions for their preservation if they were present. Mochizuki *et al.* (2014) visited Fortune Head as well as successions in Meishucun (China) and Gobi-Altai (Mongolia) and suggested that *Planolites* Nicholson increased in size through Member 2. Tarhan & Droser (2014) gathered a trace-fossil dataset from the basal 18 m of Member 2 at Fortune Head as well as from other Cambrian successions worldwide and argued that a sediment mixed layer was not developed at that time (see also Tarhan *et al.* 2015). Herringshaw *et al.* (2017) advocated that burrowing organisms of the Chapel Island Formation became more efficient ecosystem engineers during the Cambrian. Gougeon *et al.* (2018a) demonstrated from polished samples that a sediment mixed layer similar in overall structure to that of modern seafloors was established in the Chapel Island Formation around the base of Cambrian Stage 2. Laing *et al.* (2018) revised the taxonomy of *Gyrolithes* de Saporta and erected a new ichnospecies, *G. scintillus* Laing, Buatois, Mángano, Narbonne & Gougeon. Laing *et al.* (2019) then characterised the autecology of organisms at Fortune Head by comparing Fortunian modes of life with those of the Ediacaran and early to middle Cambrian. Gougeon *et al.* (2023) compared ichnofabrics from four sections of the Chapel Island Formation hosting the Ediacaran–Cambrian boundary interval and evaluated the importance of outcrop bias on trace-fossil datasets. Gougeon *et al.* (2025a)

recently discriminated evolutionary from environmental controls in the succession by designing fourteen time-environment matrices, and identified three ecological stages in shallow-marine waters that are globally distributed. Gougeon *et al.* (2025b) published detailed ichnologic and sedimentolgic datasets from six sites hosting strata of the Chapel Island Formation.

In addition, studies on other aspects of the Chapel Island Formation have been published since the mid-eighties. Myrow & Hiscott (1991) described sediment gravity flow deposits encountered within Member 2 at Fortune Head and Grand Bank Head. Narbonne *et al.* (1991) recorded 'Kullingia delicata' from basal Member 2 at Grand Bank Head which was considered at the time as an impression of a pelagic chondrophorine fossil, but Jensen *et al.* (2002a, 2018a) later re-interpreted this structure as an inorganic scratch circle. Brasier *et al.* (1992) evaluated the $\delta^{13}C$ and $\delta^{18}O$ isotope records of carbonates from upper Member 3 and Member 4, considering that $\delta^{18}O$ values were flawed by thermal alteration, but $\delta^{13}C$ had reliable values for worldwide carbon isotope excursion correlation. Myrow (1992a, 1994) described and interpreted a variety of pot and gutter casts encountered within Member 2 that were created during storms. Myrow (1992b) proposed a 'tempestite facies model' based on Member 2 at Fortune Head characterised by sediment bypass on the proximal shelf and deeper sand accumulation, just above storm wave base. Myrow & Landing (1992) developed a mixed carbonate-siliciclastic facies model for upper Member 3 and Member 4, represented by large-scale shoaling upward cycles of siliciclastic mudstone and peritidal limestone deposited in an oxygen-stratified basin. Strauss *et al.* (1992) attempted a stable isotope geochemistry study from the entire Chapel Island Formation and noted that isotopic fluctuations were mostly controlled by changing depositional environments. Myrow & Hiscott (1993) described the different sedimentary facies of this unit and developed depositional history and sequence stratigraphical models based on a composite section. Rabu *et al.* (1993, 1994) described the geology of Saint-Pierre-et-Miquelon and recorded Members 3 to 5 strata at Langlade (southern part of Miquelon), with small shelly fossils similar to material found at Little Dantzic Cove. Brasier *et al.* (1994a), Fåhræus (1994), and Landing (1994) commented on the ratification of the Cambrian Global Stratotype Section and Point at Fortune Head. Hantsoo *et al.* (2018) performed a chemostratigraphical analysis of the Chapel Island Formation and recorded a positive $\delta^{13}C$ excursion starting at the Ediacaran–Cambrian boundary point, later returning to stable values at the top of Member 2. In addition, pyrite sulfur showed a significant ^{34}S depletion at the Ediacaran–Cambrian boundary point. Both variations in carbon and sulfur isotopes were interpreted as resulting from increased ventilation and oxygenation of the seafloor in concordance with increased bioturbation.

Body fossils

Although trace fossils are some of the most striking biogenic remains of the Chapel Island Formation, other fossils were recorded in the succession both in Ediacaran and Cambrian strata. Greene & Williams (1974) first mentioned that *Epiphyton* sp., possible *Volborthella* Schmidt, hyolithids and other fossilized remains were present in strata below the Random Formation. Bengtson & Fletcher (1983) later described small shelly fossils from southeastern Newfoundland that defined two assemblages (Fig. 1): (1) an *Aldanella attleborensis* assemblage from the Chapel Island (Members 4 and 5) and Random formations; and (2) a *Coleoloides typicalis* assemblage from the overlying Bonavista and Brigus formations. At Little Dantzic Cove, the *Aldanella attleborensis* assemblage is characterised by *Halkieria* sp. (within the second limestone bed of Member 4, or LS2 *sensu* Myrow 1987) and *Aldanella* cf. *A. attleborensis* (Shaler & Foerste), *Fomitchella* cf. *F. acinaciformis* Missarzhevsky, *Ginella* sp., *Halkieria* sp., *Lapworthella* sp., *Latouchella* sp., and other helcionellids and orthothecids (within the third limestone bed of Member 4, or LS3 *sensu* Myrow 1987). *Aldanella attleborensis* is a dextrally coiled shell of gastropod or hyolith affinity and is a candidate index fossil for the base of Cambrian Stage 2 (Parkhaev & Karlova 2011; Dzik & Mazurek 2013; Landing *et al.* 2013; Fig. 2G). Narbonne *et al.* (1987) expanded the biozonation scheme of Bengtson & Fletcher (1983) and focussed solely on data from the Chapel Island Formation. Narbonne *et al.* (1987) described three assemblages (Fig. 1): (1) a *Sabellidites* assemblage ranging from top of Member 1 to middle of Member 2A, with the sole occurrence of *Sabellidites cambriensis* Yanishevsky; (2) a *Circotheca*? sp. assemblage ranging from top of Member 2B to the Member 3/Member 4 contact, with only the name bearer recovered; and (3) an *Aldanella attleborensis* assemblage in Members 4 and 5, with molluscs (*Aldanella attleborensis*, *Igorella* sp. aff. *I. ungulata* Missarzhevsky, *Latouchella* sp., *Watsonella crosbyi* Grabau), phosphatic problematica (*Eccentrotheca kanesia* Landing, Nowlan & Fletcher, *Torellella* sp., *Lapworthella ludvigseni* Landing), hyoliths (*Turcutheca* Missarzhevsky, *Laratheca impur*?), and other forms recovered. *Sabellidites cambriensis* is a compressed ribbon-shaped film with transverse wrinkling of annelid affinity and was recently suggested as an index fossil for the lowermost Cambrian (Ivantsov 1990; Moczydłowska *et al.* 2014; Ebbestad *et al.* 2022; Fig. 2B). *Watsonella crosbyi* is a univalve conch looking

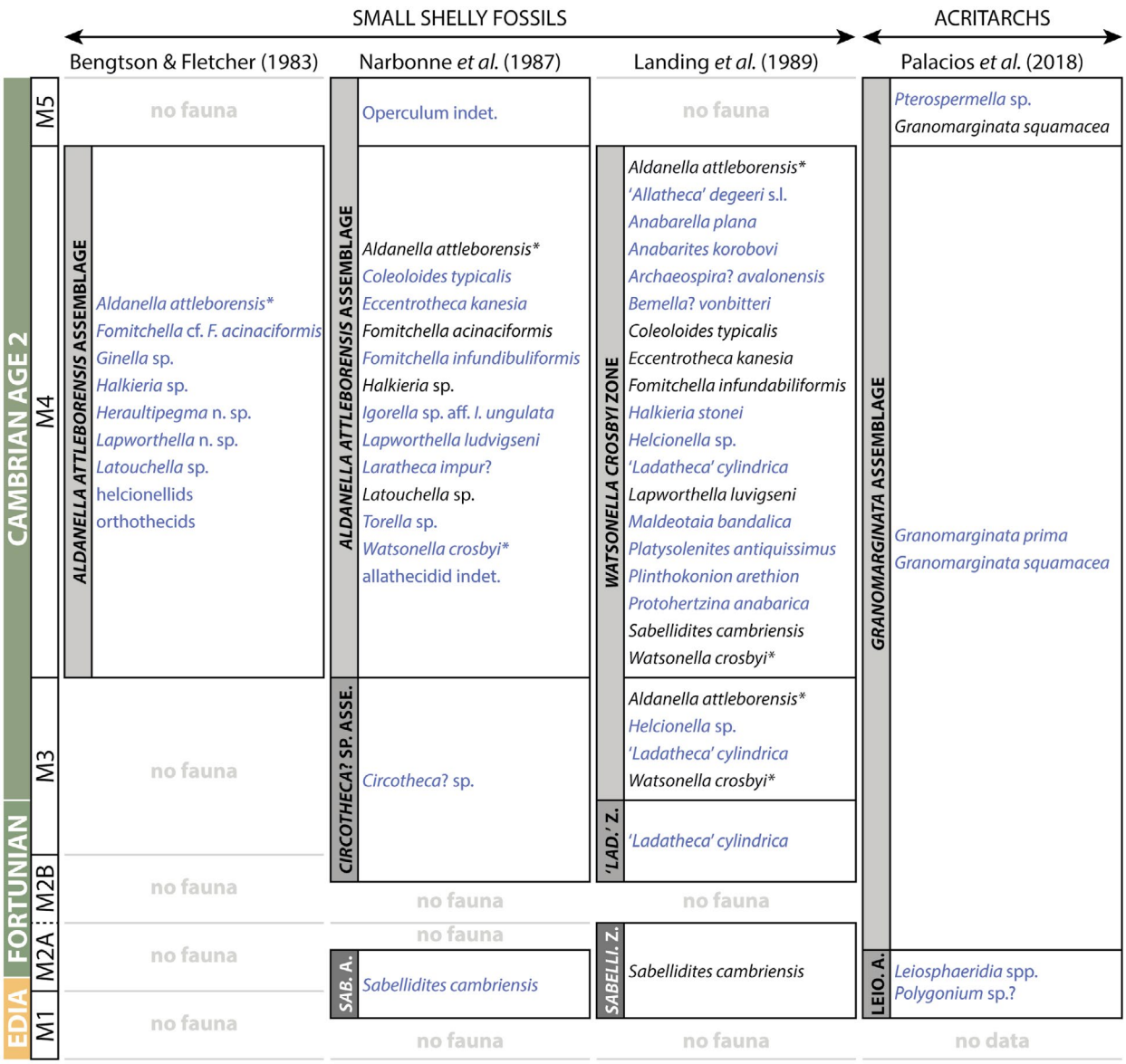

Fig. 1. Summary of biozonation models for the Chapel Island Formation based on small shelly fossils and acritarchs. Bengtson & Fletcher (1983) defined a second biozone with *Coleoloides typicalis* Walcott from the younger Bonavista and Brigus formations that became obsolete as *C. typicalis* was later recorded stratigraphically lower, within Member 4 (Narbonne *et al.* 1987; Landing *et al.* 1989). Preliminary studies on acritarchs (Downie 1982; Strauss *et al.* 1992) are not included but are discussed in the main text. Key: newly described taxa in purple; candidate index fossils for the base of the Cambrian Stage 2 with asterix (*). Abbreviations: Edia, Ediacaran; M1 to M5, Members 1 to 5 of the Chapel Island Formation; *Sab.* a., *Sabellidites* assemblage; *Circotheca*? sp. asse., *Circotheca*? sp. assemblage; *Sabelli.* Z., *Sabellidites cambriensis* Zone; '*Lad.*' Z., '*Ladatheca*' *cylindrica* Zone; and leio. A., leiosphaerids Assemblage. Vertical extension of members not to scale.

like a 'laterally compressed hood' of molluscan affinity and is a candidate index fossil for the base of the Cambrian Stage 2 (Li *et al.* 2011; Devaere *et al.* 2013; Landing *et al.* 2013; Jacquet *et al.* 2017). Narbonne *et al.* (1987) also recorded the algal carbonaceous compression *Tyrasotaenia* sp. within Member 1 (Hofmann & Chen 1981; Fig. 2A). *Harlaniella podolica* Sokolov and *Palaeopascichnus delicatus* Palij were first described as Ediacaran trace fossils in the succession (Narbonne *et al.* 1987) and were later reconsidered as body fossils (Jensen 2003). *Harlaniella podolica* is a rope-like tube of possible algal affinity (Ivantsov 2013) that is recovered at Grand Bank Head and Fortune Head (Fig. 2C). *Palaeopascichnus delicatus* is composed of sausage-like units on bedding surfaces and may have a protozoan affinity (Seilacher *et al.* 2003; Antcliffe *et al.* 2011; Kolesnikov *et al.* 2018; Hawco *et al.* 2021; Fig. 2D). Both *Harlaniella* and *Palaeopascichnus* are found 0.2 m below the Global Stratotype Section and Point at Fortune Head (Narbonne *et al.* 1987). Landing *et al.* (1989) refined the biozonation scheme of Narbonne *et al.* (1987) by describing twenty different types of

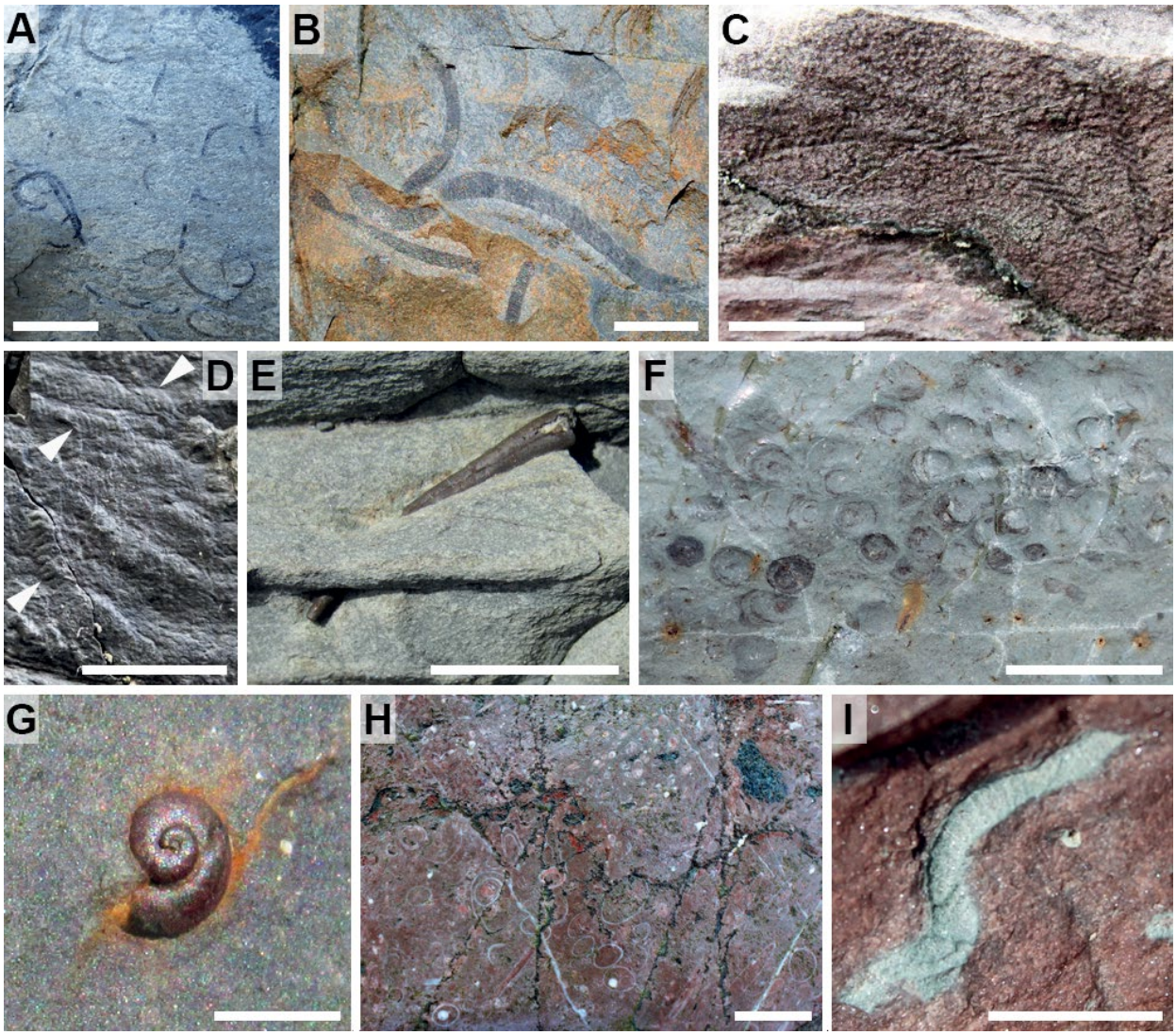

Fig. 2. Body fossils from the Chapel Island Formation. Scale bars are 2 mm (G), 5 mm (I) and 1 cm (A–F, H). **A**, *Tyrasotaenia* sp. Point May, Member 1 (Ediacaran). **B**, *Sabellidites cambriensis* Yanishevsky. Fortune Head, Member 1 (Ediacaran). **C**, *Harlaniella podolica* Sokolov. Grand Bank Head, Member 1 (Ediacaran). **D**, *Palaeopascichnus delicatus* Palij (arrows) found 0.2 m below the Ediacaran–Cambrian boundary point. Fortune Head, Member 2A (Ediacaran). **E**, '*Ladatheca*' *cylindrica* (Grabau). Little Dantzic Cove, Member 4 (Cambrian Age 2). **F**, Cluster of '*Ladatheca*' *cylindrica* opercula. Little Dantzic Cove, Member 3 (Fortunian). **G**, *Aldanella attleborensis* (Shaler & Foerste). Little Dantzic Cove, Member 4 (Cambrian Age 2). **H**, Hyoliths and other small shelly fossils accumulated in a limestone bed (LS3). Grand Bank Head, Member 4 (Cambrian Age 2). **I**, Possible *Platysolenites* sp. Little Dantzic Cove, Member 4 (Cambrian Age 2).

body fossils from Fortune Head, Fortune North and Little Dantzic Cove (Fig. 1). Landing *et al.* (1989) erected a '*Ladatheca*' *cylindrica* Zone (previously referred as *Circotheca*? sp. assemblage in Narbonne *et al.* 1987) and a *Watsonella crosbyi* Zone in Member 4 (previously partially referred as *Aldanella attleborensis* assemblage in Narbonne *et al.* 1987). '*Ladatheca*' *cylindrica* (Grabau) is an elongate tapering conch with a calcareous operculum of polychaete affinity (Landing 1993; Fig. 2E, F). Myrow & Conoglio (1991) described *Frutexites* Maslov cryptobionts in sheet cracks from the stromatolitic limestone bed of Member 4 at Little Dantic Cove. McIlroy *et al.* (2001) recorded *Platysolenites cooperi* McIlroy, Green & Brasier from Members 3 and 4 at Little Dantzic Cove (also mentioned in Landing *et al.* 1989), which was interpreted as a straight agglutinated tube of foraminiferan affinity (Fig. 2I). In a preliminary study, Downie (1982) recovered the acritarchs *Protoleiosphaeridium* Timofeyev, *Granomarginata squamacea* Volkova, and *Archaeodiscina umbonulata* Volkova from a unit near St Lawrence that is coeval with the Rencontre and basal Chapel Island formations (see also Conway Morris 1989). Downie (1982) suggested a Cambrian age for this assemblage. Later, Strauss *et al.* (1992) recovered acritarchs from four samples of the Chapel Island Formation, but only *Granomarginata squamata* from Member 5 was

considered relevant as Cambrian index fossil. Palacios *et al.* (2018) significantly expanded the dataset on these microfossils and erected four biozones spanning the Chapel Island and Random formations, with notably leiosphaerid acritarchs appearing in Member 1 and *Granomarginata* Naumova recovered from Member 2 through Member 5 (Fig. 1).

Regional and stratigraphical framework

The Avalon terrane corresponds to Neoproterozoic–Ordovician volcanic, plutonic, and clastic sedimentary rocks that are today exposed from eastern North America to southern Great Britain (Keppie *et al.* 2003; Landing *et al.* 2022). During the late Neoproterozoic, Avalonia formed an insular microcontinent or a composite terrane that was the located at the periphery of the northern margin of West Gondwana (Landing *et al.* 2022; Murphy *et al.* 2023). Avalonia developed along an active plate margin, with widespread arc-related magmatism attributed to subduction beneath Amazonia, West Africa, or Baltica (Williams 1979; Thompson *et al.* 2007; Murphy *et al.* 2008, 2023). During the Early Ordovician, Avalonia separated from Gondwana and later accreted with Laurentia by the Late Ordovician (Pollock *et al.* 2009; Keppie *et al.* 2021).

Rocks of the Avalon terrane are best exposed in its type area in eastern Newfoundland (i.e. in the Avalon Zone *sensu* O'Brien *et al.* 1996) and can be recovered from five distinctive regions (Mills *et al.* 2021): (1) westernmost Connaigre Peninsula; (2) southwestern Burin Peninsula; (3) central Eastport Area; (4) eastern Bonavista Peninsula; and (5) easternmost Avalon Peninsula. In Burin Peninsula, the Burin Group represents a Proterozoic basement dated at *ca.* 763 Ma and composed of submarine basalts and ophiolites (Fig. 3A; Krogh *et al.* 1988; O'Driscoll *et al.* 2001; Murphy *et al.* 2008). The younger Connecting Point Group consists of sandstone and mudstone of deep-marine and deltaic origin and is dated at *ca.* 610–605 Ma (Fig. 3A; Knight & O'Brien 1988; Mills *et al.* 2016). The Marystown Group exposed in Burin Peninsula forms a large-scale anticline that is juxtaposed geographically to the Burin Group (Sparkes & Dunning 2014). It is composed of subaerial volcanic and sedimentary rocks dated at *ca.* 590–565 Ma (Fig. 3A; Strong *et al.* 1978; Skipton *et al.* 2013). The Long Harbour Group overlays the Marystown Group to the west and north in Burin Peninsula and is composed of subaerial felsic volcanic rocks and minor siliciclastic rocks constrained by dating at *ca.* 568–552 Ma (Fig. 3A; O'Brien *et al.* 1996; Sparkes & Dunning 2014). However, to the east of Burin Peninsula, the Marystown Group is overlain by the Musgravetown Group, a succession of marine to terrestrial sedimentary rocks and minor bimodal volcanic rocks dated at *ca.* 605–569 Ma (Fig. 3A; Sparkes & Dunning 2014; Mills & Sandeman 2021; Mills *et al.* 2021).

An arc-to-platform transition took place from the late Neoproterozoic to Cambrian in relation to the development of strike-slip faults and a transform regime (Murphy *et al.* 2019; van Staal *et al.* 2021). Consequently, siliciclastic deposits unconformably accumulated on the Avalon terrane in a series of newly opened pull-apart basins (Murphy & Nance 1989; Landing 1996a; Nance *et al.* 2002). Landing (1996b) identified marginal, inner, and off platform areas on the Avalon terrane, with deposits of Burin Peninsula corresponding to marginal settings (see also Landing *et al.* 2022). These deposits correspond to the Rencontre, Chapel Island, and Random formations (Landing 1996a, b; Landing *et al.* 2022). The Ediacaran Rencontre Formation consists of conglomerate, sandstone, and mudstone deposited in braided stream, fan delta, floodplain, and tidal and wave-influenced settings, and represents the early filling stage of a fault-bounded basin (Smith & Hiscott 1984). King (1982) provided a 565 ± 26 Ma dating on K-Ar isotopes from the Rencontre Formation at Western Fortune Bay. The Cambrian Stage 2 Random Formation is dominated by cross-bedded quartzarenite sandstone and subordinate heterolithic mudstone and sandstone deposited in subtidal sandbars and tidal flats (Anderson 1981; Hiscott 1982).

The Chapel Island Formation was primarily defined on Chapel Island by Widmer (1950) as being more than 500 m thick. Widmer (1950) identified a basal 18 m-thick interval of thin-bedded sandstone and mudstone in conformity with underlying strata, followed by 61 m of green mudstone with rare red sandstone and mudstone intercalations. This green mudstone passes into an 18 m-thick interval of red mudstone, then followed by 427 m of green and grey-green sandstone and mudstone (Widmer 1950, p. 195). Later, Bengtson & Fletcher (1983) focussed on strata from Burin Peninsula and considered the Chapel Island Formation as a continuous succession 915 m thick. Bengtson & Fletcher (1983) subdivided the formation into five informal members (from base to top): (1) 400 m of red and grey green mudstone and sandstone representing Member 1; (2) 50 m of grey-green mudstone and sandstone representing Member 2; (3) 150 m of grey-green mudstone with large calcite concretions, as well as a basal 5 m-thick red mudstone representing Member 3; (4) 165 m of red, purple and green mudstone with calcite concretions and white stromatolitic limestone representing Member 4; and (5) 150 m of red and grey-green sandy mudstone representing Member 5. In his doctoral thesis, Myrow (1987) revisited sections

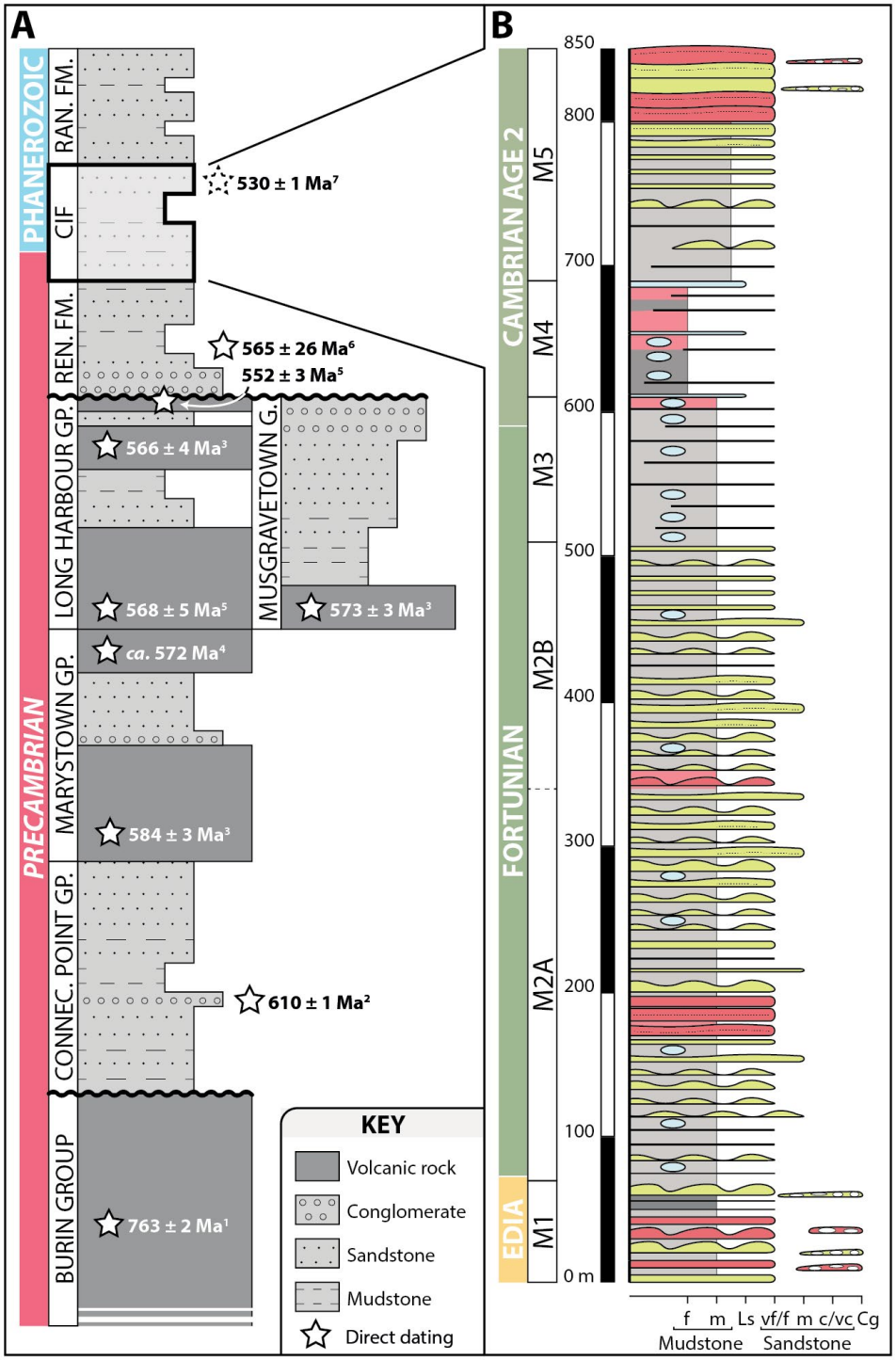

Fig. 3. **A**, Simplified stratigraphy at Burin Peninsula from the Neoproterozoic basement to the lower Cambrian. Based on Mills *et al.* (2021). Groups and formations are not to scale. Connecting Point Group sedimentology and stratigraphy are based on Dec *et al.* (1992), Marystown Group on O'Brien (1979), Long Harbour Group on Williams (1971), Musgravetown Group on Pu *et al.* (2016), Rencontre Formation on Smith & Hiscott (1984), and Random Formation on Hiscott (1982). Note that the simplified stratigraphy within each group or formation is built from ideal/type sections and may not actually outcrop completely at Burin Peninsula. Data on direct dating from: Krogh *et al.* (1988)[1], Dec *et al.* (1992)[2], Ferguson (2017)[3], O'Brien *et al.* (1999)[4], O'Brien *et al.* (1995)[5], King (1982)[6], and Schmitz (2020)[7]. **B**, Composite stratigraphic column of the Chapel Island Formation compiled from Grand Bank Head (basal 59.1 m), Fortune Head (middle 451.1 m), and Little Dantzic Cove (upper 333.6 m). Discrepancies with Myrow's (1987) measurements result from unvisited intervals of strata in Member 1 at Grand Bank Head (about 120 m) and in basal Member 3 at Little Dantzic Cove (about 40 m). Abbreviations: Connect. Point Gp., Connecting Point Group; Gp. and G., Group; Ren. Fm., Rencontre Formation; CIF, Chapel Island Formation; Ran. Fm., Random Formation; Edia, Ediacaran; M1 to M5, Members 1 to 5 of the Chapel Island Formation; f and m mudstone, fine and medium mudstone; Ls, limestone; vf/f, m, c/vc sandstone, very fine-/fine-grained, medium-grained, coarse-/very coarse-grained sandstone; and Cg, conglomerate.

from Burin Peninsula and clarified some discrepancies with the scheme of Bengtson & Fletcher (1983). Myrow (1987) noted that at Fortune Head, strata from Member 3 *sensu* Bengtson & Fletcher (1983) above the basal red mudstone were identical to strata from Member 2; Myrow (1987) decided to place Member 3 *sensu* Bengtson & Fletcher (1983) into a Member 2B. Therefore, Member 2 *sensu* Bengtson & Fletcher (1983) became Member 2A (see also Narbonne *et al.* 1987). Member 3 *sensu* Myrow (1987) represents a distinctive package dominated by mudstone that is well exposed at Little Dantzic Cove. Moreover, Myrow (1987) noted that the definition of the contact between Member 1 and underlying red beds of the Rencontre Formation was unclear. Myrow (1987) then followed the suggestion of Potter (1949) and considered Member 1 to start at the first green interval thicker than 1 m at Grand Bank Head. Myrow's (1987) measurements on member thicknesses at Grand Bank Head (Member 1), Fortune Head (Members 1 and 2) and Little Dantzic Cove (Members 3–5) correspond to: (1) 180 m of alternating red and green sandstone and mudstone representing Member 1; (2) 430 m of grey-green mudstone and sandstone with two intercalated red bed packages representing Member 2 (265 m of Member 2A, 165 m of Member 2B); (3) 135 m of laminated mudstone representing Member 3; (4) 85 m of red and green mudstone intercalated by three limestone beds representing Member 4; and (5) 178 m of sandy mudstone and red and green micaceous sandstone representing Member 5. Because there is no overlap between the highest strata at Fortune Head and lowest strata at Little Dantzic Cove, measured thicknesses of Members 2 and 3 represent minimum values for these members. Therefore, the minimum thickness of the Chapel Island Formation as measured by Myrow (1987) is 1008 m. Our measurement of a total thickness of 843.8 m agrees closely with Myrow (1987) after considering strata that were not logged in our study but were added by Myrow (1987) in his composite section (which correspond to about 160 m, see caption in Fig. 3B). A 530.02 ± 1.07 Ma date was recovered from a volcanic ash bed in New Brunswick (Isachsen *et al.* 1994, later corrected by Schmitz 2012, 2020; see also Compston *et al.* 2008) that was suspected by Landing (2004) to be coeval with the upper part of Member 5. Recent zircon dating on an ash bed located 10 m below the previous one revealed an age of 532.3 ± 0.3 Ma, while a third dating from a coeval section provided an age of 531.5 ± 0.3 Ma (Hamilton *et al.* 2024). However, the stratigraphical correlation of the New Brunswick strata with the Chapel Island Formation in southeastern Newfoundland as proposed by Landing (2004) has not been agreed by the research community (Barr *et al.* 2023). Therefore, the related dating need to be treated with caution, and the stratigraphical subdivision of the Chapel Island Formation into a lower Quaco Road Member and an upper Mystery Lake Member as defined in New Brunswick (Landing 1996a, 2004) will not be applied in this study.

Outcrop locations, accessibility, and stratigraphical measurements

Outcrops of the Chapel Island Formation are in southeastern Newfoundland, eastern Canada (Fig. 4A). Easily accessible sections are located at Burin Peninsula and can be reached by car from Highway 220 which defines an overall loop running parallel to the coastline (Fig. 4B). The type section of the Chapel Island Formation is located on Chapel Island which is facing Burin Peninsula on the other side of Fortune Bay. Similarly, other sections of this unit can be found on Brunette and Sagona islands in Fortune Bay. Although the three islands have been visited and logged previously by Myrow (1987), they were not added to our study as their access is arduous, their stratal extension limited, and covered intervals and faults are in places common (Myrow 1987, figs 1.5, 1.6). Another section included in previous studies (Bengtson & Fletcher 1983; Myrow 1987) is Duck Point, at the southern tip of Burin Peninsula. This outcrop is also affected by abundant faults and has problematic stratigraphical correlations (Myrow 1987; Bengtson & Fletcher 1983; Brasier *et al.* 1992). Finally, sections on the French island of Langlade (southern part of Miquelon, 16 km offshore from the southwestern tip of Burin Peninsula) have difficult access and are of poor quality (Rabu *et al.* 1993, 1994). Therefore, they have not been included either in this study.

For this study, six sections were visited in coastal cliffs of Burin Peninsula. Fortune Head is the most renowned section of the Chapel Island Formation as it hosts the Cambrian Global Section and Point (Brasier *et al.* 1994a). It is located on the west side in an ecological reserve, 1.8 km west of the town of Fortune (Fig. 4B). Access is easy thanks to a car trail departing from Highway 220, and strata are conveniently attainable along the shoreline. Beds dip toward the southwest, therefore the outcrop extends from northeast (base) to southwest (top) (Fig. 4C). Seven sedimentological logs (FH-A to FH-G) were measured in Members 1 to 2B and represent 451.1 m of strata in total (Fig. 4C; 'Data 1' file in Gougeon *et al.* 2025b).

Fortune North is located 400 m northwest of Fortune and is therefore at an intermediate geographic position between the town of Fortune and Fortune Head. At Fortune North, Member 2A is difficult to access from the top of the cliff and walking trails are absent; only a small interval was visited for this study. Member 5 is more conveniently

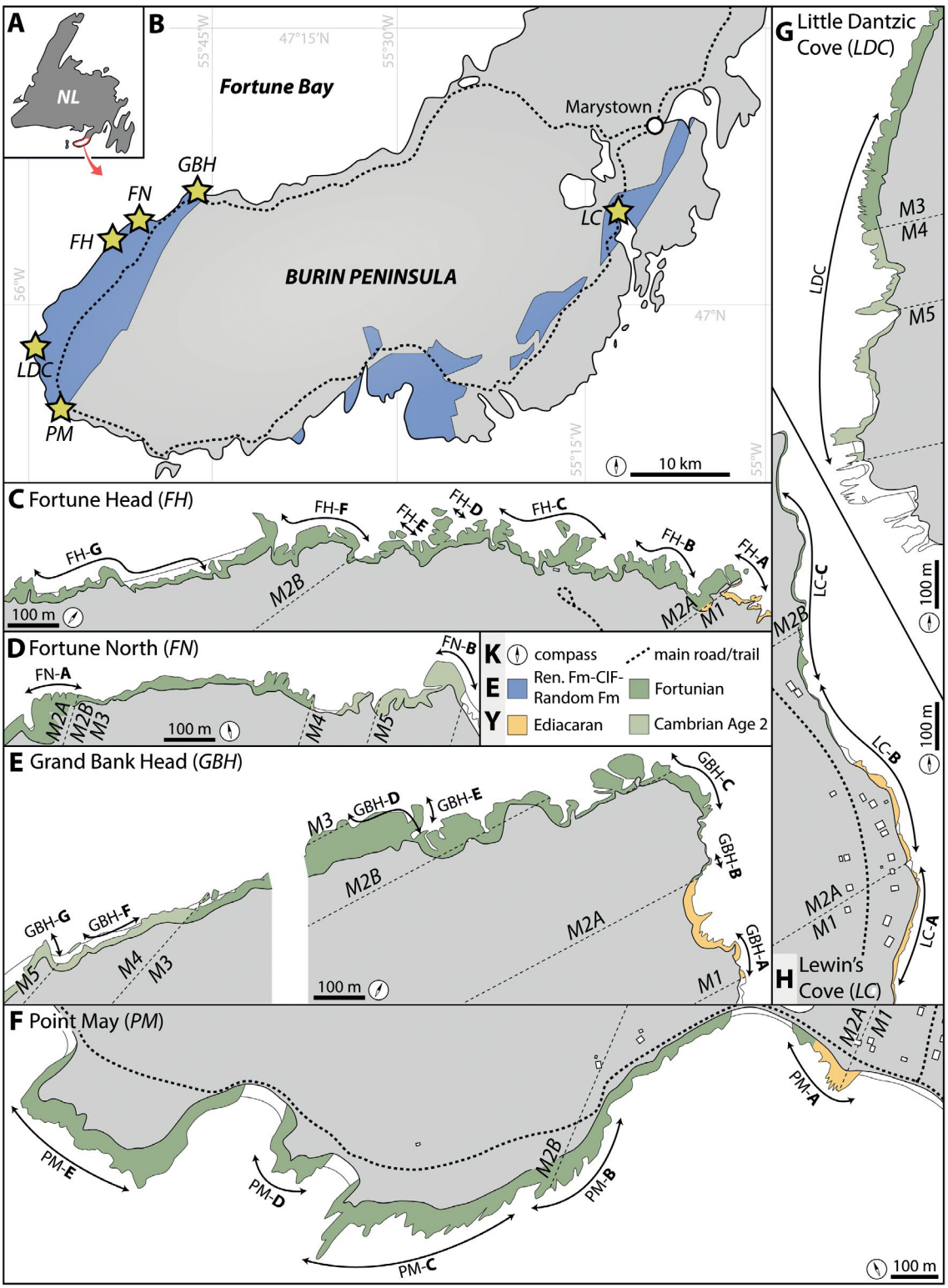

Fig. 4. Location maps of the six studied outcrops. Abbreviations: NL, Newfoundland; M1 to M5, Members 1 to 5 of the Chapel Island Formation; Ren. Fm, Rencontre Formation; CIF, Chapel Island Formation; and Random Fm, Random Formation. **A**, General map of Newfoundland, eastern Canada. **B**, General map of Burin Peninsula showing location of outcrops (stars) exposed along the coast. Coordinates of outcrops are: Fortune Head (FH), 47°04'32"N 55°51'19"W; Fortune North (FN), 47°04'42"N 55°49'56"W; Grand Bank Head (GBH), 47°06'26"N 55°46'03"W; Lewin's Cove (LC), 47°04'30"N 55°12'18"W; Little Dantzic Cove (LDC), 46°57'33"N 55°59'13"W; and Point May (PM), 46°54'19"N 55°56'57"W. **C–G**, Close-ups at each outcrop showing exposed areas and measured sedimentologic logs (see 'Data 1' and 'Data 2' files in Gougeon *et al.* 2025b for detailed logs).

attainable thanks to a trail departing from a nearby beach. Fortune North beds dip toward the east, and the section is therefore oriented west (base) to east (top) (Fig. 4D). The difference in dip between Fortune Head and Fortune North results from an anticline identified at the base of both sections. Two sedimentological logs (FN-A, FN-B) were measured in Members 2A, 2B and 5, representing 123.0 m of strata in total (Fig. 4D; 'Data 1' file in Gougeon *et al.* 2025b).

Grand Bank Head is located 500 m northwest of the town of Grand Bank, with sedimentary rocks cropping in cliffs of Grand Bank Cape (Fig. 4E). Members 1 to 2B at Grand Bank Head are easily reached through a walking trail running around Grand Bank Cape. Members 4 and 5 are also easily accessed from a side road departing from Highway 220. Beds dip northwest, and the section is therefore oriented from southeast (base) to northwest (top) (Fig. 4E). Myrow (1987) separated this section into Grand Bank Head (base) and Radio Station (top), but although some intermediate intervals are not revealed or accessible (Member 3 and basal Member 4), both sections are in stratal continuity and should then be considered altogether. Seven sedimentological logs (GBH-A to GBH-G) were measured in Members 1 to 5 and represent 393.5 m of strata in total (Fig. 4E; 'Data 1' file in Gougeon *et al.* 2025b). GBH-E may repeat partially with GBH-D (Fig. 4E), but a fault renders stratigraphical correlations uncertain.

Lewin's Cove is exposed on the east side of Burin Peninsula, 1.1 km south of Lewin's Cove town center (Fig. 4B). Sections at Lewin's Cove are located close to Highway 220 (Fig. 4H) and are more easily accessed at low tides. Beds are oriented south (base) to north (top), and three sedimentological logs (LC-A to LC-C) were measured in Members 1 to 2A, representing 123.9 m of strata in total (Fig. 4H; 'Data 1' file in Gougeon *et al.* 2025b).

Little Dantzic Cove is located on the western shore of Burin Peninsula, in between Fortune Head (north) and Point May (south), and is not nearby Highway 220 as for the other sections (Fig. 4B). The most convenient way of access is by leaving the car at Pieduck Point and hiking along the shoreline northward for about 2 km. Beds are oriented north (base) to south (top), and one continuous sedimentological log of 333.6 m encompassing Members 3 to 5 was measured (Fig. 4G; 'Data 1' file in Gougeon *et al.* 2025b).

Finally, Point May starts on the beach northwest of town. This outcrop extends from southeast (base) to northwest (top) (Fig. 4F). Five sedimentological logs (PM-A to PM-E) were measured in Members 1 to 2B, representing 260.1 m of strata in total (Fig. 4F; 'Data 1' file in Gougeon *et al.* 2025b).

Methodology

Six outcrops were selected based on information from Myrow (1987), Narbonne *et al.* (1987), and Landing *et al.* (1988). They were visited over thirteen weeks of fieldwork during summers of 2016, 2017, 2019, and 2021. For each outcrop, sedimentological logs were measured meter by meter using a Jacob staff. Attention was placed on: (1) bed geometry; (2) bed thickness; (3) bed grain size; (4) sandstone/mudstone ratio; and (5) sedimentary structures. Twenty-five logs were drawn at 1:40 on field notebooks (5 meters per page), ranging from 6.7 to 334.1 m in thickness and representing 1708.2 m of strata in total ('Data 1' file in Gougeon *et al.* 2025b). The stratigraphical position of these logs can readily be correlated with the excellent work of Myrow (1987), and the content of each log has been double-checked accordingly. In addition, ten high-resolution logs were recorded at 1:1.67 from Members 2A, 2B, 3, and 5, representing 11.08 m of strata in total ('Data 2' file in Gougeon *et al.* 2025b). Outcrop quality was also assessed using the following criteria: (1) outcrop accessibility; (2) vertical continuity; (3) lateral extension of beds; (4) completeness; and (5) type of exposure (see also Shillito & Davies 2020, 2021, Gougeon *et al.* 2023, and Shillito & Gougeon 2023).

Ichnological datasets were gathered from all outcrops whenever exposure was sufficient to provide accurate observations. Exploration of a maximum of bed bases, bed tops, and vertical exposures aided in providing an extensive dataset. Ichnological dataset focussed on: (1) bioturbation index (BI); (2) bedding plane bioturbation index (BPBI); (3) burrow width; (4) burrow depth; (5) ichnotaxonomic classification; and (6) stratigraphical position of trace fossils. Bioturbation index follows Taylor & Goldring (1993) and can be summarized as: BI = 0 for no bioturbation (0%); BI = 1 for sparse bioturbation (1–5%); BI = 2 for low bioturbation (6–30%); BI = 3 for moderate bioturbation (31–60%); BI = 4 for high bioturbation (61–90%); BI = 5 for intense bioturbation (91–99%); and BI = 6 for complete bioturbation (100%). The record on bioturbation index values is typically biased toward intervals displaying burrows, but intervals lacking bioturbation (BI = 0) were also integrated to the study as commonly as possible. Bioturbation index values were best evaluated on intervals with good vertical and lateral consistency in their overall bioturbation intensity; for instance, these intervals are commonly less than or a few cm thick in Member 2 but can be pluri-cm thick in Member 5 (compare high-resolution datasets in 'Data 2' file of Gougeon *et al.* 2025b). In intervals where weathering did not allow a clear evaluation of vertical bioturbation,

emphasis was placed on naturally polished surfaces resulting from modern wave, storm, and tidal erosion that revealed the ichnofabric (cf. McIlroy & Logan 1999). Similarly, the use of water to wet surfaces by hand on unpolished areas permitted better observations. A total of 1596 individual bioturbation index values was recorded from all studied sections (446 at Fortune Head; 123 at Fortune North; 357 at Grand Bank Head; 53 at Lewin's Cove; 324 at Little Dantzic Cove; and 293 at Point May) (Fig. 5). Bedding plane bioturbation index follows Miller & Smail (1997) and can be summarized as: BPBI = 1 for no bioturbation (0%); BPBI = 2 for low bioturbation (1–10%); BPBI = 3 for low to moderate bioturbation (11–40%); BPBI = 4 for moderate to high bioturbation (41–60%); and BPBI = 5 for intense bioturbation (61–100%). Discrimination of bedding plane bioturbation index recorded from either a bed base or a top was also noted. As with the bioturbation index, the record on bedding plane bioturbation index values is biased toward surfaces displaying burrows, but surfaces with no bioturbation were also integrated to the datasets whenever possible. Burrow width and depth were recorded using a caliper. Burrow depth was considered as the maximum vertical extension of an individual burrow (cf. Droser & Bottjer 1988), without any attempt at inferring a connection between a floating burrow (*sensu* Droser *et al.* 2002) and an overlying sandstone bed that could have filled the burrow and, hence, would have been originally in contact. A total of 714 bedding plane bioturbation index values was recorded from bed tops (259 at Fortune Head; 27 at Fortune North; 69 at Grand Bank Head; 101 at Lewin's Cove; 227 at Little Dantzic Cove; and 32 at Point May), and 767 values for bed bases (357 at Fortune Head; 35 at Fortune North; 348 at Grand Bank Head; 3 at Lewin's Cove; 1 at Little Dantzic Cove; and 23 at Point May) (Fig. 5). Trace-fossil taxonomy was standardized using ichnotaxobases (Bromley 1996; Bertling *et al.* 2006, 2022; Buatois & Mángano 2011; Rindsberg 2018) which consist of: (1) general form; (2) wall and lining; (3) branching; (4) fill; and (5) presence/absence of spreiten. The review of ichnospecies previously erected for each ichnogenus was done by: (1) accessing all the literature available from commonly cited papers on the ichnotaxon; (2) researching extensively on Google Scholar to track additional papers dealing with that ichnotaxon; (3) creating requests to the Interlibrary Loan System at the University of Saskatchewan (Canada) to get access to original descriptions and publications outside the mainstream journals; and (4) contacting colleagues directly for additional literature. Sixty-four polished samples and seventeen thin sections were prepared to support observations from the field. Finally, all sedimentological and ichnological datasets were double-checked with the aid of *ca.* 20,000 photographs that were taken by all authors during the four field seasons.

Outcrop quality

Outcrops are of variable quality among localities and within each section studied (Fig. 5) (see also Gougeon *et al.* 2023). Fortune Head, Fortune North, and Grand Bank Head (Members 2A and 5 for the latter) possess the best exposures, with vertical sections and bed bases and tops fully accessible for investigation, as well as extensive lateral continuity of beds. These outcrops correspond to stepped sections *sensu* Shillito & Davies (2020) and Shillito & Gougeon (2023). However, at Grand Bank Head, Members 1 and 2B lack good bed top exposures due to the peculiar orientation of beds. In addition, Member 4 at Grand Bank Head is dominated by mudstone which weathers heavily and erases bed junctions; therefore, bed surface data are limited. Lewin's Cove is distinctive by its absence of bed base exposure. In addition, lateral continuity of beds is restricted to narrow exposures because of important weathering from modern waves and tides, as well as the negative impact of modern vegetation and root systems from land. Beds are mostly subhorizontal, and erosion abraded bed tops obliquely which proved to be an asset in unravelling preservational variation in trace fossils (Gougeon *et al.* 2023). Members 4 and 5 at Little Dantzic Cove have good exposures of vertical sections and bed tops, as well as good lateral continuity of beds. However, bed base exposure is lacking. In addition, Member 3 at Little Dantzic Cove is dominated by bed top exposure, resulting in a stepped plateau section *sensu* Shillito & Davies (2021) and Shillito & Gougeon (2023). Finally, Point May displays more commonly vertical sections than bed top surfaces. This setting corresponds to a coastal section *sensu* Shillito & Davies (2020) and Shillito & Gougeon (2023). Bed bases are not exposed. In addition, Member 2B at Point May displays a strong metamorphic cleavage which impacts negatively on the study of horizontal trace fossils (Gougeon *et al.* 2023).

Sedimentary facies

Five facies associations subdivided into fourteen sedimentary facies have been defined in this study. Whereas facies associations correspond to broad depositional environments, sedimentary facies refer to subdivisions within these environments. Sedimentary facies are characterised based on

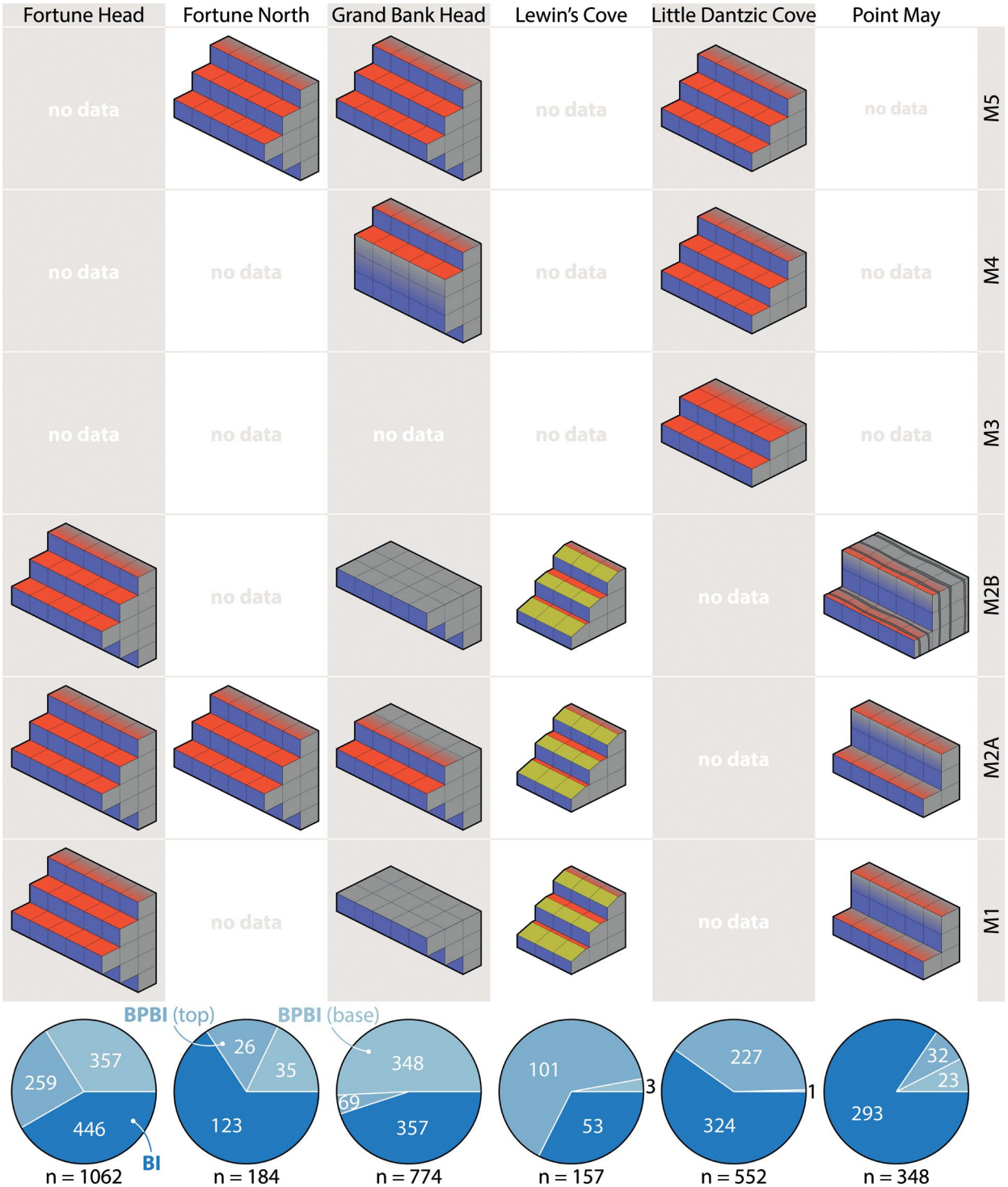

Fig. 5. Block diagrams assessing outcrop quality, and circular diagrams evaluating proportions of bioturbation index values (BI), bedding plane bioturbation index values observed on bed tops [BPBI (top)], and bedding plane bioturbation index values observed on bed bases [BPBI (base)] recovered from the six studied outcrops. The lateral and vertical continuity of outcrops is expressed by lateral/vertical extension of cubes. Red: horizontal surface with trace fossils; blue: vertical surface with trace fossils; yellow; oblique surface with trace fossils; grey: no rock exposure. Overall, Fortune Head, Fortune North, and Grand Bank Head have common vertical sections and bed base and top exposures that are laterally extensive. Lewin's Cove has a restricted lateral exposure of beds, and bed top surfaces are eroded obliquely because of modern waves and tides. Little Dantzic Cove lacks bed base exposure, and Member 3 reveals wide and common bed tops. Point May displays mostly vertical sections, and bed tops are either restricted in area or are hampered by a metamorphic overprint. See main text, Shillito & Davies (2020, 2021), Gougeon *et al.* (2023), and Shillito & Gougeon (2023), for further explanations.

lithology, physical sedimentary structures, geometry, bed contacts, and fossil content. Distribution of sedimentary facies is based on logs provided in the 'Data 1' file of Gougeon *et al.* (2025b). The subdivision of tidal environments follows the scheme by Dalrymple (2010), and that of wave-dominated shallow-marine environments the scheme by MacEachern *et al.* (1999). Terminology for sandstone is based on Wentworth (1922), for mudstone on Lazar *et al.* (2015), for heterolithic bedding on Reineck & Wunderlich (1968), for gutter and pot casts on Myrow (1992a), and for hummocky cross-stratification on Cheel & Leckie (1993) (see 'Data 1' and 'Data 2' files in Gougeon *et al.* 2025b for detailed logs, and Table 1 for a summary of sedimentary facies description and interpretation).

Table 1. Summary of facies associations and sedimentary facies description and interpretation. Abbreviations: FA = facies association; Subfac. = subfacies.

FA	Facies	Subfac.	Occurrence	Lithology	Sedimentary Structures	Depositional Processes	Depositional environment
A	A1		Members 1, 2A	Red and green, medium mudstone, with thinly laminated to very thin-bedded, very fine- to fine-grained sandstone, 5–35% sandstone	Parallel lamination, current ripple cross-lamination, starved current ripples, wavy and lenticular bedding, phosphate pebbles, syneresis cracks, injections structures, reticulated and wrinkled microbially induced sedimentary structures, calcite concretions	Low energy, dominant sediment suspension fall-out related to slack-water periods	Intertidal mud-flat
	A2		Members 1, 2A	Red and green, thin- to medium-bedded, very fine- to medium-grained sandstone, 35–75% sandstone	Massive, parallel lamination, current, combined-flow and climbing ripple cross-lamination, flaser, wavy and lenticular bedding, asymmetrical and near-symmetrical ripples, low-angle planar cross-bedding (rare), hummocky cross-stratification-like structures (rare), rhythmites (rare), flat and ovoid pebbles, tool marks, load casts, ball-and-pillows, syneresis cracks, gas domes, pustular, reticulated and wrinkled microbially induced sedimentary structures	Low to moderate energy, alternation of episodic sand deposition (tidal currents) and suspension fall-out (slack-water periods)	Intertidal mixed-flat
	A3		Members 1, 2A	Red medium- to thick-bedded, very fine- to fine-grained sandstone, 75–90% sandstone	Massive, parallel lamination, current ripple cross-lamination, low-angle planar cross-bedding (rare), sigmoidal cross-bedding (rare), hummocky cross-stratification-like structures (rare), rhythmites (rare), channel-like bases and large scouring, sandstone chips, syneresis cracks	Moderate to high energy, dominant sand deposition (tidal currents and tidal channel discharges)	Intertidal sand-flat to subtidal
	A4		Member 1	Black, thinly laminated medium mudstone, with thinly laminated to medium-bedded, very fine- to fine-grained sandstone, 10–40% sandstone	Massive, parallel lamination, pin-striped lamination, contorted beds, channel-like bases, flat and oval mudstone pebbles, phosphate and pyrite pebbles, tool marks, syneresis cracks, injection structures, gas domes, reticulated and wrinkled microbially induced sedimentary structures	Low energy, dominant sediment suspension fall-out	Tide-dominated or -influenced embayment
B	B1		Member 5	Red and green, thick- to very thick-bedded, fine-grained sandstone, >90% sandstone	Massive, amalgamation, hummocky and swaley cross-stratifications, low-angle planar cross-bedding (rare), symmetrical ripple crests, granules/ phosphate pebbles in conglomeratic beds and lenses	High energy, dominant sand deposition through oscillatory flows (storms)	Middle shoreface
	B2		Members 2A, 2B, 5	Red, grey and green, thin- to thick-bedded, fine- to medium-grained sandstone, 70–90% sandstone	Massive, amalgamation, hummocky cross-stratification, parallel lamination, (low-angle) planar cross-bedding (rare), wave and combined-flow ripple cross-lamination, symmetrical ripple crests, convolute bedding, phosphate pebbles/granules/flat mudstone pebbles/ shell debris in conglomeratic beds and lenses, tool and flute marks, pustular microbially induced sedimentary structures, calcite concretions (rare)	Moderate to high energy, dominant sand deposition through oscillatory flows (storms)	Lower shoreface

FA	Facies	Subfac.	Occurrence	Lithology	Sedimentary Structures	Depositional Processes	Depositional environment
C	C1	C1a	Members 2A, 2B, 3	Brown and grey, very thin- to medium-bedded, very fine- to medium-grained sandstone with silver-green medium mudstone, 40–70% sandstone	Massive, amalgamation (rare), parallel lamination, hummocky cross-stratification, wave and combined-flow ripple cross-lamination (in Subfacies C1a), symmetrical and near-symmetrical ripple crests (in Subfacies C1a), normal grading (in Subfacies C1b), tool marks, flute and load casts, pustular microbially induced sedimentary structures (in Subfacies C1a), isolated calcite concretions (rare)	Low to moderate energy, alternance of suspension fall-out and oscillatory flows (storms) transporting sand	Offshore transition
		C1b	Member 5	Grey, very thin- to medium-bedded, very fine- to fine-grained sandstone with grey-green sandy mudstone, 40–70% sandstone			
	C2	C2a	Members 2A, 2B	Silver-green, medium mudstone, with thinly laminated to very thin-bedded, very fine- to fine-grained sandstone, 20–40% sandstone	Massive, parallel lamination, normal grading, starved wave and current ripples, wave and combined-flow ripple cross-lamination and (micro-) hummocky cross-stratification (in Subfacies C2a), symmetrical ripple crests (in Subfacies C2a), current ripple cross-lamination (in Subfacies C2b, C2c), small- and large-scale scours (in Subfacies C2b), granules/rounded pebbles in conglomeratic beds and lenses (in Subfacies C2a), gutter and pot casts (in Subfacies C2a), tool marks, flute and load casts, scratch circles, injection structures (in Subfacies C2a), pustular, reticulated or subparallel microbially induced sedimentary structures (in Subfacies C2a), isolated calcite concretions	Low energy, alternance of sediment suspension fall-out and oscillatory flows (distal storms) transporting sand	Upper offshore
		C2b	Member 2B	Red, medium mudstone, with thinly laminated to very thin-bedded, very fine- to fine-grained sandstone, 20–40% sandstone		Low energy, alternance of sediment suspension fall-out and unidirectional flows (offshore currents) transporting sand	
		C2c	Member 5	Grey-green, sandy mudstone, with thinly laminated to very thin-bedded, very fine- to fine-grained sandstone, 20–40% sandstone			
	C3	C3a	Members 2A, 2B, 3	Green and silver-green, medium mudstone, with thinly to thickly laminated, very fine- to fine-grained sandstone, 5–20% sandstone	Massive, normal grading, parallel lamination, starved wave and current ripples, wave and combined-flow ripple cross-lamination and micro-hummocky cross-stratification (in Subfacies C3a), symmetrical and near-symmetrical ripple crests (in Subfacies C3a), current ripple cross-lamination (rare, in Subfacies C3b and C3c), phosphate pebbles (in Subfacies C3d), gutter and pot casts (in Subfacies C3a), small-scale scours (in Subfacies C3d), tool marks, scratch circles, flute and load casts, parting lineation (rare), injection structures (in Subfacies C3a), reticulated or wrinkled microbially induced sedimentary structures (in Subfacies C3a), isolated calcite concretions	Low energy, dominant sediment suspension fall-out deposited between oscillatory flows (distal storms) transporting sand	Lower offshore
		C3b	Member 2B	Red, medium mudstone, with thinly to thickly laminated, very fine- to fine-grained sandstone, 5–20% sandstone		Low energy, dominant sediment suspension fall-out deposited between unidirectional flows (offshore currents) transporting sand	
		C3c	Member 4	Red, purple, grey and green, fine mudstone, with thinly to thickly laminated, very fine- to fine-grained sandstone, 5–20% sandstone			
		C3d	Member 5	Grey-green, sandy mudstone, with thinly to thickly laminated, very fine- to fine-grained sandstone, 5–20% sandstone			

(*continued*)

Table 1. (*Continued*)

FA	Facies	Subfac.	Occurrence	Lithology	Sedimentary Structures	Depositional Processes	Depositional environment
D	D1		Members 2B, 3	Green and grey-green, medium mudstone (∅ = 3–70 μm), with rare thinly laminated, very fine- to fine-grained sandstone, <5% sandstone	Massive sandstone, bioturbated or parallel-laminated mudstone with normal grading (rare), soft-sediment deformation structures, phosphate nodules, isolated and bedded calcite concretions, small shelly fossils	Very low energy, dominant sediment suspension fall-out	Shelf
	D2		Member 4	Red, purple, grey and green, fine mudstone (∅ = 3–52 μm), with rare thinly laminated, very fine- to fine-grained sandstone, <5% sandstone	Bioturbated, massive or parallel-laminated (rare) mudstone, phosphate and pyrite pebbles, isolated and bedded calcite concretions, small shelly fossils		
	D3		Member 5	Grey-green, sandy mudstone (∅ = 3–104 μm), with rare very fine- to fine-grained sandstone laminae, <5% sandstone	Massive sandstone, bioturbated or parallel-laminated sandy mudstone		
E	E1		Member 4	Micritic limestone, wackestone and packstone lenses	Oncoids, burrow mottling, small shelly fossils	Low to moderate energy (waves and tides)	Subtidal
	E2		Member 4	Micritic limestone, wackestone, and packstone lenses	Oncoids, planar and columnar stromatolites, inversely graded calcite crystals, intraclasts/phosphatic clasts/volcanic clasts in conglomerates, sheet cracks, tepee structures, desiccation cracks, small shelly fossils	Low to moderate energy, alternance of moments of quiescence and energetic events (waves and tides)	Intertidal

Facies Association A

Facies association A is recorded from Member 1 (Ediacaran) and Member 2A (Fortunian). It represents intertidal deposits encompassing the intertidal mud-flat (Facies A1), the mixed-flat (Facies A2), and sand-flat to subtidal settings (Facies A3). In addition, tide-dominated or -influenced embayments formed in nearshore areas (Facies A4).

Facies A1: Mudstone-dominated heterolithics with wavy and lenticular bedding

Description. – Facies A1 consists of red and green, medium mudstone, with subordinate thinly laminated to very thin-bedded, very fine- to fine-grained sandstone (Fig. 6). Thin- and medium-bedded sandstone is rare. Sandstone makes up 5–35%. Sandstone beds are typically 0.1–1 cm thick, and mudstone layers are 0.5–3 cm thick. Facies A1 forms units 0.2–6.8 m thick and represents 44.0 m of strata in total.

Mudstone is massive or parallel laminated. Sandstone displays parallel lamination and common starved current ripple cross-lamination. Lenticular bedding is single or connected, with thick or flat lenses. Wavy bedding has also been noted. Syneresis cracks are common within mudstone intervals and can be wide (up to 1.8 cm) and deep (up to 11.0 cm) in cross-section. Sandstone bed tops display straight, arcuate, and circular syneresis cracks ('Manchuriophycus'-type). Phosphate pebble lenses are rare. Finally, reticulated (i.e. 'Kinneyia'-type) and wrinkled surfaces suggestive of microbial stabilisation can be pervasive on bedforms, in places shaping large sinuous ripples. A rare structure made of multiple circular elements has also been found associated with microbially modified surfaces.

Ichnology. – *Palaeophycus tubularis* Hall, *Palaeophycus* isp., and *Treptichnus pedum* are present in Facies A1.

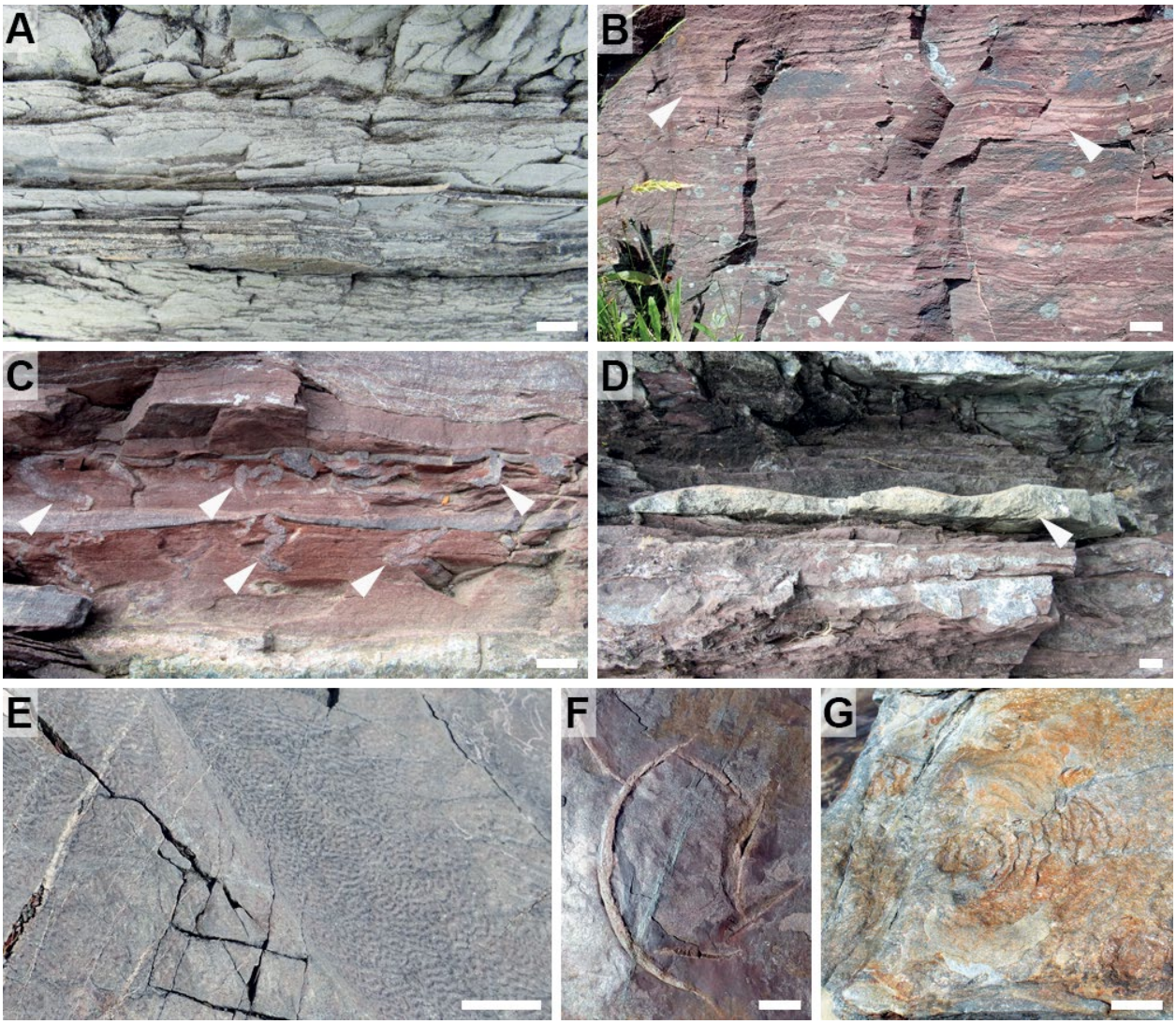

Fig. 6. Facies A1 (intertidal mud-flat). Scale bars are 1 cm (A, C, D, F, G) and 2 cm (B, E). All photographs are from Member 1 (Ediacaran). **A**, Green mudstone with subordinate thin sandstone laminae. Grand Bank Head. **B**, Red mudstone intercalated by wavy and lenticular (arrows) sandstone. Lewin's Cove. **C**, Injection structures (arrows) filled with fine-grained sandstone. Grand Bank Head. **D**, Starved current ripples. Note the ripple cross-lamination (arrow). Grand Bank Head. **E**, Top view with 'Kinneyia' associated with large ripples. Lewin's Cove. **F**, Top view showing arcuate syneresis cracks. Lewin's Cove. **G**, Top view with circular structure associated with a microbially modified surface. Lewin's Cove.

Distribution and equivalents. – Facies A1 occurs in Member 1 (Ediacaran) and Member 2A at Fortune Head (3.6 m in total; FH-A 4.3–4.5, 6.1–6.7, FH-B 81.7–82.1, 91.1–91.5, FH-C 8.4–8.6, 18.5–19.7, 20.5–20.8, 21.7–22.0), Grand Bank Head (17.2 m in total; GBH-A 5.3–6.0, 7.0–8.1, 10.6–11.2, 11.9–14.1, 14.6–16.0, 17.8–18.9, 20.4–22.0, 25.8–26.3, 35.7–36.0, 41.5–42.5, 43.6–44.1, 45.2–46.0, 46.3–47.4, 48.0–48.6, 60.0–60.5, 60.9–64.1), Lewin's Cove (22.4 m in total; LC-A 0.0–2.7, 10.0–13.4, 14.0–16.2, 16.8–18.5, 19.2–21.1, 29.1–29.4, LC-B 0.0–6.8, 14.0–17.2, 19.3–19.5), and Point May (0.8 m in total; PM-A 4.2–5.0). At Lewin's Cove, poor exposure quality precludes accurate observations. Facies A1 is commonly gradational and intercalated with Facies A2, which renders their delineation difficult in places.

Facies A1 corresponds to Facies 1.2 of Myrow (1987).

Interpretation. – The high mudstone/sandstone ratio, and wavy and lenticular bedding argue for a

mud-flat subenvironment (Klein 1977; Flemming & Ziegler 1995; Hertweck *et al.* 2005; Dalrymple 2010; Gao 2019). Facies A1 represents the finer-grained equivalent of Facies A2, and the vertical relationship between the two facies can be best appreciated at Grand Bank Head. Dominant mud deposition resulted from prolonged slack-water periods and gravitational settling of finer particles (Ashley 1990), punctuated by episodic transport of sand through unidirectional flows (Counts *et al.* 2016). Wavy and lenticular bedding are typical of tidal areas with high suspended sediment concentrations and lesser current influence (Dalrymple 2010). Thinly laminated sandstone and starved ripples highlight low sand supply (Jenkins *et al.* 1983). 'Kinneyia' is traditionally interpreted as a microbially modified surface (Porada *et al.* 2008), although a polygenetic origin has also been suggested (Davies *et al.* 2016). Circular structures associated with microbially modified surfaces developed through shrinkage of a cohesive sediment (Pflüger 1999; Neto de Carvalho *et al.* 2016a). The presence of syneresis cracks is suggestive of salinity fluctuations (Plummer & Gostin 1981).

Facies A2: Sandstone-dominated heterolithics with flaser, wavy, and lenticular bedding

Description. – Facies A2 consists of red and green, thin- to medium-bedded, very fine- to medium-grained sandstone, intercalated with thin-bedded medium mudstone (Fig. 7). Sandstone makes up 35–75%. Sandstone beds are typically 5–30 cm thick, and mudstone layers are 2–10 cm thick. Facies A2 forms units 0.4–6.9 m thick and represents 59.7 m of strata in total.

Sandstone is massive, in places amalgamated, or displays planar-lamination and current and combined-flow ripple cross-lamination. Low-angle planar cross-bedding and hummocky cross-stratification-like structures are less common. Hummocky cross-stratification-like structures consist of subparallel undulating laminae that are difficult to trace laterally. They can pass vertically into combined-flow ripple cross-lamination, and in places display symmetrical and near-symmetrical rippled tops. Flaser, wavy, and lenticular bedding are conspicuous components. Flaser bedding is simple or wavy, formed by discontinuous mudstone drapes developed within sandstone beds, or in between amalgamated sandstone intervals. Wavy bedding consists of sharp-based, very thin- to thin-bedded sandstone alternating with mudstone, and in places displaying pinch-and-swell morphologies. Lenticular bedding is single or connected, with common thick lenses.

Very rare rhythmites are composed of repeated bundles of horizontal dark thinly laminated mudstone and red thickly laminated fine-grained sandstone. Distinct mudstone laminae in rhythmites delineate up to nine repeated bundles. Rhythmites made of mudstone and sandstone bundles are also present within intervals dominated by climbing ripple cross-lamination (cf. Tessier *et al.* 1995, fig. 7). A common vertical succession in thin- to medium-bedded sandstone is, from base to top: (1) an erosive base followed by massive sandstone; (2) planar-lamination; and (3) current ripple cross-lamination, in places with asymmetric ripples on top.

Sandstone bed bases are commonly erosive, with in places deeper erosive scours. Deep loading features, commonly of ball-and-pillow type, can deform underlying sandstone and mudstone layers. Subparallel, straight to slightly curved tool marks criss-cross on large surfaces. Flat, ovoid, and rounded pebbles are also found at the base or within sandstone beds. Large flat mudstone pebbles, up to 5.0 cm wide, and sandstone chips can mantle basal surfaces, in common association with microbially modified surfaces. Circular pits and domes can form aggregates. Microbially modified surfaces are pustular, wrinkled, or reticulated (i.e. 'Kinneyia'-type), and typically cover large surfaces. Sandstone bed tops are flat or display straight to sinuous, in places bifurcating, round-crested or flat-toped, near-symmetrical and symmetrical ripples. Sharp-crested asymmetrical ripples and interference ripples have also been noted.

On bed surfaces, syneresis cracks are irregular, filled with very fine- to fine-grained sandstone and can be thin and elongated, or short with a thick median part. Rarely, they are polygonal, with elongated, straight to slightly curved segments tapering at each end, and filled with fine-grained sandstone. In vertical section, very irregular and sinuous forms may represent injection structures. Palaeocurrent data recorded by Myrow (1987) and Myrow & Hiscott (1993) from current ripples (n = 58) indicate a bimodal flow with NE-SW orientation, showing a stronger mode toward the SW. Palaeocurrent data from ripple crests (n = 19) are polymodal, with a weak NE-SW orientation.

Ichnology. – *Circulichnis montanus* Vialov, *Helminthoidichnites tenuis* Fitch, *Palaeophycus* isp.,

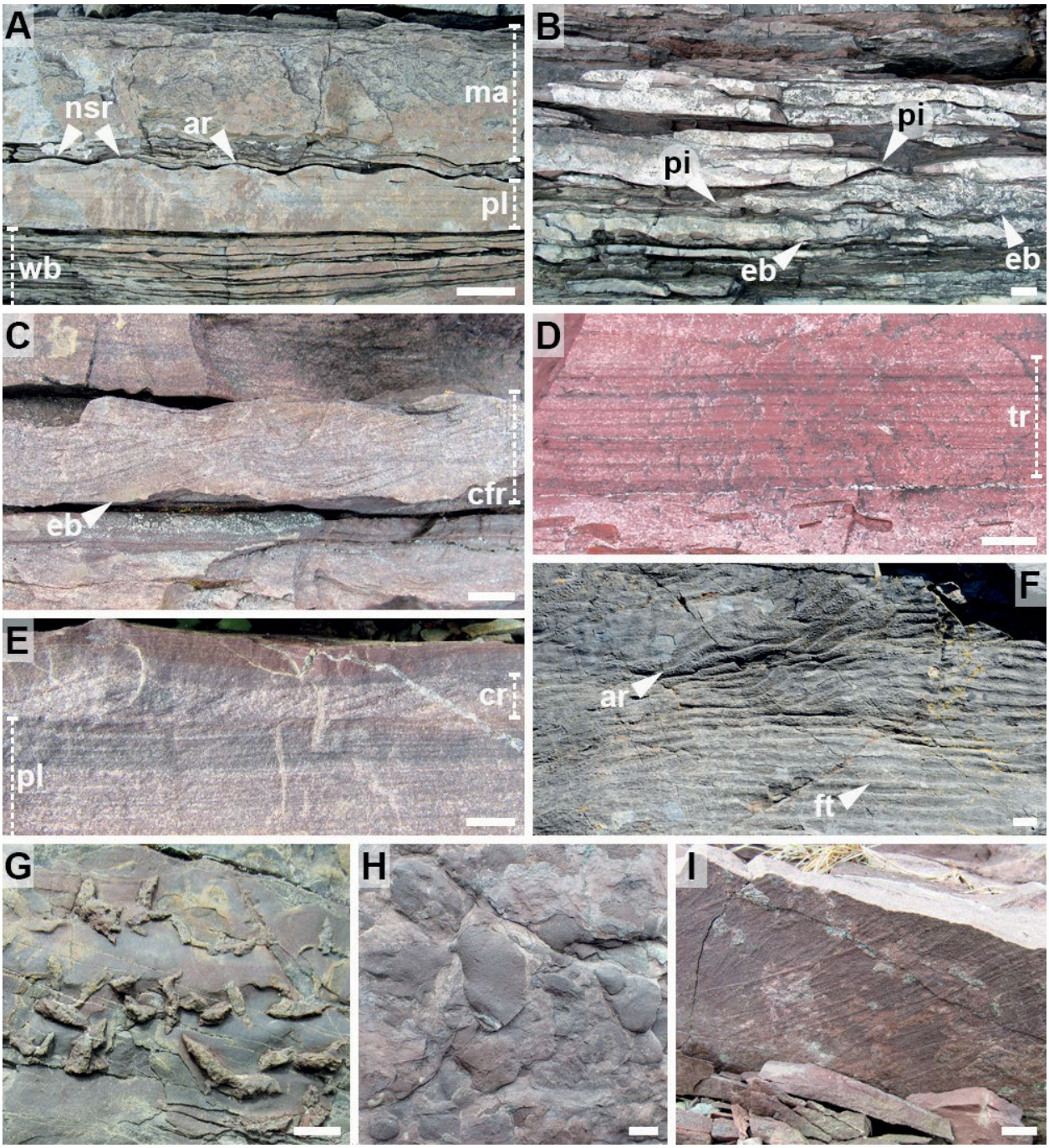

Fig. 7. Facies A2 (intertidal mixed-flat). Scale bars are 1 cm (C–E, G–I) and 5 cm (A, B, F). All photographs are from Grand Bank Head, Member 1 (Ediacaran). **A**, General view of green, very thin- to medium-bedded sandstone showing wavy bedding (wb), parallel lamination (pl) capped by asymmetrical (ar) and near-symetrical (nsr) ripples; the bed above is massive (ma). **B**, General view of red and green, thin- to medium-bedded sandstone intercalated with red mudstone, showing lateral pinching (pi) and erosive bases (eb). **C**, Combined-flow ripple cross-lamination (cfr) in a sandstone bed. Note the erosive base (eb). **D**, Tidal rhythmites (tr) with distinctive dark thin mudstone laminae delineating bundles. Note flat mudstone pebbles at the base. **E**, Common vertical succession with lower parallel lamination (pl) to upper current ripple cross-lamination (cr) in a sandstone bed. Note mudstone draping on the lee side of some of the current ripples. **F**, Top view with straight flat-topped symmetrical ripples (ft) and sinuous asymmetrical ripples (ar), oriented at different angles. Note that asymmetrical ripples are covered by microbially modified surfaces ('Kinneyia'-type). **G**, Base view with short and thick syneresis cracks. **H**, Base view with sandstone chips associated with a microbially modified surface. **I**, Base view with subparallel tool marks.

Psammichnites gigas circularis, *Saerichnites kutscheri* comb. nov., and *Treptichnus pedum* are present in Facies A2.

Distribution and equivalents. – Facies A2 occurs in Member 1 (Ediacaran) and Member 2A (Fortunian) at Fortune Head (21.1 m in total; FH-A 1.7–2.2, 3.8–4.3, 7.5–9.5, 11.2–12.1, FH-B 79.1–79.8, 80.8–81.7, 82.1–84.2, 88.2–91.1, 91.5–92.1, FH-C 1.9–8.3, 8.6–9.6, 18.2–18.5, 19.7–20.5, 20.8–21.7, 22.0–22.6), Grand Bank Head (34.9 m in total; GBH-A 5.0–5.3, 6.0–7.0, 8.1–10.6, 11.2–11.9, 16.0–17.8, 19.9–20.4, 22.0–25.8, 26.3–30.2, 33.0–35.7, 36.0–41.5, 42.5–43.6, 44.1–45.2, 46.0–46.3, 47.4–48.0, 48.6–54.5, 57.2–60.0, 60.5–60.9), Lewin's Cove (2.8 m in total; LC-C 9.3–10.2, 30.5–31.8, 38.9–39.5), and Point May (0.9 m in total; PM-A 1.1–1.4, 2.4–3.0).

Facies A2 corresponds to Facies 1.1 of Myrow (1987).

Interpretation. – The sandstone/mudstone ratio, flaser, wavy and lenticular bedding, horizontal and rippled rhythmites, and bimodal palaeocurrents are consistent with a mixed-flat subenvironment (Klein 1977; Flemming & Ziegler 1995; Tessier *et al.* 1995; Dalrymple 2010; Fan 2013; Gao 2019). Wavy bedding develops where tractive sand deposition alternates with mud settlement under the influence of current/wave action and slack-water periods, respectively (Bajard 1966; Reineck & Wunderlich 1968; Fan 2013; Chen *et al.* 2015). Lenticular bedding demonstrates energy fluctuations, with more quiescent water periods in the system. Tidal currents are inferred as the dominant processes of bedload movement, represented by current- and climbing-ripple cross-lamination and low-angle planar cross-bedding. The common vertical division starting with erosive base, massive deposition of sand followed by parallel lamination and current-ripple cross-lamination is typical of current decelerating flows (Banks 1973; Counts *et al.* 2016). In tidal setting, rhythmites indicate cyclic changes in tidal current velocities, with thicker sandstone laminae representing deposition during spring tides, and thinner mudstone laminae forming during neap tides (Tessier *et al.* 1995; Mazumder & Arima 2005; Dalrymple 2010; Choi 2011; Kvale 2012; Allport *et al.* 2022). Their rarity in the mixed-flat system can be explained by low sediment supply, weak tidal currents, and deposition within an unprotected area affected by storm waves and wind tides (Dalrymple 2010; Fan 2013), the latter being supported by the record of structures indicative of oscillatory flows (see below). Bimodal and subordinate polymodal palaeocurrent data have been recorded from tidal flats elsewhere (e.g. Eriksson *et al.* 1995; Fedo & Cooper 2001) and emphasize the role of changing current directions from ebb to flood. Polymodal currents may be the result of additional controls on sediment transport by wind and channel discharge (channels are evidenced in the genetically related Facies A3, see below). The stronger SW mode noted by Myrow (1987) and Myrow & Hiscott (1993) demonstrates a time-velocity asymmetry in ebb and flood currents (Klein 1970; de Raaf & Boersma 1971; Nio & Yang 1991; Myrow & Hiscott 1993; Lee *et al.* 2004; Dalrymple 2010), with flood being the dominant current (if the shoreline is directed to the SW, as suggested by Myrow & Hiscott 1993).

Flat-topped ripples are formed by the scouring of ripple crests during increased current velocity or during tidal retreat at low tide, indicating periodic emergence of the mixed flat (Tanner 1958; Klein 1963). Another evidence of subaerial exposure are mudstone intraclasts preserved at the base of sandstone beds, which were primarily formed during desiccation of the substrate, then incorporated to the flow and transported during the next flooding event (Mathieu 1966; Gugliotta *et al.* 2018). On the contrary, syneresis cracks formed under water where variations in salinity are important (Plummer & Gostin 1981). In tidal settings, salinity fluctuations result from the mixing of freshwater coming from precipitation and channel discharge with marine waters. The formation of syneresis cracks may also be linked to cyanobacterial and microbial binding of the seafloor (Pflüger 1999; Bouougri & Porada 2002; McMahon *et al.* 2017). Circular pits and domes can be interpreted as fluid or gas escapement structures trapped in microbial mats (Menon *et al.* 2016) or sand buildups (MacNaughton *et al.* 2019). Ball-and-pillow structures result from reverse density mechanisms applying on the sediment (Mills 1983).

Finally, the local presence of hummocky cross-stratification-like structures and bedforms with near-symmetrical ripple crests demonstrates that high-energy oscillatory flows took place. Open coast tidal flats can alternate between tide-dominated in the summer and wave-dominated in the winter, which permits the development of hummocky cross-stratification in the middle and outer parts of the flat (Yang & Chun 2001; Yang *et al.* 2005, 2006, 2021; Fan 2013). In addition, climbing ripple cross-lamination can be generated on tidal flats by wave action (Yang *et al.* 2005, 2008). Combined flows inferred from near-symmetrical rippled tops (Yokokawa 1995; Yamaguchi & Sekiguchi 2010) can

develop their asymmetry from the swash and backwash in shallow waters (MacNaughton *et al.* 2019). However, the paucity of evidence of storm and fair-weather waves in Facies A2 limits comparison with modern open coast tidal flats to small intervals.

Facies A3: Medium- to thick-bedded tabular to lenticular sandstone

Description. – Facies A3 consists of red, medium- to thick-bedded, very fine- to fine-grained sandstone, intercalated with subordinate medium mudstone (Fig. 8). Sandstone makes up 75–90%. Sandstone beds are typically 20–50 cm thick, and mudstone layers are 1–5 cm thick. Facies A3 forms units 0.8–4.0 m thick and represents 11.7 m of strata in total.

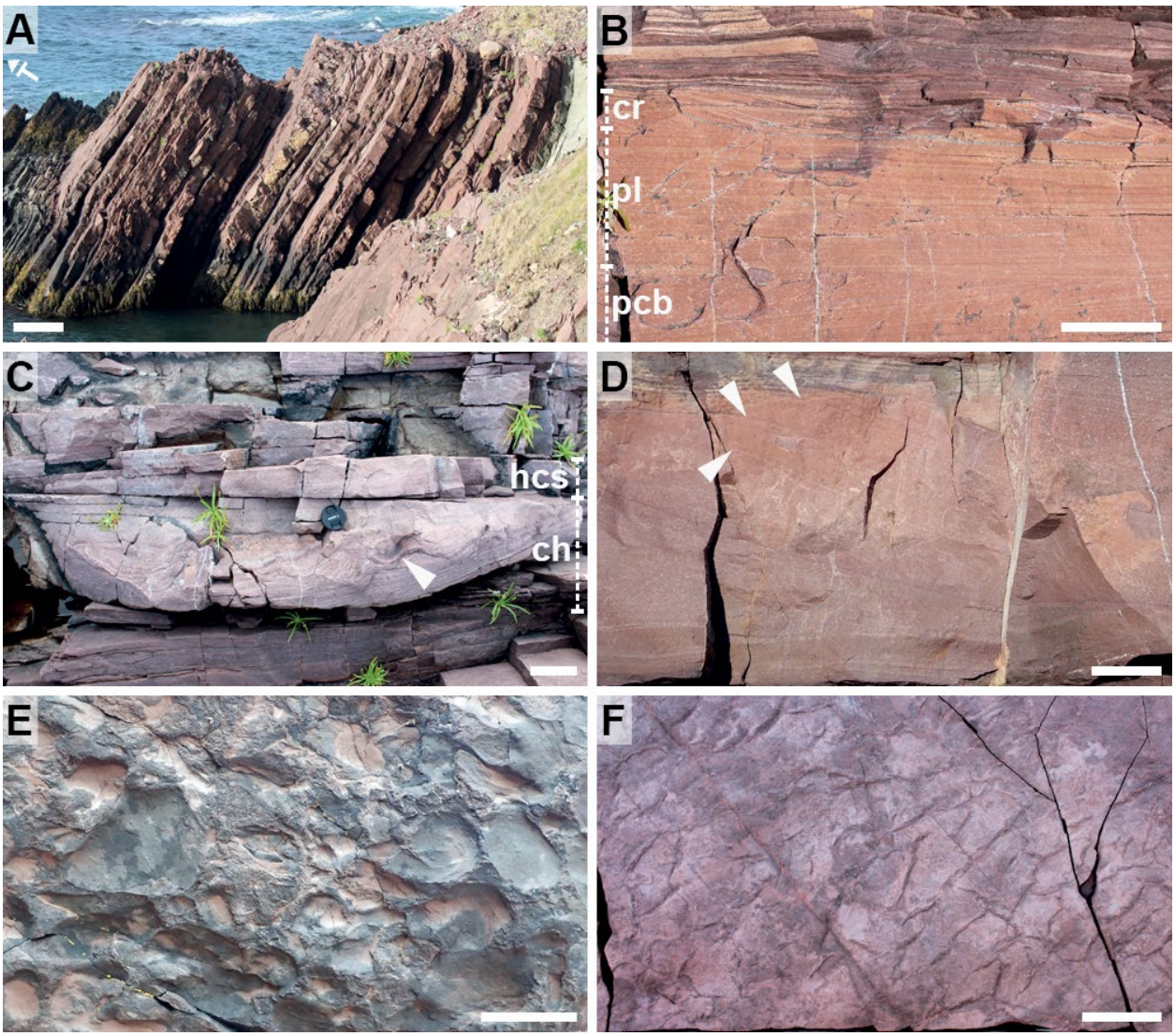

Fig. 8. Facies A3 (intertidal sand-flat/subtidal). Scale bars are 5 cm (B, D–F), 10 cm (C), and 100 cm (A). All photographs are from Fortune Head, Member 2A (Fortunian). **A**, General view of tabular, medium- to thick-bedded sandstone. Stratigraphic top is indicated by the 'T'. **B**, Transition from low angle planar cross-bedding (pcb) to parallel lamination (pl) to current ripple cross-lamination (cr) in a sandstone bed. **C**, Large-scale scour (i.e. channel, 'ch') with convoluted laminae (arrow). Note the overlying hummocky cross-stratification-like structure. **D**, Sandstone bed displaying sigmoidal cross-bedding, with tangential orientation of laminae at their tops (arrows). **E**, Large flat mudstone intraclasts covering a sandstone base. **F**, Base view of syneresis cracks.

Sandstone is massive and commonly amalgamates or shows parallel lamination, current ripple cross-lamination, and more rarely (low angle) planar cross-bedding, sigmoidal cross-bedding, and hummocky cross-stratification-like structures. Very rare horizontal rhythmites are composed of dark thin mudstone laminae and green thick very fine-grained sandstone laminae that develop up to five bundles. Most sandstone beds are tabular with small variations in thickness and extend up to 12 m laterally. Sandstone bed bases are sharp or irregular, strongly erosional. Sandstone bed tops are mostly flat or undulating. Mudstone is thinly laminated. Mudstone commonly drapes individual sandstone laminae within cross-bedded sandstone. Reticulated microbially modified surfaces and sandstone chips are in places noted. Syneresis cracks are very common and are distinguished on bed surfaces by their sinuosity, strong variation in width with tapering ends, and poor branching development. Facies A3 also displays scours at the base of medium- and thick-bedded sandstone forming lenticular geometries 1.5–2.0 m wide and 0.3–0.4 m thick, in places with basal mudstone intraclasts. These bodies are composed of undulating thin sandstone laminae, in places draping the base of the lense. Small-scale convolute bedding occurs.

Ichnology. – Trace fossils are absent in Facies A3.

Distribution and equivalents. – Facies A3 occurs in Member 1 (Ediacaran) and Member 2A (Fortunian) at Fortune Head (13.3 m in total; FH-A 2.2–3.8, 4.5–6.1, 6.7–7.5, 9.5–11.2, FH-B 79.8–80.8, 84.2–88.2) and Grand Bank Head (1.0 m in total; GBH-A 18.9–19.9).

Facies A3 corresponds to Facies 1.4 of Myrow (1987).

Interpretation. – The very high sandstone/mudstone ratio, the presence of medium- and thick-bedded sandstone, current-produced cross-stratification and cross-lamination, rhythmites, syneresis cracks, and large-scale scours with basal intraclasts argue for a sand-flat subenvironment with local formation of tidal channels (Klein 1977; Flemming & Ziegler 1995; Hertweck *et al.* 2005; Dalrymple 2010; Gao 2019; Sleveland *et al.* 2020). In addition, large planar and sigmoidal cross-bedding indicates the rare development of subtidal sand dunes (Desjardins *et al.* 2010a, 2012). Facies A3 corresponds to the sandier equivalent of Facies A2. Current-ripple cross lamination and planar cross-bedding demonstrate the influence of unidirectional flows responsible for the migration of ripples and dunes, respectively. In addition, planar-lamination within sandstone indicates an upper-flow regime moving very fine- to fine-grained sand as flat beds (Driese *et al.* 1981; Ashley 1990). Mudstone partings highlight periods of short-time quiescence, with fine-grained particles highly concentrated in the water column settling down and draping the seafloor (Amos 1995; Gao 2019).

During ebb, scouring and gouging can erode previously deposited sediment, transporting sandstone and mudstone clasts distally and resulting in the formation of tidal channels (Goodwin & Anderson 1974; Gehling 2000; Counts *et al.* 2016; Vaucher *et al.* 2020). Fan (2013) noted that open-coast tidal flats may possess less channels and thinner sand-flat deposits than sheltered tidal flats, which was probably the case in the Chapel Island Formation. Open-coast tidal flats are prone to be affected by storm-wave action (Yang *et al.* 2005, 2021) which is suggested by hummocky cross-stratification-like structures in Facies A3.

An alternative interpretation of tabular sandstone beds of Facies A3 is the development of a sheet-braided system (see also Shahkarami *et al.* 2020). During pre-Devonian times, the absence of pervasive land vegetation favored the development of sheet-braided systems with channel bodies of high width-to-thickness ratios (MacNaughton *et al.* 1997; Davies & Gibling 2010; Lowe & Arnott 2016; Went & McMahon 2018; Ielpi *et al.* 2022). Davies & Gibling (2010) summarized criteria for the recognition of sheet-braided systems: (1) < 5% mudstone and > 95 % sandstone or coarser lithologies; (2) predominance of 'sheet-braided' style where calculation of width/thickness ratio depends of rock exposure; (3) rarity of inclined or laterally impersistent beds; (4) abundance of trough cross-bedding, planar lamination, massive sandstone and pebble lags, common soft-sediment deformation structures, but rarity of other structures; and (5) common (sub)arkosic sandstone. Some of the criteria fit the description of sandstone in Facies A3, notably points (1), (2), and (3). Limitation of outcrop exposure at Fortune Head precludes a clear evaluation of lateral variation of sandstone bodies, as sheet-braided channels can reach width/thickness ratios of 20:1 (Cotter 1977) to more than 1000:1 (Long 2004). However, trough cross-bedding and pebble lags were not observed in Facies A3. In addition, sheet-braided systems tended to display coarser-grained lithologies and to lack mudstone intraclasts in the early Palaeozoic (Davies & Gibling 2010; Went & McMahon 2018), which are features that are not consistent with observations made in Facies A3. In Facies A3, distinct narrow and deep channels are identified as well as features typical of tidal influence (e.g. rythmites, sigmoidal cross-bedding, mudstone draping) which favor the former interpretation as sand-flat with tidal channels.

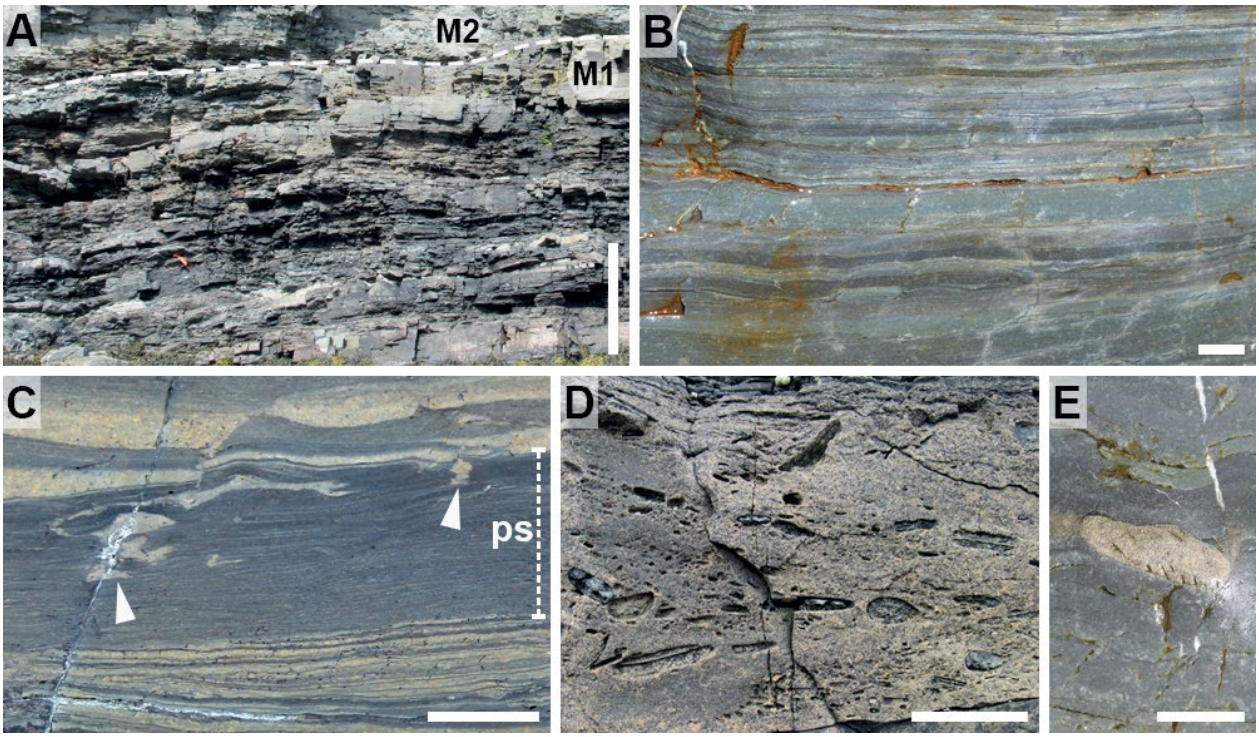

Fig. 9. Facies A4 (tide-dominated or -influenced embayment). Scale bars are 1 cm (B, C, E), 5 cm (D), and 1 m (A). All photographs are from Member 1 (Ediacaran). **A**, General view of Facies A4 at the Member 1 (M1)/Member 2 (M2) contact at Fortune Head. **B**, Polished surface showing alternation of dark grey and black, thinly laminated to thin-bedded sandstone and mudstone. Fortune Head. **C**, Polished surface showing a typical pin-striped interval (ps) and injection structures (arrows). Point May. **D**, Pebbly conglomerate with a sandstone matrix. Fortune Head. **E**, Pyrite nodule. Fortune Head.

Facies A4: Thinly laminated, pin-striped mudstone with syneresis cracks

Description. – Facies A4 consists of dark grey to black, parallel-laminated medium mudstone, intercalated with thinly laminated to medium-bedded, very fine- to fine-grained sandstone (Fig. 9). Medium-grained sandstone is uncommon. Sandstone makes up 10–40%. Sandstone beds are typically 0.1–2 cm thick, and mudstone layers are 0.1–1 cm thick. Facies A4 forms units 3.1–4.6 m thick and represents 7.7 m of strata in total.

Sandstone beds are commonly slightly contorted and massive, in places amalgamated, or display parallel lamination. A typical feature is the presence of pin-striped intervals made of parallel, thinly laminated black mudstone and quarzitic sandstone. Laterally, sandstone beds can show important variations in thickness, developing lenses and channel-like morphologies. Flat and oval mudstone pebbles aggregate in lenses within sandstone. Phosphate and pyrite pebbles have also been noted. Syneresis cracks are common on sandstone bed bases, with irregular straight to curved shapes, tapering at their ends. In vertical section, injection structures are squashed and very tortuous, in places very deep (down to 7.0 cm), and taper at their tops and bases.

Sandstone bed bases are either sharp or irregularly erosive, and display gas domes, pustular microbially modified surfaces, and subparallel, curved tool marks. Sandstone bed tops are rarely exposed. An important surface delineating the Member 1/Member 2 contact at Fortune Head displays irregular, sinuous near-symmetrical ripples, whereas other areas on that surface are less deformed, showing wrinkled, microbially modified patches. Another surface at Point May shows weathered, straight, round-crested symmetrical ripples. Carbonaceous algal filaments are also common on bed surfaces.

Ichnology. – *Archaeonassa fossulata* Fenton & Fenton, *Circulichnis ligusticus* Uchman & Rattazzi, *Palaeophycus* isp., *Torrowangea rosei* Webby, and *Treptichnus* indet. are present in Facies A4.

Distribution and equivalents. – Facies A4 occurs in Member 1 (Ediacaran) at Fortune Head (3.1 m in total; FH-A 12.4–15.5 m) and Point May (4.6 m; PM-A

9.4–14.0). Myrow (1987) also recorded Facies A4 at Grand Bank Head (*ca.* 50 m) and Lewin's Cove (*ca.* 16 m) in areas that have not been accessed in this study.

Facies A4 corresponds to Facies 1.3 of Myrow (1987).

Interpretation. – The dominance of parallel-laminated mudstone suggests low energy, with suspended particles settling on the seafloor. Intercalated thin sandstone laminae and very fine-grained sandstone lacking erosive bases may have been also deposited from suspension (Eriksson *et al.* 1995). Pin-striped lamination is formed through weak tidal currents with daily variations in flow regimes (Reif & Slatt 1979; Chen *et al.* 2015). Small-scale convolution may have resulted from overpressure on water-enriched sediments (Vernhet & Reijmer 2010). The dark color of mudstone is typically interpreted as organic enrichment, either resulting from water-column anoxia or high organic production (Wignall & Myers 1988; Brenchley *et al.* 1993; Vernhet & Reijmer 2010; Jiang *et al.* 2011). Vendotaenid algae and cyanobacterial and microbial bindings may have been responsible for the enrichment in organic material in Facies A4. Parallel-laminated sandstone and the presence of pyrite nodules indicate sulfur enrichment and anoxic conditions (Baird & Brett 1986; Wignall & Hallam 1991; Machhour *et al.* 1994; Smith & Bustin 1995).

Possible shallow- and marginal-marine depositional environments for this type of facies are a protected lagoon (Chafetz 1978; Vernhet & Reijmer 2010; Jiang *et al.* 2011), the central basin of a wave-dominated estuary (Dalrymple *et al.* 1992; Boyd 2010), and a tide-dominated or -influenced embayment (MacEachern & Gingras 2007; Durbano *et al.* 2015; Dashtgard *et al.* 2021). Lagoons typically develop where wave action is dominant, tidal influence is minimal to absent, and fluvial input is negligible (Boyd *et al.* 1992), which are not characteristics of Facies A4. Identification of estuaries relies in part on the narrow lateral extension of the facies, and their predictability in terms of proximal-distal trends (Dalrymple *et al.* 1992; Zaitlin *et al.* 1994; Dalrymple 2006; Desjardins *et al.* 2012). In the Chapel Island Formation, Facies A4 is recorded from Point May, Grand Bank Head, Fortune Head, and Lewin's Cove, spanning a lateral extension of at least 50 km from SW to NE at Burin Peninsula. In addition, none of the typical facies transitions that characterise estuarine systems have been identified. In the Chapel Island Formation, a tide-dominated or -influenced embayment is regarded as the most consistent depositional scenario with the sedimentological features present in Facies A4, and with the vertical facies transitions observed. Evidence of emersion (e.g. desiccation cracks) is absent. Moreover, this embayment may have developed on an area sheltered from wave and storm action, as demonstrated by the lack of associated sedimentary structures. The distal part of a restricted bay, as defined by MacEachern & Gingras (2007), displays typical elements of Facies A4, with common convolution, dark mud typical of anaerobic and dysaerobic conditions, abundant syneresis cracks, and a low sand content. Open bays are less sheltered, possessing a higher sand content than restricted bays because of storm action (MacEachern & Gingras 2007). Small channels could have developed on the mud-dominated embayment and would have carried sand and pebbles (cf. Frey *et al.* 1989).

Facies Association B

Facies association B occurs in Members 2A and 2B (Fortunian) and Member 5 (Cambrian Stage 2). It represents shallow-marine shoreface subenvironments deposited below the breaker zone and above fair-weather wave base, encompassing the middle shoreface (Facies B1) and the lower shoreface (Facies B2).

Facies B1: Thick- to very thick-bedded sandstone with swaley cross-stratification

Description. – Facies B1 consists of red and green, thick- to very thick-bedded, fine-grained micaceous sandstone (Fig. 10). Sandstone makes up more than 90%. Sandstone beds are typically 0.5–5.7 m thick. Mudstone partings are very rare. Facies B1 forms units 1.7–19.2 m thick and represents 30.1 m of strata in total.

Sandstone is massive or displays swaley cross-stratification. Low-angle planar cross-bedding is rare. Within each sandstone bed, concave-up subparallel laminae form laminasets with common second-order truncation surfaces typifying swaley cross-stratification. Truncation of hummocks and difficulties in tracing each bed laterally render detailed measurements on swaley cross-stratification complicated. Sandstone bed bases and tops are rarely accessible, but in places display straight, round- and sharp-crested symmetrical ripples. Conglomeratic intervals form discontinuous and continuous thin beds made of granules and purple phosphate pebbles, floating within the massive sandstone matrix.

Ichnology. – *Rosselia erecta* (Torell) is present in Facies B1.

Distribution and equivalents. – Facies B1 occurs in Member 5 (Cambrian Age 2) at Fortune North (9.2 m

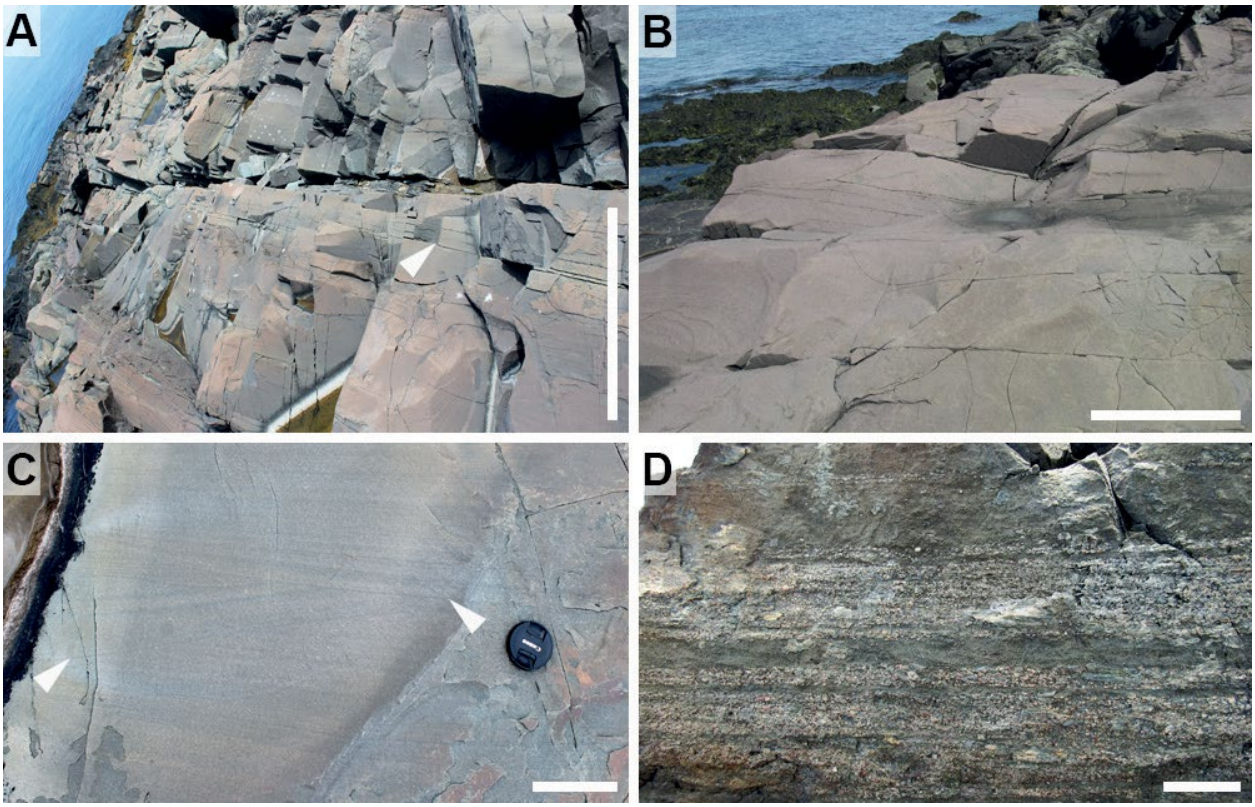

Fig. 10. Facies B1 (middle shoreface). Scale bars are 5 cm (D), 10 cm (C), and 50 cm (A, B). All photographs are from Member 5 (Cambrian Age 2). **A**, General view of Facies B1. Note low angle planar cross-bedding (arrow). Fortune North. **B**, Top view with typical preservation of swaleys. Little Dantzic Cove. **C**, Swaley cross-stratification within a sandstone bed. Note second-order, concave-up truncation surfaces (arrows). Fortune North. **D**, Horizontal, discontinuous and continuous thin conglomeratic beds made of granules. Little Dantzic Cove.

in total; FN-B 31.1–40.3) and Little Dantzic Cove (20.9 m in total; LDC 291.4–310.6, 324.0–325.7).

Facies B1 corresponds to Subfacies 6.1B of Myrow (1987).

Interpretation. – Swaley cross-stratification is typical of the middle shoreface (Leckie & Walker 1982; Swift *et al.* 1987; Dalrymple & Choi 2007; Herbers *et al.* 2016; Jelby *et al.* 2020; Dashtgard *et al.* 2021). Swaley cross-stratification results from hummocky cross-stratification amalgamation and truncation of hummocks during storms (Kumar & Sanders 1976; MacEachern & Pemberton 1992; Dumas & Arnott 2006). The upper shoreface is not represented in Facies B1, as trough cross-bedding and medium- to coarse-grained sandstone are absent (Clifton *et al.* 1971; Dumas & Arnott 2006). Preservation of fair-weather mudstone is hindered by erosion taking place during sustained storms or by the absence of a window for fine-grained particle settlement (Leckie & Walker 1982). Gravel and pebble lags are common in storm deposits and result from the shoaling of waves occasionally accumulating large clasts on hummocky scour surfaces (Kumar & Sanders 1976; Dott & Bourgeois 1982; Hunter & Clifton 1982; DeCelles & Cavazza 1992; Simpson *et al.* 2002; Ghienne *et al.* 2007).

Facies B2: Thin- to thick-bedded sandstone with hummocky cross-stratification

Description. – Facies B2 consists of red, grey, and green, thin- to thick-bedded, fine- to medium-grained sandstone, in places with thin mudstone intervals (Fig. 11). Coarse-grained sandstone is more uncommon. Sandstone makes up 70–90%. Sandstone beds are typically 2.0–100.0 cm thick, and mudstone layers are 0.1–3.0 cm thick. Facies B2 forms units 0.1–14.8 m thick and represents 139.2 m of strata in total.

Sandstone is massive or displays hummocky cross-stratification, wave and combined-flow ripple cross-lamination, parallel lamination, and convolute bedding. Low-angle planar cross-bedding is rare. Sandstone beds are tabular and commonly amalgamate. In places, planar cross-bedded sandstone pinches out to develop lenses. Hummocky cross-stratification is isotropic with scour-and-drape morphologies. A typical succession in beds having

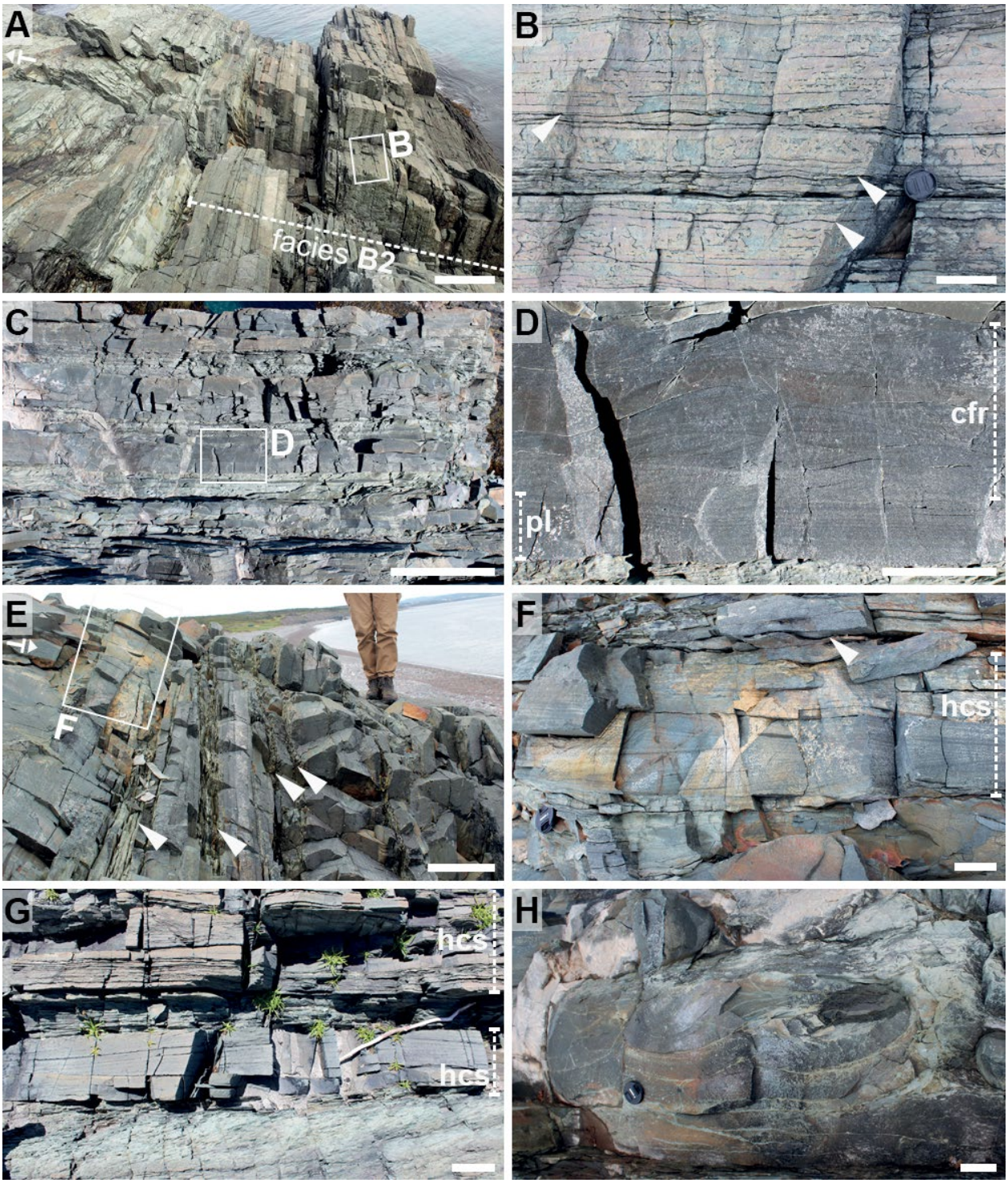

Fig. 11. Facies B2 (lower shoreface). Scale bars are 5 cm (D), 10 cm (B, F–H), 50 cm (C, E), and 100 cm (A). Stratigraphic tops are indicated by the 'T'. **A**, General view showing tabular sandstone of Facies B2. Grand Bank Head, Member 2A (Fortunian). **B**, Close-up from Figure 11A showing amalgamation of very thin- and thin-bedded sandstone. Note the irregular wavy bed tops (arrows). **C**, An interval dominated by very thin- to medium-bedded sandstone, intercalated by mudstone. Fortune Head, Member 2A (Fortunian). **D**, Close-up from Figure 11C showing parallel-lamination (pl) followed by combined-flow ripple cross-lamination (cfr). **E**, General view with intercalated thin- and medium-bedded sandstone, and mudstone (arrows). Grand Bank Head, Member 5 (Cambrian Age 2). **F**, Close-up from Figure 11E showing a hummocky cross-stratification (hcs) capped by symmetrical ripples (arrow). **G**, Interval dominated by isotropic hummocky cross-stratification (hcs) with low dip angles. Fortune Head, Member 2B (Fortunian). **H**, Soft-sediment deformation structure. Grand Bank Head, Member 5 (Cambrian Age 2).

hummocky cross-stratification is composed of: (1) an erosive base; (2) planar-lamination; (3) hummocky cross-stratification, with second-order truncation surfaces; and (4) a rare interval on top, either massive or displaying combined-flow ripple cross-lamination. Hummocky cross-stratification has spacings between hummocks of 1.8–4.4 m and height of 10–12 cm from swale to hummock. In addition, combined-flow ripple cross-lamination can develop directly over a basal planar-laminated interval, without intercalation of any hummocky interval. Locally, convolute bedding forms ball-and-pillow structures or larger-scale slumps. Conglomeratic beds and lenses are common, made of purple phosphatic pebbles, granules, flat mudstone pebbles, or shell debris. Calcite concretions are locally present and can be repeated laterally. In places, a white diagenetic mottling within sandstone beds is visible in Member 5, resulting from local carbonate cementation. In contrast to burrow mottling, this diagenetic mottling does not disrupt the sedimentary fabric and can end abruptly in contact to internal sandstone laminae. Sandstone bed bases are typically sharp and erosive, with rare tool and flute marks. Sandstone bed tops are flat, undulating, or show straight, round- and sharp-crested symmetrical ripples. Microbially modified surfaces are pustular and form patches.

Ichnology. – *Archaeonassa fossulata*, *Arenicolites* isp., *Circulichnis ligusticus*, *C. montanus*, *Cochlichnus luguanensis* Zhang, *Curvolithus multiplex* Fritsch, *C. simplex* Buatois, Mángano, Mikuláš & Maples, *Dendroidichnites* aff. *D. irregulare* (Holub & Kozur), *Didymaulichnus miettensis* Young, *Dimorphichnus* isp. B, ?*Diplocraterion* isp., *Gyrolithes gyratus* (Hofmann), *G. scintillus*, *Helminthoidichnites tenuis*, *Helminthopsis abeli* Książkiewicz, *H. hieroglyphica* Wetzel & Bromley, *H. tenuis* Książkiewicz, *Monomorphichnus lineatus* Crimes, Legg, Marcos & Arboleya, *Palaeophycus annulatus* Badve, *P. tubularis*, *Palaeophycus* isp., *Psammichnites gigas circularis*, *Rosselia* isp., *Rusophycus avalonensis* Crimes & Anderson, *Saerichnites kutscheri*, *Teichichnus rectus* Seilacher, *Treptichnus coronatum* (Crimes & Anderson), *T. pedum*, and *Treptichnus* indet. are present in Facies B2.

Distribution and equivalents. – Facies B2 occurs in Members 2A and 2B (Fortunian) and Member 5 (Cambrian Age 2) at Fortune Head (21.2 m in total; FH-C 13.7–14.8, 16.9–17.4, 22.6–23.1, 24.4–26.2, 44.6–45.8, 66.0–66.3, 88.0–88.2, 88.8–89.5, 101.6–102.2, 102.5–103.3, 103.7–104.2, 108.2–108.6, 114.7–115.2, 117.9–119.7, 128.2–128.8, 131.0–132.2, 139.0–139.4, 146.5–147.3, 148.6–148.9, FH-E 5.6–6.0, 7.1–7.6, FH-F 23.5–23.8, 37.4–39.2, 40.1–42.1, 51.2–52.2, 84.6–85.0, FH-G 3.8–4.4), Fortune North (58.1 m in total; FN-A 7.2–8.5, 18.4–18.7, 19.6–19.8, FN-B 0.2–4.1, 6.2–13.2, 13.4–16.2, 16.6–26.4, 26.7–31.1, 40.5–48.2, 48.3–49.7, 53.2–55.1, 55.7–70.6, 71.0–71.6, 71.8–72.4, 75.0–75.4, 75.6–76.5), Grand Bank Head (40.4 m in total; GBH-C 5.9–9.2, 9.5–10.8, 11.0–11.3, 42.2–42.8, 49.1–49.3, 74.6–75.3, 76.0–76.2, 87.6–87.7, 90.0–92.2, 107.6–107.9, 113.8–114.0, 115.8–117.0, 117.6–117.9, GBH-E 15.4–15.6, GBH-G 7.5–21.0, 21.1–22.2, 22.4–29.5, 30.5–33.0, 33.1–36.2, 36.5–37.6, 38.4–39.3), Lewin's Cove (0.2 m in total; LC-C 24.8–25.0), Little Dantzic Cove (18.4 m in total; LDC-257.8–258.2, 279.4–279.8, 280.0–291.4, 325.7–328.3, 329.1–332.7), and Point May (0.9 m in total; PM-C 118.0–118.6, PM-E 6.5–6.8).

Facies B2 corresponds to the sandier part of Subfacies 2.2B and Subfacies 6.1A of Myrow (1987).

Interpretation. – Amalgamated sandstone and the sedimentary structures argue for a lower shoreface dominated by storms (MacEachern & Pemberton 1992; Buatois & Mángano 2003a; Bann *et al.* 2004; Plint 2010; Dashtgard *et al.* 2012, 2021). On the shoreface, sand is transported by shoaling waves (Plint 2010), and strong and sustained storms allow the formation of hummocky cross-stratification (Dott & Bourgeois 1982; Arora *et al.* 2018; Jelby *et al.* 2020). Amalgamated hummocky cross-stratification is typical of the lower shoreface (MacEachern & Pemberton 1992; Midtgaard 1996; Buatois & Mángano 2003a; Myrow *et al.* 2004; Morsilli & Pomar 2012; Vaucher *et al.* 2017), and mudstone intervals result from background sedimentation in between storm events (Dashtgard *et al.* 2012; Counts *et al.* 2016). The vertical succession in beds having hummocky cross-stratification highlights initial transport of sediment under high-energetic conditions followed by a waning stage with development of hummocks, until the progressive return to fair-weather conditions allowing the formation of combined-flow ripple cross-lamination (Dott & Bourgeois 1982; Walker *et al.* 1983; Morsilli & Pomar 2012; Jelby *et al.* 2020). Massive intervals in hummocky cross-stratification represent rapid settlement of suspended sediment (DeCelles & Cavazza 1992). Combined-flow ripples are common on the shoreface and result from ebb surges created by storms superimposing on oscillatory flows generated by waves (Yokokawa 1995). Preservation of mudstone parting demonstrates that fair-weather deposits were not always fully destroyed during storm events (Myrow *et al.* 2006a). Ball-and-pillow structures and large-scale slumps developed through liquefaction and fluidization of sediment and were arguably triggered by storm-wave activity (Dalrymple 1979; Molina *et al.* 1998; Chen & Lee 2013; Jelby *et al.* 2020). MacEachern

& Pemberton (1992) identified three types of wave-dominated shorefaces, namely storm-influenced, moderately storm-dominated, or strongly storm-dominated, depending on the overall energy (see also Dashtgard *et al.* 2012, 2021 and Wesolowski *et al.* 2018). With the presence of both bedded and amalgamated sandstone of storm origin and the common record of mudstone partings, Facies B2 reflects more likely a moderately or strongly storm-dominated shoreface. Notably, identification of a moderately storm-dominated shoreface relies in part on the presence of lam-scram intervals, which in Facies B2 would be difficult to form due to the evolutionary control on bioturbation (Gougeon *et al.* 2025a).

Facies Association C

Facies association C is recorded from Member 2A (Ediacaran), Members 2A, 2B, and 3 (Fortunian), and Member 5 (Cambrian Stage 2). It represents offshore subenvironments deposited below fair-weather wave base and above storm-weather wave base, encompassing

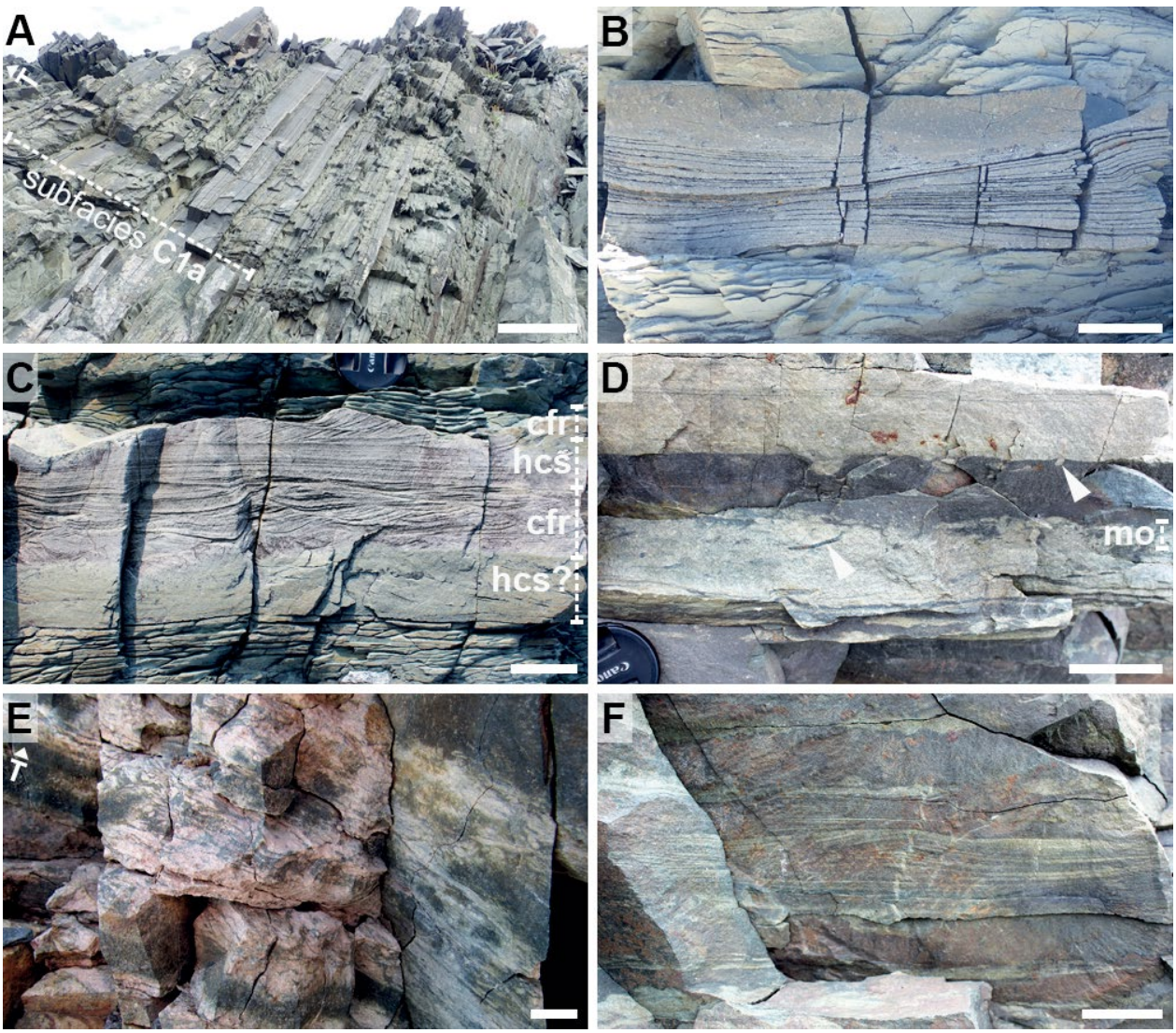

Fig. 12. Facies C1 (offshore transition). Scale bars are 2 cm (E, F), 5 cm (B–D), and 50 cm (A). Stratigraphic tops are indicated by the 'T'. **A**, General view of Subfacies C1a showing tabular, very thin- to thin-bedded sandstone and common hummocky cross-stratification. Fortune Head, Member 2B (Fortunian). **B**, Close-up on an isotropic hummocky cross-stratification in Subfacies C1a, with thickening of laminae on the hummocky (right) and swale (left) intervals (i.e. accretionary morphology). Fortune Head, Member 2A (Fortunian). **C**, A complex hummocky cross-stratification (hcs) in Subfacies C1a, with two combined-flow ripple cross-lamination intervals (cfr) intercalated. Fortune Head, Member 2B (Fortunian). **D**, Subfacies C1b with massive and planar-laminated sandstone. Note the mottled top (mo) and distinctive open burrows filled with sediment from above (arrows). Little Dantzic Cove, Member 5 (Cambrian Age 2). **E**, An intensely bioturbated interval in Subfacies C1b, with bedding hardly preserved. Little Dantzic Cove, Member 5 (Cambrian Age 2). **F**, A rarely preserved hummocky cross-stratification in Subfacies C1b. Little Dantzic Cove, Member 5 (Cambrian Age 2).

the offshore transition (Facies C1), the upper offshore (Facies C2), and the lower offshore (Facies C3).

Facies C1: Very thin- to medium-bedded sandstone and mudstone

Description. – Facies C1 is composed of Subfacies C1a and C1b. Subfacies C1a consists of brown and grey, rarely red, very thin- to medium-bedded, very fine- to medium-grained sandstone intercalated by silver-green medium mudstone (Fig. 12A–C). Subfacies C1b is composed of grey very thin- to medium-bedded, very fine- to fine-grained sandstone intercalated by grey-green sandy mudstone (Fig. 12D–F). Coarse-grained sandstone is uncommon. Sandstone makes up 40–70%. Sandstone beds are typically 0.1–50.0 cm thick, and mudstone layers are 0.1–10.0 cm thick. Facies C1 forms units 0.1–1.6 m thick and represents 67.8 m of strata in total.

Sandstone is massive or displays parallel lamination and hummocky cross-stratification. Sandstone beds are mostly tabular and rarely pinch-and-swell like in Facies C2 and C3. Amalgamation of thin-bedded sandstone is also noted. Hummocky cross-stratification is isotropic with low dip angles, displaying scour-and-drape and accretionary morphologies. A vertical succession in beds with hummocky cross-stratification is typically composed of: (1) an erosive base; (2) planar-lamination, rarely with normal grading; (3) hummocky cross-stratification, with second-order truncation surfaces; and (4) a rare interval on top, either massive or displaying combined-flow ripple cross-lamination. Hummocky cross-stratification has spacings between hummocks of 1.1–4.2 m and heights of 5–25 cm from swale to hummock. Hummocky cross-stratification can also form large-scale lenses. Hummocky cross-stratification is better preserved and more common in Subfacies C1a. Isolated calcite concretions are very rare. In places, sandstone beds are carbonate cemented. Sandstone bed bases are erosive, either sharp or irregular, and display tool marks, flute casts, and load casts.

In addition, wave and combined-flow ripple cross-lamination is recorded in Subfacies C1a, as well as sandstone bed tops showing straight, round- and sharp-crested, symmetrical and near-symmetrical ripples. Pustular, patchy microbially modified surfaces are rare in Subfacies C1a. Normal grading is more common in Subfacies C1b. Moreover, a common sequence in sandstone of Subfacies C1b is: (1) a sharp base, with or without scouring; (2) a parallel-laminated interval; and (3) a diffuse top. Current ripple cross-lamination is in places found in close association to the parallel-laminated interval. Bioturbation can heavily obliterate the sedimentary fabric in Subfacies C1b.

Ichnology. – cf. *Allocotichnus dyeri* Osgood, *Archaeonassa fossulata*, *Arenicolites* isp., *Circulichnis ligusticus*, *Cochlichnus anguineus* Hitchcock, *C. luguanensis*, *Cruziana problematica* (Schindewolf), *Curvolithus simplex*, *Dendroidichnites* aff. *D. irregulare*, *Didymaulichnus miettensis*, *Dimorphichnus* isp. A, cf. *Dimorphichnus* isp., *Gyrolithes gyratus*, *G. scintillus*, *Helminthoidichnites tenuis*, *Helminthopsis hieroglyphica*, *H. tenuis*, *Monomorphichnus bilinearis* Crimes, *M. lineatus*, *Palaeophycus annulatus*, *P. tubularis*, *Palaeophycus* isp., *Psammichnites gigas circularis*, *Rusophycus dabardae* isp. nov., *Saerichnites kutscheri*, *Teichichnus rectus*, *Torrowangea rosei*, *Treptichnus bifurcus* Miller, *T. coronatum*, *T. pedum*, *T. pollardi* Buatois & Mángano, *Treptichnus* indet., and *Trichichnus linearis* Frey are present in Facies C1.

Distribution and equivalents. – Facies C1 occurs in Members 2A, 2B, and 3 (Fortunian), and Member 5 (Cambrian Age 2) at Fortune Head (39.5 m in total; FH-B 38.8–39.1, 43.4–43.8, 44.8–45.1, 46.1–46.4, 48.6–49.1, 61.5–61.9, 62.3–62.6, 69.5–70.0, FH-C 15.3–15.8, 16.7–16.9, 17.4–18.2, 23.1–24.4, 44.2–44.6, 54.7–54.9, 65.9–66.0, 70.0–70.2, 75.5–76.0, 82.8–84.1, 88.2–88.8, 89.5–90.0, 92.2–92.3, 93.1–93.4, 95.0–95.7, 101.4–101.6, 102.2–102.5, 103.3–103.7, 105.3–105.9, 110.5–111.4, 114.3–114.7, 116.1–116.3, 116.8–117.9, 123.8–125.1, 126.1–126.5, 126.8–127.1, 129.8–130.0, 138.3–139.0, 139.4–140.2, 142.9–143.5, 146.1–146.5, 147.8–148.6, 151.7–152.1, 153.5–153.7, FH-D 0.0–0.8, 1.9–2.7, FH-E 0.4–1.0, 2.5–3.9, 5.2–5.6, 6.3–7.1, 10.1–11.3, FH-F 2.8–3.0, 4.0–4.2, 9.4–9.6, 17.4–17.5, 18.0–19.1, 19.7–20.2, 21.8–22.2, 23.4–23.6, 23.8–24.2, 28.0–28.1, 28.9–29.2, 34.5–34.7, 39.2–40.1, 47.0–47.3, 49.6–49.8, 50.3–51.2, 52.6–53.3, 54.7–55.0, 60.4–60.6, 61.3–61.5, 64.8–65.0, 67.3–67.5, 71.2–71.8, 86.1–86.5, FH-G 2.6–3.8, 5.4–5.7, 7.7–8.3, 10.5–11.2, 12.5–12.7, 15.0–15.2, 16.9–17.8, 55.0–55.1, 55.5–56.2), Fortune North (4.2 m in total; FN-A 5.7–6.3, 7.0–7.2, 9.7–10.0, 15.4–15.5, 18.2–18.4, 23.1–23.5, 23.9–24.2, 24.7–24.8, 25.5–25.7, 39.0–39.4, 40.4–40.6, FN-B 13.2–13.4, 16.2–16.6, 26.4–26.7, 40.3–40.5, 48.2–48.3), Grand Bank Head (11.8 m in total; GBH-B 10.7–11.0, 12.5–13.3, GBH-C 5.6–5.9, 18.0–18.2, 22.5–22.9, 29.5–30.0, 40.4–40.7, 41.6–42.2, 49.0–49.1, 59.2–59.5, 62.1–62.3, 63.2–63.3, 66.2–66.8, 67.4–68.0, 74.1–74.6, 76.2–77.4, 87.0–87.6, 89.6–90.0, 100.3–100.4, 103.0–103.3, 107.4–107.6, 112.3–113.2, 113.5–113.8, 117.0–117.6, GBH-E 2.7–3.0, 5.3–5.5, 13.5–13.7, GBH-G 21.0–21.1, 22.2–22.4, 33.0–33.1, 36.2–36.5), Lewin's Cove (2.5 m in total;

LC-C 8.9–9.3, 10.6–11.0, 12.1–12.2, 23.1–23.4, 35.2–35.5, 36.4–37.2, 38.0–38.2), Little Dantzic Cove (5.5 m in total; LDC 66.5–66.6, 243.8–244.0, 244.6–245.0, 247.4–247.8, 248.8–249.1, 255.6–256.0, 257.4–257.8, 261.4–262.3, 271.1–271.6, 272.8–273.0, 273.8–273.9, 277.8–279.4), and Point May (4.3 m in total; PM-B 1.0–1.3, 7.2–7.4, 9.5–10.7, PM-C 9.0–9.3, 18.7–19.0, 123.5–123.9, 128.4–128.5, 130.5–130.7, 131.5–132.3, PM-D 1.2–1.6, PM-E 3.0–3.1).

Subfacies C1a is found in Members 2A, 2B, and 3 (Fortunian), and Subfacies C1b in Member 5 (Cambrian Age 2). Subfacies C1a corresponds to the finer-grained intervals of Subfacies 2.2B and the sandier intervals of Facies 2.3 of Myrow (1987), whereas Subfacies C1b represents the sandier intervals of Facies 5.2 of Myrow (1987).

Interpretation. – The sandstone/mudstone ratio and the prevalence of hummocky cross-stratification are consistent with an offshore transition (Howard & Reineck 1981; MacEachern *et al.* 1999; Buatois & Mángano 2003a; Bann *et al.* 2004; Eide *et al.* 2015; Wesolowski *et al.* 2018). The offshore transition is typified by an alternation in energy and processes, with oscillatory and unidirectional flows dominating during storms, and fine-grained suspended particles settling on the seafloor during quiescent moments (MacEachern & Pemberton 1992; Buatois & Mángano 2003a; Bann *et al.* 2004; Wesolowski *et al.* 2018). Hummocky cross-stratification is typically developed during strong storms, hurricanes, or tsunamis (Dott & Bourgeois 1982; Hunter & Clifton 1982; Duke 1985). Notably, isotropic hummocky cross-stratification develops under pure oscillatory flows or with the addition of a very weak unidirectional current (Arnott & Southard 1990; Dumas *et al.* 2005; Dumas & Arnott 2006). Therefore, isotropic hummocky cross-stratification is prevalent on low-gradient shelves, where the development of unidirectional currents is less important and storm-induced oscillatory flows prevail (Jelby *et al.* 2020; Grundvåg *et al.* 2021). Moreover, the sequence observed in hummocky cross-stratification demonstrates a deceleration in flow velocity, from basal upper-flow regime with parallel-lamination grading into the typical hummocky stratification, then followed by lower flow-regime combined-flow ripple cross-lamination resulting from the late stage of the storm surge (Simpson & Eriksson 1990; Runkel 1994; Myrow *et al.* 2006b). Thicker hummocky cross-stratification develops from the stacking of several erosive depositional storm events (Aigner 1982). In Subfacies C1b, offshore transition with reduced intensity and frequency of storms can display higher bioturbation levels, as a result of long-term colonisation windows opened in a well oxygenated environment (MacEachern & Pemberton 1992; Wesolowski *et al.* 2018).

Subfacies C1a represents a typical storm-dominated offshore transition, whereas subfacies C1b relates more likely to a weakly storm-affected offshore transition as described by Wesolowski *et al.* (2018). In the Chapel Island Formation, early stages in animal evolutionary innovations would have played a significant role in the low bioturbation intensities observed in Subfacies C1a which are only recorded from Member 2 (i.e. Fortunian), contrary to Subfacies C1b which displays more thoroughly churned intervals (Fig. 12E; Gougeon *et al.* 2018a) and which is recorded from Member 5 (i.e. Cambrian Age 2) (Gougeon *et al.* 2025a).

Facies C2: Mudstone with thinly laminated to very thin-bedded sandstone

Description. – Facies C2 is composed of Subfacies C2a, C2b, and C2c. Subfacies C2a consists of dominant silver green, medium mudstone, intercalated with brown and dark grey thinly laminated to very thin-bedded, very fine- to fine-grained sandstone (Fig. 13A–D). Subfacies C2b is composed of dominant red medium mudstone, intercalated with green thinly laminated to very thin-bedded, very fine- to fine-grained sandstone (Fig. 13E, F). Subfacies C2c is dominated by grey green sandy mudstone, intercalated with thinly laminated to very thin-bedded, very fine- to fine-grained sandstone (Fig. 13G, H). Medium- and coarse-grained sandstone is less common. Sandstone makes up 20–40%. Sandstone beds are typically 0.05–5.0 cm thick, and mudstone layers are 0.1–10.0 cm thick. Facies C2 forms units 0.1–4.1 m thick and represents 231.3 m of strata in total.

Sandstone beds are massive or display parallel-lamination and normal grading. Sandstone beds are either laterally continuous with common pinch-and-swell or discontinuous, in places developing starved wave and current ripples. Sandstone beds are in places calcite cemented and can also be quartzitic. Sandstone bed bases are erosive, either sharp or irregular, and display tool marks, load casts, and scratch circles ('Kullingia').

Subfacies C2a shows wave and combined-flow ripple cross-lamination and (micro-) hummocky cross-stratification. Wave ripple cross-lamination can follow a basal planar-laminated interval. In Subfacies C2a, sandstone bed tops are flat or show symmetrical ripples that are typically round-crested, straight to sinuous, in places bifurcating. Hummocky cross-stratification is isotropic with scour-and-drape morphologies and commonly forms large-scale lenses. A vertical succession in beds

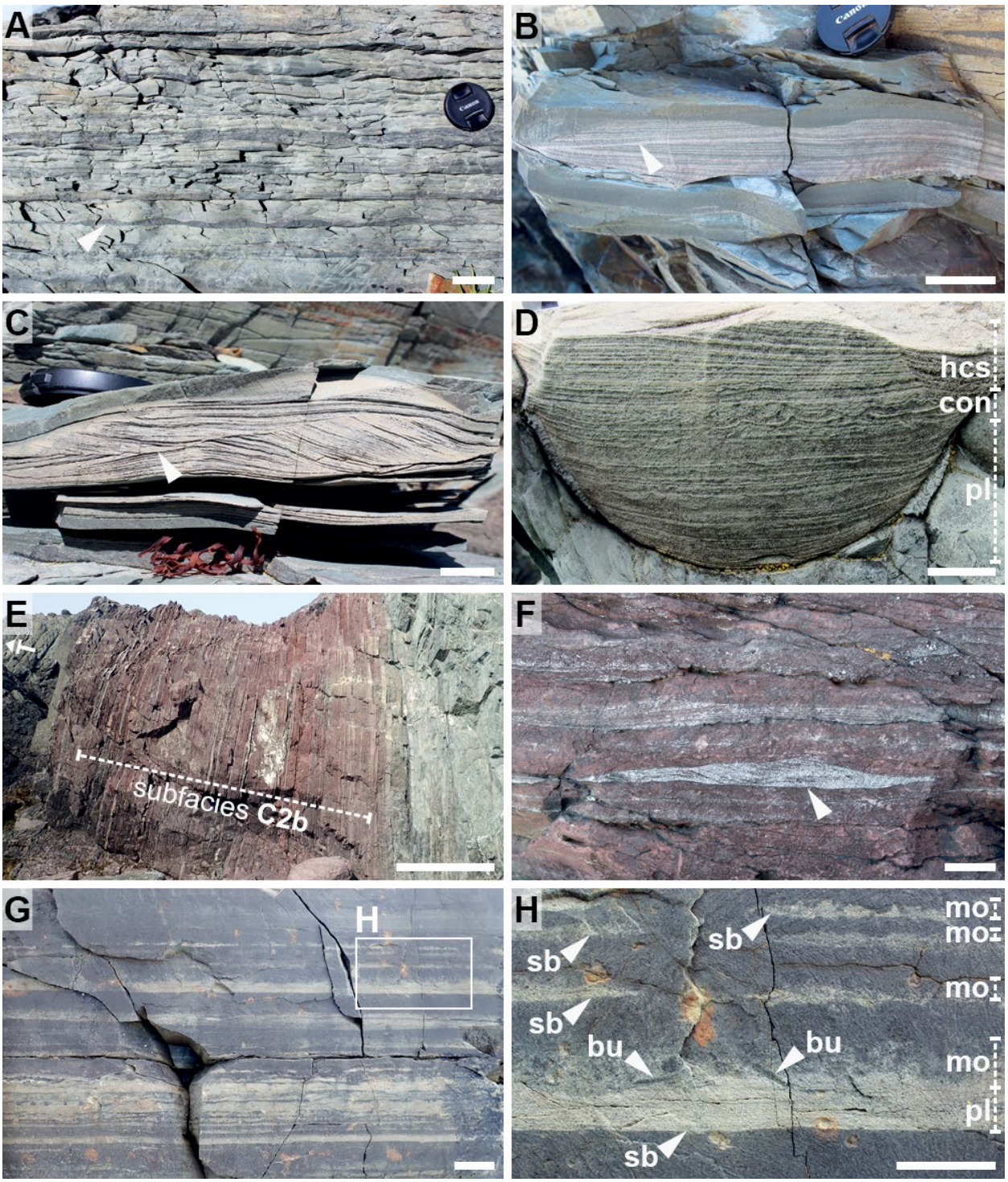

Fig. 13. Facies C2 (upper offshore). Scale bars are 2 cm (C, D, F), 5 cm (A, B, H), 10 cm (G), and 100 cm (E). **A**, General view of Subfacies C2a showing tabular, thinly laminated to very thin-bedded sandstone. Note the sandstone bed with symmetrical rippled top (arrow). Fortune Head, Member 2A (Fortunian). **B**, Lenticular isotropic hummocky cross-stratification in Subfacies C2a. Note the second-order truncation surface (arrow). Fortune Head, Member 2A (Fortunian). **C**, Calcite concretion in Subfacies C2a showing combined-flow ripple cross-lamination, with basal aggregation of undulated laminae displaying lateral deviation (right side) crosscut by a truncation surface (arrow) and capped by undulated subparallel laminae. Fortune Head, Member 2A (Fortunian). **D**, Gutter cast in Subfacies C2a with basal parallel lamination (pl), small-scale convolution (con), and hummocky cross-stratification (hcs) on top. Fortune Head, Member 2A (Fortunian). **E**, General view of Subfacies C2b. Stratigraphic top is indicated by the 'T'. Fortune Head, Member 2B (Fortunian). **F**, Starved current ripple cross-lamination in Subfacies C2b (arrow). Note that sandstone laminae and beds are calcite cemented. Grand Bank Head, Member 2B (Fortunian). **G**, General view of Subfacies C2c. Little Dantzic Cove, Member 5 (Cambrian Age 2). **H**, Close-up from Figure 13G showing the common sequence with sharp erosive base (sb), parallel lamination (pl), and burrow mottling (mo). Note the presence of distinctive burrows (bu). See also Figure 64 for further interpretation.

with hummocky cross-stratification is composed of: (1) an erosive base; (2) planar-lamination, with in places normal grading; (3) hummocky cross-stratification, with second-order truncation surfaces; and (4) a rare interval on top, either apparently massive or displaying combined-flow ripple cross-lamination. Weak convolution within the hummocky interval (3) has been noted. (Micro-) hummocky cross-stratification has spacing between hummocks of 0.3–1.7 m and height of 2–15 cm from swale to hummock. Distinction between large combined-flow ripple cross-lamination and micro-hummocky cross-stratification can be difficult. Isolated calcite concretions are common. In places, granules and rounded pebbles form conglomeratic lenses and beds that can be normal graded (especially in basal Member 2A). Microbially modified surfaces are either pustular, reticulated (i.e. 'Kinneyia'-type), or rarely made of subparallel linear elements (i.e. 'Arumberia'-like), and can be patchy or covering larger areas.

Gutter casts, pot casts, and injection structures are conspicuous elements of Subfacies C2a, notably in the lower half of Member 2A. Gutter casts are 3–24 cm wide, 3–19 cm deep, and are filled with fine-grained sandstone and, to a lesser extent, with medium-grained sandstone and granular to pebbly conglomerate. Gutter casts are mostly horizontal, narrow to wide, straight to sinuous. In cross-section, gutter casts are U- to V-shaped with common wide upper openings and are either isolated or connected to an overlying sandstone bed (see Myrow 1992a for a detailed description of gutter cast morphologies). Infill of gutter casts is massive, normally graded, parallel-laminated, or hummocky cross-stratified. Wave and climbing ripple cross-lamination has been noted in the upper portion. On gutter cast bases and sides, tool and flute marks are commonly aligned to the gutter orientation. Myrow (1987, 1992a) noted that gutter casts are mostly oriented NE-SW at Fortune Head (n = 90). Pot casts are 3–17 cm wide, 1–4 cm deep, and form short to tall pillars filled with fine-grained sandstone and shale-chip conglomerate (Myrow 1992a), in places displaying longitudinal circular markings on their walls. Pot casts have semi-circular, flat, or widened bases in cross-section. Injection structures are straight to very irregular (ptygmatic) in vertical section and are filled with very fine- to fine-grained sandstone. They are typically connected to sandstone beds at their tops and taper at their bases.

Subfacies C2b and C2c are notable for the prevalence of current ripple cross-lamination in sandstone. In Subfacies C2c, intense burrow mottling commonly disrupts or homogenizes sandstone and sandy mudstone intervals. In vertical sections, Subfacies C2c shows small- and large-scale scours filled with current-ripple cross-laminated sandstone. Sandstone bed soles and tops are rarely exposed in Subfacies C2c. However, sandstone tops in vertical section are commonly diffuse because of intense bioturbation. In Subfacies C2c, a common vertical succession in thin-bedded sandstone is: (1) a sharp base, with or without scouring; (2) a parallel-laminated interval, with in places normal grading; and (3) a diffuse top.

Palaeocurrent data recorded by Myrow (1992b) from Member 2 (Subfacies C2a) argue for a NE-SW orientation, with a strong unimodal orientation toward the NE displayed by flute casts. Palaeocurrent data from Member 5 (Subfacies C2c) are scarce as bed soles and tops are poorly exposed, and do not show any preferential orientation (Myrow 1987).

Ichnology. – *Archaeonassa fossulata*, *Arenicolites* aff. *A. carbonarius* (Binney), *Arenicolites* isp., *Bergaueria perata* Prantl, *B.* cf. *B. radiata* Alpert, *Circulichnis montanus*, *Cochlichnus luguanensis*, *Conichnus conicus* Männil, *Cruziana problematica*, *Curvolithus multiplex*, *C. simplex*, *Curvolithus* isp., *Dendroidichnites* aff. *D. irregulare*, *Didymaulichnus miettensis*, *Dimorphichnus* isp. A, *Gordia marina* Emmons, *Gyrolithes gyratus*, *G. scintillus*, *Helminthoidichnites tenuis*, *Helminthopsis abeli*, *H. hieroglyphica*, *H. tenuis*, *Monomorphichnus bilinearis*, *M. lineatus*, *M. needleiunm* Wang, *Palaeophycus annulatus*, *P. tubularis*, *Palaeophycus* isp., *Psammichnites gigas circularis*, *Rusophycus dabardae*, *Saerichnites kutscheri*, *Teichichnus rectus*, *Treptichnus bifurcus*, *T. coronatum*, *T. pedum*, *T. pollardi*, *Treptichnus* indet., *Trichichnus linearis*, *Trichichnus* isp., and radial probing burrow are present in Facies C2.

Distribution and equivalents. – Facies C2 occurs in Member 2A (Ediacaran), Members 2A and 2B (Fortunian), and Member 5 (Cambrian Age 2) at Fortune Head (103.8 m in total; FH-A 16.0–16.1, 18.6–19.3, 21.2–21.8, 26.0–26.2, 29.6–29.7, FH-B 5.7–5.8, 17.6–18.3, 21.0–21.1, 23.3–23.7, 25.6–25.7, 27.0–27.1, 28.0–28.9, 31.8–32.3, 33.2–33.8, 36.2–36.7, 38.6–38.8, 39.6–39.8, 40.1–40.3, 42.0–42.1, 42.5–42.8, 43.8–44.8, 45.1–46.1, 46.4–47.3, 47.7–47.9, 50.6–50.9, 51.5–51.9, 53.1–53.9, 54.4–54.6, 54.9–56.1, 56.6–57.7, 59.6–60.2, 60.5–61.5, 61.9–62.4, 63.0–63.8, 65.6–66.1, 67.8–68.2, 68.9–69.5, 71.0–71.5, 72.0–72.2, 73.0–74.1, FH-C 13.3–13.7, 15.1–15.3, 16.2–16.3, 26.2–27.7, 29.4–31.9, 45.8–46.6, 47.5–47.8, 48.3–49.2, 53.0–53.5, 54.5–54.7, 55.7–56.0, 67.4–67.6, 69.5–70.0, 71.3–72.0, 72.5–72.7, 73.3–73.8, 74.8–75.5, 76.0–76.2, 77.8–78.8, 82.4–82.8, 84.0–85.2, 90.2–92.2, 92.3–93.1, 95.7–96.7, 97.9–99.7, 100.7–100.8, 101.3–101.4, 104.9–105.3, 106.4–107.8, 109.9–110.5, 114.0–114.3, 115.8–116.1, 116.3–116.8, 120.3–120.7, 121.1–121.3, 123.2–123.8, 125.9–126.1, 127.1–127.6, 129.6–129.8, 130.7–131.0, 132.8–133.3, 134.4–134.8, 141.7–142.9, 143.5–143.9, 144.6–145.1,

145.8–146.1, 147.3–147.8, 148.9–150.4, 150.9–151.7, 152.5–152.7, 152.9–153.1, FH-D 0.8–1.9, 2.7-6.0, 6.5–6.7, FH-E 0.0–0.4, 1.2–2.5, 4.6–5.2, 6.0–6.3, 7.6–10.0, FH-F 1.7–2.0, 4.8–5.0, 5.6–6.1, 8.1–8.3, 9.0–9.4, 10.2–10.8, 12.4–12.7, 14.2–14.5, 16.9–17.4, 20.2–21.8, 23.0–23.4, 24.2–25.1, 26.3–28.0, 28.6–28.9, 29.7–30.3, 33.4–33.7, 35.3–35.5, 43.7–47.0, 48.6–49.6, 49.8–50.3, 52.2–52.6, 53.3–54.7, 55.0–55.7, 57.0–57.1, 60.6–61.3, 62.0–62.6, 64.1–64.8, 67.0–67.3, 67.9–68.4, 73.3–74.3, 74.7–78.0, 80.3–80.4, 81.2–81.3, 82.8–83.5, 84.3–84.6, 85.0–85.6, 85.9–86.1, 86.8–87.0, 87.2–89.6, FH-G 1.2–2.6, 4.4–5.4, 6.2–6.8, 7.2–7.7, 8.8–9.8, 10.2–10.5, 11.6–12.5, 13.7–15.0, 15.2–16.9, 18.7–19.0, 22.2–22.5, 50.9–55.0, 55.1–55.5, 56.8–57.7), Fortune North (15.9 m in total; FN-A 1.9–2.2, 3.1–3.8, 9.2–9.7, 11.4–11.6, 13.3–15.4, 16.4–18.2, 18.7–19.6, 19.2–21.8, 22.3–23.1, 23.5–23.9, 24.2–24.6, 24.8–25.5, 25.7–27.1, 27.8–28.4, 29.4–30.0, 38.9–39.0, 40.2–40.4, 40.6–42.2), Grand Bank Head (36.8 m in total; GBH-B 0.0–0.1, 1.7–2.2, 3.1–3.4, 5.3–5.4, 6.9–7.1, 10.5–10.7, GBH-C 4.2–5.6, 17.6–18.0, 21.2–22.5, 23.4–23.8, 25.2–26.3, 26.8–27.1, 27.6–28.4, 29.1–29.5, 30.4–31.2, 32.6–36.1, 36.7–36.8, 38.0–38.2, 39.9–40.0, 44.0–44.3, 45.3–45.6, 47.0–48.0, 48.5–49.0, 57.5–59.2, 59.8–60.1, 61.8–62.1, 62.3–63.2, 63.7–64.3, 65.4–66.2, 66.8–67.4, 68.0–69.0, 73.6–74.1, 83.2–83.7, 86.8–87.0, 87.7–89.6, 92.6–93.8, 99.2–100.3, 102.8–103.0, 103.3–103.8, 105.0–107.4, 113.2–113.5, GBH-D 0.0–0.8, 33.8–33.9, 47.5–49.1, GBH-E 1.1–2.7, 4.0–5.3, 7.5–8.1, 8.6–9.1, 9.5–9.6, 10.5–11.3, 14.4–14.5), Lewin's Cove (20.6 m in total; LC-B 22.0–23.0, 24.5–24.7, 25.3–25.8, 27.7–28.9, 29.4–29.5, 32.2–33.4, 43.4–43.6, 45.2–45.5, LC-C 0.9–1.9, 3.8–5.7, 8.4–8.9, 11.1–12.1, 12.2–15.8, 19.0–19.9, 20.5–22.6, 23.4–24.8, 25.0–25.2, 30.2–30.5, 31.8–32.5, 36.0–36.4, 37.2–38.0, 40.0–41.1), Little Dantzic Cove (17.7 m in total; LDC 180.5–180.9, 188.8–189.1, 212.7–212.9, 224.4–224.6, 227.9–228.4, 228.8–229.1, 236.3–238.3, 242.1–242.2, 242.7–243.8, 244.0–244.5, 247.2–247.4, 250.6–250.7, 253.0–253.4, 254.9–255.6, 256.6–257.4, 258.8–261.4, 262.3–263.4, 266.3–270.4, 270.8–271.1, 275.5–277.3), and Point May (36.5 m in total; PM-A 25.8–26.5, 27.9–28.9, PM-B 3.6–3.7, 6.7–7.2, 7.9–8.3, 11.4–12.8, 15.3–15.9, 17.7–19.0, 21.7–23.0, PM-C 7.3–7.8, 8.7–9.0, 11.8–12.3, 14.3–14.8, 15.5–16.2, 19.0–19.4, 22.7–22.8, 24.2–24.5, 25.4–25.9, 27.2–27.9, 29.4–30.3, 32.3–33.0, 33.3–33.4, 35.9–36.0, 43.0–43.3, 44.3–44.8, 47.6–48.2, 62.0–62.1, 69.2–69.4, 70.6–71.0, 73.8–74.8, 75.5–76.4, 78.0–78.9, 82.2–83.5, 116.4–116.5, 119.2–119.5, 119.9–122.8, 123.9–124.6, 128.2–128.4, 128.5–130.5, 130.7–131.5, 133.9–135.3, 137.6–138.2, 139.2–139.6, PM-D 6.4–7.1, 8.9–9.1, 13.5–14.7, PM-E 0.8–3.0, 6.8–7.6, 13.3–14.7, 16.1–16.9).

Subfacies C2a is found in Member 2A (Ediacaran) and Members 2A and 2B (Fortunian), Subfacies C2b in Member 2B (Fortunian), and Subfacies C2c in Member 5 (Cambrian Age 2). Subfacies C2a, C2b and C2c correspond, in parts, to Facies 2.1/Subfacies 2.2A, Facies 2.3, and Subfacies 5.1B/Facies 5.2 of Myrow (1987), respectively.

Interpretation. – The sandstone/mudstone ratio and the sedimentary structures indicate deposition in an upper offshore (MacEachern & Pemberton 1992; Bann *et al.* 2004; Buatois & Mángano 2011; Chen & Lee 2013; Łabaj & Pratt 2016; Vaucher *et al.* 2020). Heterolithic bedding demonstrates rapid changes in flow velocities, with sandstone deposited during energetic events and mudstone mostly settling from suspension fallout during quiescent moments. In addition, some of the tabular, thinly to thickly laminated sandstone may also have formed through suspension fallout (Myrow 1992b). Scratch circles ('Kullingia') are physical structures formed by the passive rotation of an anchored object on the substrate (Jensen *et al.* 2002a, 2018a).

In Subfacies C2a, oscillatory flows generated by fair-weather wave and storm-wave action are the dominant processes in the upper offshore. Isotropic hummocky cross-stratification can form during storms, tsunamis, and hurricanes (Dott & Bourgeois 1982; Duke 1985; Arora *et al.* 2018), either from pure oscillatory flows or combined flows resulting from the superimposition of a low-velocity unidirectional current (Arnott & Southard 1990; Dumas *et al.* 2005; Dumas & Arnott 2006). Isotropic hummocky cross-stratification commonly prevails on low-gradient shelves having a large proportion of their seafloor above storm wave base (Jelby *et al.* 2020; Grundvåg *et al.* 2021). Micro-hummocky cross-stratification and lenticular hummocky cross-stratification demonstrate limited sand supply and distalward transport of sand relatively to the main storm activity affecting the shoreface. Starved wave ripples and symmetrical ripple crests indicate that wave action developed during fair-weather conditions or during the waning stage following storms (Dott & Bourgeois 1982; Walker *et al.* 1983; Arnott 1993; Basilici *et al.* 2012). Convolution within hummocky cross-stratification results from liquefaction of sediment triggered by stress related to storm wave (Molina *et al.* 1998; Jelby *et al.* 2020). In fact, gutter casts oriented perpendicular to the shoreline (Myrow 1992a), in addition to hummocky cross-stratification and combined-flow ripple cross-lamination, indicate that subsidiary unidirectional currents were present as well. Considering the dominance of storm-wave action, these currents may have been related to storm-generated offshore-directed flows (Myrow *et al.* 2002; Pattison *et al.* 2007; Basilici *et al.* 2012; Grundvag *et al.* 2021). Such currents can develop during storm surge,

with coastal sea-level set-up causing major downwelling of currents carrying sediment offshore along the bottom seafloor (Leckie & Krystinik 1989; Cheel & Leckie 1993). In addition, wave-modified turbidity currents display basal normal grading followed by hummocky cross-stratification and combined-flow ripple cross-lamination similarly to some sandstone beds of Subfacies C2a; they are interpreted as resulting from excess-weight forces during storms that can carry sediment offshore (Myrow & Southard 1996; Myrow *et al.* 2002; Lamb *et al.* 2008). Across-shelf transport of sediment through wave-modified turbidity currents are potentially related to seasonal increased storm activity and enhanced river discharge after rainfall (Pattison *et al.* 2007). Normal graded beds with gravel conglomerate and coarse-grained sandstone at their bases, albeit in low proportion and mostly restricted to the base of Member 2A, suggest traction of sediment followed by a waxing stage that is more typical of hyperpycnal flows, preferentially generated directly on the shelf with the aid of storm-wave action (Mulder *et al.* 2003; Pattison & Hoffman 2008; Bhattacharya & MacEachern 2009; Jelby *et al.* 2020; Lin & Bhattacharya 2021; Zavala *et al.* 2021, 2024). Hyperpycnal flows generated by waves only require low-gradient slopes to develop (Bhattacharya & MacEachern 2009), which corroborates interpretations on isotropic hummocky cross-stratification. Dewatering cracks (i.e. injections structures) as observed in basal Member 2A are also commonly associated with hyperpycnal deposits, suggesting slight freshwater inputs in the system (Bhattacharya & MacEachern 2009; Birgenheier *et al.* 2017).

Subfacies C2b and C2c display current ripple cross-lamination, in addition to tool marks and small- and large-scale scours (in Subfacies C2c), which indicate dominance of unidirectional flows in the upper offshore. Prevalence of unidirectional currents over oscillatory flows can be related to the presence of a moderate- to high-gradient shelf, where shelf-crossing, gravity-driven currents are more prone to develop (Jelby *et al.* 2020; Grundvåg *et al.* 2021). Several mechanisms have been invoked to explain current development below fair-weather wave base. In addition to the offshore-directed, storm-related currents described above, geostrophic currents are formed offshore during storms, triggered by wind stress on the water surface (Swift *et al.* 1983, 1987; Niedoroda *et al.* 1984, 1985). Geostrophic currents are parallel to oblique to the shoreline (Swift *et al.* 1983; Plint 2010). Considering that palaeocurrent datasets from Subfacies C2b and C2c are limited (Myrow 1987), definitive conclusions on the origin of these offshore currents are difficult. Nevertheless, the more intense bioturbation both in Subfacies C2b (abundant *Teichichnus*) and Subfacies C2c (mottled ichnofabrics) indicate that these currents were able to provide good oxygen and nutrient levels, allowing the endobenthos to thrive.

Myrow (1987) noted similarities between the common vertical succession of Subfacies C2c and the classic Bouma sequence of deep-marine turbidites, notably with the presence of normal grading within parallel-laminated intervals. Similarities between Bouma sequences of turbidites and sequences in distal tempestites have also been noted by other authors (e.g. Cheel & Leckie 1993; Mulder *et al.* 2009). However, classic Bouma sequences are typically more complex, notably with the presence of a basal T_a division with normal grading in coarser-grained lithologies and a T_c division with ripple cross-lamination (Middleton & Hampton 1973; Nichols 2009; Peakall *et al.* 2020). Wave-modified turbidites, which tend to show similar vertical successions, display oscillatory-flow structures (small-scale hummocky cross-stratification, combined-flow ripples; Myrow *et al.* 2002) that are absent in Subfacies C2c. However, the basal portion of wave-modified turbidites, with an erosive base followed by normal grading (Myrow *et al.* 2002), is similar to the common succession of Subfacies C2c. Hyperpycnal flows display both inverse and normal grading, common climbing ripples, and coarser-grained intervals evidencing sustained and prolonged supply of sediment (Mulder & Alexander 2001; Mulder *et al.* 2003; Bhattacharya & MacEachern 2009; Zavala & Arcuri 2016) that are absent in Subfacies C2c. Consequently, the parallel-laminated interval of the common vertical succession is interpreted as being deposited from sheet flows generated by storm-waves (Clifton 1981; DeCelles & Cavazza 1992), whereas the return to fair-weather conditions permitted recolonisation of the seafloor by organisms (MacEachern & Pemberton 1992; Bann *et al.* 2004).

Facies C3: Interlaminated mudstone and sandstone

Description. – Facies C3 is composed of Subfacies C3a, C3b, C3c, and C3d. Subfacies C3a consists of dominant green and silver green, medium mudstone, intercalated with brown and dark grey, thinly to thickly laminated, very fine- to fine-grained sandstone (Fig. 14A–G). Subfacies C3b is composed of dominant red medium mudstone, intercalated with green thinly to thickly laminated, very fine- to medium-grained sandstone (Fig. 14H). Subfacies C3c consists of red, purple, grey, and green fine mudstone, intercalated with thinly laminated to very thin-bedded, very fine- to fine-grained sandstone (Fig. 14I, J). Subfacies C3d is dominated by grey green sandy mudstone, intercalated with dark grey thinly to thickly laminated, very fine- to fine-grained sandstone (Fig. 14K). Medium- and coarse-grained

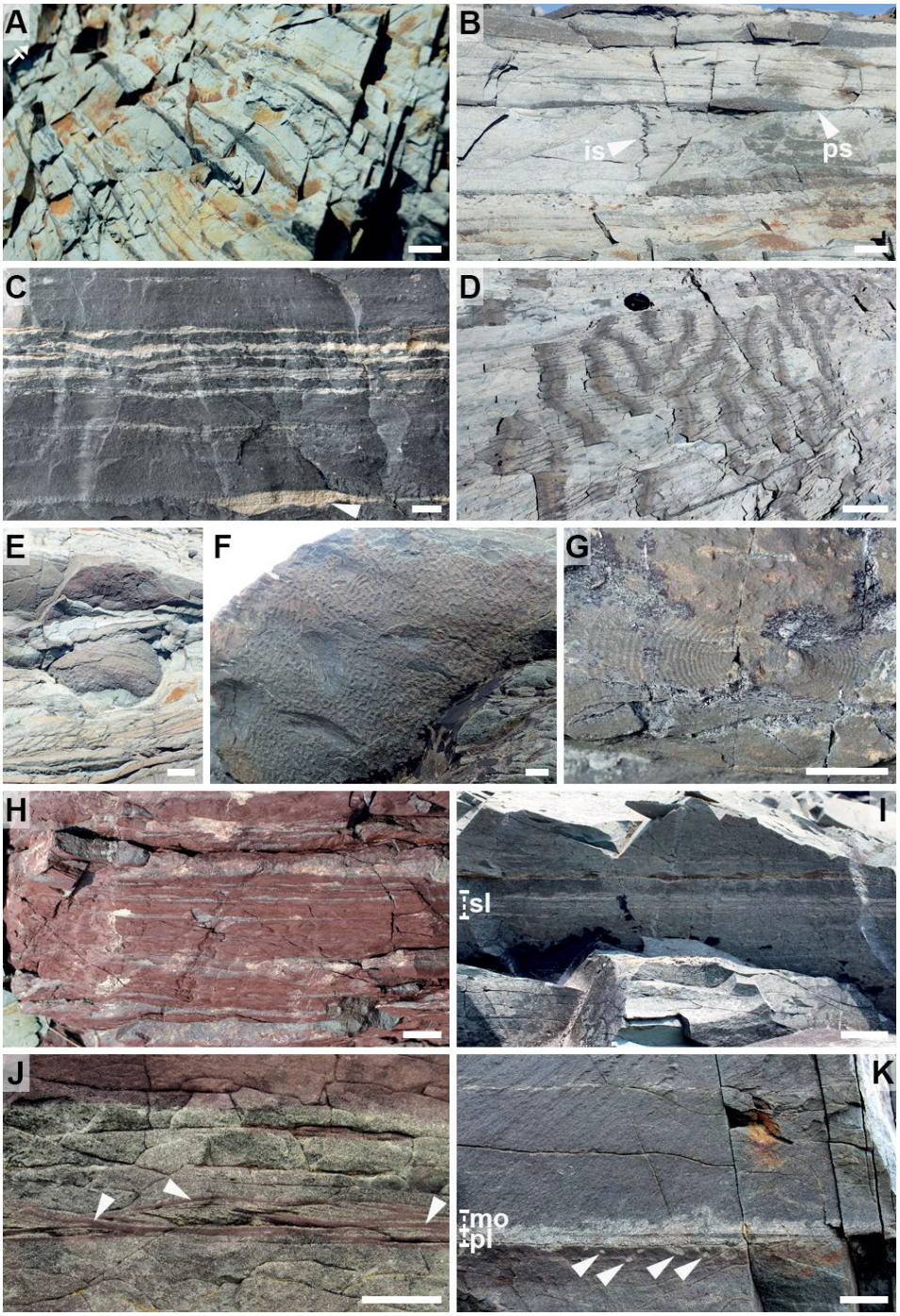

Fig. 14. Facies C3 (lower offshore). Scale bars are 1 cm (G), 2 cm (A–C, E, F, H, J, K), and 10 cm (D, I). **A**, General view of Subfacies C3a showing laterally extensive, thinly to thickly laminated sandstone. Stratigraphic top is indicated by the 'T'. Grand Bank Head, Member 2A (Fortunian). **B**, Subfacies C3a showing pinch-and-swell (ps) within a thickly laminated sandstone, and an injection structure (is). Fortune Head, Member 2A (Fortunian). **C**, Subfacies C3a with closely spaced, cemented thin sandstone laminae, some developing blebby patterns. Note the erosive base (arrow). Grand Bank Head, Member 2B (Fortunian). **D**, Top view with sinuous, in places bifurcating, round-crested symmetrical ripples in Subfacies C3a. Fortune Head, Member 2A (Fortunian). **E**, Large pot cast with coarse-grained sandstone at the base, and longitudinal circular markings on the wall. Grand Bank Head, Member 2A (Fortunian). **F**, Top view of a reticulated, microbially modified surface ('Kinneyia'-type) in Subfacies C3a, covering a large area. Grand Bank Head, Member 2A (Fortunian). **G**, Top view of scratch circles ('Kullingia') in Subfacies C3a. Fortune Head, Member 2A (Fortunian). **H**, General view of Subfacies C3b showing red medium mudstone. Fortune Head, Member 2B (Fortunian). **I**, General view of Subfacies C3c showing grey fine mudstone. Note closely spaced thin sandstone laminae (sl). Little Dantzic Cove, Member 4 (Cambrian Age 2). **J**, Close-up on current ripple cross-lamination having thick fine mudstone draping in Subfacies C3c (arrows). Note transition from green to red fine mudstone. Little Dantzic Cove, Member 4 (Cambrian Age 2). **K**, General view of Subfacies C3d, with a common sequence of sharp erosive base, parallel lamination (pl), and burrow mottling (mo). Note the distinctive burrows filled from above (arrows), and the thin sandstone laminae at the top. Little Dantzic Cove, Member 5 (Cambrian Age 2).

sandstone is uncommon. Sandstone makes up 5–20%. Sandstone beds are typically 0.05–2.0 cm thick, and mudstone layers are 0.1–20.0 cm thick. Facies C3 forms units 0.1–11.4 m thick and represents 408.0 m of strata in total.

Sandstone is massive or displays normal grading and parallel lamination. Thin sandstone laminae are either faint or clearly distinctive and are commonly laterally extensive. Thick sandstone laminae are tabular or discontinuous laterally with pinch-and-swell morphologies, in places with starved wave and current ripples. Thick sandstone laminae can have diffuse tops, with normal grading fading within the overlying mudstone. Sandstone bed bases are erosive, either sharp or irregular, and display tool marks, flute casts, load casts, and scratch circles ('Kullingia'). Sandstone bed tops are flat or undulating, in places displaying parting lineation. Pyritization of burrows is common, and pyrite rosettes have been recorded at Point May.

Subfacies C3a shows rare wave and combined-flow ripple cross-lamination and micro-hummocky cross-stratification. Sandstone bed tops can have symmetrical to near-symmetrical, straight to sinuous, round- to sharp-crested ripples in Subfacies C3a. Polished slabs reveal that mudstone is massive, parallel-laminated, or intensely bioturbated (Gougeon *et al.* 2018a). Microbially modified surfaces are wrinkled or reticulated (i.e. 'Kinneyia'-type), forming patches or dominating larger surfaces. Pot casts, gutter casts, and injection structures are common in Subfacies C3a, in the lower half of Member 2A (see detailed description in Facies C2). Thin sandstone laminae in Subfacies C3a can form packages of horizontal sheets, stacked on top of each other and separated by very thin mudstone veneers, in places with irregular blebby patterns. Calcite concretions may form along these laminated packages. Isolated calcite concretions are conspicuous in mudstone intervals of Subfacies C3a.

Subfacies C3b, C3c, and C3d display rare current-ripple cross-lamination. Cementation of beds is locally abundant in these subfacies. Subfacies C3c also hosts calcite concretions in the lower half of Member 4. In Subfacies C3c, Myrow (1987) and Myrow & Landing (1992) noted that rare sandstone beds greater than 2 cm thick demonstrate a transition from lower parallel lamination to upper current ripple cross-lamination. Subfacies C3d poorly exposes sandstone bed soles and tops. In Subfacies C3d, small-scale scours visible in cross-section and filled with current ripple cross-lamination represent erosive equivalents to gutter casts of Subfacies C3a. A vertical succession with sharp erosive base, parallel-laminated sandstone topped by biogenic mottling is very rarely observed in Subfacies C3d. Purple phosphate pebbles have been noted in Subfacies C3d.

Ichnology. – *Archaeonassa fossulata*, *Arenicolites* aff. *A. carbonarius*, *Bergaueria perata*, *Cochlichnus luguanensis*, *Conichnus conicus*, *Cruziana problematica*, *Curvolithus multiplex*, *C. simplex*, *Dendroidichnites* aff. *D. irregulare*, *Gordia marina*, *Helminthoidichnites tenuis*, *Helminthopsis tenuis*, *Gyrolithes gyratus*, *G. scintillus*, *Monomorphichnus bilinearis*, *M. lineatus*, *M. needleiunm*, *Monomorphichnus* isp., *Palaeophycus annulatus*, *P. tubularis*, *Palaeophycus* isp., *Psammichnites gigas circularis*, *Psammichnites* cf. *P. saltensis* (Aceñolaza & Durand), *Rusophycus* isp., *Saerichnites kutscheri*, *Teichichnus rectus*, *Treptichnus bifurcus*, *T. coronatum*, *T. pedum*, *Treptichnus* indet., *Trichichnus linearis*, *Trichichnus* isp., and radial probing burrow are present in Facies C3.

Distribution and equivalents. – Facies C3 occurs in Member 2A (Ediacaran), Members 2A, 2B, and 3 (Fortunian), and Members 4 and 5 (Cambrian Age 2) at Fortune Head (140.4 m in total; FH-A 15.5–16.0, 16.1–18.6, 19.7–21.2, 21.8–26.0, 26.6–27.0, 27.4–29.6, 29.7–31.7, 32.0–32.4, 33.2–34.1, FH-B 5.8–6.4, 6.8–8.3, 12.3–12.5, 13.0–17.6, 18.3–21.0, 21.9–22.1, 22.6–23.2, 23.7–23.8, 24.4–25.6, 25.7–26.3, 26.7–27.0, 27.1–28.0, 28.9–30.1, 30.6–31.8, 32.6–33.2, 33.8–34.5, 36.7–38.6, 39.1–39.6, 39.8–40.1, 40.3–40.6, 41.4–41.6, 41.9–42.0, 42.1–42.5, 43.2–43.4, 49.5–49.9, 50.2–50.6, 50.9–51.5, 51.9–53.1, 54.1–54.4, 54.6–54.9, 56.1–56.6, 57.7–59.6, 60.2–60.5, 62.6–63.0, 63.8–64.1, 65.4–65.6, 66.1–67.8, 68.2–68.9, 70.0–71.0, 71.5–72.0, 72.2–73.0, 74.1–75.2, FH-C 12.6–13.3, 14.8–15.1, 15.8–16.2, 16.3–16.7, 38.1–43.6, 46.6–47.5, 47.8–48.3, 49.7–50.2, 51.2–51.8, 52.3–53.0, 54.9–55.7, 56.0–57.3, 66.3–67.4, 67.6–69.5, 70.2–71.7, 72.0–72.6, 72.7–73.3, 73.8–74.8, 77.5–77.8, 78.8–82.4, 96.7–97.9, 100.2–100.7, 100.8–101.3, 104.2–104.9, 105.9–106.4, 107.8–108.2, 109.0–109.9, 113.3–114.0, 115.2–115.8, 119.7–120.3, 120.7–121.1, 121.3–123.2, 125.1–125.9, 127.6–128.2, 128.8–129.6, 130.0–130.7, 132.2–132.8, 133.3–134.4, 140.2–141.7, 143.9–144.6, 145.1–145.8, 152.1–152.5, 153.1–153.5, FH-D 6.0–6.5, FH-E 1.0–1.2, 3.9–4.6, FH-F 0.0–1.7, 2.0–2.8, 3.0–4.0, 4.2–4.8, 5.0–5.6, 6.1–8.1, 8.3–9.0, 9.6–10.2, 10.8–12.4, 12.7–14.2, 14.5–16.9, 17.5–18.0, 19.1–19.7, 22.2–23.0, 25.1–26.3, 28.1–28.6, 29.2–29.7, 30.3–33.4, 33.7–34.5, 34.7–35.3, 35.5–37.4, 42.1–43.7, 47.3–48.6, 55.7–57.0, 57.1–57.7, 61.5–62.0, 62.6–64.1, 65.0–67.0, 67.5–67.9, 68.4–69.6, 70.0–71.2, 71.9–73.3, 74.3–74.7, 78.0–80.3, 80.8–81.2, 81.3–82.8, 83.5–84.3, 85.6–85.9, 86.5–86.8, 87.0–87.8, 89.6–89.8, FH-G 0.5–1.2, 5.7–6.2, 6.8–7.2, 8.3–8.8, 9.8–10.2, 11.2–11.6, 12.7–13.7, 17.8–18.7,

22.5–23.0, 56.2–56.8, 57.7–58.1), Fortune North (12.5 m in total; FN-A 1.4–1.9, 2.2–3.1, 3.8–5.7, 8.5–9.2, 11.6–13.3, 15.5–16.4, 21.8–22.3, 27.1–27.8, 28.4–29.4, 38.4–38.9, 39.4–40.1, 42.2–44.7), Grand Bank Head (86.0 m in total; GBH-B 0.4–1.7, 2.2–3.1, 3.4–5.3, 5.4–5.7, 6.6–6.9, 7.1–7.5, 10.1–10.5, 11.0–11.8, 13.3–13.7, GBH-C 0.0–4.2, 9.2–9.5, 11.3–16.7, 17.0–17.6, 18.2–18.8, 22.9–23.4, 23.8–25.2, 26.3–26.8, 27.1–27.6, 28.4–29.1, 30.0–30.4, 31.2–32.6, 36.1–36.7, 36.8–38.0, 38.2–39.9, 40.0–40.4, 40.7–41.6, 42.8–44.0, 44.3–45.3, 45.6–47.0, 48.0–48.5, 54.2–55.5, 59.5–59.8, 61.2–61.7, 63.3–63.7, 64.3–65.4, 69.0–70.4, 71.9–72.4, 75.3–76.0, 77.4–77.9, 82.9–83.2, 83.7–83.8, 86.4–86.8, 92.2–92.6, 117.9–122.8, 133.3–133.4, 137.1–139.5, GBH-D 31.2–33.8, 33.9–43.0, 45.3–47.5, 49.1–50.8, 51.4–51.8, 52.6–53.0, 55.4–57.9, GBH-E 3.2–4.0, 5.5–7.5, 8.1–8.6, 9.4–9.5, 9.8–10.5, 11.2–13.0, 13.3–13.5, 13.7–14.4, 14.6–15.4, 15.6–27.0, GBH-F 45.2–45.9), Lewin's Cove (23.6 m in total; LC-B 21.1–22.0, 23.0–24.5, 24.7–25.3, 25.8–26.0, 27.0–27.7, 28.9–29.4, 29.5–31.3, 35.1–35.4, 37.4–39.5, 40.0–43.4, 43.6–44.2, 44.8–45.2, 45.5–47.5, LC-C 0.0–0.9, 1.9–2.7, 3.1–3.8, 5.7–6.4, 8.0–8.4, 10.2–10.6, 19.9–20.5, 22.6–23.1, 25.2–27.1, 35.5–36.0, 38.2–38.9, 39.5–40.0), Little Dantzic Cove (53.5 m in total; LDC 0.5–0.7, 9.3–9.5, 24.2–24.8, 27.0–27.4, 28.7–30.0, 31.5–32.2, 33.4–36.6, 39.4–39.6, 40.8–42.8, 44.9–45.8, 46.5–47.4, 50.1–53.1, 54.2–55.8, 60.2–60.7, 63.4–64.2, 71.0–72.3, 72.8–75.1, 76.0–76.3, 77.1–77.5, 78.4–79.1, 81.3–82.0, 82.5–83.4, 83.8–84.1, 84.6–85.1, 85.4–85.5, 85.9–86.3, 86.6–87.7, 88.9–89.5, 90.2–90.3, 90.7–91.7, 92.1–92.2, 92.9–93.0, 94.1–96.0, 96.7–97.4, 98.3–98.6, 99.3–99.7, 100.4–102.0, 108.2–109.7, 131.2–132.2, 136.7–136.9, 160.6–160.7, 162.3–162.4, 166.5–167.3, 168.0–168.2, 170.1–171.2, 173.5–173.8, 175.0–175.1, 184.1–184.2, 187.5–188.8, 189.6–190.0, 197.9–198.4, 201.7–201.9, 202.3–202.4, 205.4–205.6, 206.7–206.9, 207.6–207.9, 211.4–212.7, 213.3–213.6, 215.2–215.3, 216.0–216.3, 216.9–218.1, 218.8–219.0, 221.0–221.2, 222.0–222.3, 224.9–225.2, 230.7–231.0, 232.7–233.5, 234.0–234.3, 235.3–235.4, 240.6–240.8, 241.3–242.1, 245.0–245.4, 245.8–246.1, 248.1–248.3, 248.7–248.8, 249.5–249.6, 250.2–250.6, 253.8–254.9, 258.6–258.8, 265.4–266.3, 272.0–272.2, 272.5–272.8, 274.5–274.7, 275.1–275.5), and Point May (92.0 m in total; PM-A 15.5–25.8, 26.5–27.9, 28.9–33.6, PM-B 0.0–1.0, 1.3–3.6, 3.7–6.7, 7.4–7.9, 8.3–9.5, 10.7–11.4, 12.8–14.1, 15.0–15.3, 17.3–17.7, 20.9–21.7, PM-C 3.0–3.5, 4.5–7.3, 7.8–8.7, 9.3–10.9, 11.4–11.8, 12.3–13.3, 13.6–14.3, 14.8–15.5, 16.2–18.7, 23.2–24.2, 24.5–25.4, 25.9–26.9, 27.9–29.4, 30.3–32.3, 33.4–35.9, 36.0–37.9, 39.6–42.9, 43.7–44.3, 44.8–47.6, 48.2–52.4, 57.6–62.0, 62.1–63.7, 68.1–69.2, 69.4–70.6, 71.0–73.8, 74.8–75.5, 76.4–78.0, 78.9–79.1, 81.6–82.2, 83.5–83.8, 114.9–116.4, 116.9–117.2, 117.6–118.0, 118.6–119.2, 119.5–119.9, 122.8–123.4, 124.6–125.0, 127.8–128.2, 132.3–132.9, 135.3–137.6, 138.2–139.2, 139.6–140.0, PM-D 0.8–1.2, 6.0–6.4, 7.1–8.9, 9.1–10.1, 14.7–15.1, PM-E 0.0–0.8, 3.1–4.1, 6.1–6.5, 14.7–16.1, 19.5–20.0).

Subfacies C3a is found in Member 2A (Ediacaran) and Members 2A, 2B, and 3 (Fortunian), Subfacies C3b in Member 2B (Fortunian), Subfacies C3c in Member 4 (Cambrian Age 2), and Subfacies C3d in Member 5 (Cambrian Age 2). Subfacies C3a, C3b, and C3d correspond respectively to the finer-grained intervals of Facies 2.1/Subfacies 2.2A, Facies 2.3, and Subfacies 5.1A of Myrow (1987). Subfacies C3c corresponds to the sandier intervals of Facies 4.1/4.2 of Myrow (1987).

Interpretation. – The dominant fine-grained sedimentation associated with incipient thinly to thickly laminated sandstone tempestites argues for deposition in a lower offshore (MacEachern & Pemberton 1992; Bann *et al.* 2004; Buatois & Mángano 2011; Dashtgard *et al.* 2012; Jelby *et al.* 2020). Suspension fallout during quiescent moments is an important process responsible for deposition of mudstone, especially for parallel-laminated intervals (Pattison *et al.* 2007). Additional processes have been invoked for the deposition of mud on the shelf, notably traction of flocculated fine mud behaving as larger particles (Schieber *et al.* 2007; Schieber 2011; Shchepetkina *et al.* 2018), hyperpycnal mud plumes (Bhattacharya & MacEachern 2009; Schieber 2016), or wave-enhanced sediment gravity flows (Wright & Friedrichs 2006; Ichaso & Dalrymple 2009; Macquaker *et al.* 2010; Plint 2014; Denommee *et al.* 2016; Saleh *et al.* 2022). Identifying mud flocculation requires the use of a scanning electron microscope, which is outside the scope of this study. Hyperpycnal mud plumes and wave-enhanced sediment gravity flows display more complex features than that recorded in mudstone of Facies C3. Some of the thin sandstone laminae may have been deposited from suspension fallout after storms (Reineck & Singh 1972; Dott & Bourgeois 1982). Crinkly stacked sandstone laminae separated by thin mudstone veneers in Subfacies C3a result from microbial stabilization of the seafloor (cf. Noffke *et al.* 2006). In these intervals, microbes triggered the formation of bedded concretions through early diagenetic processes (Coleman 1993). Planar lamination records traction deposition that conforms with tempestites deposited from oscillatory sheet flows (DeCelles & Cavazza 1992; Jelby *et al.* 2020). Pot casts are formed by vertical vortices drilling the substrate

through the grinding action of sand and larger clasts (Myrow 1992a). Normal graded beds with erosive bases are either deposited from simple waning flows and suspension fallout (Reineck & Singh 1972; Simpson *et al.* 2002; Desjardins *et al.* 2010a; Grundvåg *et al.* 2021), from storm-initiated turbidity currents (Hayes 1967; Basilici *et al.* 2012; Jelby *et al.* 2020), or from hyperpycnal flows (Mulder *et al.* 2003; Pattison 2005; Birgenheier *et al.* 2017).

Processes involved in the origin and deposition of sand are different in Subfacies C3a and C3b/d. The presence of symmetrical ripples and micro-hummocky cross-stratification in Subfacies C3a demonstrates that oscillatory flows were transporting sand, most notably from the distalmost reach of storms (Bann *et al.* 2004). Subfacies C3b/d only display rare current ripples, indicating that unidirectional currents were involved in sand transportation. In the lower offshore, unidirectional flows may have resulted from geostrophic currents, rip currents, or the distalmost reach of downwelling currents after storm surges (Swift *et al.* 1983, 1987; Niedoroda *et al.* 1984, 1985; Leckie & Krystinik 1989). Whereas rip currents have more influence on the shoreface (Swift *et al.* 1987), downwelling currents after storms can transport sediment further offshore if shoaling from wave orbital currents is not strong enough to keep the sand on the shoreface (Niedoroda *et al.* 1984, 1985). The lack of conclusive palaeocurrent datasets for Subfacies C3b and C3d (Myrow 1987) hinders a full understanding of sand deposition in these settings. However, palaeocurrents perpendicular to the shoreline in Subfacies C3a (Myrow 1992a; Myrow & Hiscott 1993) indicate that sand was carried through similar processes as detailed for the upper offshore Subfacies C2a.

Subfacies C3c differs from Subfacies C3a/b/d by its fine mudstone content and its stratal relationship with Facies D2. Hence, Subfacies C3c is linked to the development of a mud depocenter along the shoreline with reduced sand inputs most likely provided through wind-driven currents that are active during winters (e.g. Lee & Chu 2001; see Facies D2 interpretation). Subfacies C3c is better exposed in the upper part of Member 4 at Little Dantzic Cove, characterised by the distinct development of current ripple cross-lamination (Fig. 14J) demonstrating a slight increase in energy (in comparison to suspension fallout sedimentation of Facies D2, which is dominantly recorded in Member 4). This follows the suggestion of Myrow & Landing (1992) that Member 4 depicts a progressive shallowing at Little Dantzic Cove, although this conclusion is not based on the same evidences (see Facies D2 interpretation). At Grand Bank Head, Subfacies C3c is absent in Member 4, which suggests that this locality depicts deeper water conditions unaffected by wind-driven currents.

Finally, although red beds are more common in continental deposits, they have also been recorded in fully marine settings in relation to oxidation events (Hu *et al.* 2012; Wetzel & Uchman 2018; Li *et al.* 2019; Rasmussen & Muhling 2019). The formation of hematite pigments necessitates a small initial organic matter fraction coupled with a significant quantity of unstable ferruginous minerals or rock fragments (Blodgett *et al.* 1993). Red beds of Subfacies C3b originated in a marine environment, as demonstrated by their stratal position and genetic relationship with Facies C1 and C2 and their higher bioturbation intensities.

Facies Association D

Facies association D is recorded from Members 2A, 2B, and 3 (Fortunian), and Members 4 and 5 (Cambrian Stage 2). It represents shelf settings (*stricto sensu*) deposited below storm-weather wave base and is composed of Facies D1 (massive medium mudstone), Facies D2 (massive fine mudstone), and Facies D3 (massive sandy mudstone).

Facies D1: Massive medium mudstone

Description. – Facies D1 consists of massive green and grey green, medium mudstone, sparsely intercalated with thinly laminated, very fine- to fine-grained sandstone (Figs 15A–C, 17A, B). Sandstone makes up less than 5%. Sandstone laminae are typically 0.05–0.1 cm thick, and mudstone layers are 0.2–9.2 m thick. Facies D1 forms units 0.2–14.7 m thick and represents 120.0 m of strata in total.

Thin sandstone laminae are massive and typically discontinuous laterally. Mudstone grains have ∅ = 3–70 μm (based on four thin sections). Medium mudstone is the dominant lithology, but fine and coarse mudstones are recorded to a lesser degree. Another thin section (S1.LDC16) has ∅ = 4–96 μm, is heavily bioturbated and poorly sorted. On polished samples (cf. supplementary material in Gougeon *et al.* 2018a), mudstone intervals are either biogenically mottled or planar laminated, in places with normal grading. Within Member 2, soft-sediment deformation structures have been noted. Carbonate concretions are conspicuous. These large nodules, typically two to three times wider than thick, are oriented parallel to the bedding and can host small shelly fossils. Large purple phosphate nodules are also preserved in clusters. In thin section, organic carbonaceous material is common, and burrows and algal body fossils are typically pyritized.

Ichnology. – *Bergaueria perata*, *Cochlichnus anguineus*, *Gyrolithes gyratus*, *G. scintillus*, *Helminthoidichnites tenuis*, *Helminthopsis tenuis*, *Monomorphichnus bilinearis*,

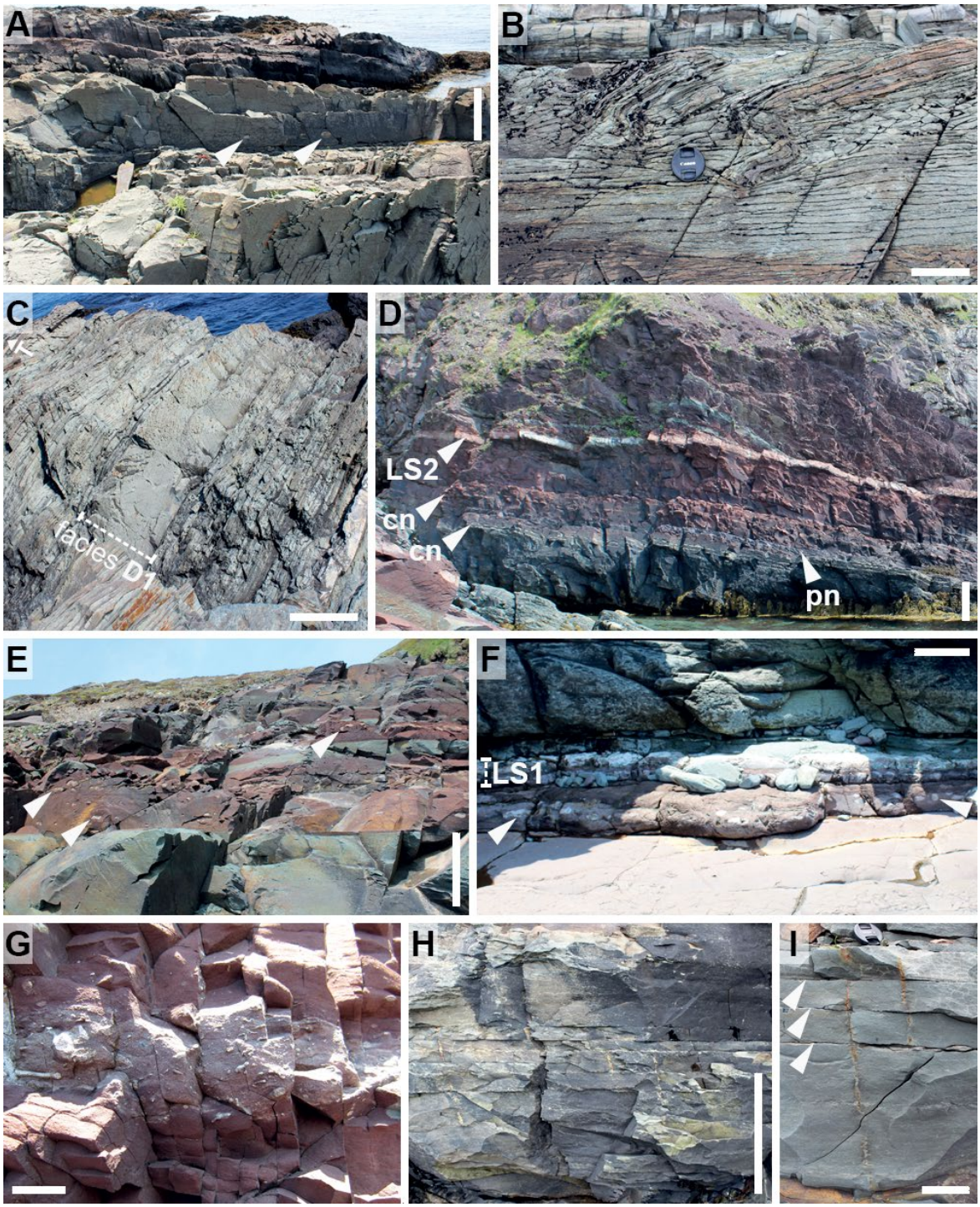

Fig. 15. Facies D1 (A–C), Facies D2 (D–G), and Facies D3 (H, I) (shelf). Scale bars are 1 cm (G), 10 cm (B, I), 30 cm (F), 50 cm (H), and 100 cm (A, C–E). **A**, General view of Facies D1 showing dominance of medium mudstone. Note calcite concretions (arrows). Little Dantzic Cove, Member 3 (Fortunian). **B**, Soft-sediment deformation structure within mudstone of Facies D1. Fortune Head, Member 2A (Fortunian). **C**, Stratal relationship of Facies D1 with other facies. Stratigraphic top is indicated by the 'T'. Fortune Head, Member 2A (Fortunian). **D**, General view of Facies D2 showing dominance of fine mudstone. Note intercalation of LS2, bedded calcite nodules (cn), bedded phosphate nodules (pn), and red intervals both below and above LS2. Little Dantzic Cove, Member 4 (Cambrian Age 2). **E**, Banded alternance of green and red mudstone in Facies D2. Note disorganized calcite nodules (some are arrowed). Little Dantzic Cove, Member 4 (Cambrian Age 2). **F**, LS1, made of two beds of coalesced calcite nodules delineating the base of Member 4. Note other calcite nodules (arrows). Little Dantzic Cove, Member 4 (Cambrian Age 2). **G**, Distinct calcite-cemented burrows recorded just above LS2. Little Dantzic Cove, Member 4 (Cambrian Age 2). **H**, General view of Facies D3 showing dominance of sandy mudstone. Note black-colored cover on the exposure. Little Dantzic Cove, Member 5 (Cambrian Age 2). **I**, Close-up on a clean sandy mudstone exposure of Facies D3, showing vertical pyritized burrows (*Trichichnus* isp.) and sparse thin sandstone laminae (arrows). Little Dantzic Cove, Member 5 (Cambrian Age 2).

Palaeophycus tubularis, *Palaeophycus* isp., *Psammichnites gigas circularis*, *Saerichnites kutscheri*, *Teichichnus rectus*, *Torrowangea rosei*, *Treptichnus pedum*, *Treptichnus* indet., *Trichichnus linearis*, *Trichichnus* isp., and radial probing burrow are present in Facies D1.

Distribution and equivalents. – Facies D1 occurs in Members 2A, 2B, and 3 (Fortunian) at Fortune Head (18.7 m in total; FH-A 19.3–19.7, 26.2–26.6, 27.0–27.4, 31.7–32.0, 32.4–33.2, FH-B 6.4–6.8, 8.3–9.0, 11.1–12.3, 12.5–13.0, 21.1–21.9, 22.1–22.6, 26.4–26.7, 30.1–30.6, 32.3–32.6, 40.6–41.4, 41.6–41.9, 42.8–43.2, 47.3–47.7, 47.9–48.6, 49.1–49.5, 49.9–50.2, 53.9–54.1, 64.1–65.4, FH-C 43.6–44.2, 49.2–49.7, 50.2–51.2, 51.8–52.3, 53.5–54.5, 57.3–57.6, 99.7–100.2, 108.6–109.0, 126.5–126.8, FH-F 69.6–70.0, 80.4–80.8, FH-G 0.0–0.5), Grand Bank Head (18.6 m in total; GBH-B 0.1–0.4, 5.8–6.6, 7.5–8.0, GBH-C 10.8–11.0, 16.7–17.0, 72.4–73.6, 124.1–133.3, 133.4–137.1, GBH-D 50.8–51.4, 51.8–52.6, GBH-E 3.0–3.2, 9.1–9.4, 9.6–9.8, 13.0–13.3), Lewin's Cove (2.3 m in total; LC-B 26.2–27.0, 34.2–34.4, 35.4–35.8, 39.5–40.0, LC-C 2.7–3.1), Little Dantzic Cove (66.6 m in total; 0.0–0.5, 0.7–9.3, 9.5–24.2, 24.8–27.0, 27.4–28.7, 30.0–31.5, 32.2–33.4, 36.6–39.4, 39.6–40.8, 42.8–44.9, 45.8–46.5, 47.4–50.1, 53.1–54.2, 55.8–60.2, 60.7–63.4, 64.2–66.5, 66.6–71.0, 72.3–72.8, 75.1–76.0, 76.3–77.1, 77.5–78.4, 79.1–81.3, 82.0–82.5, 83.4–83.8, 84.1–84.6, 85.1–85.4, 85.5–85.9, 86.3–86.6, 87.7–88.9, 89.5–90.2, 90.3–90.7, 91.7–92.1, 92.2–92.9, 93.0–94.1, 96.0–96.7, 97.4–97.7), and Point May (13.8 m in total; PM-B 14.1–14.6, 23.0–24.2, PM-C 3.5–4.5, 10.9–11.4, 13.3–13.6, 22.3–22.7, 22.8–23.2, 26.9–27.2, 33.0–33.3, 37.9–39.6, 43.3–43.7, 52.4–57.6, 116.5–116.9, 117.2–117.6, PM-D 0.0–0.8).

Facies D1 corresponds to the finer-grained intervals of Facies 2.4/3.1 of Myrow (1987).

Interpretation. – Thick mudstone intervals and the stratigraphical position of Facies D1 indicate deposition on a shelf (*stricto sensu*) below storm-weather wave base (MacEachern *et al.* 1999; Buatois & Mángano 2011; Hutsky & Fielding 2016; Birgenheier *et al.* 2017). Processes that can be invoked for mudstone transport or deposition are suspension fallout, mud flocculation, hyperpycnal mud plumes, or wave-enhanced sediment gravity flows (Schieber *et al.* 2007; Bhattacharya & MacEachern 2009; Macquaker *et al.* 2010; Saleh *et al.* 2022). Identification of mud floccules requires scanning electron microscope imaging (e.g. Schieber *et al.* 2007, fig. 1), which is outside the scope of this study. Hyperpycnal flows are typified by inverse and normal grading, climbing ripples, and coarser-grained intervals (Mulder & Alexander 2001; Mulder *et al.* 2003; Bhattacharya & MacEachern 2009; Zavala & Arcuri 2016) that are overall not observed in Facies D1. Wave-enhanced sediment gravity flows are identified based on a specific tripartite small-scale succession (see Macquaker *et al.* 2010, fig. 2) which has not been noted in polished samples from Facies D1. Therefore, passive mud settlement from the water column possibly related to repetitive changes in fluid viscosity (Al-Mufti & Arnott 2023) is suggested as the main process of deposition for mudstone of Facies D1, which permitted the development of planar-lamination and normal grading. Discontinuous thin sandstone laminae undisrupted by burrows indicate sand starvation (Birgenheier *et al.* 2017). Intensely bioturbated intervals represent fully marine, well-oxygenated conditions (Savrda *et al.* 1991; Savrda 2007; Wilson & Schieber 2015). In addition, some laminated intervals may also have been oxygenated, although at lower levels, allowing meiofauna to thrive and feed in between clastic grains without disrupting the sedimentary fabric (Schieber & Wilson 2021). Thick convoluted intervals were studied in detail by Myrow (1987) and Myrow & Hiscott (1991) and were interpreted as gravity-flow deposits (unifite and raft-bearing beds). Carbonate concretions are early diagenetic structures exposing the original depositional fabric (Chafetz 1979; Marshall & Pirrie 2013), whose formation can be initiated by microbial activity related to organic material decay (Berner 1968; Grice *et al.* 2019). The common intercalation of lower offshore (i.e. Facies C3) and shelf strata (i.e. Facies D1) in Member 3 demonstrates their genetic relationship.

Facies D2: Massive fine mudstone

Description. – Facies D2 consists of massive red, purple, grey, and green, fine mudstone, sparsely intercalated with thinly laminated, very fine- to fine-grained sandstone (Figs 15D–G, 16, 17C). Sandstone beds are typically 0.05–0.1 cm thick, and mudstone intervals are 0.1–27.0 m thick. Sandstone makes up less than 2%. Facies D2 forms units 0.4–37.3 m thick and represents 112.3 m of strata in total.

Mudstone grains have ∅ = 3–52 μm (based on six thin sections). Fine mudstone is the dominant lithology, but medium mudstone is also recorded. Mudstone is massive or heavily bioturbated (BI = 4–6) and displays banded alternation in colors. Colored bands are laterally pervasive and consistent in thickness, or patchy. In the field, intense biomixing is striking at green-to-red interfaces, where the color contrast is the highest. Polished samples reveal high bioturbation intensities in either red, green, or grey mudstone. One polished sample (S1.LDC28, collected 1.9 m below LS3 at Little Dantzic Cove) also displays parallel lamination. Thin sandstone laminae are commonly calcite cemented, typically discontinuous laterally and forming local packages. Phosphate and pyrite pebbles are isolated or in clusters.

Fig. 16. Polished sample recovered 1.9 m below the base of LS3 at Little Dantzic Cove (sample S1.LDC28; stratigraphic level LDC 177.2). Note red fine mudstone with distinct parallel lamination (some laminae are arrowed). Member 4 (Cambrian Age 2). Scale bar is 1 cm.

Bedding planes are poorly exposed. Grey and green intervals display small shelly fossils, notably *Aldanella attleborensis*, *'Ladatheca' cylindrica*, and *Watsonella crosbyi* (see also Landing *et al.* 1989 and Landing 1993). Algal filaments are also commonly preserved.

Calcite concretions are either isolated, arranged chaotically, or forming laterally extensive layers. Concretions are structureless or display parallel lamination. They are notably lacking in the upper half of Member 4, both at Grand Bank Head and Little Dantzic Cove. Concretions can coalesce and develop laterally extensive beds of micritic limestone, 3–18 cm thick, that vary greatly in thickness. At Little Dantzic Cove, a thicker limestone bed defining the base of Member 4 (i.e. LS1 of Myrow 1987) consists of: (1) basal coalescent calcite nodules (6 cm thick); (2) a red mudstone interval (3 cm thick); and (3) a homogeneous micritic limestone bed (6 cm thick).

Ichnology. – *Conichnus conicus*, *Palaeophycus tubularis*, *Palaeophycus* isp., *Psammichnites gigas circularis*, *Teichichnus rectus*, *Trichichnus linearis*, and *Trichichnus* isp. are present in Facies D2.

Distribution and equivalents. – Facies D2 occurs in Member 4 (Cambrian Stage 2) at Grand Bank Head (41.5 m in total; GBH-F 0.0–37.3, 40.1–44.3) and Little Dantzic Cove (70.8 m in total; LDC 97.9–98.3, 98.7–99.3, 99.7–100.4, 102.0–108.2, 109.7–131.2, 132.2–136.7, 136.9–145.1, 145.3–156.5, 158.5–160.6, 160.7–162.3, 162.4–166.5, 167.3–168.0, 168.2–170.1, 171.2–173.5, 173.8–175.0, 175.1–178.7).

Myrow (1987) also recorded Facies D2 at Fortune North (*ca.* 85 m) in an area that has not been accessed in this study. Facies D2 corresponds to finer-grained intervals of Facies 4.1/4.2 of Myrow (1987).

Interpretation. – A model was developed by Myrow & Landing (1992) to explain the deposition of mudstone and limestone of Member 4. They argued that grey mudstone was deposited in the distal portion of a ramp under dysaerobic conditions, whereas green and red mudstone were more typical of proximal aerobic settings (see also Brasier *et al.* 1992 and Landing & Westrop 2004). An important line of evidence for this model was the interpretation of bioturbated intervals, which were thought to be more important in red and green mudstone. Indeed, in the field, red and green mudstone interfaces provide an important color contrast that aids in spotting intense biomixing. However, polished samples also demonstrate elevated bioturbation intensities in grey mudstone (Gougeon *et al.* 2018a, fig. 2d). Moreover, Myrow & Landing (1992) emphasized different trends in carbonate, phosphate, and pyrite nodule occurrences, with: (1) phosphate and pyrite nodules found in grey mudstone, in intervals lacking carbonate nodules; (2) small carbonate nodules found in red mudstone; and (3) large carbonate nodules found in green mudstone. However, from our observations, carbonate nodules do not follow a preferential arrangement with regard to the colored mudstone they are found in. Carbonate nodules are, for instance, abundant in red mudstone of upper Member 3 (LDC 94.5–97.7) and in the lower half of Member 4 (GBH-F 9.6–12.2, LDC 134.9–135.7, LDC 143.1–145.1), whereas they are absent in other red intervals from the lower half of Member 4 (GBH-F 17.5–21.0, LDC 135.7–136.9). Red mudstone from the upper half of Member 4 (i.e. in between LS2 and LS3) is lacking calcite concretions, both at Grand Bank Head and Little Dantzic Cove. Phosphatic nodules are recorded either from red, purple, grey, or green mudstone, while pyritic nodules are found

both in grey and green mudstone (Myrow & Landing 1992, fig. 2). Myrow & Landing (1992) further argued that facies trends at Little Dantzic Cove depict a progressive shallowing from distal dysaerobic grey/green mudstone to more proximal aerobic red mudstone, with two peaks of coastal strata represented by peritidal limestone of LS2 and LS3. However, red mudstone is found just below and above LS2 (Fig. 15D; Myrow & Landing 1992, fig. 2, and our dataset LDC 142.9–151.1) and LS3 (Myrow & Landing 1992, fig. 2, and our dataset LDC 176.3–181.3) at Little Dantzic Cove. Similarly, at Grand Bank Head, LS3 (GBH-F 43.1–45.8) is intercalated within red mudstone. The absence of carbonate concretions in the upper half of Member 4 at Little Dantzic Cove, Grand Bank Head, and apparently at Fortune North (Myrow & Landing 1992, fig. 2), is problematic and does not agree with the progressive shallowing sequence as suggested in the archetypal model of Myrow & Landing (1992, fig. 8). Finally, red mudstone below LS3 can be heavily bioturbated, but it also displays parallel lamination (Fig. 16) that does not suggest aerobic conditions.

Using calcite nodules in a sedimentary model is problematic as these are diagenetic features, not sedimentologic. In the Chapel Island Formation, calcite nodules are recorded in lower shoreface (e.g. FN-B 1.4, FN-B 7.3), offshore transition (e.g. FH-F 18.1, GBH-B 12.9), upper offshore (e.g. FH-A 26.1, FH-B 17.9), lower offshore (e.g. FH-A 30.1, FH-B 15.5), and shelf (e.g. FH-A 33.1, FH-C 50.5) settings. In addition, calcite concretions have been recorded in continental, marginal-marine, and deep-marine environments elsewhere (e.g. Blodgett *et al.* 1993; Allison & Pye 1994; Marshall & Pirrie 2013; Gaines & Vorhies 2016). Similarly, bedding color can be diagenetic (Blodgett *et al.* 1993; Hu *et al.* 2012). For instance, red-colored mudstone is recorded from continental, marginal-, shallow-, and deep-marine environments (e.g. Blodgett *et al.* 1993; Sheldon 2005; Hu *et al.* 2006, 2012; Wetzel & Uchman 2018; Li *et al.* 2019). To summarize, it is difficult to reconcile the conceptual model of Myrow & Landing (1992) with direct observations in the field and from polished samples.

In this study, we propose a different interpretation for the deposition of Facies D2 that is not based on bed color nor on carbonate, phosphate, or pyrite nodule arrangements. From field and polished sample observations, important elements to account for are: (1) the dominance of fine mudstone; (2) the intense bioturbation in some intervals; (3) the stratal relationship with Subfacies C3c that shows thinly laminated sandstone, planar-laminated sandstone, and current ripple cross-laminated sandstone; and (4) the stratal relationship with Facies E1 and E2 that have subtidal and intertidal origins. The most likely interpretation for Facies D2 is deposition in a mud depocenter detached from its source (cf. Lantzsch *et al.* 2009; Hanebuth *et al.* 2015). Mud depocenters typically form below storm wave base during highstands when the continental shelf is widely inundated, with the main agent of sediment transport being hyperpycnal plumes (Cattaneo *et al.* 2003; Hanebuth *et al.* 2015). Wind-driven and geostrophic currents can carry suspended particles along the shoreline (e.g. Foster & Carter 1997; Cattaneo *et al.* 2003; Liu *et al.* 2018), a phenomenon aided by the lack of flocculation of fine-grained particles (Liu *et al.* 2014). Therefore, mud can be transported far from the fluvial source and be accumulated along to the coast in an area of low energy that can be no more than 10–20 m in water depth (e.g. Lee & Chu 2001). These mud depocenters are known as mud belts, shallow-water contourite drifts, mud entrapments, or mud wedges (Hanebuth *et al.* 2015). In Member 4, the mud depocenter was probably detached, as sandstone is absent (i.e. Facies D2) or limited to thin laminae (i.e. Subfacies C3c); coarsening upward successions that are observed in prodeltaic settings are also absent (Lantzsch *et al.* 2009; Hanebuth *et al.* 2015). Currents transporting mud can provide nutrients and organic materials to the euphotic zone, hence triggering proliferation of a diverse and abundant benthic life (Oliver *et al.* 2011; Cheriton *et al.* 2014) aiding in the development of a sediment mixed layer (e.g. Park *et al.* 2000; Lesueur *et al.* 2001; Cattaneo *et al.* 2003). Benthic life was also thriving at the time of deposition of Facies D2, as depicted by high bioturbation intensities and the formation of thick mottled intervals (Gougeon *et al.* 2018a, 2025a).

A modern analogue to the mud depocenter of Member 4 is the Huksan Mud Belt (also referred to as Southeastern Yellow Sea Mud Belt) from the southwestern coast of South Korea (Park *et al.* 2000; Lee 2015). The Huksan Mud Belt is exclusively composed of mud, spanning a geographic area of 20–50 km in width and 200 km in length with water depths of 10–110 m, and is located far from any significant river discharge (Lee & Chu 2001; Lee 2015). For comparison, Facies D2 (and more generally Member 4) has a minimal extension of 40 km as it is recorded in Grand Bank Head and Langlade (Saint-Pierre-et-Miquelon; Rabu *et al.* 1993, 1994). The maximum Huksan Mud Belt thickness reaches 50 m (Park *et al.* 2000; Lee 2015) which is also comparable to the maximum thickness of 37.2 m recorded for Facies D2. Sediment of the Huksan Mud Belt is provided in part from the Korean Keum river and carried by the wind-driven Korean Coastal Current, but also from the Chinese Huanghe or Changjiang rivers and transported offshore by the

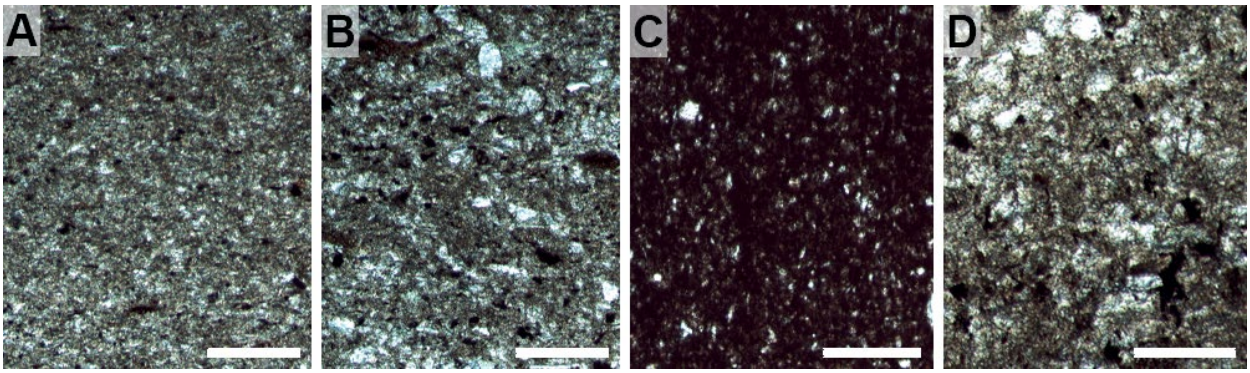

Fig. 17. Thin sections from Facies D1 (A, B), Facies D2 (C), and Facies D3 (D) (shelf). Scale bars are 200 μm. All thin sections are from Little Dantzic Cove. **A**, Typical medium mudstone of Facies D1. Grain ∅ = 5–40 μm. Sample S1.LDC13, Member 3 (Fortunian). **B**, Thin section from a bioturbated interval in Facies D1. Note poor grain sorting. Grain ∅ = 4–96 μm. Sample S1.LDC16, Member 3 (Fortunian). **C**, Typical fine mudstone of Facies D2 recovered from a red interval. Grain ∅ = 3–24 μm. Sample S1.LDC25, Member 4 (Cambrian Age 2). **D**, Typical sandy mudstone of Facies D3. Note poor grain sorting and similarities with Figure 17B. Grain ∅ = 3–104 μm. Sample S1.LDC30, Member 5 (Cambrian Age 2).

Yellow Sea Warm Current, both currents being notably active during winters (Alexander *et al.* 1991; Park *et al.* 2000; Lee & Chu 2001; Lim *et al.* 2007; Wang *et al.* 2010; Lee 2015). The Huksan Mud Belt is generally highly bioturbated especially in the southern part of the belt, but some other areas remain mostly parallel-laminated (Park *et al.* 2000; Lee & Chu 2001). Notably, Park *et al.* (2000) recorded a well-developed sediment mixed layer in many of the cores studied. Areas with good preservation of laminated sedimentary fabric result from higher sedimentation rates and possible anoxia precluding benthic colonisation (Leithold 1993; Cattaneo *et al.* 2003). In sedimentary cores, shell lags were found in close association to bioturbated intervals (Park *et al.* 2000; Lee & Chu 2001), but their origin is unclear. Member 4 also possesses two shell lags composed of small shelly fossils (as part of Facies E1 and E2) that are intercalated within Facies D2.

Facies D3: Massive sandy mudstone

Description. – Facies D3 is composed of massive grey green, sandy mudstone, rarely intercalated with dark grey, thinly laminated, very fine- to fine-grained sandstone (Figs 15H, I, 17D). Sandstone makes up less than 5%. Sandstone beds are typically 0.05–0.1 cm thick, and sandy mudstone layers are 0.1–4.5 m thick. Facies D3 forms units 0.1–4.5 m thick and represents 55.5 m of strata in total.

Mudstone grains are poorly sorted and have ∅ = 3–104 μm (based on two thin sections). Sandy mudstone is the dominant lithology, but fine to coarse mudstone is also recorded. Thin sandstone laminae are massive, commonly calcite cemented, and are discontinuous laterally. Rare naturally polished vertical sections in the field show that sandy mudstone is either parallel-laminated or heavily bioturbated, which is confirmed on polished samples. However, many vertical exposures in the field are covered and do not allow further detailed analysis.

Ichnology. – *Arenicolites* isp., *Curvolithus simplex*, *Helminthopsis tenuis*, *Palaeophycus* isp., *Psammichnites gigas circularis*, *Teichichnus rectus*, *Trichichnus linearis*, and *Trichichnus* isp. are present in Facies D3.

Distribution and equivalents. – Facies D3 occurs in Member 5 (Cambrian Age 2) at Grand Bank Head (0.4 m in total; GBH-F 45.9–46.3) and Little Dantzic Cove (55.1 m in total; 179.3–180.5, 181.0–184.1, 184.2–187.5, 189.1–189.6, 190.0–194.5, 196.5–197.9, 198.4–201.7, 201.9–202.3, 202.4–205.4, 205.6–206.7, 206.9–207.6, 207.9–211.4, 212.9–213.3, 213.6–215.2, 215.3–216.0, 216.3–216.9, 218.1–218.8, 219.0–221.0, 221.2–222.0, 222.3–224.4, 224.6–224.9, 225.2–227.9, 228.4–228.8, 229.1–230.7, 231.0–232.7, 233.5–234.0, 234.3–235.3, 235.4–236.3, 238.3–239.7, 240.0–240.6, 240.8–241.3, 242.2–242.7, 245.4–245.8, 246.1–247.3, 247.8–248.1, 248.3–248.7, 249.1–249.5, 249.6–250.2, 250.7–250.8, 253.4–253.8, 258.2–258.6, 263.4–265.4, 270.4–270.8, 271.6–272.0, 273.9–274.5, 277.3–277.8).

Facies D3 corresponds to the finer-grained interval of Subfacies 5.1A of Myrow (1987).

Interpretation. – Thick sandy mudstone intervals and the stratigraphical position of Facies D3 argue for shelf deposition (*stricto sensu*) below storm-weather wave base (MacEachern *et al.* 1999; Aitken & Flint 1995). Thick sandy mudstone intervals may be related to important biogenic reworking of sand and mud particles (e.g. Moslow & Pemberton 1988; McKay & Longstaffe 2003; Bann *et al.* 2004), or from immature

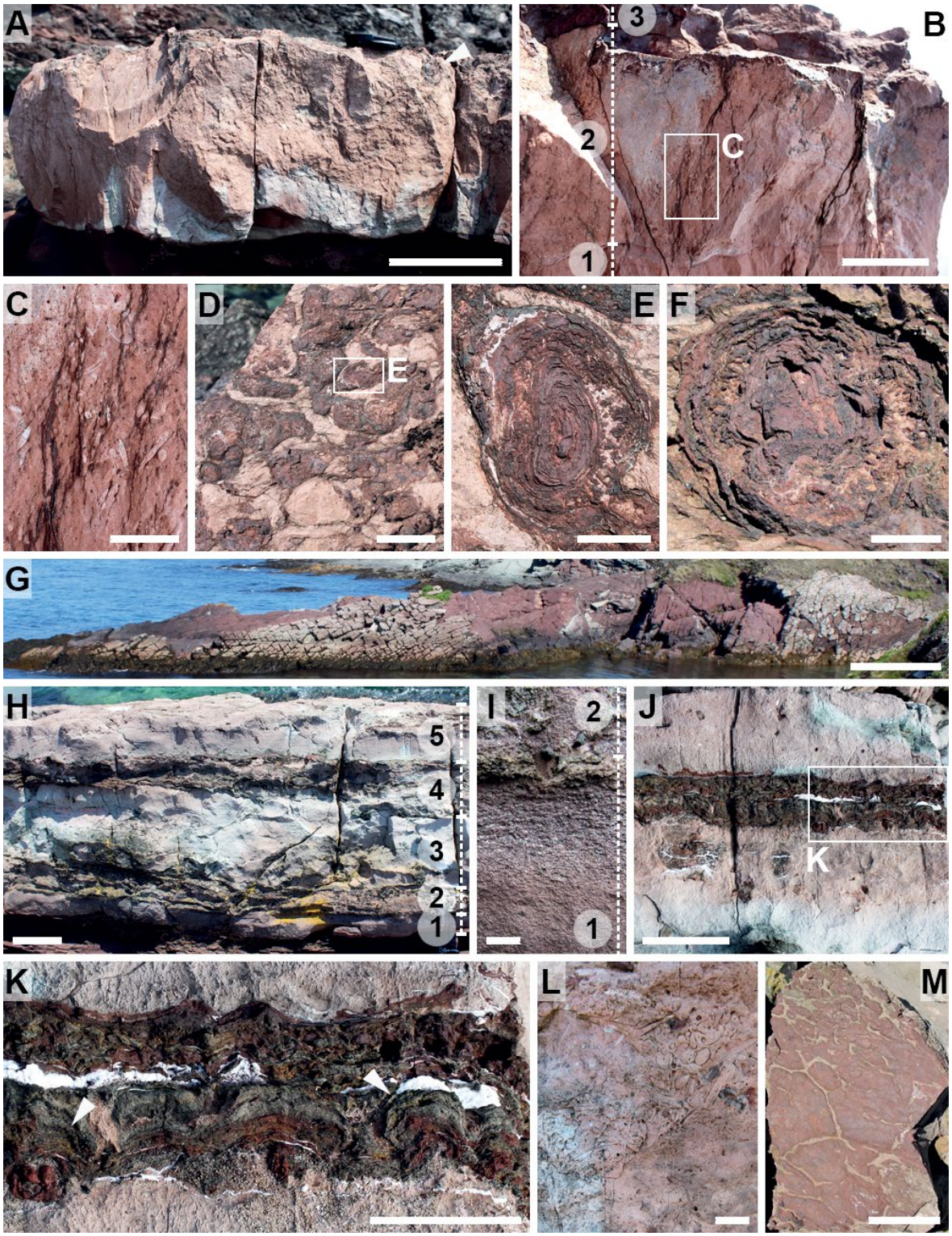

Fig. 18. Facies E1 (A–F) (subtidal) and Facies E2 (G–M) (intertidal). Scale bars are 1 cm (C, E, F, I, L), 5 cm (B, D, K, M), 10 cm (A, H, J), and 10 m (G). All photographs are from Little Dantzic Cove, Member 4 (Cambrian Age 2). **A**, General view of LS2. Note rare oncoid preserved in cross-section (arrow). **B**, Units (1) to (3) of LS2. Note sharp contact between units (1) and (2). Unit (3) is only partially preserved (left side). **C**, Close-up from Figure 18B showing small shelly fossil accumulation. **D**, Upper surface view of LS2 showing aggregation of oncoids. **E**, Close-up from Figure 18D showing a disc-shaped oncoid with well-developed cortex and a mudstone clast as nucleus. **F**, Irregular lobate oncoid from LS2. **G**, General top view of LS3. **H**, General cross-section view of LS3 with the five units preserved. **I**, Transition from units (1) to (2) in LS3 showing inverse graded calcite crystals in unit (1) and clasts in basal part of unit (2). **J**, Transition from units (3) to (5) in LS3. **K**, Close-up from Figure 18J showing prominent domal stromatolite of unit (4) (arrows). **L**, Small shelly fossil accumulation in unit (5) of LS3. **M**, Top view of desiccation cracks in LS3.

and poorly sorted sediment. Direct evidence in the field (Fig. 64), on polished samples (Gougeon *et al.* 2018a), and on thin sections (compare Fig. 17B and 17D) suggest that intense bioturbation is the main contributor to the development of sandy mudstone in Facies D3 (see also Gougeon *et al.* 2025a). Different mechanisms are invoked for the transport of fine-grained sediments onto the shelf (see Facies C3 interpretation). In Facies D3, passive suspension fallout is the most probable mechanism considering the stratigraphical relationship of this facies with lower offshore deposits of Subfacies C3d.

Facies Association E

Facies association E is recorded from Member 4 (Cambrian Stage 2). It corresponds to two limestone beds deposited in shallow subtidal (Facies E1) and intertidal (Facies E2) environments.

Facies E1: Medium-bedded limestone with oncoids

Description. – Facies E1 consists of a limestone bed (LS2 of Myrow 1987) showing a moderate degree of complexity (Figs 15D, 18A–F). LS2 is located 47.4 m above the base of Member 4 at Little Dantzic Cove. LS2 is 24 cm thick, does not vary much in thickness, and extends 23+ m laterally. LS2 consists of four units: (1) a basal red homogeneous micritic limestone (10 cm thick); (2) red wackestone with packstone lenses of small shelly fossil bioclasts (9 cm thick); (3) a black mudstone interval mineralized by iron and manganese and displaying prominent oncoids (1 cm thick); and (4) a red nodular micritic limestone (4 cm thick). Myrow & Landing (1992) recorded burrow mottling within micritic intervals (1) and (4). Small shelly fossils from LS2 were identified by Landing *et al.* (1989, table 1) and are composed of *Aldanella attleborensis*, '*Allatheca*' *degeeri* (Holm), *Anabarites korobovi* (Missarzhevsky), *Archaeospira*? *avalonensis* Landing, *Bemella*? *vonbitteri* Landing, *Coleoloides typicalis*, *Fomitchella infundabiliformis* Missarzhevsky, *Halkieria stonei* Landing, *Helcionella* sp., '*Ladatheca*' *cylindrica*, *Lapworthella ludvigseni*, *Maldeotaia bandalica* Singh & Shukla, and *Watsonella crosbyi*. Oncoids are of low-relief, disc-shaped to more elongated, some having irregular morphologies, and are densely aggregated. Concentric layers of red mud form their cortex, whereas the nucleus rarely exposes a mudstone clast (see Álvaro & Mills 2024 for detailed oncoid description). Oncoids have ∅ = 1–7 cm and layers forming the cortex are submillimetric in thickness.

Ichnology. – Individual trace fossils have not been identified in Facies E1.

Distribution and equivalents. – Facies E1 occurs in Member 4 (Cambrian Age 2) at Little Dantzic Cove (24 cm thick; LDC 145.1–145.3). Facies E1 corresponds to Facies 4.3 (LS2) of Myrow (1987).

Interpretation. – The presence of large disc-shaped oncoids and the stratigraphical position of Facies E1 suggest deposition in a marine shallow subtidal environment (Peryt 1981; Olszewski 1996; Schaefer *et al.* 2001; Flügel 2010; Alshuaibi *et al.* 2012; Riaz *et al.* 2020). Oncoids are coated grains formed by the binding of clastic particles thanks to algal mats or biofilms, which secondarily trigger calcite precipitation (Aitken 1967; Dahanayake *et al.* 1985; Jones & Goodbody 1985; Garcia-Pichel *et al.* 2004; Flügel 2010; Jones 2010). Oncoids are typically developed in continental (e.g. Dean & Eggleston 1984; Smith & Mason 1991; Verrecchia *et al.* 1997) and marine intertidal or subtidal areas (e.g. Pratt 1979; Védrine *et al.* 2007; Alshuaibi *et al.* 2012). Considering the stratigraphical position of Facies E1, a shallow marine environment is envisioned (see also Álvaro & Mills 2024). Oncoids have also been recorded in association with shells and bioturbated intervals in open-marine settings within the photic zone, above storm wave base (Massari & Dieni 1983; Olszewski 1996; Beraldi-Campesi *et al.* 2018). Small subspherical oncoids result from important rolling and overturning in high-energy conditions, whereas larger, lobate, and more irregular oncoids are formed in low-energy environments allowing the development of microbial meshwork (Védrine *et al.* 2007; Flügel 2010). Therefore, large, irregular, and disc-shaped oncoids of Facies E1 are more typical of lower-energetic conditions within the photic zone. Oncoid formation and accumulation can be associated with transgressive (Fürsich *et al.* 1992; Védrine *et al.* 2007) or regressive events (Jiang *et al.* 1998; Shi & Chen, 2006; Riaz *et al.* 2020). Flügel (2010) noted that oncolitic wackestone associated with whole fossils may represent regressive conditions, an opinion suggested here for Facies E1 considering the bioclastic content and Member 4 depositional model.

At Grand Bank Head, a *ca.* 20 cm-thick limestone bed, very irregular in thickness, is found within Member 4 (GBH-F 22.4–22.6). This bed consists of micritic limestone and lacks oncoids and small shelly fossils that would undoubtedly affiliate it to LS2. However, the stratigraphical position of this bed delineates a lower interval of Member 4 hosting calcite nodules and an upper interval lacking nodules, an arrangement similar to that of Member 4 at Little Dantzic Cove (see 'Data 1' file in Gougeon *et al.* 2025b). In addition, the thickness of the bed at Grand Bank Head is comparable to that of LS2 at Little Dantzic Cove, which suggests a potential stratigraphical correlation between the two localities.

Facies E2: Thick-bedded limestone with oncoids, desiccation cracks, and stromatolites

Description. – Facies E2 consists of a limestone bed (LS3 of Myrow 1987) showing a high degree of complexity (Fig. 18G–M). LS3 defines the top of Member 4 at Grand Bank Head and Little Dantzic Cove. LS3 is 60 cm thick, does not vary much in thickness, and extends 80+ m laterally. LS3 is composed of five units: (1) a basal pink green interval with inverse graded, fine- to coarse-grained elongated calcite crystals in a green to red mudstone matrix (5–8 cm thick); (2) an interval with basal conglomerate capped by planar stromatolites (7–15 cm thick); (3) a pink micritic limestone with local wackestone of red and green mudstone clasts and oncoids (5–25 cm thick); (4) an interval with basal conglomerate capped by columnar stromatolites, sheet cracks, and tepee structures (2–15 cm thick); and (5) a pink white wackestone with packstone lenses made of small shelly fossil bioclasts (6–15 cm thick). Conglomerates of intervals (2) and (4) are composed of limestone intraclasts, red mudstone clasts, phosphatic clasts, rounded volcanic clasts, oncoids, and small shelly fossils. Stromatolites of interval (4) consist of horizontal, parallel mineralized laminae that develop domes and distinct columns. The top of interval (5) displays large polygonal desiccation cracks that extend into intervals (3) and (4). Small shelly fossils from LS3 were identified by Landing *et al.* (1989, table 1) and are composed of *Aldanella attleborensis*, '*Allatheca*' *degeeri*, *Anabarella plana* Vostokova, *Anabarites korobovi*, *Archaeospira*? *avalonensis*, *Bemella*? *vonbitteri*, *Eccentrotheca kanesia*, *Fomitchella infundabiliformis*, *Halkieria stonei*, *Helcionella* sp., '*Ladatheca*' *cylindrica*, *Lapworthella ludvigseni*, *Maldeotaia bandalica*, *Plinthokonion arethion* Landing, *Protohertzina anabarica* Missarzhevsky, and *Watsonella crosbyi*. Oncoids are similar in shape to those described in Facies E1.

Ichnology. – Trace fossils are absent in Facies E2.

Distribution and equivalents. – Facies E2 occurs in Member 4 (Cambrian Age 2) at Grand Bank Head (60 cm thick; GBH-F 44.6–45.2) and Little Dantzic Cove (60 cm thick; LDC 178.7–179.3). Myrow (1987) also recorded Facies E2 at Fortune North in an area that has not been accessed in this study. Facies E2 corresponds to Facies 4.3 (LS3) of Myrow (1987).

Interpretation. – The presence of stromatolites, oncoids, sheet and desiccation cracks, and tepee structures argues for deposition in an intertidal environment (Awramik 1971; Halley 1975; Dravis 1983; Dill *et al.* 1986; Feldman & McKenzie 1998; Flügel 2010). Stromatolites are formed by the trapping and binding of sediment by photozoan and heterozoan bacteria and their *in-situ* calcification (Golubic & Focke 1978; Awramik 1992; Grotzinger & James 2000; Jones 2010; Pace *et al.* 2018). Oncoids are coated grains also made by microbes, algae, and other encrusting organisms (Flügel 2010; Jones 2010). Although similar in shape, oncoids are less abundant in LS3 than LS2, and are associated with mudstone clasts. Their shape suggests a formation in a lower-energetic environment (Védrine *et al.* 2007) and their association with mudstone clasts implies subsequent transportation and accumulation. Oncoids are easily transported on tidal flats because of their light structure (Alshuaibi *et al.* 2012). Sheet cracks are planar to undulatory cracks, parallel to bedding, and are interpreted as desiccation structures that are commonly developed on tidal flats (Flügel 2010; Hoffman & Macdonald 2010; Cui *et al.* 2019). Tepee structures are inverted, depressed V-shaped structures in cross-section that originate from desiccation (but see Pratt 2002), and are notably recorded in supratidal and intertidal areas (Burri *et al.* 1973; Assereto & Kendall 1977; Kendall & Warren 1987; Flügel 2010). Desiccation cracks are formed by the dewatering of mud during subaerial exposure (Bajard 1966). Finally, mudstone intraclasts indicate early lithification in shallow subtidal and tidal flats and secondary transport close to their place of origination (Gevirtzman & Mount 1986; Jones 2010; Pratt 2010). The stratigraphical position of Facies E2 suggests that a rapid regressive event took place between mud depocenter deposits of Facies D2/Subfacies C3c and intertidal limestone of Facies E2, which is comparable to the interpretation of Facies E1.

Systematic palaeontology

The ichnotaxonomic analysis performed is in accordance with common procedures in ichnology and is standardized using ichnotaxobases (Bromley 1990, 1996; Bertling *et al.* 2006, 2022; Buatois & Mángano 2011). Overall, the revision of ichnotaxa done here follows a conservative philosophy, keeping valid ichnospecies that provide distinctive morphological characters reflecting a function of behaviour and identifying redundant ichnospecies that can be synonymized, but giving less weight to superficial differences that could be taphonomic (Bertling *et al.* 2006, 2022; Buatois & Mángano 2011). The use of trace-fossil metrics (e.g. width, depth, degree of curvature – but not ratios) and the clustering of elements are generally considered poor ichnotaxobases and, therefore, have not been considered to discriminate ichnospecies in this study (see Bertling *et al.* 2006, 2022). New ichnospecies that were erected in master and doctoral dissertations

(i.e. *Arenicolites skeltonensis* Farrow, 1967, *Diplocraterion arkelli* Farrow, 1967, *D. statheri* Farrow, 1967, *Rosselia motivus* Bann, 1998, *Teichichnus sinuosus* Bann, 1998, *Arenicolites yunnanensis* Li, 2014, and *Cochlichnus plegmaeidos* Hogue, 2018) have no status with the International Code of Zoological Nomenclature and therefore are not discussed in detail. However, some of these ichnospecies could be useful if formally erected in peer-reviewed publications (e.g. *Arenicolites skeltonensis*, *Teichichnus sinuosus*). Synonymies of previous reports for each ichnospecies only focus on papers dealing with Chapel Island Formation material. Terminology on what is a burrow, a trail, or a trackway follows Bromley (1996) and Buatois & Mángano (2011). Terminology on individual elements composing trackways follows Trewin (1994).

Repository. – The material analysed in this work was mostly investigated in the field, although samples curated at the Geological Survey of Canada (GSC) in Ottawa (Canada) were also added to the study, for completeness.

Ichnogenus *Allocotichnus* Osgood, 1970

Discussion. – *Allocotichnus* is an asymmetric trackway with imprints arranged *en echelon* (Osgood 1970) included in the category of architectural design of 'trackways and scratch imprints' (Buatois *et al.* 2017). *Allocotichnus* was first described from the Ordovician Latonia Formation of eastern USA (Miller 1880; Osgood 1970). Originally, Miller (1880) proposed the ichnogenus *Asaphoidichnus* and erected two ichnospecies based on imprint morphology: *A. trifidus* with trifid imprints and merged ridges at their bases, and *A. dyeri* with quadrifid imprints and unconnected ridges. Later, Osgood (1970) re-examined type and newly collected specimens and explored whether imprints of a pair are dimorphic or not. Although *Asaphoidichnus trifidus* is composed of similar imprints within pairs, this is not the case for *A. dyeri*. Therefore, Osgood (1970) removed *Asaphoidichnus dyeri* from *Asaphoidichnus* and placed it within the new ichnogenera *Allocotichnus*. Two ichnospecies attributed to *Allocotichnus* have been erected: *A. dyeri* (Miller, 1880) and *A. palmatus* Aceñolaza & Gutiérrez-Marco, 1999. The type ichnospecies, *Allocotichnus dyeri*, has subparallel, unconnected ridges in each imprint (Miller 1880; Osgood 1970). *Allocotichnus palmatus* has up to ten radiating ridges per imprint (Aceñolaza & Gutiérrez-Marco 1999).

Allocotichnus shows similarities with *Asaphoidichnus* Miller, 1880, *Dimorphichnus* Seilacher, 1955a, *Monomorphichnus* Crimes, 1970, and *Tasmanadia* Chapman, 1928. *Asaphoidichnus* is composed of two series of similar opposite imprints, whereas imprints in *Allocotichnus* are asymmetric and arranged *en echelon* (Osgood 1970). *Dimorphichnus* is an asymmetric trackway with series of delicate elongated ridges and short blunt imprints (Seilacher 1955a, 1990a). In contrast, *Allocotichnus* imprints are never composed of elongated ridges, and imprints are arranged *en echelon* and in pairs. *Monomorphichnus* consists of a series of subparallel ridges of similar shape that may repeat laterally (Crimes 1970). Contrary to *Allocotichnus*, scratch imprints in *Monomorphichnus* are not dimorphic. Finally, *Tasmanadia* is composed of elongate imprints forming series with opposite symmetry, an organization that is not observed in *Allocotichnus* (Chapman 1928; Glaessner 1957; Durand & Aceñolaza 1990; Seilacher *et al.* 2005).

Allocotichnus ranges from the Cambrian (this study) to the Ordovician (Osgood 1970; Aceñolaza & Gutiérrez-Marco 1999). Other recordings from the Ordovician (Aceñolaza & Aceñolaza 2002), Devonian (Sutcliffe *et al.* 1999; Acker 2013) and Permian (Gand *et al.* 2008) need re-evaluation. Trilobites have been indicated as possible producers (Miller 1880; Osgood 1970). *Allocotichnus* is recorded in shallow-marine environments (Osgood 1970; this study). In the Chapel Island Formation, *Allocotichnus* has only been documented recently (see synonym list below).

cf. *Allocotichnus dyeri* (Miller, 1880)

Figure 19A–C

2014 *Allocotichnus dyeri* (Miller); Buatois, Narbonne, Mángano, Carmona & Myrow, p. 3, fig. 1a–g.
2014 *Dimorphichnus* Seilacher; Tarhan & Droser, p. 318, fig. 9G.
2016 *Allocotichnus dyeri* (Miller); Mángano & Buatois, p. 93, fig. 3.11a, b.
2017 *Allocotichnus dyeri* (Miller); Buatois, Wisshak, Wilson & Mángano, p. 112, fig. 6A.
2017 *Allocotichnus dyeri* (Miller); Landing *et al.*, p. 51, fig. 19A, C, D.
2018 *Dimorphichnus* Seilacher; Tarhan, p. 189, fig. 8G.

Material. – Two trackways from Member 2B (Fortunian) in Fortune Head.

Description. – Trackway with one series of imprints arranged *en echelon*. Preserved as negative epirelief. Imprints are composed of 3 to 7 elongate to crescentic grooves. Each groove is subparallel to the neighbouring ones, but grooves commonly have shorter distances at one end of the imprint therefore creating a slight radial arrangement. Grooves located in the medium position of the imprint are longer than the other ones. Submillimetric, elongate grooves that overlap with the main grooves are locally observed. Imprints are positioned at a

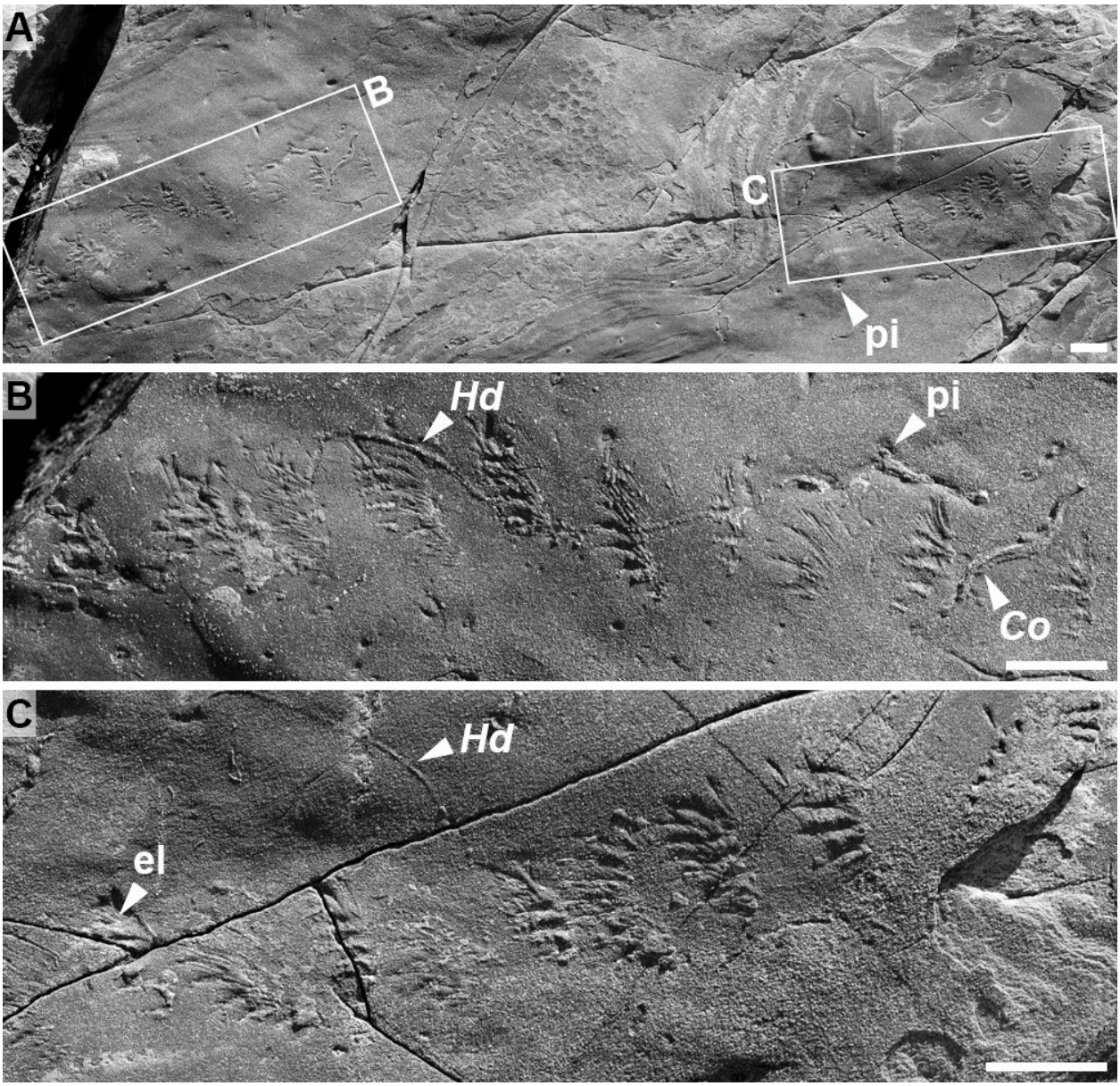

Fig. 19. cf. *Allocotichnus dyeri* (Miller). Scale bars are 1 cm. All photographs are negative epireliefs from Fortune Head, Member 2A (Fortunian). **A**, Surface with the two trackways. Note the aligned pits (pi) of *Treptichnus* Miller affinity. **B**, Close-up from Figure 19A. Note the presence of *Cochlichnus luguanensis* (Co), *Helminthoidichnites tenuis* (Hd) and aligned pits (pi) of *Treptichnus* affinity. **C**, Close-up from Figure 19A showing elongated ridges (el). Note the presence of *Helminthoidichnites tenuis* (Hd).

regular distance from one-another forming a linear arrangement. Maximum imprint width is 0.9–1.5 cm; distance between imprints is 0.6–1.8 cm; maximum number of imprints per trackway is 10; maximum trackway length is 9.7 cm.

Associated trace fossils. – cf. *Allocotichnus dyeri* co-occurs with *Cochlichnus anguineus*, *Helminthoidichnites tenuis*, and *Helminthopsis tenuis*.

Remarks. – Imprints aligned *en echelon* allow comparison with *Allocotichnus dyeri*. However, the absence of a second asymmetric track row and the high number of grooves per imprints precludes a more precise identification. The type material of *Allocotichnus dyeri* photographed by Osgood (1970, pl. 72, fig. 1) shows that imprints are oriented obliquely from the trackway axis. In the Chapel Island Formation, imprints are not oblique but almost parallel, hence the distinct *en echelon* arrangement. Paratype specimens of *Allocotichnus dyeri* (Osgood 1970, pl. 72, fig. 2, pl. 73, fig. 7, pl. 74, figs 6, 7) suggest that the higher the obliquity of paired imprints, the lower the preservational quality of one row of imprints, reaching a critical point where one

row of imprints is undetectable. This critical point was arguably reached in the Chapel Island Formation specimens, resulting in the preservation of only one row of imprints. Palacios (1989) also mentioned the presence of ?*Allocotichnus* in the Cambrian of Spain, but without providing an illustration.

Ichnogenus *Archaeonassa* Fenton & Fenton, 1937a

Discussion. – *Archaeonassa* is a horizontal trail with lateral levees (Jensen 2003) included in the category of architectural design of 'simple horizontal trails' (Buatois *et al.* 2017). *Archaeonassa* was first described from the Cambrian Mt. Whyte Formation of western Canada (Fenton & Fenton 1937a; Yochelson & Fedonkin 1997). Buckman (1994a) attempted a revision based on material from the Carboniferous of Ireland. However, this work was subsequently contested as the trace fossils studied may belong to other ichnotaxa (Yochelson & Fedonkin 1997; Mángano *et al.* 2002a; Melchor *et al.* 2003). Two ichnospecies attributed to *Archaeonassa* have been erected: *A. fossulata* Fenton & Fenton, 1937a and *A. jamisoni* Hammersburg, Hasiotis & Robison, 2018. The type ichnospecies, *Archaeonassa fossulata*, has an elongated course with distinctive lateral levees (Fenton & Fenton 1937a; Yochelson & Fedonkin 1997). *Archaeonassa jamisoni* is a short asymmetric structure with unclear morphology, and its affinity to *Archaeonassa* is unsupported (Mángano *et al.* 2022). Consequently, only the type ichnospecies, *Archaeonassa fossulata*, is here considered valid.

Archaeonassa shows similarities with *Dendroidichnites* Demathieu, Gand & Toutin-Morin, 1992, *Nereites* MacLeay in Murchison, 1839, *Protovirgularia* M'Coy, 1850, *Psammichnites* Torell, 1870, and various ichnogenera included in the category of simple horizontal trails. *Dendroidichnites* is a trackway with elongate to crescentic imprints forming two rows not organized into series (Demathieu *et al.* 1992; Buatois *et al.* 1998a; Minter & Braddy 2009). Rarely, *Dendroidichnites* can develop levees associated with its lateral imprints, which can be reminiscent of *Archaeonassa* (Fig. 29A, B; see *Dendroidichnites* section, p. 75). Although levees in *Archaeonassa* can be continuous and regular or segmented or more irregular, they do not display incisive, nested, crescentic imprints. In addition, a detailed analysis of the morphology of these ichnotaxa allows to reconstruct two very different modes of formation reflecting contrasting locomotion mechanisms and disparate biological affinity (see *Dendroidichnites* section, p. 75). Accordingly, we propose to exclude from *Archaeonassa* those leveed trails that record the presence of associated imprints. *Nereites* is a horizontal trail that is more complex than *Archaeonassa* by displaying a median backfilled tunnel surrounded by an even to lobate zone of reworked sediment (Orr & Pickerill 1995; Uchman 1995; Mángano *et al.* 2000). The loss of substrate stiffness may create lobate-like levees in *Archaeonassa* that superficially resemble *Nereites* lobes (Jensen 2003), but the regular reworked lobes of *Nereites* differ from the discontinuous, sort of segmented levees of *Archaeonassa* generated by simple wedging through the sediment. *Protovirgularia* is a horizontal trail with a median line and chevrons expanding laterally (Han & Pickerill 1994a; Seilacher & Seilacher 1994; Mángano *et al.* 1998; Knaust 2023). Some preservational variants of *Protovirgularia* can develop lateral levees, but they correspond to nested chevrons, a feature distinctive from the smooth levees in *Archaeonassa*. *Psammichnites* is a backfilled structure with a dorsal median furrow/ridge (Mángano *et al.* 2002a, 2022). Morphological and behavioural similarities have been noted between *Archaeonassa* and *Psammichnites* depending on the position of the tracemaker within the sediment (Hagadorn *et al.* 2000; Jensen 2003; McIlroy & Brasier 2017; Mángano *et al.* 2022). Distinguishing between the two may be difficult in some preservational variants, such as collapsed *Psammichnites*. However, the more complex infill of *Psammichnites* and the local presence of a thin axial structure may help in separation from *Archaeonassa* (Mángano *et al.* 2022). Simple horizontal trails (i.e. *Circulichnis* Vialov, 1971, *Gordia* Emmons, 1844, *Helminthoidichnites* Fitch, 1850, and *Helminthopsis* Heer, 1877) all lack distinctive lateral levees. However, Hofmann *et al.* (2012) noted that *Archaeonassa* can form compound trails with *Helminthoidichnites* and *Helminthopsis*.

Archaeonassa ranges from the Ediacaran (e.g. Sokolov 1973; Fedonkin 1990; Jensen 2003; Hofmann & Mountjoy 2010; Buatois & Mángano 2016; Uchman & Martyshyn 2020) to the Holocene (e.g. Abel 1935; Bajard 1966; Miller 1997; Matz *et al.* 2008; Baucon & Felletti 2013; Schatz *et al.* 2013). In the Ediacaran, inorganic structures resulting from the surficial displacement of microbial flocs can mimic *Archaeonassa* (Mariotti *et al.* 2016; Warren *et al.* 2020). However, pseudotraces produced by microbial flocs can be identified based on a number of criteria (Warren *et al.* 2020) including: (1) their morphology and orientation (i.e. microbial floc pseudotraces are typically straight and subparallel to one another due to onshore wind and wave action); and (2) facies characterisation (i.e. microbial floc pseudotraces are more prone to form in lake margins, low-energy intertidal or subtidal shallow marine settings where physical transport processes can move them). Potential producers of *Archaeonassa* are arthropods (Moussa 1970; Metz 1987a; Lan *et al.* 2021), cnidarians (Collins *et al.* 2000), gastropods (e.g. Fenton & Fenton

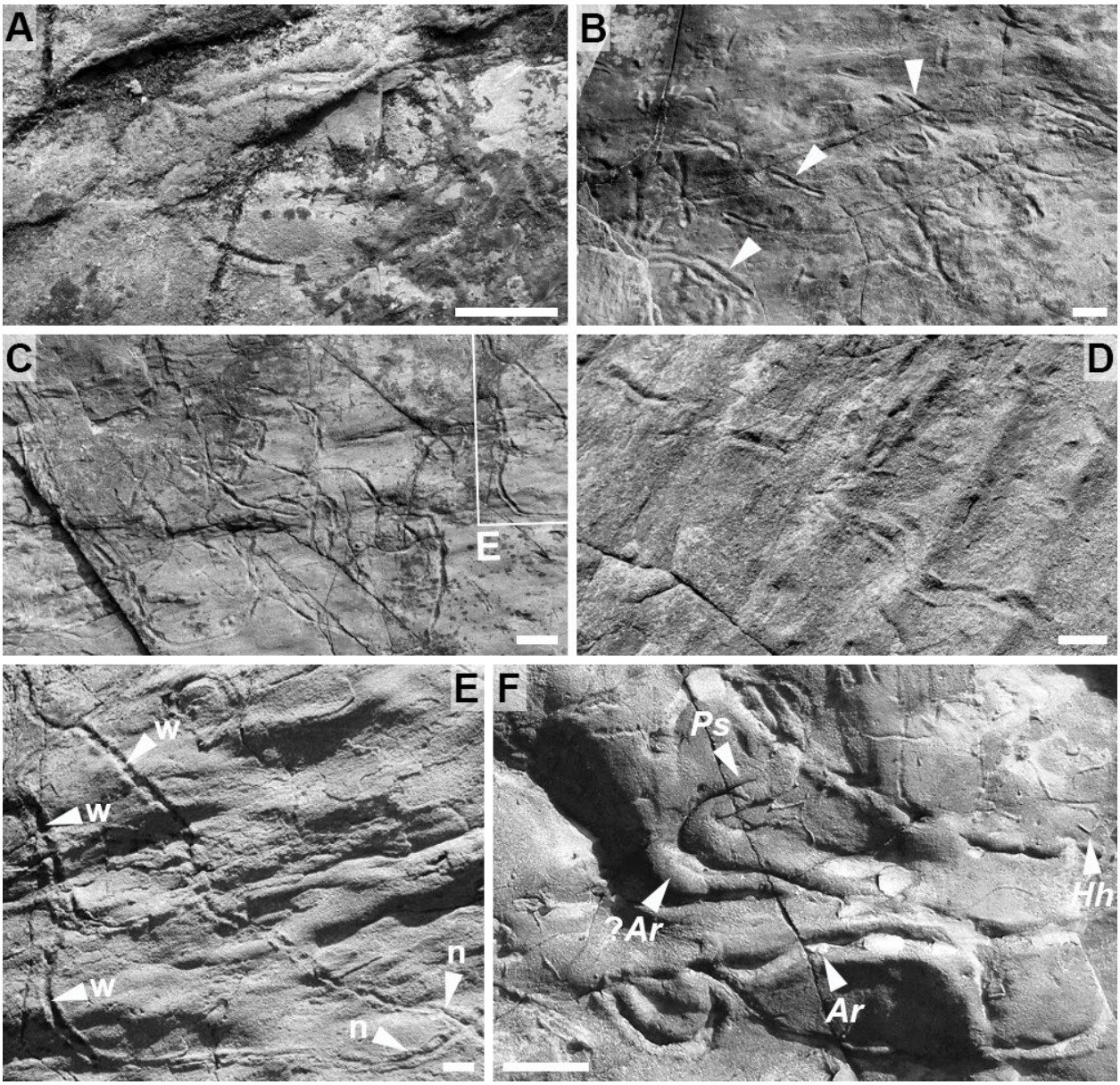

Fig. 20. Archaeonassa fossulata Fenton & Fenton (A–F) and a problematic specimen (F). Scale bars are 1 cm (A, B, D, E), 2 cm (F), and 3 cm (C). All photographs are negative epireliefs from Fortune Head. **A**, Two Ediacaran specimens. Member 1 (Ediacaran). **B**, Many short specimens with distinct V-shaped median furrows (arrows). Member 2A (Fortunian). **C**, Long, curved, and meandering specimens. Member 2A (Fortunian). **D**, A discontinuous specimen on a wave-rippled bedform. Member 2A (Fortunian). **E**, Close-up from Figure 20C showing transitions from wide (w) to narrow (n) median furrows. **F**, Complex specimen showing transition from bilobed trace fossil with incising median furrow (morphology similar to *Psammichnites*, 'Ps') to a trail with bulging lateral levees and wider median furrow (morphology close to *Archaeonassa*, '?Ar'). Note *Archaeonassa fossulata* (Ar) and *Helminthopsis hieroglyphica* (Hh) on the same surface. Member 2A (Fortunian).

1931; Abel 1935; Lessertisseur 1955; Knox & Miller 1985; Miller 1997; Wang *et al.* 2024), holothurians (Schatz *et al.* 2013), protists (Buchanan & Hedley 1960; Matz *et al.* 2008), and several clades of worms (e.g. annelids, flatworms; Lessertisseur 1955; Bajard 1966; Collins *et al.* 2000; Martin 2009; Schatz *et al.* 2013; Wang *et al.* 2019). Further precisions on possible producers need to be addressed on a case-by-case basis. *Archaeonassa* is recorded in continental (e.g. Buatois & Mángano 2002, 2009; Melchor *et al.* 2003; Genise *et al.* 2010; Netto *et al.* 2012; Scott *et al.* 2012), marginal-marine (e.g. Fenton & Fenton 1937a; Johnson *et al.* 1997; Stanley & Feldmann 1998; Baldwin *et al.* 2004; Demircan & Uchman 2016; Neto de Carvalho *et al.* 2016b), shallow-marine

(e.g. Buatois & Mángano 2004a; Chen *et al.* 2011; Mángano *et al.* 2013; Carbone & Narbonne 2014; Rodríguez-Tovar *et al.* 2014; Hanken *et al.* 2016), and deep-marine (e.g. Ewing & Davis 1967; Heezen & Hollister 1971; Lemche *et al.* 1976; Kitchell & Clark 1979; Matz *et al.* 2008; Buatois & Mángano 2016) environments. In the Chapel Island Formation, *Archaeonassa* has only been recorded recently (Landing *et al.* 2017; Laing *et al.* 2019).

Archaeonassa fossulata Fenton & Fenton, 1937a

Figure 20A–F

1985 *Gordia* sp. Crimes & Anderson, p. 316, fig. 5.8.
2019 *Archaeonassa fossulata* Fenton & Fenton; Laing, Mángano, Buatois, Narbonne & Gougeon, p. 1626, fig. 2a.

Material. – About 180 specimens from Member 1 (Ediacaran) and Members 2A and 2B (Fortunian) in Fortune Head, Grand Bank Head, and Lewin's Cove.

Emended diagnosis. – Horizontal trail with a narrow to wide, U- to V-shaped median furrow and two distinctive, smooth lateral levees (modified from Yochelson & Fedonkin 1997).

Description. – Horizontal trails with a median furrow and two distinctive lateral levees. Preserved as negative epirelief. The course is straight, curving, meandering to looping, in places cross-cutting other specimens. The median furrow is smooth, either narrow and V-shaped, or flat, wide, and U-shaped; transition from V to U shapes is common. Lateral levees are smooth forming a continuous rim but can change in thickness and morphology. Width is 0.2–1.7 cm; median furrow width is 0.05–0.4 cm; levees width is 0.05–0.3 cm; maximum length is 27.6 cm.

Associated trace fossils. – *Archaeonassa fossulata* occurs together with *Circulichnis ligusticus*, *Dendroidichnites* aff. *D. irregulare*, *Gordia marina, Helminthoidichnites tenuis*, *Helminthopsis hieroglyphica*, *H. tenuis*, and *Palaeophycus tubularis*.

Remarks. – The presence of a median furrow flanked by distinctive smooth lateral levees allows placement in *Archaeonassa fossulata*. The shape of the median furrow (i.e. U- or V-shaped) merits further discussion. Fenton & Fenton (1937a) described *Archaeonassa fossulata* with a wide median furrow and narrow lateral levees. Yochelson & Fedonkin (1997) recorded a broader variety of forms on the holotype slab and confirmed that V-shaped median furrows are also present (Fenton & Fenton 1937a, pl. 1, fig. 1). V-shaped *Archaeonassa* are extensively recorded in ancient (e.g. Yochelson & Fedonkin 1997; Buatois & Mángano 2002; Mángano & Buatois 2003a; Melchor *et al.* 2003; Mángano *et al.* 2005a; Demircan & Uchman 2016) and modern settings (e.g. Knox & Miller 1985; Miller 1997; Desai 2010). In that regard, the diagnosis of *Archaeonassa fossulata* is emended to include both U- and V-shaped furrows.

Similar forms from the Ediacaran and Cambrian records have previously been mentioned as *Aulichnites* sp. (Fedonkin 1990; Narbonne & Aitken 1990; Jenkins 1995), *Gordia* sp. (Liñán 1984), *Nereites* sp. (Crimes & Germs 1982), cf. *Nereites* (Jenkins 1995), and cf. *Palaeobullia* isp. (Bryant & Pickerill 1990). All of these reports display smooth furrows with lateral levees that allow their assignments to *Archaeonassa*. In addition, the type materials of *Aulichnites* Fenton & Fenton and *Palaeobullia* Götzinger & Becker are junior synonyms of *Psammichnites* and *Scolicia* de Quatrefages, respectively (Uchman 1995; Mángano *et al.* 2002a, 2022), and their further use is not recommended.

Jensen (2003) noted morphological similarities between *Archaeonassa* and Cambrian *Psammichnites*. *Archaeonassa* represents the surficial movement of a mollusk-like animal pushing though the sediment surface, whereas *Psammichnites* records its infaunal expression involving packing of an active filling. Therefore, transitional forms between *Archaeonassa* and *Psammichnites* should not be uncommon and have been noted in the Chapel Island Formation (Fig. 20F). Collapse of the median area in *Psammichnites* may render taxonomic decisions problematic, particularly in the case of shallow tier *P. gigas circularis* characterised by an absence of a clear active infill. In any case, the depth of the animal in the sediment, mode of construction, and nature of the sediment (i.e. grain size and consistency) play significant roles on the fine morphologies of these ichnotaxa (Knox & Miller 1985; Miller 1997; Jensen 2003).

In the Chapel Island Formation, some specimens of *Archaeonassa fossulata* display discontinuous levees. This can be explained by their mode of construction and sediment properties. Classic *Archaeonassa* results from the wedging action of the producer as it moves through the sediment relatively close or at the sediment surface. The interaction with sediment having high tensile strength creates a rupture in sediment cohesiveness and aids in the formation of irregularities on levees, in places forming sediment pads along the structure (Jensen 2003). The presence of a pre-existing topography and lateral displacement by wave action interacting with the trail in production can explain some discontinuous forms displaying irregular levees (Fig. 20D). Oblique striae

have been observed in trace fossils referred to as *Archaeonassa* (Demircan & Uchman 2016), but these striae are incising the substrate and resulted from a different mode of construction that is more typical of *Dendroidichnites* (see above and in *Dendroidichnites* section, p. 75).

Ichnogenus *Arenicolites* Salter, 1857

Discussion. – *Arenicolites* is a vertical U-shaped burrow without spreiten (Häntzschel 1975; Fillion & Pickerill 1990) included in the category of architectural design of 'vertical single U- and Y-shaped burrows' (Buatois *et al.* 2017). *Arenicolites* was first described from the Ediacaran Longmyndian Supergroup of western England (Salter 1856, 1857; McIlroy *et al.* 2005). Recent revision of the material collected by Salter revealed that these structures were, in fact, pseudo-fossils (McIlroy *et al.* 2005; Menon *et al.* 2016, 2017). Regardless, Richter (1924) selected *Arenicolites carbonarius* (Binney) as type ichnospecies, a burrow that displays the typical vertical U-shape morphology (see also Häntzschel 1975).

Arenicolites ichnospecies have only been partially reviewed so far (cf. Fürsich 1974a; Chamberlain 1977; Buckman 1992; Hammersburg *et al.* 2018; Oligmueller & Hasiotis 2024). The main difficulty is to select appropriate ichnotaxobases that reflect variations in behaviours, and not taphonomic artifacts (Buckman 1992). Fürsich (1974a) considered that burrow depth and the presence of funnel shaped apertures should not be used to discriminate ichnospecies because their morphology and preservation depend on erosion. To that, we add that the shape of the burrow in cross-section should not be used as well as it can result from lateral compaction and tectonic processes; the shape of the causative burrow in cross-section is also not always easy to decipher (e.g. Mángano *et al.* 2002b) (see also Matthew 1891, Buckman 1992). For this review, we have distinguished *Arenicolites* ichnospecies based on the overall morphology of the causative burrow, the lining, and the presence of branching. A 'distance between openings/depth' ratio could potentially be used to discriminated ichnospecies further (see *Arenicolites brevis* Matthew below), but this requires a clear identification of the colonisation surface to avoid taphonomic bias and a revision of type materials.

At least 40 ichnospecies attributed to *Arenicolites* have been erected in the literature: *A. compressus* (Sowerby, 1829); *A. carbonarius* (Binney, 1852); *A. didymus* (Salter, 1856); *A. sparsus* Salter, 1857; *A. subcompressus* (Eichwald, 1860); *A. gigas* Torell, 1868; *A. spiralis* Torell, 1869; *A. lyelli* (Torell, 1870); *A. parallelus* (Torell, 1870); *A. antiquatus* (Billings, 1872); *A. robustus* Nicholson, 1873; *A. kenta* (de Tromelin & Lebesconte, 1876); *A. woodi* Whitfield, 1882; *A. brevis* Matthew, 1891; *A. chemungensis* Whitfield, 1904; *A. lunaeformis* (Blanckenhorn, 1916); *A. kahlaensis* Kolesch, 1922; *A. zimmermanni* Kolesch, 1922; *A. statheri* Bather, 1925; *A. communis* Czarnocki, 1927; *A. obliquiforans* Hundt, 1928; *A. pfeifferi* Hundt, 1928; *A. simplex* Hundt, 1928; *A. lymensis* Coysh, 1931; *A. graptolithoformis* Hundt, 1931; *A. pascholdi* Hundt, 1931; *A. franconicus* Trusheim, 1934; A. *solignaci* Mathieu, 1949; *A. fourmarieri* Graulich, 1961; *A. curvatus* Goldring, 1962; *A. silvestris* Ortolam, 1967; *A. variabilis* Fürsich, 1974a; *A. naraensis* Badve & Ghare, 1978; *A. yunnanensis* Yang, 1990; *A. hunanensis* Zhang, 1991; *A. phataensis* Nayak, 2000; *A. longistriatus* Rindsberg & Kopaska-Merkel, 2005; *A. tenuis* Kulkarni, Borkar & Petare, 2008; *A. tanhrilensis* Rajkumar, Khaidem, Soibam & Sanasam, 2012; and *A. helixus* Rajkonwar, Tiwari & Patel, 2013. The type ichnospecies, *Arenicolites carbonarius*, formerly *Arenicola carbonaria*, is a simple vertical U-shaped burrow with subparallel limbs (Binney 1852, fig. 2). Rindsberg & Kopaska-Merkel (2005) noted that the type material of *Arenicolites carbonarius* is branched, which could be an issue as it does not comply with the archetypal morphology of *Arenicolites*. However, from the sandstone block figured by Binney (1852, fig. 2), only one of the three specimens or *Arenicolites carbonarius* illustrated possesses a branching (the one to the right). Therefore, after revision and publication of photographs of the type material, we suggest that the holotype is referred to either the left or middle specimens from that block, in order to maintain the status of this ichnospecies. *Arenicolites compressus*, formerly *Serpula compressa*, is an elongated fossil with an elliptical cross-section and a tapering end (Sowerby 1829, pl. 598, fig. 3). Its vertical development is not demonstrated, and an affinity to *Solemyatuba subcompressa* should also be envisioned (but see Seilacher 1990b). *Arenicolites didymus*, formerly *Arenicola didyma*, was described and illustrated as parallel oval structures on the rock surface (Salter 1856, pl. 4, fig. 1), while *A. sparsus* was represented as simple pits and depressions of variable sizes on the rock surface (Salter 1857, pl. 5, figs 1–4). McIlroy *et al.* (2005) first reviewed both types and additional materials from that locality and interpreted *Arenicolites didymus* and *A. sparsus* as the Ediacaran body fossil *Beltanelliformis minutae* McIlroy (see also Callow *et al.* 2011). However, these were later re-interpreted as fluid escape structures, loading structures, and sediment volcanoes associated with microbial mats (Menon *et al.* 2016, 2017). *Arenicolites subcompressus*, formerly *Serpula subcompressa*, is a simple curved structure with elliptical cross-section oriented

at various angles (Eichwald 1860, pl. 34, fig. 7). Its vertical development is not demonstrated in the figured specimen nor mentioned in the text by Eichwald (1860), yet Seilacher (1990b) erected it as type ichnospecies of *Solemyatuba* Seilacher. This ichnospecies is not retained as valid here. The material figured by Eichwald (1860, pl. 34, fig. 7) is also highly reminiscent of *Oblongichnus solodukhoi* Bel Haouz, Lagnaoui & Silantiev. *Arenicolites gigas* is a horizontal trace fossil that was later reassigned to *Psammichnites gigas* by Torell (1870) (see also Mángano *et al.* 2022). *Arenicolites spiralis* is a coiled structure that was only mentioned in Torell (1869) (see also Linnarsson 1869) before being formally described as *Spiroscolex spiralis* Torell. The type material of *Spiroscolex* Torell from Sweden is a *nomen nudum* potentially synonymous with *Gyrolithes* (Jensen 1997), whereas Canadian material (e.g. Billings 1872) was affiliated to *Helminthoidichnites spiralis* Walcott which is probably an algal body fossil (Hofmann 1971; Walter *et al.* 1990; Sharma & Shukla 2009). *Arenicolites lyelli* and *A. parallelus*, formerly *Diplocraterion lyelli* and *D. parallelum*, respectively, are vertical U-shaped burrows with spreiten (Westergård 1931; Fürsich 1974b) that were placed in synonymy with *Arenicolites* by Matthew (1890). However, Fürsich (1974b) reviewed *Diplocraterion* Torell in depth and considered *D. parallelum* valid, while *D. lyelli* was referred as its junior synonym. *Arenicolites antiquatus*, formerly *Arthraria antiquata*, is a dumb-bell-shaped trace fossil (Billings 1872). *Arthraria* Billings was placed in synonymy with *Arenicolites* by Matthew (1899). *Arthraria* was later reviewed in detail by Fillion & Pickerill (1984a) and is currently considered valid, although its vertical development is unknown (see also Buatois *et al.* 2017; Gougeon *et al.* 2025c). *Arenicolites robustus* was neither described nor figured by Nicholson (1873) and is therefore considered a *nomen nudum* (Benton & Trewin 1978). *Arenicolites kenta*, formerly *Arenicola kenta*, was described by de Tromelin & Lebesconte (1876) as thin, elongated, horizontal structures on the rock surface. Although Lebesconte (1886) suggested relocation within the newly erected ichnotaxa *Montfortia rhedonensis* Lebesconte and *M. filiformis* Lebesconte, holotype and topotype materials were recently restudied by Gougeon *et al.* (2018b) and correspond to simple horizontal trails *Helminthoidichnites tenuis* and *Helminthopsis tenuis*. *Arenicolites woodi* is a simple vertical burrow with semi-lunate openings and a rim at the top (Whitfield 1882, pl. 2, figs 1–3). The U-shaped morphology is not demonstrated, and James (1892) placed it in synonymy with *Skolithos* Haldeman (see also Alpert 1974). *Arenicolites brevis* is a shallow vertical U-shaped burrow (Matthew 1891, pl. 11, fig. 13). Although Fürsich (1974b) placed it in synonymy with *Diplocraterion*, the description does not mention spreiten and this is not apparent in the figured material of Matthew (1891) either. This ichnospecies is here tentatively placed in synonymy with *Arenicolites carbonarius*, although it could be retained as valid after revision of the type material if a 'distance between opening/depth' ratio is used as ichnotaxobase. *Arenicolites chemungensis* is a vertical U-shaped burrow with a thick lining and funnel-shaped apertures surrounded by raised rims (Whitfield 1904, pl. 14, figs 1, 2). The presence of a thick lining is considered an important ichnotaxobase that is well illustrated by Whitfield (1904, pl. 14, fig. 1) and, therefore, *Arenicolites chemungensis* is retained as valid. *Arenicolites lunaeformis*, formerly *Arenicoloides luniformis*, is a vertical U-shaped burrow with spreiten (Kolesch 1922, fig. 4) and belongs to *Diplocraterion* (Knox 1973; Häntzschel 1975; Pollard 1981; Buckman 1992). *Arenicolites kahlaensis* was only figured by Kolesch (1922, fig. 15) as individual pits aggregated on a bed surface (see also Knox 1973), which does not provide enough morphological elements to retain it as valid. *Arenicolites zimmermanni* was not figured by Kolesch (1922) and should therefore be regarded as a *nomen nudum*, although drawn specimens (Kolesch 1922, figs 7–13) suggest an affinity to *Diplocraterion* (Knox 1973; Häntzschel 1975; Pollard 1981; Buckman 1992). *Arenicolites statheri* is a vertical U-shaped burrow with parallel limbs and a thin lining (Bather 1925; Chamberlain 1977; Fürsich 1974a). As drawn by Bather (1925), this ichnospecies does not differ from *Arenicolites carbonarius* and should be considered its junior synonym; other specimens from the type locality correspond to *Diplocraterion* (Häntzschel 1975; Buckman 1992). *Arenicolites communis* is neither figured nor described (Czarnocki 1927) and is a *nomen nudum* (S. Jensen, pers. comm., 2024). *Arenicolites obliquiforans* is made of a simple oblique tube developing within the casting rock (Hundt 1928, p. 35) and may be related to *Palaeophycus tubularis*. *Arenicolites pfeifferi* is a U-shaped oblique burrow without spreiten (Hundt 1928, p. 38, 39). As the oblique orientation may be related to schistosity of the metamorphic rock hosting the burrow (Hundt 1928) and therefore would be a taphonomic artifact, we consider this ichnospecies a junior synonym of *Arenicolites carbonarius*. *Arenicolites simplex* does not display the vertical U-shaped form typical of *Arenicolites* (Hundt 1928, p. 33), and its exact ichnotaxonomic affiliation requires restudy of the type material. *Arenicolites lymensis* is a vertical U-shaped burrow with spreiten (Coysh 1931, fig. 1) and corresponds to *Diplocraterion* (Fürsich 1974b; Buckman 1992; Moghadam & Paul 2000). *Arenicolites graptolithoformis* consists of two parallel, subvertical and unconnected tubes with faint transverse striations and was erected based on its superficial

resemblance to graptolites (Hundt 1931, pp. 184, 185). Although considered to be affiliated to *Diplocraterion* (Buckman 1992) or *Solemyatuba* (Mángano *et al.* 2002b), the U-shaped morphology of *Arenicolites* is not displayed and revision is needed (see also Fürsich 1974a). *Arenicolites pascholdi* was only mentioned by Hundt (1931, p. 185) without description or illustration, and is therefore a *nomen nudum*. *Arenicolites franconicus* is an irregular, vertical to oblique burrow with a terminal bulbous chamber (Trusheim 1934; Schlirf 2006) that was relocated in *Trusheimichnus franconicus* (Trusheim) after re-evaluation of the type material (Schlirf 2006). *Arenicolites solignaci* is a horizontal backfilled trace fossil (Mathieu 1949) that is unrelated to *Arenicolites* and shows affinities to *Parataenidium* and *Protovirgularia*. *Arenicolites fourmarieri* is a very irregular structure, oriented horizontal to oblique from bedding and with an inconsistent width (Graulich 1961, figs 1–3). Re-evaluation of this structure is needed, but it seems to be inorganic. *Arenicolites curvatus* is a vertical burrow with inclined limbs and an elliptical cross-section (Goldring 1962; Chamberlain 1977). Seilacher (1990b) considered *Arenicolites curvatus* a synonym of *Solemyatuba subcompressa*, but issues related to the type material of the latter (see above) render this interpretation problematic. In this study, we provisionally retain *Arenicolites curvatus* as valid, pending further revision of *Solemyatuba* (but see Knaust 2019 for a different view). *Arenicolites silvestris* was described by Ortolam (1967, p. 538) as a simple vertical U-shaped burrow with a fill mostly composed of mudstone, except in the upper part of one limb which is composed of sandstone. The type of passive infill in open burrows is considered a weak ichnotaxobase (Bertling *et al.* 2022), and therefore this ichnospecies is placed in synonymy with *Arenicolites carbonarius*. *Arenicolites variabilis* is described as either narrow or wide, vertical or oblique, in places with variable distance in between limbs, a lateral deviation at its base, or even possessing spreiten (Fürsich 1974a). The holotype, however, is a simple vertical U-shaped burrow displaying a shortening of the distance between limbs toward the top (Fürsich 1974a, figs 4e, 5b), a diagnostic feature also emphasized in the text. Therefore, we suggest to restrict *Arenicolites variabilis* to forms showing a variable distance in between limbs (cf. Pickerill & Keppie 1981). *Arenicolites naraensis* is a vertical U-shaped burrow with subparallel limbs (Badve & Ghare 1978, pl. 3, figs 1, 2) that does not differ from *A. carbonarius* and should be regarded as its junior synonym. *Arenicolites yunnanensis* is a wide vertical U-shaped burrow with limbs mostly inclined (Yang *et al.* 2004, pl. 2, fig. 1) and may represent a junior synonym of *A. curvatus*. Zhang (1991) described *Arenicolites hunanensis* as a simple, unlined, vertical U-shaped burrow with subparallel limbs that is distinguished from other ichnospecies based on morphometric parameters. As burrow width and depth are not considered good ichnotaxobases for *Arenicolites*, this ichnospecies is regarded as a junior synonym of *A. carbonarius*. *Arenicolites phataensis* was described by Nayak (2000) as a vertical U-shaped burrow with one funnel-shaped limb. The vertical expression is not demonstrated in the figured material and the infill is unclear (Nayak 2000, pl. 1, fig. 1), and a revision is needed. *Arenicolites longistriatus* is a subhorizontal burrow with longitudinal striae (Rindsberg & Kopaska-Merkel 2005). Re-evaluation of the type material by Lucas & Stimson (2013) revealed that the U-shaped morphology is not expressed in the type and other material from that locality, and that *Arenicolites longistriatus* is a junior synonym of *Palaeophycus striatus* Hall. *Arenicolites tenuis* is a vertical U-shaped burrow with parallel limbs (Kulkarni *et al.* 2008) and is a junior synonym of *A. carbonarius* (but see Knaust 2019 for an alternative view). Rajkumar *et al.* (2012) did not provide a reason to differentiate *Arenicolites tanhrilensis* from other ichnospecies. The simple vertical U-shaped morphology with parallel limbs as figured by Rajkumar *et al.* (2012, fig. 2a) suggests a synonymy of *Arenicolites tanhrilensis* with *A. carbonarius*. *Arenicolites helixus* was described by Rajkonwar *et al.* (2013) as having helically coiled limbs with a basal branching. However, the figured specimen (Rajkonwar *et al.* 2013, pl. 2, fig. c) shows a complex infill of thick lamina oriented obliquely and delineated by thin laminae of different lithology. This type of infill is similar to tubular tidalites as described by Gingras & Zonneveld (2015) in *Arenicolites* (see also Wetzel *et al.* 2014 and Rodríguez-Tovar *et al.* 2019) and fits well with the interpreted tidal depositional setting (Singh *et al.* 2010) (but see Knaust 2019 for an alternative opinion). Therefore, this distinction is taphonomic, not morphological, and should not be used as an ichnotaxobase. However, the presence of branching, which is clearly visible in their photographed specimen (Rajkonwar *et al.* 2013, pl. 2, fig. c), is diagnostic and supports the validity of this ichnospecies (if we considered the holotype of *A. carbonarius* to be unbranched, as suggested above). Consequently, five ichnospecies, *Arenicolites carbonarius*, *A. chemungensis*, *A. curvatus*, *A. helixus*, and *A. variabilis*, are provisionally retained as valid in this study until revision of type materials.

Arenicolites shows similarities with *Diplocraterion* Torell, 1870, *Lapispira* Lange, 1932, *Skolithos* Haldeman, 1840, *Solemyatuba* Seilacher, 1990b, *Teichichnus* Seilacher, 1955b, and *Tisoa* de Serres, 1840. *Arenicolites* is distinguished from *Diplocraterion* by the absence of spreiten (Fürsich 1974b). *Lapispira* is a vertical burrow made of two limbs connected at their base but forming

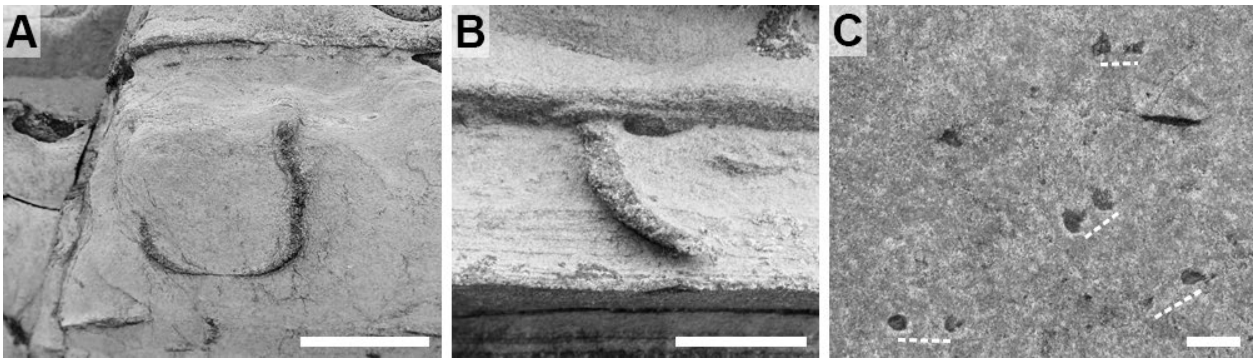

Fig. 21. Arenicolites aff. *A. carbonarius* (Binney) (A, B) and *Arenicolites* isp. (C). Scale bars are 1 cm (A, B) and 2 cm (C). **A**, *Arenicolites* aff. *A. carbonarius* showing two parallel limbs connected at their base. Note the thinning of the burrow in its basal portion. Full relief, Point May, Member 2A (Fortunian). **B**, Partially preserved *Arenicolites* aff. *A. carbonarius*. Full relief, Grand Bank Head, Member 2A (Fortunian). **C**, Multiple *Arenicolites* isp. on a bed top composed of paired burrow openings. Full relief, Little Dantzic Cove, Member 5 (Cambrian Age 2).

an overall helix shape (Lanés *et al.* 2007; de Gibert *et al.* 2012). *Skolithos* is a simple vertical burrow without pairing and basal connection (Alpert 1974; Schlirf & Uchman 2005; Knaust *et al.* 2018). *Solemyatuba* is a wide vertical U-shaped burrow with an elliptical cross-section, commonly with a tube extending at its base (Seilacher 1990b). However, the type material of *Solemyatuba*, *S. subcompressa*, is not representative of the ichnogenus as diagnosed by Seilacher (1990b) (see comments above). Therefore, we suggest *Solemyatuba* to be restricted to forms displaying the basal extension (i.e. *S. ypsilon* Seilacher), awaiting further revision of *S. subcompressa*. Wide and shallow *Arenicolites* can be reminiscent of *Teichichnus* (e.g. Goldring 1962; Bjerstedt 1987). However, *Teichichnus* always displays vertical spreiten, which is absent in *Arenicolites*. Recently, Knaust (2019) included simple vertical U-shaped burrows as part of the morphological range of *Tisoa*. Although the holotype of *Tisoa* is lost, topotype material demonstrates that *Tisoa* is a deep vertical U-shaped burrow with a low-amplitude helicoidal morphology and faint spreiten (Wetzel & Blouet 2023), the latter features being absent in *Arenicolites*.

Arenicolites ranges from the Cambrian (e.g. Kennedy & Droser 2011; Hofmann *et al.* 2012; Mángano & Buatois 2016, 2020; Korovnikov *et al.* 2019; Liu *et al.* 2022) to the Holocene (e.g. Bajard 1966; Hertweck & Reineck 1966; Howard & Dörjes 1972; Ekdale & Lewis 1991; Gingras *et al.* 2002; Dashtgard 2011). *Arenicolites* from the Ediacaran of Mongolia (Oji *et al.* 2018) awaits further investigation as the morphology of the illustrated specimen is not typical of *Arenicolites*, with a flat base forming 90° angles with respect to vertical limbs (Oji *et al.* 2018, figs 5, 7). In addition, the position of the Ediacaran–Cambrian boundary in this area is highly debated (Smith *et al.* 2016a, 2017; Landing & Kruse 2017; Topper *et al.* 2022). Continental *Arenicolites* are produced by insect larvae (Chamberlain 1975; McLachlan & Cantrell 1976; Wallace & Merritt 1980), whereas marine forms are affiliated to amphipods (e.g. Seilacher 1953, 1967a; Lessertisseur 1955; Bajard 1966; Gingras *et al.* 2002; MacEachern *et al.* 2007), decapods (Farrow 1971), enteropneusts (Lessertisseur 1955; Howard & Dörjes 1972), holothurians (Bromley 1996), and sipunculid (Baucon & Felletti 2013), polychaete (e.g. Fisher & MacGinitie 1928; Bajard 1966; Seilacher 1967b; Aller & Yingst 1978; Bromley 1996; Dashtgard 2011), and priapulid worms (Turk *et al.* 2024a). *Arenicolites* is found in continental (e.g. Chamberlain 1975; Bromley & Asgaard 1991; Buatois & Mángano 2004b; Fernandes & Carvalho 2006; Netto 2007; Gingras *et al.* 2016), marginal-marine (e.g. Howard & Dörjes 1972; Hakes 1976; Kamola 1984; Eagar *et al.* 1985; Gingras *et al.* 1999; Liu *et al.* 2022), shallow-marine (e.g. Frey & Chowns 1972; Heinberg & Birkelund 1984; Dam 1990; MacEachern & Pemberton 1992; Droser *et al.* 1994; Schlirf 2000), and deep-marine (e.g. Jansa 1974; Crimes 1977; Pickerill & Keppie 1981; Savrda *et al.* 1984; Buatois & Mángano 1992; Leszczynski *et al.* 1996) environments. *Arenicolites* was previously mentioned in the Chapel Island Formation (Crimes & Anderson 1985; Narbonne *et al.* 1987; Landing *et al.* 1988; Droser *et al.* 2002; Herringshaw *et al.* 2017).

Arenicolites aff. *A. carbonarius* (Binney, 1852)

Figure 21A, B

? 1987 *Arenicolites* sp. Narbonne, Myrow, Landing & Anderson, p. 1287, fig. 6H.
2002 'curved burrow' Droser, Jensen, Gehling, Myrow & Narbonne, p. 9, fig. 6F.

Material. – Five specimens from Members 2A and 2B (Fortunian) in Fortune Head, Grand Bank Head, and Point May.

Description. – Simple, unlined, vertical U-shaped burrow. Preserved as full relief. Cross-section of limbs is circular. Limbs are parallel in the most complete specimen. In that specimen, the base forms a U shape with angular corners; the burrow width of that base is also thinner than the limbs. Infill is massive, composed of fine-grained sandstone different from the mudstone host rock. Width of burrow is 0.01–0.3 cm; maximum depth is 1.1 cm; distance between limbs is 1.3 cm.

Associated trace fossils. – *Arenicolites* aff. *A. carbonarius* co-occurs with *Trichichnus linearis*.

Remarks. – The simple vertical U-shaped morphology with parallel limbs and absence of lining or branching allow comparison with *Arenicolites carbonarius*. However, the lack of complete specimens and their limited number do not permit definitive conclusions, and hence these burrows are referred to as *Arenicolites* aff. *A. carbonarius*. Curved burrows with a vertical component (as in Fig. 21B) are commonly referred to *Arenicolites* in the literature, especially when recovered from cores (e.g. Chamberlain 1978; Virtasalo *et al.* 2006; Davison & MacEachern 2007; Gingras *et al.* 2016). The thinning of the burrow width in one specimen at its base (Fig. 21A) certainly resulted from compaction after burial. *Arenicolites carbonarius* has rarely been recorded in the Cambrian: (1) Yin *et al.* (1993) mentioned a lower Cambrian specimen from China without illustration; and (2) Hammersburg *et al.* (2018, fig. 6.4) figured a middle Cambrian specimen that is Y-shaped with a basal extension and is certainly of different affinity than *Arenicolites*. *Arenicolites* isp. from the Cambrian of Poland (Stachacz 2016, fig. 17A, B) does not show an important vertical component and should be regarded as *Palaeophycus tubularis*. In the Chapel Island Formation, Narbonne *et al.* (1987, fig. 6H) figured *Arenicolites* sp. in vertical section that may represent a partially preserved specimen of *Arenicolites* aff. *A. carbonarius* as described herein.

Arenicolites isp.

Figure 21C

Material. – Eleven specimens from Member 5 (Cambrian Age 2) in Little Dantzic Cove.

Description. – Simple pair of burrow openings. Preserved as full relief (on bed tops). Cross section of burrow opening is circular. Unlined, or showing a thin pyritized lining. Infill is massive, composed of very fine- to fine grained sandstone different from the sandy mudstone host rock. Width of burrow opening is 0.3–0.8 cm; distance between burrow openings is 0.6–2.6 cm.

Associated trace fossils. – *Arenicolites* isp. co-occurs with *Trichichnus linearis*.

Remarks. – The pairing of burrow openings on bed bases or tops is commonly referred to *Arenicolites* in the literature (e.g. Crimes & Jiang 1986; Brasier & Hewitt 1979). However, in the absence of vertical expression, an ichnospecific assignation is not possible. In the Chapel Island Formation, paired burrow openings were also recorded by Crimes & Anderson (1985) as *Arenicolites* sp. from Member 2 at Grand Bank Head without illustration.

Ichnogenus *Bergaueria* Prantl, 1945

Discussion. – *Bergaueria* is a cylindrical to hemispherical plug-shaped burrow (Prantl 1945; Pemberton *et al.* 1988) included in the category of architectural design of 'vertical plug-shaped burrows' (Buatois *et al.* 2017). *Bergaueria* was first described from the Ordovician Letná Formation ('Chrustenice Beds') of central Czech Republic (Prantl 1945). Pemberton *et al.* (1988) reviewed the ichnotaxonomy of plug-shaped burrows and considered four ichnospecies attributed to *Bergaueria* valid: *B. perata* Prantl, 1945; *B. langi* (Hallam, 1960); *B. radiata* Alpert, 1973; and *B. hemispherica* Crimes, Legg, Marcos & Arboleya, 1977. The type ichnospecies, *Bergaueria perata,* is thinly lined or unlined, has a central knob or depression, and can display concentric ridges (Prantl 1945; Pemberton *et al.* 1988; Pickerill 1989). *Bergaueria langi*, formerly *Kulindrichnus langi*, has a very thick lining and is unornamented (Hallam 1960; Pemberton *et al.* 1988). *Bergaueria radiata* has a thin lining and prominent basal radial ridges surrounding a central depression (Alpert 1973; Pemberton *et al.* 1988). *Bergaueria hemispherica* has a thin lining, lacks a central depression, and is unornamented (Crimes *et al.* 1977; Pemberton *et al.* 1988). Jensen (1997) considered it a preservational variant of *Bergaueria perata*, but *B. hemispherica* could be retained as valid if a width/depth ratio was used to discriminate further ichnospecies of *Bergaueria*. Since the review of Pemberton *et al.* (1988), at least ten *Bergaueria* ichnospecies have been erected or re-described: *B. klieni* (Geinitz, 1871); *B. major* Palij, 1976; *B. prantli* Książkiewicz, 1977; *B. sucta* Seilacher, 1990a; *B. elliptica* Orłowski & Żylińska, 1996; *B. baltica* Pacześna, 1996; *B. corniculata* Pacześna, 1996; *B. irregulara* Pacześna, 1996; *B. phallica* Seilacher-Drexler & Seilacher, 1999; *B. thangjingi* Singh & Kushwaha, 2008; and *B. lagingi* Zessin, 2009. *Bergaueria klieni*, formerly *Tremospongia klieni*, is a simple vertical plug-shaped burrow with concentric

ridges and a slight angle formed with the overlying casting rock (Geinitz 1871; Niebuhr & Wilmsen 2016). Although Niebuhr & Wilmsen (2016) advocated that type materials of *Bergaueria klieni* and *B. perata* were identical and therefore that *B. klieni* should be retained as the senior synonym, we suggest here to maintain *B. perata* as the valid ichnospecies for this form to comply with nomenclatural stability. *Bergaueria major* is a long vertical burrow without basal central depression (Palij 1976; Pacześna 1996, 2010). While Pemberton *et al.* (1988) placed it in synonymy with *Bergaueria perata*, Pacześna (1996, 2010) kept the use of this ichnospecies. *Bergaueria major* could potentially be retained as valid if a width/depth ratio was used to further discriminate *Bergaueria* ichnospecies. *Bergaueria prantli* is irregular with two basal, connected depressions (Książkiewicz 1977; Uchman 1998). Although Pemberton *et al.* (1988) placed it in synonymy with *Bergaueria perata*, other authors disagreed (Pickerill 1989; Uchman 1998), and we follow the latter opinion as the basal features are distinctive and not taphonomic. *Bergaueria sucta* has a very high width/depth ratio, is closely overlapping and laterally repeated (Seilacher 1990a; Jensen 1997). *Bergaueria elliptica* has an oval base with a longitudinal furrow (Orłowski & Żylińska 1996). Its affinity to *Bergaueria* is considered dubious (Uchman 1998; Demircan & Uchman 2010). *Bergaueria baltica* has a flat base with concentric ridges (Pacześna 1996) and should be considered a junior synonym of *B. hemispherica* as they are morphologically similar (cf. Crimes *et al.* 1977, pl. 6, fig. c; Pemberton *et al.* 1988, fig. 8). *Bergaueria corniculata* is described as a conical burrow with smooth walls (Pacześna 1996). These morphological traits are typical of *Conichnus* Männil rather than *Bergaueria*. *Bergaueria irregularia* is a vertical-to- or oblique-to-horizontal irregular cylindrical trace fossil with net-like sculptures and concentric swellings (Pacześna 1996), and its affinity to *Bergaueria* is dubious. *Bergaueria phallica* has a constriction ring close to the base of the burrow (Seilacher-Drexler & Seilacher 1999). *Bergaueria thangjingi* was described by Singh & Kushwaha (2008) as having radially arranged tubercles on its surface, which are not obvious from the figured material (Singh & Kushwara 2008, pl. 1, fig. a). Revision of this ichnospecies is needed. *Bergaueria lagingi* comprises conical structures with very irregular sizes and shapes (Zessin 2009, figs 27–34). Although Hoffmann & Grimmberger (2011) affiliated these structures to *Conichnus*, we consider its biogenicity dubious. In addition to these ichnospecies, Seilacher-Drexler & Seilacher (1999, fig. 3) mentioned *Bergaueria conica* without further description. From their drawing, this conical burrow seems closer to *Conichnus* in overall shape. However, the presence of a basal knob is not a diagnostic feature of *Conichnus* (see *Conichnus* section, p. 66) and may place this form closer to *Conostichus* Lesquereux, although transversal and longitudinal ridges of the latter are missing. Consequently, six ichnospecies, *Bergaueria langi*, *B. phallica*, *B. perata*, *B. prantli*, *B. radiata*, and *B. sucta*, are considered valid here. The ichnotaxonomic status of *Bergaueria hemispherica and B. major* requires additional work, and their validity would depend on the use of a width/depth ratio as ichnotaxobase.

Bergaueria shows similarities with *Astropolichnus* Crimes & Anderson, 1985, *Cheiichnus* Jensen & Bergström, 2000, *Conichnus* Männil, 1966, *Conostichus* Lesquereux, 1876, and *Piscichnus* Feibel, 1987. *Astropolichnus* is characterised by a ring-like structure ornamented with prominent regular radial ridges surrounding an axial cylinder (Crimes *et al.* 1977; Crimes & Anderson 1985; Pemberton *et al.* 1988). Contrastingly, radial ridges in *Bergaueria* are only recorded in *B. radiata* and originate from the axial area (Alpert 1973). *Cheiichnus* is a plug-shaped burrow that differs from *Bergaueria* by the presence of scratch imprints (Jensen & Bergström 2000). While *Bergaueria* is cylindrical to hemispherical, *Conichnus* has a conical shape (Männil 1966; Pemberton *et al.* 1988). *Conostichus* differs from *Bergaueria* by its conical shape and prominent ornamentation made of transversal and longitudinal ridges (Chamberlain 1971; Pemberton *et al.* 1988). *Piscichnus* is a large simple dish-shaped burrow (Feibel 1987; Gregory 1991) that lacks the typical morphology of *Bergaueria*.

Bergaueria – and more generally small plug-shaped structures – can also be difficult to differentiate from body fossils (Jensen 2003; McIlroy *et al.* 2005; Mángano & Buatois 2020), gas or fluid escape structures (Karcz *et al.* 1974; Dornbos *et al.* 2007; Banerjee *et al.* 2010; Menon *et al.* 2016, 2017), spherical mineral concretions (Geyer & Uchman 1995), and physical sedimentary structures (e.g. pot casts; Jensen 1997; Lerner & Lucas 2015; Knaust 2017).

Bergaueria ranges from the Ediacaran (Bekker 2013; Menon *et al.* 2013; Kolesnikov *et al.* 2015) to the Holocene (e.g. Lessertisseur 1955; Ansell & Trueman 1968; Mangum 1970; Seilacher-Drexler & Seilacher 1999). Other Ediacaran occurrences (e.g. Crimes & Germs 1982; Kumar *et al.* 1984; Tarhan *et al.* 2020) need careful re-evaluation (Pickerill 1989; Jensen *et al.* 2006). *Bergaueria* has been classically regarded as produced by cnidarians (sea anemones, sea pens; Lessertisseur 1955; Ansell & Trueman 1968; Mangum 1970; Seilacher-Drexler & Seilacher 1999), but other tracemakers are possible sponges (Dashtgard & Gingras 2012). *Bergaueria* is recorded in marginal-marine (e.g. Crimes *et al.* 1977; Narbonne 1984; Miller & Knox 1985; Mikuláš 1993; Mángano & Buatois 2004a; Mata *et al.* 2012),

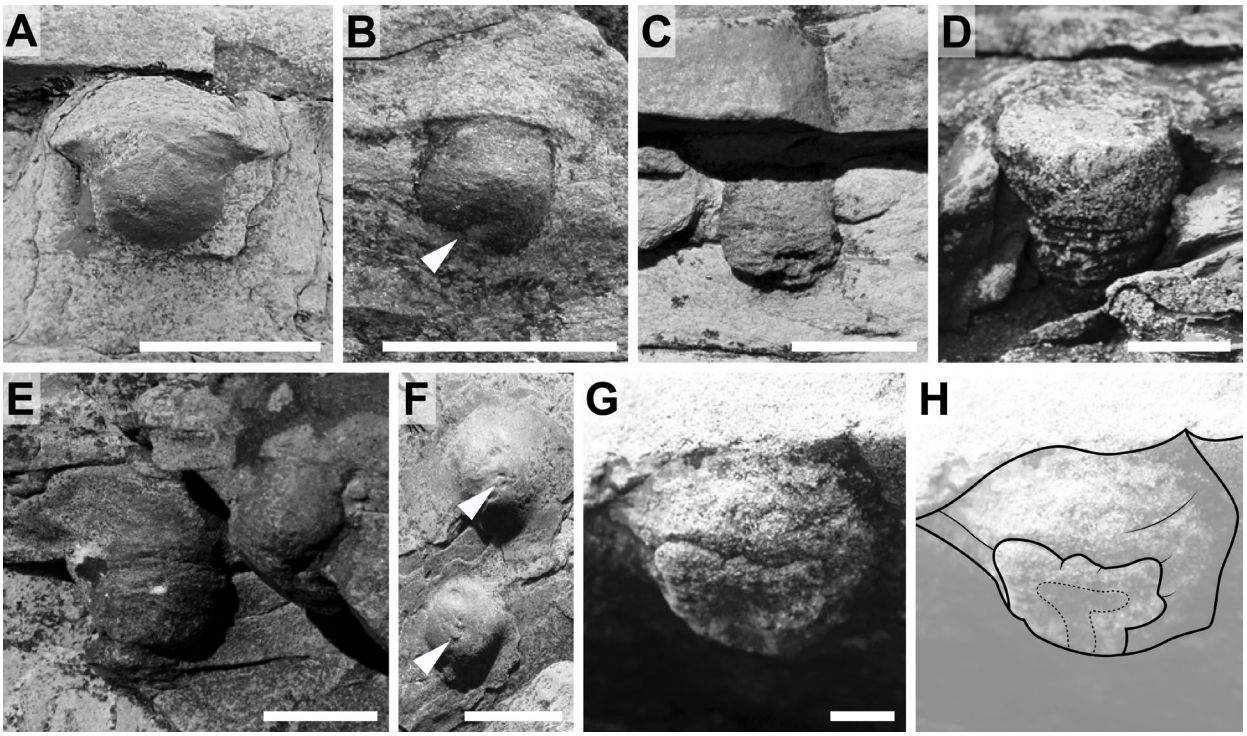

Fig. 22. Bergaueria perata Prantl (A–F) and *B.* cf. *B. radiata* Alpert (G, H). Scale bars are 1 cm. All specimens are from Member 2A (Fortunian). **A**, Smooth *Bergaueria perata* with a regular hemispherical shape and no basal feature. Full relief, Point May. **B**, Smooth *Bergaueria perata* with a regular hemispherical shape and a possible basal depression (arrow). Full relief, Fortune Head. **C**, *Bergaueria perata* with a regular cylindrical shape showing massive infill. Full relief, Fortune Head. **D**, *Bergaueria perata* with thick, parallel, concentric ridges filled with medium-grained sandstone. Full relief, Fortune Head. **E**, Two *Bergaueria perata* with irregular shapes and ornamented with delicate concentric ridges. Full relief, Grand Bank Head. **F**, Two smooth *Bergaueria perata* with regular hemispherical shapes and basal knobs (arrows). Positive hyporelief, Fortune Head. **G**, Smooth *Bergaueria* cf. *B. radiata* with a hemispherical shape and an irregular basal ornamentation surrounding a central depression. Positive hyporelief, Fortune Head. **H**, Line drawing of *Bergaueria* cf. *B. radiata* shown in Figure 22G.

shallow-marine (e.g. Fürsich 1974a; Orłowski 1989; Pemberton & Magwood 1990; Mángano *et al.* 2005a; Pacześna 2010; Shitole *et al.* 2019; Cherif *et al.* 2022), and deep-marine (e.g. Książkiewicz 1977; Eagar *et al.* 1985; Uchman 1995; Tchoumatchenco & Uchman 2001; Leszczyński 2004; Buatois *et al.* 2009) environments. Shone (1978) mentioned a continental occurrence that is lacking description or photograph. In the Chapel Island Formation, *Bergaueria* was first recorded by Crimes & Anderson (1985) and has been regularly mentioned (e.g. Narbonne *et al.* 1987; Herringshaw *et al.* 2017).

***Bergaueria perata* Prantl, 1945**

Figure 22A–F

2017 *Bergaueria* isp. Landing *et al.*, p. 45, fig. 17E.
? 2019 *Bergaueria perata* Prantl; Laing, Mángano, Buatois, Narbonne & Gougeon, p. 1626, fig. 2p.

Material. – Seventeen specimens from Members 2A and 2B (Fortunian) in Fortune Head, Fortune North, Grand Bank Head, and Point May.

Description. – Simple cylindrical to hemispherical plug-shaped burrows. Preserved as positive hyporelief and full relief. Burrows are circular in cross-section, with or without a basal depression/knob. They are solitary or in pair. Unlined to very-thinly lined; walls are smooth or with concentric ridges. Infill is massive, composed of very fine- to medium-grained sandstone different from the mudstone to very fine-grained sandstone host rock. Width is 0.3–1.2 cm; depth is 0.2–1.6 cm; width/depth ratio is 0.8–1.5.

Associated trace fossils. – *Bergaueria perata* co-occurs with *Conichnus conicus*, *Palaeophycus* isp., and *Trichichnus linearis*.

Remarks. – The cylindrical to hemispherical morphology allows comparison with *Bergaueria perata*. Pemberton *et al.* (1988) considered the small depression to be diagnostic of *Bergaueria perata*, whereas Prantl (1945) mentioned the presence of both knob and depression. Specimens from the Chapel Island Formation display both features. Buck & Goldring (2003) considered the basal knob/depression to be

the strongest evidence for a biogenic origin. In the Chapel Island Formation, *Bergauria perata* is mostly recorded from Member 2A; this part of the section belongs to the Gutter Cast Facies of Myrow (1987, p. 259) where large pot casts are very common. Myrow (1987, p. 201) noted that the basal portion of pot casts is commonly deeper on the outside, which looks like the base of a wine bottle; this contrasts with the structures describe here. Concentric ridges in *Bergaueria* result from the peristaltic burrowing mechanism of sea anemones, or simply from the casting of their outer bodies (Shinn 1968; Mangum 1970; Chamberlain 1971). Whereas ridges are concentric and subparallel in biogenic structures such as *Bergaueria* (Fig. 22D; Pickerill 1989; Pemberton & Magwood 1990), they would be theoretically more oblique and criss-crossing for pot casts as a consequence of their mode of formation, with eddies transporting sediment and marking the surface helicoidally (Alexander 1932; Myrow 1992a). Similar Cambrian trace fossils have been recorded under the names *Bergaueria* isp. (Arai & McGugan 1968), *Bergaueria hemispherica* (Pemberton & Magwood 1990; Hammersburg *et al.* 2018), *Bergaueria perata* (Radwański & Roniewicz 1963; Pemberton & Magwood 1990; Orłowski & Żylińska 1996; Jensen 1997; Singh *et al.* 2024a), and *Bergaueria* cf. *B. perata* (Mángano & Buatois 2004a). Records of Cambrian *Bergaueria perata* in association with microbially stabilized surfaces in Hoşgör & Yılmaz (2018) most probably correspond to gas or fluid escape structures (cf. Karcz *et al.* 1974).

Bergaueria cf. *B. radiata* Alpert, 1973

Figure 22G, H

Material. – Two specimens from Member 2A (Fortunian) in Fortune Head.

Description. – Plug-shaped, unlined burrows with a basal ornamentation. Preserved as positive hyporelief. Burrows are irregular and hemispherical in shape, circular in cross-section. The basal ornamentation consists of two or more, very irregular lobes. A basal central depression is also observable in one specimen. Infill is massive, composed of very fine- to medium-grained sandstone different from the mudstone to very fine-grained sandstone host rock. Width is 3.0–3.9 cm; depth is 1.3–1.8 cm; width/depth ratio is 2.2–2.3.

Associated trace fossils. – *Bergaueria* cf. *B. radiata* does not occur with other formally described ichnotaxa.

Remarks. – The basal ornamentation allows comparison with *Bergaueria radiata*. However, Alpert (1973) described *Bergaueria radiata* with prominent basal ridges regularly organized around a central depression (see also Pemberton *et al.* 1998 and Pemberton & Magwood 1990). In the Chapel Island Formation, the basal ornamentation is more disorganized, but a central depression is visible. Therefore, *Bergaueria* cf. *B. radiata* is more appropriate. This basal ornamentation results from the contraction and enlargement of a physa in burrowing anemones (Ansell & Trueman 1968; Chamberlain 1971) and is considered as a strong evidence for biogenicity (Pickens 1988; Buck & Goldring 2003). *Bergaueria radiata* is rare in the fossil record.

Ichnogenus *Circulichnis* Vialov, 1971

Discussion. – *Circulichnis* is a circular horizontal trail (Vialov 1971; Uchman & Rattazzi 2019) included in the category of architectural design of 'simple horizontal trails' (Buatois *et al.* 2017). *Circulichnis* was first described from the Triassic Istyk series of southwestern Russia (Vialov 1971). Keighley & Pickerill (1997) proposed to correct the name *Circulichnis* for *Circulichnus*. However, in their recent review of this ichnotaxon, Uchman & Rattazzi (2019) considered this correction inadequate based on the International Code of Zoological Nomenclature and recommended to keep the original designation of *Circulichnis*. Uchman & Rattazzi (2019) considered two *Circulichnis* ichnospecies valid: *C. montanus* Vialov, 1971 and *C. ligusticus* Uchman & Rattazzi, 2019. The type ichnospecies, *Circulichnis montanus*, has a regular circular to elliptical course (Vialov 1971; Uchman & Rattazzi 2019). *Circulichnis ligusticus* is circular with a winding irregular course (Uchman & Rattazzi 2019). To the list of ichnospecies discussed in their review, we should add *Circulichnis zhanwaensis* Hu, 1991. *Circulichnis zhanwaensis* occurs as dense assemblages, but trace-fossil density is regarded as a weak ichnotaxobase (Schlirf & Uchman 2005; Knaust *et al.* 2018). Solitary *Circulichnis zhanwaensis* does not show significant difference with *C. montanus* and is regarded as its junior synonym. Recently, Fan *et al.* (2021) resurrected *Circulichnis sinensis* Yang in Yang *et al.*, 1990. *Circulichnis sinensis* is a circular horizontal structure with regular tangential branches departing laterally (Yang *et al.* 2004; Fan *et al.* 2021). As noted by Fan *et al.* (2021), the taxonomic affinity of these trace fossils to either *Circulichnis* or *Treptichnus* (cf. *T. coronatum*) is problematic. Their detailed taphonomic analysis based on a large

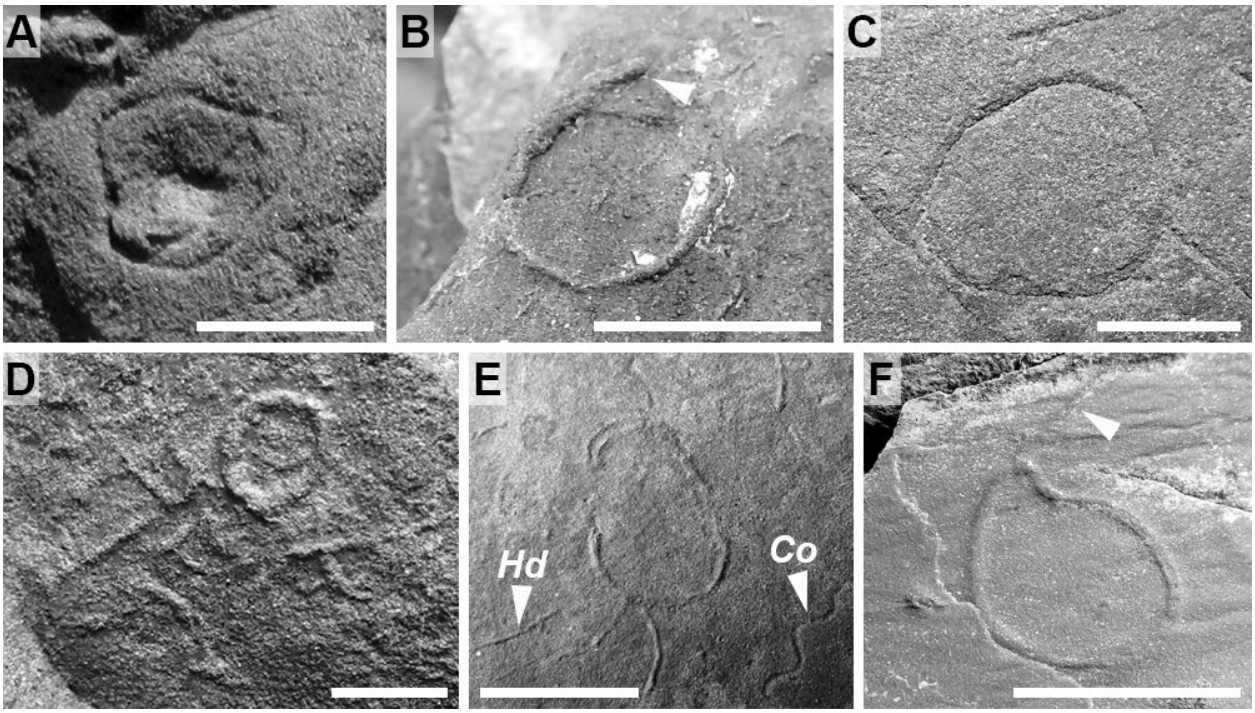

Fig. 23. *Circulichnis ligusticus* Uchman & Rattazzi (A, B), *C. montanus* Vialov (C–E), and a problematic circular trace fossil (F). Scale bars are 0.5 (B) and 1 cm (A, C–F). **A**, *Circulichnis ligusticus* with a closed course. Negative epirelief, Fortune Head, Member 2A (Fortunian). **B**, *Circulichnis ligusticus* with a short segment departing from the ring (arrow). Positive relief, collected on a loose slab in Fortune Head, within a Member 2A (Fortunian) interval. **C**, *Circulichnis montanus* with a closed course. Negative hyporelief, Grand Bank Head, Member 2A (Fortunian). **D**, *Circulichnis montanus* with a closed course associated with undetermined burrows. Positive hyporelief, Grand Bank Head, Member 1 (Ediacaran). **E**, *Circulichnis montanus* with an opened course. Note the presence of *Cochlichnus anguineus* (Co) and *Helminthoidichnites tenuis* (Hd). Positive and negative epirelief, Grand Bank Head, Member 2B (Fortunian). **F**, Problematic trace fossil with an almost circular course and a straight short segment. A faint segment extending from the main ring is observed (arrow). Positive epirelief, Grand Bank Head, Member 2A (Fortunian).

number of specimens (Fan *et al.* 2021, figs 4, 5, 7, 8) and reconstruction of the tracemaker behaviour (Fan *et al.* 2021, fig. 8) suggest a discontinuous mode of formation through repeated probing, which therefore agrees with a *Treptichnus* affinity. In addition, *Circulichnis leomonti* Morgan, Juntunen, Scott & Landreth, 2023 was recently erected as a circular to ovoid ring made of connected, straight to curved segments (Morgan *et al.* 2023). This diagnosis is problematic as it suggests the burrow to be constructed discontinuously, which does not comply with the revision of the type material of *Circulichnis* by Uchman & Rattazzi (2019). Moreover, considering the irregular outlines of each burrow of *Circulichnis leomonti*, their different infill from the host rock, their large burrow width, the potential presence of a median feature along the burrow (see left side of holotype specimen in fig. 2, lower left in Morgan *et al.* 2023), and the overlap of burrows ('double ring pattern' of Morgan *et al.* 2023, p. 7), there is a strong possibility that these burrows correspond to scribbling *Psammichnites gigas circularis* as recorded here (Fig. 45) and elsewhere (e.g. Yang *et al.* 1982, pl. 2, fig. 1). Nevertheless, the poor quality of preservation of the holotype slab and the report of material from only one bed surface preclude definitive conclusions and call for additional material to support the case of *Circulichnis leomonti*. Therefore, the two ichnospecies *Circulichnis ligusticus* and *C. montanus* are here retained as valid.

Circulichnis shows similarities with *Gordia* Emmons, 1844. *Gordia marina*, the type ichnospecies of *Gordia*, forms an α-shaped course with a distinct self-overcrossing (Keighley & Pickerill 1997). However, the proposed ichnospecies *Gordia arcuata* Książkiewicz, 1977 is an arc-shaped horizontal trace fossil which is problematic as no self-overcrossing is apparent. As a consequence, unclosed circular trails have been included by different authors either in *Circulichnis* (e.g. McCann & Pickerill 1988; Feng *et al.* 2017) or in *Gordia* (e.g. Fritz & Crimes 1985; Crimes *et al.* 1992). We propose to keep *Gordia* for circular trails displaying a distinct self overcrossing, and to consider unclosed circular trails as preservational variant of *Circulichnis montanus* (see 'Remarks' below).

Circulichnis ranges from the Ediacaran (e.g. Zhang 1986; Gibson 1989; Narbonne & Aitken 1990; Hagadorn & Waggoner 2000; Bekker 2013) to the Holocene (e.g. Kitchell *et al.* 1978; Kitchell & Clark 1979; Young *et al.* 1985; Metz 1987a). Suggested producers are arthropods (Metz 1987a) and annelid worms (Pickerill & Keppie 1981; Young *et al.* 1985; Buatois *et al.* 1998a). *Circulichnis* is recorded in continental (e.g. Metz 1987a; Buatois & Mángano 1993a, 1998; Keighley & Pickerill 1997; Buatois *et al.* 1998a; Avanzini *et al.* 2011), marginal-marine (e.g. Fillion & Pickerill 1984b, 1990; Pickerill *et al.* 1984a; Davies *et al.* 2010), shallow-marine (e.g. Maples & Suttner 1990; Zhao *et al.* 2015; Feng *et al.* 2017), and deep-marine (e.g. McCann & Pickerill 1988; Pickerill *et al.* 1988; Tunis & Uchman 1996a; Tchoumatchenco & Uchman 1999; Buatois & Mángano 2003b; Wetzel *et al.* 2007) environments. In the Chapel Island Formation, *Circulichnis* has never been identified before.

Circulichnis ligusticus Uchman & Rattazzi, 2019

Figure 23A, B

Material. – Four specimens from Member 1 (Ediacaran) and Members 2A and 2B (Fortunian) in Fortune Head and Grand Bank Head.

Description. – Horizontal, unlined, circular to elliptical trails or burrows with an irregular winding course. Preserved as positive hyporelief and negative epirelief. The ring is closed or left opened. Typically unbranched, although rarely a short segment departs from the ring. Infill is massive, composed of very fine- to fine-grained sandstone similar to the host rock. Width is 0.05–0.1 cm; internal diameter of the ring is 0.3–2.0 cm.

Associated trace fossils. – *Circulichnis ligusticus* co-occurs with *Archaeonassa fossulata*, *Helminthoidichnites tenuis*, *Helminthopsis tenuis*, and *Palaeophycus tubularis*.

Remarks. – The irregular course allows placing these trace fossils in *Circulichnis ligusticus*. *Circulichnis ligusticus* is also present in the Ediacaran Blueflower Formation of northwestern Canada ('knotted circular trail' in Narbonne & Aitken 1990, text-fig. 7D). In the Chapel Island Formation, *Circulichnis ligusticus* can display a short segment departing from the main ring (Fig. 23B). A single branch in *Circulichnis* has also been recorded elsewhere (Hakes 1976, pl. 11, fig. 2; Pickerill & Keppie 1981, fig. 3a). This could be problematic as it is reminiscent of *Gordia marina*. However, two 'branches' are required in *Gordia marina* to form an overall α-shaped course. Moreover, a branching entrance or exit point is theoretically required in *Circulichnis* if the producer accessed the ring more laterally (Keighley & Pickerill 1997; Uchman & Rattazzi 2019). Problematic circular trace fossils like *Circulichnis ligusticus* have been found transitional with *Helminthopsis hieroglyphica* (Fig. 41C). These more likely represent taphonomic variants of treptichnids where the projections (i.e. probes) are not clearly displayed (compare with Fig. 52H) (see also Fan *et al.* 2021).

Circulichnis montanus Vialov, 1971

Figure 23C–E

Material. – Five specimens from Member 1 (Ediacaran) and Members 2A and 2B (Fortunian) in Fortune Head and Grand Bank Head.

Description. – Horizontal, unlined, unbranched, circular to elliptical trails or burrows with a regular course. Preserved as positive and negative hyporelief and epirelief. The ring is closed or left opened. Infill is massive, composed of very fine- to fine-grained sandstone similar to the host rock. Trail width is 0.1–0.2 cm; internal diameter of the ring is 0.6–2.3 cm.

Associated trace fossils. – *Circulichnis montanus* co-occurs with *Cochlichnus anguineus* and *Helminthoidichnites tenuis*.

Remarks. – The regular course allows placing these trace fossils in *Circulichnis montanus*. *Circulichnis montanus* is also recorded from the Ediacaran of China (Zhang 1986, pl. 4, fig. 10), Urals (Bekker 2013, pl. 1, fig. 9), and USA (Gibson 1989, fig. 3.1; Hagadorn & Waggoner 2000, fig. 3.4). *Circulichnis* figured in Gibson (1989) forms an incomplete circle similarly to one of the Chapel Island Formation specimens (Fig. 23E). *Gordia arcuata* from the Stelkuz Formation of Canada (Fritz & Crimes 1985, pl. 4, figs 4–6) may represent additional Ediacaran material, although these specimens never form complete circles and have only been recovered from float samples. *Helminthoidichnites* isp. from the Ediacaran Dzhezhim Formation of Russia (Kolesnikov *et al.* 2023a, fig. 2h) is a semi-circular horizontal trail that may also correspond to a partially preserved *Circulichnis montanus*. The Ediacaran specimen from the Chapel Island Formation (Fig. 23D) is suggested to be of biogenic origin, as very similar specimens have been described elsewhere (Fillion & Pickerill 1990, pl. 2, figs 2, 3; Buatois *et al.* 1998a, fig. 4.1). Finally, a problematic circular trace fossil from the Chapel Island Formation displays an affinity with *Circulichnis montanus*, although the course

has a straight segment only on a short portion of the ring (Fig. 23F). A faint lateral branch is also observable, with bare relief, and its relationship to the ring is unclear. This specimen is retained in *Circulichnis montanus* with caution.

Previous reports mentioned *Gordia arcuata* in the Chapel Island Formation (Narbonne *et al.* 1987; Landing *et al.* 1988). Książkiewicz (1977) erected *Gordia arcuata* for partial arc-shaped loops displaying a prominent apical segment representing the deeper burrowing of the organism. As mentioned above, the affiliation of these trace fossils to *Gordia* is problematic, as self-overcrossing is not observed. Fillion & Pickerill (1990) considered that incompletely looping trails should be referred to *Gordia* isp. This approach has been followed in the Chapel Island Formation recently (Herringshaw *et al.* 2017; Landing *et al.* 2017; Laing *et al.* 2019). In the literature, incompletely looping trails have been described as *Gordia arcuata* (Fritz & Crimes 1985, figs 4.4–6; Walter *et al.* 1989, fig. 8G), *Gordia* aff. *G. arcuata* (Crimes *et al.* 1992, fig. 2E; Vidal *et al.* 1994a, fig. 3C), and *Gordia* cf. *G. arcuata* (Weber & Brady 2004, fig. 10). However, an incomplete loop is also a feature that can be expressed in partially preserved *Circulichnis montanus*. Here, we suggest that the use of *Gordia* is restricted to trails displaying a distinct α-shaped morphology. Arc-shaped trails should be compared to *Circulichnis montanus* (i.e. cf. *C. montanus*), and ring-like trails be affiliated more confidently to *C. montanus*.

Ichnogenus *Cochlichnus* Hitchcock, 1858

Discussion. – *Cochlichnus* is a horizontal sinusoidal trace fossil (Elliott 1985; Fillion & Pickerill 1990; Buatois & Mángano 1993a) included in the category of architectural design of 'simple horizontal trails' (Buatois *et al.* 2017). *Cochlichnus* was first described from the Jurassic Turners Falls Formation of northeastern USA (Hitchcock 1858; Goldstein *et al.* 2017). In the original diagnosis by Hitchcock (1858), analogy to a corkscrew led to taxonomic confusion (Głuszek 1995; Metz 1998). However, distinctive horizontal sinusoidal trace fossils were also figured (Hitchcock 1858, pl. 26, fig. 6, pl. 28, fig. 1; see also Uchman *et al.* 2004a). Although three ichnospecies are typically considered valid (see review below), Uchman *et al.* (2004a) suggested that smooth *Cochlichnus* could be discriminated at ichnospecific rank based on different wavelength/amplitude ratios (i.e. λ/2A; Fig. 24). Morphological variation in smooth *Cochlichnus* has also been documented elsewhere (e.g. Crimes & Anderson 1985; Hofmann *et al.* 1994; Buatois *et al.* 1997; Bordy *et al.* 2011; Won & Kong 2023). Uchman *et al.* (2004a) argued that changes in ratio could highlight differences in producers or changing substrates. The difference of ratio could also result from changes in speed by the tracemaker, as stretched forms (i.e. high λ/2A) are theoretically made by organisms moving faster and more efficiently within the substrate, and *vice versa*. Hence, the change of ratio would then correspond to a change of behaviour. Uchman *et al.* (2004a) recorded three peaks of *Cochlichnus* morphotypes in their study of continental Oligocene trace fossils from Switzerland: a peak for tight forms ($1 < \lambda/2A < 1.5$), a peak for normal forms ($2.5 < \lambda/2A < 3.0$), and a peak for stretched forms ($3.5 < \lambda/2A < 4.0$). However, their stretched forms are not easily distinguishable from normal forms by the naked eye (see Fig. 24), and this could be problematic when

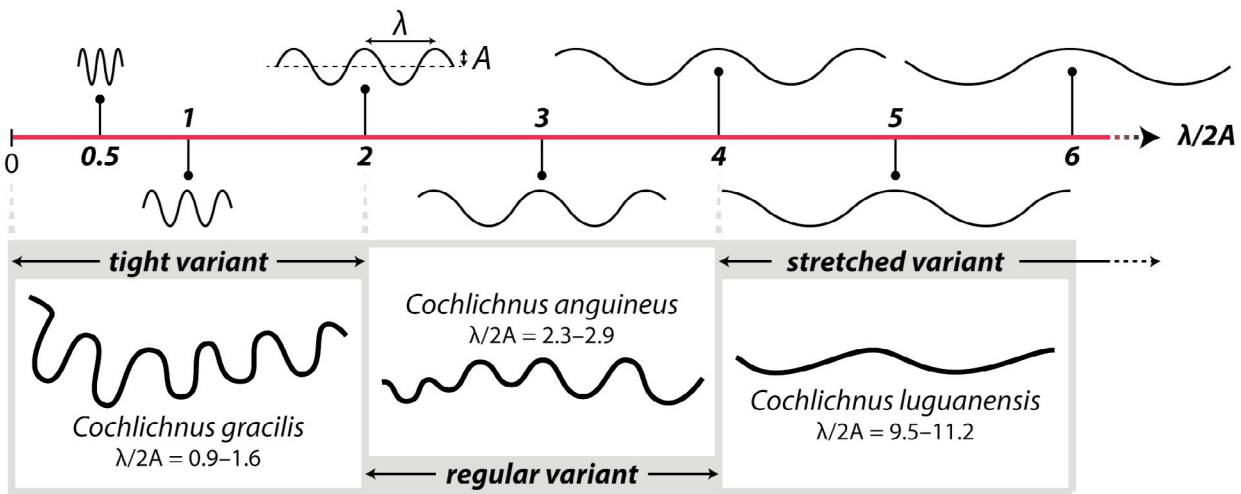

Fig. 24. Morphometric parameters of smooth *Cochlichnus* and distinction between the three valid ichnospecies. Course of *Cochlichnus gracilis* based on Vialov (1979, pl. 2, fig. 11), of *C. anguineus* on Hitchcock (1858, pl. 27, fig. 1), and of *C. luguanensis* on Zhang (1991, pl. 1, fig. 2).

discriminating smooth *Cochlichnus* ichnospecies in the field. We suggest combining these two peaks together, therefore creating a broader morphometric range for normal forms. We then reserve the term 'stretched forms' for those *Cochlichnus* that are clearly flatten, such as is the case of *Cochlichnus luguanensis*. Consequently, three morphotypes of smooth *Cochlichnus* can be related to previously erected ichnospecies (Fig. 24). Tight forms have *Cochlichnus gracilis* Vialov as typical ichnospecies and have $\lambda/2A < 2.0$. Regular forms have *Cochlichnus anguineus* as typical ichnospecies and have $2.0 < \lambda/2A < 4.0$. Stretched forms have *Cochlichnus luguanensis* as typical ichnospecies and have $\lambda/2A > 4.0$. Morphometric boundaries for each form were based on Uchman *et al.* (2004a, fig. 3) and on our taxonomic revision (see below).

Fillion & Pickerill (1990), Buatois & Mángano (1993a), and Stanley & Pickerill (1998) discussed the ichnotaxonomy of *Cochlichnus*, concluding that three ichnospecies were valid: *C. anguineus* Hitchcock, 1858; *C. antarcticus* Tasch, 1968; and *C. annulatus* Orłowski, 1989. The type ichnospecies, *Cochlichnus anguineus*, is smooth with $\lambda/2A = 2.3–2.9$ (Hitchcock 1858, pl. 27, fig. 1). *Cochlichnus antarcticus* has lateral marks (Tasch 1968; Fillion & Pickerill 1990). *Cochlichnus annulatus* has an annulated outer wall (Orłowski 1989; Buatois & Mángano 1993a). Eight additional ichnospecies attributed to *Cochlichnus* have been erected in the literature, which are discussed here: *C. gracilis* Vialov, 1979; *C. lagartensis* Muniz, 1980; *C. sousensis* Muniz, 1985; *C. luguanensis* Zhang, 1991; *C. xinhuaensis* Zhang, 1991; *C. ciliensis* Zhang & Wang, 1996; *Cochilichnus* (sic) *hanyangensis* Yang, Zhang & Yang, 2004; and *C. karlae* Zessin, 2009. *Cochlichnus gracilis* is smooth with $\lambda/2A = 0.9–1.6$ (Vialov 1979, pl. 2, fig. 11). *Cochlichnus lagartensis* is a sinusoidal horizontal structure with rare sharp angles preserved exclusively in ripple troughs (Muniz 1980; Corrêa & Fernandes 2002; Barreto *et al.* 2014). Corrêa & Fernandes (2002) correctly re-interpreted the type material as a syneresis crack. *Cochlichnus ciliensis* ($\lambda/2A = 3.3$), *C. karlae* ($\lambda/2A = 3.7$), and *C. sousensis* ($\lambda/2A = 2.7–3.0$) are all smooth sinusoidal trails (Muniz 1985; Zhang & Wang 1996; Zessin 2009) with $\lambda/2A$ fitting the morphometric limits of their senior synonym *C. anguineus*. *Cochlichnus luguanensis* is described by Zhang (1991) as having large length and width. The figured specimen (Zhang 1991, pl. 1, fig. 2) is smooth and shows $\lambda/2A = 9.5–11.2$. *Cochlichnus xinhuaensis* is distinguished by Zhang (1991) by its high width, wavelength, and amplitude, displaying two surficial furrows. Re-evaluation of the type material is needed, as it is unclear if the surficial furrows are real morphological features or if they resulted from the collapse of the structure. *Cochlichnus hanyangensis* is a poorly preserved horizontal structure that possibly represents a sinusoidal burrow (Yang *et al.* 2004, pl. 9, figs 5, 6). However, the photographed specimens do not allow measurements on $\lambda/2A$, and an in-depth revision of the material is needed. Consequently, five ichnospecies, *Cochlichnus anguineus*, *C. annulatus*, *C. antarcticus, C. gracilis,* and *C. luguanensis*, are here retained as valid.

Cochlichnus shows different degrees of similarities with *Belorhaphe* Fuchs, 1895, *Cosmorhaphe* Fuchs, 1895, *Cymataulus* Rindsberg, 1994, *Helminthopsis* Heer, 1877, *Protopaleodictyon* Książkiewicz, 1970, *Psammichnites* Torell, 1870, *Sinusichnus* de Gibert, 1996, and *Undichna* Anderson, 1976. *Belorhaphe* is an unbranched horizontal graphoglyptid trace fossil with angular turns (Hakes 1976; Seilacher 1977; Buatois & Mángano 1993a), this latter feature being absent in *Cochlichnus*. *Cosmorhaphe* is also an unbranched graphoglyptid burrow with two orders of meander: the first order displays large meanders whereas the second order is sinusoidal, similarly to *Cochlichnus* (Seilacher 1977; Fan *et al.* 2018). *Protopaleodictyon*, in particular *P. incomposum* Książkiewicz, is a branched graphoglyptid burrow with two orders of meanders: the second order is sinusoidal similarly to *Cochlichnus*, but with lateral branches departing at each sine (Seilacher 1977). Only very fragmentary specimens of *Cosmorhaphe* and *Protopaleodictyon* may be in principle confused with *Cochlichnus*. Rindsberg (1994) introduced *Cymataulus* for horizontal sinusoidal burrows. Most authors (e.g. Pickerill & Narbonne 1995; Buatois *et al.* 1997; Stanley & Pickerill 1998; de Gibert *et al.* 2000; Melchor *et al.* 2003; Gaigalas & Uchman 2004) agreed to retain both trails and burrows within *Cochlichnus* because their differentiation is not always possible. *Helminthopsis* is a simple horizontal trace fossil with irregular meanders (Wetzel & Bromley 1996), and the absence of a regular sinusoidal course allows distinction from *Cochlichnus*. The dorsal sinusoidal funnel of some *Psammichnites* can be reminiscent of *Cochlichnus* (Goldring & Jensen 1996; McIlroy & Heys 1997). For example, Crimes *et al.* (1977) referred to as *Cochlichnus* sinusoidal trails that in one case intergrades with the central component of *Psammichnites* (their *Taphrhelminthopsis circularis*) and are, therefore, partially preserved *Psammichnites* (Mángano *et al.* 2022). *Psammichnites* is, however, a more complex structure with an internal backfill and two dorsal lobes formed on the sediment surface that are visible on more complete specimens. *Sinusichnus* is a horizontal sinusoidal burrow that, unlike *Cochlichnus*, also displays common branching and

short shafts (de Gibert 1996; de Gibert *et al.* 1999a). *Undichna*, in particular *U. unisulca* de Gibert, Buatois, Fregenal-Martínez, Mángano, Ortega, Poyato-Ariza & Wenz, is a slightly asymmetrical sinusoidal trace fossil that differs from *Cochlichnus* by its sharp incision of the substrate (de Gibert *et al.* 1999b).

Cochlichnus ranges from the Cambrian (e.g. Orłowski 1989; Fillion & Pickerill 1990; Hofmann *et al.* 1994; Goldring & Jensen 1996; Buatois & Mángano 2003b; Shahkarami *et al.* 2017a) to the Holocene (e.g. Rode & Staar 1961; Sandstedt *et al.* 1961; Chamberlain 1975; Metz 1987b; Jensen 1996; Martin 2009). Reports from the Ediacaran can be dismissed as follow: (1) *Cochlichnus serpens* Webby (a junior synonym of *C. anguineus* according to our revision of smooth forms; see also Fillion & Pickerill 1990) recorded by Webby (1970, fig. 16) as Ediacaran is now thought to occur in Cambrian strata (Walter *et al.* 1989); (2) *Cochlichnus* sp. 2 recorded by Palij *et al.* (1979, 1983, pl. 54, fig. 6) is irregular, and the sinusoidal course is not clearly demonstrated (cf. Jensen *et al.* 2006); (3) *Cochlichnus* isp. recorded by Cope (1982, pl. 2, fig. 3) does not show the regular sinusoidal course of *Cochlichnus* (Runnegar 1992; Jensen *et al.* 2006; Liu & McIlroy 2015); (4) *C. serpens* recorded by Aitken (1989, fig. 6F), although of debatable Ediacaran or Cambrian age (cf. Runnegar 1992; MacNaughton *et al.* 2000; Carbone & Narbonne 2014), is irregular with angularities along its course; (5) *C. anguineus* recorded by Kulkarni & Borkar (1996, figs 2–5) is preserved in ripple troughs and is a sinusoidal syneresis crack (Seilacher *et al.* 2005); (6) *C. anguineus* recorded by Kulkarni & Borkar (1997a) is not sinusoidal and should be affiliated to filamentous body fossils; (7) *C. serpens* recorded by MacNaughton & Narbonne (1999), although considered Ediacaran at the time, was recorded from strata that are now regarded as Cambrian (Carbone & Narbonne 2014); and (8) *Cochlichnus* isp. recorded by Jensen *et al.* (2006, fig. 2E) is irregular with angularities along its course. *Cochlichnus* is recorded in continental (e.g. Elliott 1985; Głuszek 1995; Metz 2000; Melchor *et al.* 2003; Lerner *et al.* 2007; de Gibert & Sáez 2009), marginal-marine (e.g. Hakes 1976; Narbonne 1984; Eagar *et al.* 1985; Greb & Archer 1995; Braddy & Briggs 2002; Lucas & Lerner 2005), shallow-marine

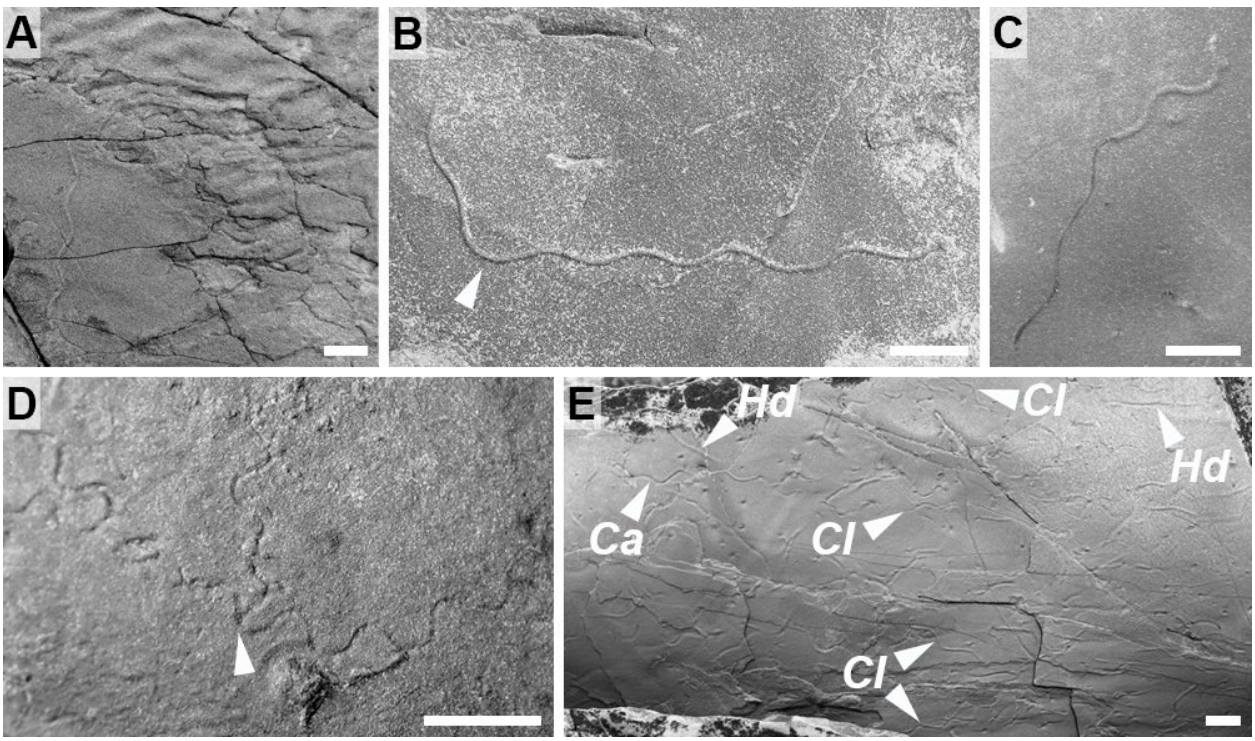

Fig. 25. Cochlichnus anguineus Hitchcock (D, E) and *C. luguanensis* Zhang (A–C, E). Scale bars are 1 cm. **A**, Straight *Cochlichnus luguanensis* (λ/2A = 6.0–8.2) associated with a microbially stabilized surface. Positive epirelief, Fortune Head, Member 2A (Fortunian). **B**, *Cochlichnus luguanensis* (λ/2A = 4.6–8.3) with a sharp bend along its course (arrow). Positive epirelief, Fortune Head, Member 2A (Fortunian). **C**, *Cochlichnus luguanensis* (λ/2A = 4.4–6.2) displaying a pyritized infill that grades into a full relief, preserved on bed top. Note the change in amplitude along the course. Positive epirelief/full relief, Fortune Head, Member 2B (Fortunian). **D**, Two *Cochlichnus anguineus* (λ/2A = 2.1–3.2) showing secondary successive branching (arrow). Negative epirelief, Grand Bank Head, Member 2B (Fortunian). **E**, Surface with multiple specimens of *Cochlichnus anguineus* (Ca) and *C. luguanensis* (Cl) associated with *Helminthoidichnites tenuis* (Hd) and pits of uncertain affinity. Note the transition from positive to negative epirelief in one specimen (upper left arrow). Positive and negative epirelief, Grand Bank Head, Member 2A (Fortunian).

(e.g. Hakes 1976; Dam 1990; Rindsberg 1994; Stanley & Pickerill 1998; de Gibert & Ekdale 2002; Shahkarami *et al.* 2017a), and deep-marine (e.g. McCann & Pickerill 1988; Tunis & Uchman 1996b; Uchman 1998; Buatois & Mángano 2003b, 2012b; Bayet-Goll *et al.* 2014) environments. In continental environments, potential producers are both arthropods (insect larvae; Metz 1987b) and nematode worms (Rode & Staar 1961; Sandstedt *et al.* 1961; Gray & Lissmann 1964; Chamberlain 1975; Jensen 1996), but only the latter are candidates in the case of marine environments (Cullen 1973; Baliński *et al.* 2013). *Cochlichnus* was first recorded in the Chapel Island Formation by Crimes & Anderson (1985) and has been regularly mentioned since then (see synonym lists below).

Cochlichnus anguineus Hitchcock, 1858

Figure 25D, E

1985 *Cochlichnus* sp. Crimes & Anderson, p. 318, fig. 6.1.

Material. – Twelve specimens from Members 2A, 2B, and 3 (Fortunian) in Fortune Head, Grand Bank Head, and Little Dantzic Cove.

Description. – Smooth, unlined, unbranched horizontal burrows or trails with a sinusoidal course and $2.0 < \lambda/2A < 4.0$. Preserved as positive hyporelief, positive and negative epirelief, and full relief. The course is straight to curved. Transition from negative to positive epirelief on a single course occurs. The amplitude of sines is typically constant or can vary along a single course. Secondary successive branching has been observed. Infill is massive, composed of very fine- to fine-grained sandstone similar to the host rock; in rare cases, infill is pyritized. Trace fossil width is 0.1 cm; maximum length is 12.5 cm; number of sines is 1¼–19; $\lambda/2A = 2.1–3.6$.

Associated trace fossils. – *Cochlichnus anguineus* co-occurs with *Circulichnis montanus*, *Cochlichnus luguanensis*, *Helminthoidichnites tenuis*, *Helminthopsis tenuis*, and *Palaeophycus tubularis*. *Cochlichnus anguineus* can be transitional with *C. luguanensis*.

Remarks. – The smooth outline and $\lambda/2A = 2.1–3.6$ allow placement in *Cochlichnus anguineus*. *Cochlichnus anguineus* is less common in the Chapel Island Formation than *C. luguanensis*. Sines of *Cochlichnus anguineus* in this unit never curve as tightly as in *C. gracilis*, although $\lambda/2A$ gets close to 2 in some specimens. The 'bell-curve' morphology in *Cochlichnus anguineus* is a consequence of locomotion through stiffer sediment involving increased frictional resistance (Elliott 1985). This morphology is typical of nematodes, as observed experimentally by Sandstedt *et al.* (1961, fig. 1). Reverse movement in nematodes leads to secondary successive branching (Sandstedt *et al.* 1961), a feature also observed in the Chapel Island Formation (Fig. 25D). Secondary successive branching is typically interpreted as produced for feeding purposes. However, Sandstedt *et al.* (1961) noted that modern nematodes produce similar trails solely for locomotory purposes (i.e. without feeding behaviour associated). Accordingly, secondary successive branching in *Cochlichnus* may suggest the need to re-use a previously opened trail to increase movement performance and to limit energetic costs associated with locomotion.

Crimes & Anderson (1985, figs 6.1, 6.2) also noted two morphologies in *Cochlichnus* from the Chapel Island Formation (they draw them distinctively), and their specimen fig. 6.1 fits within the morphometric limits of *C. anguineus* ($\lambda/2A = 2.5–3.8$). *Cochlichnus* in Narbonne *et al.* (1987), Landing *et al.* (1988), and Herringshaw *et al.* (2017) are only mentioned without illustration, and their affinity is unknown.

Cochlichnus luguanensis Zhang, 1991

Figure 25A–C, E

1985 *Cochlichnus* sp. Crimes & Anderson, p. 318, fig. 6.2.
2014 *Cochlichnus anguineus* Hitchcock; Buatois, Narbonne, Mángano, Carmona & Myrow, p. 3, fig. 1a, b.
2016 *Cochlichnus anguineus* Hitchcock; Mángano & Buatois, p. 93, fig. 3.11c.
2017 *Cochlichnus anguineus* Hitchcock; Landing *et al.*, p. 45, fig. 17D.
2019 *Cochlichnus anguineus* Hitchcock; Laing, Mángano, Buatois, Narbonne & Gougeon, p. 1626, fig. 2e.

Material. – 69 specimens from Members 2A and 2B (Fortunian) in Fortune Head and Grand Bank Head.

Description. – Smooth, unlined, unbranched horizontal burrows or trails with a sinusoidal course and $\lambda/2A > 4.0$. Preserved as positive and negative hyporelief, positive and negative epirelief, and full relief. Transition from negative to positive epirelief on a single course occurs. The course is typically straight, in places curved and rarely developing sharp bends. In rare cases, the course disappears along regular and specific intervals, in between the low and high points of a sine. The amplitude of sines is mostly constant or can vary along a single course. A small depression can end a course. Secondary successive branching has been observed. Infill is massive, composed of very

fine- to fine-grained sandstone similar to the host rock; in rare cases, infill is pyritized. Trace fossil width is 0.05–0.1 cm; maximum length is 7.3 cm; number of sines is 1¼–5¾; λ/2A = 4.6–16.0.

Associated trace fossils. – *Cochlichnus luguanensis* co-occurs with *Archaeonassa fossulata*, *Cochlichnus anguineus*, *Curvolithus simplex*, *Helminthopsis tenuis*, *Monomorphichnus lineatus*, *Palaeophycus tubularis*, *Saerichnites kutscheri*, *Treptichnus coronatum*, and *T. pedum*. *Cochlichnus luguanensis* can be transitional with *C. anguineus*.

Remarks. – The smooth outline and λ/2A = 4.6–16.0 allow placement in *Cochlichnus luguanensis*. In the Chapel Island Formation, *Cochlichnus luguanensis* is more common than *C. anguineus*. The high wavelength/amplitude ratio demonstrates relatively low friction with the sediment resulting in efficient movement. Therefore, transitional specimens between *Cochlichnus luguanensis* and *C. anguineus* point to a change in locomotion behaviour and increased speed in the former. The association with microbially stabilized surfaces (Fig. 25A) suggests that *Cochlichnus* represents a grazing strategy, and the question is left opened on whether the food resource was mostly bacteria (i.e. bacteriotrophs) or other type of organic matter. The depression at the end of some *Cochlichnus* specimens shows that the tracemaker was able to change vertical position within the sediment, suggesting that these structures could be made infaunally.

The disappearance of certain intervals along the course has been noted in specimens from the Carboniferous of Germany (Uchman & Geyer 2020), the Cambrian of Norway (Högström *et al.* 2013), the Cambrian of northwestern Canada (R. MacNaughton, pers. comm., 2022), and was also figured in the Chapel Island Formation (Laing *et al.*, 2019, fig. 2e). Högström *et al.* (2013) and Uchman & Geyer (2020) interpreted these forms to be slightly helical. In the Chapel Island Formation, the material is mostly sinusoidal in aspect, and should not be mistaken with Cambrian *Helicolithus* Häntzschel (McIlroy & Brasier 2017, fig. 4c), which are less stretched and clearly display a vertical component.

Cochlichnus luguanensis has been commonly recorded in the Cambrian (e.g. Webby 1970, fig. 16C–F; Hofmann *et al.* 1994, fig. 5J; Goldring & Jensen 1996, fig. 2b, upper specimen; Seilacher *et al.* 2005, fig. 8B; Shahkarami *et al.* 2017a, fig. 2.1). In the Chapel Island Formation, previous reports by Crimes & Anderson (1985, fig. 6.2, λ/2A = 7.7–8.2), Buatois *et al.* (2014, fig. 1a, λ/2A = 5.8), Mángano & Buatois (2016, fig. 3.11c, λ/2A = 5.8), Landing *et al.* (2017, fig. 17D, λ/2A = 4.9–6.3), and Laing *et al.* (2019, fig. 2e, λ/2A = 6–8.3) can be relocated within *Cochlichnus luguanensis* as well.

Ichnogenus *Conichnus* Männil, 1966

Discussion. – *Conichnus* is a conical unornamented plug-shaped burrow (Männil 1966; Frey & Howard 1981; Pemberton *et al.* 1988) included in the category of architectural design of 'vertical plug-shaped burrows' (Buatois *et al.* 2017). *Conichnus* was first described from the Ordovician Kahula Formation of northern Estonia (Männil 1966; Vinn *et al.* 2015). Four ichnospecies attributed to *Conichnus* have been described in the literature: *C. conicus* Männil, 1966; *C. papillus* (Männil, 1966); *C. conosinus* Nielsen, Hansen & Simonsen, 1996; and *C. wudangensis* Chen, Wang, Bai, Nie & Wang, 2005. The type ichnospecies, *Conichnus conicus*, has a conical shape with a rounded base (Männil 1966; Pemberton *et al.* 1988; Vinn *et al.* 2015). *Conichnus papillus*, formerly *Amphorichnus papillus*, has an amphora shape with a distinct basal protuberance (Männil 1966; Pemberton *et al.* 1988; Vinn *et al.* 2015). Frey & Howard (1981) placed *Amphorichnus* Männil in synonymy with *Conichnus*. However, Vinn *et al.* (2015) re-studied material from the type locality and considered the amphora shape and distinct termination to be significant at ichnogenus rank (see also Ershova *et al.* 2006). *Conichnus conosinus* is composed of a basal cone topped by a very wide opening (Nielsen *et al.* 1996). *Conichnus wudangensis* is a vertical funnel-shaped burrow with a central tube (Chen *et al.* 2005, pl. I, figs 1b, 8) that may represent a preservational variant of *Rosselia socialis*. In addition, Swift *et al.* (1987, p. 433) mentioned *Conichnus concentricus*, but without providing further detail or photograph. This may have resulted from a typo, the authors possibly referring to *Cylindrichnus concentricus* Toots. Consequently, two ichnospecies, *Conichnus conicus* and *C. conosinus*, are here considered valid.

Conichnus shows similarities with *Bergaueria* Prantl, 1945, *Conostichus* Lesquereux, 1876, and *Cornulatichnus* Carroll & Trewin, 1995. Contrary to the conical morphology of *Conichnus*, *Bergaueria* is cylindrical to hemispherical (Prantl 1945; Pemberton *et al.* 1988). *Conostichus* is a conical plug-shaped burrow with regular transversal and longitudinal ridges (Chamberlain 1971; Pemberton *et al.* 1988), whereas *Conichnus* is typically smooth or rarely with concentric ridges. *Cornulatichnus* is a vertical conical burrow with a blade-like termination (Carroll & Trewin 1995) which is absent in *Conichnus*.

Conichnus can resemble body fossils of sponges (Klug & Hoffmann 2018). However, Klug & Hoffmann (2018) considered that sponges can be differentiated

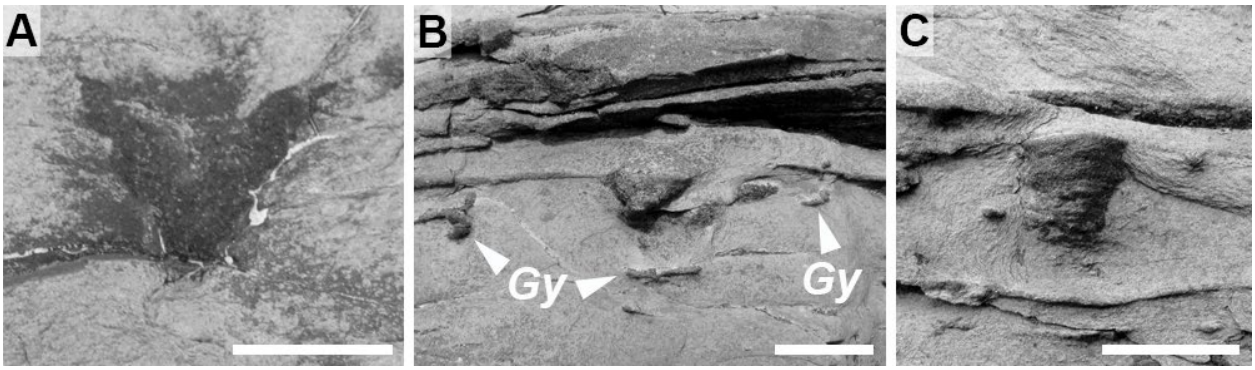

Fig. 26. Conichnus conicus Männil. Scale bars are 1 cm. All specimens are full reliefs. **A**, Specimen with a concave upper surface. Fortune Head, Member 2A (Fortunian). **B**, Specimen with a flat upper surface. Note *Gyrolithes scintillus* (Gy). Fortune Head, Member 2A (Fortunian). **C**, Specimen with concentric ridges on the wall. Fortune Head, Member 2A (Fortunian).

by their distinct skeleton, their different orientation after death, and their gradual fading with the casting sedimentary rock. Conical structures can also be formed by physical processes, with the fluidization of sediment resulting in collapsing (e.g. Plint 1983; Jensen & Miller 1990; Pemberton *et al.* 1992; Knaust & Langbein 1995; Dionne & Pérez Alberti 2000; Buck & Goldring 2003). Although the distinction is not always easy to resolve, the cone-in-cone morphology of physical structures widens upward, whereas cone-in-cone *Conichnus* tend to have a relatively steady width (Buck & Goldring 2003).

Conichnus ranges from the Ediacaran (Jensen & Runnegar 2005; Darroch *et al.* 2016, 2021; Cribb *et al.* 2019) to the Holocene (e.g. Shinn 1968; Schäfer 1972; Halley & Evans 1983; Gingras *et al.* 2008; Ayranci *et al.* 2014). Convincing Ediacaran occurrences (e.g. Darroch *et al.* 2021) are all from the Nama Group. In any case, extreme care is needed when evaluating these forms, as conical physical sedimentary structures have also been recorded from Precambrian strata (Dionne & Pérez Alberti 2000). Producers are burrowing cnidarians (actinarians and ceriantharians; Shinn 1968; Schäfer 1972; Halley & Evans 1983; Bromley 1996; Gingras *et al.* 2008) and possible holothurians (Weissbrod & Barthel 1998). *Conichnus* is recorded in marginal-marine (e.g. Curran & Frey 1977; Hiscott *et al.* 1984; Savrda *et al.* 1998; Weissbrod & Barthel 1998; Savrda 2003; Mata *et al.* 2012) and shallow-marine (e.g. MacEachern & Pemberton 1992; Pemberton *et al.* 1992; Nielsen *et al.* 1996; Bann *et al.* 2004; Mayoral *et al.* 2013; Vinn *et al.* 2015) environments. A report from continental settings (Keighley & Pickerill 1997) is controversial and awaits documentation of additional material. In the Chapel Island Formation, *Conichnus* was first recorded by Narbonne *et al.* (1987) and has been regularly mentioned since then (see synonym list below).

***Conichnus conicus* Männil, 1966**

Figure 26A–C

1987 *Conichnus conicus* Männil; Narbonne, Myrow, Landing & Anderson, p. 1287, fig. 6J.
2017 *Conichnus conicus* Männil; Landing *et al.*, p. 45, fig. 17E.
2019 *Conichnus conicus* Männil; Laing, Mángano, Buatois, Narbonne & Gougeon, p. 1626, fig. 2q.

Material. – Seventeen specimens from Members 2A and 2B (Fortunian) and Member 4 (Cambrian Age 2) in Fortune Head, Fortune North, Grand Bank Head, Little Dantzic Cove, and Point May.

Emended diagnosis. – Conical plug-shaped burrow with rounded base; smooth or displaying rare concentric ridges (modified from Pemberton *et al.* 1988).

Description. – Simple conical plug-shaped burrows. Preserved as full relief. Burrows are regular cones, circular in cross-section, with a rounded base. The upper part of the cone can be flat or concave. Their orientation is mostly vertical, and rarely slightly inclined. They are solitary or in pair. One specimen displays a poorly developed cone-in-cone morphology. Unlined to very thinly lined; walls are smooth or made of concentric ridges. Infill is massive, composed of mudstone or very fine- to fine-grained sandstone different from the mudstone to medium-grained sandstone host rock. Collapsing of sediment is absent. Rare specimens are preserved in calcite concretions. Widest part of each cone is 0.3–10.0 cm; depth is 0.3–10.5 cm; width/depth ratio is 0.5–2.8.

Associated trace fossils. – *Conichnus conicus* co-occurs with *Bergaueria perata*, *Gyrolithes scintillus*, *Palaeophycus tubularis*, *Palaeophycus* isp., and *Trichichnus linearis*.

Remarks. – The conical morphology allows placing the specimens studied in *Conichnus conicus*. Many Phanerozoic reports of *Conichnus conicus* display a cone-in-cone morphology (e.g. Buck & Goldring 2003; Savrda 2003; Abad *et al.* 2006; Desai & Saklani 2015), depicting a readjustment of the tracemaker to the sediment-water interface while keeping pace with the aggrading substrate. These differ mainly from inorganic cones by the absence of sediment collapse and absence of wider opening at the top (Curran & Frey 1977; Buck & Goldring 2003). In the Chapel Island Formation, a cone-in-cone morphology is poorly developed in a single specimen, arguing for an equilibrium structure. Collapsing has also not been observed in any specimen. Specimens of the Chapel Island Formation display simple, distinct conical geometries with sharp boundaries that strongly point toward a biogenic origin. Additionally, some of the specimens from this unit display a very thin lining, which could depict mucus secretion from an organism resting in its burrow.

Some Chapel Island Formation specimens display concentric ridges on their walls (Fig. 26C), which are features not diagnostic of *Conichnus* as reviewed by Pemberton *et al.* (1988). The ridges are biogenic and do not result from the intersection with sandstone laminae or thin beds, as *Conichnus* is preserved within massive mudstone intervals (e.g. Fig. 26C). *Conostichus* is a close relative to these forms, as it possesses a conical shape and transversal ridges, but longitudinal ridges are also diagnostic (Chamberlain 1971; Pemberton *et al.* 1988). We consider that the absence of longitudinal ridges in the Chapel Island Formation specimens does not support comparison with *Conostichus*. Consequently, we emend the diagnosis of *Conichnus conicus* to accommodate the rare record of concentric ridges. These ridges may depict the re-adjustment of the organism within its burrow in relation to changes in sedimentation rates.

Pemberton *et al.* (1988) gave a width/depth ratio of 0.26–0.67 for *Conichnus conicus*. This ratio is consistent with other reports (e.g. Savrda 2003; Mayoral *et al.* 2013; Vinn *et al.* 2015) and some of the Chapel Island Formation material, especially from Member 4. Conical burrows from Member 4 have typically larger dimensions, which would imply that a very large organism was living in the cone, well beyond the sizes of other trace-making organisms of the section. Large Cambrian conical burrows are not unusual (Hiscott *et al.* 1984; Hoffmann & Grimmberger 2011; Mata *et al.* 2012). In the Chapel Island Formation, the width/depth ratio is of 0.5–2.8, which is overall greater than the values recorded by Pemberton *et al.* (1988). Pemberton *et al.* (1988) did not suggest the possibility of discriminating further ichnospecies of smooth *Conichnus* based on variable ratios, neither did other authors. Some other Cambrian reports of *Conichnus conicus* (Pacześna 2010; Hammersburg *et al.* 2018) are doubtful as they do not display a clear conical morphology.

Ichnogenus *Cruziana* d'Orbigny, 1842

Discussion. – *Cruziana* is a horizontal bilobed burrow with scratch imprints (d'Orbigny 1842; Seilacher 1970; Keighley & Pickerill 1996) included in the category of architectural design of 'bilobate trails and paired grooves' (Buatois *et al.* 2017). *Cruziana* was first described from the Ordovician Anzaldo Formation of central Bolivia (d'Orbigny 1842, 1846; Egenhoff *et al.* 2007). Although early interpretations suggested a bivalve (Say in Dekay 1824; d'Orbigny 1842), a crustacean (Pictet 1854), a plant (de Tromelin & Lebesconte 1876; Lebesconte 1883; de Saporta & Marion 1881; de Saporta 1882, 1884, 1887; Delgado 1886; Schimper 1890), or a sponge (Lebesconte 1886) origin, Nathorst (1881, 1886) convincingly demonstrated that similar structures were made by arthropod scratching the sediment surface (see also Dawson 1864, 1890, James 1885, Bureau 1886, and Maillard 1887). *Cruziana* is an iconic trace fossil that is very common in shallow-marine Palaeozoic rocks and gave its name to a classic Seilacherian ichnofacies (Seilacher 1967a).

As a result of its high diversity and distinctive 'fingerprints' (*sensu* Seilacher 1970), Crimes (1968, 1969, 1975a, 1981) and Seilacher (1960, 1970, 1990a, 1992, 1993, 1994, 1996, 2007) suggested that ichnospecies of *Cruziana* could be useful as biostratigraphical markers in strata lacking body fossils (see also Häntzschel 1975; Aceñolaza & Durand 1978; Ekdale *et al.* 1984; Zonneveld *et al.* 2002; MacNaughton 2007; Buatois & Mángano 2011; Memória *et al.* 2023). This approach was originally designed for Gondwana and peri-Gondwana terranes and worked particularly well in some strata of late Cambrian–Ordovician age (e.g. Baldwin 1978; Blaise & Bouyx 1980; Pickerill & Fillion 1983; Wycisk *et al.* 1990; Mángano *et al.* 1996a, 2001; Aceñolaza & Milana 2005; Singh *et al.* 2019; Meischner *et al.* 2020; Elicki & Magnus 2021), having been refined in subsequent studies (Cooper 1984; Egenhoff *et al.* 2007; Hofmann *et al.* 2012). Focus in other palaeocontinents, such as Baltica (Knaust 2004; Jensen *et al.* 2011) and Laurentia (Magwood & Pemberton 1990; Gibb *et al.* 2017), have challenged some of the tenants of this ichnostratigraphy (but see also Seilacher 1994). However, limited number of studies and, in some cases, poor preservation of specimens or a small sample size lacking sufficient

morphological variability (i.e. non-representative sampling) call for the need of additional, detailed investigations.

Another debate focussed on the position of formation of *Cruziana*, either at the sediment-water interface (Radwański & Roniewicz 1963, 1972; Cowie & Spencer 1970; Crimes 1970, 1975b; Baldwin 1977a; Crimes *et al.* 1977; Gutschick & Rodriguez 1977), or at a sand-mud interface below a thin veneer of sediment (Seilacher 1955a, 1970, 1982, 1983, 1985, 1990a, 1994, 1996; Birkenmajer & Bruton 1971; Goldring 1985). The question was reviewed by Mángano *et al.* (1996a) and, although uncontroversial evidence is not always available, interpretations should be based on a case-by-case basis (see also Sadlok 2014 and Kesidis *et al.* 2019a).

Taxonomic controversies revolved around the validity of *Rusophycus* Hall and *Isopodichnus* Bornemann. Although Seilacher (1955a) first treated *Cruziana* and *Rusophycus* separately, he later decided to synonymize both ichnogenera from 1970 onward. This approach led to some confusion in the community, as most ichnologists dealt with *Cruziana* and *Rusophycus* separately, acknowledging clear morphological and behavioural differences (e.g. Lessertisseur 1955; Radwański & Roniewicz 1963; Crimes 1970; Osgood 1970; Birkenmajer & Bruton 1971; Häntzschel 1975; Alpert 1976a; Bergström 1976; Bromley & Asgaard 1979; Pickerill & Fillion 1983; Durand 1985). In this study, we agree with Keighley & Pickerill (1996) and separate *Cruziana* from *Rusophycus* based on a length/width ratio, with *Cruziana* ratio being greater than 2. We also add that *Rusophycus* displays, in places, morphological elements at their anterior end, posterior end, or in axial position, representing casts of skeletal body parts of their tracemaker. The other taxonomic issue concerns *Isopodichnus*, which has been retained as valid by some authors based on: (1) its intermediate status between *Cruziana* and *Rusophycus*, as it can display both coffee-bean and bilobed elongated shapes along the same specimen; (2) its smaller size; (3) its continental facies dependence; (4) its extension into the post-Palaeozoic; and (5) its non-trilobitic origin (Seilacher 1953, 1970, 1985; Bromley & Asgaard 1972, 1979; Bergström 1976; Trewin 1976; Hakes 1985; Pollard 1985; Manca 1986; Fillion & Pickerill 1990; Keighley & Pickerill 1996; Zonneveld *et al.* 2002). All these arguments are not taxonomically sound (Bromley 1996; Bertling *et al.* 2006, 2022; Buatois & Mángano 2011), and *Isopodichnus* is therefore synonymized with either *Cruziana* or *Rusophycus* depending on the overall morphology of the trace fossil.

At least 119 ichnospecies attributed to *Cruziana* have been either mentioned, described, or erected in the literature (pers. data, see also Gougeon 2023). Although synonymy of ichnospecies (Kolb & Wolf 1979) or description of ichnosubspecies (Seilacher 1996; Mángano & Buatois 2003a) have been suggested, it emerges that significant work is awaiting to clarify *Cruziana* ichnotaxonomy and determine its valid ichnospecies. Many of the forms erected by Seilacher (1970, 1990a) representing a stationary position of the tracemaker [e.g. *Cruziana carleyi* James, *C. leifeirikssoni* (Bergström), *C. pudica* (Hall), or *C. polonica* Seilacher] are regarded as *Rusophycus* by most other authors. For this work, only *Cruziana problematica*, an ichnospecies that was recovered in the Chapel Island Formation, is discussed in more detail below.

Cruziana shows similarities with *Didymaulichnus* Young, 1972, *Dimorphichnus* Seilacher, 1955a, *Diplichnites* Dawson, 1873, *Diplopodichnus* Brady, 1947, *Gyrochorte* Heer, 1865, and *Rusophycus* Hall, 1852. *Didymaulichnus* is a problematic ichnotaxon currently under revision. The typical morphology, as seen in *Didymaulichnus miettensis*, is quite distinct; this ichnospecies comprises smooth forms with two ventral lobes and lateral bevels (Young 1972). Specimens of *Didymaulichnus* displaying scratch imprints [e.g. type material of *D. lyelli* (Rouault) and *D. nankervisi* Bradshaw] should be relocated elsewhere (Jensen 1997) and may belong in *Cruziana*. *Dimorphichnus* and *Diplichnites* are trackways with two series of imprints that are not organized into two lobes as in *Cruziana* (Seilacher 1955a; Keighley & Pickerill 1998). *Diplopodichnus* is composed of two ridges in positive hyporelief or grooves in negative epirelief that are distinguished from *Cruziana* by their distinct spacing and lack of scratch imprints (Keighley & Pickerill 1996; Buatois *et al.* 1998b). *Gyrochorte* is a bilobed trace fossil that, unlike *Cruziana*, is preserved as positive epirelief or negative hyporelief (Heinberg 1970, 1973; Wetzel *et al.* 2020). Finally, *Rusophycus* is a short, bilobed burrow with scratch imprints that has a coffee bean morphology (Fillion & Pickerill 1990) and can display morphological skeletal features defining anterior, posterior, or axial elements.

Cruziana ranges from the Cambrian (e.g. Radwański & Roniewicz 1963; Crimes *et al.* 1977; Magwood & Pemberton 1990; Seilacher 1990a; MacNaughton & Narbonne 1999; Kesidis *et al.* 2019a) to the Cretaceous (Buatois *et al.* 2000; Oligmueller & Hasiotis 2024). Muñiz *et al.* (2015) also recorded *Cruziana*-like trace fossils made by fish from a modern estuary. However, these have sharp outlines with

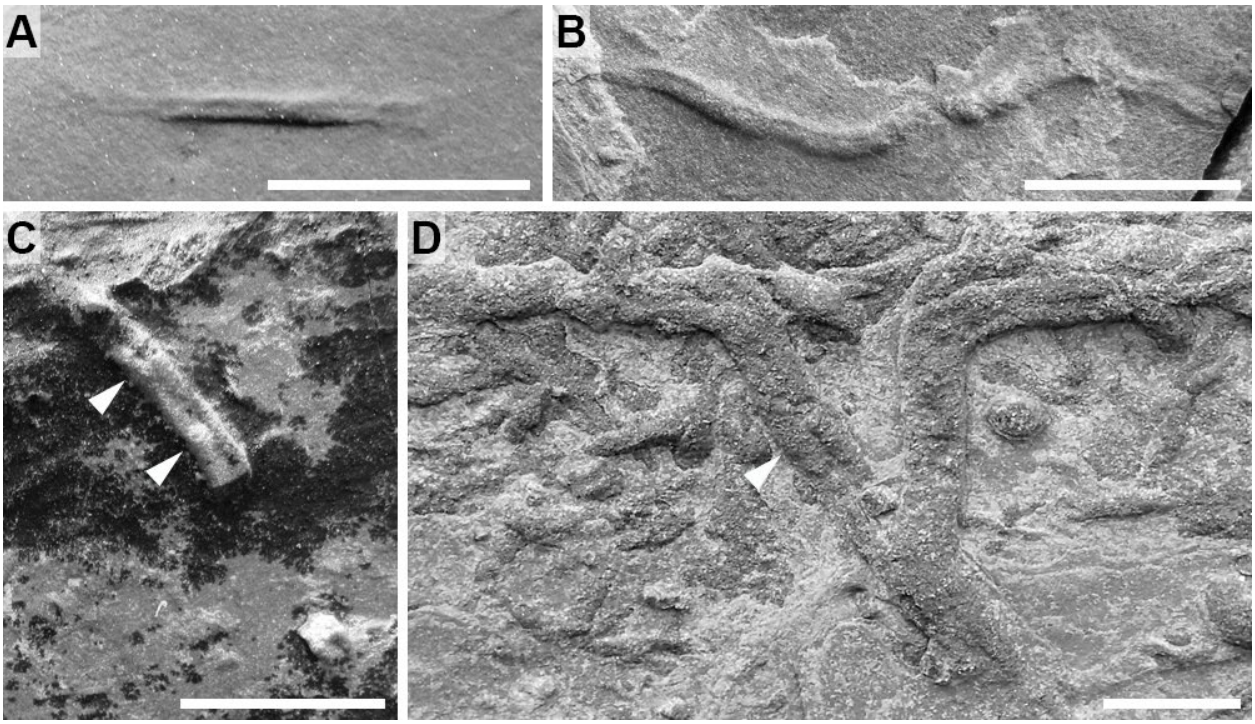

Fig. 27. Cruziana problematica (Schindewolf). Scale bars are 1 cm. All photographs are positive hyporeliefs. **A**, Straight specimen (morphotype A). Grand Bank Head, Member 2A (Fortunian). **B**, Loosely meandering specimen (morphotype A). Fortune Head, Member 2B (Fortunian). **C**, Straight specimen showing bulging (arrows) (morphotype A). Note that the specimen is broken (bottom right), and that the sharp terminations allow the observation of the squarish cross-section in the field. Fortune Head, Member 2A (Fortunian). **D**, Two flat specimens showing overlapping and angular turns (morphotype B). Note that the surface is not clearly smooth, and bulging suggests possible resting of the tracemaker (arrow). Grand Bank Head, Member 2A (Fortunian).

flat lobes, and are either smooth or with delicate longitudinal striae (Muñiz *et al.* 2015, fig. 4B–D) which differs from typical *Cruziana*. *Cruziana* is recorded in continental (e.g. Bromley & Asgaard 1972; Trewin 1976; Pollard 1985; Pickerill 1992; Schlirf *et al.* 2001; Minter & Lucas 2009), marginal-marine (e.g. Baldwin 1977b; Narbonne 1984; Legg 1985; Fillion & Pickerill 1990; Mángano *et al.* 2002b, 2021), shallow-marine (e.g. Radwański & Roniewicz 1963; Seilacher 1964; Crimes 1968; Zonneveld *et al.* 2002; Stachacz *et al.* 2015; Heward *et al.* 2018), and deep-marine (Pickerill *et al.* 1988; Pickerill 1995) environments. Producers are arthropods, including branchiopods in continental settings (e.g. Seilacher 1960; Bromley & Asgaard 1972; Pollard 1985; Gand *et al.* 2008; Minter & Lucas 2009; Sadlok 2014) and trilobites (e.g. Birkenmajer & Bruton 1971; Bergström 1973; Seilacher 1985; Fortey & Seilacher 1997; Fortey & Owens 1999; Mángano *et al.* 2021) and aglaspidids (Fischer 1978) in marine environments. More unusual tracemakers that were suggested include gastropods (Linck 1942; Seilacher 1960) and polychaete worms (Schindewolf 1928; Seilacher 1960). *Cruziana* has never been recorded in the Chapel Island Formation before.

Cruziana problematica (Schindewolf, 1921)

Figure 27A–D

Material. – Eight specimens of morphotype A from Member 2A (Fortunian) in Grand Bank Head; five specimens of morphotype B from Members 2A and 2B (Fortunian) in Fortune Head and Grand Bank Head.

Description. – Horizontal bilobed trail locally displaying faint transverse striae. Preserved as positive hyporelief. The course is straight, winding, to curved at deep angles. Terminations are not sharp, and the lobes progressively disappear within the host rock. Morphotype A has raised lobes with a narrow, shallow, incising median furrow and steep, deep, well-defined margins. Morphotype B is flat with a discontinuous median furrow and well-defined margins. In places, corrugations or bulging form at irregular intervals along the lobes. Cross-section is squarish in morphotype A. Overcrossing and secondary successive branching have been observed. Infill is massive, composed of very fine- to fine-grained sandstone similar to the host rock for morphotype A, and different

from the mudstone host rock for morphotype B. Morphotype A has width of 0.1–0.2 cm and maximum length of 3.1 cm. Morphotype B has width of 0.4–0.6 cm and maximum length of 15.2 cm.

Associated trace fossils. – Morphotype A co-occurs with *Palaeophycus tubularis*; morphotype B co-occurs with *Curvolithus simplex*, *Palaeophycus tubularis*, *Psammichnites gigas circularis*, *Rusophycus avalonensis*, *Treptichnus coronatum*, and *Treptichnus* indet.

Remarks. – Schindewolf (1921) first erected *Ichnium problematicum* Schindewolf for horizontal trace fossils 3–8 mm wide, up to 40 cm long, made of two lobes with oblique striae, and with a smooth median furrow. Later, Schindewolf (1928) reassigned this material to *Isopodichnus* Bornemann and provided illustrations. *Isopodichnus*, however, is now considered a junior synonym of *Cruziana* (see 'Discussion' above, p. 69). Schindewolf (1928) included both coffee-bean shaped and elongated bilobed structures within *Isopodichnus* (i.e. *Rusophycus* and *Cruziana* in modern ichnotaxonomy, respectively). Schindewolf (1928, p. 28) emphasized the presence of a narrow median furrow and steep lateral margins in a specimen, which corresponds to morphotype A in the Chapel Island Formation. A flat specimen similar to morphotype B in the Chapel Island Formation was also figured (Schindewolf, 1928, fig. 8, left specimen), although its margins are more irregular due to striae terminating at different positions laterally. Flat specimens with irregular lateral margins have commonly been recorded in *Cruziana problematica* (e.g. Bromley & Asgaard 1979, fig. 16A; Pickerill 1992, fig. 2B; Bromley 1996, fig. 8.13; Minter & Lucas 2009, fig. 3A, B; Fillmore *et al.* 2017, fig. 26). Certain reports of *Cruziana problematica* with more oblique striae and wider median furrow (e.g. Fillion & Pickerill 1990, pl. 3, fig. 4) may be, however, more closely affiliated with *C. bagnolensis* Morière, 1878. The sharp margins in morphotype B may be a taphonomic artifact as striae are not distinct. Both morphotypes from the Chapel Island Formation are included confidently within *Cruziana problematica*.

There is, however, a debate regarding the validity of *Cruziana problematica* in relation to *C. tenella* (Linnarsson, 1871). Material from the type locality of *Cruziana tenella*, formerly *Fraena tenella* Linnarsson, is composed of narrow horizontal trace fossils with a shallow incising median furrows, sharp and steep margins, and faint striae on lobes (Linnarsson 1871, pl. 1, fig. 5; Jensen 1997, figs 31, 32; Kesidis *et al.* 2019a, figs 1–4). Therefore, this material has a morphology close to morphotype A in the Chapel Island Formation. Jensen (1997) regarded *Cruziana problematica* as a more stable ichnospecies than *C. tenella* despite the seniority of the latter and, therefore, suggested that it could be retained as valid for nomenclatural stability, an opinion followed by Mángano *et al.* (2002b). Nevertheless, Jensen (1997) still resurrected *Cruziana tenella* because of the issues related with the former placement of *Cruziana problematica* in *Isopodichnus* by Schindewolf (1928) (see 'Discussion' above for a treatment of the issues with *Isopodichnus*, p. 69). The similarity of *Cruziana tenella* with *C. acadica* Dawson, 1864 was also noted by Keighley & Pickerill (1996) and would merit further exploration, as *C. acadica* was erected before *C. tenella*. *Cruziana problematica* was and still is a regularly cited ichnotaxon in the literature (e.g. Bromley & Asgaard 1972; Fillion & Pickerill 1990; Keighley & Pickerill 1996; Schlirf *et al.* 2001; Mikuláš & Lehotský 2002; Mángano *et al.* 2005a; Minter & Lucas 2009; Hofmann *et al.* 2012; Lima & Netto 2012; Shahkarami *et al.* 2017a; Hammersburg *et al.* 2018; Elicki & Altumi 2019; Kaur *et al.* 2021; Singh *et al.* 2024b). However, since the revision of the type material by Jensen (1997), *Cruziana tenella* has also been commonly used in the literature (e.g. MacNaughton & Narbonne 1999; Sadlok 2010; Pandey *et al.* 2014; Rodríguez-Tovar *et al.* 2014; Gibb *et al.* 2017; Kesidis *et al.* 2019a; Metz 2022). In this study, we follow the suggestion of Mángano *et al.* (2002b) and apply the name *Cruziana problematica* for both morphotypes recovered in the Chapel Island Formation. However, future revision of the type material published in Schindewolf (1921, 1928) may relocate part of this material in *Cruziana tenella* (i.e. material similar to morphotype A in the Chapel Island Formation) considering its recent rise in use.

Bilobated, horizontal, continuous, smooth structures without lateral bevels are commonly assigned to *Didymaulichnus lyelli*. This ichnospecies is extensively recorded, ranging from the Cambrian (Walter *et al.* 1989; Mángano & Buatois 2016; Buatois *et al.* 2017) to the Cretaceous (Vossler *et al.* 1989), and is present in continental (Aceñolaza & Buatois 1991, 1993; Trewin & McNamara 1995; Buatois & Mángano 2002), marginal-marine (Hakes 1977; Bradshaw 1981; Fillion & Pickerill 1990), shallow-marine (El-Khayal & Romano 1988; Vossler *et al.* 1989; Walter *et al.* 1989; Kumpulainen *et al.* 2006), and deep-marine (Han & Pickerill 1994b) environments. However, the morphology of recorded *Didymaulichnus lyelli* is highly variable and is represented by: (1) very flat specimens with sharp edges and an incising median furrow (Buatois & Mángano 2002; da Silva *et al.* 2003); (2) specimens with more relief and steeper lobes (Hakes

1977; Bradshaw 1981; Walter *et al.* 1989; Aceñolaza & Buatois 1993; Kumpulainen *et al.* 2006); (3) very short specimens with 'lobes' of variable width (Neef 2004); (4) trace fossils with very wide median furrow (Walter *et al.* 1989; Buatois *et al.* 2017); or (5) specimens with unclear transverse scratch imprints (Bradshaw 1981; Vossler *et al.* 1989). This variety of forms demonstrates that the morphological boundaries of *Didymaulichnus lyelli* are poorly defined. The type material may actually represent a taphonomic variant of *Cruziana* (Durand 1985), and this ichnotaxon needs revision.

In the Chapel Island Formation, Crimes & Anderson (1985) recorded two forms as *Didymaulichnus* isp.: a flattened form with incising median furrow similar to what is called *Didymaulichnus lyelli* in the literature (Crimes & Anderson 1985, fig. 5.6), and a form made of two rounded, connected strings (only drawn; Crimes & Anderson 1985, fig. 6.3). This latter morphology is intriguing as it passes into a unilobed burrow, which has been observed in morphotype B of *Cruziana problematica* as described herein. Herringshaw *et al.* (2017) also recorded *Didymaulichnus* isp. from Member s 2A and 2B without providing illustration.

Similar forms to morphotype A have been recorded in the literature as *Cruziana problematica* (Fillion & Pickerill 1990; Keighley & Pickerill 1996; Mángano *et al.* 2002b; Shahkarami *et al.* 2017a, b), *Cruziana tenella* (Jensen 1997; Sadlock 2010; Kesidis *et al.* 2019a; Novis *et al.* 2022), *Didymaulichnus* (Eagar *et al.* 1985), *Isopodichnus* isp. (Bergström 1976), and *Planolites* cf. *P. serpens* Alpert (Fedonkin 1990). Transverse striations are commonly recorded (Jensen 1997; Shahkarami *et al.* 2017a), which warrant an affinity to *Cruziana*. In the Chapel Island Formation, these are lacking, but it is commonly assumed that smaller specimens of *Cruziana* may not preserve striae due to the size of sediment grains impacting taphonomy (Bromley & Asgaard 1979; Jensen *et al.* 2005; Sadlock 2010; Schatz *et al.* 2011). Kesidis *et al.* (2019a) considered that *Cruziana tenella* from the type locality recorded repeated resting stages by the tracemaker, i.e. the continuous alignment of *Rusophycus* burrows. In the Chapel Island Formation, large corrugations on some specimens may represent similar resting behaviours (Fig. 27C), but lobes are typically connected and favor continuous locomotion.

Ichnogenus *Curvolithus* Fritsch, 1908

Discussion. – *Curvolithus* is a subhorizontal trail with a trilobed dorsal surface displaying a vertical undulatory component in its course (Buatois *et al.* 1998c; Seilacher 2007) and is included in the category of architectural design of 'trilobate flattened trails' (Buatois *et al.* 2017). *Curvolithus* was first described from the Ordovician Kosov Formation of central Czech Republic (Fritsch 1908; Buatois *et al.* 1998c). Buatois *et al.* (1998c) reviewed the ichnotaxonomy of *Curvolithus* and considered two ichnospecies valid: *C. multiplex* Fritsch, 1908 and *C. simplex* Buatois, Mángano, Mikuláš & Maples, 1998c. The type ichnospecies, *Curvolithus multiplex*, has a quadrilobed ventral surface (Fritsch 1908; Buatois *et al.* 1998c). *Curvolithus simplex* has a uni- to trilobed ventral surface (Buatois *et al.* 1998c).

Curvolithus shows similarities with *Psammichnites* Torell, 1870, *Treptichnus* Miller, 1889, and *Trisulcus* Hitchcock, 1865. *Psammichnites* is a subhorizontal trail with a median dorsal structure and a flat uni- to trilobed ventral surface like *Curvolithus* (Mángano *et al.* 2002a). However, *Psammichnites* also displays a distinctive backfilling. In addition, *Psammichnites* typically represents long structures with a meandering course, whereas *Curvolithus* is typically short and straight (Buatois *et al.* 1998c; Mángano *et al.* 2002a). *Treptichnus triplex* consists of repeated trilobed segments (Palij 1976; Buatois & Mángano 1993b). Taken alone, these segments may be reminiscent of *Curvolithus* (e.g. Jensen & Grant 1998; Wilson *et al.* 2012), but branching is absent in *Curvolithus*. *Trisulcus* is composed of three thin grooves separated by two wide ridges on bed top (Hitchcock 1865; Getty & Goldstein 2022). Contrary to *Curvolithus*, *Trisulcus* is a surficial trail that also displays, in places, short lateral imprints (Getty & Goldstein 2022).

Curvolithus ranges from the Cambrian (e.g. Banks 1970; Walter *et al.* 1989; Bryant & Pickerill 1990; Systra & Jensen 2006; Högström *et al.* 2013; Shahkarami *et al.* 2017a) to the Miocene (Keij 1965). A report of an alleged incipient *Curvolithus* (Lawfield & Pickerill 2006) is an epifaunal trail and therefore is unrelated to full relief, clearly endichnial structures belonging to *Curvolithus*. Potential producers are gastropods (e.g. Heinberg 1973; Alpert 1976b; Hakes 1976; Fürsich & Heinberg 1983; Heinberg & Birkelund 1984), holothurians (Lockley *et al.* 1987), and worms (annelids, flatworms, and nemerteans; Lockley *et al.* 1987; Seilacher *et al.* 2005; Seilacher 2007; Knaust 2010). *Curvolithus* is typically recorded from marginal-marine (e.g. Keij 1965; Hakes 1985; Martino 1989; Maples & Suttner 1990; Greb & Chesnut 1994; Mángano & Buatois 2004b) and shallow-marine (e.g. Chamberlain 1971; Walter *et al.* 1989; Rindsberg 1994; Stanley & Pickerill 1998; Mángano *et al.* 2002b; Krobicki & Uchman 2003) environments. Seilacher & Mrinjek (2011) also

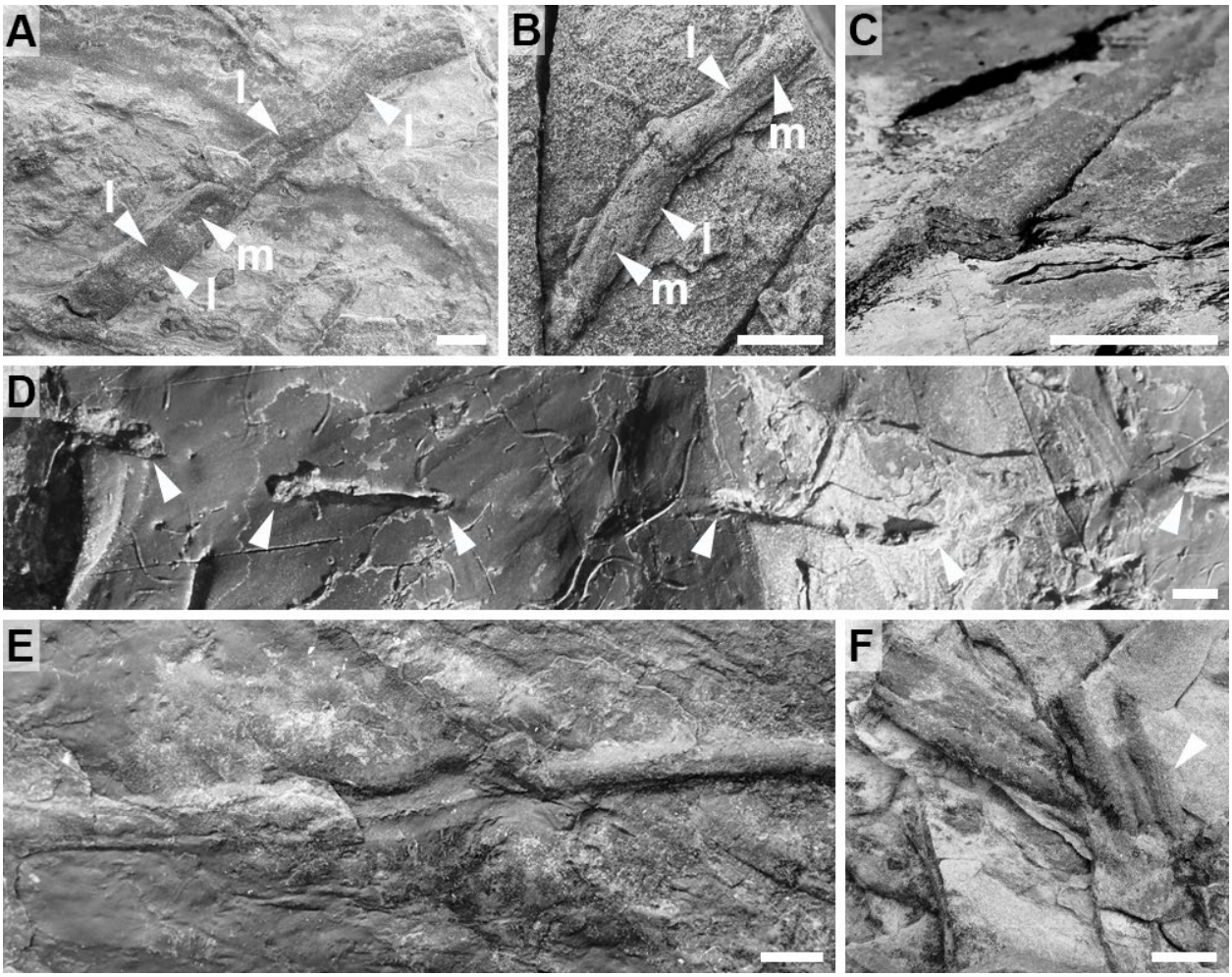

Fig. 28. Curvolithus multiplex Fritsch (A, B), *Curvolithus simplex* Buatois, Mángano, Mikuláš & Maples (C–E), and *Curvolithus* isp. (F). Scale bars are 1 cm. **A, B**, *Curvolithus multiplex* with discontinuous grooves separating the median (m) and lateral (l) lobes. Positive hyporelief, Grand Bank Head, Member 2A (Fortunian, D) and Member 5 (Cambrian Age 2, E). **C**, Flattened *Curvolithus simplex* with a trilobed dorsal surface and a unilobed ventral surface. Full relief, Lewin's Cove, Member 2A (Fortunian). **D**, *Curvolithus simplex* showing vertical undulation, with appearance and disappearance of the specimen along its course (arrows). Note the simple horizontal trails on the same surface. Full relief observed on bed top, Fortune Head, Member 2B (Fortunian). **E**, *Curvolithus simplex* with a trilobed dorsal surface (left side) and a bilobed ventral surface (middle). Note that the dorsal surface grades into a unilobed surface (right side). Full relief, Grand Bank Head, Member 2B (Fortunian). **F**, *Curvolithus* isp. with distinct longitudinal striae along a lateral lobe (arrow). Positive hyporelief, Fortune Head, Member 2B (Fortunian).

mentioned a possible deep-marine occurence. In the Chapel Island Formation, *Curvolithus* was first recorded by Crimes & Anderson (1985) and has been commonly mentioned since then (e.g. Narbonne *et al.* 1987; Herringshaw *et al.* 2017).

***Curvolithus multiplex* Fritsch, 1908**

Figure 28A, B

Material. – Three specimens from Members 2A and 2B (Fortunian) and Member 5 (Cambrian Age 2) in Fortune Head and Grand Bank Head.

Description. – Smooth, unlined, unbranched, subhorizontal trails with a quadrilobed ventral surface. Preserved as positive hyporelief. The course is straight to curving. The trail is ovoid to flattened in cross-section. Ventral median lobes bulge or are at the same level with respect to lateral lobes. Infill is massive, composed of very fine-grained sandstone similar to the host rock, or different where encased in mudstone. Width is 0.5–1.1 cm; maximum length is 13.5 cm.

Associated trace fossils. – *Curvolithus multiplex* co-occurs with *Curvolithus simplex*, *Didymaulichnus miettensis*, *Palaeophycus tubularis*, and *Treptichnus pedum*.

Remarks. – Mángano *et al.* (2002b) described a specimen of *Curvolithus multiplex* with a quadrilobed ventral surface lacking a dorsal expression. These authors noted that the quadrilobed ventral surface is very distinctive of *Curvolithus multiplex,* and we agree with this opinion. *Curvolithus multiplex* is uncommon from the trace-fossil record (cf. synonym list in Buatois *et al.* 1998c) and has not been recorded from the Cambrian before. In the Chapel Island Formation, grooves separating the lobes are typically faint and can disappear along the course: other reports in the literature display either distinctive ridges and quadra-lobation (Buatois *et al.* 1998c, fig. 6; Maples & Suttner 1990, figs 10.1, 10.3; Muszer 2020, fig. 4B), or discontinuous ridges if the preservation is partial (Mángano *et al.* 2002b, fig. 30).

Curvolithus simplex **Buatois, Mángano, Mikuláš & Maples, 1998c**

Figure 28C–E

Material. – About 55 specimens from Members 2A and 2B (Fortunian) and Member 5 (Cambrian Age 2) in Fortune Head, Grand Bank Head, and Lewin's Cove.

Description. – Smooth, unlined, unbranched horizontal trails with a trilobed dorsal surface and a uni- to trilobed ventral surface. Preserved as positive hyporelief, positive and negative epirelief, and full relief. The course is typically short, straight to curved, and can display a vertical undulatory component on well exposed slabs. The width is constant along the trail. The trail is ovoid to flattened in cross-section. The dorsal surface has a wider median lobe, and the three dorsal lobes can grade into a unilobed surface. The ventral surface can display transitions from uni- to bi- and trilobed surfaces. The ventral median lobe can bulge with respect to lateral lobes. Trails are isolated or aggregated, in places significantly overlapping. Infill is massive, composed of very fine- to fine-grained sandstone similar to the host rock, or different where encased in mudstone or fine-grained sandstone. Width is 0.5–1.3 cm; maximum length is 20.7 cm.

Associated trace fossils. – *Curvolithus simplex* co-occurs with *Cruziana problematica*, *Curvolithus multiplex*, *Helminthoidichnites tenuis*, *Helminthopsis tenuis*, *Monomorphichnus lineatus*, *Palaeophycus tubularis*, *Psammichnites gigas circularis*, *Rusophycus avalonensis*, *Treptichnus bifurcus*, *T. pedum*, and *Trichichnus linearis*.

Remarks. – The trilobed dorsal surface and uni-, bi-, or trilobed ventral surface allow placing these trace fossils in *Curvolithus simplex*. Short specimens displaying a tendency to change vertical level within the sediment are also typical (Buatois *et al.* 1998c; Mángano *et al.* 2002b; Seilacher 2007). Where only a bilobed ventral surface is visible, *Curvolithus* shares similarities with *Psammichnites* (cf. Jensen & Palacios 2016; Mángano *et al.* 2022), as well as with *Cruziana problematica* (both morphotypes A and B) as described in this study. Uchman (1995) stated that Palaeozoic *Taphrhelminthopsis* Sacco are most likely washed-out casts of *Curvolithus* or *Cruziana*. However, re-evaluation of lower Palaeozoic occurrences of *Taphrhelminthopsis* indicates that these are instead preservational variants of *Psammichnites* (Mángano *et al.* 2022). In the Chapel Island Formation, *Psammichnites* is typically unilobed on its ventral surface (see *Psammichnites* section, p. 111). Consequently, if material is showing a bilobed ventral surface, only specimens also demonstrating a distinct trilobed dorsal surface are included in *Curvolithus simplex*. Moreover, as trilobed ventral surfaces are not demonstrated in *Psammichnites* from the Chapel Island Formation, specimens displaying that feature and lacking exposure of their dorsal surface are included in *Curvolithus simplex* as well.

Curvolithus sp. was described by Crimes & Anderson (1985) from Member 2A without figured specimens. Their description emphasized the presence of a trilobed ventral surface, which corresponds to *Curvolithus simplex* as described herein. Additional *Curvolithus* and *Curvolithus* sp. materials were mentioned in the Chapel Island Formation without illustration (e.g. Narbonne *et al.* 1987; Landing *et al.* 1988; Herringshaw *et al.* 2017), and their affinity is unknown.

Curvolithus **isp.**

Figure 28F

Material. – Two specimens from Member 2B (Fortunian) in Fortune Head.

Description. – Smooth, unlined, unbranched, subhorizontal trails with a trilobed ventral surface, and longitudinal striae along lateral lobes. Preserved as positive hyporelief. The median lobe is in places wider than lateral lobes, and slightly depressed relatively to lateral lobes. Longitudinal striae are clear on lateral lobes of one specimen and are only faint on the other specimen. The two specimens are overlapping. Infill is massive, composed of very fine-grained sandstone different from the mudstone host rock. Width is 1.0–1.2 cm; maximum length is 3.5 cm.

Associated trace fossils. – *Curvolithus* isp. does not occur with other formally described ichnotaxa.

Remarks. – These specimens display a trilobed ventral surface, which is a feature typical of *Curvolithus* in the Chapel Island Formation (see Remarks in *Curvolithus simplex* section above). However, diagnoses of previously erected *Curvolithus* ichnospecies do not mention longitudinal striae. Striae may have resulted from the marking of body parts of the producer during locomotion. With the record of only two specimens in the Chapel Island Formation and in the absence of dorsal exposure, the erection of a new *Curvolithus* ichnospecies is not envisioned.

Ichnogenus *Dendroidichnites* Demathieu, Gand & Toutin-Morin, 1992

Discussion. – *Dendroidichnites* is a trackway with two symmetric rows of oblique, incisive, elongate to crescentic imprints not organized into series (Demathieu *et al.* 1992; Buatois *et al.* 1998a; Minter & Braddy 2009) included in the category of architectural design of 'trackways and scratch imprints' (Buatois *et al.* 2017). *Dendroidichnites* was first described from the Permian Motte Formation of southeastern France (Demathieu *et al.* 1992). The complicated taxonomic status of *Dendroidichnites*, *Mirandaichnium* Aceñolaza, and *Permichnium* Guthörl was summarized by Buatois *et al.* (1998a) and Minter & Braddy (2009), who considered *Dendroidichnites* valid based on its lack of V-shaped series (see also Kozur & Lemone 1995). Further difficulties arose with the description of intergradational specimens of *Diplichnites*, *Diplopodichnus*, and *Dendroidichnites*, which resulted from variations in substrate cohesiveness (Braddy 1998; Bertling *et al.* 2006; Minter *et al.* 2007; Minter & Braddy 2009). Minter *et al.* (2007) recommended retaining each ichnotaxon valid where they occur in isolation, an approach that has been followed by subsequent authors (e.g. Minter & Braddy 2009; Lucas & Lerner 2010; Buatois *et al.* 2017). Two ichnospecies attributed to *Dendroidichnites* have previously been described in the literature: *D. irregulare* (Holub & Kozur, 1981) and *D. elegans* Demathieu, Gand & Toutin-Morin, 1992. *Dendroidichnites elegans*, originally designated as type ichnospecies, consists of symmetric crescentic imprints separated by a median area with or without longitudinal striae (Demathieu *et al.* 1992). However, the type material of *Dendroidichnites irregulare* (Holub & Kozur 1981, pl. 12, fig. 1), formerly *Mirandaichnium irregulare*, is undistinguishable from *D. elegans* (Buatois *et al.* 1998a). Consequently, Buatois *et al.* (1998a) considered *Dendroidichnites irregulare* as the type ichnospecies of *Dendroidichnites*, a decision endorsed here. Therefore, only *Dendroidichnites irregulare* is considered valid in this study.

Dendroidichnites shows similarities with *Archaeonassa* Fenton & Fenton, 1937a, *Diplichnites* Dawson, 1873, *Diplopodichnus* Brady, 1947, *Mirandaichnium* Aceñolaza, 1978, *Protichnites* Owen, 1852, and *Protovirgularia* M'Coy, 1850. *Archaeonassa* is a horizontal trail with lateral levees (Jensen 2003). Although levees in *Archaeonassa* are typically smooth and continuous, their collapse can in places result in irregularities that are reminiscent of imprints in *Dendroidichnites*. However, the latter incise the substrate sharply and are regularly repeated and nested, normally not associated with lateral lobes (but see below), and with a mode of construction that is fundamentally different (wedging of a glide-crawling organism in *Archaeonassa* versus displacing sediment using legs in *Dendroidichnites*) (see also *Archaeonassa* section, p. 49). Unlike the nested crescentic imprints of *Dendroidichnites,* imprints in *Diplichnites* are simple, but also form a trackway with two parallel rows (Keighley & Pickerill 1998). *Diplopodichnus* consists of two to three parallel grooves/ridges without displaying imprints as in *Dendroidichnites* (Brady 1947; Buatois *et al.* 1998b). *Mirandaichnium* is a trackway composed of two rows of imprints forming series of eight imprints, whereas *Dendroidichnites* is not organized into series (Aceñolaza & Buatois 1993; Buatois *et al.* 1998c). *Protichnites* is a trackway with a central part made of one or many grooves and lateral rows of short oblique imprints that are not crescentic (Keighley & Pickerill 1998). *Protovirgularia* is a horizontal trail with a median line and chevrons extending laterally (M'Coy 1850; Han & Pickerill 1994a; Mángano *et al.* 2002b; Carmona *et al.* 2010; López Cabrera *et al.* 2019; Knaust 2023). In *Dendroidichnites*, converging imprints from each row can mimic the median line of *Protovirgularia* (e.g. Buatois *et al.* 1998a). However, Carmona *et al.* (2010) noted that staggered imprints and curling of their lateral ends were more typical of *Dendroidichnites*.

Dendroidichnites superficially resembles some aspects of abiogenic chevron grooves. Chevron grooves are U- to V-shaped imprints produced by tools moving on or above a cohesive substrate (Craig & Walton 1962; Allen 1982) and are distinguished by their straighter course, broader size range, preservation on bed soles, presence of other current-made structures on the same surface, and absence of trace fossils on the same surface (Benton 1982a; Lucas *et al.* 2005a; Minter & Braddy 2009).

Dendroidichnites is recorded from the Cambrian (this study) to the Holocene (Davis *et al.* 2007). Producers are arthropods (isopods, myriapods and possible dragonfly nymphs, hymenopterans, and

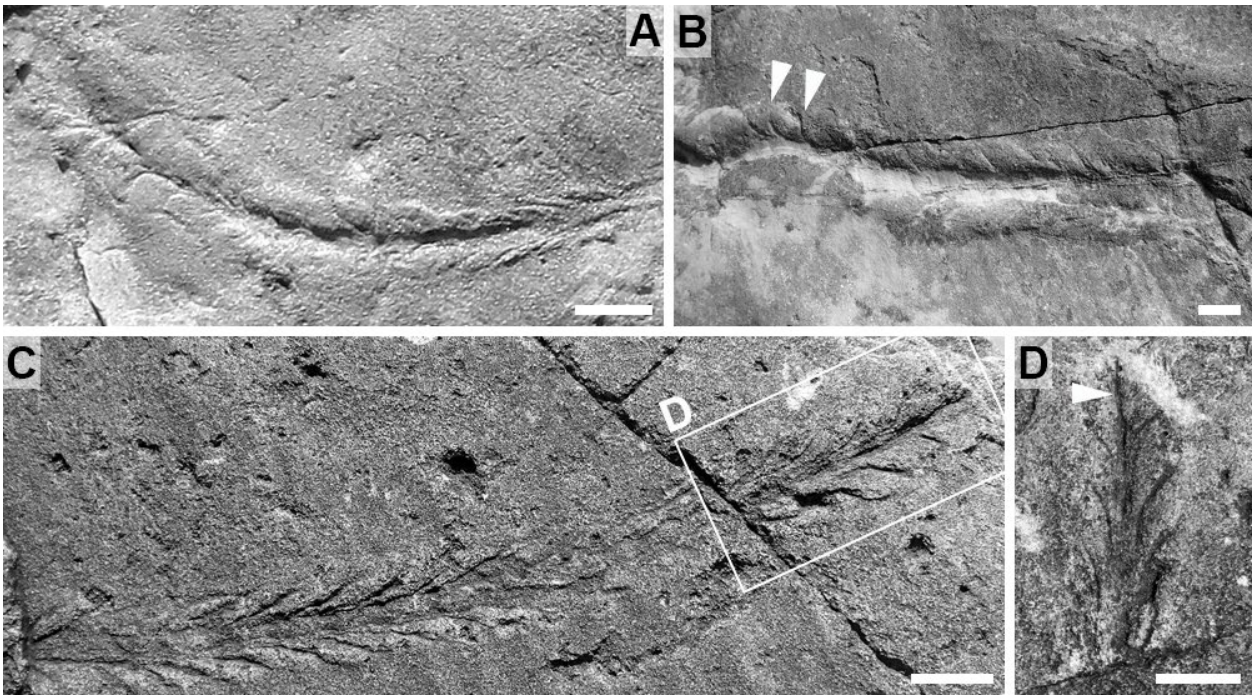

Fig. 29. Dendroidichnites aff. *D. irregulare* (Holub & Kozur). Scale bars are 1 cm. **A**, Specimen with widely spaced (left) and nested imprints (right). Note transition from leveed (left) to flat morphology (right). Negative epirelief, Fortune Head, Member 2A (Fortunian). **B**, Asymmetric specimen with levees on both sides, but incisive imprints are present on the upper side only. Note lateral ends of imprints bent perpendicular to the trackway axis (arrows). Negative epirelief, Little Dantzic Cove, Member 5 (Cambrian Age 2). **C**, Specimen with regularly spaced nested imprints. Negative epirelief, Little Dantzic Cove, Member 5 (Cambrian Age 2). **D**, Close-up from Figure 29C showing incisive, paired crescentic imprints and a median part reduced to a simple line (arrow).

pygocephalomorphs; Gibbard & Stuart 1974; Buatois *et al.* 1998a; Davis *et al.* 2007; Melchor & Cardonatto 2014). *Dendroidichnites* is most exclusively recorded in continental (e.g. Demathieu *et al.* 1992; Ronchi & Santi 2003; Minter & Braddy 2009; Marchetti *et al.* 2015; Fillmore *et al.* 2017; Pedernera *et al.* 2021) settings. Marginal-marine (Buatois *et al.* 1998a) and shallow-marine (this study) occurrences are less common. *Dendroidichnites* has never been recorded in the Chapel Island Formation before.

***Dendroidichnites* aff. *D. irregulare* (Holub & Kozur, 1981)**

Figure 29A–D

Material. – Six specimens from Member 2A (Fortunian) and Member 5 (Cambrian Age 2) in Fortune Head and Little Dantzic Cove.

Description. – Mostly symmetric trackways with two rows of paired imprints that tend to converge in their median part. The course is curved or slightly sinuous. The median part is typically wide (deep or flat) but can also be reduced to a simple axial line. Imprints are incisive, oblique to the trackway axis, elongate to crescentic, and nested to more widely spaced. In leveed specimens, imprint morphology can be highly crescentic with lateral endings oriented perpendicular to the trackway axis. Organization of imprints in series is absent. Development of levees associated to imprints as well as transition from leveed-to-flat morphology have been noted. Such transition is associated with a narrowing of the trackway width. Trackway width is 0.8–2.2 cm; median furrow width is 0.05–0.7 cm; imprints length is 0.5–1.3 cm; maximum trackway length is 13.8 cm.

Associated trace fossils. – *Dendroidichnites* aff. *D. irregulare* co-occurs with *Archaeonassa fossulata*, *Circulichnis ligusticus*, *Helminthoidichnites tenuis*, *Helminthopsis hieroglyphica*, *H. tenuis*, and *Psammichnites gigas circularis*.

Remarks. – The presence of two rows of crescentic imprints allows placement in *Dendroidichnites*. However, levees have not been described previously in *Dendroidichnites irregulare*, which does not permit a complete agreement with an affiliation to this ichnospecies (i.e. *Dendroidichnites* aff. *D. irregulare*). Leveed imprints develop from the passing of the body of a legged animal through a soft substrate, fairly enhanced in water content but still allowing plastic deformation. Hence, leveed-to-flat transition most likely results from

a change in substrate stiffness, from soft to firm, possibly related to local microbial stabilization. Levees are typical of *Archaeonassa*. Demircan & Uchman (2016) described *Archaeonassa* with levees and oblique striae that they suggested to be made from body appendages of an arthropod. Striae in Demircan & Uchman (2016) are shorter and straighter than crescentic forms typically recorded in *Dendroidichnites*, but they are incising the substrate and their mode of formation as interpreted by the authors is similar. Therefore, we suggest these forms to be morphologically and functionally closer to *Dendroidichnites* than *Archaeonassa*. This conclusion is supported by the report of modern leveed trails with imprints made by appendages of amphipods and isopods that in places display nested imprints with crescentic morphologies (Uchman & Pervesler 2006, fig. 4B, C).

Ichnogenus *Didymaulichnus* Young, 1972

Discussion. – *Didymaulichnus* is a smooth horizontal trail with two raised ventral lobes and a median furrow (Young 1972) included in the category of architectural design of 'bilobate trails and paired grooves' (Buatois *et al.* 2017). *Didymaulichnus* was first described from the Cambrian part of the Miette Group of western Canada (Young 1972; Buatois & Mángano 2016). The type ichnospecies, however, was designated from the Ordovician Armorican Sandstone Formation of western France, and was first described under the ichnogenus name *Fraena* Rouault (Young 1972). *Fraena* covers a broad variety of trace fossils that comprise unilobed smooth trails, bilobed smooth trails, and bilobed trails with striae (Rouault 1850; Lebesconte 1883; Durand 1985). The ichnogenus *Fraena* has rarely been used to designate smooth unilobed trails (de Tromelin & Lebesconte 1876; Durand 1985). Other forms have been relocated in *Cruziana* and *Didymaulichnus*. After Young (1972) erected *Didymaulichnus*, Durand (1985) designated a lectotype from Rouault's collection as no holotype was defined. There is, however, an important debate surrounding the validity of *Didymaulichnus* and its distinction from *Cruziana* (Fillion & Pickerill 1990; Jensen 1997; Jensen *et al.* 2005; Sadlock 2010; Schatz *et al.* 2011). Three arguments merit discussion: (1) the type ichnospecies, *Didymaulichnus lyelli*, is associated with horizontal bilobed trace fossils with scratch imprints of *Cruziana* affinity (Durand 1985); (2) partially preserved marginal ridges can be seen on the type material which are typical of some *Cruziana* ichnospecies (Durand 1985); and (3) sediment grain-size can affect the preservation of scratch imprints and could in places renders the distinction of *Cruziana* from *Didymaulichnus* difficult (Jensen *et al.* 2005; Schatz *et al.* 2011). These observations suggest that *Didymaulichnus* could be a junior synonym of *Cruziana*, and that an in-depth revision of *Didymaulichnus* is necessary to resolve this problem (D. Muñoz, pers. comm., 2022). In turn, Dzik (2005) rejected the standard taxonomy of trace fossils and referred *Didymaulichnus* to *Mattaia* Dzik, conflating ichnotaxonomic and biological classifications. This approach has been contested in the literature and is rejected here as trace fossils should not be treated in the same fashion as body fossils (Bertling *et al.* 2006, 2022; Buatois & Mángano 2011; Buatois 2018).

At least ten ichnospecies attributed to *Didymaulichnus* have been described: *D. lyelli* (Rouault, 1850); *D. rouaulti* (Lebesconte, 1883); *D. furnai* (Lange, 1942); *D. miettensis* Young, 1972; *D. tirasensis* Palij, 1974; *D. nankervisi* Bradshaw, 1981; *D. alternatus* Pickerill, Romano & Meléndez, 1984b; *D. meanderiformis* Fedonkin, 1985; *D. dailyi* (Hofmann & Patel, 1989); and *D. nerodenkoi* Grytsenko, 2016. The type ichnospecies, *Didymaulichnus lyelli*, formerly *Fraena lyelli*, is smooth with two simple lobes (Rouault 1850; Jensen & Mens 2001) and is currently under revision. *Didymaulichnus rouaulti*, formerly *Cruziana rouaulti*, has narrow marginal grooves/ridges (Pickerill *et al.* 1984b), and its affinity to either *Didymaulichnus* or *Cruziana* has to be re-evaluated. *Didymaulichnus furnai*, formerly *Fraena furnai*, is smooth and bilobed (Lange 1942) and is considered a junior synonym of *D. lyelli* (Fernandes *et al.* 2002; Sedorko *et al.* 2013). *Didymaulichnus miettensis* is a distinctive form displaying lateral bevels (Young 1972). *Didymaulichnus tirasensis* consists of repeated and overlapping bilobed segments (Palij 1974; Jensen & Mens 2001). *Didymaulichnus alternatus* has a variable depth along its course (Pickerill *et al.* 1984b). *Didymaulichnus meanderiformis* is smooth, bilobed and meandering (Fedonkin 1990). Although it was compared to *Taphrhelminthoida* Książkiewicz (Hofmann & Patel 1989; Aceñolaza & Buatois 1993), the latter was placed in synonymy with *Scolicia* (Uchman 1995). Palaeozoic forms have, however, a different affinity (Mángano *et al.* 2022). Accordingly, re-evaluation of the type material of *Didymaulichnus meanderiformis* is needed to explore its potential relationship to *Psammichnites*. Barr *et al.* (2023) recently proposed the new combination *Didymaulichnus dailyi* (formerly *Taphrhelminthoida dailyi*) for similar forms. We suggest retaining provisionally *Didymaulichnus meanderiformis* for these trails, awaiting re-evaluation of the type material. According to Bradshaw (1981), *Didymaulichnus nankervisi* has regular transverse scratch imprints on its lobes, and Pickerill *et al.* (1984b) considered this ichnospecies a preservational variant of *Cruziana*. *Didymaulichnus nerodenkoi* is a horizontal structure with a median furrow and irregular lateral levees (Grytsenko 2016). The toponomy of this ichnospecies was not provided by Grytsenko (2016), and its affinity to *Didymaulichnus* is doubtful.

Consequently, four ichnospecies, *Didymaulichnus alternatus*, *D. lyelli*, *D. miettensis*, and *D. tirasensis*, are provisionally retained as valid, awaiting re-evaluation of *D. lyelli* and *D. meanderiformis*.

Didymaulichnus shows similarities with *Cruziana* d'Orbigny, 1842, *Didymaulyponomos* Bradshaw, 1981, *Diplopodichnus* Brady, 1947, *Gyrochorte* Heer, 1865, and *Psammichnites* Torell, 1870. *Cruziana* is a bilobed trail with scratch imprints (Crimes 1968, 1970, 1975a; Fillion & Pickerill 1990; Keighley & Pickerill 1996; Fortey & Seilacher 1997). As mentioned above, its relationship to *Didymaulichnus* needs to be re-evaluated on a case-by-case basis. *Didymaulyponomos* is a passively filled horizontal burrow with a ventral median groove and, in places, a beaded appearance on the ventral surface (Bradshaw 1981; Trewin & McNamara 1995). *Didymaulyponomos* is typically preserved as negative epireliefs, making difficult to observe its fine morphology. However, the apparent absence of scratch imprints and general bilobated morphology makes it difficult to be distinguish from *Didymaulichnus*, and re-evaluation is needed. *Diplopodichnus* has two well-spaced furrows in negative epirelief or two well-spaced ridges and a wide central depression in positive hyporelief (Keighley & Pickerill 1996; Buatois *et al.* 1998b). The wide spacing between furrows is distinctive from *Didymaulichnus*. *Gyrochorte* is a smooth bilobed trail preserved in positive epirelief (Heinberg 1970, 1973), whereas *Didymaulichnus* is bilobed in positive hyporelief. Although the dorsal surface of *Didymaulichnus* is poorly known, cross-sections in Dzik (2005) suggest it was made of two lobes separated by a median furrow, which

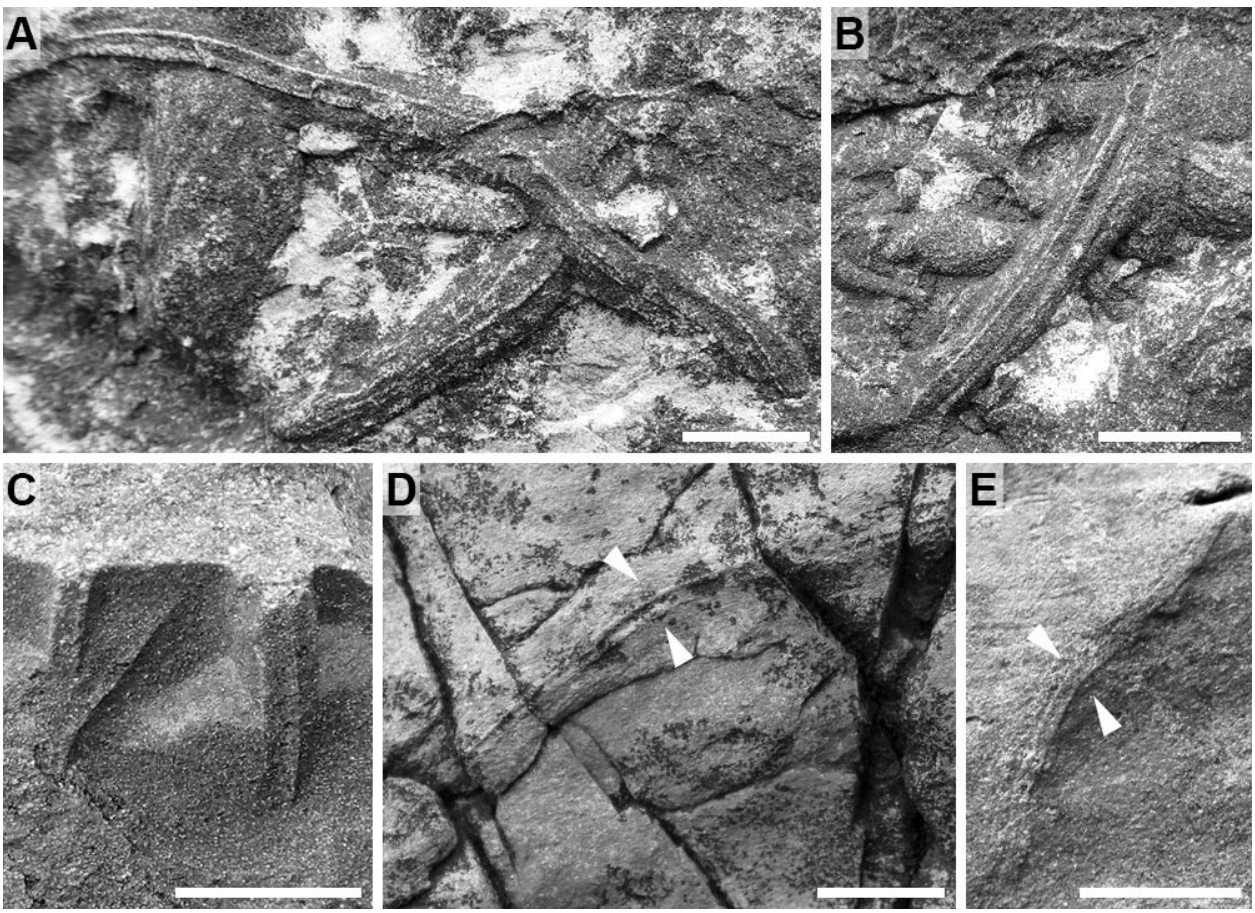

Fig. 30. Didymaulichnus miettensis Young. Scale bars are 1 cm. All photographs are positive hyporeliefs. **A**, Two specimens crossing each other. Note the variable distance between the lobes in the bottom specimen. Fortune North, Member 5 (Cambrian Age 2). **B**, Specimen with an incising median furrow, two well-spaced lobes and lateral bevels. Fortune North, Member 5 (Cambrian Age 2). **C**, Two specimens in cross-section: the left specimen only displays two parallel ridges, whereas right specimen has more depth and preserves lateral bevels. Grand Bank Head, Member 5 (Cambrian Age 2). **D**, A flattened specimen with closely spaced lobes and wide lateral bevels (arrows). Grand Bank Head, Member 5 (Cambrian Age 2). **E**, Lowermost specimen in the succession with distinct median ridges and, in places, faint bulging reminiscent of lateral bevels (arrows). Compare with specimens Figure 30C (left) and 30D. Fortune Head, Member 2A (Fortunian).

could make it close to *Gyrochorte* and *Psammichnites*. *Gyrochorte*, however, typically displays a negative relief in sandstone soles, and *Psammichnites* exhibits a complex backfill and additional morphological elements such as an axial ridge/groove (Mángano *et al.* 2002a). Finally, as noted by Seilacher *et al.* (2005), neighbouring simple horizontal trails oriented in parallel may be mistaken for *Didymaulichnus* (e.g. Bordonaro *et al.* 1992).

According to our taxonomic revision, convincing examples of *Didymaulichnus* have been recorded from the Cambrian (e.g. Jiang *et al.* 1982; Palij *et al.* 1983; Walter *et al.* 1989; Goldring & Jensen 1996; Jensen & Mens 2001; Dzik 2005) and the Ordovician (Pickerill *et al.* 1984b). Notably, simple bilobed forms need re-evaluation as some of these may display faint scratch imprints (e.g. Garcia-Ramos 1976, pl. 3, fig. f; El-Khayal & Romano 1988, fig. 5h; Vossler *et al.* 1989, fig. 2.1; Han & Pickerill 1994b, fig. 4F) that would allow their placement in *Cruziana*. In addition, *Didymaulichnus* has been mentioned in the Precambrian (Poiré *et al.* 1984; Grytsenko 2016; Kolesnikov & Bobkov 2019; Kolesnikov *et al.* 2023b). The morphology of these forms is typically very irregular, in many cases with unclear bilateral symmetry and absence of well-developed lobes. These structures are most likely related to shrinkage of microbial mats (Porada & Bouougri 2008; Buatois & Mángano 2016; see also Seilacher *et al.* 2005 and Jensen *et al.* 2006). *Didymaulichnus* has been attributed to arthropod producers (Collette *et al.* 2010), mollusks (Glaessner 1969; Young 1972), and priapulid worms (Dzik 2005, 2007). *Didymaulichnus* is recorded in marginal-marine (Collette *et al.* 2010) and shallow-marine (Young 1972; Pickerill *et al.* 1984b; Crimes & Jiang 1986; Walter *et al.* 1989; this study) environments. Crimes & Anderson (1985) first described and illustrated *Didymaulichnus* in the Chapel Island Formation, but subsequent reports were rare (Landing *et al.* 1988; Gehling *et al.* 2001).

***Didymaulichnus miettensis* Young, 1972**

Figure 30A–E

1985 *Didymaulichnus miettensis* Young; Crimes & Anderson, p. 316, fig. 5.5.

Material. – About sixty specimens from Member 2A (Fortunian) and Member 5 (Cambrian Age 2) in Fortune Head, Fortune North, and Grand Bank Head.

Description. – Horizontal, unlined, unbranched trails with two deep and sharp ventral ridges separated by a median furrow, and two lateral bevels. Preserved as positive hyporelief. The course is straight to slightly curving. Trails are either isolated or overlapping in dense associations. The median furrow can form a V shape in cross-section. The two ventral ridges are distinctly spaced or close together; these ridges are thin and sharp with clear outlines. Lateral bevels are deep and account for most of the height of the trail. Rarely, bevels are flattened or absent. Infill is massive, composed of very fine- to medium-grained sandstone similar from the host rock, or different from the mudstone host rock. Trail width is 0.2–1.4 cm; lobe width is 0.05–0.1 cm; distance between lobes is 0.1–0.3 cm; bevel width is 0–0.4 cm; maximum length is 34.0 cm.

Associated trace fossils. – *Didymaulichnus miettensis* co-occurs with *Curvolithus multiplex*, *Palaeophycus tubularis*, and *Psammichnites gigas circularis*.

Remarks. – The two ventral ridges and distinctive lateral bevels allow placing these trace fossils in *Didymaulichnus miettensis*. *Didymaulichnus miettensis* has only been found in the Cambrian, with recordings in Australia (Glaessner 1969; Walter *et al.* 1989), Canada (Young 1972; Fritz & Crimes 1985), China (Jiang *et al.* 1982; Sun 1985; Crimes & Jiang 1986), Iran (Shahkarami *et al.* 2017a), Mongolia (Goldring & Jensen 1996), Russia (Dzik 2005, 2007), and USA (Jensen *et al.* 2002b). The worldwide distribution of this ichnospecies has been highlighted by Jensen *et al.* (2013). Young (1972) noted that bevels can disappear along the course. This observation makes the revision of *Didymaulichnus miettensis* difficult when bevels are only mentioned in the text and are not clearly displayed in figures (e.g. Fritz & Crimes 1985). In the absence of bevels, these trace fossils do not differ fundamentally from *Didymaulichnus lyelli*, which is problematic. Lateral bevels are in places absent in Chapel Island Formation specimens. In these rare cases, it is still possible to identify the ventral ridges of *Didymaulichnus miettensis* because they are perfectly parallel, incise the sediment surface sharply (Fig. 30C, E), and are therefore comparable to the ventral ridges of more complete specimens possessing bevels. ?*Subphyllochorda* isp. in Hofmann & Patel (1989, fig. 2d) consists of two narrow ventral lobes and wide flat lateral bevels, which fits the diagnosis of *Didymaulichnus miettensis*. This form is similar to a specimen of *Didymaulichnus miettensis* found in the Chapel Island Formation (Fig. 30D). Similarly, *Scolicia* isp. in Palij *et al.* (1983, pl. 63, fig. 1) has two narrow median ridges and two distinct, deep and wide lateral bevels and belongs to *Didymaulichnus miettensis*.

In the Chapel Island Formation, the two ventral lobes are reduced to narrow ridges, which is unusual when compared to the wide lobes recorded in the type material (Young 1972) and elsewhere (e.g. Walter *et al.* 1979; Crimes & Jiang 1986; Dzik 2005), but is comparable to lobes observed in *Didymaulichnus tirasensis* (Palij 1974, fig. 1). Crimes & Anderson (1985) included Chapel Island Formation specimens within *Didymaulichnus miettensis*. We concur with their decision and do not consider the ratio 'width of the median lobes/total width' as relevant to erect a new ichnospecies. In the Chapel Island Formation, Crimes & Anderson (1985) only recorded *Didymaulichnus miettensis* from Member 5. This ichnotaxon is indeed more abundant in that part of the succession, but it is also found in Member 2A (Fig. 30E) where facies and environmental conditions are appropriate for its formation and preservation (i.e. in thicker sandstone beds representing higher-energetic conditions). With their narrow median lobes and wide lateral bevels, *Didymaulichnus miettensis* from the Chapel Island Formation match the morphology of trails produced by euthycarcinoid arthropods as recorded from the Cambrian of eastern Canada and USA (Collette *et al.* 2010).

Ichnogenus *Dimorphichnus* Seilacher, 1955a

Discussion. – *Dimorphichnus* is an asymmetric trackway with two types of series, one made of delicate elongated ridges (i.e. rakers) and the other made of short blunt imprints (i.e. pushers) (Seilacher 1955a). It is included in the category of architectural design of 'trackways and scratch imprints' (Buatois *et al.* 2017). *Dimorphichnus* was first described from the Cambrian Jutana Formation of northeastern Pakistan (Seilacher 1955a). Confusion arose when Crimes (1970) defined *Monomorphichnus*, a similar trace fossil displaying only rakers. Seilacher (1985, 1990a, 2007) considered the absence of pushers in *Monomorphichnus* as a taphonomic artifact (i.e. his 'undertrack deficiency') and placed it in synonymy with *Dimorphichnus*. However, *Monomorphichnus* has been repeatedly described in the literature, and we suggest maintaining this ichnotaxon for nomenclatural stability until further revision (see also *Monomorphichnus* section, p. 102).

At least nine *Dimorphichnus* ichnospecies have been erected: *D. obliquus* Seilacher, 1955a; *D. bontempii* Borrello, 1966; *D. hunanensis* Zhang & Wang in Zhang *et al.*, 1986; *D. quadrifidus* Seilacher, 1990a; *D. ebianensis* Shen & Zeng in Shen *et al.*, 1990; *D. reticularis* Shen & Zeng in Shen *et al.*, 1990; *D. ctenidos* Gámez-Vintaned, 1995; *D. suoxiyuensis* Zhang & Wang, 1996; and *D. juchemi* Zessin, 2008. The type ichnospecies, *Dimorphichnus obliquus*, has rakers forming bundles of two ridges (Seilacher 1955a; Hofmann *et al.* 2012). Borrello (1966) described *Dimorphichnus bontempii* as a single series of curved, subparallel, staggered ridges. The figured specimen (Borrello 1966, pl. 20, fig. 2) does not display the typical morphology of *Dimorphichnus*, with the second series of asymmetric imprints lacking, and *Dimorphichnus bontempii* may be better relocated within *Monomorphichnus* after revision of the type material. Zhang & Wang (1996) described *Dimorphichnus hunanensis* as two series of scratch imprints, the pushers having a tadpole shape whereas the rakers are curved, parallel to each other and can be split along their course (Zhang *et al.* 1986; Zhang & Wang 1996). Zhang & Wang (1996) did not clearly specify on which ground this ichnospecies was distinctive from others, and the photographs available (Zhang *et al.* 1986, pl. 1, figs 12–14; Zhang & Wang 1996, pl. 1, fig. 11) display closer similarities to *Cruziana* than to *Dimorphichnus* (see also Zhang *et al.* 1986, fig. 6.1, 6.2). *Dimorphichnus quadrifidus* has rakers forming bundles of four ridges (Seilacher 1990a). *Dimorphichnus ebianensis* has subparallel ridges/wrinkles (Shen *et al.* 1990, pl. 1, fig. 4). Its affinity to *Dimorphichnus* is dubious, and the photographed specimen is reminiscent of a partially preserved *Cruziana*. *Dimorphichnus reticularis* has oblique ridges oriented in V shapes and arranged onto two lobes (Shen *et al.* 1990, pl. 1, fig. 5). It should be relocated within *Cruziana*. *Dimorphichnus ctenidos* has large fusiform rakers with delicate subridges, and disorganized pushers (Gámez-Vintaned 1995). Zhang & Wang (1996) described *Dimorphichnus suoxiyuensis* as two series of scratch imprints, the pushers being reduced to dots, whereas the rakers are thin and elongated. It is difficult, however, to observe those features on the figured specimens (Zhang & Wang 1996, pl. 2, figs 6, 7), and re-evaluation of the type material is required. The holotype of *Dimorphichnus juchemi* has three subparallel ridges arranged in bundles repeated laterally (Zessin 2008, figs 9–11). The second asymmetric series of imprints typical of *Dimorphichnus* is absent, and therefore this material cannot be retained as an ichnospecies of *Dimorphichnus*. Consequently, only three ichnospecies, *Dimorphichnus ctenidos*, *D. obliquus*, and *D. quadrifidus*, are here considered valid. *Dimorphichnus suoxiyuensis* awaits re-evaluation of its type material.

Dimorphichnus shows similarities with *Allocotichnus* Osgood, 1970, *Diplichnites* Dawson, 1873, and *Monomorphichnus* Crimes, 1970. *Allocotichnus* is an asymmetric trackway with paired imprints arranged

en echelon that do not display the rakers and pushers arrangement of *Dimorphichnus* (Osgood 1970). *Diplichnites* is a trackway with two parallel series of imprints (Keighley & Pickerill 1998), and confusion with *Dimorphichnus* exists where imprints of each series are asymmetric (e.g. Pickerill *et al.* 1987; Such *et al.* 2007; Parcha & Singh 2010). *Monomorphichnus* has only a series of elongated rakers, whereas *Dimorphichnus* possesses two series of asymmetric imprints (Crimes 1970).

Dimorphichnus ranges from the Cambrian (e.g. Seilacher 1955a; Radwanski & Roniewicz 1963; Crimes 1970; Gámez-Vintaned 1995; Hofmann *et al.* 2012; Jago & Gatehouse 2014) to the Ordovician (e.g. Baldwin 1977b; Pickerill 1977; Fillion & Pickerill 1990; Mángano *et al.* 2005a). Pickerill *et al.* (1987, fig. 4a) described and illustrated a potential occurrence in the Silurian, although the figure caption refers to *Diplichnites* and indeed the trace fossil looks like a trackway without lateral repetition of series. Wang (1992, pl. 1, fig. 10) described a specimen from the Devonian, but the illustration is too poor to confirm that occurrence. Feng *et al.* (2019, fig. 7a–c, f) described material from the Triassic that is mostly made of elongated imprints, and the formation of asymmetric series is not demonstrated. Potential producers are arthropods, particularly trilobites or trilobitomorphs (e.g. Seilacher 1955a; Martinsson 1965; Osgood 1970; Bergström 1973; Baldwin 1978; Mikuláš 1995). *Dimorphichnus* is recorded in marginal-marine (e.g. Fillion & Pickerill 1990; Mikuláš 1995; Ghienne *et al.* 2010; Mángano *et al.* 2013, 2014; Jago & Gatehouse 2014) and shallow-marine (e.g. Radwanski & Roniewicz 1963; Crimes 1970; Pickerill & Peel 1990; Gámez-Vintaned 1995; MacNaughton & Narbonne 1999; Such *et al.* 2007) environments. *Dimorphichnus* has previously been mentioned in the Chapel Island Formation (e.g. Narbonne *et al.* 1987; Landing *et al.* 1988; Hantsoo *et al.* 2018).

***Dimorphichnus* isp. A**

Figure 31A, B

Material. – Two specimens from Members 2A and 2B (Fortunian) in Fortune Head and Grand Bank Head.

Description. – Horizontal scratch imprints made of two types of series: (1) deep, punctuate imprints; and (2) subparallel elongated ridges. Preserved as positive hyporelief. Punctuate imprints are clustered together in groups of 8–15 imprints. Elongated ridges form either one series or two series in parallel. Punctuate imprints and elongated ridges incise the surface sharply. Dimension of the punctuate imprint cluster is 0.7–5.0 cm wide; individual punctuate imprint is 0.05–0.3 cm. Width of elongated ridges series is 0.4–9.5 cm; individual elongated ridge width is 0.01–0.5 cm; maximum elongated ridge length is 7.0 cm; number of elongated ridges per series is 4–10. Maximum distance covered is 25.4 cm.

Associated trace fossils. – *Dimorphichnus* isp. A co-occurs with *Palaeophycus tubularis*.

Remarks. – Two asymmetric series made of elongated ridges and deep punctuate imprints allow comparison with *Dimorphichnus suoxiyuensis*. However, because the type material of *Dimorphichnus suoxiyuensis* needs to be re-evaluated (see above), we refer to specimens from the Chapel Island Formation as *Dimorphichnus* isp. A. Elongated ridges imply the sidling of the tracemaker, and the sharp punctuate imprints indicate the vertical contact of the tips of the producer's limbs with the sediment. To form punctuate imprint aggregates, the producer used either a small set of limbs repeatedly, or a large set of limbs all at once. Contrary to the Chapel Island Formation material, pusher imprints in *Dimorphichnus obliquus* and *D. quadrifidus* are forming a series and have an elongated to tapered shape. A similar morphology to the Chapel Island Formation material has been recorded by Fillion & Pickerill (1990, pl. 6, fig. 9) as *Dimorphichnus obliquus* with 'dotlike pushing imprints to the left and elongate, straight raking scratch marks to the right'. In the Chapel Island Formation, the parallel orientation of the elongated ridges in one specimen (Fig. 31A) is also reminiscent of *Monomorphichnus biserialis* as described by Mikuláš (1995). However, Mikuláš (1995) did not mention the additional presence of punctuate imprints. Simón López-Villalta (2019) described *Dimorphichnus* isp. from the Cambrian with elongated subparallel ridges associated with small knobs. The circular shape of knobs and the absence of clustering of the knobs in the figured material (Simón López-Villalta 2019, fig. 6A) do not allow to confirm the interpretation as pusher imprints that would be related to the elongated ridges (rakers) on that surface.

***Dimorphichnus* isp. B**

Figure 31C–F

2017 *Monomorphichnus* isp. Landing *et al.*, p. 45, fig. 17B.

Material. – Two specimens from Member 2A (Fortunian) in Grand Bank Head and Lewin's Cove (on a loose slab).

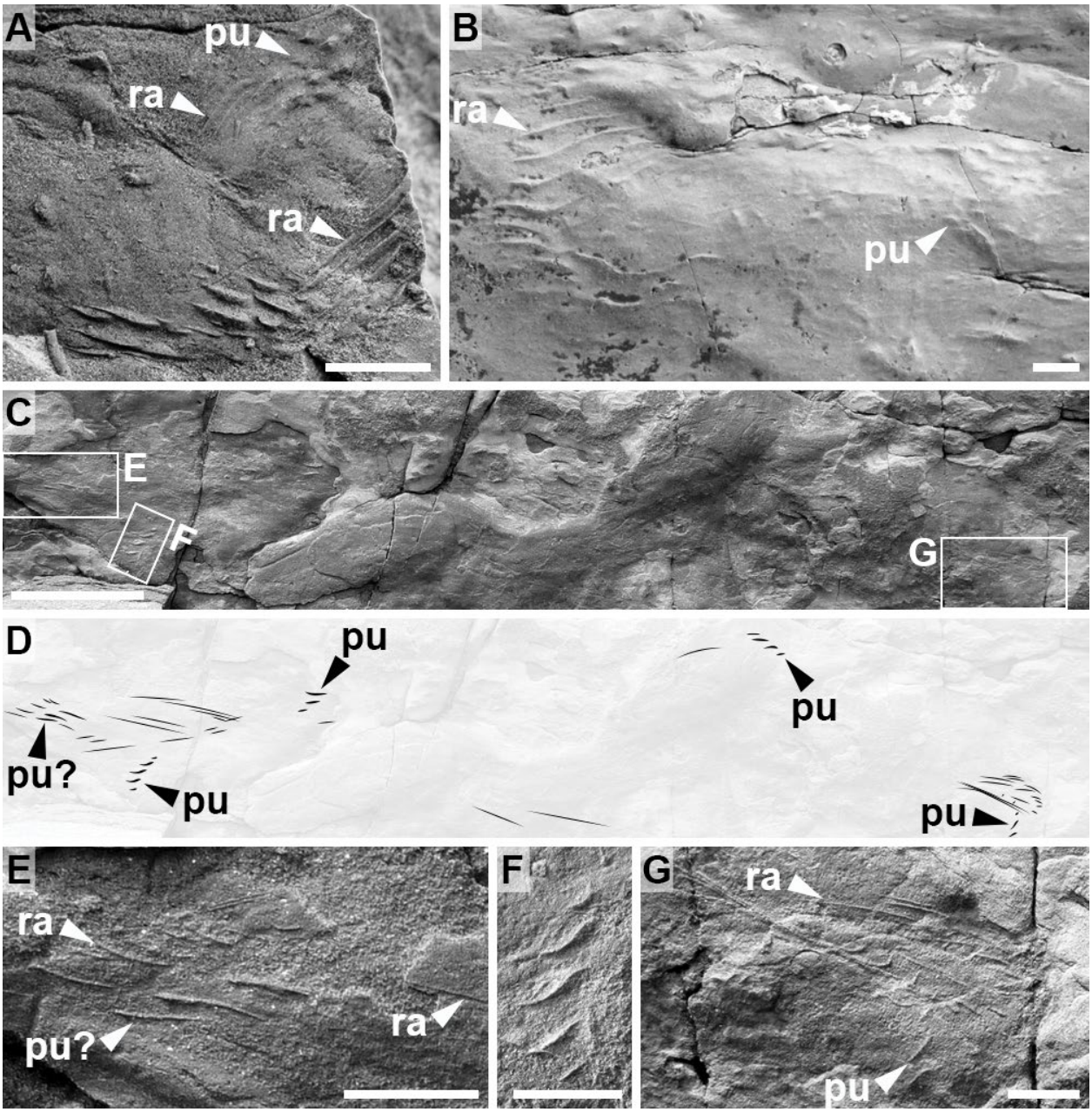

Fig. 31. Dimorphichnus isp. A (A, B) and *Dimorphichnus* isp. B (C–G). 'pu' corresponds to pusher imprints; 'ra' to elongated raker ridges. Scale bars are 1 cm (A, B, D–G) and 5 cm (C). All specimens are positive hyporeliefs. **A**, *Dimorphichnus* isp. A with two parallel series of elongated raker ridges, and a cluster of punctuate pusher imprints. Note the additional series of deep and short imprints oriented at a different angle (bottom); these may represent a partially preserved *Dimorphichnus* isp. B specimen, although their lack of arrangement into series precludes a definitive conclusion. Fortune Head, Member 2B (Fortunian). **B**, *Dimorphichnus* isp. A with raker ridges starting slightly deeper, then becoming elongated and ending by an aggregate of punctuate pusher imprints. Grand Bank Head, Member 2A (Fortunian). **C**, General view of a specimen showing the overall distance traveled by the producer. Grand Bank Head, Member 2A (Fortunian). **D**, Line drawing from Figure 31C. **E**, Close-up from Figure 31C showing possible pusher imprints and raker ridges. **F**, Close-up from Figure 31C showing pusher imprints. **G**, Close-up from Figure 31C showing pusher imprints and crisscrossing raker ridges.

Description. – Horizontal scratch imprints made of two types of series: (1) series of subparallel, prominent imprints; and (2) series of subparallel to disorganized, delicate, elongated ridges. Preserved as positive hyporelief. Both types of series are preserved on the same surface and are oriented in the same direction or slightly obliquely (about 30°–50° of deviation). Prominent imprints are either very short, slightly curved, or sigmoidal. The thickness of those imprints is variable, but they are always more deeply printed than the elongated ridges. Elongated ridges are straight or gently curved. Distance between prominent imprints within a series is mostly constant, whereas elongated ridges have either a constant distance (i.e. subparallel) or can be

crisscrossing. Specimens are only identifiable on largely exposed surfaces. Width of prominent imprint series is 0.9–1.5 cm; individual prominent imprint width is 0.05–0.15 cm (at the thickest part); individual prominent imprint length is 0.2–0.8 cm; number of prominent imprints per series is 3–5. Width of elongated ridge series is 1.0–1.3 cm; individual elongated ridge width is 0.01 cm; maximum elongated ridge length is 3.8 cm; number of elongated ridges per series is 3–12. Maximum distance covered is 47.6 cm.

Associated trace fossils. – *Dimorphichnus* isp. B does not occur with other formally described ichnotaxa.

Remarks. – Series with two distinctive types of imprints are diagnostic of *Dimorphichnus*. However, the organization of elongated ridges in the Chapel Island Formation specimens is different from that of the valid *Dimorphichnus* ichnospecies: *D. ctenidos* has large fusiform elongated ridges with delicate subridges, *D. obliquus* has elongated ridges forming bundles of two, and *D. quadrifidus* has elongated ridges forming bundles of four. Although Fillion & Pickerill (1990) only emphasized the sigmoidal nature of elongated ridges as the key feature in *Dimorphichnus obliquus*, the holotype clearly demonstrates the formation of bundles of two elongated ridges (Seilacher 1955a, pl. 17). This has also been indicated in other reports (Seilacher 1990a; Hofmann *et al.* 2012; Mángano *et al.* 2013). Consequently, a specimen of *Dimorphichnus obliquus* figured in Fillion & Pickerill (1990, pl. 6, fig. 6), where the elongated ridge series are composed of a single bundle of two ridges, may require re-evaluation.

In the Chapel Island Formation, the formation of bundles within elongated ridge series is extremely rare. These ridges are either disorganized or parallel to each other without distinctive pattern. Disorganized ridges, if they were to be found alone, would have been difficult to distinguish from tool/drag marks (see also *Monomorphichnus* section, p. 102). This illustrates the difficulty in demonstrating the biogenicity of such structures, and large exposures are essential to provide confident interpretations. Here, the association of two types of imprint morphologies advocates for biogenicity.

cf. *Dimorphichnus* isp.

Figure 32A, B

2019 *Dimorphichnus* cf. *D. obliquus* Seilacher; Laing, Mángano, Buatois, Narbonne & Gougeon, p. 1626, fig. 2r.

Material. – One specimen from Member 2A (Fortunian) in Grand Bank Head.

Description. – Horizontal scratch imprints made of two types of series: (1) shallow, subparallel, elongated ridges; and (2) slightly deeper, parallel, elongated imprints. Preserved as positive hyporelief. Deeper imprints are forming groups of 3 ridges. Shallow ridges are subparallel and not organized in bundles. Group of deeper imprints is 0.3 cm wide; individual deeper imprint width is 0.05 cm; maximum deeper imprint length is 0.7 cm. Individual shallow ridge width is 0.05 cm; maximum individual shallow ridge length is 1.5 cm; number of subparallel shallow ridges is 12+. Maximum distance covered is 5.6 cm.

Associated trace fossils. – cf. *Dimorphichnus* isp. co-occurs with *Helminthoidichnites tenuis*.

Remarks. – Two asymmetric series made of shallower elongated ridges and deeper imprints allow comparison with *Dimorphichnus*. However, the lack of clear arrangement with each type of imprints, the poor lateral repetition of series, and the presence of tool marks on the same surface (Fig. 32) warrant caution. As for other *Dimorphichnus* specimens, deeper imprints are interpreted as pushers from a primitive benthic arthropod, and shallow ridges as rakers (Fig. 32B).

Ichnogenus *Diplocraterion* Torell, 1870

Discussion. – *Diplocraterion* is a U-shaped, vertical to oblique burrow with spreiten (Fürsich 1974b; Schlirf 2011) included in the category of architectural design of 'vertical single U- and Y-shaped burrows' (Buatois *et al.* 2017). *Diplocraterion* was first described from the Cambrian File Haidar Formation of southern Sweden (Torell 1870; Westergård 1931; Jensen 1997). In his classic review, Fürsich (1974b) considered five ichnospecies attributed to *Diplocraterion* valid: *D. parallelum* Torell, 1870; *D. biclavatum* (Miller, 1875); *D. polyupsilon* (Smith, 1893); *D. habichi* (Lissón, 1904); and *D. helmerseni* (Öpik, 1929). The type ichnospecies, *Diplocraterion parallelum*, has parallel limbs (Torell 1870; Schlirf 2011). *Diplocraterion biclavatum*, formerly *Arthraria biclavata*, has limbs extending below the base of the deepest 'U' (Miller 1875; Fürsich 1974b). *Diplocraterion polyupsilon*, formerly *Corophioides polyupsilon*, has bidirected spreiten, both expanding vertically and laterally (Smith 1893; Fürsich 1974b). *Diplocraterion habichi*, formerly *Tigillites habichi*, is very narrow with the upward portion of limbs diverging laterally (Lissón 1904; Fürsich 1974b). *Diplocraterion helmerseni*, formerly *Corophioides helmerseni*, has an expanded base (Öpik 1929; Fürsich 1974b). Fürsich (1974b) did not comment on the status of *Diplocraterion morgani* Fleming, 1973. *Diplocraterion morgani* has

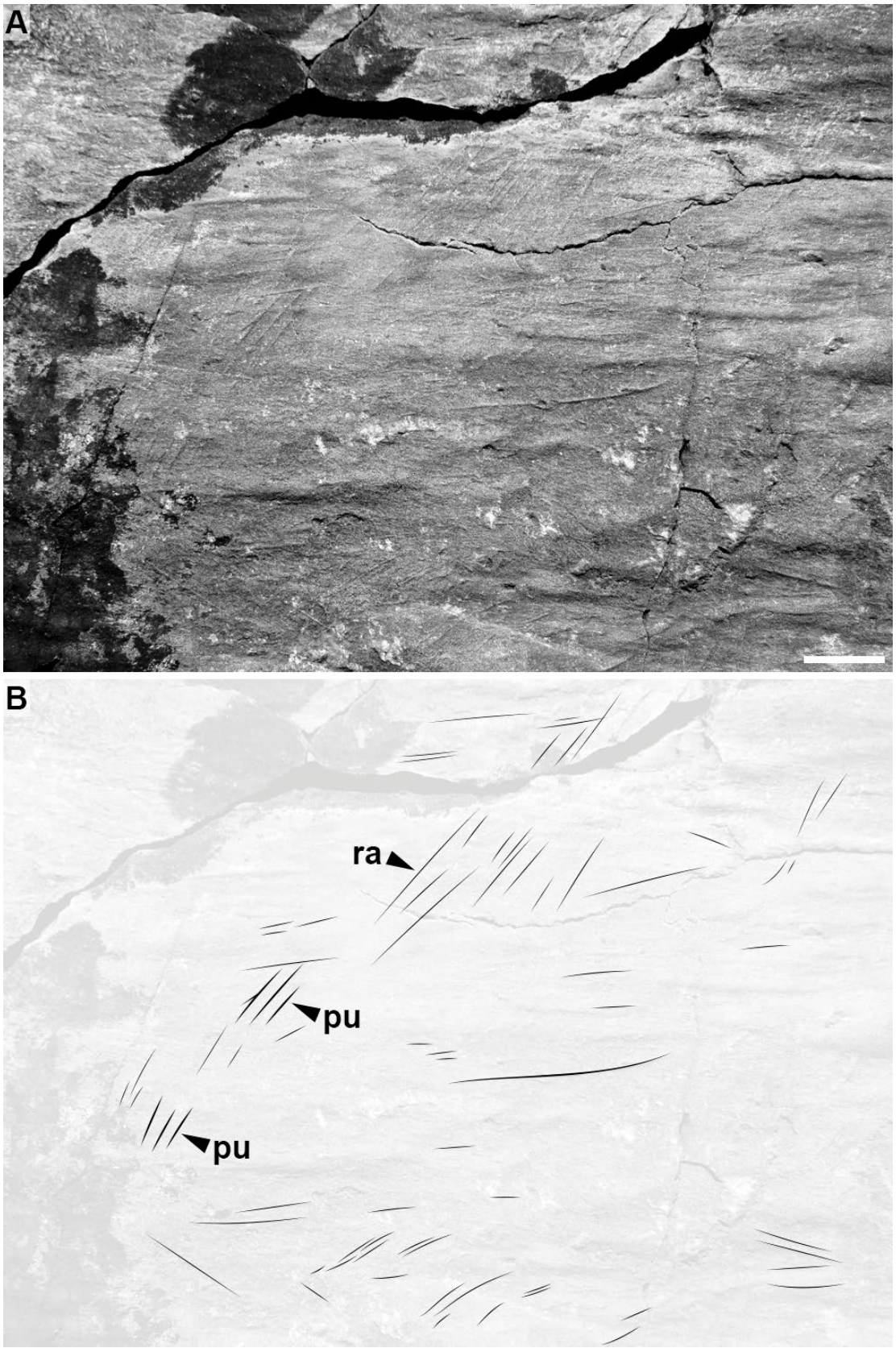

Fig. 32. cf. *Dimorphichnus* isp. Scale bar is 1 cm. Positive hyporelief, Grand Bank Head, Member 2A (Fortunian). **A**, General view of the slab. **B**, Line drawing from Figure 32A. Note pusher imprints (pu) and raker (ra) ridges.

closely spaced parallel limbs (Fleming 1973) and should therefore be regarded as a junior synonym of *D. parallelum* (but see Knaust 2019 for an alternative view). Since Fürsich (1974b) review, at least five more *Diplocraterion* ichnospecies have been described or re-evaluated: *D. ultimum* (de Saporta & Marion, 1883); *D. luniforme* (Blanckenhorn, 1916); *D. emiensis* Li & Yang, 1988; *D. asymmetrium* Ekdale & Lewis, 1991; and *D. dushanensis* Wang, 2005. According to Schlirf (2011), *Diplocraterion ultimum*, formerly *Taonurus ultimus*, is oriented obliquely. However, Knaust (2013) placed this ichnospecies in junior synonymy with *Rhizocorallium jenense*, a proposal endorsed here (see also Fernández & Pazos 2012). Pollard (1981) resurrected *Diplocraterion luniforme*, formerly *Arenicoloides luniformis*, for material with parallel limbs and a luniform morphology on bed surfaces. This latter distinction is taphonomic, and we agree with Fürsich (1974b) in the synonymy of *Diplocraterion luniforme* with *D. parallelum*. Yang *et al.* (2004) described *Diplocraterion emiensis* as having two limbs expanding below the causative U-shaped tube, which makes it a junior synonym of *D. biclavatum*. *Diplocraterion asymmetrium* has a very irregular causative burrow and poorly developed spreiten (Ekdale & Lewis 1991). Wang (2005) described *Diplocraterion dushanensis* as having a short distance between limbs that are composed of 'nodositial tubes'. The casting rock experienced a strong metamorphic cleavage that may have affected the morphology of burrows (see Wang 2005, pl. 1, figs 7, 8, pl. 2, figs 1–3, 5, 8). Knaust (2019) considered *Diplocraterion dushanensis* a junior synonym of *Tisoa siphonalis* de Serres without providing further explanation. Therefore, *Diplocraterion dushanensis* needs revision. In addition, Knaust (2019) considered *Diplocraterion habichi* to belong to *Tisoa* rather than *Diplocraterion*, proposing the new combination *Tisoa habichi*. However, Wetzel & Blouet (2023) recently reviewed topotype material of the type ichnospecies *Tisoa siphonalis* and considered the low-amplitude helicoidal course to be diagnostic, a feature that is absent in *Diplocraterion*. Consequently, six ichnospecies, *Diplocraterion asymmetrium*, *D. biclavatum*, *D. habichi*, *D. helmerseni*, *D. parallelum*, and *D. polyupsilon*, are here retained as valid.

Diplocraterion shows similarities with *Arenicolites* Salter, 1857, *Arthraria* Billings, 1872, *Bifungites* Desio, 1940, *Rhizocorallium* Zenker, 1836, *Teichichnus* Seilacher, 1955b, and *Tisoa* de Serres, 1840. *Arenicolites* is also a vertical U-shaped burrow (Salter 1857; Häntzschel 1975), but the absence of spreiten distinguishes it from *Diplocraterion*. The dumb-bell-shaped horizontal expression of *Diplocraterion* has led to a debate regarding the validity of *Arthraria* and *Bifungites*. However, *Arthraria* has no significant vertical development, whereas *Bifungites* is a U-shaped burrow without spreiten and with basal lateral chambers (Fillion & Pickerill 1984a; Gougeon *et al.* 2025c). With its U-shaped causative burrow and spreiten, *Diplocraterion* compares with *Rhizocorallium*. However, *Rhizocorallium* is oriented horizontally (Schlirf 2011; Knaust 2013). *Teichichnus* is characterised by a vertical spreite system produced by the displacement of a subhorizontal causative burrow (Seilacher 1955b; Knaust 2018a). This ichnogenus can be reminiscent of *Diplocraterion* depending on the degree of curvature of the causative burrow (Corner & Fjalstad 1993). In addition, specimens of *Diplocraterion* observed in vertical section and cut perpendicularly through the spreiten may look like *Teichichnus* (e.g. Goldring 1962). Therefore, detailed analysis of taphonomic variants can be required to discriminate between those forms. Finally, and as discussed above, *Tisoa* differs from *Diplocraterion* by the low-amplitude helicoidal course of the former (Wetzel & Blouet 2023).

Diplocraterion ranges from the Cambrian (e.g. Westergård 1931; Palij *et al.* 1983; Clausen & Vilhjálmsson 1986; Cornish 1986; Bromley & Hanken 1991; Zhang *et al.* 2017a) to the Holocene (e.g. Seilacher 1967a; Ekdale & Lewis 1991; Gingras *et al.* 1999, 2001, 2008; Hauck *et al.* 2009). Producers are arthropods (e.g. Seilacher 1967a; Bromley 1996; Dashtgard *et al.* 2008, 2017; Gingras *et al.* 1999, 2008) and annelid worms (e.g. Seilacher 1967a; Schäfer 1972; Gingras *et al.* 2001; Pemberton *et al.* 2001; Hauck *et al.* 2009). *Diplocraterion* is typically recorded in marginal-marine (e.g. Fürsich 1975; Cornish 1986; Pollard 1981; Goldring *et al.* 2005; Higgs & Higgs 2015; Zhang *et al.* 2017a) and shallow-marine (e.g. Heinberg & Birkelund 1984; Mason & Christie 1986; Orłowski 1989; Dam 1990; Gaillard & Racheboeuf 2006; Rodríguez-Tovar *et al.* 2007) environments. Continental (Kim & Paik 1997) and deep-marine (Leszczynski *et al.* 1996; Hubbard & Shultz 2008; Riahi *et al.* 2014) occurrences are less common. In the Chapel Island Formation, *Diplocraterion* was first recorded in Members 3 and 5 by Narbonne *et al.* (1987), but illustrated material has not been provided so far (see also Landing *et al.* 1988, 2017, and Gougeon *et al.* 2018a).

?*Diplocraterion* isp.

Figure 33A, B

Material. – Five specimens from Members 4 and 5 (Cambrian Age 2) in Grand Bank Head and Little Dantzic Cove.

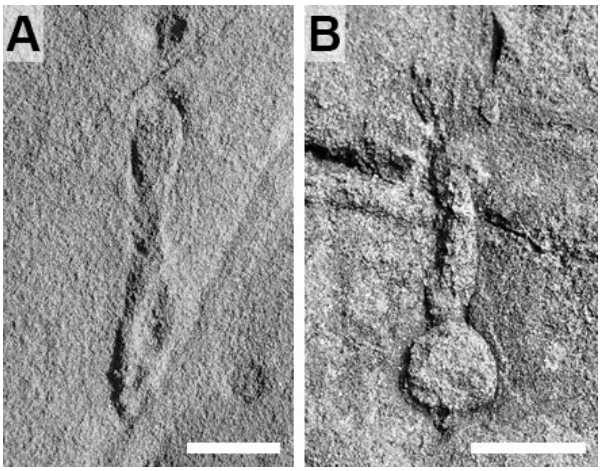

Fig. 33. ?*Diplocraterion* isp. Scale bars are 1 cm. All photographs are full reliefs from Little Dantzic Cove, Member 5 (Cambrian Age 2). **A**, Specimen with narrow terminations. Note the surrounding pits of unknown affinity. **B**, Specimen with wide terminations connected by a thin bar.

Description. – Dumb-bell-shaped trace fossils made of circular terminations and a connecting bar. Preserved as full relief (on bed bases and tops). Terminations are typically wider than the connecting bar. Burrows are unlined or surrounded by a thin lining. Infill is massive, composed of fine-grained sandstone similar to the host rock; infill can also be pyritized. Termination width is 0.5–1.6 cm; connecting bar width is 0.2–0.4 cm; connecting bar length is 1.4–2.4 cm; length of combined terminations and connecting bar is 2.4–4.9 cm.

Associated trace fossils. – ?*Diplocraterion* isp. co-occurs with *Psammichnites gigas circularis* and *Palaeophycus tubularis*.

Remarks. – ?*Diplocraterion* isp. is interpreted to represent the horizontal expression of a U-shaped causative burrow (i.e. the marginal terminations) connected by inner spreiten (i.e. the connecting bar). Because the vertical expression of the trace fossil is not exposed, we adopt a conservative approach and designate these burrows as ?*Diplocraterion* isp., although similar reports from the Cambrian were referred to as *Diplocraterion* isp. (e.g. Crimes *et al.* 1977; Fritz & Crimes 1985; Crimes & Jiang 1986; Walter *et al.* 1989; Mángano *et al.* 2013). Zonneveld *et al.* (2012, fig. 4A) noted that some specimens of *Diplocraterion* do not develop spreiten through the whole length of the causative U-shaped burrow, and the resulting horizontal expression would correspond, in part, to a pair of unconnected circular burrows. In Members 4 and 5 of the Chapel Island Formation, large *Trichichnus* isp. are common but are not observed as pairs. Pairing of burrows on bed tops in that part of the succession can be confidently affiliated to *Arenicolites* isp. because multiple specimens present on the same surface never display spreiten (Fig. 21C). At Burin Peninsula, Crimes & Anderson (1985) recorded similar ?*Diplocraterion* isp. but only from the overlying Random Formation.

Ichnogenus *Gordia* Emmons, 1844

Discussion. – *Gordia* is a horizontal trace fossil with self-overcrossing (Emmons 1844; Hofmann & Patel 1989) included in the category of architectural designs of 'simple horizontal trails' (Buatois *et al.* 2017). *Gordia* was first described from the Ordovician 'Hudson River Group' of northeastern USA (Emmons 1844; Hall 1847; Schneer 1978). Häntzschel (1975) placed *Helminthoidichnites* in synonymy with *Gordia*. However, the holotype of *Gordia* displays a distinctive looping pattern (Emmons 1844, pl. 2, fig. 2), a feature mostly absent in *Helminthoidichnites* (Fitch 1850, p. 866). Later, Hofmann & Patel (1989) restored the taxonomic separation of *Gordia* and *Helminthoidichnites* (see also Hofmann 1990), which has been followed by subsequent authors (e.g. Fillion & Pickerill 1990; MacNaughton & Pickerill 1995; Pickerill & Fyffe 1999; Uchman *et al.* 2009), although with rare exceptions (e.g. Gaillard & Racheboeuf 2006, fig. 5.5; Villegas-Martín & Netto 2019, fig. 4).

Buatois *et al.* (1998a) considered four *Gordia* ichnospecies valid: *G. marina* Emmons, 1844; *G. indianensis* (Miller, 1889); *G. arcuata* Książkiewicz, 1977; and *G. nodosa* Pickerill & Peel, 1991. The type ichnospecies, *Gordia marina*, has a smooth outline (Emmons 1844; Hofmann & Patel 1989). *Gordia indianensis*, formerly *Haplotichnus indianensis*, has sharp angles along its course (Buatois *et al.* 1998a). Re-examination of the type material by Getty & Bush (2017) revealed the presence of projections at each angle which are diagnostic of *Treptichnus bifurcus*. *Gordia arcuata* has a partial arc-shaped loop (Książkiewicz 1977). Absence of self-overcrossing is problematic, and *Gordia arcuata* may be better regarded as a preservational variant of *Circulichnis montanus* (see *Circulichnis* section, p. 59). *Gordia nodosa* has annulations (Pickerill & Peel 1991). In addition, at least nine other ichnospecies attributed to *Gordia* have been described and are discussed here: *G. molassica* (Heer, 1865); *G. vermicularis* (Fritsch, 1908); *G. carickensis* (Smith, 1909); *G. maeandria* Jiang in Jiang *et al.*, 1982; *G. hanyangensis* Yang & Hu in Yang *et al.*, 1987; *G. gyratus* Hu & Meng in Hu *et al.*, 1991; *G. lushanensis* Hu & Meng in Hu *et al.*, 1991; *G. multilaqua* Yin, Li & He, 1993; and *G. iramica* Vilmova, 2012. *Gordia molassica*, formerly *Helminthoida molassica*, has meanders and self-overcrossing (Heer 1865; Książkiewicz 1977)

and has been considered a junior synonym of *Gordia marina* (Pickerill 1981; Uchman 1998). *Gordia vermicularis*, formerly *Spongolithus vermicularis*, is a sinusoidal to loosely meandering trail without self overcrossing (Fritsch 1908, pl. 12, fig. 2; see also Mikuláš 1992) and is unrelated to *Gordia*. *Gordia carickensis*, formerly *Mermia carickensis*, displays dense loops forming scribbles (Smith 1909). Uchman *et al.* (2009) transferred *Mermia carickensis* to *Gordia*, regarding abundant loops and scribbles as significant at ichnospecific level (see also Pickerill & Peel 1991 and Getty *et al.* 2017). However, other authors (e.g. Buatois & Mángano 1993a; Pazos *et al.* 2007; Alonso-Muruaga *et al.* 2012; Hofmann *et al.* 2012; Lima *et al.* 2017) regarded these as diagnostic features at ichnogenus level, therefore retaining *Mermia* as a valid ichnogenus with *M. carickensis* as its type ichnospecies, a decision endorsed here. *Gordia maeandria* is an irregular meandering trail with lateral levees or lobes (Jiang *et al.* 1982, pl. 2, fig. 1; Crimes & Jiang 1986, fig. 4h), which are features absent in *Gordia* and reminiscent of other ichnotaxa such as *Archaeonassa* or *Psammichnites*. *Gordia hanyangensis* is smooth with self-overcrossing (Yang *et al.* 1987) and is considered a junior synonym of *G. marina* (Fillion & Pickerill 1990). *Gordia gyratus* (see Hu *et al.* 1991, pl. 1, figs 4–6, 8, 9, 12, 14) and *G. lushanensis* (see Hu *et al.* 1991, pl. 1, fig. 16) are sinusoidal to circular structures identical to 'Manchuriophycus'-type syneresis cracks. Therefore, both are here regarded as microbially induced sedimentary structures rather than trace fossils. *Gordia multilaqua* consists of dense, curving and subparallel horizontal segments, with at least one instance of self-overcrossing displayed in the type material (Yin *et al.* 1993, pl. 3, fig. 1). Pokorný *et al.* (2017) placed it in synonymy with *Helminthoidichnites*, but the presence of at least one self-overcrossing is problematic. Re-evaluation of the type material of *Gordia multilaqua* is required, and this ichnospecies is provisionally not retained as valid. *Gordia iramica* was neither figured nor described (Vilmova 2012) and is a *nomen nudum*. Finally, Runnegar (1992) briefly mentioned the ichnospecies *Gordia antiqua* from Ediacara (Australia) without formally erecting it. Later, material refered to as *Gordia antiquaria* from Flinders Ranges (Australia) was figured in Fedonkin & Vickers-Rich (2007, fig. 398), and may correspond to the same material as *G. antiqua*. This specimen displays a simple overcrossing course which corresponds to the diagnostic feature of *Gordia marina*. In any case, absence of formal erection makes *Gordia antiqua* (or *G. antiquaria*) a *nomen nudum*. To summarize, only the two ichnospecies *Gordia marina* and *G. nodosa* are here considered valid.

Gordia shows similarities with *Archaeonassa* Fenton & Fenton, 1937a, *Circulichnis* Vialov, 1971, *Helminthoidichnites* Fitch, 1850, *Helminthopsis* Heer, 1877, and *Mermia* Smith, 1909. Some authors (e.g. Crimes & Anderson 1985; Walter *et al.* 1989) mentioned lateral levees along trails attributed to *Gordia*, but this feature is more typical of *Archaeonassa* (Fenton & Fenton 1937a; Jensen 2003) and is considered of higher ichnotaxonomic rank as it informs about the mode of construction. *Circulichnis* is a horizontal trail with a circular course (Uchman & Rattazzi 2019) but, unlike *Gordia*, does not show self-overcrossing. In the same vein, self-overcrossing in *Gordia* distinguishes it from straight to curved *Helminthoidichnites* and irregularly meandering *Helminthopsis* (Hofmann & Patel 1989; Narbonne & Aitken 1990; Vidal *et al.* 1994a; Uchman *et al.* 2009; Pokorný *et al.* 2017; Gougeon *et al.* 2018b). *Mermia* is a trail with intense crossovers (Smith 1909; Pollard & Walker 1984; Walker 1985; Buatois & Mángano 1993a), whereas crossovers in *Gordia* are solitary.

Gordia ranges from the Ediacaran (e.g. Glaessner 1969; Fritz & Crimes 1985; Narbonne & Hofmann 1987; Gibson 1989; Vidal *et al.* 1994a; Buatois & Mángano 2016) to the Holocene (e.g. Bajard 1966; Ratcliffe & Fagerstrom 1980; Metz 1987a; Martin 2009; Scott *et al.* 2009; Zachos & Platt 2019). Inferred producers are arthropods (including insect larvae in continental settings; Bajard 1966; Metz 1987a; Zachos & Platt 2019), gastropods (Abel 1935), and worms (nematomorphs and annelids; Chamberlain 1975; Książkiewicz 1977; Martin 2009). *Gordia* is recorded in continental (e.g. Metz 1987a; Aceñolaza & Buatois 1993; Gradziński & Uchman 1994; MacNaugthon & Pickerill 1995; Melchor *et al.* 2003; Netto *et al.* 2012), marginal-marine (e.g. Narbonne 1984; Buatois *et al.* 1998a; Balistieri *et al.* 2002; Lucas *et al.* 2004), shallow-marine (e.g. Narbonne & Hofmann 1987; Geyer & Uchman 1995; Knaust 2004; Gaillard & Racheboeuf 2006; Mángano 2011), and deep-marine (e.g. Książkiewicz 1977; Pickerill 1981; Crimes *et al.* 1992; McCann 1993; Uchman 1998; McIlroy 1999) environments. In the Chapel Island Formation, *Gordia* was first recorded by Crimes & Anderson (1985) and has been subsequently mentioned regularly (e.g. Narbonne *et al.* 1987; Laing *et al.* 2019).

***Gordia marina* Emmons, 1844**

Figure 34A–C

1985 *Gordia marina* Emmons; Crimes & Anderson, p. 318, fig. 6.6.

Material. – Seven specimens from Members 2A and 2B (Fortunian) in Fortune Head and Grand Bank Head.

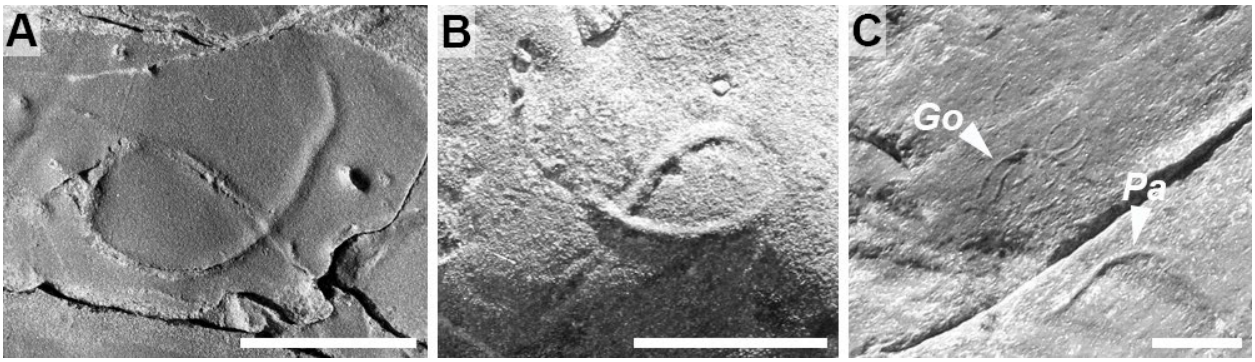

Fig. 34. Gordia marina Emmons. Scale bars are 0.5 cm (C) and 1 cm (A, B). **A**, Slightly irregular *Gordia marina*. Negative epirelief, Fortune Head, Member 2B (Fortunian). **B**, Regular *Gordia marina*. Positive hyporelief, Grand Bank Head, Member 2B (Fortunian). **C**, Minute regular *Gordia marina* (Go) associated with *Palaeophycus tubularis* (Pa). Positive epirelief, Fortune Head, Member 2A (Fortunian).

Description. – Smooth, unlined, unbranched, horizontal trails with a self-overcrossing. Preserved as positive hyporelief and positive and negative epirelief. The course is regular or irregular. The self-overcrossing forms an α-shape. Infill is massive, composed of very fine- to fine-grained sandstone similar to the host rock. Width is 0.05–0.2 cm; maximum length is 41.5 cm.

Associated trace fossils. – *Gordia marina* co-occurs with *Helminthoidichnites tenuis*, *Helminthopsis abeli*, *H. tenuis*, and *Palaeophycus tubularis*.

Remarks. – The presence of self-overcrossing and lack of annulations allow placing these trace fossils in *Gordia marina*. Another important feature of *Gordia marina* is the development of an α-shape (Keighley & Pickerill 1997). In the Chapel Island Formation, *Gordia marina* was only figured as a drawing by Crimes & Anderson (1985, fig. 6.6).

Ichnogenus *Gyrolithes* de Saporta, 1884

Discussion. – *Gyrolithes* is a vertical burrow forming a single helix (Bromley & Frey 1974; de Gibert *et al.* 2012) included in the category of architectural design of 'vertical helicoidal burrows' (Buatois *et al.* 2017). *Gyrolithes* was first described from the Cretaceous Vaals Formation of northeastern Belgium (de Saporta 1884; Bromley & Frey 1974). In a former review, Uchman & Hanken (2013) concluded that: (1) ichnospecies of *Gyrolithes* are first discriminated based on their wall and ornamentation (i.e. smooth, pelletal, striated, or with a thick lining), and (2) for unornamented walls, morphometric parameters are to be used. Two morphometric parameters are relevant for the characterisation of *Gyrolithes* (Uchman & Hanken 2013; De Renzi *et al.* 2017; Laing *et al.* 2018; De Renzi & Mayoral 2024): (1) the burrow radius r (2r representing the width of the burrow), and (2) the whorl radius R (2R representing the whorl diameter). The r/R ratio defines κ, a dimensionless parameter that is fitted to discriminate ichnospecies (Laing *et al.* 2018). However, the κ range offset of valid ichnospecies still displays extensive overlap, whether this was plotted in one (Laing *et al.* 2018, fig. 9) or two dimensions (Uchman & Hanken 2013, fig. 2). This is problematic because the selection process of the valid ichnospecies for a given *Gyrolithes* specimen or a group of taxonomically related specimens is not straightforward and can rely on a subjective decision made by the investigator. In addition, some of the decisions on the type of wall or ornamentation as described in Uchman & Hanken (2013) are not in agreement with the descriptions and illustrations of original materials (Fig. 35 and see below).

These issues prompted us to review extensively the literature on published material of *Gyrolithes*. In this study, primary decisions on valid ichnospecies are based on wall and ornamentation, as suggested by Uchman & Hanken (2013). Secondarily, κ was calculated for all holotype and topotype materials available, rarely for lectotypes (Bromley & Frey 1974) and neotypes (Muñiz & Belaústegui 2019), regardless of their wall and ornamentation types. The restriction of measurements to type materials is intended to provide an objective evaluation of the range offset of κ coming from one locality only, and to avoid biases created by the measurements of κ values from specimens of other localities. We emphasize that difficulties in measuring κ arise when dealing with burrows with variable width along the spiral [e.g. *Gyrolithes babkovi* (Hecker), *G. okinawaensis* Myint & Noda] (see also Bromley & Frey 1974). In those cases, a mean width was used for the calculation. In addition, measurements were only done where at least half of a whorl was illustrated. Finally, other morphological criteria than the ones retained by Uchman & Hanken

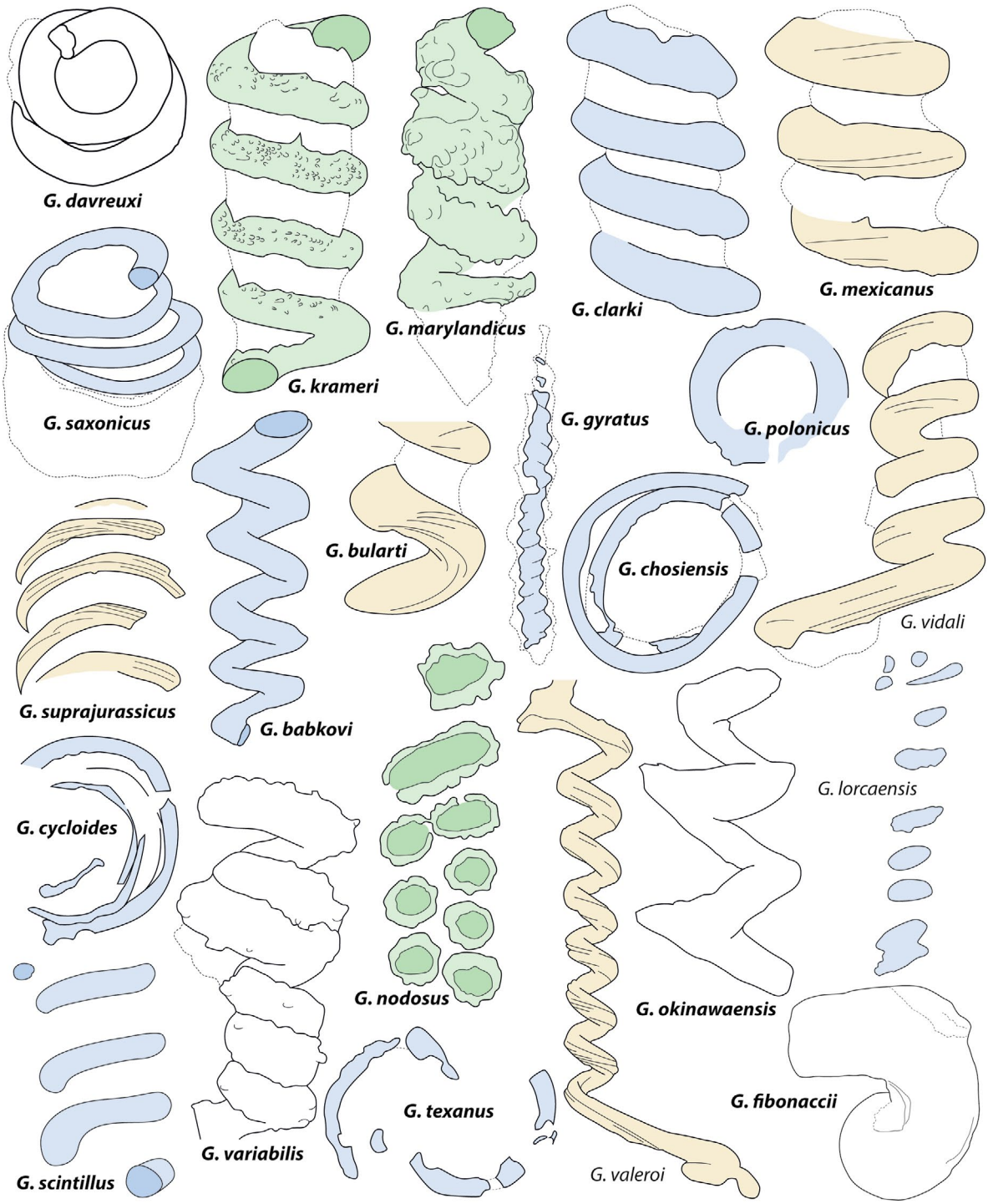

Fig. 35. Line drawings of holotype or lectotype materials of *Gyrolithes* de Saporta. *Gyrolithes dewalquei*, *G. krymensis*, *G. kunradensis*, and *G. triassica* are not illustrated as they do not display a helical morphology. Valid ichnospecies (after our revision) are in bold. Note the presence of pellets in *Gyrolithes krameri* and of longitudinal striae in *G. bularti*, *G. mexicanus*, *G. valeroi*, and *G. vidali*. Color code is the same as in Figure 36. Drawing of *Gyrolithes davreuxi* based on de Saporta (1884, pl. 5, fig. 3), of *G. krameri* on von Ammon (1900, fig. 4), of *G. marylandicus* on Mansfield (1927, pl. 2, fig. 1), of *G. clarki* on Mansfield (1930, pl. 1, fig. 1), of *G. mexicanus* on Mansfield (1930, pl. 1, fig. 3), of *G. saxonicus* on Häntzschel (1934, fig. 2), of *G. suprajurassicus* on Schneid (1938, p. 313), of *G. babkovi* on Hecker *et al.* (1962, pl. 22, fig. 4), of *G. bularti* on Macsotay (1967, pl. 12, fig. 49, left specimen), of *G. gyratus* on Hofmann (1979, pl. 15, fig. A), of *G. chosiensis* on Omori *et al.* (1992, pl. 1, fig. 1), of *G. polonicus* on Fedonkin (1977, pl. 5, fig. a), of *G. vidali* on Mayoral (1986, fig. 5), of *G. cycloides* on Mikuláš & Pek (1994, fig. 2), of *G. scintillus* on Laing *et al.* (2018, fig. 5A), of *G. variabilis* on Mayoral & Muñiz (1995, pl. 1, fig. 1), of *G. nodosus* on Mayoral & Muñiz (1998, pl. 1, fig. 1), of *G. texanus* on Morgan (2019, fig. 4A), of *G. valeroi* on Mendiola *et al.* (1998, pl. 4, fig. 1), of *G. okinawaensis* on Myint & Noda (2000, fig. 2A), of *G. lorcaensis* on Uchman & Hanken (2013, fig. 3a), and of *G. fibonacci* on Conti & Serventi (2023, fig. 6b).

(2013) are used to discriminate two additional ichnospecies: (1) *Gyrolithes variabilis* Mayoral & Muñiz with its conical shape, and (2) *G. okinawaensis* with its sharp lateral extensions (see below).

Twenty-six ichnospecies attributed to *Gyrolithes* were previously described in the literature: *G. davreuxi* de Saporta, 1884; *G. dewalquei* de Saporta, 1884; *G. krameri* (von Ammon, 1900); G. *kunradensis* Umbgrove, 1925; *G. marylandicus* (Mansfield, 1927); *G. clarki* (Mansfield, 1930); *G. mexicanus* (Mansfield, 1930); *G. saxonicus* (Häntzschel, 1934); *G. suprajurassicus* (Schneid, 1938); *G. babkovi* (Hecker in Hecker *et al.*, 1962); *G. bularti* Macsotay, 1967; *G. krymensis* Vialov, 1969; *G. gyratus* (Hofmann, 1979); *G. polonicus* Fedonkin, 1981; *G. triassica* Yang & Sun, 1982; *G. vidali* Mayoral, 1986; *G. chosiensis* Omori, Ishida & Adachi, 1992; *G. cycloides* (Mikuláš & Pek, 1994); *G. variabilis* Mayoral & Muñiz, 1995; *G. nodosus* Mayoral & Muñiz, 1998; *G. valeroi* Mendiola, Martinez, Blasco & Lopez, 1998; *G. okinawaensis* Myint & Noda, 2000; *G. lorcaensis* Uchman & Hanken, 2013; *G. scintillus* Laing, Buatois, Mángano, Narbonne & Gougeon, 2018; *G. texanus* Morgan, 2019; and G. *fibonaccii* Conti & Serventi, 2023. The type ichnospecies, *Gyrolithes davreuxi*, has a thick wall with a lectotype κ = 0.23–0.30 and topotype κ = 0.20–0.27 (de Saporta 1884, pl. 5, figs 1–4; Bromley & Frey 1974, pl. 1). *Gyrolithes dawalquei* is a burrow with either straight or U-shaped elements (de Saporta 1884, pl. 6, figs 3–5) and may represent partial *Thalassinoides* Ehrenberg segments (see also Bromley & Frey 1974). *Gyrolithes krameri*, formerly *Daemonhelix krameri*, has a holotype κ = 0.28–0.33 and topotype κ = 0.42 (von Ammon 1900, figs 4, 5). Uchman & Hanken (2013) recorded smooth outlines for *Gyrolithes krameri*, but the type material of von Ammon (1900, fig. 4) shows rugosities on its surface that could potentially correspond to remnants of pellets (see also Fig. 35). We provisionally retain it as a pellet-wall form until revision of the type material is done. *Gyrolithes kunradensis* is a straight fossil with circular cross-section (Umbgrove 1925, figs 1–5) that is unrelated to *Gyrolithes*. *Gyrolithes marylandicus*, formerly *Xenohelix marylandica*, has a pelletal wall with a holotype κ = 0.57–0.73 and topotype κ = 0.52–0.93 (Mansfield 1927, pl. 2, fig. 1, pl. 3, fig. 1). Other topotypical materials show smooth outlines (with κ = 0.54–0.60, Mansfield 1927, pl. 3, fig. 2) and longitudinal striations (with κ = 0.66–0.73, Gernant 1972, pl. 1, fig. 2), but these features should not be included in the diagnosis of *Gyrolithes marylandicus* to maintain consistency with the taxonomic rationale proposed in this study. Therefore, the variants with smooth and striated walls should be relocated in *Gyrolithes babkovi* and be ground for a new ichnospecies, respectively (following our revision Fig. 36B). *Gyrolithes clarki*, formerly *Xenohelix clarki*, has smooth outlines with a holotype κ = 0.27–0.30 and topotype κ = 0.32–0.42 (Mansfield 1930, pl. 1, fig. 1, pl. 2, fig. 1). *Gyrolithes mexicanus*, formerly *Xenohelix mexicana*, has a holotype κ = 0.29–0.32 (Mansfield 1930, pl. 1, fig. 3). Although Uchman & Hanken (2013) considered it smooth, the holotype has longitudinal striae that were correctly identified by Mansfied (1930) (see also Fig. 35). *Gyrolithes saxonicus*, formerly *Spongites saxonicus*, has smooth outlines with a holotype κ = 0.17–0.20 and topotype κ = 0.11–0.16 (Häntzschel 1934, figs 1, 2, 4). Uchman & Hanken (2013) considered that only material of small dimensions (i.e. Häntzschel 1934, figs 1, 2) should be retained as valid, and material of large dimensions (i.e. Häntzschel 1934, fig. 4) be placed in synonymy with *Gyrolithes cycloides*. However, the κ of holotype or topotype materials of *Gyrolithes saxonicus* never overlap with measurements from *G. cycloides*, and the synonymy is therefore not retained here (Fig. 36A, B). *Gyrolithes suprajurassicus*, formerly *Xenohelix suprajurassica*, has longitudinal striations with a holotype κ = 0.12 (Schneid 1938, p. 313; Uchman & Hanken 2013). *Gyrolithes babkovi*, formerly *Xenohelix babkovi*, has smooth outlines with a holotype κ = 0.40–0.66 (Hecker *et al.* 1962, pl. 22, fig. 4). *Gyrolithes bularti* has a holotype κ = 0.58 and topotype κ = 0.28–0.40 (Macsotay 1967, figs 49, 61). Uchman & Hankel (2013) mentioned smooth outlines and placed *Gyrolithes bularti* in synonymy with *G. krameri*, but Macsotay (1967, figs 49, 61–63) only described and figured specimens with distinct longitudinal striations (see also Fig. 35). *Gyrolithes krymensis* is a problematic burrow that does not display a helical morphology (Vialov 1969, p. 108) and, therefore, is not retained as valid. *Gyrolithes gyratus*, formerly *Skolithos gyratus*, has smooth outlines with a holotype κ = 0.63–1.00 and topotype κ = 0.50–1.00 (Hofmann 1979, pl. 5, figs A, B). *Gyrolithes polonicus* has smooth outlines with a holotype κ = 0.21 and topotype κ = 0.22–0.51 (Fedonkin 1977, pl. 5, figs a, b, g, 1981, pl. 22, figs 1–5, 8). Uchman & Hanken (2013) mentioned the presence of local perpendicular striations, but this is not observed in material figured by Fedonkin (1977, pl. 5, figs a, b, 1981, pl. 22, figs 1–5) and may be taphonomic (Jensen 1997). *Gyrolithes triassica* is a S-shaped burrow with only one specimen recovered (Yang & Sun 1982, pl. 2, fig. 6), and the development of a vertical helix is not demonstrated (Uchman & Hanken 2013). *Gyrolithes vidali* has a holotype κ = 0.23–0.43 and topotype κ = 0.44–0.54 (Mayoral 1986, pl. 1, figs 8–11). Uchman & Hankel (2013) mentioned smooth outlines and placed *Gyrolithes vidali* in synonymy with *G. krameri*, but Mayoral (1986, pl. 1, figs 8–11) recorded distinct longitudinal striations (see also Fig. 35). *Gyrolithes chosiensis* has smooth outlines with a holotype κ = 0.09–0.11 (Omori *et al.* 1992, pl. 1, fig. 1). *Gyrolithes cycloides*, formerly *Spirocircus cycloides*, has smooth outlines with a

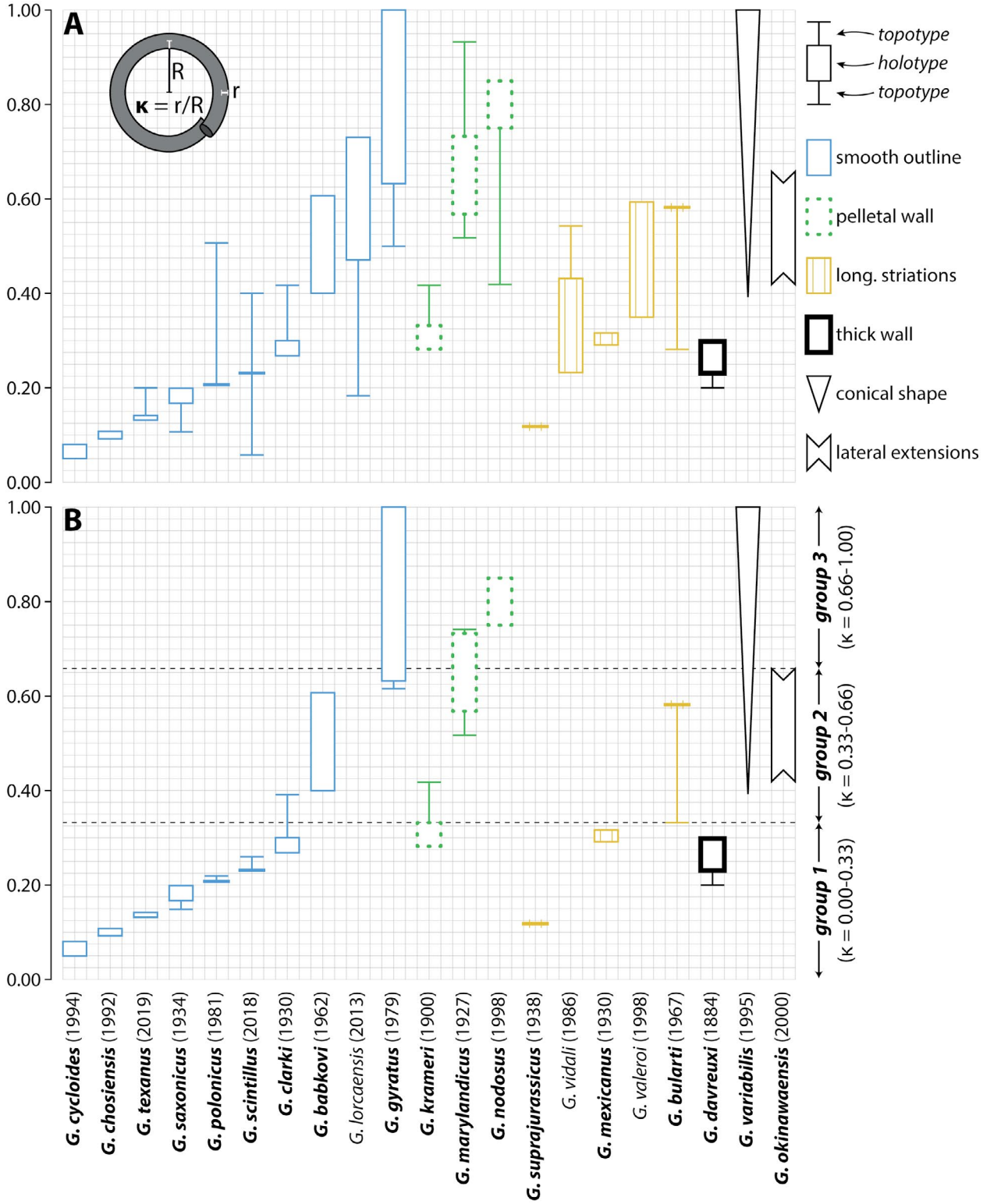

Fig. 36. Comparison of κ values calculated from type materials of *Gyrolithes* ichnospecies. **A**, Plot of all κ values. **B**, Discrimination of valid ichnospecies based on (by order of priority): (1) seniority where holotype ranges overlap (e.g. *G. mexicanus* versus *G. vidali*); (2) holotype range over topotype range (e.g. *G. babkovi* versus *G. gyratus*); and (3) seniority where topotype ranges overlap (e.g. *G. marylandicus* versus *G. nodosus*). Note that within each wall type, κ ranges never overlap across valid ichnospecies.

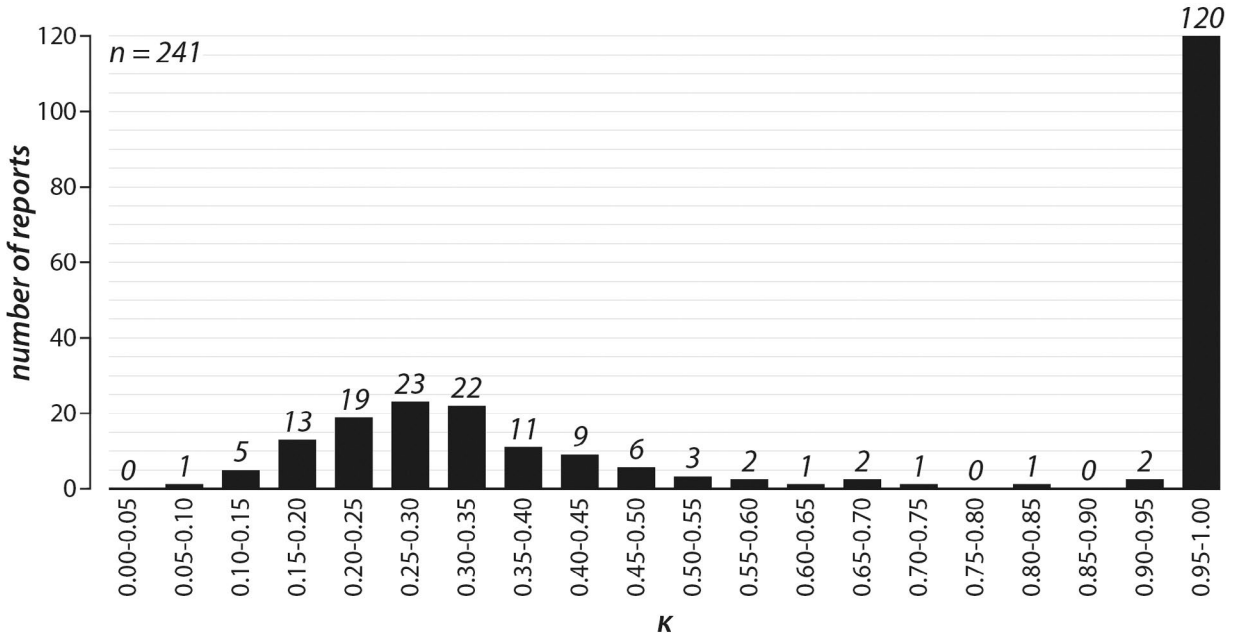

Fig. 37. Histogram showing the number of reports per categories of κ values highlighting a bimodal distribution (modes at κ = 0.20–0.35 and κ = 0.95–1.00). The two modes correspond to the range offsets of *Gyrolithes polonicus*/*G. scintillus*/*G. clarki* and *G. gyratus* as defined in this study (Fig. 36B); however, we adopt a conservative approach and consider the first mode to represent material belonging to *G. scintillus* solely (see text for further explanations).

holotype κ = 0.06–0.08 (Mikuláš & Pek 1994, fig. 2; Uchman & Hanken 2013). *Gyrolithes variabilis* has a holotype κ = 0.39–1.00 with a conical morphology (Mayoral & Muñiz 1995, pl. 1, fig. 1). Uchman & Hanken (2013) considered it smooth, but the holotype and some topotype materials (with κ = 0.45–0.90) show local pellets (Mayoral & Muñiz 1995, pl. 1, figs 1, 2, 4) (see also Fig. 35), whereas further topotypes have either smooth (with κ = 0.58–0.63, Mayoral & Muñiz 1995,pl. 1, fig. 3) or longitudinal striations (with κ = 0.39–1.00, Mayoral & Muñiz 1995, pl. 1, fig. 5). We suggest keeping the conical feature as diagnostic element of *Gyrolithes variabilis* and relocate non-conical smooth forms in *G. babkovi* and non-conical striated forms in *G. bularti* or a new ichnospecies depending on κ values (Fig. 36B). *Gyrolithes nodosus* has a pelletal wall with a holotype κ = 0.75–0.85, neotype κ = 0.42–0.71, and topotype κ = 0.45–0.70 (Mayoral & Muñiz 1998, pl. 1, figs 1–3, 6; Muñiz & Belaústegui 2019, fig. 6A). *Gyrolithes valeroi* has a holotype κ = 0.35–0.59 (Mendiola *et al.* 1998, pl. 4).Although Uchman & Hanken (2013) considered it smooth and synonym of *Gyrolithes krameri*, the type specimen clearly displays longitudinal striations that were accurately noted by Mendiola *et al.* (1998) (see also Fig. 35). *Gyrolithes okinawaensis* has smooth outlines with a holotype κ = 0.42–0.66 and sharp lateral extensions (Myint & Noda 2000, fig. 2). Although Uchman & Hanken (2013) considered *Gyrolithes okinawaensis* valid based on its mudstone wall, Myint & Noda (2000) emphasized the peculiar pointed-shape lateral extensions, and both features should be used as ichnotaxobases. *Gyrolithes lorcaensis* has smooth outlines with a holotype κ = 0.47–0.73 and topotype κ = 0.18–0.63 (Uchman & Hanken 2013, figs 3a, c, e, 4b). *Gyrolithes scintillus* has smooth outlines with a holotype κ = 0.23 and topotype κ = 0.11–0.40 (Laing *et al.* 2018, table 1). *Gyrolithes texanus* has a smooth wall, supposedly with rare pellets, and a holotype κ = 0.13–0.14 and topotype κ = 0.18–0.20 (Morgan 2019, figs 3A, 4A, C). *Gyrolithes fibonaccii* stands alone among *Gyrolithes* ichnospecies, as it is made of a single whorl with a burrow width tapering downward (Conti & Serventi 2023).

Figure 36A shows a graph of all κ values measured from type materials of *Gyrolithes* ichnospecies. κ range offsets demonstrate some overlap, notably: (1) κ from the holotype of *Gyrolithes lorcaensis* (κ = 0.47–0.73) overlaps with κ from both holotypes of *G. babkovi* (κ = 0.40–0.66) and *G. gyratus* (κ = 0.63–1.00); (2) κ from the holotype of *G. vidali* (κ = 0.23–0.43) overlaps with κ from the holotype of *G. mexicanus* (κ = 0.29–0.32); and (3) κ from the holotype of *G. valeroi* (κ = 0.35–0.59) overlaps with κ from both holotypes of *G. vidali* (κ = 0.23–0.43) and *G. bularti* (κ = 0.58). In addition, *Gyrolithes babkovi*/*G. gyratus*, *G. mexicanus*, and *G. bularti* have seniority over *G. lorcaensis*, *G. vidali*, and *G. valeroi*, respectively. Therefore, we consider *Gyrolithes lorcaensis* a junior synonym of *G. babkovi* or *G. gyratus* depending on the κ range

offset, *G. vidali* a junior synonym of *G. mexicanus*, and *G. valeroi* a junior synonym of *G. bularti* (Fig. 36B).

Furthermore, we refined the limits of κ range offset for each ichnospecies to avoid overlap with other ichnospecies (Fig. 36B). In practice, material recovered from one locality may cover the κ range offset of more than one ichnospecies. In those cases, we suggest to first identify the number of modes of κ values from that locality (e.g. Fig. 37), and secondarily to assign each mode to a valid ichnospecies based on its closest affinity with the κ range offset of valid ichnospecies (using Fig. 36B as a basis for ichnospecies selection). An example is provided below with the description of *Gyrolithes gyratus* and *G. scintillus* in the Chapel Island Formation (see also Fig. 37).

Gyrolithes shows similarities with *Augerinoichnus* Minter, Lucas, Lerner & Braddy, 2008, *Avetoichnus* Uchman & Rattazzi, 2011, *Daimonhelix* Barbour, 1892, *Helicodromites* Berger, 1957, *Helicolithus* Häntzschel, 1962, *Ichnogyrus* Bown & Kraus, 1983, *Lapispira* Lange, 1932, and *Megagyrolithes* Gaillard, 1980. *Augerinoichnus*, *Avetoichnus*, and *Helicodromites* are helical burrows oriented horizontally (Poschmann 2015; Buatois *et al.* 2017), which differs from the vertical orientation of *Gyrolithes*. *Helicolithus* is also a horizontal helix with regular meanders and lateral branches (i.e. uniramous graphoglyptid: Książkiewicz 1977; Seilacher 1977). *Daimonhelix* is a meter-scale vertical helical burrow placed in synonymy with *Gyrolithes* by some authors (Fillion & Pickerill 1990; Jensen 1997), and its ichnotaxonomic validity is still pending further revision (Laing *et al.* 2018). *Ichnogyrus* is a vertical helical burrow with whorls in contact (Bown & Kraus 1983) that awaits revision as whorls can also be in contact in *Gyrolithes gyratus* (see also 'Remarks' in *G. gyratus* below). The single vertical helix of *Gyrolithes* differs from the connected double helices of *Lapispira* (Lanés *et al.* 2007; Gibert *et al.* 2012). *Megagyrolithes* is a meter-scale vertical helical burrow with horizontal branching segments (Gaillard 1980) and is potentially a junior synonym of *Gyrolithes* (Jensen 1997; Buatois *et al.* 2017).

Gyrolithes typically ranges from the Cambrian (e.g. Banks 1970; Fedonkin 1977; Liñan 1984; Jensen 1997; Hofmann *et al.* 2012; Mángano & Buatois 2014) to the Holocene (e.g. van der Horst 1934; Powell 1977; Dworschak & Rodrigues 1997; Felder 2001; Wetzel *et al.* 2010; Dashtgard & Gingras 2012). However, *Gyrolithes gyratus* has been recorded a few meters below the Ediacaran–Cambrian boundary point in the Chapel Island Formation (Gehling *et al.* 2001; this study). Another Ediacaran report by Jenkins (1981) needs re-evaluation (Baghiyan-Yazd 1998). Producers are crustacean arthropods (e.g. Dworschak & Rodrigues 1997; Felder 2001; Pervesler 2002; Belaústegui & Muñiz 2016), enteropneusts (van der Horst 1934; Gingras *et al.* 1999; Hauck *et al.* 2009; Dashtgard & Gingras 2012), and annelid worms (Hertweck & Reineck 1966; Howard & Frey 1975; Powell 1977; Gingras *et al.* 1999). *Gyrolithes* is typically recorded in marginal-marine (e.g. Keij 1965; Ranger & Pemberton 1988; Buatois *et al.* 2005; Wetzel *et al.* 2010; Rodríguez-Tovar *et al.* 2019; Melnyk & Gingras 2020) and shallow-marine (e.g. Banks 1970; Jensen 1997; Systra & Jensen 2006; Belaústegui & Muñiz 2016; Muñiz & Belaústegui 2019) environments. Deep-marine reports are more unusual (Conti & Serventi 2023; Hovikoski *et al.* 2025), some being regarded as produced by doomed pioneers (Föllmi & Grimm 1990; Grimm & Föllmi 1994). *Gyrolithes* was first recorded in the Chapel Island Formation by Crimes & Anderson (1985, fig. 6.7, 6.8), and was later mentioned either as *Skolithos annulatus* (= *G. gyratus*) (e.g. Narbonne *et al.* 1987; Herringshaw *et al.* 2017), *G. polonicus* (e.g. Gehling *et al.* 2001; Hantsoo *et al.* 2018), or *G. scintillus* (Laing *et al.* 2018, 2019).

Gyrolithes gyratus (Hofmann, 1979)

Figure 38A, B

1987 *Skolithos annulatus* (Howell); Narbonne, Myrow, Landing & Anderson, p. 1287, fig. 6H.

2001 *Skolithos annulatus* (Howell); Gehling, Jensen, Droser, Myrow & Narbonne, p. 216, fig. 2c.

2016 *Gyrolithes* de Saporta; Mángano & Buatois, p. 115, fig. 3.27e, f.

2017 *Skolithos annulatus* (Howell); Herringshaw, Callow & McIlroy, p. 375, fig. 3a.

2018 *Gyrolithes gyratus* (Hofmann); Laing, Buatois, Mángano, Narbonne & Gougeon, pp. 176, 178, 179, figs 5D, F, 6, 8.

2019 *Gyrolithes gyratus* (Hofmann); Laing, Mángano, Buatois, Narbonne & Gougeon, p. 1626, fig. 2h.

Material. – About one hundred specimens from Member 2A (Ediacaran) and Members 2A and 2B (Fortunian) in Fortune Head, Grand Bank Head, and Point May.

Description. – Vertical, unlined, unbranched, sinistral, or dextral helical burrow with r = 0.025–0.1 cm, R = 0.025–0.15 cm and κ = 0.40–1.00 (mean κ = 0.81). Preserved as full relief. Whorls can be clearly distinct and distant from one another or compacted and in contact. Burrows are oriented vertically or, more rarely, obliquely. Burrows are found isolated or forming aggregates repeated laterally at the same stratigraphical level. In places, burrows are pyritized. Burrows can develop a horizontal extension departing from the deepest whorl. Infill is massive, composed of very fine- to fine-grained sandstone different from

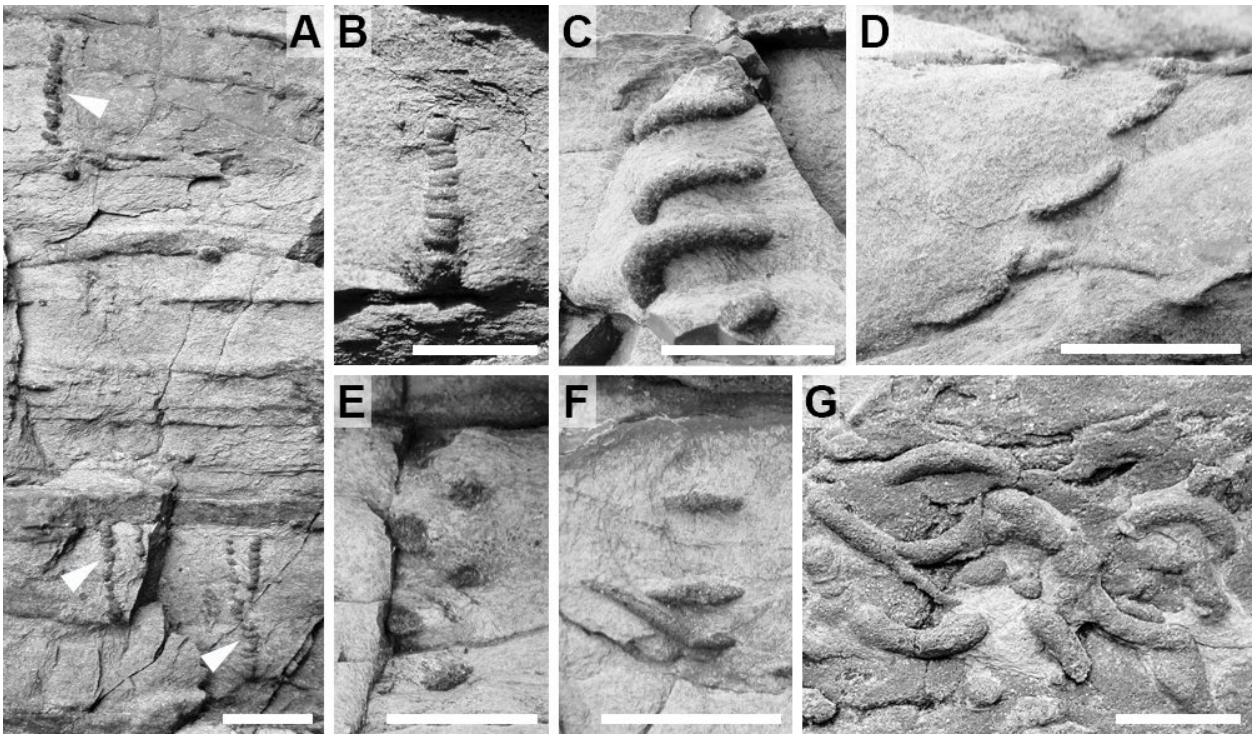

Fig. 38. Gyrolithes gyratus (Hofmann) (A, B) and *G. scintillus* Laing, Buatois, Mángano, Narbonne & Gougeon (C–G). Scale bars are 1 cm (A, C–G) and 3 mm (B). All photographs are from Member 2A (Fortunian). **A**, *Gyrolithes gyratus* at different stratigraphic levels (arrows). κ = 0.67–1.00. See also Laing *et al.* (2018, figs 6, 8) for close-ups. Full relief, Fortune Head. **B**, *Gyrolithes gyratus* with distinct horizontal whorls. Orientation of whorls is interpreted as a result of compaction. κ = 0.83–1.00. Full relief, Fortune Head. **C**, Holotype of *Gyrolithes scintillus*. κ = 0.27–0.31. Full relief, Fortune Head. **D**, *Gyrolithes scintillus* showing lateral deviation of the whorls. κ = 0.14–0.20. Full relief, Fortune Head. **E**, Cross-section through the whorls of *Gyrolithes scintillus*. κ = 0.31–0.37. Full relief, Fortune Head. **F**, *Gyrolithes scintillus* with a basal extension. κ = 0.32–0.35. Full relief, Fortune Head. **G**, Partially preserved *Gyrolithes scintillus*. It is not possible to calculate κ from this material. Positive hyporelief, Grand Bank Head.

the mudstone host rock. Maximum depth is 3.9 cm; maximum number of whorls is 16.

Associated trace fossils. – *Gyrolithes gyratus* co-occurs with *G. scintillus*, *Palaeophycus* isp., and *Trichichnus linearis*.

Remarks. – Morphometric parameters (κ = 0.40–1.00) overall agree with an affiliation to *Gyrolithes gyratus* (Fig. 36B). The lower κ values (from 0.40 to 0.62) are outside the range of our revision on *Gyrolithes* ichnospecies (Fig. 36B) but are not too far from the limits of topotype material of *G. gyratus* (Fig. 36A; Hofmann 1979). Therefore, we consider that overall, this material is closer in affinity to the second mode of κ values recorded in the Chapel Island Formation, with its peak at κ = 1.00 (Fig. 37). *Gyrolithes gyratus* is not a common ichnospecies and is only recorded from the Cambrian (Laing *et al.* 2018, 2019; Gougeon *et al.* 2023; this study) and the Ordovician (Hofmann 1979). The type material of *Skolithos annulatus*, to which this material was previously assigned (see synonym list above), consists of distinct transverse ring-like annulations that do not develop a helix (Howell 1957, fig. 1; Alpert 1974). *Ichnogyrus nididens* Bown & Kraus has a κ = 1.00 (Bown & Kraus 1983, fig. 7B) and overlaps in morphometric parameters with *Gyrolithes gyratus*. However, *Ichnogyrus* never deviates from this extreme κ value and has every whorl in contact, two morphological characters that could discriminate *Ichnogyrus* from *Gyrolithes*.

Gyrolithes scintillus Laing, Buatois, Mángano, Narbonne & Gougeon, 2018

Figure 38C–G

? 2001 *Gyrolithes polonicus* Fedonkin; Gehling, Jensen, Droser, Myrow & Narbonne, p. 216, fig. 2c.
? 2002 *Gyrolithes* de Saporta; Droser, Jensen, Gehling, Myrow & Narbonne, p. 9, fig. 6C.
2014 *Gyrolithes* de Saporta; Tarhan & Droser, p. 319, fig. 9B.
2016 *Gyrolithes* isp. Mángano & Buatois, p. 90, fig. 3.9c.
2017 *Gyrolithes polonicus* Fedonkin; Herringshaw, Callow & McIlroy, p. 375, fig. 3b.
2017 *Gyrolithes* isp. Landing *et al.*, p. 45, fig. 17C.
2018a *Gyrolithes* de Saporta; Gougeon, Mángano, Buatois, Narbonne & Laing (supplementary material), pp. 6, 8, 10, figs 4a, b, d, 5a, d, 6a, e.
2018 *Gyrolithes polonicus* Fedonkin; Hantsoo, Kaufman, Cui, Plummer & Narbonne, p. 1243, fig. 2i.

2018 *Gyrolithes scintillus* isp. nov. Laing, Buatois, Mángano, Narbonne & Gougeon, p. 176, fig. 5A-C, E.
2019 *Gyrolithes scintillus* Laing, Buatois, Mángano, Narbonne & Gougeon; Laing, Mángano, Buatois, Narbonne & Gougeon, p. 1626, fig. 2i.
2020 *Gyrolithes scintillus* Laing, Buatois, Mángano, Narbonne & Gougeon; Mángano & Buatois, p. 14, fig. 3b.

Material. – About 105 specimens from Members 2A, 2B, and 3 (Fortunian) in Fortune Head, Fortune North, Grand Bank Head, Lewin's Cove, Little Dantzic Cove, and Point May.

Description. – Vertical, unlined, unbranched, sinistral, or dextral helical burrow with r = 0.025–0.05 cm, R = 0.1–0.55 cm and κ = 0.11–0.50 (mean κ = 0.26). Preserved as full relief. Whorls are horizontal to oblique and are typically well separated or in proximity (but not in contact). Burrows are vertical to slightly oblique. Burrows are rarely pyritized. Burrows can develop a horizontal to oblique extension departing from the deepest whorl. Infill is massive, composed of very fine- to medium-grained sandstone different from the mudstone host rock. Maximum depth is 5.0 cm; maximum number of whorls is 9.

Associated trace fossils. – *Gyrolithes scintillus* co-occurs with *Conichnus conicus*, *G. gyratus*, *Palaeophycus* isp., *Treptichnus pedum*, and *Trichichnus linearis*.

Remarks. – Morphometric parameters (κ = 0.11–0.50) overall agree with holotype and topotype measurements on *Gyrolithes scintillus* (Fig. 36A). Extreme lower and upper values are more unusual, and the mean κ value of our specimens (i.e. κ = 0.26, Laing *et al.* 2018) falls within the range offset of *Gyrolithes scintillus*. The first mode of κ values in the Chapel Island Formation is spanning the 0.20–0.35 interval (Fig. 37), which corresponds to most of the range of *G. scintillus*. *Gyrolithes scintillus* is a recently introduced ichnospecies (Laing *et al.* 2018) that belongs to the group 1 of *Gyrolithes* ichnospecies possessing low κ values (Uchman & Hankel 2013; Laing *et al.* 2018; Fig. 36B). Partially preserved Cambrian specimens displaying less than a whorl (e.g. *Gyrolithes* sp. in Liñán 1984, pl. 2, figs 2–4; *Gyrolithes* cf. *G. polonicus* in Baghiyan-Yazd 1998, pl. 10, fig. B; *Gyrolithes* isp. in Jensen & Grant 1998, fig. 5b, Jensen & Mens 1999, fig. 3, Jensen *et al.* 2018a, fig. 6B; *Gyrolithes* in Högström *et al.* 2013, fig. 5H; McIlroy & Brasier 2017, fig. 6b) require further investigation of more complete material for accurate taxonomic affiliation. A basal straight extension in *Gyrolithes* as seen in some specimens of the Chapel Island Formation (Fig. 38F) was also recorded in younger material (e.g. Gernant 1972; Muñiz & Belaústegui 2019), but its purpose is unknown in the lower Cambrian. *Gyrolithes scintillus* has recently been described from suspected coeval strata (cf. Landing 2004) of the Chapel Island Formation in Nova Scotia (Barr *et al.* 2020). Material described in open nomenclature by Banks (1970, pl. 2, fig. c) displays three whorls and potentially represents additional Cambrian *Gyrolithes scintillus*. Moczydłowska *et al.* (2001, fig. 6h) recorded *Gyrolithes* isp. in Cambrian cores from Sweden, but the helical vertical development in the figured specimen is difficult to confirm.

Ichnogenus *Halopoa* Torell, 1870

Discussion. – *Halopoa* is a horizontal burrow with inflated segments covered with irregular ridges or wrinkles (Uchman 1998; Mángano *et al.* 2002b) included in the category of architectural design of 'horizontal burrows with simple vertically oriented spreiten' (Buatois *et al.* 2017). *Halopoa* was first described from the Cambrian File Haidar Formation of central Sweden (Torell 1870; Jensen 1997). Torell (1870) erected *Halopoa composita* and *H. imbricata* without providing photographed specimens or a type ichnospecies. Later, Andrews (1955) designated *Halopoa imbricata* as the type ichnospecies, and Martinsson (1965) figured and discussed a lectotype slab and additional material from the museum of the Geological Survey of Sweden. Jensen (1997) re-studied the collected material of *Halopoa* and evaluated its potential similarities with *Fucusopsis* Palibin and *Palaeophycus* Hall. Subsequently, Uchman (1998) reviewed the type material of *Fucusopsis* and regarded it as a junior synonym of *Halopoa*. The presence of inflated, vertically stacked segments in *Halopoa* (Uchman 1998; Mángano *et al.* 2002b) does not fit the diagnosis of *Palaeophycus* (cf. Pemberton & Frey 1982), although these are not evident in the type material (S. Jensen, pers. comm., 2024). *Halopoa* is here retained as valid, following the proposal of Uchman (1998, 1999).

Five *Halopoa* ichnospecies have been previously described in the literature: *H. composita* Torell, 1870; *H. imbricata* Torell, 1870; *H. annulata* (Książkiewicz, 1970); *H. indica* Badve & Ghare, 1978; and *H. storeana* Uchman, 2001. The type ichnospecies, *Halopoa imbricata*, is unbranched with long furrows and wrinkles (Torell 1870; Jensen 1997; Uchman 1998). The slab containing the type material of *Halopoa composita* (Jensen 1997, fig. 50) displays different burrows that can be assigned to *Halopoa imbricata*, *Phycodes* Richter, and *Treptichnus*, which prevents the retention of *H. composita* as valid (Martinsson 1965; Jensen 1997). *Halopoa annulata*, formerly *Fucusopsis annulata*, is commonly branched with perpendicular constrictions (Uchman 1998). The diagnostic features of *Halopoa indica* are unclear from the description and illustration of Badve & Gadve (1978). However, they noted that *Halopoa indica*

differs from *H. imbricata* by 'being plaited', which suggests that it may represent a senior synonym of *H. storeana* (cf. Uchman 2001). Accordingly, re-evaluation of the type material of *Halopoa indica* is needed. *Halopoa storeana* has oblique, plait-like wrinkles (Uchman 2001). In addition, Bayet-Goll *et al.* (2015, p. 633) mentioned *Halopoa hieroglyphica* without further description, but this was probably a typo referring to *Helminthopsis hieroglyphica*. Consequently, three ichnospecies, *Halopoa annulata*, *H. imbricata*, and *H. storeana*, are provisionally retained, pending re-evaluation of the type material of *H. indica*.

Halopoa shows similarities with *Asterosoma* von Otto, 1854, *Palaeophycus* Hall, 1847, and *Teichichnus* Seilacher, 1955b. *Asterosoma* is composed of horizontal concentric bulbs, and mainly differs from *Halopoa* by its branching tendency and the pronounced fusiform shape of its elements (Seilacher 2007; Monaco 2014). *Palaeophycus* is a simple passively filled, lined, subhorizontal burrow (Pemberton & Frey 1982; Keighley & Pickerill 1995). Some ichnospecies of *Palaeophycus* possess longitudinal wrinkles and striae (see *Palaeophycus* section, p. 107) which created confusion with *Halopoa* (e.g. Osgood 1970; Crimes & McCall 1995; Jensen 1997). However, *Palaeophycus* does not display the bulging and stacking pattern (i.e. vertical spreiten) observed in *Halopoa*. *Teichichnus* is a vertical spreite system formed by the displacement of a subhorizontal burrow (Knaust 2018a) and differs from *Halopoa* by the absence of bulging and more regular and developed vertical spreiten (Uchman 1998).

Halopoa ranges from the Cambrian (e.g. Martinsson 1965; Poulsen 1967; Seilacher 1990a; Jensen 1997; Orłowski & Żylińska 2002; Davies *et al.* 2009) to the Miocene (e.g. Crimes & McCall 1995; Monaco & Checconi 2010; Monaco & Trecci 2014). Ediacaran *Halopoa* isp. recorded by Hofmann & Mountjoy (2010) does not display inflated elements nor wrinkles on the surface of the structure. Based on its overall morphology, it would fit best within *Palaeophycus*. Possible producers are crustacean arthropods (Nathorst 1881; Seilacher 2007) and annelid worms (priapulids; Birkenmajer 1959; Hakes 1976; Książkiewicz 1977; Seilacher 2007). *Halopoa* is recorded in marginal-marine (Hakes 1976; Mángano *et al.* 2002b; Desjardins *et al.* 2010b), shallow-marine (e.g. Orłowski & Żylińska 2002; Knaust 2004; Davies *et al.* 2009; Astibia *et al.* 2017; Darngawn *et al.* 2018) and deep-marine (e.g. Crimes & McCall 1995; Uchman 1998; Monaco *et al.* 2010; Knaust *et al.* 2014; Wetzel & Uchman 2018; Adserá *et al.* 2020) environments. A possible continental occurrence was recorded by Hagdorn (2014) as ?*Halopoa*, although D. Knaust (pers. comm. in Hagdorn, 2014) considered it as *Asterosoma*. Examination of the specimen figured does not allow to confirm any of these assignments. *Halopoa* had not been recorded in the Chapel Island Formation previously.

***Halopoa imbricata* Torell, 1870**

Figure 39A–C

Material. – Seven specimens from Member 2B (Fortunian) in Grand Bank Head.

Description. – Horizontal elongated burrows with inflated intervals and partially preserved longitudinal striae. Preserved as positive hyporelief and negative epirelief. Burrows are circular to elliptical in cross-section, with a straight to curved course. Burrows are isolated or imbricated, commonly forming pairs. Longitudinal striations are subparallel to each other and discontinuous. Burrow width can be highly variable, with almost invariably thinning and tapering at both ends. A very thin lining is observable in few specimens. Branching is absent, although paired burrows can be in close proximity. Infill is massive, composed of fine-grained sandstone similar to the host rock. Width is 0.6–1.2 cm; maximum length is 9.0 cm.

Associated trace fossils. – *Halopoa imbricata* co-occurs with *Palaeophycus tubularis*, *Psammichnites gigas circularis*, and *Treptichnus pedum*.

Remarks. – The presence of inflated intervals and longitudinal striae allows comparison with *Halopoa imbricata*. Striae in *Halopoa imbricata* have been described as subparallel ridges and wrinkles (e.g. Jensen 1997; Uchman 1998), both features observed in the Chapel Island Formation specimens. Overlapping of burrows without branching in *Halopoa imbricata* is also typical (e.g. Jensen 1997; Uchman 1998; Knaust 2004; Monaco 2014; Kilibarda & Schassburger 2018; Madon 2021). Distinction from *Palaeophycus striatus* relies mostly on the inflated intervals along the burrow, and the common pairing and imbrication of specimens.

The lectotype slab of *Halopoa imbricata* (Martinsson 1965, fig. 29; Jensen 1997, fig. 45) displays specimens of variable sizes and shapes, with many burrows seemingly flattened and wrinkles typically visible on their outlines. *Halopoa imbricata* from the Cambrian of Poland (Orłowski & Żylińska 2002) and *Halopoa* cf. *H. imbricata* from the Cambrian of Denmark (Poulsen 1967) are conspecific with the Chapel Island Formation material, presenting elongated burrows tapering at their ends and subparallel longitudinal striae. Weber *et al.* (2013) recorded '*Palaeophycus* (*Halopoa*) type traces' from the

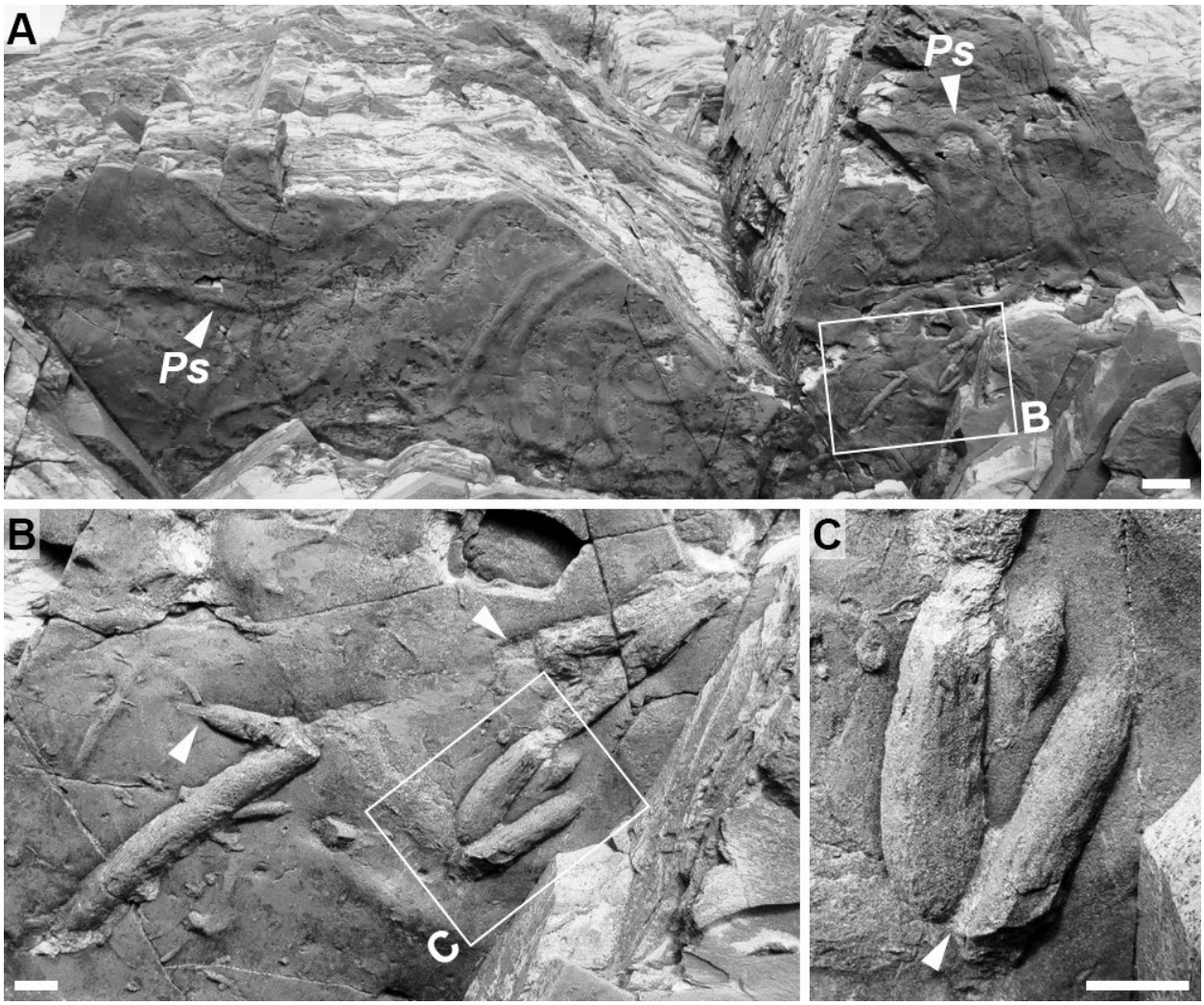

Fig. 39. Halopoa imbricata Torell. Scale bars are 5 cm (A) and 1 cm (B, C). All photographs are positive hyporeliefs from Grand Bank Head, Member 2B (Fortunian). **A**, Specimens associated with *Psammichnites gigas circularis* (Ps). **B**, Close-up from Figure 39A. Note the imbricated nature of the burrows, and their inflated shape with narrowing terminations (arrows). **C**, Close-up from Figure 39B. Note the coarse striae along the burrows, and the paired arrangement with distinct separation (arrow).

Cambrian of Kazakhstan that display inflated intervals and longitudinal striae and wrinkles diagnostic of *Halopoa imbricata*. Specimens recorded as cf. *Halopoa imbricata* from a Cambrian erratic boulder of Sweden (Weidner *et al.* 2015) are spindle-shaped with very regular, parallel longitudinal ridges, and their affinity to *Halopoa* is dubious. *Halopoa* aff. *H. imbricata* from the Cambrian of Utah, USA (Hammersburg *et al.* 2018) is very poorly preserved without identifiable outlines and should be kept in open nomenclature. cf. *Trichophycus venosus* Miller from the Cambrian of Sweden (McLoughlin *et al.* 2021, fig. 9J) displays one bulging elongated segment with parallel longitudinal striae and may represent a preservational variant of *Halopoa imbricata*. *Halopoa* isp. from the Cambrian of Estonia (Palij *et al.* 1983) has an irregular width, but the presence of inflated intervals and longitudinal ridges or wrinkles is unclear. Inflated segments and longitudinal features in *Halopoa* isp. from the Cambrian of India (Singh & Rai 1983) are not demonstrated. Finally, specimens of Cambrian *Palaeophycus striatus* from Scotland (Davies *et al.* 2009) and China (Bai *et al.* 2012) display inflated segments with longitudinal striae and are best relocated within *Halopoa imbricata*.

Ichnogenus *Helminthoidichnites* Fitch, 1850

Discussion. – *Helminthoidichnites* is a horizontal trail with a straight to curved course (Hofmann & Patel 1989; Hofmann 1990) included in the category of architectural design of 'simple horizontal trails' (Buatois *et al.* 2017). *Helminthoidichnites* was first described

from the Ordovician 'Hudson River Group' of north-eastern USA (Hall 1847; Fitch 1850; Schneer 1978). Whereas Emmons (1844) considered *Gordia marina* as the remains of worms, Fitch (1850) believed these were trace fossils and defined *Helminthoidichnites marinus* and *H. tenuis*. Häntzschel (1975) considered *Helminthoidichnites* a junior synonym of *Gordia*, but Hofmann & Patel (1989) contested this conclusion, an opinion endorsed here (see *Gordia* section, p. 86).

At least eight ichnospecies attributed to *Helminthoidichnites* have been described: *H. marinus* (Emmons, 1844); *H. tenuis* Fitch, 1850; *H. meeki* Walcott, 1899; *H. neihartensis* Walcott, 1899; *H. spiralis* Walcott, 1899; *H. multilaqueatus* (Yin, Li & He, 1993); *H. sangshuanensis* (Du, 1986) in Yan & Liu, 1998; and *H. ornatus* (Rindsberg & Kopaska-Merkel, 2005). The type ichnospecies, *Helminthoidichnites tenuis,* is a simple trail with smooth outline (Hofmann & Patel 1989; Hofmann 1990). *Gordia marina* was ascribed to *Helminthoidichnites marinus* by Fitch (1850). However, *Gordia* has a characteristic self-overcrossing (Emmons 1844; Hofmann & Patel 1989). *Helminthoidichnites multilaqueatus*, formerly *Gordia multilaqua*, consists of dense, curving, and subparallel horizontal segments (Pokorný *et al.* 2017). The type material displays at least one case of self-overcrossing (Yin *et al.* 1993, pl. 3, fig. 1), but other specimens are mostly curved without overcrossing. *Helminthoidichnites multilaqueatus* needs re-evaluation of its type material and is provisionally not retained as valid here. *Helminthoidichnites ornatus*, formerly *Haplotichnus ornatus*, has lateral levees with corrugations at short intervals (Rindsberg & Kopaska-Merkel 2005; Demircan & Uchman 2016). Although Demircan & Uchman (2016) transferred *Haplotichnus ornatus* to *Helminthoidichnites*, distinctive lateral levees are typical of *Archaeonassa* and do not support their current taxonomic position. Finally, *Helminthoidichnites meeki*, *H. neihartensis*, *H. sangshuanensis*, and *H. spiralis* are flat, filamentous and/or coiled (Walcott 1899; Du *et al.* 1986; Yan & Liu 1998) and are all regarded as algal body fossils (Cloud 1968; Walter *et al.* 1976, 1990; Hofmann 1983; Niu 1998). Consequently, only the type ichnospecies *Helminthoidichnites tenuis* is here retained as valid.

Helminthoidichnites shows similarities with *Archaeonassa* Fenton & Fenton, 1937a, *Gordia* Emmons, 1844, and *Helminthopsis* Heer, 1877. Although some *Helminthoidichnites* can be flanked by faint levees (e.g. Fitch 1850; Hofmann *et al.* 1994; Schlirf *et al.* 2001; Droser *et al.* 2005; Carbone & Narbonne 2014; Gougeon *et al.* 2018b), well-developed levees are diagnostic of *Archaeonassa* (Fenton & Fenton 1937a; Jensen 2003). Most notably, Ediacaran horizontal trace fossils from Australia previously recorded as *Helminthoidichnites* (e.g. Droser *et al.* 2017, fig. 3e; Gehling & Droser 2018, fig. 1F; Gehling *et al.* 2019, fig. 1c; Evans *et al.* 2020, fig. 2A) all display well-developed lateral levees and belong to *Archaeonassa*. Self-overcrossing horizontal trails are assigned to *Gordia* (Emmons 1844; Hofmann & Patel 1989). Some authors figured *Helminthoidichnites* with irregular meanders (e.g. Narbonne & Aitken 1990; Uchman *et al.* 2005), but these features are more typical of *Helminthopsis* (Hofmann & Patel 1989; Jensen 1997; Buatois *et al.* 1998a).

Helminthoidichnites ranges from the Ediacaran (e.g. Narbonne & Aitken 1990; Vidal *et al.* 1994a; Carbone & Narbonne 2014; Jensen & Palacios 2016; Shahkarami *et al.* 2017a; Mángano & Buatois 2020) to the Holocene (e.g. Bajard 1966; Ewing & Davis 1967; Scott *et al.* 2009). Producers are possible arthropods in continental settings (insect larvae and small insects; Buatois *et al.* 1997; Metz 2000; Uchman *et al.* 2009) and worms (annelids; Bajard 1966; and possible nematodes; Buatois *et al.* 1997; Olivero & López Cabrera 2023). *Helminthoidichnites* is recorded in continental (e.g. Buatois & Mángano 1995; Schlirf *et al.* 2001; Melchor *et al.* 2003; Uchman *et al.* 2004a; de Gibert & Sáez 2009; Netto *et al.* 2009), marginal-marine (e.g. Buatois *et al.* 1998a, d; MacNaughton & Narbonne 1999; Mángano & Buatois 2004a; Desjardins *et al.* 2012; Hofmann *et al.* 2012), shallow-marine (e.g. Hofmann & Patel 1989; Droser *et al.* 2005; Knaust 2007; Gehling & Droser 2009; Buatois & Mángano 2012a; Villegas-Martín & Netto 2019), and deep-marine (e.g. Narbonne & Aitken 1990; Hofmann *et al.* 1994; Buatois & Mángano 2003c; Uchman *et al.* 2005; Buatois *et al.* 2009; Carbone & Narbonne 2014) environments. *Helminthoidichnites* has been regularly mentioned in the Chapel Island Formation (see synonym list below).

Helminthoidichnites tenuis **Fitch, 1850**

Figure 40A, B

1985	*Helminthopsis tenuis* Książkiewicz; Crimes & Anderson, p. 322, fig. 7.8.
2014	*Helminthoidichnites tenuis* Fitch; Buatois, Narbonne, Mángano, Carmona & Myrow, p. 3, fig. 1c, d, f.
2016	*Helminthoidichnites tenuis* Fitch; Mángano & Buatois, p. 93, fig. 3.11d.
non 2017	*Helminthoidichnites* isp. Herringshaw, Callow & McIlroy, p. 375, fig. 3d.
2017	*Helminthoidichnites tenuis* Fitch; Landing *et al.*, pp. 45, 51, figs 17A, 19A, B.
2018	*Helminthoidichnites tenuis* Fitch; Hantsoo, Kaufman, Cui, Plummer & Narbonne, p. 1243, fig. 2f.
2019	*Helminthoidichnites tenuis* Fitch; Laing, Mángano, Buatois, Narbonne & Gougeon, p. 1626, fig. 2d.

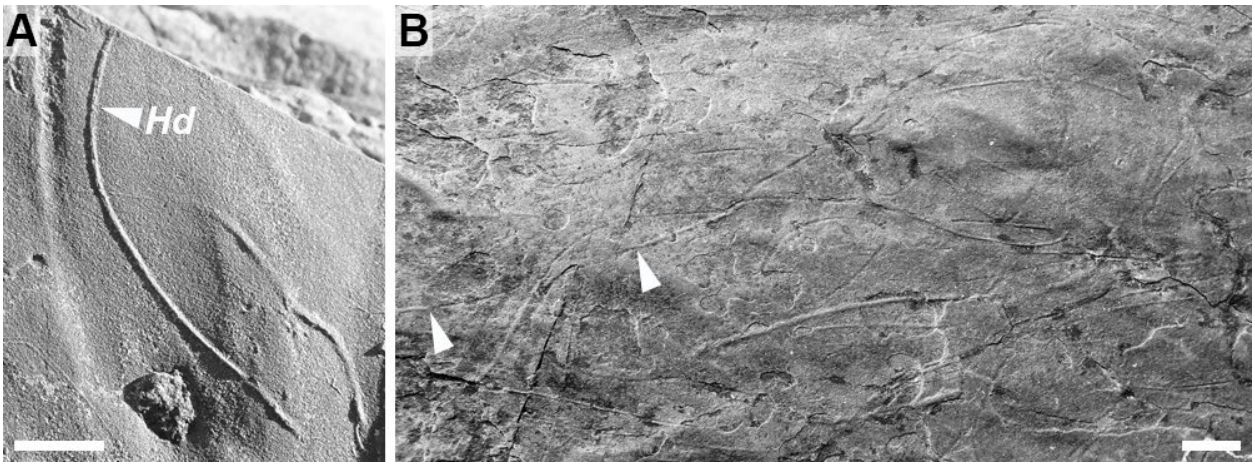

Fig. 40. Helminthoidichnites tenuis Fitch. Scale bars are 1 cm. **A**, Solitary *Helminthoidichnites tenuis* (Hd). Positive epirelief, Fortune Head, Member 2B (Fortunian). **B**, *Helminthoidichnites tenuis* densely covering a surface. Note transitions from positive to negative reliefs along individual courses (arrows). Positive and negative epirelief, Lewin's Cove, Member 2A (Fortunian).

Material. – About 140 specimens from Member 1 (Ediacaran), Members 2A, 2B and 3 (Fortunian), and Member 5 (Cambrian Age 2) in Fortune Head, Fortune North, Grand Bank Head, Lewin's Cove, Little Dantzic Cove, and Point May.

Description. – Smooth, unlined, unbranched, horizontal trails with a straight, curved to semicircular course. Preserved as positive and negative hyporelief and epirelief. Transition from positive to negative relief on a single course may occur. The course may develop small changes of direction, but never turns more than about 45°. Few specimens have faint lateral furrows or levees. Trails are isolated or crowded forming patches of higher density and showing common overlap. Infill is massive, composed of very fine- to fine-grained sandstone similar to the host rock. Width is 0.05–0.3 cm; maximum length is 13.5 cm.

Associated trace fossils. – *Helminthoidichnites tenuis* co-occurs with *Archaeonassa fossulata*, *Circulichnis ligusticus*, *C. montanus*, *Cochlichnus anguineus*, *Gordia marina*, *Helminthopsis abeli*, *H. hieroglyphica, H. tenuis*, *Monomorphichnus bilinearis*, *Palaeophycus tubularis*, *Psammichnites gigas circularis*, and *Treptichnus pedum*.

Remarks. – A straight to gently curving horizontal course allows placing these trace fossils in *Helminthoidichnites tenuis*. In the Chapel Island Formation, *Helminthoidichnites tenuis* was mentioned for the first time by Landing & Westrop (1998) but was not figured, and some older reports of *Gordia* and *Helminthopsis* that predate Hofmann & Patel's (1989) landmark paper may in fact correspond to *Helminthoidichnites* (as for instance Crimes & Anderson 1985, fig. 7.8). *Helminthoidichnites* isp. in Herringshaw *et al.* (2017, fig. 3d) is sinuous to slightly meandering and may be better affiliated to *Helminthopsis tenuis*. *Helminthoidichnites tenuis* is a common trace fossil from the Ediacaran and Cambrian worldwide. Transition from positive to negative relief on a single course is common (Fig. 40B), suggesting the presence of microbial mats. True branching is absent, but occasional secondary successive branching occurs on densely covered surfaces (Fig. 40B).

Ichnogenus *Helminthopsis* Heer, 1877

Discussion. – *Helminthopsis* is a horizontal trail with irregular meanders (Han & Pickerill 1995; Wetzel & Bromley 1996) included in the category of architectural design of 'simple horizontal trails' (Buatois *et al.* 2017). *Helminthopsis* was first described from the Palaeocene–Eocene Ruchberg series of eastern Switzerland (Heer 1877; Wetzel & Bromley 1996). The history of *Helminthopsis* is complicated and has been well summarized by Wetzel & Bromley (1996). Heer (1877) erected three ichnospecies (*Helminthopsis magna*, *H. intermedia*, and *H. labyrinthica*) that were considered junior synonyms of *Scolicia* isp. (*Helminthopsis magna* and *H. intermedia*) and *Spirocosmorhaphe helicoidea* Seilacher (*H. labyrinthica*) by Wetzel & Bromley (1996). As *Helminthopsis magna* was designated type ichnospecies by several authors but deemed unsuitable for representing the ichnogenus, Wetzel & Bromley (1996) designated a new type ichnospecies, *Helminthopsis hieroglyphica*, selected from Heer's collection to maintain nomenclature stability. To complicate things further, another revision of *Helminthopsis* was conducted independently at the same time by Han & Pickerill (1995),

leading to different conclusions. Han & Pickerill (1995) used statistical analyses to consider three valid ichnospecies: *Helminthopsis abeli*, *H. granulata* Książkiewicz, and *H. hieroglyphica*. On the other hand, Wetzel & Bromley (1996) used simple morphological criteria to consider *Helminthopsis abeli*, *H. hieroglyphica*, and *H. tenuis* valid. Uchman (1998) maintained the distinction of *Helminthopsis tenuis* from *H. abeli*, but also retained *H. granulata* as potentially valid. By integrating these reviews, four *Helminthopsis* ichnospecies are here considered valid: *H. granulata* Książkiewicz, 1968; *H. tenuis* Książkiewicz, 1968; *H. abeli* Książkiewicz, 1977; and *H. hieroglyphica* Wetzel & Bromley, 1996. The type ichnospecies, *Helminthopsis hieroglyphica,* has straight segments along its course (Wetzel & Bromley 1996). *Helminthopsis granulata* has a tuberculate surficial ornamentation (Książkiewicz 1968; Han & Pickerill 1995). *Helminthopsis tenuis* has wide, shallow meanders (Książkiewicz 1968; Wetzel & Bromley 1996). *Helminthopsis abeli* has deep horseshoe-like, bulged meanders (Książkiewicz 1977; Wetzel & Bromley 1996).

Helminthopsis shows similarities with *Archaeonassa* Fenton & Fenton, 1937a, *Cochlichnus* Hitchcock, 1858, *Gordia* Emmons, 1844, *Helminthoidichnites* Fitch, 1850, *Multina* Orłowski, 1968, *Palaeophycus* Hall, 1847, and *Planolites* Nicholson, 1873. Although some specimens of *Helminthopsis* may develop narrow lateral levees (Jensen *et al.* 2006), distinctive and well-developed levees are features more typical of *Archaeonassa* (Fenton & Fenton 1937a; Jensen 2003). With its irregular meandering course, *Helminthopsis* differs from other simple horizontal trails, such as *Cochlichnus* (sinusoidal course), *Gordia* (self-overcrossing course), and *Helminthoidichnites* (straight to curved course) (Hofmann & Patel 1989; Buatois *et al.* 1998a; Gougeon *et al.* 2018b). *Multina* is a horizontal branching burrow that can be mistaken for *Helminthopsis* if partially preserved (Buatois & Mángano 2012a). Finally, *Helminthopsis* differs from *Palaeophycus* and *Planolites* by being non-penetrative (Keighley & Pickerill 1997).

Helminthopsis ranges from the Ediacaran (e.g. Fritz & Crimes 1985; Narbonne & Aitken 1990; Seilacher *et al.* 2005; Jensen *et al.* 2006; Hofmann & Mountjoy 2010; Carbone & Narbonne 2014) to the Holocene (e.g. Swinbanks & Murray 1981; Metz 1987a; Mángano *et al.* 1996b; Schatz *et al.* 2013; Muñiz Guinea *et al.* 2014). *Helminthopsis* is recorded in continental (e.g. Metz 1987a, 2000; Pickerill 1992; Keighley & Pickerill 1997; Buatois & Mángano 2003d; Buatois *et al.* 2006), marginal-marine (e.g. Archer 1984; Miller & Knox 1985; Fillion & Pickerill 1990; Raychaudhuri & Pemberton 1992; Buatois *et al.* 1998a), shallow-marine (e.g. Archer 1984; Fritz & Crimes 1985; Stanley & Pickerill 1998; Pickerill & Blissett 1999; Dam 1990; Gong & Droser 2001), and deep-marine (e.g. Książkiewicz 1968; Bottjer 1981; Pickerill 1981; Crimes & Crossley 1991; Uchman 1998; Lehane & Ekdale 2016) environments. In continental settings, suggested producers are insect larvae, nematomorphs, and nematodes (Metz 1987a; Mángano *et al.* 1996b; Muñiz Guinea *et al.* 2014). In marine environments, it is typically attributed to various types of worms, such as annelids, nematodes, and priapulids (Książkiewicz 1977; Miller & Knox 1985; Fillion & Pickerill 1990; Olivero & López Cabrera 2023). In the Chapel Island Formation, *Helminthopsis* has been regularly recorded (see synonym lists below) since its first description by Crimes & Anderson (1985).

***Helminthopsis abeli* Książkiewicz, 1977**

Figure 41A

1985 *Helminthopsis abeli* Książkiewicz; Crimes & Anderson, p. 322, fig. 7.6.

1985 *Helminthoida miocenica* Sacco; Crimes & Anderson, p. 322, fig. 7.5.

Material. – Four specimens from Members 2A and 2B (Fortunian) and Member 5 (Cambrian Age 2) in Fortune Head and Grand Bank Head.

Description. – Smooth, unlined, unbranched, horizontal trails with an irregular meandering course showing deep, bulged meanders. Preserved as positive hyporelief and positive epirelief. Bulged meanders have regular bell shapes, or more irregular morphologies. Infill is massive, composed of fine-grained sandstone similar to the host rock. Width is 0.1 cm; maximum length is 5.7 cm.

Associated trace fossils. – *Helminthopsis abeli* co-occurs with *Gordia marina*, *Helminthoidichnites tenuis*, *Helminthopsis tenuis*, *Palaeophycus tubularis*, and *Treptichnus pedum*.

Remarks. – The presence of deep, bulged meanders allows placing these trace fossils in *Helminthopsis abeli*. The evaluation of what represents a 'deep meander' is subject to interpretation: while both Han & Pickerill (1995) and Wetzel & Bromley (1996) argued for the presence of distinct horseshoe-like turns at intervals along the course, this has not always been clearly followed by authors (e.g. Tiwari *et al.* 2011). Here, we only consider an affiliation to *Helminthopsis abeli* where deep horseshoe-like turns are distinct (see also Crimes & Crossley 1991, Tchoumatchenco & Uchman 2001,

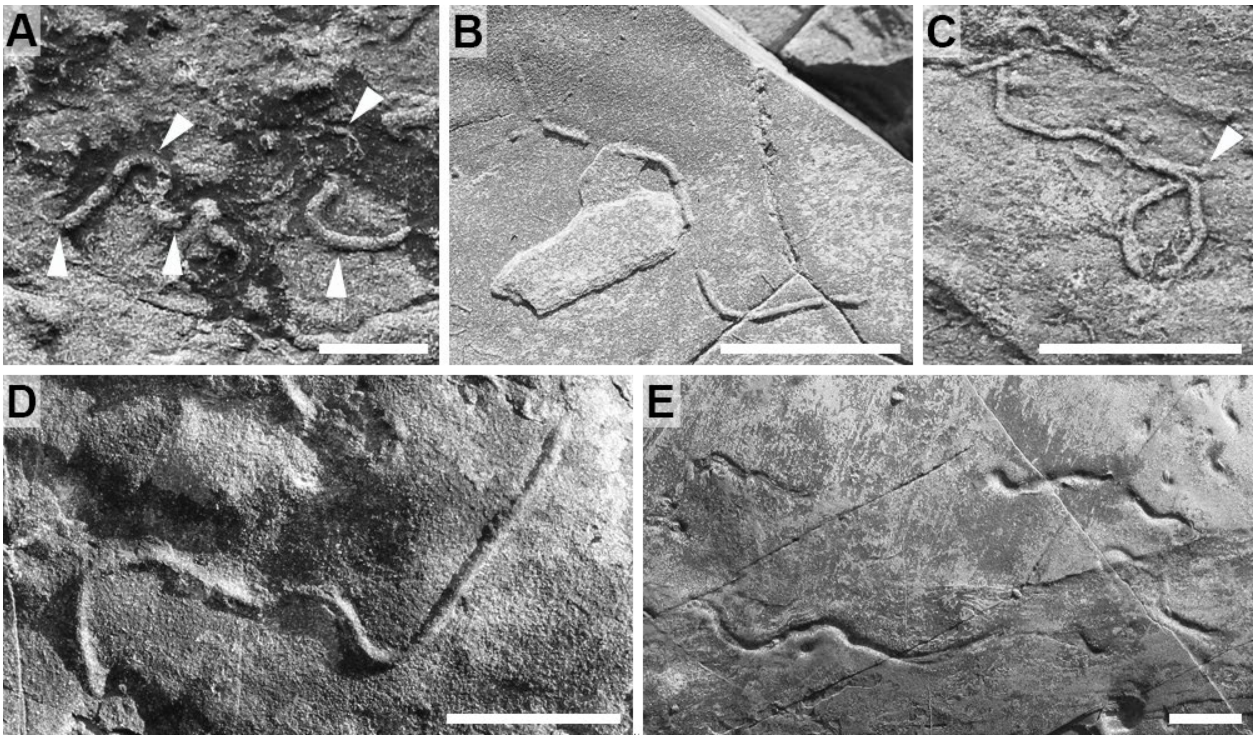

Fig. 41. Helminthopsis abeli Książkiewicz (A), *H. hieroglyphica* Wetzel & Bromley (B, C), and *H. tenuis* Książkiewicz (D, E). Scale bars are 1 cm. **A**, *Helminthopsis abeli* with deep, bulged meanders (arrows). Positive hyporelief, Grand Bank Head, Member 5 (Cambrian Age 2). **B**, *Helminthopsis hieroglyphica* with straight intervals. Positive epirelief, Fortune Head, Member 2B (Fortunian). **C**, Problematic *Helminthopsis hieroglyphica* with a possible branching (arrow) and a *Gordia*-like ending on one side. Positive hyporelief, Grand Bank Head, Member 2A (Fortunian). **D**, *Helminthopsis tenuis* with shallow meanders. Positive hyporelief, Grand Bank Head, Member 2B (Fortunian). **E**, Tortuous *Helminthopsis tenuis* gathered on a surface. Negative epirelief, Fortune Head, Member 2A (Fortunian)

Uchman 2004, and Vaziri & Fürsich 2007). Otherwise, irregularly meandering trace fossils with shallow meanders are placed in *Helminthopsis tenuis*. In addition, the distinction between *Helminthopsis abeli* and some specimens of *Cochlichnus anguineus* and *C. gracilis* is not always straightforward, especially where the sinusoidal course turns out to be irregular along some intervals.

Helminthopsis abeli has rarely been recorded and figured from the Ediacaran (Narbonne & Aitken 1990; Hofmann & Mountjoy 2010) and the Cambrian (Orłowski & Żylińska 2002; Weber *et al.* 2007). In the Chapel Island Formation, only Crimes & Anderson (1985, fig. 7.6) figured *Helminthopsis abeli* from Member 2B; *Helminthoida miocenica* Sacco (Crimes & Anderson 1985, fig. 7.5) is very loose and irregular, and should also be considered as *Helminthopsis abeli*.

Helminthopsis hieroglyphica Wetzel & Bromley, 1996

Figure 41B, C

Material. – Nine specimens from Members 2A and 2B (Fortunian) in Fortune Head and Grand Bank Head.

Description. – Smooth, unlined, horizontal trails with an irregular meandering course made of straight intervals. Preserved as positive hyporelief and positive epirelief. Angle of turn varies from few degrees to about 90°; rarely, straight intervals end up forming a loop. Unbranched, although one specimen displays a possible branch. Infill is massive, composed of very fine- to fine-grained sandstone similar to the host rock. Width is 0.1–0.2 cm; maximum length is 6.9 cm.

Associated trace fossils. – *Helminthopsis hieroglyphica* co-occurs with *Archaeonassa fossulata*, *Circulichnis ligusticus*, *Cochlichnus anguineus*, *Helminthoidichnites tenuis*, *Helminthopsis tenuis*, and *Palaeophycus tubularis*.

Remarks. – Han & Pickerill (1995) and Wetzel & Bromley (1996) considered *Helminthopsis hieroglyphica* a valid ichnospecies based on its box-like appearance with straight intervals. Some forms of *Treptichnus* preserving only a horizontal basal burrow without showing clear projections can develop highly angular courses reminiscent of *Helminthopsis hieroglyphica*

(e.g. Archer & Maples 1984, fig. 5C; Archer *et al.* 1995, fig. 7b; Gámez Vintaned *et al.* 2006, figs 9.7, 8). *Helminthopsis hieroglyphica* has rarely been recorded in the Cambrian (Webby 1970; Pickerill & Blissett 1999; Mángano *et al.* 2019). Ediacaran *Helminthopsis hieroglyphica* in Bekker (2013, pl. 2, fig. 2) has a straight course without meanders and fits better within *Helminthoidichnites*. Cambrian *Helminthopsis hieroglyphica* in Orłowski & Żylińska (2002, fig. 5c, e) is leveed and is closer to *Archaeonassa*, and in Bai *et al.* (2012, fig. 3.1) does not display straight intervals and is closer to *Palaeophycus*.

Helminthopsis tenuis Książkiewicz, 1968

Figure 41D, E

2014 *Helminthopsis tenuis* Książkiewicz; Buatois, Narbonne, Mángano, Carmona & Myrow, p. 3, fig. 1b.
2017 *Helminthoidichnites* isp. Herringshaw, Callow & McIlroy, p. 375, fig. 3d.
2017 *Helminthopsis tenuis* Książkiewicz; Landing *et al.*, pp. 45, 51, figs. 17A, 19I.
2019 *Helminthopsis tenuis* Książkiewicz; Laing, Mángano, Buatois, Narbonne & Gougeon, p. 1626, fig. 2b.

Material. – About 110 specimens from Members 2A, 2B and 3 (Fortunian) and Member 5 (Cambrian Age 2) in Fortune Head, Grand Bank Head, Lewin's Cove, Little Dantzic Cove, and Point May.

Description. – Smooth, unlined, unbranched, horizontal trails with wide, shallow meanders. Preserved as positive and negative hyporelief and epirelief. In rare cases, irregular meanders are more tortuous. A knob can be preserved at the end of the course. Overlap with adjacent specimens is rare. Infill is massive, composed of very fine- to fine-grained sandstone similar to the host rock; rarely, infill is pyritized. Width is 0.05–0.2 cm; maximum length is 18.7 cm.

Associated trace fossils. – *Helminthopsis tenuis* co-occurs with *Archaeonassa fossulata*, *Cochlichnus anguineus*, *Gordia marina*, *Helminthoidichnites tenuis*, *Helminthopsis abeli*, *H. hieroglyphica*, *Monomorphichnus bilinearis*, and *M. needleiunm*.

Remarks. – Although Han & Pickerill (1995) synonymized *Helminthopsis tenuis* with *H. abeli*, Wetzel & Bromley (1996) retained the former as a valid ichnospecies on the basis of its shallow turns and the absence of horseshoe-like patterns, a decision endorsed here. *Helminthopsis tenuis* is easily identifiable in the field, being commonly recorded in the Ediacaran and the Cambrian (e.g. Buatois & Mángano 2003c, 2016; Carbone & Narbonne 2014; Shahkarami *et al.* 2017a; Gougeon *et al.* 2018b; Mángano & Buatois 2020). In the Chapel Island Formation, *Helminthopsis tenuis* is a common trace fossil typically associated with other simple grazing trails. The presence of a terminal knob reveals the ability of the tracemaker to change vertical level. Tortuous specimens (Fig. 41E) can be reminiscent of *Cochlichnus*, but they are too irregular to be considered sinusoidal. *Helminthopsis tenuis* was also mentioned in the succession by Narbonne *et al.* (1987) and Landing *et al.* (1988) without providing illustration.

Ichnogenus *Monomorphichnus* Crimes, 1970

Discussion. – *Monomorphichnus* consists of a series of subparallel ridges in places repeated laterally (Crimes 1970) included in the category of architectural design of 'trackways and scratch imprints' (Buatois *et al.* 2017). *Monomorphichnus* was first described from the Cambrian Ffestiniog Formation of northern Wales (Crimes 1970; Hawkins & Jones 1981). Fillion & Pickerill (1990) mentioned the existence of a possible senior synonym for *Monomorphichnus*, namely *Ctenichnites* Matthew, 1891, which needs revision. Another debate started when Seilacher (1985, 1990a) considered *Monomorphichnus* a junior synonym of *Dimorphichnus*. Seilacher (1985) argued that the type material of *Monomorphichnus* displays a second set of blunt imprints typical of *Dimorphichnus*. This suggestion was discarded by Fillion & Pickerill (1990). Pending further revision, Jensen (1997) and Mángano & Buatois (2003a) temporarily retained *Monomorphichnus*, arguing that some of its ichnospecies would be difficult to relocate within *Dimorphichnus*.

At least nineteen ichnospecies attributed to *Monomorphichnus* have been erected: *M. bilinearis* Crimes, 1970; *M. multilineatus* Alpert, 1976a; *M. lineatus* Crimes, Legg, Marcos & Arboleya, 1977; *M. cretacea* Badve & Ghare, 1980; *M. gaopoensis* Yang & Yin in Yang *et al.*, 1982; *M. monolinearis* Shah & Sudan, 1983; *M. pectenensis* Legg, 1985; *M. devonicus* Yang & Hu in Yang *et al.*, 1987; *M. biscolus* Chu, 1988; *M. intersectus* Fillion & Pickerill, 1990; *M. henanensis* Yang & Wang, 1991; *M. biserialis* Mikuláš, 1995; *M. semilineatus* Mikuláš, 1995; *M. podolicus* Uchman, Drygant, Paszkowski, Porębski & Turnau, 2004b; *M. taenia* Wang, Zhang, Yang, Li & Wang, 2006; *M. kailiensis* Wang, 2007; *M. needleiunm* Wang, 2007; *M. sinus* Gibb, Chatterton & Pemberton, 2009; and *M. gregarius* Pandey, Uchman, Kumar & Shekhawar, 2014. The type ichnospecies, *Monomorphichnus*

bilinearis, has bundles of two ridges within a series (Crimes 1970). *Monomorphichnus multilineatus* has five or six ridges per series with more prominent central ridges (Alpert 1976a). *Monomorphichnus lineatus* has subparallel ridges forming series sometimes repeated laterally (Crimes *et al.* 1977). *Monomorphichnus cretacea* is made of subparallel wrinkles (Badve & Ghare 1980, pl. 2, fig. 4) and is not a trace fossil but a microbially stabilized surface (cf. Fillion & Pickerill 1990). *Monomorphichnus gaopoensis* does not display any subparallel ridges typical of *Monomorphichnus* (Yang *et al.* 1982, pl. 1, fig. 4) and has a dubious biogenic affinity (Uchman *et al.* 2004b). *Monomorphichnus monolinearis* has simple ridges organized in a series (Shah & Sudan 1983), which is already diagnostic of *M. lineatus* (Fillion & Pickerill 1990). *Monomorphichnus pectenensis* has bundles of two ridges with intervening finer striations (Legg 1985). Yang *et al.* (1987) described *Monomorphichnus devonicus* as groups of parallel ridges. The poor quality of the illustrated material (Yang *et al.* 1987, pl. II, fig. 1) and loose description call for its re-evaluation. *Monomorphichnus biscolus* is composed of ridges not arranged in a series (Chu 1988, fig. 9, pl. II, fig. 4) and is unrelated to *Monomorphichnus*. *Monomorphichnus intersectus* has cross-cutting ridges within individual series (Fillion & Pickerill 1990). *Monomorphichnus henanensis* has series of subparallel ridges repeated laterally (Yang & Wang 1991, pl. 2, fig. 7), and is a junior synonym of *M. lineatus*. *Monomorphichnus biserialis* has ridges paired in two series oriented in parallel (Mikuláš 1995). *Monomorphichnus semilineatus* has irregular ridges oriented in various direction (Mikuláš 1995). The absence of clear pattern for the series, and the random orientation of ridges preclude an affinity to *Monomorphichnus*. *Monomorphichnus podolicus* has series of dense ridges arranged in bundles of four to six ridges (Uchman *et al.* 2004b) and may be a synonym of *Cruziana omanica* Seilacher (Gibb *et al.* 2009). *Monomorphichnus taenia* has dense subparallel ridges/wrinkles (Wang *et al.* 2006, pl. 1, fig. 3) and may be a microbially stabilized surface. Wang (2007) described *Monomorphichnus kailiensis* as having two thin ridges in between two wider ridges within a single series. This feature is not obvious from the figured specimens (Wang 2007, pl. 3, figs 9, 10), and this ichnospecies may be a junior synonym of *M. lineatus*. *Monomorphichnus needleiunm* has ridges oriented in a fan shape (Wang 2007). *Monomorphichnus sinus* has six to seven prominent curved ridges (Gibb *et al.* 2009). This ichnospecies needs further investigation to be clearly distinguished from *Monomorphichnus multilineatus* (compare with Gibb *et al.* 2009, fig. 8D). *Monomorphichnus gregarius* has bundles of four ridges that densely cover surfaces (Pandey *et al.* 2014). Sharma *et al.* (2018a) named *Monomorphichnus multilineatus* similar specimens from the same area, and *M. gregarius* features are also typical of *M. podolicus* (see also Hammersburg *et al.* 2018). Consequently, seven ichnospecies, *Monomorphichnus bilinearis*, *M. biserialis*, *M. intersectus*, *M. lineatus*, *M. multilineatus*, *M. needleiunm*, and *M. pectenensis*, are here retained as valid until further revision.

Monomorphichnus shows similarities with *Allocotichnus* Osgood, 1970, *Asaphoidichnus* Miller, 1880, *Dimorphichnus* Seilacher, 1955a, *Diplichnites* Dawson, 1873, and *Rusophycus* Hall, 1852. *Allocotichnus* is an asymmetric trackway with paired imprints oriented obliquely to the main direction (Osgood 1970). Pairing of imprints is absent in *Monomorphichnus*. Contrary to *Monomorphichnus*, *Asaphoidichnus* consists of parallel series, with bifid to trifid imprints (Miller 1880; Weber & Braddy 2004). *Dimorphichnus* has a first series of thin elongated ridges and a distinctive second series of blunt, shorter imprints (Seilacher 1955a). *Rusophycus* consists of a short bilobed burrow typically covered with scratch imprints (Dawson 1864), and single-sided *Rusophycus* can be misinterpreted for *Monomorphichnus* (Jensen 1997; Jensen *et al.* 2002b). *Diplichnites* is distinctive from *Monomorphichnus* by the arrangement of simple imprints into two parallel rows within a trackway (Keighley & Pickerill 1998).

Monomorphichnus can be difficult to differentiate from inorganic features in some cases. Tool marks are made by the contact of objects with the seafloor through unidirectional flows and can be subdivided into drag marks (protracted contact with the substrate), roll marks (a rounded object rolling over the substrate), prod marks (brief contact with the substrate), tumble marks (saltation of the object onto the substrate), skim marks (gouging of the substrate through a curved trajectory), chevron marks (combination of drag and skim marks), and brush marks (sweeping action over the substrate) (Dżułyński & Walton 1965; Allen 1982; Peakall *et al.* 2020). Jensen (1997) discussed 'Eophyton'-type tool marks which are delicate, closely spaced subparallel ridges along a wider elongated groove, and noted that those may have been formed by intraclasts of coarser-grained lithology. This arrangement of delicate ridges is similar to some features of Chapel Island Formation *Monomorphichnus* isp. (Fig. 42F). However, *Monomorphichnus* isp. also displays larger fusiform elements repeated in parallel, a level of organization that is hard to reconcile with an inorganic mode of formation. Overall, *Monomorphichnus* in this study is distinguished from any of the tool marks listed above by one or many of the following features: (1) the

formation of series of at least three subparallel ridges of comparable width and length that are mostly equidistant from one-another; (2) the lateral repetition of series; (3) the sigmoidal pattern of ridges; and (4) the pairing of ridges. The first point is the most important as tool marks do not form arrangements of ridges and has been observed in all the specimens recovered in this study.

Monomorphichnus ranges from the Cambrian (e.g. Crimes 1970; Alpert 1976a; Brasier *et al.* 1979; Pickerill & Peel 1990; Jensen & Mens 2001; Hofmann *et al.* 2012) to the Holocene (Muñiz & Gámez Vintaned 2008). Reports from the Ediacaran can be dismissed as follow: (1) *Monomorphichnus bilinearis* and *M. lineatus* recorded by Walter *et al.* (1989), although stated to be found in the Ediacaran, are only figured from the Cambrian; (2) cf. *Monomorphichnus* recorded by Jenkins (1995, pl. 1, fig. C) consists of dense subparallel ridges that were re-interpreted as *Kimberichnus* Ivantsov (Seilacher *et al.* 2005; Jensen *et al.* 2006; Gehling *et al.* 2014); and (3) cf. *Monomorphichnus* recorded by Waggoner & Hagadorn (2002, fig. 7; also figured in Waggoner 1999, fig. 4g) is very poorly preserved, irregular, and may be inorganic (Jensen *et al.* 2006). Producers are possible arthropods (crustaceans, eurypterids, trilobites, xiphosurids; e.g. Martinsson 1965; Crimes 1970; Mikuláš 1995; Jensen 1997; Weber & Braddy 2004), and vertebrates (birds; Muñiz & Gámez Vintaned 2008). *Monomorphichnus* is recorded in continental (e.g. Shone 1979; Pickerill 1992; Keighley & Pickerill 1998; Lucas *et al.* 2005b; Minter & Lucas 2009), marginal-marine (e.g. Narbonne 1984; Legg 1985; Uchman *et al.* 2004b; Weber & Braddy 2004; Buatois *et al.* 2005; Pandey *et al.* 2014), and shallow-marine (e.g. Crimes 1970; Pickerill & Peel 1990; Stanley & Pickerill 1998; Mángano *et al.* 2005a; Gibb *et al.* 2009; Hammersburg *et al.* 2018) environments. In the Chapel Island Formation, *Monomorphichnus* was commonly mentioned in previous studies (e.g. Crimes & Anderson 1985; Narbonne *et al.* 1987; Laing *et al.* 2019).

Monomorphichnus bilinearis **Crimes, 1970**

Figure 42A, B

1985 *Monomorphichnus bilinearis* Crimes; Crimes & Anderson, pp. 318, 324, figs 6.11, 8.2.
? 2017 *Monomorphichnus* isp. Herringshaw, Callow & McIlroy, p. 375, fig. 3f.

Material. – Eight specimens from Members 2A and 2B (Fortunian) in Fortune Head and Grand Bank Head.

Description. – Horizontal, straight, gently curved to sigmoidal subparallel ridges arranged in bundles of two ridges, which in turn form series of 4 to 10 bundles. Preserved as positive hyporelief. Series are rarely repeated laterally and extend at great length or remain short. Ridges are close together within a bundle, and the distance in between bundles is more important. Ridges of a bundle extend along the whole course of the specimen, or one ridge of the bundle can fade away within the host rock and be shorter. In places, the two ridges of a bundle merge and result in a single ridge. One ridge of the bundle can be more prominent than the other one. Series width is 1.3–3.1 cm; ridge width is 0.05–0.1 cm; distance in between bundles is 0.2–0.4 cm; maximum ridge length is 27.5 cm.

Associated trace fossils. – *Monomorphichnus bilinearis* co-occurs with *Helminthoidichnites tenuis*, *Helminthopsis tenuis*, *Monomorphichnus lineatus*, and *Palaeophycus tubularis*.

Remarks. – The formation of bundles of two ridges within a series allows placing these trace fossils in *Monomorphichnus bilinearis*. Reports of *Monomorphichnus bilinearis* show that ridges can be short (e.g. Crimes 1970; Pickerill 1992; Baghiyan-Yazd 1998) or extend over a greater distance (e.g. Crimes & Anderson 1985; Mikuláš 1995). For short specimens, difficulties arise where they are also slightly bulbous, and can be mistaken for half-lobed *Rusophycus* (Mángano *et al.* 1996a; Mángano & Buatois 2003a). Crimes (1970) noted that one ridge of the bundle can be more prominent than the other, which is also noted in some Chapel Island Formation specimens as well as in other reports (e.g. Pickerill 1992). The prominence of one ridge over the other is, however, not always clearly visible (Mángano *et al.* 1996a). The formation of bundles of two ridges argues for a producer having at least two claws per limb (Legg 1985). The number of bundles per series is arguably controlled by the number of limbs of the producer (Weber & Braddy 2004), but this only provides the minimum number of appendages, as not all appendages may have been in contact with the substrate, or their imprints may have been lost due to undertrack fall-out effect. *Monomorphichnus bilinearis* in Hammersburg *et al.* (2018) consists of only one bundle of two ridges, which is taxonomically problematic. Finally, the distinction of *Dimorphichnus obliquus* from *Monomorphichnus bilinearis* is not always clear, especially where the series of blunt imprints is not well identified. This led to confusion in some studies (e.g. Orłowski 1992).

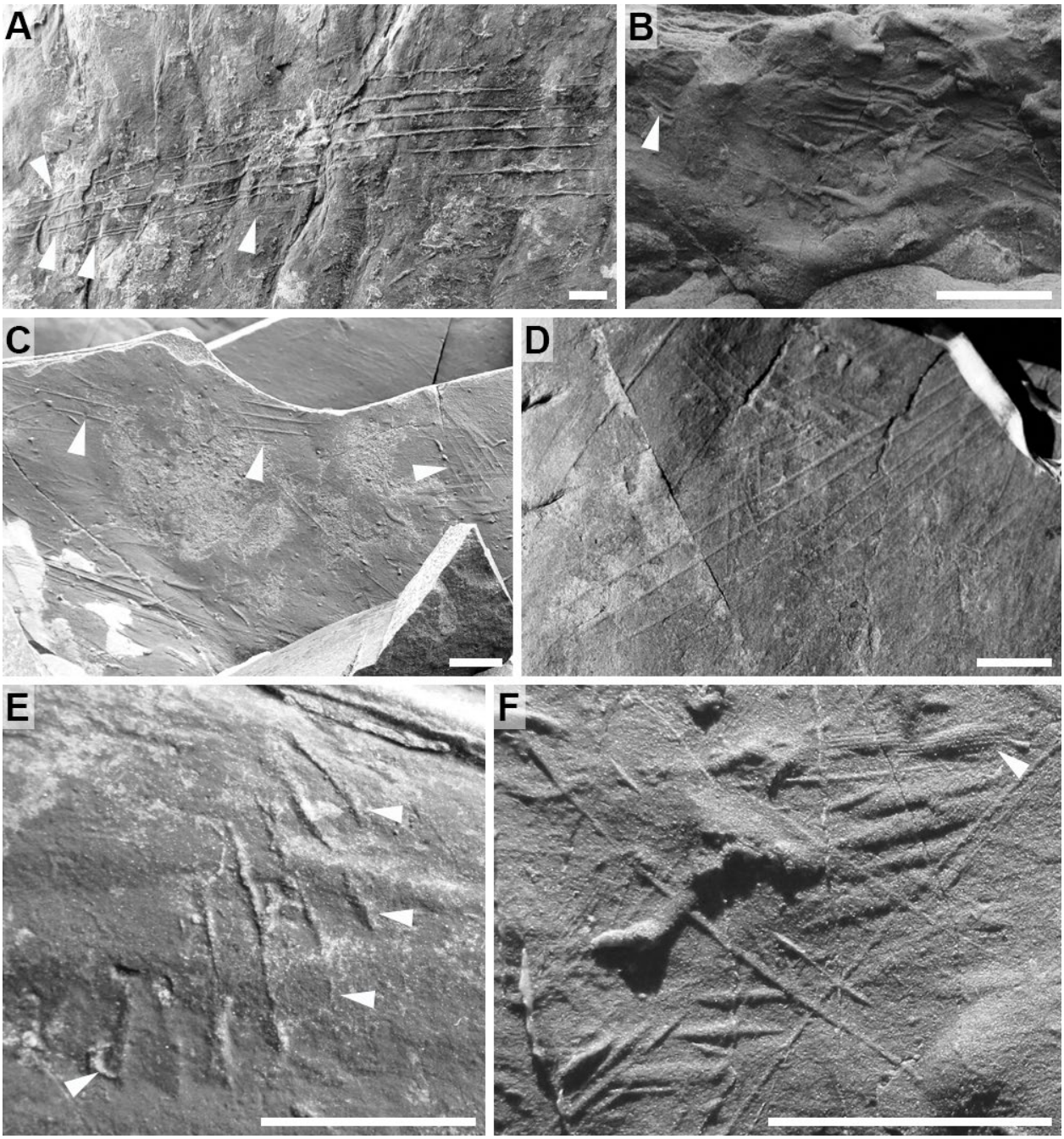

Fig. 42. Monomorphichnus bilinearis Crimes (A, B), *M. lineatus* Crimes, Legg, Marcos & Arboleya (C, D), *M. needleiunm* Wang (E), and *Monomorphichnus* isp. (F). Scale bars are 1 cm. All photographs are positive hyporeliefs from Member 2A (Fortunian). **A**, *Monomorphichnus bilinearis* with slightly curved, elongated ridges. Note bundles of paired ridges (arrows). Grand Bank Head. **B**, *Monomorphichnus bilinearis* with short and slightly sigmoidal ridges. Note the re-appearance of ridges on the left (arrow). Fortune Head. **C**, Short *Monomorphichnus lineatus* repeated laterally (arrows). Fortune Head. **D**, Overlapping of two *Monomorphichnus lineatus* with different orientation. Lewin's Cove. **E**, Fan-shaped *Monomorphichnus needleiunm*. Note that some ridges form an angle of deviation from their adjacent ridges (arrows). Fortune Head. **F**, *Monomorphichnus* isp. with fusiform ridges. Note the delicate, parallel subridges (arrow). Grand Bank Head.

Monomorphichnus lineatus Crimes, Legg, Marcos & Arboleya, 1977

Figure 42C, D

1985 *Monomorphichnus lineatus* Crimes, Legg, Marcos & Arboleya; Crimes & Anderson, pp. 318, 324, figs 6.12, 8.4.
2017 *Monomorphichnus* isp. Budd & Jensen, p. 462, fig. 7E.
2019 *Monomorphichnus* isp. A Laing, Mángano, Buatois, Narbonne & Gougeon, p. 1626, fig. 2n.

Material. – Thirty-four specimens from Members 2A and 2B (Fortunian) in Fortune Head, Grand Bank Head, and Lewin's Cove.

Description. – Horizontal, gently curved and subparallel simple ridges forming series of 4 to 9 ridges. Preserved as positive hyporelief and negative epirelief. Series are isolated or repeated laterally. The distance between ridges is typically constant. Individual ridges are commonly thicker and prominent in their middle part and get thinner and taper laterally. Series width is 0.9–3.1 cm; ridge width is 0.05–0.1 cm; distance in between ridges is 0.1–1.1 cm; maximum ridge length is 7.5 cm.

Associated trace fossils. – *Monomorphichnus lineatus* co-occurs with *Curvolithus simplex*, *Helminthopsis tenuis*, *Monomorphichnus bilinearis*, *Palaeophycus tubularis*, and *Palaeophycus* isp.

Remarks. – Series of simple ridges in places repeated laterally allow placing these trace fossils in *Monomorphichnus lineatus*. The holotype from the Cambrian of northern Spain has short and deep ridges closely spaced together (Crimes *et al.* 1977, pl. 3, fig. b); a second specimen from the same locality shows series repeated laterally over a greater distance (Crimes *et al.* 1977, fig. 5a) similarly to some Chapel Island Formation specimens (Fig. 42C). Reports of short and deep imprints similar to the holotype (e.g. Pickerill & Peel 1990, fig. 8a; Orłowski 1992, fig. 13.5; Stanley & Pickerill 1998, pl. 5, fig. 4) require careful examination of larger areas as they could also represent *Dimorphichnus* pushers. Most of the Chapel Island Formation specimens have, however, delicate and shallow ridges that cannot be mistaken for *Dimorphichnus* pushers. Reports of *Monomorphichnus linearis* with series of three ridges or less (e.g. Mikuláš 1995; Baghiyan-Yazd 1998; Hammersburg *et al.* 2018) are less convincing.

Monomorphichnus needleiunm Wang, 2007

Figure 42E

Material. – Two specimens from Members 2A and 2B (Fortunian) in Fortune Head.

Description. – Horizontal, straight ridges forming a series of 7 ridges arranged in a fan shape. Preserved as positive hyporelief and negative epirelief. Ridges are very thin and shallow. Although some ridges are subparallel, others deviate from their adjacent ridges by about 10°. Ridges do not depart from the same point, but instead are staggered from one another. Series width is 1.5–1.7 cm; ridge width is 0.05–0.1 cm; distance in between ridges is 0.1–0.3 cm; maximum ridge length is 1.6 cm.

Associated trace fossils. – *Monomorphichnus needleiunm* co-occurs with *Helminthopsis tenuis*.

Remarks. – The organization of ridges in a fan shape allows placing these trace fossils in *Monomorphichnus needleiunm*. Besides the type material, *Monomorphichnus needleiunm* has not been previously recorded. The holotype (Wang 2007, pl. 3, fig. 3) displays 15 ridges arranged in a series: although some are subparallel, others display a small angle of deviation from their adjacent ridges. Similar observations are visible in the Chapel Island Formation material, although the fan development is less obvious due to the lower number of ridges.

Monomorphichnus isp.

Figure 42F

2019 *Monomorphichnus* isp. B Laing, Mángano, Buatois, Narbonne & Gougeon, p. 1626, fig. 2m.

Material. – Four specimens from Member 2A (Fortunian) in Grand Bank Head.

Description. – Horizontal, parallel, fusiform ridges arranged in a series of 4 to 7 ridges. Preserved as positive hyporelief. Ridges are very wide at one end and taper at the other end. One ridge is overprinted by extremely delicate, perfectly straight and parallel subridges that extend outside the limits of the larger fusiform ridge outline. Series width is 0.4–0.7 cm; ridge width is 0.05–0.15 cm (at the widest part); maximum ridge length is 0.7 cm.

Associated trace fossils. – *Monomorphichnus* isp. co-occurs with *Palaeophycus tubularis*.

Remarks. – The fusiform shape of the ridges is unusual for *Monomorphichnus*. *Monomorphichnus pectenensis* also has intervening subridges (Legg 1985, p. 157), but they are found in between more prominent ridges, whereas in the Chapel Island Formation specimens they are found within the fusiform ridges.

Similarities exist between *Monomorphichnus* isp. from the Chapel Island Formation and *Dimorphichnus ctenidos* of Gámez-Vintaned (1995), both developing series of fusiform ridges with delicate subridges within them. *Dimorphichnus ctenidos*, however, has additional smaller pusher imprints (Gámez-Vintaned 1995, fig. 3).

Ichnogenus *Palaeophycus* Hall, 1847

Discussion. – *Palaeophycus* is a subhorizontal burrow with a lining (Pemberton & Frey 1982; Keighley & Pickerill 1995) included in the category of architectural design of 'passively filled horizontal burrows' (Buatois *et al.* 2017). *Palaeophycus* was first described from the Ordovician 'Calciferous Sandstone' of northeastern USA (Hall 1847; Osgood 1970). In an in-depth review, Pemberton & Frey (1982) considered five *Palaeophycus* ichnospecies valid: *P. tubularis* Hall, 1847; *P. striatus* Hall, 1852; *P. heberti* (de Saporta, 1872); *P. sulcatus* (Miller & Dyer, 1878a); and *P. alternatus* Pemberton & Frey, 1982. The type ichnospecies, *Palaeophycus tubularis*, has a smooth, thin lining (Hall 1847; Pemberton & Frey 1982). *Palaeophycus striatus* has continuous longitudinal striae on the outer wall (Hall 1852; Pemberton & Frey 1982). *Palaeophycus heberti*, formerly *Siphonites heberti*, has a smooth, thick lining (de Saporta 1872; Pemberton & Frey 1982). *Palaeophycus sulcatus*, formerly *Trichophycus sulcatus*, has irregular anastomosing striae on the wall (Miller & Dyer 1878a; Pemberton & Frey 1982). Jensen (1997) considered that the striae could represent a taphonomic artifact resulting from sediment properties (see also Pemberton & Frey 1984) and argued that similar striae are produced biogenetically in *Palaeophycus imbricatus*. However, this view was not followed by other authors (e.g. Uchman 1999; Knaust 2004; Hammersburg *et al.* 2018). In addition, *Palaeophycus imbricatus*, formerly *Halopoa imbricata*, also displays bulges along its course that are clearly distinctive at ichnogeneric rank (see *Halopoa* section, p. 95). *Palaeophycus alternatus* has both transversal and longitudinal striae located at intervals along the length of the burrow (Pemberton & Frey 1982). Later, Buckman (1995) reviewed the literature on *Palaeophycus* possessing annulated walls and considered previously erected ichnospecies (i.e. *P. annulatus* Badve, 1987, *P. anulatus* McCann & Pickerill, 1988, and *P. serratus* McCann, 1993) invalid or as *nomina dubia*. Buckman (1995) then erected a new ichnospecies, *P. crenulatus*, to account for these forms. However, it is unclear why *Palaeophycus annulatus* was considered a *nomen dubium*: Badve (1987, pl. 3, figs 1, 4) figured specimens both in cross-section and bedding view that depict the massive infill and the distinct lining and annulations. Consequently, we retain here *Palaeophycus annulatus* as the senior synonym, and therefore as the valid ichnospecies for annulated *Palaeophycus*. Since the reviews by Pemberton & Frey (1982) and Buckman (1995), at least twelve other ichnospecies attributed to *Palaeophycus* have been erected or re-described: *P. tortuosus* Hall, 1852; *P. imbricatus* (Torell, 1870); *P. angulata* (Palibin in Vassoevich, 1932); *P. curvatus* Yang, 1983; *P. ferrovittatus* Hofmann, 1983; *P. wutingensis* Yang & Fu, 1985; *P. subornatus* Ghare & Kulkarny, 1986; *P. canalis* Elphinstone & Walter in Walter *et al.*, 1989; *P. hongshiyanensis* Luo, 1993; *P. beifengwanensis* Luo in Luo *et al.*, 1994; *P. bolbitermilus* Kim, Pickerill & Wilson, 2000; and *P. tiefengshanensis* Zhang, Zhou, Ge, Hu, Xiong & Yi, 2018. *Palaeophycus tortuosus* has a tortuous course and a thin lining (Hall 1852; Collette *et al.* 2011). It was placed in synonymy with *Palaeophycus tubularis* by Pemberton & Frey (1982) but re-considered valid by Collette *et al.* (2011). *Palaeophycus imbricatus*, formerly *Halopoa imbricata*, has irregular interweaving longitudinal striae and bulges along its course (Torell 1870; Jensen 1997), and is better located in *Halopoa* (see above, and in *Halopoa* section, p. 95). *Palaeophycus angulata*, formerly *Fucusopsis angulata*, has discontinuous longitudinal wrinkling striae and oblique step-like breaks on the surface of the burrow (Książkiewicz 1977; Crimes & McCall 1995). Although *Palaeophycus angulata* was considered valid by Crimes & McCall (1995) based on new material, this ichnospecies should be placed either within *Palaeophycus sulcatus* (Pemberton & Frey 1982) or *Halopoa imbricata* (Uchman 1998, 1999), based on a case-by-case re-study of each specimen. *Palaeophycus curvatus* has a curved course (Yang 1983; Bai *et al.* 2012), which is also diagnostic of *P. tubularis* (Pemberton & Frey 1982). *Palaeophycus ferrovittatus* has longitudinal striae on the internal side of the lining only (Hofmann 1983; Buckman 1995). MacNaughton & Narbonne (1999) suspected this structure might represent a tubular body fossil. *Palaeophycus wutingensis* has irregular striae and local swelling (Yang & Fu 1985; Zhang *et al.* 2018). Although these features are characteristic of *Halopoa imbricata*, swelling is not clearly displayed on the figured specimens (Yang & Fu 1985, pl. 2, figs 5b, 6a, 7) which would make it a junior synonym of *Palaeophycus sulcatus*. *Palaeophycus subornatus* has a thick wall and transverse striae (Ghare & Kulkarli 1986). These features are not clear from the figured holotype (Ghare & Kulkarli 1986, pl. 2, fig. 2), and this ichnospecies is regarded as a *nomen dubium* (Mángano *et al.* 1996a; Buatois *et al.* 1997). *Palaeophycus canalis* has one to four longitudinal grooves (Walter *et al.* 1989). This ichnospecies was suggested to be a junior synonym of *Palaeophycus*

heberti (Buckman 1992) or a potential *nomen dubium* (Buckman 1995) without clear justification (see also Kim *et al.* 2000). Re-evaluation of the type material is needed, and it may also represent a junior synonym of *Palaeophycus striatus*. *Palaeophycus hongshiyanensis* is a wide, smooth, and curved passively filled burrow (Luo 1993) and should be regarded as a junior synonym of *P. tubularis*. *Palaeophycus beifengwanensis* is smooth with a thin lining (Luo *et al.* 1994, pl. 2, fig. 2), and is a junior synonym of *P. tubularis*. *Palaeophycus bolbitermilus* has a wide bulbous termination at one extremity (Kim *et al.* 2000). *Palaeophycus tiefengshanensis* has a wall made of nodules and bivalve shell fragments (Zhang *et al.* 2018). This ichnospecies needs detailed re-evaluation, but the wall organisation is not diagnostic of *Palaeophycus* and may instead represent an example of an armored burrow (cf. Buatois *et al.* 2017). Consequently, eight ichnospecies, *Palaeophycus alternatus*, *P. annulatus*, *P. bolbitermilus*, *P. heberti*, *P. striatus*, *P. sulcatus*, *P. tortuosus*, and *P. tubularis*, are here considered valid.

Palaeophycus shows similarities with *Halopoa* Torell, 1870, *Macaronichnus* Clifton & Thompson, 1978, *Oblongichnus* Bel Haouz, Lagnaoui & Silantiev, 2020, and *Planolites* Nicholson, 1873. *Halopoa* is an actively filled horizontal burrow with longitudinal wrinkles and inflated segments (Uchman 1998; Mángano *et al.* 2002b). *Macaronichnus* is a lined, actively filled simple burrow (Clifton & Thompson 1978; Quiroz *et al.* 2010; Seike *et al.* 2015). *Oblongichnus* is a simple lined burrow randomly oriented and differs from *Palaeophycus* by its subrectangular cross-section (Bel Haouz *et al.* 2020). *Planolites* is a simple actively filled burrow without a lining (Pemberton & Frey 1982; Keighley & Pickerill 1995).

Palaeophycus ranges from the Ediacaran (e.g. Narbonne & Aitken 1990; Geyer & Uchman 1995; Jenkins 1995; Warren *et al.* 2014; Buatois & Mángano 2016; Mángano & Buatois 2020) to the Holocene (e.g. Ahlbrandt *et al.* 1978; Ratcliffe & Fagerstrom 1980; Pemberton & Frey 1985; Wetzel 2008; Dashtgard & Gingras 2012; Yang *et al.* 2021). A pre-Ediacaran example (Kulkarni & Borkar 1997b) has been later rejected in the light of subsequent revisions (Mángano & Buatois 2016, 2020). Moreover, Ediacaran shrinkage structures and tubular fossils (e.g. Poiré *et al.* 1984; Jenkins 1995) have also been mistaken for *Palaeophycus* (Jensen *et al.* 2006; Porada & Bouougri 2008). Producers are arthropods (Ahlbrandt *et al.* 1978; Ratcliffe & Fagerstrom 1980), enteropneusts (Gingras *et al.* 1999), possible mollusks (bivalves, gastropods; Osgood 1970), and annelid worms (e.g. Elder 1973; Howard & Frey 1975; Pemberton & Frey 1985; Bromley 1996; Gingras *et al.* 1999; Dashtgard & Gingras 2012). *Palaeophycus* is recorded in continental (e.g. Aceñolaza & Buatois 1993; MacNaughton & Pickerill 1995; Gillette *et al.* 2003; Melchor *et al.* 2003; Tanner *et al.* 2006; Krapovickas *et al.* 2009), marginal-marine (e.g. Pollard 1981; Beynon *et al.* 1988; Stanley & Feldmann 1998; Mángano *et al.* 2002b; Lucas & Lerner 2004; Palma-Ramírez *et al.* 2019), shallow-marine (e.g. Frey & Chowns 1972; Pemberton & Frey 1984; Maples & Suttner 1990; Mángano *et al.* 1996a; Schlirf 2000; Gaillard & Racheboeuf 2006), and deep-marine (e.g. D'Alessandro *et al.* 1986; Bjerstedt 1988; McCann & Pickerill 1988; Mángano *et al.* 1996c; Uchman 1998; Buatois & Mángano 2003c) environments. In the Chapel Island Formation, *Palaeophycus* was first recorded by Crimes & Anderson (1985) and has been regularly mentioned since then (e.g. Narbonne *et al.* 1987; Laing *et al.* 2019).

***Palaeophycus annulatus* Badve, 1987**

Figure 43A–C

Material. – Four specimens from Member 2A (Fortunian) in Fortune Head, Grand Bank Head, and Lewin's Cove.

Description. – Horizontal, unbranched burrows with delicate annulations. Preserved as full relief observed on bed top. Burrows are circular in cross-section, with a straight to curved course. Annulations are millimetric, tightly spaced, straight to slightly bent, and can be partially weathered along the burrow surface. Burrows are thinly lined. Infill is massive, composed of very fine- to fine-grained sandstone different from the mudstone host rock. Width is 0.2–0.4 cm; maximum length is 5.2 cm.

Associated trace fossils. – *Palaeophycus annulatus* co-occurs with *Palaeophycus tubularis*.

Remarks. – The presence of annulations allows placing these trace fossils in *Palaeophycus annulatus*. The millimetric thickness of annuli is comparable to the type material of *Palaeophycus annulatus* (cf. Badve 1987, pl. 2, fig. 4). The assignment of simple annulated burrows to either *Palaeophycus annulatus* or *Planolites annularis* Walcott can be subjective (cf. Fillion & Pickerill 1990; McCann 1993). In Member 2 of the Chapel Island Formation, many burrows were left open thanks to stiff sediments and were later passively filled (Droser *et al.* 2002). Consequently, an affinity to *Palaeophycus annulatus* is more likely. *Palaeophycus tubularis* from the Cambrian Mickwitzia Sandstone of Sweden (Jensen 1997, fig. 47C) displays annulations which are diagnostic of *P. annulatus*, although those could have also formed during compaction through

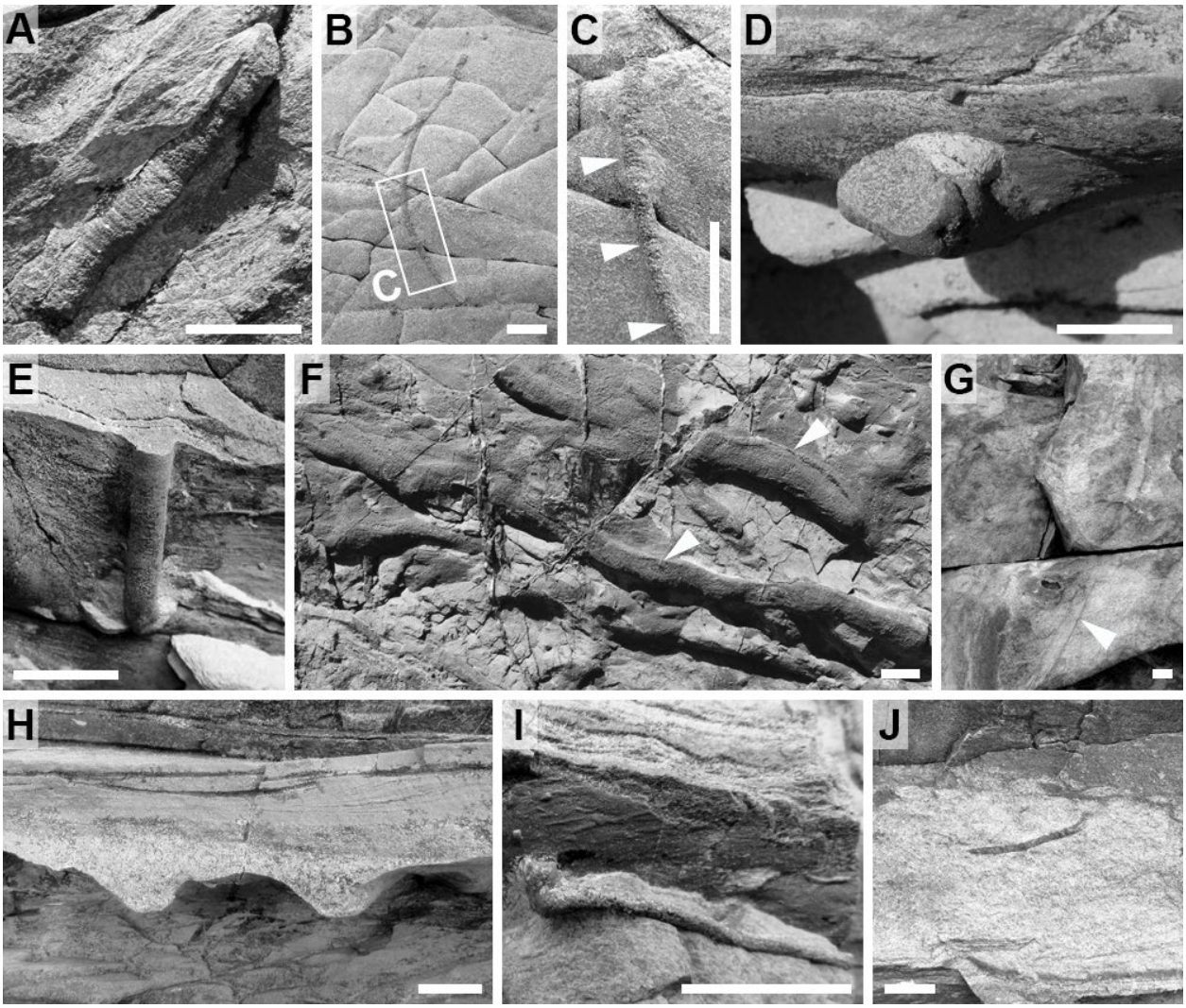

Fig. 43. Palaeophycus annulatus Badve (A–C), *P. tubularis* Hall (D–H), and *Palaeophycus* isp. (I, J). Scale bars are 1 cm. **A**, Straight *Palaeophycus annulatus* with millimetric annulations. Full relief observed on bed top, Fortune Head, Member 2A (Fortunian). **B**, Curved *Palaeophycus annulatus*. Full relief observed on bed top, Grand Bank Head, Member 2A (Fortunian). **C**, Close-up from Figure 43B showing millimetric annulations (arrows). **D**, *Palaeophycus tubularis* passively filled from the sandstone bed above. Full relief, Fortune Head, Member 2B (Fortunian). **E**, Straight *Palaeophycus tubularis*. Positive hyporelief, Fortune Head, Member 2A (Fortunian). **F**, Long, slightly tortuous *Palaeophycus tubularis*. Positive hyporelief, Fortune Head, Member 2A (Fortunian). **G**, *Palaeophycus tubularis* with a thin lining (arrow) overprinting a mottled fabric. Full relief observed on bed top, Little Dantzic Cove, Member 5 (Cambrian Age 2). **H**, Two *Palaeophycus tubularis* eroded and filled by medium-grained sand. Full relief, Fortune Head, Member 2A (Fortunian). **I**, Slightly tortuous *Palaeophycus* isp. connected to a very fine-grained sandstone bed. Full relief, Fortune Head, Member 2A (Fortunian). **J**, *Palaeophycus* isp. passively filled by sandy mud coming from the bed above. Full relief, Little Dantzic Cove, Member 5 (Cambrian Age 2).

the differential movement of sediment across the burrow (S. Jensen, pers. comm., 2024).

***Palaeophycus tubularis* Hall, 1847**

Figure 43D–H

? 1985 *Palaeophycus tubularis* Hall; Crimes & Anderson, p. 328, fig. 10.3.
? 2017 *Palaeophycus* isp. Herringshaw, Callow & McIlroy, p. 376, fig. 4a.
2019 *Palaeophycus tubularis* Hall; Laing, Mángano, Buatois, Narbonne & Gougeon, p. 1626, fig. 2f.

Material. – Hundreds of specimens from Members 2A, 2B, and 3 (Fortunian), and Members 4 and 5 (Cambrian Age 2) in Fortune Head, Fortune North, Grand Bank Head, Lewin's Cove, Little Dantzic Cove, and Point May.

Description. – Horizontal to oblique, unbranched, smooth burrows with a thin lining. Preserved as full relief, positive hyporelief, and positive and negative epirelief. Burrows are circular to elliptical in cross-section, with a straight, slightly tortuous to curved course. The width can vary slightly within a burrow. Burrow

collapse is common, revealing a distinct lining. Burrows are either isolated, oriented subparallel to each other, or densely and randomly overlapping. Infill is massive, composed of very fine- to medium-grained sandstone similar to the host rock, or different and encased in mudstone, sandy mudstone, or very fine- to fine-grained sandstone. Infill can be pyritized. Width is 0.1–1.3 cm; maximum length is 23.0 cm.

Associated trace fossils. – *Palaeophycus tubularis* co-occurs with *Conichnus conicus*, *Cruziana problematica*, *Curvolithus simplex*, *Didymaulichnus miettensis*, *Dimorphichnus* isp. A, *Halopoa imbricata*, *Helminthoidichnites tenuis*, *Helminthopsis abeli*, *H. tenuis*, *Monomorphichnus bilinearis*, *M. lineatus*, *Palaeophycus annulatus*, *Palaeophycus* isp., *Psammichnites gigas circularis*, *Rusophycus avalonensis*, *Teichichnus rectus*, *Treptichnus bifurcus*, *T. pedum*, *Trichichnus linearis*, and radial probing burrow.

Remarks. – Smooth simple burrows with thin linings are typical features of *Palaeophycus tubularis*. *Palaeophycus tubularis* was revised by Pemberton & Frey (1982) as possessing an infill similar to the host rock. However, they also noted that where dealing with heterolithic settings, the passive infill of *Palaeophycus* can be different from the host rock (see p. 850 in Pemberton & Frey 1982), which is notably common in Member 2 of the Chapel Island Formation. Pemberton & Frey (1982) argued that collapsing results from incomplete infill, which can be problematic ichnotaxonomically because fractures can form along the structure (compare *Palaeophycus tubularis* in Jensen 1997, fig. 47A with *P. striatus* in MacNaughton & Pickerill 1995, fig. 5.3 and Buatois *et al.* 1997, fig. 6.6). In the Chapel Island Formation, a lining is typically observed, but in rare cases it is inferred by the very sharp outlines of the burrow (cf. Keighley & Pickerill 1997; Stanley & Pickerill 1998). However, some authors considered sharp-walled burrows without a lining to belong to *Planolites* (e.g. Aceñolaza & Tortello 2003, fig. 3.9; Ahn & Babcock 2012, fig. 2A).

In the Chapel Island Formation, there is a high variety of forms and sizes in *Palaeophycus tubularis*. Crimes & Anderson (1985, fig. 10.3) only recorded one slab with *Palaeophycus tubularis* from Member 5 in Grand Bank Head which is difficult to interpret. On some of the burrow intervals, a trilobed ventral surface is observable which is typical of *Curvolithus simplex*, an ichnotaxon abundant in this part of the succession. Other burrow intervals are smooth which is more typical of *Palaeophycus tubularis*, but an interpretation as weathered *Curvolithus simplex* is also viable. Some of the previous records of *Planolites beverleyensis* (Billings) in the section (Crimes & Anderson 1985; Narbonne *et al.* 1987) may represent *Palaeophycus tubularis*, but the lack of figured specimens prevents definitive conclusions.

Overall, *Palaeophycus tubularis* is very common in the Cambrian (e.g. Jensen 1997; Goldring & Jensen 1996; Bartley *et al.* 1998; Grazhdankin & Krayushkin 2007; Shahkarami *et al.* 2017a; Ding *et al.* 2020). cf. *Palaeophycus tubularis* from the Cambrian Torneträsk Formation of Sweden (McLoughlin *et al.* 2021, fig. 10A–F) displays some distinctive features (trilobed bases, faint transverse segments, inflated segments) that are not characteristics of *Palaeophycus tubularis*.

***Palaeophycus* isp.**

Figure 43I, J

non ? 2017 *Palaeophycus* isp. Herringshaw, Callow & McIlroy, p. 376, fig. 4a.
2019 *Palaeophycus* isp. Laing, Mángano, Buatois, Narbonne & Gougeon, p. 1626, fig. 2g.

Material. – Hundreds of specimens from Members 2A, 2B, and 3 (Fortunian), and Members 4 and 5 (Cambrian Age 2) in Fortune Head, Fortune North, Grand Bank Head, Lewin's Cove, Little Dantzic Cove, and Point May.

Description. – Horizontal, oblique to rarely vertical, smooth, unbranched, passively filled burrows without clear lining. Preserved as full relief. Burrows are circular in cross-section, with a straight, curved to tortuous course. Burrows are isolated or aggregated. Infill is massive, composed of sandy mudstone and very fine- to medium-grained sandstone different from the mudstone, sandy mudstone, or very fine- to fine-grained sandstone host rock. Width is 0.1–0.5 cm; maximum length is 16.8 cm.

Associated trace fossils. – *Palaeophycus* isp. co-occurs with *Bergaueria perata*, *Conichnus conicus*, *Gyrolithes gyratus*, *G. scintillus*, *Palaeophycus tubularis*, *Teichichnus rectus*, *Treptichnus pedum*, *Trichichnus linearis*, and radial probing burrow.

Remarks. – Pemberton & Frey (1982) defined *Palaeophycus* as lined burrows with an infill similar to the host rock. However, they noted that the filling is different if 'the overlying sediment differed' (Pemberton & Frey 1982, p. 852; see also Fillion & Pickerill 1984b). In vertical exposures, Chapel Island Formation burrows with a different fill than the host rock are common in heterolithic facies. They are

either in contact with the overlying sedimentary bed ('adhering' preservation-style of Droser *et al.* 2002) or detached from it ('floating' preservation-style of Droser *et al.* 2002). These burrows described herein show evidence of passive fill from above and are therefore assigned to *Palaeophycus*. We follow here authors arguing that ichnotaxonomic decisions must be tempered by preservational considerations (Pemberton & Frey 1985; Fillion & Pickerill 1990; Keighley & Pickerill 1995). However, the absence of a lining precludes a decision at ichnospecies rank. Similar passively filled, unlined burrows were sometime described as *Planolites* elsewhere (e.g. Locklair & Savrda 1998; Hembree & Hasiotis 2007).

In the Chapel Island Formation, similar forms were drawn by Droser *et al.* (2002, fig. 4) and referred as *Planolites* and 'open burrow'. *Palaeophycus* isp. from the Chapel Island Formation described in Herringshaw *et al.* (2017, fig. 4a) are composed of short segments densely covering a lower bed surface and may probably be better affiliated to *Treptichnus*.

Ichnogenus *Psammichnites* Torell, 1870

Discussion. – *Psammichnites* is a backfilled subhorizontal trail with a median dorsal furrow/ridge (Mángano *et al.* 2002a, 2022) included in the category of architectural design of 'complex actively filled horizontal structures' (Buatois *et al.* 2017). *Psammichnites* was first described from the Cambrian Hardeberga Formation of southern Sweden (Torell 1870; Álvaro & Vizcaïno 1999). Torell (1868, 1870) erected *Psammichnites* for different types of trace fossils (see below) but did not provide a holotype. Therefore, Fischer & Paulus (1969) designated *Psammichnites gigas* as the type ichnospecies. Later, Häntzschel (1975) placed *Psammichnites* in synonymy with *Scolicia* and other horizontal backfilled trace fossils. Smith & Crimes (1983) demonstrated that only the trace fossils with double drainage tubes, which are affiliated to Mesozoic and Cenozoic spatangoid echinoids, should be included in *Scolicia* (see also Plaziat & Mahmoudi 1988, Uchman 1995, and Buatois *et al.* 2023). Uchman (1995) argued that Palaeozoic forms previously assigned to *Taphrhelminthopsis* most likely represent washed-out casts of either *Cruziana* or *Curvolithus*. Both *Cruziana* and *Curvolithus* differ significantly from Palaeozoic *Taphrhelminthopsis* in their construction. Mángano *et al.* (2002a) re-studied Palaeozoic forms based on a literature review and a critical evaluation of type specimens and new materials, concluding that these trace fossils should be assigned to *Psammichnites*. Pazos & Gutiérrez (2022) mentioned that the type material of *Psammichnites gigas* does not show the internal structure of other reports of *P. gigas*. However, as explained in Mángano *et al.* (2002a), *Psammichnites gigas* from the type locality in Sweden is preserved in quartzite, which has a negative impact on taphonomy and hampers preservation of more delicate features. As for comparison, a similar issue was discussed for small-scale *Cruziana*, where coarser-grained sediment impacts negatively on the preservation of delicate scratch imprints (Bromley & Asgaard 1979; Jensen *et al.* 2005; Sadlock 2010; Schatz *et al.* 2011). Still, material of *Psammichnites gigas* figured by Álvaro & Vizcaïno (1999, pl. 1, fig. 1) from the type locality does show, in places, crescentic laminae on the surface of the trails representing backfilling (see also Rohde 2009 and Mángano *et al.* 2022).

The ichnogenus *Olivellites* Fenton & Fenton has long been regarded a junior synonym of *Psammichnites* on the basis of shared characteristics that are considered ichnotaxobases at ichnogenus level (see discussion in Mángano *et al.* 2022). Pazos & Gutiérrez (2022) recently stated that all post-Cambrian ichnospecies of *Psammichnites* should be relocated in *Olivellites,* based on their study of specimens from the Carboniferous of Argentina. In addition to claiming that *Psammichnites gigas* does not show evidence of backfill (see above), Pazos & Gutiérrez (2022) also argued that *Psammichnites gigas* has different width and length than *Olivellites*, but size is not considered a good ichnotaxobase (Bertling *et al.* 2006, 2022). Furthermore, length is of no relevance in this type of trace fossils, as it does not convey any significant information. Pazos & Gutiérrez (2022) also mentioned that the lithological contrast with the host rock is different for *Psammichnites gigas* and *Olivellites*. This argument is dubious, as lithological contrast in *Psammichnites gigas* is variable and is essentially a reflection of its preservation in various environments, encompassing both sandstone-dominated and heterolithic bedsets (cf. Álvaro & Vizcaïno 1999; MacNaughton *et al.* 2021; Mángano *et al.* 2022). A critical evaluation of the type specimens and additional material from various stratigraphical units reinforced the widely accepted notion that *Olivellites* is a junior synonym of *Psammichnites* (Mángano *et al.* 2002a, 2022; Murray *et al.* 2024).

At least thirteen ichnospecies attributed to *Psammichnites* have been described in the literature: *P. gigas* (Torell, 1868); *P. filiformis* Torell, 1870; *P. gumaelii* Torell, 1870; *P. impressus* Torell, 1870; *P. clintonensis* Dawson, 1890; *P. biseriatus* (Clarke & Swartz, 1913); *P. plummeri* (Fenton & Fenton, 1937b); *P. saltensis* (Aceñolaza & Durand, 1973); *P. circularis* (Crimes, Legg, Marcos & Arboleya, 1977); *P. grumula*

(Romano & Meléndez, 1979); *P. sintanensis* Yang, 1984; *P. implexus* (Rindsberg, 1994); *P. pittermanni* Zessin, 2009; and *P. devonicus* Bradshaw, 2010. The type ichnospecies, *Psammichnites gigas*, formerly *Arenicolites gigas*, has a straight to looping course with a straight to sinusoidal dorsal median feature (Hofmann & Patel 1989; Seilacher & Gámez-Vintaned 1995; Álvaro & Vizcaïno 1999). Recently, Mángano *et al.* (2022) recognised three ichnosubspecies of *Psammichnites gigas* (*P. gigas arcuatus* Roedel, *P. gigas circularis*, and *P. gigas gigas* Torell) depending on slight but readily noticeable morphological differences (see 'Remarks' below in *P. gigas circularis*, p. 115). *Psammichnites filiformis* is a horizontal meandering trace fossil with annulations (Torell 1870; Jensen 1997). Although Nathorst (1881) placed this ichnotaxon in synonymy with *Fraena tenella*, Jensen (1997) disagreed and suspected a synonymy with *Olenichnus* isp. *Psammichnites gumaelii* is a curved trace fossil with a median structure and transverse ridges (Torell 1870). Torell (1870) did not provide any illustration, and this ichnospecies is currently considered a *nomen dubium* as material could not be recovered from museum collections (S. Jensen, pers. comm., 2021). *Psammichnites impressus* is a bilobed to trilobed horizontal trace fossils (Torell 1870; Jensen 1997). Jensen (1997) considered it a *nomen dubium,* as the type material could not be found in Torell's collection. *Psammichnites clintonensis* is a horizontal trail with a thick median ridge and possible transverse laminae (Dawson 1890, fig. 3), and a detailed revision is required. *Psammichnites biseriatus*, formerly *Pteridichnites biseriatus*, has a dorsal median groove, a meniscoid internal backfilling, and a ventral surface with a double row of shallow depressions, either displayed side-by-side or staggered (Clarke & Swartz 1913; Miller *et al.* 2009; Mángano *et al.* 2022). Although ventral features are not recommended for ichnospecies discrimination, the strong peculiarity of *Psammichnites biseriatus* may suffice to retain it as valid (Mángano *et al.* 2022). *Psammichnites plummeri*, formerly *Olivellites plummeri*, has a straight dorsal median feature and delicate crenulated transverse ridges (Fenton & Fenton 1937b; Mángano *et al.* 2002a). *Psammichnites saltensis*, formerly *Nereites saltensis,* has an irregular meandering course with distinctive kinks after each turn (Aceñolaza & Durand 1973; Seilacher *et al.* 2005). Although the inclusion of these forms within *Psammichnites* has been contested by some authors (Aceñolaza & Aceñolaza 2007; Aceñolaza *et al.* 2009; Pazos & Gutiérrez 2022), morphological features of *Nereites* are absent (i.e. lateral paired lobes surrounding a zone of reworked sediment; Orr & Pickerill 1995; Uchman 1995; Seilacher *et al.* 2005), whereas the median siphon mark separating the two lobes of *Psammichnites* is present in some preservational variants. *Psammichnites circularis*, formerly *Taphrhelminthopsis circularis*, was mentioned informally by Jensen & Palacios (2016) and Ebbestad *et al.* (2022) for trace fossils now referred to as *P. gigas circularis* (Mángano *et al.* 2022). *Psammichnites grumula*, formerly *Olivellites grumula*, has regularly spaced dorsal median holes/mounds (Romano & Meléndez 1979; Mángano *et al.* 2002a). Yang (1984) described *Psammichnites sintanensis* as a horizontal trail with a median ridge and irregular transverse imprints. Yang (1984) differentiated *Psammichnites sintanensis* from other *Psammichnites* ichnospecies based on its greater width and thicker transverse laminae. Size is not considered a good ichnotaxobase (Bertling *et al.* 2006, 2022), and the thickness of backfilled laminae can depend on preservation. This ichnospecies may be better located within *Psammichnites biseriatus*. *Psammichnites implexus*, formerly *Uchirites implexus*, has a sharp, continuous, and straight dorsal median structure and very fine, subtle transverse ridges (Rindsberg 1994; Mángano *et al.* 2002a). *Psammichnites pittermanni* is a structure with two parallel grooves (Zesssin 2009, figs 19, 20) and is of dubious biogenic affinity. *Psammichnites devonicus* has tight backfilled laminae, an irregular dorsal median groove, and a ventral median string (Bradshaw 2010). Bradshaw (2010) considered the ventral median string to be the most diagnostic feature of *Psammichnites devonicus*, but ventral features in *Psammichnites* are variable and are not recommended for ichnospecies discrimination (Mángano *et al.* 2002a). The tight backfilled laminae are, however, reminiscent of *Psammichnites plummeri*. Re-evaluation of *Psammichnites devonicus* could confirm the synonymy, especially knowing that the basal surface of *P. plummeri* can expose a trilobed morphology with a median string (Mángano *et al.* 2002a, fig. 3A). Consequently, six ichnospecies, *Psammichnites biseriatus, P. gigas*, *P. grumula*, *P. implexus*, *P. plummeri*, and *P. saltensis*, are here considered valid; the status of *P. clintonensis* awaits re-evaluation of the type material.

Psammichnites shows similarities with *Bichordites* Plaziat & Mahmoudi, 1988, *Cochlichnus* Hitchcock, 1858, *Curvolithus* Fritsch, 1908, *Dictyodora* Weiss, 1884, *Didymaulichnus* Young, 1972, *Parapsammichnites* Buatois, Almond, Mángano, Jensen & Germs, 2018, and *Scolicia* de Quatrefages, 1849. *Bichordites* and *Scolicia* are horizontal backfilled burrows with a single or double ventral drainage string(s), respectively (Smith & Crimes 1983; Plaziat & Mahmoudi 1988; Pickerill *et al.* 1993; Seilacher & Gámez-Vintaned 1995; Uchman 1995; Buatois *et al.* 2023). Both

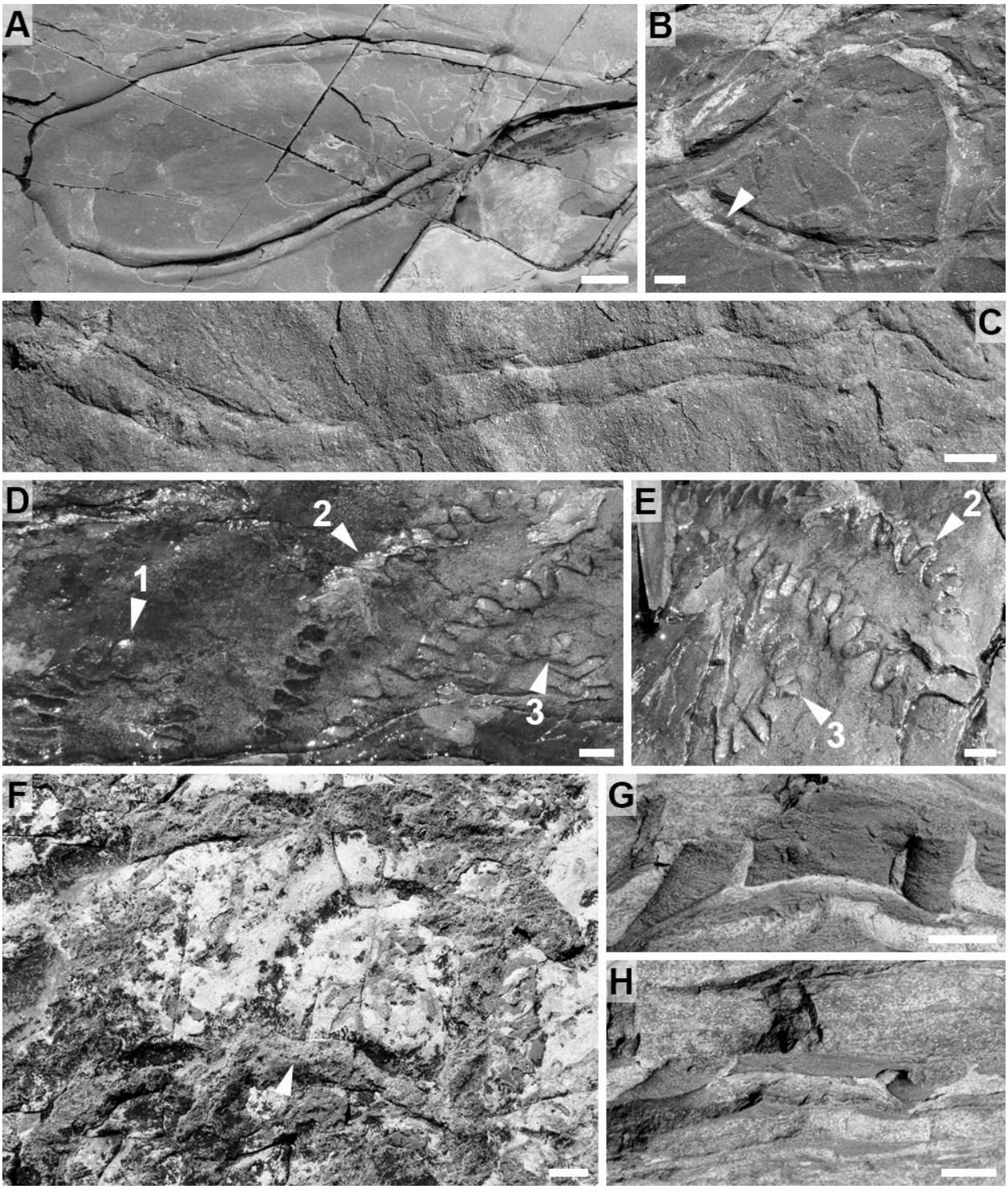

Fig. 44. Psammichnites gigas circularis (Crimes, Legg, Marcos & Arboleya). Scale bars are 1 cm (B, C, F–H) and 2 cm (A, D, E). **A**, Looping specimen showing two lobes and a slightly sinusoidal median furrow. Positive epirelief, Fortune Head, Member 2B (Fortunian). **B**, Looping specimen with a uni- to bilobed ventral surface (arrow). Negative epirelief, Fortune Head, Member 2B (Fortunian). **C**, Straight to slightly tortuous specimen with sharp outlines and a partially preserved straight dorsal ridge. Positive epirelief, Little Dantzic Cove, Member 5 (Cambrian Age 2). **D**, Specimen with three partially preserved meanders (numbered), showing a highly sinuous median furrow. Positive epirelief, Little Dantzic Cove, Member 5 (Cambrian Age 2). **E**, Close-up at the specimen Figure 44D pictured from the opposite side, showing two of the meanders (same numbers as in Fig. 44D) and the bulged area with the furrow delineating the overall trail course. **F**, Surface with many specimens displaying their internal backfilling. Note the rare preservation of a bulged dorsal surface with a median furrow (arrow). Full relief, Little Dantzic Cove, Member 3 (Fortunian). **G**, Two specimens with delicate transverse striae on their ventral surface. Positive hyporelief, Grand Bank Head, Member 2A (Fortunian). **H**, Same specimens as in Figure 44G showing flat cross-sections.

ichnogenera share complex ventral features and oval cross-sections that are different from *Psammichnites*. *Cochlichnus* is a simple horizontal sinusoidal trail (Buatois & Mángano 1993a), and the siphon mark of *Psammichnites gigas circularis* can mimic *Cochlichnus* if lobes are not developed (McIlroy & Heys 1997; Mángano *et al.* 2022). *Curvolithus* is a horizontal trail with a characteristic trilobed dorsal surface (Buatois *et al.* 1998c). The uni- to trilobed ventral surface of *Curvolithus* can be similar to *Psammichnites*, and their distinction then relies on the presence of a distinctive backfilling in *Psammichnites*. *Dictyodora* is a backfilled subhorizontal trace fossil with a prominent conical structure at its top resulting from the migration of a long vertical snorkel (Benton 1982b; Seilacher-Drexler & Seilacher 1999) that is absent in *Psammichnites*. *Didymaulichnus* is a smooth horizontal trail with two raised ventral lobes and a median furrow (Young 1972). Absence of backfilling and the poorly known dorsal surface of *Didymaulichnus* distinguish it from *Psammichnites*. *Parapsammichnites* has a uni- to bilobed ventral surface and local transversal laminae delineating inclined sediment pads (Buatois *et al.* 2018). *Parapsammichnites* does not possess the dorsal median feature of *Psammichnites* but represents a primitive form of sediment bulldozing belonging to the '*Psammichnites* evolutionary lineage' (Buatois *et al.* 2018; Mángano *et al.* 2022).

Psammichnites ranges from the Cambrian (e.g. Matthew 1890; Hofmann & Patel 1989; Bryant & Pickerill 1990; Álvaro & Vizcaïno 1999; Jago & Gatehouse 2007; MacNaughton *et al.* 2021) to the Permian (Skwarko & Seilacher 1993; Bann 1998; Luo *et al.* 2017). Ediacaran *Psammichnites* in Jenkins (1995, pl. 2, figs F, G) are complex structures displaying thin transverse laminations, and two ventral longitudinal ridges. The absence of a dorsal expression limits their comparison to *Psammichnites*. Jensen *et al.* (2006) also suggested a possible affinity to tubular body fossils. In addition, Droser *et al.* (2006) mentioned that these are float specimens, therefore casting doubts with respect to their provenance. A possible Triassic occurrence has been figured by Luo *et al.* (2016). This would represent the only post-Palaeozoic record of *Psammichnites* and, accordingly, further work on the detailed morphology of these specimens is encouraged. Potential producers are arthropods (Yochelson & Schindel 1978), molluscs (Fenton & Fenton 1937b; Häntzschel 1975; Bryant & Pickerill 1990; Mángano *et al.* 2002a; Seilacher & Hagadorn 2010), flatworms (Matthew 1888; Seilacher & Gámez-Vintaned 1995; Gámez-Vintaned *et al.* 2006; McIlroy & Heys 1997), and organisms related to halkieriids (Seilacher-Drexler & Seilacher 1999). *Psammichnites* is recorded in marginal-marine (e.g. Hofmann & Patel 1989; Greb & Chesnut 1994; Mángano & Buatois 2004b; Buatois *et al.* 2005; Alonso-Muruaga *et al.* 2012; Desjardins *et al.* 2012) and shallow-marine (e.g. McIlroy & Heys 1997; Buatois & Mángano 2012b; Weber *et al.* 2013; Carbone & Narbonne 2014; MacNaughton *et al.* 2021; Ornia *et al.* 2024) environments. Deep-marine occurrences (Gingras *et al.* 2011) are rare. *Psammichnites* has only been mentioned in the Chapel Island Formation recently (supplementary material in Mángano & Buatois 2014), and previous reports were referred to as *Helminthoida* Schafhäult, *Taphrhelminthopsis*, and possibly *Muensteria* Sternberg and *Uchirites* Macsotay (e.g. Crimes & Anderson 1985; Narbonne *et al.* 1987).

***Psammichnites gigas circularis* (Crimes, Legg, Marcos & Arboleya, 1977)**

Figures 44A–H & 45A–C

1985 ?*Taphrhelminthopsis circularis* Crimes, Legg, Marcos & Arboleya; Crimes & Anderson, p. 332, fig. 12.6.
1985 *Taphrhelminthopsis circularis* Crimes, Legg, Marcos & Arboleya; Crimes & Anderson, p. 332, fig. 12.7.
1987 *Taphrhelminthopsis circularis* Crimes, Legg, Marcos & Arboleya; Narbonne, Myrow, Landing & Anderson, p. 1287, fig. 6F.
2002 *Taphrhelminthopsis* Sacco; Droser, Jensen, Gehling, Myrow & Narbonne, p. 9, fig. 6A.
? 2002 *Taphrhelminthopsis* Sacco; Droser, Jensen, Gehling, Myrow & Narbonne, p. 11, fig. 9.
2003 '*Taphrhelminthopsis*' *circularis* Crimes, Legg, Marcos & Arboleya; Jensen, p. 222, fig. 4.
2016 *Psammichnites* Torell; Mángano & Buatois, p. 91, fig. 3.10a.
2017 ?*Psammichnites* isp. Herringshaw, Callow & McIlroy, p. 376, fig. 4c.
2017 ?*Thalassinoides* isp. Herringshaw, Callow & McIlroy, p. 376, fig. 4e.
2017 *Psammichnites* Torell; Landing *et al.*, p. 45, fig. 17J.
2018 *Psammichnites gigas* (Torell); Hantsoo, Kaufman, Cui, Plummer & Narbonne, p. 1243, fig. 2e.

Material. – About 170 specimens from Members 2A, 2B, and 3 (Fortunian) and Members 4 and 5 (Cambrian Age 2) in Fortune Head, Fortune North, Grand Bank Head, Lewin's Cove, Little Dantzic Cove, and Point May.

Description. – Horizontal to subhorizontal, unbranched, backfilled trails with a median dorsal feature. Preserved as positive hyporelief, positive and negative epirelief, and full relief. Cross-section is flat to elliptical. The course is straight, curved, winding, meandering loosely, looping, or scribbling. Ventral surface is unilobed, rarely bilobed. Dorsal surface is bilobed with an incising median furrow or ridge. The dorsal median feature is straight, slightly sinusoidal, to highly sinusoidal, with transitions from the two formers; the median feature

Fig. 45. Circling and scribbling *Psammichnites gigas circularis* (Crimes, Legg, Marcos & Arboleya), previously referred to as 'circular spreiten burrow' or 'spiral trace'. Scale bars are 2 cm. All photographs are from Member 2B (Fortunian). **A**, *In situ* specimen with overlapping circles. Note the lateral deviation of circles (arrow). Negative epirelief, Fortune Head. **B**, Loose specimen with overlapping circles (clearly visible at arrow). Photograph courtesy of P. Myrow. Positive hyporelief, Brunette Island. **C**, Loose specimen with scribbles. Positive hyporelief, Fortune Head.

can also collapse, resulting in a wider, depressed median area. Width is typically constant within a trail. Where terminations are visible, they taper in an arcuate tip, or can be broken abruptly. A thin lining is rare but has been noted. Rarely, longitudinal striae are visible on the sides of the trail. Overlapping of trails is common and can result in false branching. Avoidance of previously visited areas has also been noted. Infill is either massive or made or millimetric, straight to curved transverse laminae visible either on the ventral surface, or in longitudinal sections showing the internal organization. Infill is composed of sandy mudstone or very fine- to medium-grained sandstone similar to the host rock, or different where encased in mudstone. Width is 0.5–4.5 cm; maximum length is 124 cm; dorsal median feature is 0.05–0.1 mm wide (where not collapsed); transverse laminae are 0.05–0.3 cm thick (where visible).

Associated trace fossils. – *Psammichnites gigas circularis* co-occurs with *Archaeonassa fossulata*, *Cruziana problematica*, *Curvolithus simplex*, *Dendroidichnites* aff. *D. irregulare*, *Didymaulichnus miettensis*, ?*Diplocraterion* isp., *Halopoa imbricata*, *Helminthoidichnites tenuis*, *Palaeophycus tubularis*, *Rosselia erecta*, *Rusophycus avalonensis*, *Teichichnus rectus*, *Treptichnus pedum*, *Trichichnus linearis*, and radial probing burrow.

Remarks. – In a recent review, Mángano *et al.* (2022) defined three ichnosubspecies of *Psammichnites gigas*. *Psammichnites gigas gigas*, which comprises the type material from the Cambrian of Sweden (Torell 1868, 1870), is characterised by a high convexity, a straight median feature, and a straight, sinuous, or bent course without systematic circling or scribbling. *Psammichnites gigas circularis*, formerly *Taphrhelminthopsis circularis*, has a low convexity, a straight to local sinusoidal median feature, and tends to develop circular courses that can loop and scribble. A typical example of *Psammichnites gigas circularis* is the 'lasso trail' first recorded by Seilacher & Gámez-Vintaned (1995) from the Cambrian of central Spain (see also Seilacher 1997a, 2007, and Mángano *et al.* 2022). *Psammichnites gigas arcuatus*, formerly *Plagiogmus arcuatus*, has a typical basal ladder-trail made of thick transverse elements. In the Chapel Island Formation, a basal ladder-trail is never observed, which rules out identification of *Psammichnites gigas arcuatus*. Some specimens show straight courses and straight median features which are shared by *Psammichnites gigas circularis* and *P. gigas gigas*, but a high convexity in cross-section has not been observed. Specimens of the Chapel Island Formation are almost exclusively of low relief, in places displaying sinusoidal median furrows, and tend to bend or loop. Consequently, we assign confidently the Chapel Island Formation material to *Psammichnites gigas circularis*.

Negative epireliefs with two concave lobes and a straight median ridge are common in the Chapel Island Formation (e.g. Figs 28E, 44B). Their interpretation is ambiguous, as they can either represent the ventral surface of *Psammichnites* or *Curvolithus*. Ventrally bilobed *Psammichnites* have been recorded from the Cambrian elsewhere (e.g. Álvaro & Vizcaïno 1999; Jensen & Palacios 2016). The correct affiliation then relies on their association with other preservational variants of *Psammichnites* or *Curvolithus* on the same surfaces, or on the presence of transverse laminae, which are typical of *Psammichnites* backfilling. In addition, distinction of *Psammichnites gigas circularis* from *Teichichnus rectus* may also be

difficult, if the latter is wide and extending at length on bedding surfaces; these forms are fairly common around the base of Member 2B (e.g. Fig. 50B). Key distinctive features are the more irregular width, and the careful identification of oblique internal laminae in *Teichichnus*.

The first report of *Psammichnites gigas circularis* in the section was from Crimes & Anderson (1985, fig. 12.6), which shows collapsing of the median furrow. Another report by Crimes & Anderson (1985, fig. 12.7) is a meandering specimen that displays the typical bilobed dorsal preservation. Narbonne *et al.* (1987) recorded 'circular spreiten burrows' close to the base of Member 2B at Fortune Head. These trace fossils have been spotted *in situ* and recovered from loose samples (Fig. 45A–C). Although these specimens were interpreted as spiral trace fossils in Crimes & Fedonkin (1994, fig. 2I), they display abundant overlapping (i.e. looping and scribbling), with evidence of backfilling, and most likely represent preservational variants of *Psammichnites gigas circularis* (cf. Gougeon *et al.* 2022). Similar forms may have been recorded recently under the name *Spirocircus* isp. by Bokr *et al.* (2021) from the Ordovician of Czech Republic. Finally, it is possible that the reports of *Muensteria* sp. and ?*Uchirites* sp. by Narbonne *et al.* (1987) from Members 3 and 5 represent preservational variants of *Psammichnites gigas circularis* as well.

Psammichnites cf. *P. saltensis* (Aceñolaza & Durand, 1973)

Figure 46A–G

	1985	*Helminthoida crassa* Schafhäutl; Crimes & Anderson, p. 322, fig. 7.1, 7.2.
	1985	*Helminthoida miocenica* Sacco; Crimes & Anderson, p. 322, fig. 7.3, 7.4.
?	1985	*Helminthoida miocenica* Sacco; Crimes & Anderson, p. 322, fig. 7.5.
partim	1987	*Helminthoida* Schafhäult; Conway Morris, p. 163, fig. 8.
	2016	*Psammichnites* isp. Mángano & Buatois, p. 100, fig. 3.18c.
	2017	*Psammichnites* isp. Landing *et al.*, p. 45, fig. 17F.
	2018	*Psammichnites* isp. Hantsoo, Kaufman, Cui, Plummer & Narbonne, p. 1243, fig. 2k.
	2020	*Psammichnites* isp. Mángano & Buatois, p. 14, fig. 3c.
	2022	*Psammichnites* isp. Mángano *et al.*, fig. 7A, B.

Material. – About 45 specimens from Member 2B (Fortunian) in Fortune Head and Grand Bank Head.

Description. – Horizontal, unlined, unbranched trails with regular meanders, in places displaying kinks after U-turns. Preserved as positive hyporelief and negative epirelief. Specimens are in places isolated, or densely cover bed surfaces. Cross-section is rarely exposed but is circular in positive hyporelief. The course consists of regular U-turns that delineate segments; segments have variable lengths and typically run in parallel to each other. Rarely, specimens start as loose meanders and progressively build-up regular meanders. In places, a kink is visible close to a U-turn; the kink is typically small, and the course stays parallel to the previous segment. Rarely, the kink forms a V-shape with a higher angle. Infill is typically massive, or displays backfilling made of coarse arcuate elements in positive hyporelief. Infill is composed of very fine- to fine-grained sandstone similar to the host rock. Width of the trail is 0.3–0.7 cm; maximum length of the trail is 67.0 cm; width of the meandering system is 6.3–10.2 cm; length of the meandering system is 4.2–17.3 cm.

Associated trace fossils. – *Psammichnites* cf. *P. saltensis* co-occurs with *Palaeophycus tubularis* and *Treptichnus pedum*.

Remarks. – Diagnostic features of *Psammichnites saltensis* are: (1) a meandering system with U-turns; (2) large U-turns; (3) a kink after each turn; (4) a loose or guided course after the kink; and (5) two lobes and a median furrow in positive epirelief (Aceñolaza & Durand 1973; Seilacher *et al.* 2005). In the Chapel Island Formation, U-turns are not as large as in the type material, and the course is mostly guided. However, although the kink is less pronounced as in the type material, larger V-shaped kinks occur in places in the studied specimens (Fig. 46D). The nature of the upper surface of the trail is unknown, as the specimens are not exposed in positive epirelief. In addition, most specimens of the Chapel Island Formation are weathered, which renders their analysis difficult. For these reasons, we refer to the Chapel Island Formation material as *Psammichnites* cf. *P. saltensis*.

Reports of *Psammichnites saltensis* are scarce, with specimens only identified from Argentina (Aceñolaza & Durand 1973; Seilacher *et al.* 2005) and western Canada (under the name *Helminthorhaphe* isp. in Hofmann *et al.* 1994, fig. 3A, but assigned to *Psammichnites saltensis* by Seilacher *et al.* 2005). *Helminthoida* isp. in Goldring & Jensen (1996, fig. 3a) displays regular meanders and rare small kinks, which are similar features to *Psammichnites* cf. *P. saltensis*. Moreover, this material shows an incising median furrow and two lobes along short intervals, which reinforce their affiliation to *Psammichnites*. Additional material interpreted as *Helminthoida* sp. (Narbonne

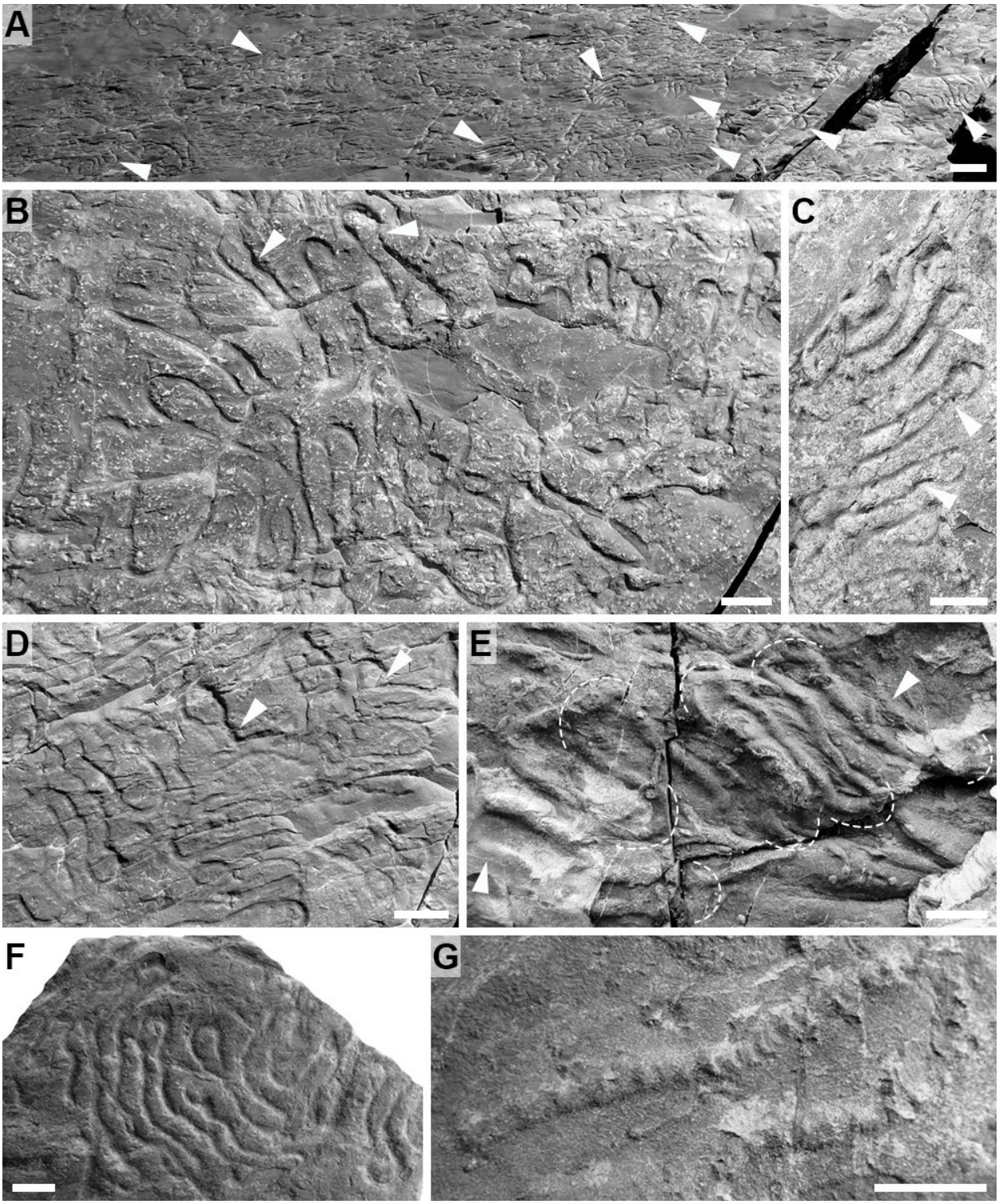

Fig. 46. Psammichnites cf. *P. saltensis* (Aceñolaza & Durand). Scale bars are 1 cm (C, E–G), 2 cm (B, D), and 10 cm (A). All photographs are from Member 2B (Fortunian). **A**, Large surface with multiple specimens (arrows). Negative epirelief, Fortune Head. **B**, Surface with loosely to regularly meandering specimens, some displaying small kinks (arrows). Negative epirelief, Fortune Head. **C**, Regularly meandering specimen, with small distinctive kinks after each U-turn (arrows). Negative epirelief, Fortune Head. **D**, Surface covered with specimens, some displaying large V-shaped kinks (arrows). Negative epirelief, Fortune Head. **E**, Specimen with regular meanders. Start and end points are arrowed, and U-turns are enhanced with dashed lines. Positive hyporelief, Fortune Head. **F**, Specimen with regular meanders. GSC 73327. Negative epirelief, Grand Bank Head. **G**, Specimen showing backfilling made of thick arcuate elements. GSC 73330. Positive hyporelief, Grand Bank Head.

& Aitken 1990, pl. 4, fig. 1) and ?*Helminthoida* isp. (Goldring & Jensen 1996, fig. 2e) display meanders with U-turns, distinct lobes, and collapsed median furrows, which are features of *Psammichnites*.

Crimes & Anderson (1985) described *Helminthoida crassa* Schafhäutl and *H. miocenica* in the Chapel Island Formation, both assignments followed in subsequent studies (Narbonne *et al.* 1987; Landing *et al.* 1988; Herringshaw *et al.* 2017). Uchman (1995) placed *Helminthoida crassa* of Crimes & Anderson (1985, fig. 7.1, 7.2) in synonymy with *Helminthorhaphe flexuosa* Uchman. *Helminthorhaphe* Seilacher is a meandering system with a smooth surface and a high amplitude at each U-turn, with its type ichnospecies, *H. japonica* (Tanaka), also lacking kinks along its course (Uchman 1995). These features do not agree with the morphology of the Chapel Island Formation material as recorded herein. *Helminthorhaphe reflecta* Seilacher, however, is another ichnospecies that displays a kink after each turn followed by a thigmotaxic component (Raup & Seilacher 1969; Seilacher 1977). Although similarities with the Chapel Island Formation material are more evident, high amplitude of the turns, important variations in segment length, and absence of backfilling do not support the comparison. In addition, the validity of *Helminthorhaphe reflecta* and its affinity with other material of *Helminthorhaphe*, and notably to its lectotype, has not been discussed and revised since the review by Uchman (1995). To complicate further, the type material of *Helminthoida* is now considered a junior synonym of *Nereites* (Uchman 1995). The paired lateral lobes surrounding a central zone of reworked sediment, which are features typical of *Nereites*, have not been observed in the Chapel Island Formation material. In addition, backfilling in the Chapel Island Formation is composed of closely spaced, thick arcuate elements of regular width (Fig. 46G), which is different from the well-separated fecal pellets of *Nereites* (i.e. *Scalarituba* Weller preservational variant, Seilacher 2007). Therefore, comparisons of the Chapel Island Formation material with either *Helminthorhaphe* or *Nereites* are discarded. Instead, the development of a regular meandering system with distinct kinks in negative epirelief, and diagnostic backfilling in positive hyporelief, support the comparison with *Psammichnites saltensis*.

Ichnogenus *Rosselia* Dahmer, 1937

Discussion. – *Rosselia* is a vertical spindle-shaped burrow (Nara 1995; Liou *et al.* 2022) included in the category of architectural design of 'vertical concentrically filled burrows' (Buatois *et al.* 2017). *Rosselia* was first described from the Devonian 'Taunus Quartzite' of western Germany (Dahmer 1937; Schlirf *et al.* 2002; Nara *et al.* 2004). Five ichnospecies attributed to *Rosselia* have been formally proposed: *R. erecta* (Torell, 1870); *R. socialis* Dahmer, 1937; *R. rotatus* McCarthy, 1979; *R. prolifera* (Fournier, Pemberton & Risk, 1980); and *R. chonoides* Howard & Frey, 1984. The type ichnospecies, *Rosselia socialis*, has nested concentric laminae (Dahmer 1937; Nara 1995). *Rosselia erecta*, formerly *Micrapium erectum*, has an enlarged causative tube within the funnel-shaped aperture (Torell 1870; Knaust 2021). *Rosselia rotatus* has crescentic structures within the funnel resulting from the rotary movement of the central tube (McCarthy 1979; Knaust 2021). *Rosselia chonoides* has helicoid swirls of reworked sediment (Howard & Frey 1984). Uchman & Krenmayr (1995) questioned the validity of both *Rosselia rotatus* and *R. chonoides*, which they regarded as junior synonyms of *R. socialis*. These authors suggested that the absence of concentric laminae in *Rosselia chonoides* was the result of secondary reworking of the funnel, a decision endorsed here as it is also observed in the Chapel Island Formation (Fig. 47B). Uchman & Krenmayr (1995) regarded *Rosselia rotatus* as an intraspecific variant of *R. socialis*, whereas MacEachern & Bann (2020) and Knaust (2021) recently retained it as valid. We consider that the crescentic infill structures of *Rosselia rotatus* record a constructional difference resulting from the distinctive lateral displacement of the producing organism, which could be considered a valid ichnotaxobase at ichnospecies rank. However, the holotype was only drawn by McCarty (1979, text-fig. 4e, f), and revision and convincing illustration is required before leading to a definitive conclusion. *Rosselia prolifera*, formerly *Polycylindrichnus prolifer*, is a branched vertical burrow with subconical individual elements (Fournier *et al.* 1980; Knaust 2021). Knaust (2021) considered the branching diagnostic, but the morphology of concentric laminae is not forming a bulb (like in *Rosselia*) but instead has a subconical shape (like in *Cylindrichnus*), as it was clearly stated in the original diagnosis by Fournier *et al.* (1980). *Cylindrichnus candelabrus* Głuszek, 1998 is currently considered the valid ichnospecies for branched *Cylindrichnus* (Knaust 2021). The morphology of the concentric laminae in *Rosselia prolifera* and *Cylindrichnus candelabrus* is similar, as well as their dichotomous branching pattern (compare branching of *R. prolifera* in Fournier *et al.* 1980, fig. 1 with branching at right side of the type material of *C. candelabrus* in Głuszek 1998, fig. 7A). Therefore, *Rosselia prolifera* should either remain within *Polycylindrichnus* or be considered as the senior synonym for branched *Cylindrichnus* over *C. candelabrus*. Consequently, *Rosselia erecta* and *R. socialis*

are considered valid here, whereas *R. rotatus* awaits further revision of its type material.

Rosselia shows similarities with *Asterosoma* von Otto, 1854, *Cylindrichnus* Toots in Howard, 1966, and *Monocraterion* Torell, 1870. *Asterosoma* has bulbs made of concentric laminae oriented horizontally, whereas *Rosselia* is oriented vertically (Martino 1989; Schlirf 2000). *Cylindrichnus* is a vertical, subcylindrical burrow with concentrically layered infill, but lacks the bulbous upper burrow portion that is diagnostic of *Rosselia* (Howard & Frey 1984; Ekdale & Harding 2015). A recent revision of the type ichnospecies of *Cylindrichnus*, *C. concentricus*, showed that the burrow is in fact U-shaped (Ekdale & Harding 2015; see also Belaústegui & de Gibert 2013). Therefore, there is a need to erect another *Cylindrichnus* ichnospecies for simple vertical morphologies to maintain the nomenclature stability of those forms that are typically attributed to *Cylindrichnus* (e.g. D'Alessandro & Bromley 1986; Gingras *et al.* 2016). *Monocraterion* is a vertical burrow with a conical aperture and tentacle-like structures at its top, the latter being absent in *Rosselia* (Jensen 1997).

Rosselia ranges from the Cambrian (e.g. Orłowski 1989; Pickerill & Peel 1990; Jensen 1997; Desjardins *et al.* 2010c; Mángano *et al.* 2013; Dias da Silva *et al.* 2014) to the Holocene (Nara & Haga 2007; Gingras *et al.* 2008). Typical producers are terebellid polychaete worms (Nara 1995; Gingras *et al.* 2008); others possible tracemakers are arthropods (Frey 1970; Rindsberg & Gastaldo 1990), bivalves (D'souza *et al.* 2024), cnidarians (Chamberlain & Clark 1973; Uchman & Krenmayr 1995), and cirratulid and spionid polychaete worms (Olivero *et al.* 2012; Luo *et al.* 2017). *Rosselia* is mostly recorded in marginal-marine (e.g. Wescott & Utgaard 1987; Martino 1989; Fillion & Pickerill 1990; MacEachern & Hobbs 2004; Mello *et al.* 2021) and shallow-marine (e.g. Howard & Frey 1984; MacEachern & Pemberton 1992; Nara 1995; Uchman & Krenmayr 2004; Netto *et al.* 2014; Buatois *et al.* 2016b) environments. Reports from deep-marine environments are rare (Książkiewicz 1970, 1977). *Rosselia* has not been recorded in the Chapel Island Formation previously.

***Rosselia erecta* (Torell, 1870)**

Figure 47A

Material. – Five specimens from Member 5 (Cambrian Age 2) in Grand Bank Head and Little Dantzic Cove.

Description. – Vertical, unbranched burrows with a funnel-shaped aperture and made of lateral concentric laminae surrounding a wide central tube. Preserved

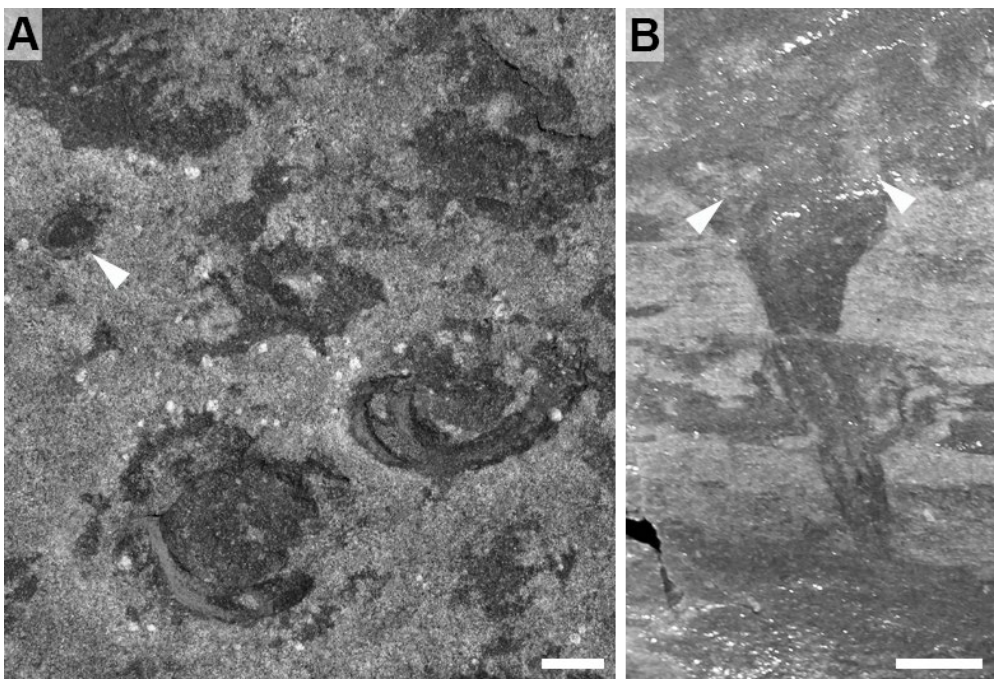

Fig. 47. Rosselia erecta (Torell) (A) and *Rosselia* isp. (B). Scale bars are 1 cm. All photographs are from Member 5 (Cambrian Age 2). **A**, Cluster of *Rosselia erecta* displaying concentrically laminated fill and wide circular central tubes. Note the smaller specimen with a thinner laminated fill (arrow). Full relief (on bed top), Little Dantzic Cove. **B**, *Rosselia* isp. in vertical cross-section showing the spindle-shaped morphology. Note the secondary reworking of the uppermost funnel portion by burrowing (arrows). Full relief, Grand Bank Head.

as full relief. In vertical section, the burrow is curved and oriented obliquely (40° of deviation). Burrows are found isolated or crowded. The central tube is circular in bedding view and occupies a major fraction of the overall width of the funnel. Infill of the central tube is massive, composed of fine-grained sandstone; concentric laminae are mostly composed of very fine- to fine-grained sandstone. Width of funnel is 1.5–4.1 cm; maximum depth observed is 2.4 cm.

Associated trace fossils. – *Rosselia erecta* co-occurs with *Psammichnites gigas circularis*.

Remarks. – The vertical spindle-shaped development and wide central tube within the funnel allow assignment to *Rosselia erecta*. *Rosselia erecta* is a recently defined ichnospecies resulting from the combination with *Micrapium erectum* Torell, 1870, a poorly known ichnotaxon that is not retained as valid for nomenclatural stability despite the seniority over *Rosselia* Dahmer, 1937 (Knaust 2021). The report of *Rosselia erecta* from the Chapel Island Formation adds to the previous Cambrian reports from the Mickwitzia Sandstone of Sweden, the Hardeberga Formation of Denmark, the Burj Formation of Jordan (Knaust 2021), and potentially the Gog Group of western Canada (Desjardins *et al.* 2010c).

***Rosselia* isp.**

Figure 47B

Material. – One specimen from Member 5 (Cambrian Age 2) in Grand Bank Head.

Description. – Vertical, unbranched burrow with a funnel-shaped aperture and made of lateral concentric laminae. Preserved as full relief. In vertical section, the burrow is straight and oriented obliquely (20° of deviation). The upper part of the funnel is reworked by biogenic mottling, and the morphology of the central tube within the funnel is unknown. Burrow is found isolated. Infill of the central tube is massive, composed of very fine-grained sandstone; concentric laminae are visible in the lower and middle portions and are mostly composed of very-fine- to fine-grained sandstone. Width of funnel is 3.0 cm; depth is 4.7 cm.

Associated trace fossils. – *Rosselia* isp. does not occur with any other formally described ichnotaxa.

Remarks. – The vertical funnel-shaped development allows assignment to *Rosselia*. However, as the morphology of the central tube is unknown, an ichnospecific affiliation is not possible. Reworking of the upper part of the funnel is reminiscent of *Rosselia chonoides*. As stated by Uchman & Krenmayr (1995), this reworking is secondary to the formation of *Rosselia*: in the Chapel Island Formation, concentric laminae are observable in the lower and middle portions of the burrow, while secondary reworking by organisms leading to an undetermined mottled fabric is observed in the upper portion of the burrow and above the burrow.

Ichnogenus *Rusophycus* Hall, 1852

Discussion. – *Rusophycus* is a short bilobate burrow typically covered with scratch imprints (Hall 1852; Fillion & Pickerill 1990) included in the category of architectural design of 'bilaterally symmetrical short, scratched impressions and burrows' (Buatois *et al.* 2017). *Rusophycus* was formally erected from the Silurian Clinton Group of northeastern USA (Hall 1852; Brett *et al.* 1998). However, prior to Hall's (1852) seminal work, *Rusophycus* was popularly referred to as 'empreintes de pas de boeufs' (i.e. cattle's tracks) by local people in the region of Normandy (France) at least since 1826 (Duval 1838; Deslongchamps 1856; de la Sicotière 1866). At first, Hall (1852) regarded *Rusophycus* as a plant remain with a wrinkled surface. Dawson (1864) raised suspicion on their 'fucoid' origin and argued that *Rusophycus* was produced by benthic animals crawling on soft mud. This opinion divided the scientific community between the supporters of Dawson (e.g. Nathorst 1881, 1883) and those opposed (e.g. de Saporta 1884; Delgado 1886). Finally, further advances in ichnology during the 20th century resulted in the overall recognition of *Rusophycus* as a trace fossil (for historical reviews, see Osgood 1970, Pemberton & Frey 1991, and Baucon *et al.* 2012). At least eighty-six ichnospecies attributed to *Rusophycus* have either been erected or mentioned in the literature (pers. data, see also Gougeon 2023). In that respect, this ichnogenus needs in-depth revision. For this study, only *Rusophycus avalonensis* is reviewed in detail as it was recovered in the Chapel Island Formation.

Rusophycus shows similarities with *Arborichnus* Romano & Meléndez, 1979, *Cruziana* d'Orbigny, 1842, *Diplichnites* Dawson, 1873, and *Monomorphichnus* Crimes, 1970. *Arborichnus* is composed of paired series of individual, symmetrical scratch imprints that decrease in width toward one extremity (Romano & Meléndez 1979; Lucas & Lerner 2005).

The organization of scratch imprints and lack of lobe formation are different from *Rusophycus*. *Cruziana* is a bilobed trail with scratch imprints (Keighley & Pickerill 1996; Fortey & Seilacher 1997) that can be difficult to distinguish from *Rusophycus*, especially because transitional forms (*Isopodichnus* type) may also develop (Trewin 1976; Keighley & Pickerill 1996; Zonneveld *et al.* 2002). Although Seilacher (1970, 1985) was reticent with the idea of separating *Rusophycus* from *Cruziana*, other specialists convincingly argued in favor of keeping both ichnogenera valid (e.g. Osgood 1970; Häntzschel 1975; Crimes *et al.* 1977; Pickerill & Fillion 1983; Nowlan *et al.* 1985). *Diplichnites* is a trackway with two parallel rows of simple imprints (Keighley & Pickerill 1998), and some authors also assigned paired ridges arranged in a short series, reminiscent of very shallow *Rusophycus*, to *Diplichnites* (e.g. Pickerill & Peel 1991; Baghiyan-Yazd 1998). Keighley & Pickerill (1996) suggested the use of a length/width ratio of 2/1 to differentiate *Rusophycus* from *Diplichnites*, a decision endorsed here (see 'Remarks' below for *Rusophycus dabardae*, p. 124). *Monomorphichnus* consists of one series of subparallel ridges (Crimes 1970). Undertracks of *Rusophycus* forming a single series of ridges can be mistaken for *Monomorphichnus* and require careful evaluation (Jensen *et al.* 2002b).

Rusophycus ranges from the Cambrian (e.g. Cloud & Nelson 1966; Banks 1970; Bergström 1970; Nowlan *et al.* 1985; Jensen 1990; Smith *et al.* 2016a) to the Holocene (Gand *et al.* 2008). Producers are arthropods (notably trilobites; e.g. Osgood 1970; Campbell 1975; Draper 1980; Fortey & Owens 1999; Gand *et al.* 2008; Gibb *et al.* 2010) and possibly gastropods and polychaete worms (Osgood 1970). Muñiz *et al.* (2015) demonstrated that modern fishes can produce *Rusophycus*-like trace fossils while feeding on the seafloor. However, these incipient traces do not form coffee-bean shapes nor have transversal scratch imprints, which are features typical of *Rusophycus*. *Rusophycus* is recorded in continental (e.g. Bromley & Asgaard 1979; Maples & Archer 1989; MacNaughton & Pickerill 1995; Schlirf *et al.* 2001; Minter *et al.* 2007; Garvey & Hasiotis 2008), marginal-marine (e.g. Mángano & Buatois 2003b; Desjardins *et al.* 2012; Hofmann *et al.* 2012; Elicki *et al.* 2013; Mángano *et al.* 2013; Durbano *et al.* 2015), shallow-marine (e.g. Young 1972; Legg 1985; MacNaughton & Narbonne 1999; Pickerill & Blissett 1999; Weber & Zhu 2003; Jensen *et al.* 2010), and rarely deep-marine (Pickerill 1995) environments. In the Chapel Island Formation, *Rusophycus* has been commonly mentioned (see synonym lists below) since its first report by Narbonne *et al.* (1987).

Rusophycus avalonensis Crimes & Anderson, 1985

Figure 48A, B

1987 *Rusophycus avalonensis* Crimes & Anderson; Narbonne, Myrow, Landing & Anderson, p. 1287, fig. 6G, I.
2014 *Rusophycus avalonensis* Crimes & Anderson; Mángano & Buatois, p. 5, fig. 2d.
2016 *Rusophycus avalonensis* Crimes & Anderson; Mángano & Buatois, p. 90, fig. 3.9g.
2016 *Rusophycus* Hall; Wolfe, Daley, Legg & Edgecombe, p. 51, fig. 2A.
2017 *Rusophycus avalonensis* Crimes & Anderson; Landing *et al.*, p. 45, fig. 17G.
2018 *Rusophycus* Hall; Daley, Antcliffe, Drage & Pates, p. 4, fig. 4F.
2018 *Rusophycus avalonensis* Crimes & Anderson; Hantsoo, Kaufman, Cui, Plummer & Narbonne, p. 1243, fig. 2j.
2021 *Rusophycus avalonensis* Crimes & Anderson; Mángano & Buatois, p. 8, fig. 5B.
In press *Rusophycus avalonensis* Crimes & Anderson; Gougeon, Mángano, Buatois, Narbonne & Rindsberg, fig. 1D–F.

Neotype. – GSC 85983 housed at the Geological Survey of Canada, Ottawa. Left specimen figured in Narbonne *et al.* (1987, fig. 6I), Wolfe *et al.* (2016, fig. 2A), and Daley *et al.* (2018, fig. 4F).

Material. – Five specimens from Member 2A (Fortunian) in Brunette Island (material in collection), Fortune Head, and Grand Bank Head.

Emended diagnosis. – Two rows of scratch imprints forming symmetrical, low-relief, elongated lobes; wide median area; coarse transverse scratch imprints do not form bundles (modified after Crimes & Anderson 1985).

Description. – Symmetrical rows of scratch imprints forming two low-relief lobes, defining an overall elliptical to quadrangular outline. Preserved as positive hyporelief. Scratch imprints are coarse, transverse, and do not crisscross or form bundles. Individual scratch imprints are thicker in their median part and taper laterally. Occasionally, one lobe is more prominent, and creates an asymmetry between lobes; coarse ridges are still visible on both rows. The median area is wide and featureless. Width is 3.5–4.1 cm; length is 2.0–3.7 cm; width of median area is 0.3–1.1 cm; length/width ratio is 0.56–1.02.

Associated trace fossils. – *Rusophycus avalonensis* co-occurs with *Cruziana problematica*, *Curvolithus simplex*, *Palaeophycus tubularis*, and *Psammichnites gigas circularis*.

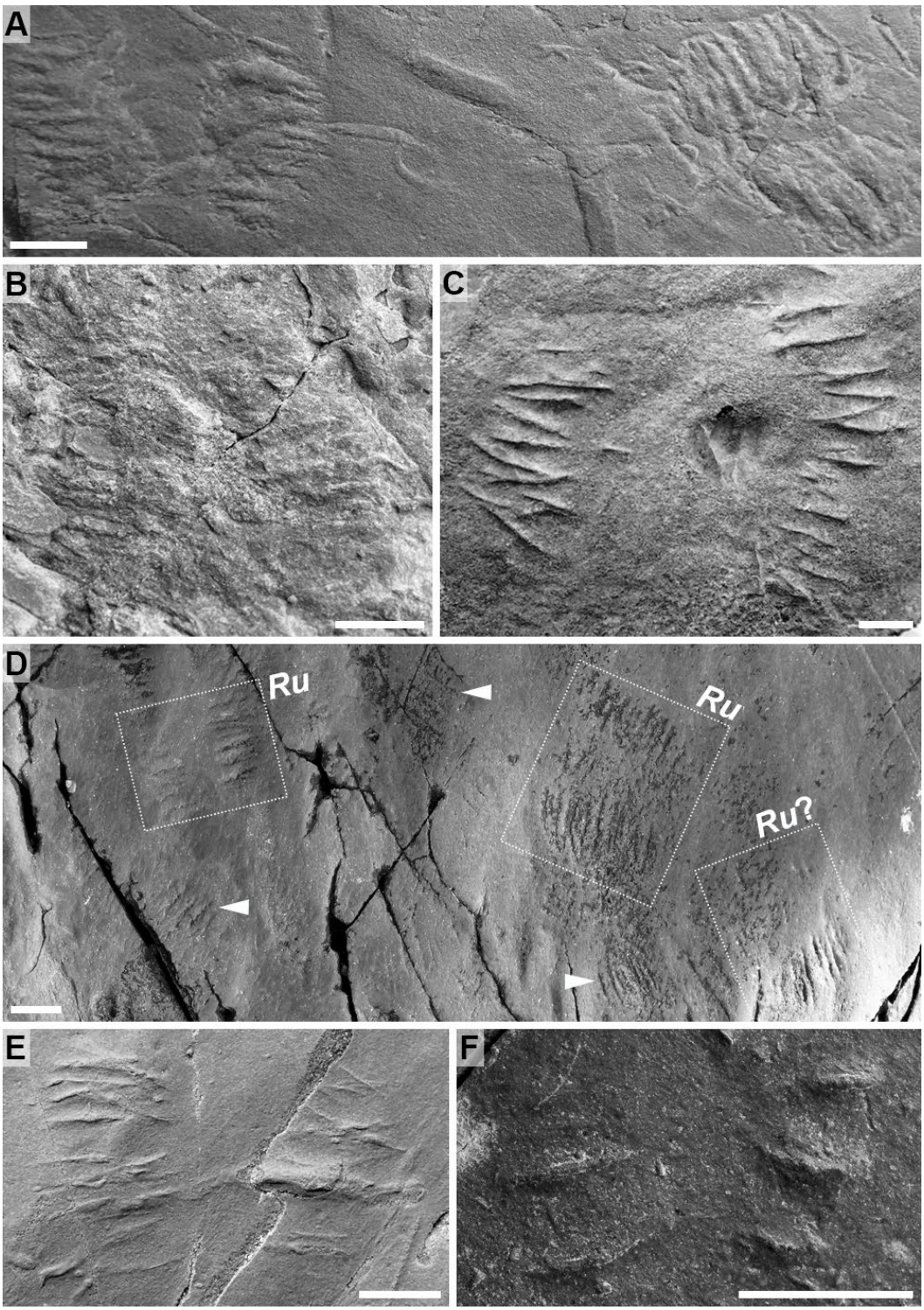

Fig. 48. *Rusophycus avalonensis* Crimes & Anderson (A, B), *Rusophycus dabardae* isp. nov. (C–E), and *Rusophycus* isp. (F). Scale bars are 1 cm. All photographs are from Member 2A (Fortunian). **A**, Specimens of *Rusophycus avalonsensis* showing two distinct lobes, a wide median area, and coarse ridges. GSC 85983. Positive hyporelief, Brunette Island. **B**, Field specimen of *Rusophycus avalonensis*. Positive hyporelief, Grand Bank Head. **C**, Holotype of *Rusophycus dabardae* that was previously referred to as *Monomorphichnus* sp. by Crimes & Anderson (1985). GSC 73337. Positive hyporelief, Lewin's Cove. **D**, Crowded surface with *Rusophycus dabardae* (Ru) displaying two distinct rows; an additional specimen (Ru?) only displays one distinct row. Note additional single rows (arrows) that may represent partially preserved *Rusophycus dabardae*. Negative epirelief, Lewin's Cove. **E**, *Rusophycus dabardae* with two rows of fine, transversal to oblique ridges. Note that the row on the right is poorly developed. Positive hyporelief, Grand Bank Head. **F**, *Rusophycus* isp. with coarse, widely spaced ridges organized in two symmetrical rows. Positive hyporelief, Fortune Head.

Remarks. – The specimen of *Rusophycus avalonensis* chosen by Crimes & Anderson (1985) as holotype was previously recorded in a paper by Seilacher (1970, p. 458, fig. 7.3) under the name *Cruziana fasciculata* Seilacher. This specimen reveals: (1) abundant delicate scratch imprints, oriented in a postero-medial direction; (2) bundles of five or more scratch imprints; (3) a moderately deep bilobate relief; (4) a length/width ratio of 1.76; and (5) lobes in contact in the midline of the burrow (Gougeon *et al.* in press). These characteristics do not correspond to the material figured by Crimes & Anderson (1985), and to other reports of *Rusophycus avalonensis* worldwide. For instance, *Rusophycus avalonensis* pictured by MacNaughton & Narbonne (1999, fig. 9A) shows two perfect lobes separated by a narrow furrow, but transversal ridges are coarse and do not form bundles. McIlroy & Brasier (2017, fig. 8g) figured a structure referred to as 'typical *Rusophycus avalonensis*', lacking any bundle formation or prominent lobes (see Gougeon *et al.* in press for more details and examples).

The diagnosis of *Rusophycus avalonensis* from Crimes & Anderson (1985) is elusive and allows a range of interpretations. According to these authors, this ichnospecies is 'consisting of fine scratch marks in bundles of five or more, arranged obliquely or transversely to the median line' (Crimes & Anderson 1985, p. 331). Arguably, the presence of bundles, which are supposedly diagnostic, is controversial as these are not observed in the material figured by Crimes & Anderson (1985) from the Random Formation (Gougeon *et al.* in press). It is also not seen in material from the Chapel Island Formation, nor mentioned by subsequent authors (Gougeon *et al.* in press). In addition, ridges in material from the Chapel Island and Random formations are coarse and transverse. Consequently, an emended diagnosis is provided herein.

We propose that a neotype of *Rusophycus avalonensis* is erected, as the holotype does not fit the description of the material recorded by Crimes & Anderson (1985) in the original publication, nor fits the emended diagnosis provided herein. The neotype corresponds to the material collected by P. Myrow (Narbonne *et al.* 1987) from Member 2 at Brunette Island and housed at the Geological Survey of Canada in Ottawa (GSC 85983). On this slab, two specimens are displayed: the left specimen both in Narbonne *et al.* (1987, fig. 6I) and herein (Fig. 48A) is the most complete, with distinct coarse ridges on both lobes, and is chosen as neotype. A petition was recently submitted to the International Commission on Zoological Nomenclature in that regard (Gougeon *et al.* in press).

After revision of the diagnosis of *Rusophycus avalonensis*, previously described material should be re-assessed on a case-by-case basis. For instance, Högström *et al.* (2013, fig. 5I) described *Rusophycus* isp. with two lobes and coarse scratch imprints that corresponds to *Rusophycus avalonensis*. Similarly, *Rusophycus* sp. documented by Nowlan *et al.* (1985, fig. 4D) displays two shallow lobes and scratch imprints not arranged in bundles, which are features pertaining to *Rusophycus avalonensis*.

***Rusophycus dabardae* isp. nov.**

Figure 48C–E

partim 1985	*Monomorphichnus* sp. Crimes & Anderson, pp. 324, 328, figs 8.7, 8.8, 10.1.
2014	*Rusophycus avalonensis* Crimes & Anderson; Buatois, Narbonne, Mángano, Carmona & Myrow, p. 3, fig. 1h.
2016	*Rusophycus avalonensis* Crimes & Anderson; Mángano & Buatois, p. 87, fig. 3.7c.
2017	*Rusophycus avalonensis* Crimes & Anderson; Landing *et al.*, p. 51, fig. 19E.
partim 2020	*Monomorphichnus* isp. Mángano & Buatois, p. 14, fig. 3e.

Etymology. – In memory of Marie-Pierre Dabard, the first ichnology instructor of the lead author at University of Rennes 1 (France).

Holotype. – GSC 73337 housed at the Geological Survey of Canada, Ottawa (Fig. 48C).

Material. – About 105 specimens from Member 2A (Fortunian) in Fortune Head, Grand Bank Head, and Lewin's Cove.

Diagnosis. – Two rows of scratch imprints without lobe formation; wide median area; thin scratch imprints are transverse to oblique, in places crisscrossing, and do not form bundles.

Description. – Paired rows of scratch imprints defining an overall elliptical to quadrangular outline. Preserved as positive hyporelief and negative epirelief. Specimens are found isolated or in clusters. Overall relief is very low, without lobe development. Scratch imprints are thin, delicate, transverse to oblique, typically distinct and well-spaced, or can crisscross. Scratch imprints do not form bundles. The median area is wide and featureless. Width is 2.3–5.9 cm; length is 1.7–4.0 cm; width of median area is 0.5–2.6 cm; length/width ratio is 0.48–1.11.

Associated trace fossils. – *Rusophycus dabardae* co-occurs with *Palaeophycus tubularis*, *Palaeophycus* isp., and *Trichichnus linearis*.

Remarks. – Paired scratch imprints and the low length/width ratio allow placement in *Rusophycus*. However, the poor organization of scratch imprints, and the absence of lobes with relief, prevent an assignation to any previously erected ichnospecies. *Rusophycus avalonensis* is the closest ichnospecies on morphological grounds (as described in this study), but it displays lobes, and scratch imprints that are coarser and mostly transverse. On the contrary, scratch imprints in *Rusophycus dabardae* are thinner and more disorganized, with common crisscrossing. The lobe relief can be a controversial feature, and Jensen *et al.* (2010) noted that taphonomy may play an important role by preserving low relief undertracks from an originally higher relief *Rusophycus*. An interpretation of *Rusophycus dabardae* as preservational variant of *R. avalonensis* is not conceivable, as the scratch imprints morphology and their arrangement are different.

Extremely shallow Cambrian *Rusophycus* have been previously referred as *Diplichnites* isp. (Pickerill & Peel 1991; Baghiyan-Yazd 1998; Weber & Zhu 2003), *Rusophycus avalonensis* (Rogov *et al.* 2015), *Rusophycus* isp. (Jensen *et al.* 2002b), and *Rusophycus* sp. (Alpert 1976a). To correctly assess the distinction between *Rusophycus* and short *Diplichnites* as described by Pickerill & Peel (1991) and Weber & Zhu (2003), the length/width ratio should be considered as a critical diagnostic feature. We decided to use the ratio of 2/1 suggested by Keighley & Pickerill (1996), which infers a coffee-bean shape, and which has been used subsequently by authors (e.g. Schlirf *et al.* 2001; Pandey *et al.* 2014), placing our specimens within *Rusophycus* morphometric limits.

In the Chapel Island Formation, similar specimens were previously referred to as *Rusophycus avalonensis* (Buatois *et al.* 2014; Mángano & Buatois 2016; Landing *et al.* 2017), *Monomorphichnus* isp. (Mángano & Buatois 2020), and *Monomorphichnus* sp. (Crimes & Anderson 1985). Interestingly, an impressive slab at Lewin's Cove displays both paired rows of scratch imprints (i.e. *Rusophycus dabardae*-type) and single rows (i.e. *Monomorphichnus lineatus*-type) on the same surface. Although negative epirelief material preserved on the bed top are still exposed and accessible in the field (Fig. 48D), casts of these imprints (i.e. positive hyporelief) have been in parts collected by Crimes & Anderson (1985) and are housed at the Geological Survey of Canada in Ottawa (GSC 73337). Rows of scratch imprints tend to be disorganized and overlapping, but a few numbers distinctly form pairs typical of *Rusophycus dabardae* (Fig. 48D).

Zoobank LSID. – urn:lsid:zoobank.org:act:608E37D2-FFB2-4D84-914D-4C8AC56EE12F

***Rusophycus* isp.**

Figure 48F

Material. – One specimen from Member 2A (Fortunian) in Fortune Head.

Description. – Two symmetrical rows of simple scratch imprints. Preserved as positive hyporelief. Scratch imprints are of very low number, well-spaced, thick, and transverse. Scratch imprints do not form bundles. The median area is wide and featureless. Width is 2.0 cm; length is 1.1 cm; width of median area is 0.5 cm; length/width ratio is 0.55.

Associated trace fossils. – *Rusophycus* isp. co-occurs with *Helminthoidichnites tenuis*, *Helminthopsis tenuis*, and *Palaeophycus tubularis*.

Remarks. – Although scratch imprints are of very low number in each row, their symmetrical arrangement and the low length/width ratio allow placement in *Rusophycus*. The thick and deep imprints are reminiscent of *Rusophycus avalonensis*, and *Rusophycus* isp. could potentially represent a preservational variant emplaced more deeply within the substrate. However, the association with simple horizontal trails (*Helminthoidichnites*, *Helminthopsis*) suggests these trace fossils were instead very shallow. In addition, a specimen of *Rusophycus avalonensis* displaying one very shallow and one deeper lobe (Narbonne *et al.* 1987, fig. 6G) demonstrates that ridges are still disorganized with variations in spacing on the very shallow lobe, which is not the case in *Rusophycus* isp. Consequently, these observations rule out an affinity to *Rusophycus avalonensis*.

Ichnogenus *Saerichnites* Billings, 1866

Discussion. – *Saerichnites* is an open burrow system made of vertical shafts connected to a basal horizontal burrow (Crimes & Anderson 1985; Uchman 1995) included in the category of architectural design of 'horizontal burrows with horizontal to vertical branches' (Buatois *et al.* 2017). *Saerichnites* was first described from the Ordovician Vauréal Formation of eastern Canada (Billings 1866; Bolton 1961; Long & Copper 1987). Although *Hormosiroidea* Schaffer and *Tuberculichnus* Książkiewicz have been in use for similar structures (e.g. Książkiewicz 1977; Seilacher 1977; Crimes & Anderson 1985), Uchman (1995) indicated *Saerichnites* was their senior synonym. Subsequently, *Hormosiroidea*, which consists of a row

of small bulbs connected by a thin string (Osgood 1970; Häntzschel 1975), was placed in synonymy with *Halimedides* Lorenz von Liburnau (Gaillard & Olivero 2009). Bromley in Uchman (1998) suggested that the type material of *Saerichnites* could represent a horizontal helical burrow exposed on a bedding plane; if that was the case, single rows of pits should be relocated in another ichnotaxon. However, Häntzschel (1975) described and figured the type material of *Saerichnites*, and did not report a potential affinity with a helical structure. Uchman (1995, 1998) placed single rows of pits within *Saerichnites canadensis* (formerly *Hormosiroidea canadensis* Crimes & Anderson). However, Uchman (1995, 1998) did not discuss *Ctenopholeus kutscheri* Seilacher & Hemleben, which is conceptually similar (Seilacher & Hemleben 1966; Fürsich *et al.* 2006). Here, we provisionally retain *Saerichnites* as valid awaiting revision of its type material, and suggest a new combination for the form made of a single row of pits (see below).

Four ichnospecies attributed to *Saerichnites* have been erected: *S. abruptus* Billings, 1866; *S. beskidensis* Plička, 1974; *S. variolatus* Chamberlain, 1977; and *S. canadensis* (Crimes & Anderson, 1985). The type ichnospecies, *Saerichnites abruptus*, has two parallel rows of closely spaced, regularly alternating pits (Billings 1866; Häntzschel 1975; Tunis & Uchman 1996b). *Saerichnites beskidensis* has two parallel rows of casts of vertical burrows (Plička 1974; Uchman 1995). Although Plička (1974) considered that the distance between pits was significant at ichnospecific rank, Uchman (1995) placed *Saerichnites beskidensis* in synonymy with *S. abruptus*. *Saerichnites variolatus* has pits arranged irregularly (Chamberlain 1977; Uchman *et al.* 2005). *Saerichnites canadensis*, formerly *Hormosiroidea canadensis*, is winding with a single row of pits (Crimes & Anderson 1985; Uchman 1995). It is morphologically and conceptually similar to the holotype of *Ctenopholeus kutscheri* (Seilacher & Hemleben 1966, pl. 3, fig. 6). However, *Saerichnites* has priority over *Ctenopholeus* as it was erected earlier and is common in the literature. Moreover, *Ctenopholeus kutscheri* was described before *Saerichnites canadensis*. Therefore, the new combination *Saerichnites kutscheri* is created here for these forms (see also 'Remarks' below, p. 126). Consequently, *Saerichnites abruptus*, *S. kutscheri*, and *S. variolatus* are here considered valid.

Saerichnites shows similarities with *Bicavichnites* Lane, Braddy, Briggs & Elliott, 2003, *Ctenopholeus* Seilacher & Hemleben, 1966, *Halimedides* Lorenz von Liburnau, 1902, *Helicodromites* Berger, 1957, *Treptichnus* Miller, 1889, and *Tuberculichnus* Książkiewicz, 1977. *Bicavichnites* has two parallel rows of circular pits (Lane *et al.* 2003). Seilacher *et al.* (2005) considered it a preservational variant of *Treptichnus pedum*. *Ctenopholeus* consists of a single row of circular pits or knobs (Seilacher & Hemleben 1966; Fürsich *et al.* 2006), and is considered a junior synonym of *Saerichnites* in this review. *Halimedides* is a burrow made of a tunnel connecting successive chambers (Gaillard & Olivero 2009; Novis *et al.* 2022). The shape of the chambers and thin strings connecting larger chambers distinguish *Halimedides* from *Saerichnites*. *Helicodromites* is a horizontal helical burrow (Poschmann 2015). Where seen on bedding plane, the burrow is composed of two parallel rows of pits (e.g. Buatois *et al.* 2017, fig. 24B), which is reminiscent of *Saerichnites abruptus* (see also Uchman 1998). However, the holotype of *Saerichnites* has yet not been convincingly demonstrated as forming a helix. *Treptichnus* is a burrow made of modular segments, pits or projections (Maples & Archer 1987; Buatois & Mángano 1993b). Some of its ichnospecies (e.g. *Treptichnus bifurcus*) can be reminiscent of *Saerichnites* when only the surficial expression is visible. Detailed observations show that *Treptichnus bifurcus* is typically made of repeated segments added one after the other and do not develop an open burrow system (see *Treptichnus* section, p. 131). Finally, *Tuberculichnus* has knobs arranged in winding rows (Książkiewicz 1977). Uchman (1998) re-assigned the type ichnospecies *Tuberculichnus meandrinus* Książkiewicz to *Protovirgularia* and did not recommend the further use of *Tuberculichnus* (see also Uchman *et al.* 2011).

Saerichnites ranges from the Cambrian (e.g. Crimes & Anderson 1985; Walter *et al.* 1989; Goldring & Jensen 1996; Gingras *et al.* 2011; Mángano & Buatois 2016; Hammersburg *et al.* 2018) to the Holocene (Heezen & Hollister 1971; Hinga 1981; Brandt *et al.* 2023). Producers have not been discussed at length so far, and previous authors suggested possible arthropods (Gomez de Llarena 1946; Brandt *et al.* 2023), holothurians (Poschmann *et al.* 2023), vertebrates (fish; Plička 1974), and worms (Lemche *et al.* 1976) as tracemakers. However, vertebrates would produce surficial trace fossils, which does not support the three-dimensional reconstruction of *Saerichnites* (cf. Crimes & Anderson 1985; Uchman 1995). *Saerichnites* is recorded in continental (Buatois *et al.* 1997; Netto *et al.* 2009; Minter *et al.* 2016), shallow-marine (Walter *et al.* 1989; Buatois & Mángano 2004a), and deep-marine (e.g. Crimes *et al.* 1981; Crimes & Crossley 1991; Tunis & Uchman 1996b; Uchman *et al.* 2005; Cummings & Hodgson 2011; Starek *et al.* 2019) environments. In the Chapel Island Formation, *Saerichnites* was originally described as *Hormosiroidea* by Crimes & Anderson

(1985), and it has rarely been mentioned since then (e.g. Narbonne *et al.* 1987; Landing *et al.* 1988).

Saerichnites kutscheri **comb. nov.**

Figure 49A–D

1985 *Hormosiroidea canadensis* isp. nov. Crimes & Anderson, pp. 324, 325, figs 8.1, 9.

Material. – Twenty specimens from Members 2A, 2B, and 3 (Fortunian), and Member 5 (Cambrian Age 2) in Fortune Head, Grand Bank Head, Lewin's Cove, and Little Dantzic Cove.

Description. – Single row of pits locally connected by a horizontal burrow. Preserved as full relief observed on bed bases and tops. In bedding-plane view, pits are typically cylindrical or elongated. The horizontal burrow is smooth with a width similar to that of the pits. The course is straight, curved, meandering to looping. Rarely, pits are not in alignment with the main course. Unlined to rarely very thinly lined. Branching is inferred at the junction between pits and the horizontal basal burrow. Infill of pits is massive, composed of very fine- to medium-grained sandstone similar to the host rock, or different where encased in mudstone or fine-grained sandstone. Width of pits is 0.2–1.4 cm; distance between pits is 0.0–4.0 cm; maximum length is 55.0 cm; maximum number of pits in a row is about 40.

Associated trace fossils. – *Saerichnites kutscheri* co-occurs with *Cochlichnus anguineus*, *Helminthoidichnites tenuis*, *Helminthopsis tenuis*, *Monomorphichnus lineatus*, *Palaeophycus tubularis*, and *Trichichnus linearis*.

Remarks. – Single rows of pits have been previously referred to as *Ctenopholeus kutscheri* (Seilacher & Hemleben 1966; Fürsich *et al.* 2006; Hughes *et al.* 2013; Kaur *et al.* 2021; Singh *et al.* 2024b), *Hormosiroidea arumbera* Elphinstone & Walter (Walter *et al.* 1989), *Hormosiroidea canadensis* (Crimes & Anderson 1985), *Hormosiroidea* cf. *H. canadensis* (only illustrated; García-Hidalgo 1993), *Saerichnites canadensis* (Uchman 1995, 1998), *Treptichnus pedum* (Gingras *et al.* 2011), and *Treptichnus vagans* (Książkiewicz) (Hammersburg *et al.* 2018). *Ctenopholeus kutscheri*, *Hormosiroidea arumbera,* and *H. canadensis* are here considered synonymous, and possess the characteristics of *Saerichnites* as described herein. Consequently, the new combination *Saerichnites kutscheri* has seniority for the ichnospecies name. A detailed revision of the type material of *Saerichnites* is still needed to further support this proposal. *Hormosiroidea* isp. from the Cambrian of northern Greenland (Bryant & Pickerill 1990, fig. 4) is recorded on a slab with both bed base and top preservations. Although the upper bedding view displays a meandering single row of pits, the sole view shows disconnected, elongated segments reminiscent of *Treptichnus*. These observations demonstrate that the interpretation of some of previously recorded *Hormosiroidea* as either *Treptichnus* or an open burrow system (as suggested for *Hormosiroidea* in the original model by Crimes & Anderson 1985; see also Uchman 1995 and Fürsich *et al.* 2006) is far from being simple and needs to be assessed on a case-by-case basis. *Treptichnus* has very distinctive features (see *Treptichnus* section, p. 131) and should not be used to describe open burrow systems.

In the Chapel Island Formation, an impressive and unique specimen (Fig. 49A) has pits in contact, which is very similar to the type material of *Saerichnites* (Häntzschel 1975, fig. 64.7). Most reports of pits aligned in rows typically possess a wide space between pits; the singularity of this Chapel Island Formation specimen reinforces its assignation to *Saerichnites*. Crimes & Anderson (1985) suggested that the burrow system could either be made of vertical shafts connected by a horizontal basal burrow, or be made by a vertically meandering burrow. The second interpretation, although favored by some authors (Bryant & Pickerill 1990; Zhu 1997), would require inclined pits intersecting the bedding plane, which have not been observed during the course of our study. Instead, our observations favor the first interpretation: most pits are circular on bedding planes, and the rare elongated pits that could infer an obliquity (e.g. Fig. 49D) resulted from the partial exposure of the basal horizontal burrow after erosion (see also Fürsich *et al.* 2006). In addition, where the basal burrow is clearly visible, it connects the pits continuously (Fig. 49C), which would not be the case if the burrow system was made by a vertically meandering structure.

Zoobank LSID. – urn:lsid:zoobank.org:act:5F5E610F-AF21-44BB-AF80-27A70CCE9C93

Ichnogenus ***Teichichnus*** **Seilacher, 1955b**

Discussion. – *Teichichnus* is a vertical spreite system formed by the displacement of a subhorizontal burrow (Seilacher 1955b; Knaust 2018a) included in the category of architectural design of 'horizontal burrows with simple vertically oriented spreiten' (Buatois *et al.* 2017). *Teichichnus* was first described

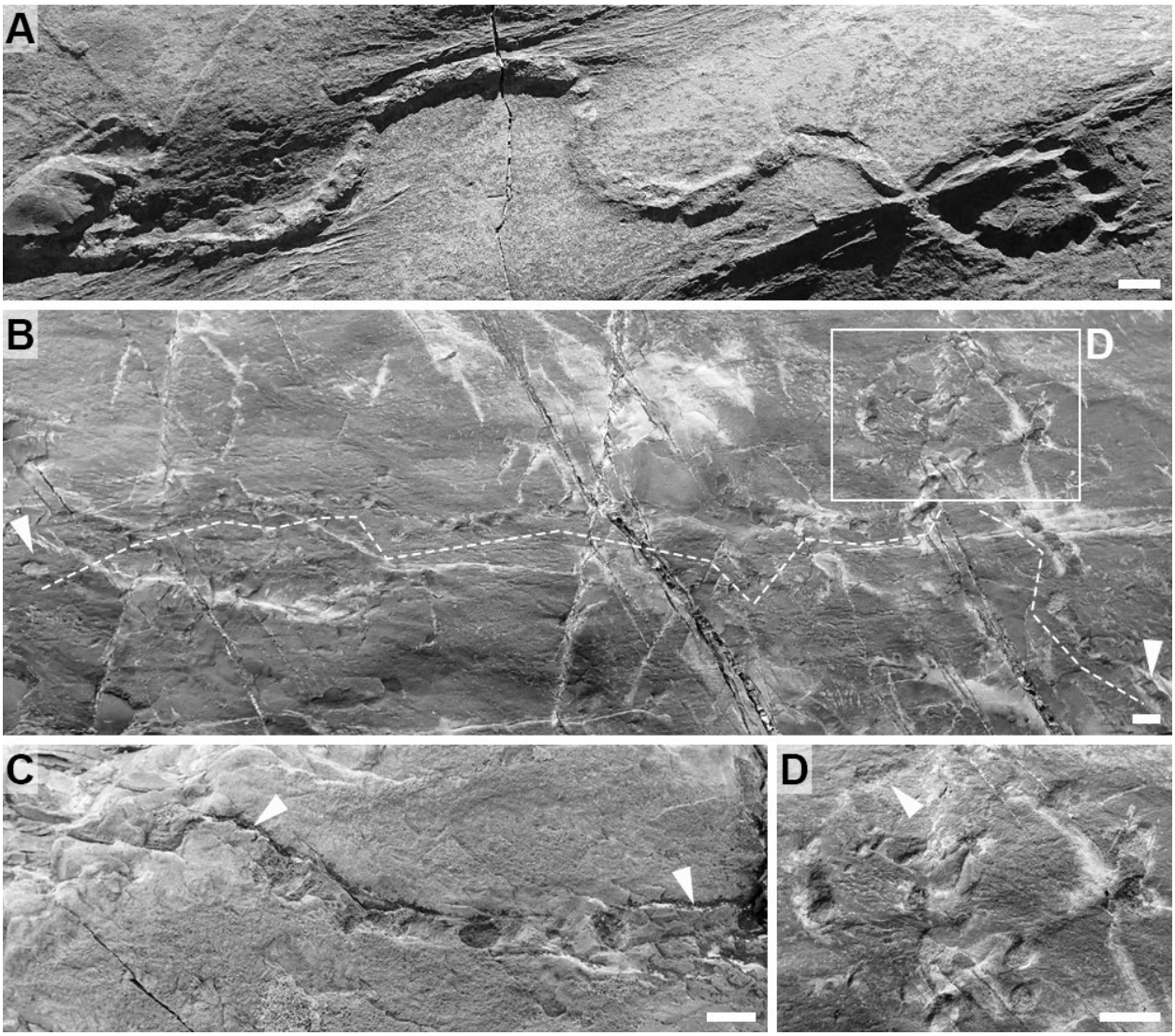

Fig. 49. Saerichnites kutscheri comb. nov. Scale bars are 1 cm. All photographs are full reliefs observed on bed tops from Member 2A (Fortunian). **A**, Specimen with a meandering to looping course and pits in close contact. Fortune Head. **B**, Specimen with a straight to looping course and widely spaced pits. Arrows designate the start and end points of the burrow. Lewin's Cove. **C**, Specimen with a continuous horizontal basal burrow (arrows) connecting the pits. Note that the width of the horizontal burrow is similar to the width of the pits. Lewin's Cove. **D**, Close-up from Figure 49B showing unconnected pits; pits are mostly circular in shape, but one is elongated (arrow). Lewin's Cove.

from the Cambrian Jutana Formation of northeastern Pakistan (Seilacher 1955b). Knaust (2018a) reviewed *Teichichnus* and considered four ichnospecies valid: *T. rectus* Seilacher, 1955b; *T. zigzag* Frey & Bromley, 1985; *T. patens* Schlirf, 2000; and *T. duplex* Schlirf & Bromley, 2007. The type ichnospecies, *Teichichnus rectus*, is a simple vertical spreite system (Seilacher 1955b). *Teichichnus patens* is branching (Schlirf 2000). *Teichichnus duplex* has bilobate spreiten with scratch imprints (Schlirf & Bromley 2007). *Teichichnus zigzag* has a zigzag pattern in vertical cross-section (Frey & Bromley 1985). In addition, *Teichichnus palmatus*, *T. sigmoidalis*, and *T. spiralis* were illustrated and briefly mentioned by Seilacher (2007), but have not been formally defined and, therefore, should not be used (Knaust 2018a). However, *Teichichnus spiralis* was subsequently mentioned in a series of papers (Lokho & Singh 2013; Tiwari & Jauhri 2014; Lokho *et al.* 2018), and the ichnospecies was incorrectly credited to Mikuláš (1990) by Lokho & Singh (2013). Specimens figured by these authors are different from the one illustrated by Seilacher (2007) and most likely represent passively filled vertical galleries rather than *Teichichnus*. Finally, *Teichichnus slendelongatus* Chu, 1988 was not discussed by Knaust (2018a). *Teichichnus slendelongatus* is a simple vertical spreite system with a long causative burrow (Chu 1988, fig. 4a, b, pl. I, fig. 6) and is a junior synonym of *T. rectus*.

Teichichnus shows similarities with *Diplocraterion* Torell, 1870, *Heimdallia* Bradshaw, 1981, *Rhizocorallium* Zenker, 1836, and *Siphonichnus* Stanistreet, Le Blanc Smith & Cadle, 1980. *Diplocraterion* has vertical spreiten made by a U-shaped causative burrow (Fürsich 1974b; Corner & Fjalstad 1993; Bland & Goldring 1995). Corner & Fjalstad (1993) used the depth/width ratio and the basal curvature of spreiten to discriminate *Teichichnus* from *Diplocraterion*. *Rhizocorallium* is a horizontal to oblique spreite system with a marginal causative burrow (Schlirf 2011; Knaust 2013). Misidentification of *Rhizocorallium* for *Teichichnus* has been previously noted (Buckman 1994b; Knaust 2018b). However, the shape and orientation of the causative burrow in *Rhizocorallium* distinguish this ichnogenus from *Teichichnus*. *Heimdallia* is a complex three-dimensional structure with an inclined to vertical causative burrow moving laterally (Bradshaw 1981; Trewin & McNamara 1995). Partially preserved *Heimdallia* may be confused with *Teichichnus*, but the more complex architecture and spreite orientation of the former are diagnostic of this ichnogenus (Fillion & Pickerill 1990; Buckman 1996; Olivero *et al.* 2004). *Siphonichnus* is a vertical burrow made of backfilled laminae and can be mistaken for *Teichichnus* when incompletely preserved (Zonneveld & Gingras 2013). Identification of the outer and inner tube in *Siphonichnus* allows distinction from *Teichichnus* (Pervesler *et al.* 2008; Zhang *et al.* 2017b).

Teichichnus ranges from the Cambrian (e.g. Martinsson 1965; Alpert 1976b; Bland & Goldring 1995; Loughlin & Hillier 2010; Jensen *et al.* 2016; McIlroy & Brasier 2017) to the Holocene (e.g. Ekdale & Berger 1978; Berger *et al.* 1979; Wetzel 1981, 1991; Corner & Fjalstad 1993). Possible producers are arthropods (Martinsson 1965; Stanton & Dodd 1984; Goldring 1985; Schlirf & Bromley 2007), holothurians (Knaust 2018b), and worms (Alpert 1976b; Hofmann 1979; Frey & Bromley 1985; Corner & Fjalstad 1993; Knaust 2018b). *Teichichnus* is recorded in marginal-marine (e.g. Martino 1989; Beynon & Pemberton 1992; Pemberton *et al.* 1992; Corner & Fjalstad 1993; Musial *et al.* 2012; Jensen *et al.* 2016), shallow-marine (e.g. Crimes 1969; Frey & Bromley 1985; Clausen & Vilhjálmsson 1986; Orłowski 1989; Jensen 1997; Loughlin & Hillier 2010), and deep-marine (e.g. Ekdale 1977; Berger *et al.* 1979; Stanton & Dodd 1984; Ineson 1987; Wetzel 1991; Leszczynski *et al.* 1996) environments. In the Chapel Island Formation, *Teichichnus* has been commonly recorded and figured (see synonym list below) since its first mention by Narbonne *et al.* (1987).

***Teichichnus rectus* Seilacher, 1955b**

Figure 50A–E

2014 *Teichichnus rectus* Seilacher; Mángano & Buatois, p. 5, fig. 2j.
2016 *Teichichnus rectus* Seilacher; Mángano & Buatois, p. 90, fig. 3.9e.
2017 *Teichichnus* isp. Herringshaw, Callow & McIlroy, p. 376, fig. 4d.
2018a *Teichichnus* Seilacher; Gougeon, Mángano, Buatois, Narbonne & Laing, p. 3, fig. 2d, e.
2018 *Teichichnus rectus* Seilacher; Hantsoo, Kaufman, Cui, Plummer & Narbonne, p. 1243, fig. 2l.
2020 *Teichichnus rectus* Seilacher; Mángano & Buatois, p. 15, fig. 4e.

Material. – Hundreds of specimens from Members 2A, 2B and 3 (Fortunian) and Members 4 and 5 (Cambrian Age 2) in Fortune Head, Fortune North, Grand Bank Head, Little Dantzic Cove, and Point May.

Description. – Vertical, unbranched, spreite burrow systems made of a subhorizontal causative burrow and stacked laminae. Preserved as full relief. In top view, burrows are straight to curved, rarely with a sharp angle along the course. Local high density of specimens results in common overcrossing. In transversal cross-section, laminae are flat to arcuate (convex-down), either distinctively spaced, or in contact. Stacked laminae are vertical to oblique in orientation. Width in transversal cross-section is mostly constant. Rarely, a bulge develops at the base. A causative burrow can be preserved at the top or, more rarely, at the base of the system. Longitudinal cross-section displays horizontal to oblique laminae, slightly curved downward. In cross-section, burrows are isolated or forming dense assemblages, either arranged patchily or extended laterally into thickly burrowed intervals. Unlined, although a diagenetic feature in calcite concretions may sharply enhance burrow boundaries. Infill is composed of very fine- to fine-grained sandstone different from the mudstone host rock. Width is 0.2–1.8 cm; laminae thickness is 0.01–0.2 cm; maximum height is 8.0 cm; maximum length is 34.0 cm.

Associated trace fossils. – *Teichichnus rectus* co-occurs with *Palaeophycus tubularis*.

Remarks. – Unbranched, vertical spreite burrow systems made of simple laminae allow placing these trace fossils in *Teichichnus rectus*. Orłowski (1989) described branched Cambrian *Teichichnus rectus*, but this characteristic is more typical of *T. patens* (Schlirf 2000; Knaust 2018a). In the Chapel Island Formation,

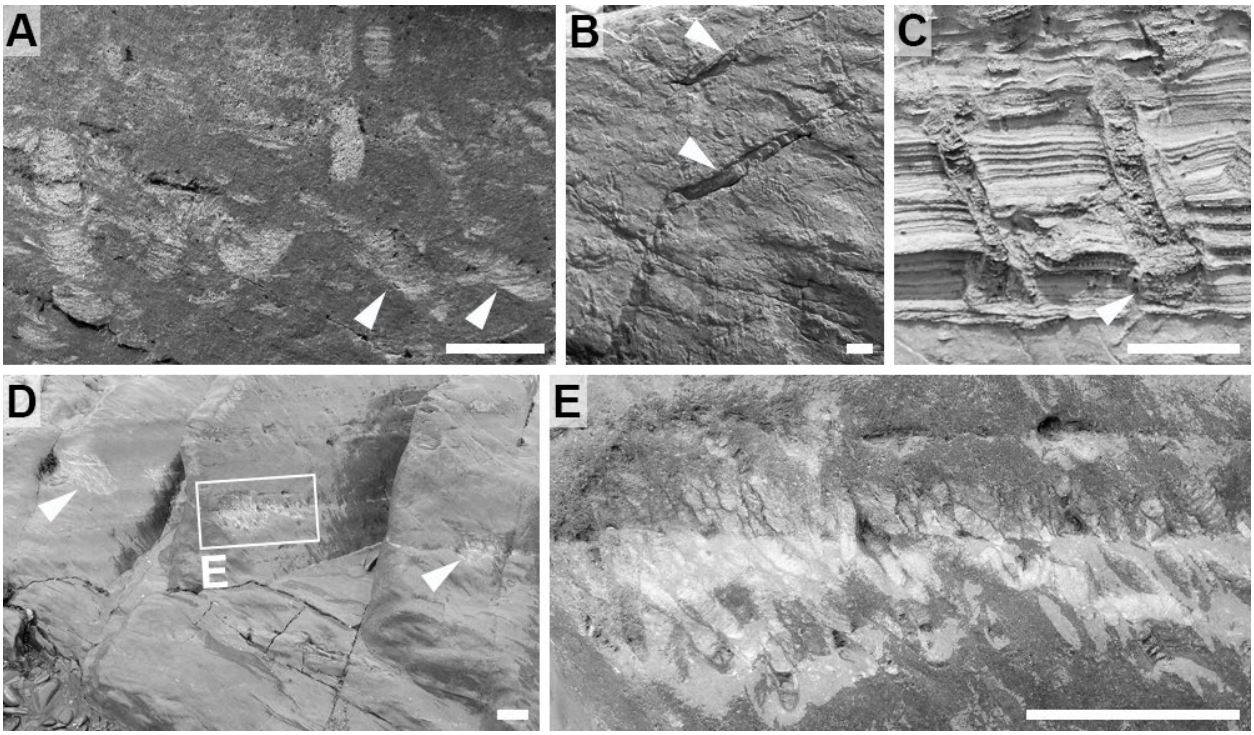

Fig. 50. Teichichnus rectus Seilacher. Scale bars are 1 cm (A, C), 2 cm (B), and 10 cm (D, E). **A**, Vertical and oblique (arrows) specimens in transversal cross-section with convex-down laminae. Full relief, Little Dantzic Cove, Member 3 (Fortunian). **B**, Top view of two long specimens with subhorizontal spreiten (arrows). Note that one specimen has a sharp angle along its course. Full relief observed on bed top, Grand Bank Head, Member 2B (Fortunian). **C**, Two specimens preserved in a calcite concretion, displaying enhanced diagenetic boundaries and bulbous bases (arrow). Full relief, Little Dantzic Cove, Member 3 (Fortunian). **D**, Grey massive mudstone displaying patchy aggregates of specimens (box and arrows). Diagenetically enhanced specimens record best visibility, but the whole deposit is bioturbated by *Teichichnus rectus*. Full relief, Point May, Member 2B (Fortunian). **E**, Close-up of Figure 50D showing a dense cluster of specimens.

aggregation of *Teichichnus rectus* can render identification of individual burrows difficult, but true branching is absent. Bulging in vertical section and straight to curving burrows on bedding plane view have been recorded in *Teichichnus rectus* elsewhere (Chisholm 1970; Fürsich 1974a; Frey & Bromley 1985; Frey & Howard 1985; Ineson 1987; Corner & Fjalstad 1993). The presence of a lining is, however, unusual. In specimens from the Chapel Island Formation, the apparent lining (Fig. 50C) is most likely a diagenetic artifact as it is only observed in calcite concretions. At Grand Bank Head, some specimens are extensive on large slabs, reaching up to 34 cm in length and displaying angular turns (Fig. 50B). These features are reminiscent of *Heimdallia chatwini* Bradshaw, which can reach 3 m in length and displays sudden changes of direction (Bradshaw 1981; Trewin & McNamara 1995). In the Chapel Island Formation, the vertical expression of these burrows is unknown, which prevents further comparison. However, the top view expression suggests a subhorizontal to slightly oblique orientation of spreiten, which is morphologically and conceptually similar to *Teichichnus*. These forms are here retained in *Teichichnus rectus* with caution.

Ichnogenus *Torrowangea* Webby, 1970

Discussion. – *Torrowangea* is a simple horizontal burrow with constrictions (Webby 1970) included in the category of architectural design of 'simple actively filled (massive) horizontal to oblique structures' (Buatois *et al.* 2017). *Torrowangea* was first described from the Cambrian Lintiss Vale Formation of southeastern Australia (Webby 1970; Walter *et al.* 1989). At least three ichnospecies attributed to *Torrowangea* have been erected: *T. rosei* Webby, 1970; *T. shamaoensis* Yang, 1984; and *T. angulata* Gámez-Vintaned & Liñán, 1993. The type ichnospecies, *Torrowangea rosei*, has a sinuous course and distinct constrictions (Webby 1970). *Torrowangea shamaoensis* consists of few ovoid beads (Yang 1984, pl. 2, fig. 3), and seems unrelated to *Torrowangea*. *Torrowangea angulata* has angular turns along its course (Gámez-Vintaned & Liñán 1993). Distinct constrictions are lacking, and an affinity to *Helminthopsis hieroglyphica* is more likely. Consequently, only the type ichnospecies *Torrowangea rosei* is here considered valid.

Torrowangea shows similarities with *Arthrophycus* Hall, 1852, *Gordia* Emmons, 1844, *Neonereites*

Seilacher, 1960, *Palaeophycus* Hall, 1847, *Planolites* Nicholson, 1873, and *Vagorichnus* Buatois, Mángano, Wu & Zhang, 1995. Uchman (1998) suggested the existence of similarities between *Torrowangea* and *Arthrophycus*. However, *Arthrophycus* differs by the presence of branching, a square cross-section, vertical spreiten, and a ventral median groove (Mángano *et al.* 2005b). *Gordia* is a simple horizontal trail with self-overcrossing (Emmons 1844; Hofmann & Patel 1989). *Gordia nodosa* displays annulations (Pickerill & Peel 1991), but these are more regular and delicate than the backfilling of *Torrowangea*. *Neonereites* is a horizontal burrow made of string(s) of beads (Seilacher 1960) reminiscent of *Torrowangea*. The type material of *Neonereites* is now regarded a junior synonym of *Nereites* (Uchman 1995; Mángano *et al.* 2000), and material previously ascribed to *Neonereites* must be re-evaluated on a case-by-case basis. *Planolites annularis* possesses transverse features along a simple burrow (Pemberton & Frey 1982). Contrary to *Torrowangea*, the burrow diameter of *Planolites annularis* is constant, and annulations are prominent (Pemberton & Frey 1982). *Palaeophycus annulatus* has annulations along its course, but a lining is diagnostic (Badve 1987; see *Palaeophycus* section, p. 107). *Vagorichnus* is an actively filled horizontal burrow system showing constrictions reminiscent of *Torrowangea*, but it also displays a diagnostic branching pattern forming an overall network (Buatois *et al.* 1995).

Several fossilized structures originally described as *Torrowangea* may belong to *Archaeonassa* (Devera 1989, pl. 2, fig. B), *Helminthoidichnites* (Liñán & Palacios 1987, pl. 1, fig. 3), or represent pseudofossils (Gámez Vintaned *et al.* 2006, fig. 10.4d). *Meanderovaleichnus* Cónsole-Gonella & Aceñolaza is a horizontal, elongated structure with constrictions and bulges that has been compared to *Torrowangea* (Cónsole-Gonella & Aceñolaza 2013). These structures are arguably inorganic, somewhat comparable to ptygmatic folding (cf. Shanmugam 2016). Finally, Jensen *et al.* (2006) also called for caution on a possible body fossil origin of some Ediacaran forms described as *Torrowangea*.

Torrowangea ranges from the Ediacaran (e.g. Hofmann 1981; Pacześna 1985; Gibson 1989; Narbonne & Aitken 1990; Geyer & Uchman 1995; Zhu 1997) to the Cretaceous (Kim *et al.* 2003). Possible producers are foraminifers (Severin *et al.* 1982; Knaust 2010) and annelid worms (Walter *et al.* 1989; Narbonne & Aitken 1990). *Torrowangea* is recorded in continental (Gámez-Vintaned & Liñán 1993; Głuszek 1995; Kim *et al.* 2003), shallow-marine (Geyer & Uchman 1995; de Gibert & Ekdale 2002; Gaillard & Racheboeuf 2006), and deep-marine (Hofmann 1981; Gibson 1989; Narbonne & Aitken 1990, 1995) environments. In the Chapel Island Formation, *Torrowangea* was figured in Narbonne *et al.* (1987, fig. 6C) and was later mentioned in a few papers (e.g. Landing *et al.* 1988; Herringshaw *et al.* 2017).

***Torrowangea rosei* Webby, 1970**

Figure 51A–C

1985 *Neonereites uniserialis* Seilacher; Crimes & Anderson, p. 328, fig. 10.2.
1987 *Torrowangea* sp. Narbonne, Myrow, Landing & Anderson, p. 1287, fig. 6C.

Material. – Seven specimens from Member 1 (Ediacaran) and Members 2A and 3 (Fortunian) in Fortune Head, Grand Bank Head, and Little Dantzic Cove.

Emended diagnosis. – Horizontal, unlined, unbranched burrow with irregular or regular constrictions; the course is straight, curved, to tortuous (modified from Webby 1970).

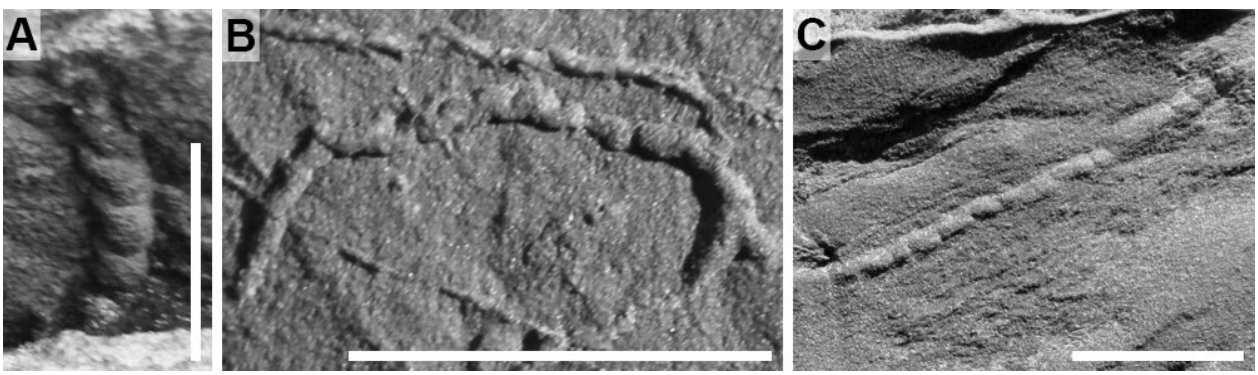

Fig. 51. Torrowangea rosei Webby. Scale bars are 1 cm. **A**, Specimen with regular constrictions. Positive hyporelief, Fortune Head, Member 1 (Ediacaran). **B**, Tortuous specimen with irregular constrictions in the middle part. Positive hyporelief, Fortune Head, Member 2A (Fortunian). **C**, Specimen with irregular constrictions. Positive epirelief, Fortune Head, Member 2A (Fortunian).

Description. – Horizontal, unlined, unbranched burrows with regular or irregular constrictions. Preserved as positive hyporelief and positive epirelief. The course is straight, slightly curved, or tortuous. Constrictions delineate segments that are elongated or more compacted; constrictions are not always preserved along the whole course. Infill is massive, composed of very fine-grained sandstone similar to the host rock. Burrow width is 0.1–0.3 cm; segment length is 0.1–0.3 cm; maximum burrow length is 2.5 cm.

Associated trace fossils. – *Torrowangea rosei* does not occur with other formally described ichnotaxa.

Remarks. – The presence of constrictions and a tortuous course are typically regarded as diagnostic of *Torrowangea rosei* (Webby 1970). However, the regularity of constrictions is a subject of debate. The type material from Australia displays mostly regular constrictions (Webby 1970, fig. 18B, D). While some authors also described regular constrictions in *Torrowangea rosei* (Jensen *et al.* 2006; Buatois & Mángano 2016), others recorded burrows with irregular constrictions as well (e.g. Mikuláš 1992; Głuszek 1995; Seilacher *et al.* 2005; Gaillard & Racheboeuf 2006; Carbone & Narbonne 2014; Jensen & Palacios 2016). For these reasons, the diagnosis of *Torrowangea rosei* is emended here, to accomodate burrows with both regular and irregular constrictions.

In numerous additional reports, the presence of constrictions in *Torrowangea* is dubious. Pseudoconstrictions can either result from the cleavage generated by shear stress texturing the surface (e.g. Liñán & Palacios 1987, pl. 1, fig. 1; Aceñolaza & Tortello 2003, fig. 3.4; see also Jensen & Palacios 2016), or from microbial textures modifying the surface of originally unornamented burrows (e.g. Zhang 1986, pl. 3, figs 2, 3; Liñán & Palacios 1987, pl. 2, fig. 2; Gámez-Vintaned & Liñán 1993, pl. 13, fig. 8; Baghiyan-Yazd 1998, pl. 29, fig. B; Gámez Vintaned et al. 2006, figs 8.6d, 9.7c; Simón 2017, fig. 5C, D). In addition, microbial mats can modify surfaces resulting in the formation of bulges, roll-ups and flip-overs superficially reminiscent of burrows (cf. Eriksson *et al.* 2007; Hagadorn & Mcdowell 2012) that were also described as *Torrowangea* (e.g. Liñán & Tejero 1988, fig. 4; Retallack 2009, fig. 9G; Hageman & Miller 2016, fig. 3D). Finally, Jensen & Palacios (2016) noted that irregular transverse constrictions could alternatively develop from the incomplete fill of a trace fossil or represent the departing point of vertical probes (which would affiliate these structures to *Treptichnus*).

A string of beads was previously considered diagnostic of *Neonereites uniserialis*. However, the type material of *Neonereites* is now regarded as a junior synonym of *Nereites* (Uchman 1995; Mángano *et al.* 2000). *Neonereites* was commonly mentioned in the Ediacaran and the Cambrian worldwide (e.g. Lin *et al.* 1986; Gibson 1989; Walter *et al.* 1989; Vidal *et al.* 1994b), but these burrows never display the internal complexity of *Nereites* (i.e. an axial backfilled tunnel flanked by paired lobes). These dissimilarities indicate different modes of construction between Ediacaran–Cambrian *Neonereites*, and *Nereites*. Furthermore, the type material of *Torrowangea rosei* locally forms a string of beads (Webby 1970, fig. 18D, bottom left). Consequently, most specimens of *Neonereites* from the Ediacaran–Cambrian should be better located within *Torrowangea*. Regarding the mode of formation of *Torrowangea*, Narbonne & Aitken (1990) argued that constrictions represented peristalsis of the tracemaker, because no internal structure was observed in longitudinal sections.

Some of the specimens from the Chapel Island Formation (Fig. 51A, C) are reminiscent of *Torrowangea rosei* as described in Walter *et al.* (1989, fig. 12A) and possibly Zhu (1997, fig. 4A). They have also been named 'complex crawling traces' in Palij *et al.* (1983, pl. 55, fig. 1; also figured in Palij, 1976, pl. 27, fig. 1). Other examples of *Torrowangea rosei* from the Chapel Island Formation (Fig. 51B), with tortuous courses and irregular constrictions, match more closely the morphology of the type specimen from Australia (Webby 1970).

Finally, the distinction between *Torrowangea rosei* and the body fossil *Harlaniella* is not always straightforward (e.g. Moczydłowska *et al.* 2001). In the Chapel Island Formation, a specimen (Fig. 51A) could be reminiscent of *Harlaniella*. However, uncontroversial *Harlaniella* specimens recorded at Fortune Head and Grand Bank Head differ by (Fig. 2C): (1) a very low, subtle relief; (2) the presence of branching; (3) delicate internal segments oriented obliquely to the main direction of the fossil; and (4) different morphometric values (segment length shorter than their width). These observations suggest that the specimen from the Chapel Island Formation (Fig. 51A) has no affinity with *Harlaniella*.

Ichnogenus *Treptichnus* Miller, 1889

Discussion. – *Treptichnus* is a three-dimensional burrow made of modular segments, pits, or projections (Buatois & Mángano 1993b) included in the category of architectural design of 'horizontal burrows with horizontal to vertical branches' (Buatois *et al.* 2017). *Treptichnus* was first described from the Carboniferous Mansfield Formation of eastern USA (Miller 1889; Maples & Archer 1987). In a pioneer work, Hitchcock (1858) erected *Halysichnus* for similar trace fossils, which should theoretically take priority as the senior synonym. However, Hitchcock (1858) description and illustration were not totally satisfactory, and *Halysichnus*

has rarely been used by subsequent authors (Goldstein *et al.* 2017). Consequently, the ichnogenus *Treptichnus* is favored for these forms, to maintain nomenclatural stability (cf. Goldstein *et al.* 2017). Miller (1889) also erected *Plangtichnus* and *Haplotichnus*, two ichnogenera now regarded as preservational variants of *Treptichnus* (Buatois & Mángano 1993b; Getty & Bush 2017). For a long time, Miller's (1889) work had been overlooked by the scientific community (Uchman *et al.* 1998), and authors referred to similar trace fossils as 'feather-stitch trails' (e.g. Wilson 1948; Seilacher 1955b; Seilacher & Hemleben 1966; Banks 1970; Cowie & Spencer 1970; Maples & Archer 1987). Maples & Archer (1987) were the first to resurrect the work of Miller (1889) on *Treptichnus*.

Buatois & Mángano (1993b) reviewed *Treptichnus* and considered four ichnospecies valid: *T. bifurcus* Miller, 1889; *T. triplex* Palij, 1976; *T. lublinensis* Pacześna, 1986; and *T. pollardi* Buatois & Mángano, 1993b. The type ichnospecies, *Treptichnus bifurcus*, has oblique projections alternating on each side (Miller 1889; Buatois & Mángano 1993b). *Treptichnus triplex* has segments divided in three parts by two narrow longitudinal grooves (Palij 1976; Palij *et al.* 1983). *Treptichnus lublinensis* has densely arranged, wide segments (Pacześna 1986). *Treptichnus pollardi* has regularly spaced vertical projections (Buatois & Mángano 1993b). Since Buatois & Mángano's (1993) review, at least eleven additional ichnospecies attributed to *Treptichnus* have been erected or resulted from new combinations: *T. pedum* (Seilacher, 1955b); *T. vagans* (Książkiewicz, 1977); *T. coronatum* (Crimes & Anderson, 1985); *T. tripleurum* (Geyer & Uchman, 1995); *T. rectangularis* Orłowski & Żylińska, 1996; *T. meandrinus* Uchman, Bromley & Leszczyński, 1998; *T. aequalternus* Schlirf, 2000; *T. apsorum* Rindsberg & Kopaska-Mekel, 2005; *T. arcus* Wang & Wang, 2006; *T. taijiangensis* Wang & Wang, 2006; and *T. streptosus* Chen & Liu, 2025. *Treptichnus pedum*, formerly *Phycodes pedum*, has curving segments typically projecting on one side (Seilacher 1955b). Hammersburg *et al.* (2018) described *Treptichnus vagans*, formerly *Tuberculichnus vagans*, as a string of beads with variable distance between each bead. However, Uchman *et al.* (2011) transferred the type material of *Tuberculichnus vagans* to *Ptychoplasma* Fenton & Fenton after careful re-evaluation. *Treptichnus coronatum*, formerly *Phycodes coronatum*, has vertical projections expanding from a basal circular burrow (Crimes & Anderson 1985; MacNaughton & Narbonne 1999). *Treptichnus tripleurum*, formerly *Trichophycus tripleurum*, has trilobate segments (Geyer & Uchman 1995), and is conceptually similar to *T. triplex*. *Treptichnus rectangularis* has segments forming perpendicular angles with one-another (Orłowski & Żylińska 1996). *Treptichnus meandrinus* has a first-order meandering course (Uchman *et al.* 1998). *Treptichnus aequalternus* has oblique projections alternating on each side (Schlirf 2000) and is conceptually similar to *T. bifurcus*. *Treptichnus apsorum* has U-shaped segments with longitudinal striations (Rindsberg & Kopaska-Mekel 2005). Lucas & Stimson (2013) re-interpreted the type material as super-imposed specimens of *Palaeophycus striatus*. *Treptichnus arcus* has arcuate, oblique segments projecting on one side (Wang & Wang 2006) and is conceptually similar to *T. pedum*. *Treptichnus taijiangensis* has oblique projections alternating on each side (Wang & Wang 2006) and is conceptually similar to *T. bifurcus*. *Treptichnus streptosus* has regular oblique ridges displayed on each segment (Chen & Liu 2025). Consequently, nine ichnospecies, *Treptichnus bifurcus*, *T. coronatum*, *T. lublinensis*, *T. meandrinus*, *T. pedum*, *T. pollardi*, *T. rectangularis*, *T. streptosus*, and *T. triplex*, are here considered valid.

Treptichnus shows similarities with *Belorhaphe* Fuchs, 1895, *Phycodes* Richter, 1850, *Saerichnites* Billings, 1866, *Spirodesmos* Andrée, 1920, *Streptichnus* Jensen & Runnegar, 2005, *Trichophycus* Miller & Dyer, 1878a, *Tuberculichnus* Książkiewicz, 1977, and *Vitichnus* Wetzel, Uchman, Blechschmidt & Matter, 2009. *Belorhaphe* is a graphoglyptid burrow made of first-order meanders and second-order zigzags (Seilacher 1977; Fan *et al.* 2018). Rindsberg & Kopaska-Merkel (2005) considered some of the 'feather-stitch trails' to be closer to *Belorhaphe* than *Treptichnus*, but the regularity of zigzags and two orders of meanders are distinctive of *Belorhaphe*. *Phycodes* is a horizontal burrow with branches forming bundles (Osgood 1970; Fillion & Pickerill 1990). Contrary to *Treptichnus*, branches in *Phycodes* tend to overlap and to depart from a single point. *Saerichnites* is an open burrow system made of aligned vertical shafts connected by a basal horizontal burrow (Crimes & Anderson 1985; Uchman 1995). The open structure and lack of repeated and connected individual segments are distinctive from *Treptichnus*. *Spirodesmos interruptus* Andrée, the holotype of *Spirodesmos*, is composed of distinct segments forming a one-way horizontal spiral (Andrée 1920; Knaust 2020; Gougeon *et al.* 2022) that can be mistaken with *Treptichnus* (cf. Archer & Maples 1984). The spiral morphology is, however, absent in *Treptichnus*. *Streptichnus* is composed of clusters of curved elements surrounding a central area that do not extend laterally or vertically as in *Treptichnus* (Jensen & Runnegar 2005). *Trichophycus* is a burrow made of U-shaped segments with delicate striae and vertical spreiten, the latter being absent in *Treptichnus* (Miller & Dyer 1878b; Geyer & Uchman 1995; Jensen 1997; Bayet-Goll *et al.* 2020). *Tuberculichnus* is a burrow composed of knobs and tubercules arranged in winding rows (Książkiewicz 1977). Although Hammersburg *et al.* (2018) placed *Tuberculichnus* in synonymy with *Treptichnus*, the validity of *Tuberculichnus* is pending further revision of the

type material (Buatois *et al.* 2017). *Vitichnus* is a burrow composed of biserially alternating short ridges arranged in a plait-like pattern (Wetzel *et al.* 2009), and its distinction from *Treptichnus* needs further re-evaluation.

Treptichnus typically ranges from the Cambrian (e.g. Seilacher 1955b; Sokolov & Fedonkin 1984; Walter *et al.* 1989; Bryant & Pickerill 1990; Jensen 1997; Zhu 1997) to the Holocene (e.g. Bajard 1966; Ewing & Davis 1967; Uchman 2005; Martin 2009; Muñiz Guinea *et al.* 2014; Kesidis *et al.* 2019b). However, trace fossils comparable to *Treptichnus* (i.e. treptichnids) have been noted in the Ediacaran (Jensen *et al.* 2000; Högström *et al.* 2013), and *Treptichnus pedum* was recorded 4.41 m below the Ediacaran–Cambrian boundary point at Fortune Head (Gehling *et al.* 2001; see also Laing *et al.* 2019, Gougeon *et al.* 2023, and 'Discussion' section of this study). *Treptichnus streptosus* and other treptichnids were also recently recovered from the latest Ediacaran Shibantan Member of the Dengying Formation in China (Chen & Liu 2025). Producers are arthropods (insect larvae; Bajard 1966; Uchman 2005; Martin 2009; Muñiz Guinea *et al.* 2014), possible enteropneusts and gastropods (Jensen *et al.* 2000), and priapulid worms (Vannier *et al.* 2010; Kesidis *et al.* 2019b; Turk *et al.* 2024a). *Treptichnus* is recorded in continental (e.g. Archer & Maples 1984; Buatois & Mángano 1993b; Metz 2000; Pazos *et al.* 2007; Martin 2009; Netto *et al.* 2009), marginal-marine (e.g. Bajard 1966; Crimes *et al.* 1977; Legg 1985; Archer *et al.* 1995; MacNaughton & Narbonne 1999; Buatois *et al.* 2013), shallow-marine (e.g. Banks 1970; Crimes 1970; Palij *et al.* 1983; Jensen 1997; MacNaughton & Narbonne 1999; Weber *et al.* 2007), and deep-marine (e.g. Ewing & Davis 1967; Crimes *et al.* 1981; Seilacher & Hemleben 1966; Wetzel & Uchman 1997; Neto de Carvalho 2008; Wilson *et al.* 2012) environments. *Treptichnus* was first recorded as *Phycodes* in the Chapel Island Formation (e.g. Crimes & Anderson 1985; Narbonne *et al.* 1987), until Gehling *et al.* (2001) reassessed its taxonomic status.

Treptichnus bifurcus Miller, 1889

Figure 52A–C

Material. – Six specimens from Members 2A and 2B (Fortunian) in Fortune Head, Grand Bank Head, and Lewin's Cove.

Description. – Three-dimensional, unlined burrows with a basal horizontal zigzagging structure and oblique projections extending at each angle. Preserved as positive hyporelief and positive epirelief. The zigzagging course is straight, slightly curving, or slightly winding. The basal zigzagging structure is forming acute (about 20°) or wider angles (about 40°); this structure can be made of distinctive segments or be fully continuous without clear delineation in between segments. At each angle, projections first extend laterally, and then obliquely to vertically. The alternating vertical projections form two parallel rows. Infill is massive, composed of very fine- to fine-grained sandstone similar to the host rock, or different where encased in mudstone. Maximum burrow length is 10.8 cm; width of basal burrow and projections is 0.1–0.4 cm.

Associated trace fossils. – *Treptichnus bifurcus* co-occurs with *Curvolithus simplex* and *Treptichnus pedum*.

Remarks. – The presence of a basal zigzagging structure and alternating oblique projections is diagnostic of *Treptichnus bifurcus*. *Treptichnus bifurcus* can be: (1) preserved as distinctive segments building up the basal horizontal structure (Fedonkin *et al.* 1983, pl. 2, fig. 1; Goldring & Jensen 1996, fig. 3d; Hammersburg *et al.* 2018, figs 21.1–6, 22.1); or (2) made of a continuous zigzagging basal structure (i.e. *Treptichnus aequalternus* preservational variant) (Chen *et al.* 2011, fig. 13A, B; Carbone & Narbonne 2014, figs 5.7, 8). Archer & Maples (1984, fig. 6) showed that both forms are taphonomic variants depending on the plane of section of the burrow system, and therefore both are recorded herein as *Treptichnus bifurcus*. *Treptichnus pollardi* also has a continuous basal burrow, in places with a zigzagging pattern; however, projections extend vertically and sharply (Buatois & Mángano 1993b). *Bicavichnites martini* Lane, Braddy, Briggs & Elliott described from the Cambrian of southwestern USA is composed of two rows of depressions (Lane *et al.* 2003), and revision could potentially make it a junior synonym of *Treptichnus bifurcus* (see also Seilacher *et al.* 2005).

Treptichnus coronatum (Crimes & Anderson, 1985)

Figure 52D, E

1985 *Phycodes coronatum* isp. nov. Crimes & Anderson, pp. 328, 329, figs 10.5, 10.6, 11.
2014 *Treptichnus coronatum* (Crimes & Anderson); Buatois, Narbonne, Mángano, Carmona & Myrow, p. 3, fig. 1i.
2016 *Treptichnus coronatum* (Crimes & Anderson); Mángano & Buatois, p. 86, fig. 3.6a.
2017 *Treptichnus coronatum* (Crimes & Anderson); Landing *et al.*, p. 51, fig. 19G.

Material. – Thirteen specimens from Members 2A and 2B (Fortunian) in Fortune Head and Grand Bank Head.

Description. – Three-dimensional, unlined burrows with a basal circular structure from which vertical projections depart. Preserved as positive hyporelief, and positive and

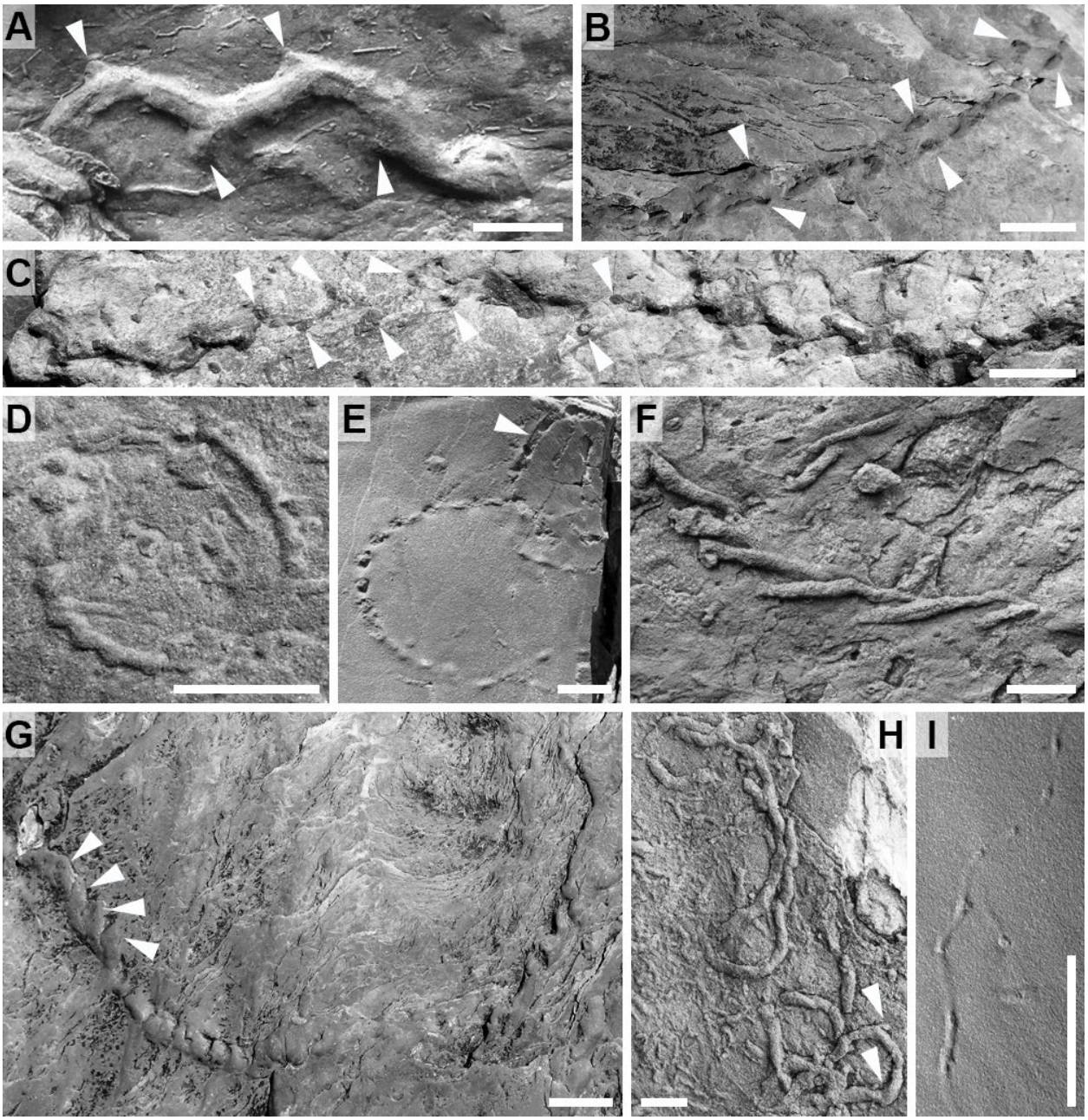

Fig. 52. *Treptichnus bifurcus* Miller (A–C), *T. coronatum* (Crimes & Anderson) (D, E), *T. pedum* (Seilacher) (F–H), and *T. pollardi* Buatois & Mángano (I). Scale bars are 1 cm. **A**, *Treptichnus bifurcus* with a zigzagging course, and small probes extending laterally (arrows). Positive hyporelief, Grand Bank Head, Member 2A (Fortunian). **B**, *Treptichnus bifurcus* with two rows of oblique probes extending upward (arrows). Positive epirelief, Lewin's Cove, Member 2A (Fortunian). **C**, *Treptichnus bifurcus* showing the basal zigzagging horizontal structure (left and right sides), and a middle interval where this structure is absent, and only the lateral pits are preserved (arrows). Positive epirelief, Fortune Head, Member 2B (Fortunian). **D**, Holotype of *Treptichnus coronatum* with a basal circular burrow connecting regularly spaced probes. GSC 73340. Positive hyporelief, Grand Bank Head, Member 2A (Fortunian). **E**, Two *Treptichnus coronatum* with vertical probes extending directly from the median part of the connective basal burrow (arrow). Negative and positive epirelief, Grand Bank Head, Member 2A (Fortunian). **F**, *Treptichnus pedum* with segments extending laterally. Positive hyporelief, Grand Bank Head, Member 2A (Fortunian). **G**, *Treptichnus pedum* with sickle-shaped segments (arrows). Positive epirelief, Lewin's Cove, Member 2A (Fortunian). **H**, *Treptichnus pedum* showing a tendency to form circles. Note that circles have an angular course, with in places lateral projections (arrows). Positive hyporelief, Grand Bank Head, Member 2A (Fortunian). **I**, *Treptichnus pollardi* with a winding course and aligned pits. Positive epirelief, Grand Bank Head, Member 2A (Fortunian).

negative epirelief. The basal structure forms a half circle, a full circle, or a '6' shape. Projections are represented by regularly spaced pits, departing slightly laterally from the basal circular structure and then extending vertically. Infill is massive, composed of very fine- to fine-grained sandstone similar to the host rock. Width of pits is 0.05–0.4 cm; width of basal circular structure (where observed) is 0.1–0.2 cm; maximum burrow length is 19.0 cm; diameter of the circle is 1.0–4.0 cm.

Associated trace fossils. – *Treptichnus coronatum* co-occurs with *Cochlichnus anguineus*, *Curvolithus simplex*, *Helminthoidichnites tenuis*, *Helminthopsis tenuis*, *Palaeophycus tubularis*, and *Treptichnus pedum*.

Remarks. – *Treptichnus coronatum* was first described from the Chapel Island Formation as *Phycodes coronatum* by Crimes & Anderson (1985). Uchman (1998) suggested that *Phycodes coronatum* may represent a primitive form of *Lorenzinia* Gabelli. However, *Lorenzinia* is clearly different, with projections extending radially and laterally; the presence of a circular basal burrow is also not clearly demonstrated (Uchman 1998). Subsequent work by MacNaughton & Narbonne (1999) placed *Phycodes coronatum* within *Treptichnus*, a decision endorsed here.

Mount & McDonald (1992) and Mount (1993) mentioned *Phycodes coronatum* in the Cambrian of south Australia without providing description, photograph or figure, and this occurrence needs re-investigation. Baghiyan-Yazd (1998, pl. 11, figs B, C) recorded *Hormosiroidea* isp. and *Phycodes coronatum* from the Cambrian of central Australia that arguably correspond to *Treptichnus coronatum*. *Treptichnus coronatum* was also recorded from many stratigraphical levels in the Cambrian of northwestern Canada (MacNaughton & Narbonne 1999, fig. 5). However, a photograph (MacNaughton & Narbonne 1999, fig. 8) shows that these specimens are closer to circular *Treptichnus pedum* as described herein (Fig. 52H). Wilson *et al.* (2012, fig. 10A) recorded circular *Treptichnus pedum* from the Cambrian of southern Namibia, with tight projections reminiscent of *T. coronatum*. These trace fossils are also found transitional with *Treptichnus pedum* (Wilson *et al.* 2012, figs 10B, C, 11A, D, E, 12A, B), and their unknown three-dimensional morphology hampers further re-evaluation of their taxonomic status. *Treptichnus coronatum* from the Cambrian of northwestern France (Coutret *et al.* 2024, fig. 16A, C) is either showing a winding course or an irregular circular pattern and may be better affiliated to *Treptichnus pedum* in which loops developed at intervals (cf. Wilson *et al.* 2012, figs 10B, 12F). *Phycodes* cf. *P. coronatum* in Bekker (2013, pl. 3, fig. 8) corresponds to crystal pseudomorphs (Kolesnikov *et al.* 2015). *Ctenopholeus kutcheri* from the Cambrian of northern India (Hughes *et al.* 2013, pl. 5, fig. 2) and the Devonian of southwestern Germany (Poschmann *et al.* 2023, figs 2–4) are forming circles with regular pits and should be re-assigned to *Treptichnus coronatum*. *Phycodes coronatum* from the Triassic of China is a horizontal circular structure with irregular bulges and pits (Bi *et al.* 1996, pl. I, fig. 9), and its affinity is unclear.

***Treptichnus pedum* (Seilacher, 1955b)**

Figure 52F–H

1987 *Phycodes pedum* Seilacher; Narbonne, Myrow, Landing & Anderson, p. 1287, fig. 6D, E.
1994a *Phycodes pedum* Seilacher; Brasier, Cowie & Taylor, p. 6, fig. 3.
2001 *Treptichnus pedum* (Seilacher); Gehling, Jensen, Droser, Myrow & Narbonne, p. 216, fig. 2b.
2007 *Treptichnus pedum* (Seilacher); MacNaughton, p. 143, fig. 8.9A.
2017 *Treptichnus pedum* (Seilacher); Herringshaw, Callow & McIlroy, p. 375, fig. 3c.
2017 *Treptichnus pedum* (Seilacher); Landing *et al.*, p. 45, fig. 17H, I.
2018 *Treptichnus pedum* (Seilacher); Hantsoo, Kaufman, Cui, Plummer & Narbonne, p. 1243, fig. 2g, h.
2019 *Treptichnus pedum* (Seilacher); Laing, Mángano, Buatois, Narbonne & Gougeon, p. 1626, fig. 2k.
2020 *Treptichnus pedum* (Seilacher); Hsieh & Plotnick, p. 67, fig. 3.
2023 *Treptichnus pedum* (Seilacher); Gougeon *et al.*, p. 9, fig. 5a–c.

Material. – About sixty specimens from Members 1 and 2A (Ediacaran), Members 2A and 2B (Fortunian), and Member 5 (Cambrian Age 2) in Fortune Head, Fortune North, Grand Bank Head, and Lewin's Cove.

Description. – Three-dimensional, unlined burrows with smooth segments added one after the other, and typically projecting on one side of the burrow. Preserved as positive hyporelief, positive epirelief, and full relief. The course is commonly straight to curving, and rarely loops. Segments are straight, arcuate, or sickle-shaped with wider bases. Infill is massive, composed of very fine- to coarse-grained sandstone similar to the host rock, or different where encased in mudstone. Maximum burrow length is 180.2 cm; width of segments is 0.05–0.6 cm; length of segments is 0.2–3.1 cm.

Associated trace fossils. – *Treptichnus pedum* co-occurs with *Curvolithus multiplex*, *C. simplex*, *Gyrolithes scintillus*, *Helminthoidichnites tenuis*, *Helminthopsis abeli*, *Palaeophycus tubularis*, *Palaeophycus* isp., *Psammichnites gigas circularis*, *P.* cf. *P. saltensis*, *Rusophycus avalonensis*, *Treptichnus bifurcus*, and *T. coronatum*.

Remarks. – *Treptichnus pedum* was first described as *Phycodes pedum* by Seilacher (1955b). Osgood (1970)

suggested to place *Phycodes pedum* within a different ichnogenus based on the morphological differences existing with other ichnospecies of *Phycodes*. Jensen & Grant (1992, 1993) noted that the type material of *Treptichnus* has segments projecting outwardly along curved courses, similarly as in *Phycodes pedum*; they proposed to relocate *P. pedum* within *Treptichnus* (see also Jensen 1997 and Jensen & Grant 1998). Geyer & Uchman (1995) argued that the type material of *Phycodes pedum* possesses vertical spreiten and fits better within *Trichophycus*. From Seilacher's (1955b, fig. 4b) drawing of the type material, a possible vertical spreite is only visible on the side of the block diagram, where the horizontal part of the burrow is cut. However, this *simili* spreite can also be interpreted as the departing point of an additional probe that was partially represented. In the same drawing, the remaining fourteen probes do not display spreiten. Consequently, we do not follow Geyer & Uchman's (1995) opinion, and agree with Jensen & Grant (1992, 1993) in that the type material of Seilacher (1955b) better fits within the morphological boundaries of *Treptichnus*. To complicate further, Dzik (2005, 2007) used the name *Manykodes pedum* (Seilacher) for these burrows, in an attempt to classify trace fossils based on their producers. This approach does not follow recommendations by the International Code of Zoological Nomenclature and has been contested (Bertling *et al.* 2006; Buatois 2018; Hammersburg *et al.* 2018).

Treptichnus pedum typically ranges from the Cambrian to the Ordovician (Seilacher 1969, 2007; Germs 1972; Baldwin 1977b; Wilson *et al.* 2012; Buatois 2018), although reports were made of specimens a few meters below the Cambrian Global Stratotype Section and Point at Fortune Head (Gelhing *et al.* 2001; Laing *et al.* 2019; Gougeon *et al.* 2023; this study). Potential reports from the Devonian (Han & Pickerill 1994b; Neto de Carvalho 2008), the Jurassic (Getty *et al.* 2016), and the Holocene (Muñiz Guinea *et al.* 2014) need further investigation. *Treptichnus pedum* has a worldwide distribution over all present-day continents: it is recorded from Africa (e.g. Seilacher 1969; Germs 1972; Crimes & Germs 1982; Geyer & Uchman 1995; Wilson *et al.* 2012), North America (e.g. Nowlan *et al.* 1985; Bryant & Pickerill 1990; Fillion & Pickerill 1990; Jensen *et al.* 2002b; Sour-Tovar *et al.* 2007; Hammersburg *et al.* 2018), South America (e.g. Durand & Aceñolaza 1990; Seilacher *et al.* 2005), Asia (e.g. Seilacher 1955b; Goldring & Jensen 1996; Zhu 1997; Wang & Wang 2006; Weber *et al.* 2012; Sharma *et al.* 2018b), Australia (e.g. Glaessner 1969; Walter *et al.* 1989; Jensen *et al.* 1998; Droser *et al.* 1999; Gehling *et al.* 2019), and Europe (e.g. Banks 1970; Palij *et al.* 1983; Pacześna 1986; Orłowski & Żylińska 1996; Jensen & Palacios 2016; McLoughlin *et al.* 2021).

In the Chapel Island Formation, Crimes & Anderson (1985) first recorded these burrows as *Phycodes* cf. *P. pedum*, with only a description provided. Following reports, either figured (see synonym list above) or non-figured, used the names *Phycodes pedum* (Narbonne *et al.* 1987; Landing *et al.* 1988; Brasier *et al.* 1994a), *Treptichnus pedum* (e.g. Gehling *et al.* 2001; Babcock *et al.* 2014; Herringshaw *et al.* 2017; Hantsoo *et al.* 2018; Laing *et al.* 2019; Hsieh & Plotnick 2020), *Treptichnus* isp. (Landing *et al.* 1988), *Treptichnus* (Droser *et al.* 2002), and *Trichophycus pedum* (Seilacher) (Landing & Westrop 1998). In the Chapel Island Formation, spreiten are never observed within the segments (i.e. as in *Trichophycus*); we therefore assign these trace fossils confidently to *Treptichnus pedum*. Circular treptichnids need to be carefully evaluated: *Treptichnus coronatum* possesses a basal circular burrow with vertical projections, whereas circling *T. pedum* are composed of distinct segments first projecting horizontally, and then extending laterally and obliquely at each angle (Fig. 52G). Circling *Treptichnus pedum* can also be transitional with straight to curving *T. pedum*. Circling *Treptichnus pedum* have been regularly recorded in the literature (Orłowski 1989, pl. 14, fig. 2; Fillion & Pickerill 1990, pl. 11, fig. 17; MacNaughton & Narbonne 1999, fig. 8; Wilson *et al.* 2012, figs 10–12; Carbone & Narbonne 2014, fig. 5.9; Wang & Wang 2006, pl. 3, fig. 1a; Getty *et al.* 2016, fig. 4.9). When projections are tight over the circle, their distinction from *Treptichnus coronatum* can be problematic (e.g. Wilson *et al.* 2012, fig. 10A).

Treptichnus pollardi **Buatois & Mángano, 1993b**

Figure 52I

Material. – Two specimens from Members 2A and 2B (Fortunian) in Fortune Head and Grand Bank Head.

Description. – Three-dimensional, unlined burrows with a basal structure from which vertical projections extend. Preserved as positive epirelief. The basal structure has a curved to winding course. Projections are represented by regularly spaced pits. Infill is massive, composed of very fine-grained sandstone similar to the host rock. Width of pits is 0.05 cm; width of basal circular structure is 0.05 cm; maximum burrow length is 2.9 cm.

Associated trace fossils. – *Treptichnus pollardi* co-occurs with *Helminthoidichnites tenuis*.

Remarks. – Regularly spaced pits extending vertically from a horizontal basal structure allow placing

these trace fossils in *Treptichnus pollardi*. Buatois & Mángano (1993b) argued that pits are preserved either at the angle of juncture of a basal zigzagging structure, or within an unguided basal structure; the second scenario is observed in the Chapel Island Formation (Fig. 52I). The holotype of *Treptichnus pollardi* displays widely spaced pits along the burrow course (Buatois & Mángano 1993b, fig. 5). However, and similarly to the Chapel Island Formation material, closely spaced pits in *Treptichnus pollardi* have also been recorded (e.g. Buatois *et al.* 2000; Metz 2009; Desjardins *et al.* 2010b). The main difference with the rather similar *Saerichnites kutscheri* is the lack of development of a permanent open gallery system in *Treptichnus pollardi*, which can be evidenced by the massive passive infill, the presence of a lining, and the robust horizontal basal burrow in the former; *Treptichnus pollardi* also tends to have a more sinuous or zigzagging course. Reports of *Treptichnus pollardi* from the Cambrian are common (e.g. Geyer & Uchman 1995; Buatois & Mángano 2003b; Wang & Wang 2006; Högström *et al.* 2013; Carbone & Narbonne 2014; Shahkarami *et al.* 2017a). In the Chapel Island Formation, *Treptichnus pollardi* has been mentioned in previous studies (Buatois *et al.* 2014; Landing *et al.* 2017) but was not figured.

Ichnogenus *Trichichnus* Frey, 1970

Discussion. – *Trichichnus* is a thread-like cylindrical burrow typically oriented vertically or obliquely (Frey 1970; Kędzierski *et al.* 2015) and included in the category of architectural design of 'burrows with shaft or bunch with downwards radiating probes' (Buatois *et al.* 2017). *Trichichnus* was first described from the Cretaceous Niobrara Chalk Formation of central USA (Frey 1970). At first, *Trichichnus* was mostly recorded from modern deep-sea cores (Bellaiche & Blanpied 1979; Thomson & Wilson 1980; Weaver & Schultheiss 1983), until it became commonly described in deep-marine trace-fossil assemblages as well (e.g. Wetzel 1981, 1983, 1984, 1991; Uchman 1995, 1999, 2001, 2007). Three ichnospecies attributed to *Trichichnus* have been erected: *T. linearis* Frey, 1970; *T. simplex* Pickerill in Fillion & Pickerill, 1990; and *T. appendicus* Uchman, 1999. The type ichnospecies, *Trichichnus linearis*, has a distinct lining (Frey 1970). *Trichichnus simplex* is unlined (Fillion & Pickerill 1990). However, the absence of lining may be related to diagenetic processes, which would make *Trichichnus simplex* a preservational variant of *T. linearis* (Uchman 1995, 1999; Monaco & Uchman 1999). *Trichichnus appendicus* has thin, short lateral extensions (Uchman 1999). Consequently, two ichnospecies, *Trichichnus appendicus* and *T. linearis*, are here considered valid.

Trichichnus shows similarities with *Multina* Orłowski, 1968, *Olenichnus* Fedonkin, 1985, *Pilichnus* Uchman, 1999, *Skolithos* Haldeman, 1840, and *Tisoa* de Serres, 1840. *Multina* is an irregular burrow network with common overlapping (Buatois & Mángano 2012a). *Multina minima* Uchman as figured by Parry *et al.* (2017, fig. 2a, b) from the Ediacaran–Cambrian of Brazil shows very thin, irregular and pyritized branching burrows oriented at different angles that are reminiscent of *Trichichnus* (see also supplementary material in Daley *et al.* 2018 and Marusin & Kuper, 2020 for alternative interpretations). Nevertheless, *Multina magna* Orłowski, the holotype of *Multina*, differs significantly from *Trichichnus* by its horizontal orientation and the formation of large polygons (Orłowski 1968). *Olenichnus* is a passively filled burrow system with sinuous meanders and horizontal and vertical branching tunnels (Fedonkin 1985; Marusin & Kuper 2020). Although it superficially resembles *Trichichnus* (cf. Marusin & Kuper 2020, figs 6, 7), the dominant horizontal orientation and sinuous course between branches are distinctive. Contrary to *Trichichnus*, *Pilichnus* is a horizontal string with dichotomous branching (Uchman 1999). *Skolithos* is a burrow that differs from *Trichichnus* by its straight vertical course and lack of branching and pyritization (Knaust *et al.* 2018). *Tisoa* is a deep, vertical and pyritized burrow that, unlike *Trichichnus*, is U-shaped with faint spreiten and a low-amplitude helicoidal morphology (Knaust 2019; Wetzel & Blouet 2023).

Other structures with informal names are also comparable to *Trichichnus*. 'Mycellia' are very thin pyritized filaments randomly oriented and found in high densities (e.g. Bellaiche & Blanpied 1979; Blanpied & Bellaiche 1981; Wetzel 1983, 1984; Baldwin & McCave 1999; Löwemark 2007). Some pyritized structures described in open nomenclature can also be reminiscent of *Trichichnus* ('string-like pyritic forms' of Jørgensen *et al.* 1981; 'pyritized cylinders' of Uchman 1999; 'ferruginous cylinders' of Rodríguez-Tovar & Uchman 2006; 'pyritized burrows' of Leonowicz 2015). Finally, thin, pyritized structures interpreted as body fossils (e.g. Hofmann 1983; Knaust & Desrochers 2019) require careful evaluation to be accurately distinguished from burrows.

Trichichnus ranges from the Cambrian (Stachacz 2012; Laing *et al.* 2019; Mángano & Buatois 2020; Gougeon *et al.* 2023) to the Holocene (e.g. Frey 1975; Werner & Wetzel 1982; Weaver & Schultheiss 1983; Wetzel 1983; Fu & Werner 1994; Löwemark 2003). Possible producers are meiofaunal arthropods (Frey 1970; Ekdale *et al.* 1984), filamentous bacteria (Virtasalo *et al.* 2010; Kędzierski *et al.* 2015), foraminifera (Frey 1975; Bellaiche & Blanpied 1979;

Blanpied & Bellaiche 1981), pogonophore and polychaete worms (Weaver & Schultheiss 1983), sipunculan worms (Romero-Wetzel 1987; McBride & Picard 1991), and nematodes (threadworms; Gingras *et al.* 2002). *Trichichnus* is recorded in marginal-marine (e.g. Pickerill *et al.* 1984a; Fillion & Pickerill 1990; Gingras *et al.* 2002; Buatois *et al.* 2005), shallow-marine (e.g. Frey 1970; Pickerill & Forbes 1979; Jordan 1985; Caruso *et al.* 2013; Leonowicz 2015; Hanken *et al.* 2016), and deep-marine (e.g. Wetzel 1983; McBride & Picard 1991; Fu & Werner 1994; Uchman 1995; Löwemark 2003; Monaco *et al.* 2012) environments. *Trichichnus* has only been recorded recently in the Chapel Island Formation (Laing *et al.* 2019; Gougeon *et al.* 2023).

***Trichichnus linearis* Frey, 1970**

Figure 53A–C

2019 *Trichichnus* cf. *T. simplex* Pickerill; Laing, Mángano, Buatois, Narbonne & Gougeon, p. 1626, fig. 2o.

Material. – Thousands of specimens from Members 2A, 2B, and 3 (Fortunian), and Members 4 and 5 (Cambrian Age 2) in Fortune Head, Fortune North, Grand Bank Head, Lewin's Cove, Little Dantzic Cove, and Point May.

Description. – Elongated cylindrical burrows oriented at various angles, but always with a significant

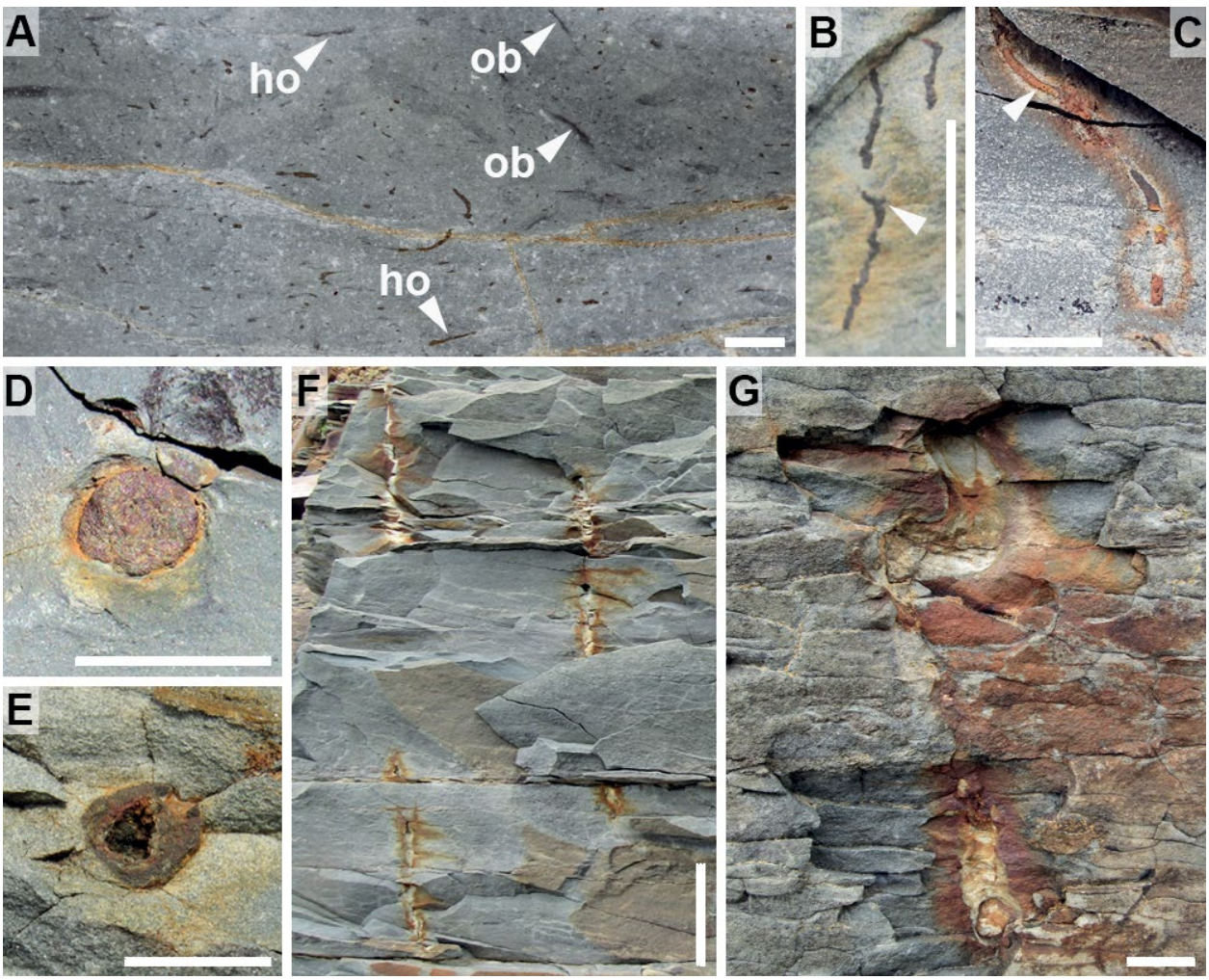

Fig. 53. Trichichnus linearis Frey (A–C) and *Trichichnus* isp. (D–G). Scale bars are 1 cm (A–E), 2 cm (G), and 10 cm (F). **A**, Dense ichnofabric of *Trichichnus linearis* oriented at various angles ('ho' for subhorizontal; 'ob' for oblique). Full relief, Point May, Member 2A (Fortunian). **B**, Vertical, unlined *Trichichnus linearis* displaying a tortuous course and possible branching (arrow). Full relief, Grand Bank Head, Member 2A (Fortunian). **C**, Horizontal, curved *Trichichnus linearis* with a thin lining (arrow). Full relief, Little Dantzic Cove, Member 4 (Cambrian Age 2). **D**, Cylindrical *Trichichnus* isp. with a thin lining. Full relief observed on bed top, Little Dantzic Cove, Member 4 (Cambrian Age 2). **E**, Subcylindrical *Trichichnus* isp. with a thick lining. Full relief observed on bed top, Little Dantzic Cove, Member 5 (Cambrian Age 2). **F**, Deep, straight *Trichichnus* isp. Full relief, Little Dantzic Cove, Member 5 (Cambrian Age 2). **G**, *Trichichnus* isp. with an elbow-shaped segment. Full relief, Little Dantzic Cove, Member 5 (Cambrian Age 2).

vertical component. Preserved as full relief. The course is straight, curved, winding, or tortuous. Burrows are isolated or forming dense aggregates. A diffuse halo is very common. Unlined or thinly lined. Branching is rare but is hinted in some specimens. Infill is massive, composed of mudstone similar to the host rock or different where encased in very fine- to fine-grained sandstone. Infill is typically darker and pyritized. Burrow diameter is 0.01–0.15 cm; maximum length is 4.1 cm; maximum halo diameter is up to 0.8 cm.

Associated trace fossils. – *Trichichnus linearis* co-occurs with *Arenicolites* aff. *A. carbonarius*, *Bergaueria perata*, *Conichnus conicus*, *Curvolithus simplex*, *Gyrolithes gyratus*, *G. scintillus*, *Palaeophycus tubularis*, *Palaeophycus* isp., *Psammichnites gigas circularis*, *Rusophycus dabardae*, *Saerichnites kutscheri*, *Trichichnus* isp., and radial probing burrow.

Remarks. – In the original description, Frey (1970) noted that walls of *Trichichnus linearis* are very distinct from the surrounding sediment and are typically pyritized. This led to confusion as pyritization of burrows is a diagenetic artifact, and hence not a valid ichnotaxobase (Bertling *et al.* 2022). Pyritization is related to the activity of sulfate-reducing bacteria (Thomsen & Vorren 1984), most notably at the oxic-anoxic transition zone within the sediment (Kędzierski *et al.* 2015). Frey (1970) described *Trichichnus* as 'thread-like', inferring burrows have a very small diameter. However, size of burrows is not a first-order ichnotaxobase either (Bertling *et al.* 2006, 2022). Here, we consider that the orientation at different angles, the variety of course shapes, true branching, and the absence of short lateral extensions, are the main ichnotaxobases of *Trichichnus linearis*. We also follow Uchman (1995, 1999) in considering *Trichichnus simplex* a junior synonym of *T. linearis* and place both lined and unlined forms within *T. linearis*.

***Trichichnus* isp.**

Figure 53D–G

Material. – About sixty specimens from Member 3 (Fortunian) and Members 4 and 5 (Cambrian Age 2) in Little Dantzic Cove.

Description. – Vertical, unbranched, simple subcylindrical burrows with a pyritized infill and/or a surrounding halo. Preserved as full relief. Burrows are found isolated. Rarely, burrow fill is weathered away, and only a lining or halo is preserved. Burrow morphology is highly variable, and is either straight, slightly inclined, slightly curved, rarely tortuous, or with a horizontal segment forming an elbow-shape along the structure. Width is mostly constant. A thin or thick lining is common. Infill is massive, composed of mudstone similar to the host rock, or different where made of very fine-grained sandstone and encased in mudstone or sandy mudstone. Burrow width (without halo) is 0.4–1.5 cm; maximum halo width is 5.6 cm; maximum depth is 57.0 cm, but typically 5.0–30.0 cm deep.

Associated trace fossils. – *Trichichnus* isp. co-occurs with *Trichichnus linearis*.

Remarks. – With their vertical development in a single tube and absence of branching, some of these burrows are reminiscent of *Skolithos*. However, the high variability of shapes and the constant pyritization is not diagnostic of *Skolithos* (cf. Alpert 1974). Pyritization and variable shapes and orientations (but with a dominant vertical component) are more typical of *Trichichnus* (cf. Frey 1970; Uchman 1999). The Chapel Island Formation material is notable for its impressive size, with burrow width and depth measurements unseen in any other *Trichichnus* ichnospecies. We retain these burrows as *Trichichnus* isp. to account for their distinctive dimensions, although size is typically not considered a good ichnotaxobase (Bertling *et al.* 2006, 2022). Similarly to *Tisoa siphonalis* (Wetzel & Blouet 2023), the dimensions of *Trichichnus* isp. and heavy pyritization suggest they formed under anoxic conditions within the substrate, and the secretion of mucus by its tracemaker resulted in the formation of a distinctive lining.

Radial probing burrow

Figure 54A–H

Material. – Sixteen specimens from Members 2B and 3 (Fortunian) in Fortune Head, Grand Bank Head, and Little Dantzic Cove.

Description. – Burrows made of probes oriented radially. Preserved in full relief. The overall structure is semispherical with irregular outlines, either plug-shaped and extending deeply within the sediment, or shallower and not very penetrative in less-developed specimens. Probes have similar widths within a specimen but variable lengths, either forming small bulges or being distinctively elongated. Where elongated, probes are straight to curved, directed laterally or upwardly, stacked on top of each other as clear individual elements or forming spreiten. Well preserved

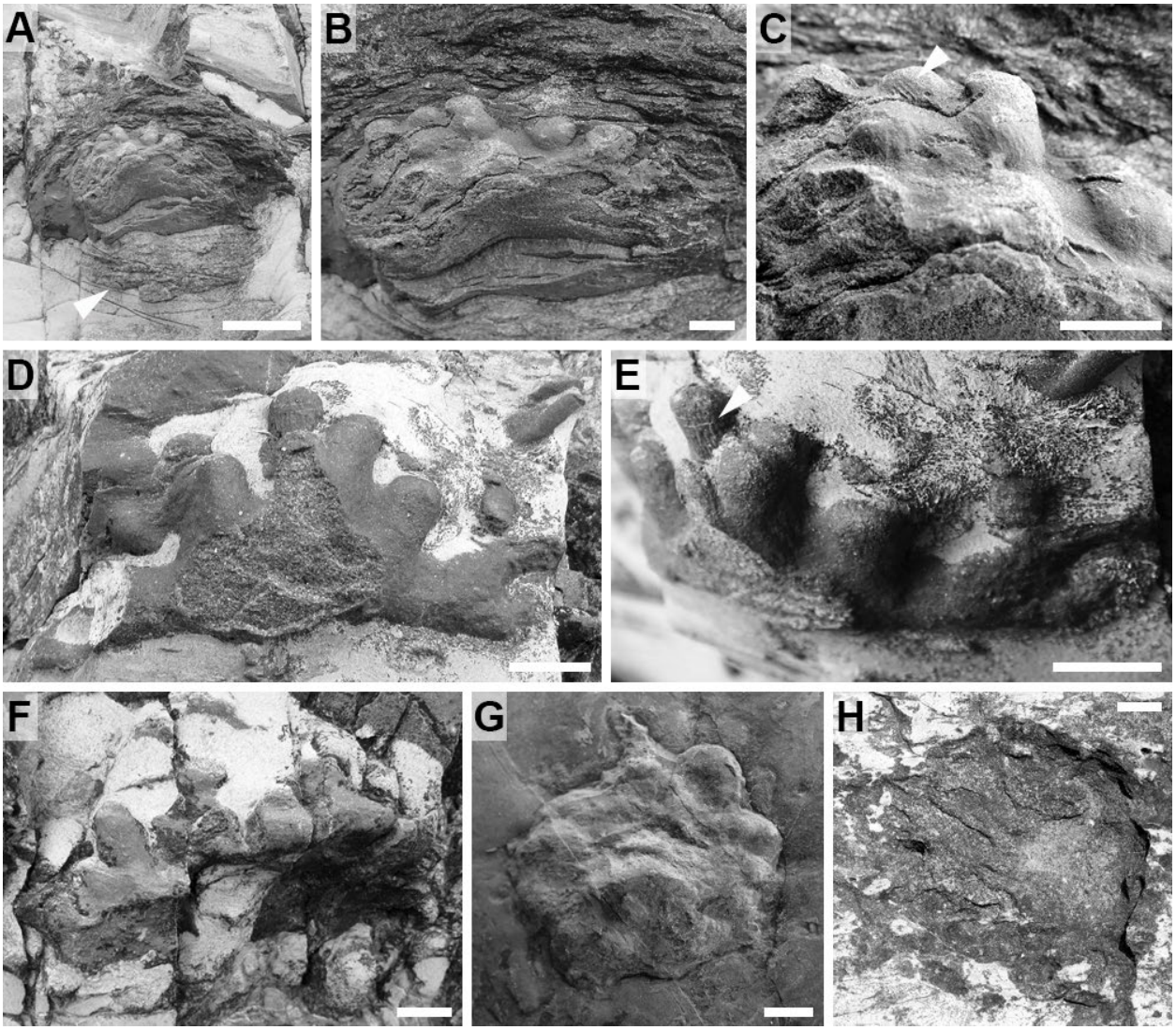

Fig. 54. Radial probing burrow. Scale bars are 1 cm (B–H) and 5 cm (A). **A**, Overall view of a large specimen, with the base extending deeply (arrow), and probes preserved on the upper part. Full relief, Grand Bank Head, Member 2B (Fortunian). **B**, Close-up view of the same specimen, with probes irregularly stacking on top of each other. Full relief, Grand Bank Head, Member 2B (Fortunian). **C**, Close-up view of the same specimen, highlighting the delicate oblique striae (arrow). Full relief, Grand Bank Head, Member 2B (Fortunian). **D**, Specimen with numerous elongated probes extending in different directions. Full relief, Grand Bank Head, Member 2B (Fortunian). **E**, Same specimen in lateral view showing the staking pattern of probes and the delicate longitudinal striae (arrow). Full relief, Grand Bank Head, Member 2B (Fortunian). **F**, Partially preserved specimen with only few probes preserved. Full relief, Grand Bank Head, Member 2B (Fortunian). **G**, Specimen showing the overall subcircular outline on a bed base. Full relief, Fortune Head, Member 2B (Fortunian). **H**, Poorly preserved specimen observed on a bed top. Full relief, Little Dantzic Cove, Member 3 (Fortunian).

specimens locally display sublongitudinal, parallel and continuous delicate striae on probes. Burrow width is 3.5–7.7 cm; burrow depth is 1.6–7.2 cm; probe width is 0.7–1.0 cm; probe length is 0.4–1.4 cm.

Associated trace fossils. – Radial probing burrow co-occurs with *Palaeophycus tubularis*, *Palaeophycus* isp., *Psammichnites gigas circularis*, and *Trichichnus linearis*.

Remarks. – The radial probing burrow as recorded from the Chapel Island Formation is unique from the trace-fossil record. Muñoz *et al.* (2019) reviewed radial and rosette trace fossils, which offers ground for comparison. Ichnotaxa with comparable morphological features are *Asterichnus* Bandel and *Dactyloidites* Hall. *Asterichnus* is a star-shaped burrow with retrusive spreiten and distinct, elongated tubes extending from a central point (Bandel 1967; Chamberlain 1971). *Dactyloidites* is a stellate to palmate rosette with branched or unbranched tubes with spreiten, and displays a radiating pattern developing from a central tube (Hall 1886; Boyd & McIlroy 2016). Specimens

from the Chapel Island Formation are more irregular than these two ichnotaxa, and probes never depart from a central point. Another similar ichnotaxon to the Chapel Island Formation material is *Phycodes*, a horizontal burrow with branches forming bundles (Osgood 1970; Fillion & Pickerill 1990). However, radial forms in *Phycodes* have not been described so far (cf. Seilacher 2007).

In fact, Crimes & Anderson (1985) described *Buthotrephis* isp. from the Chapel Island Formation, an ichnotaxon with a branching pattern now considered junior synonym of *Chondrites* Sternberg or *Phycodes* (Seilacher 1955b; Häntzschel 1975; Uchman 1998), although the synonymy is not fully accepted (Osgood 1970; Książkiewicz 1977; Clausen & Vilhjálmsson 1986). *Buthotrephis* isp. in Crimes & Anderson (1985) is neither photographed nor drawn, which complicates comparison to our material. Their description does not match the radial morphology described herein, and these authors did not specifically refer to the material coming from Member 2B at Grand Bank Head, which is the stratigraphical interval with the best-preserved specimens of radial probing burrows. By emphasizing irregular branching in their description and by considering their stratigraphical occurences (recorded in Members 1, 2, and 5), it is herein suggested that *Buthotrephis* isp. recorded by Crimes & Anderson (1985) may correspond to overlapping specimens of *Palaeophycus* and is unrelated to radial probing burrows.

Radial burrows have been recorded from the Cambrian worldwide. The 'stellate structure' figured in Walter *et al.* (1989, fig. 17C) may represent a specimen of *Asterichnus*, with well-organised and distinct radiating tubes. Carbone & Narbonne (2014, fig. 6.5) recorded a 'radiating probing' burrow, which is flattened with radial probes departing from a central point. Davies *et al.* (2009, fig. 5G) recorded *Dactylophycus* Miller & Dyer from the Cambrian of Scotland, but their figured specimen seems to represent overlapping horizontal burrows, and do not show any radial arrangement (cf. Muñoz *et al.* 2019). Hammersburg *et al.* (2018, fig. 13) recorded multiple specimens of *Gyrophyllites* Glocker that are star-shaped with well-organized lateral tubes. Perhaps the 'radiating trace' of Legg (1985, pl. 1, fig. D) from the middle Cambrian of Spain represents the closest morphology to the Chapel Island Formation material. Observed on a bed base, it possesses irregular radiating probes, arranged in a large (5 cm wide), overall circular structure extending deeply within the sediment. However, Legg (1985) did not report any ornamental feature on the surface of the probes.

The radial probing burrow from the Chapel Island Formation displays longitudinal striae (Fig. 54C, E). Their parallel arrangement, without crisscrossing, argues for body imprints from the tracemaker, rather than representing scratch imprints left by appendages used during the digging process. These striae are reminiscent of the ones described in *Treptichnus* (Kesidis *et al.* 2019b) and may suggest priapulid worms as candidates for the formation of these burrows. However, contrary to the *Treptichnus* probing behaviour which produces elongated segments added one after the other, the organism at the origin of the radial probing burrow foraged laterally and in different directions over a localized area (see also Legg 1985).

Vertical J-shaped burrow with spreiten

Figure 55

Material. – One specimen from Member 5 (Cambrian Age 2) in Little Dantzic Cove.

Fig. 55. Vertical J-shaped burrow with spreiten. Note the spreiten (arrow), only developed on the lower part. Full relief, Little Dantzic Cove, Member 5 (Cambrian Age 2). Scale bar is 1 cm.

Description. – Vertical, unbranched, J-shaped burrow with poorly developed spreiten. Preserved as full relief. The causative burrow is straight in its upper part and curved around its base where it becomes oriented horizontally. Spreiten are only developed on the lower part of the structure, and consist of oblique, slightly curved and stacked laminae. A lining is present in the causative burrow. Infill of the causative burrow is composed of very fine-grained sandstone different from the sandy mudstone host rock. Width of causative burrow is 0.4 cm; depth of the burrow is 3.7 cm.

Associated trace fossils. – Vertical J-shaped burrow with spreiten does not occur with other formally erected ichnotaxa.

Remarks. – This burrow presents features reminiscent of *Diplocraterion* and *Syringomorpha* Nathorst, two ichnogenera first appearing in the Cambrian (Mángano & Buatois 2020). *Diplocraterion* possesses a U-shaped causative burrow with spreiten. When part of the causative burrow is not preserved, the structure can form a J-shaped morphology similar to the specimen recorded here. The comparison is relevant as ?*Diplocraterion* isp. is recorded from Member 5 in Little Dantzic Cove (see *Diplocraterion* section, p. 83). *Syringomorpha* is a vertical J-shaped burrow with spreiten (Mángano & Buatois 2004a; Noffke *et al.* 2022). However, the curvature of the causative burrow in Cambrian *Syringomorpha* is less sharp, and spreiten typically start higher on the overall structure. In short, the preservation of only one specimen in the Chapel Island Formation does not allow a definitive conclusion on its ichnotaxonomic affinity.

Trace-fossil distribution

Trace fossils are distributed all through the five members, although variations were noted within specific stratigraphical intervals and in between localities (Figs 56–59).

Trace fossils in Member 1 (heterolithic sandstone and mudstone) are sparse and appear mostly within the uppermost interval. Trace fossils are horizontal and restricted to bed bases and tops. Grand Bank Head hosts the earliest appearance of simple passively filled burrows, *Palaeophycus* isp., close to the base of Member 1 (Fig. 57). Other biogenic structures noted higher in Member 1 correspond to simple horizontal trails (*Circulichnis montanus*, *Helminthoidichnites tenuis*) and undetermined burrows (Fig. 57). Toward the top of Member 1, at Fortune Head and Point May, simple actively filled structures (*Torrowangea rosei*), other passively filled burrows (*Palaeophycus tubularis*), and horizontal burrows with horizontal to vertical branches (*Treptichnus* indet.) made their appearance and are visible on the base of sandstone beds (Figs 56, 59C). Bed tops rarely display simple horizontal trace fossils (*Archaeonassa fossulata*). Trace-fossil suites are typically monospecific.

Abundance, diversity, and disparity of trace fossils significantly increases within Member 2A (heterolithic sandstone and mudstone) at all localities. Notably, trace fossils visible in vertical sections become more common and result from firm substrates allowing the pristine casting of passively filled burrows (Droser *et al.* 2002). Infaunal trace fossils cover a broad range of architectural designs, represented by trilobed flattened trails (*Curvolithus multiplex, C. simplex*), bilobed trails and paired grooves (*Cruziana problematica*, *Didymaulichnus miettensis*), passively filled horizontal burrows (*Palaeophycus annulatus*, *P. tubularis*, *Palaeophycus* isp.), complex actively filled horizontal structures (*Psammichnites gigas circularis*), horizontal burrows with horizontal to vertical branches (*Saerichnites kutscheri*, *Treptichnus bifurcus, T. coronatum*, *T. pedum*, *T. pollardi*, *Treptichnus* indet.), vertical plug-shaped burrows (*Bergaueria perata*, *B.* cf. *B. radiata*, *Conichnus conicus*), vertical single U-shaped burrows (*Arenicolites* aff. *A. carbonarius*), vertical helicoidal burrows (*Gyrolithes gyratus*, *G. scintillus*), and burrows with shaft or bunch with downwards radiating probes (*Trichichnus linearis*). Epifaunal trace fossils are found on both bed tops and bases and are composed of simple horizontal trace fossils (*Archaeonassa fossulata*, *Cochlichnus anguineus*, *C. luguanensis*, *Circulichnis ligusticus*, *C. montanus*, *Gordia marina*, *Helminthoidichnites tenuis*, *Helminthopsis abeli*, *H. hieroglyphica*, *H. tenuis*), trackways and scratch imprints (*Dendroidichnites* aff. *D. irregulare*, *Dimorphichnus* isp. A, *Dimorphichnus* isp. B, cf. *Dimorphichnus* isp., *Monomorphichnus bilinearis*, *M. lineatus*, *M. needleiunm*, *Monomorphichnus* isp.), and bilaterally symmetrical short and scratched burrows (*Rusophycus avalonensis*, *R. dabardae*, *Rusophycus* isp.). However, differencies exist in between localities when compared to Fortune Head at a finer resolution: (1) Grand Bank Head shows the low stratigraphical occurrence of *Psammichnites gigas circularis* within the *Treptichnus pedum* Ichno-Assemblage Zone (GBH-B 11.2) and of *Cruziana problematica* within the *Rusophycus avalonensis*

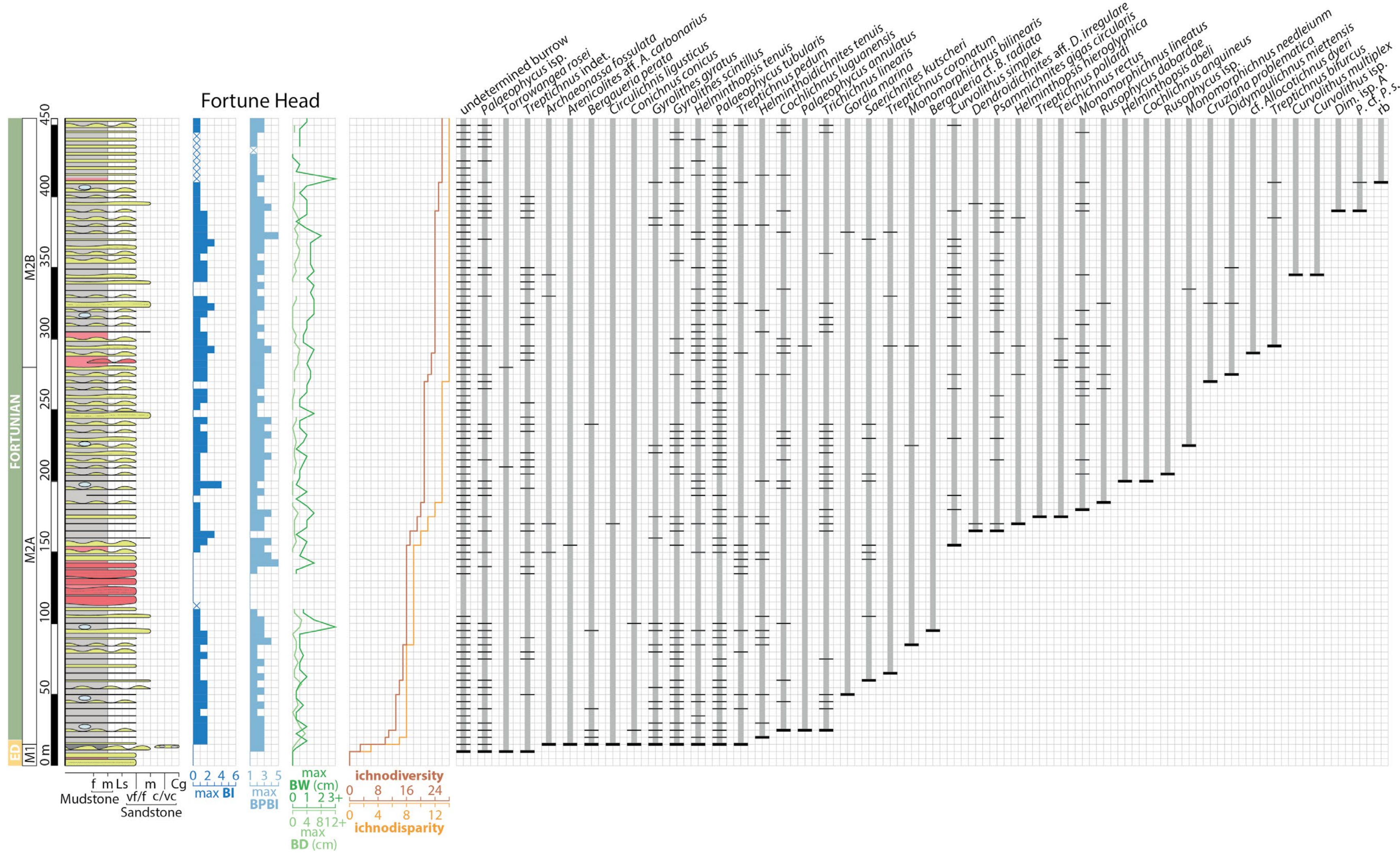

Fig. 56. Trace-fossil dataset from Fortune Head. A detail on the Ediacaran–Cambrian boundary interval can be found in Figure 65. From left to right: age; member; sedimentary log (scale in meters); maximum bioturbation index (BI); maximum bedding plane bioturbation index (BPBI); maximum burrow width (BW); maximum burrow depth (BD); ichnodiversity and ichnodisparity; and stratigraphic position of ichnotaxa. Abbreviations: Ed, Ediacaran; M1 and M2, Members 1 and 2 of the Chapel Island Formation; f and m mudstone, fine and medium mudstone; Ls, limestone; vf/f, m, c/vc sandstone, very fine-/fine-grained, medium-grained, coarse-/very coarse-grained sandstone; Cg, conglomerate; *Dim.* isp. A, *Dimorphichnus* isp. A; *P.* cf. *P. s.*, *Psammichnites* cf. *P. saltensis*; and rb, radial probing burrow.

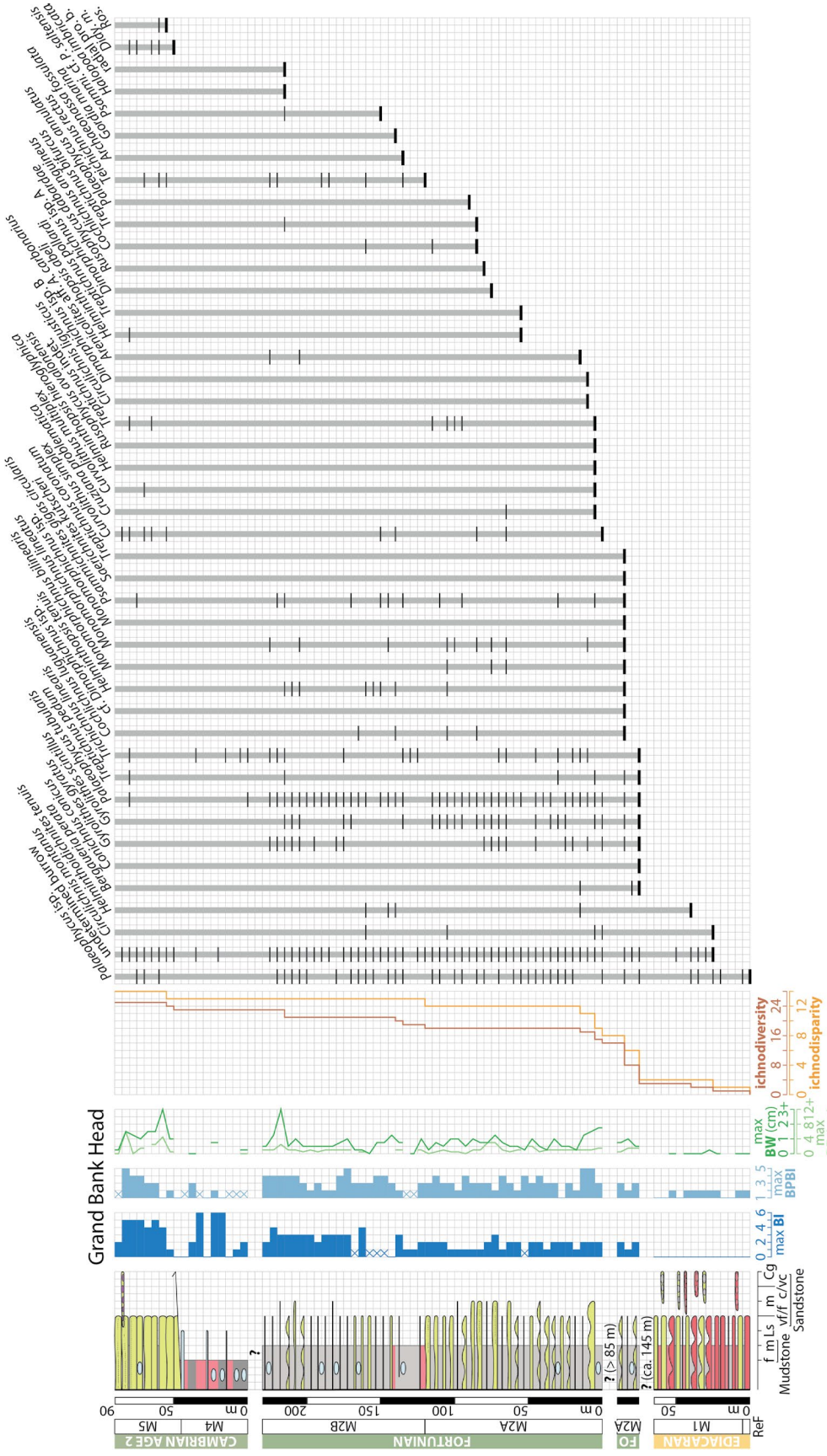

Fig. 57. Trace-fossil dataset from Grand Bank Head. From left to right: age; member; sedimentary log (scale in meters); maximum bioturbation index (BI); maximum bedding plane bioturbation index (BPBI); maximum burrow width (BW); maximum burrow depth (BD); ichnodiversity and ichnodisparity; and stratigraphic position of ichnotaxa. Abbreviations: Fo, Fortunian; ReF, Rencontre Formation; M1 to M5, Members 1 to 5 of the Chapel Island Formation; f and m mudstone, fine and medium mudstone; Ls, limestone; vf/f, m, c/vc sandstone, very fine-/fine-grained, medium-grained, coarse-/very coarse-grained sandstone; Cg, conglomerate; *Didy. m.*, *Didymaulichnus miettensis*; *Psammi.* cf. *P. saltensis*, *Psammichnites* cf. *P. saltensis*; radial pro. b., radial probing burrow; and *Ros.*, *Rosselia* isp.

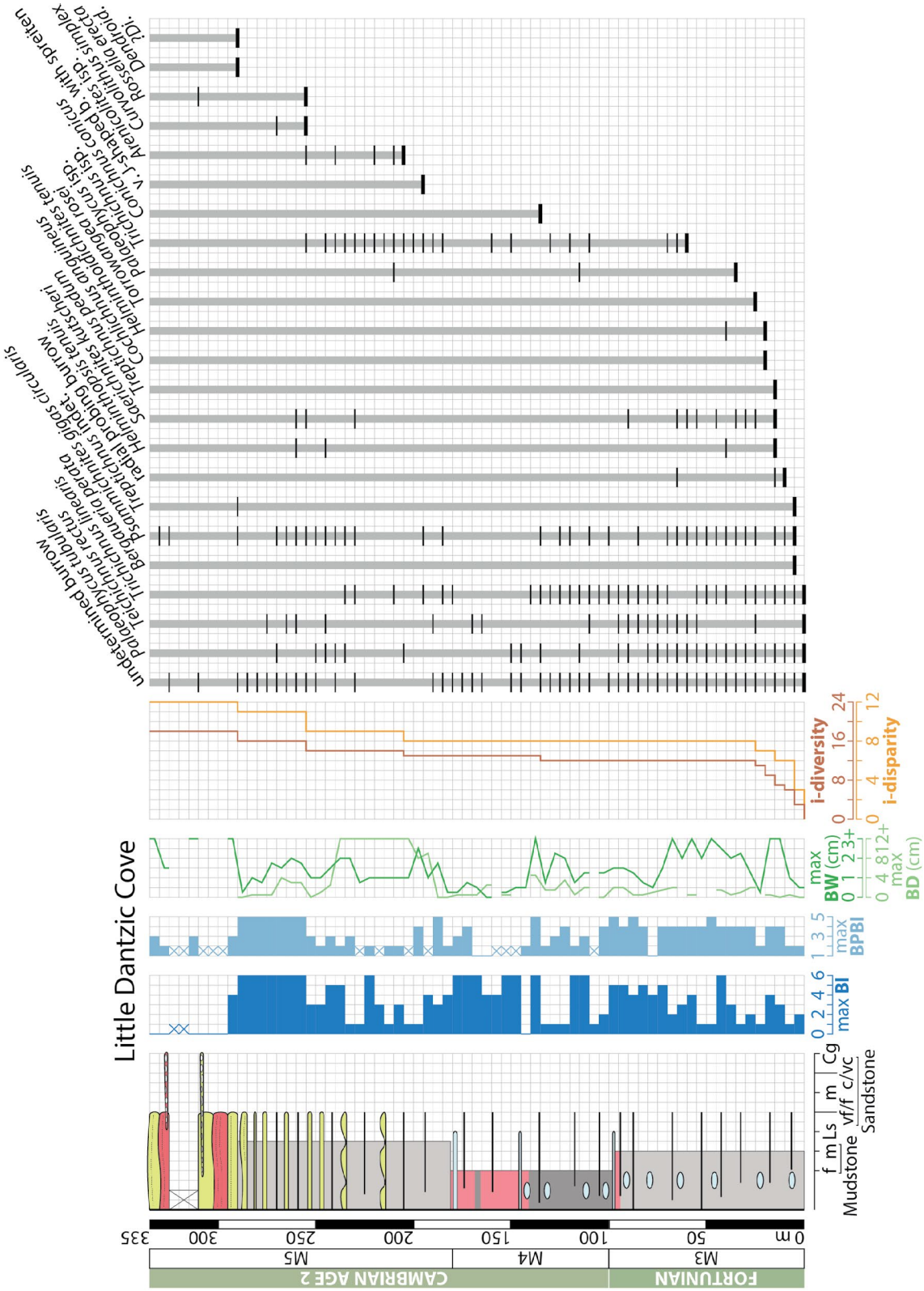

Fig. 58. Trace-fossil dataset from Little Dantzic Cove. From left to right: age; member; sedimentary log (scale in meters); maximum bioturbation index (BI); maximum bedding plane bioturbation index (BPBI); maximum burrow width (BW); maximum burrow depth (BD); ichnodiversity (i-diversity) and ichnodisparity (i-disparity); and stratigraphic position of ichnotaxa. Abbreviations: M3 to M5, Members 3 to 5 of the Chapel Island Formation; f and m mudstone, fine and medium mudstone; Ls, limestone; vf/f, m, c/vc sandstone, very fine-/fine-grained, medium-grained, coarse-/very coarse-grained sandstone; Cg, conglomerate; *Dendroid.*, *Dendroidichnites* aff. *D. irregulare*; ?*Di.*, ?*Diplocraterion* isp.; and v. J-shaped b. with spreiten, vertical J-shaped burrow with spreiten.

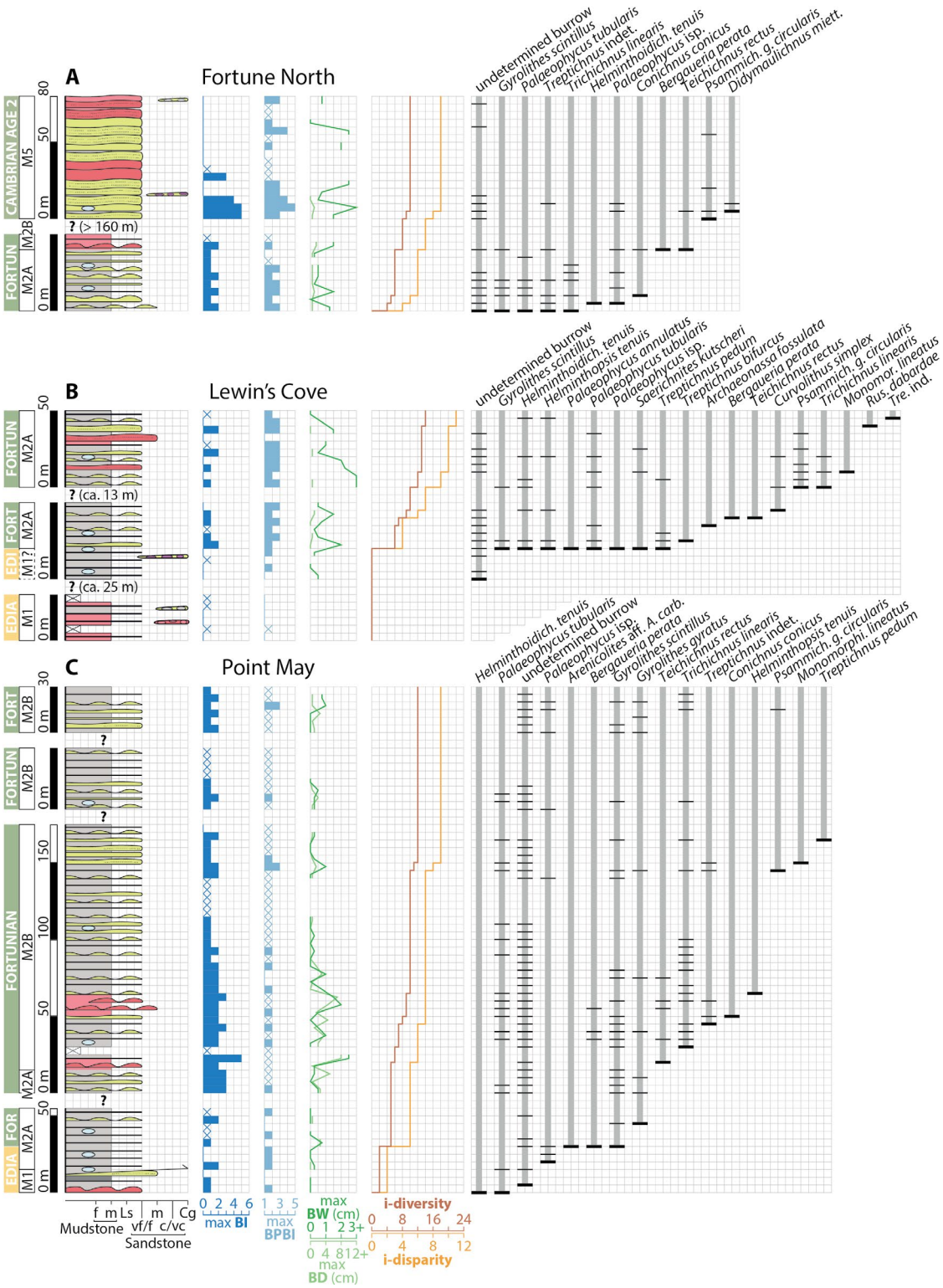

Fig. 59. Trace-fossil datasets from Fortune North (A), Lewin's Cove (B), and Point May (C). From left to right: age; member; sedimentary log (scale in meters); maximum bioturbation index (BI); maximum bedding plane bioturbation index (BPBI); maximum burrow width (BW); maximum burrow depth (BD); ichnodiversity (i-diversity) and ichnodisparity (i-disparity); and stratigraphic position of ichnotaxa. Abbreviations: Edi/Edia, Ediacaran; For/Fort/Fortun, Fortunian; M1 to M5, Members 1 to 5 of the Chapel Island Formation; f and m mudstone, fine and medium mudstone; Ls, limestone; vf/f, m, c/vc sandstone, very fine-/fine-grained, medium-grained, coarse-/very coarse-grained sandstone; Cg, conglomerate; *Arenicolites* aff. *A. carb.*, *Arenicolites* aff. *A. carbonarius*; *Didymaulichnus miette.*, *Didymaulichnus miettensis*; *Helminthoidich. tenuis*, *Helminthoidichnites tenuis*; *Monomor. lineatus*/*Monomorphi. lineatus*, *Monomorphichnus lineatus*; *Psammich. g. circularis*, *Psammichnites gigas circularis*; *Rus. dabardae*, *Rusophycus dabardae*; and *Tre.* ind., *Treptichnus* indet.

Ichno-Assemblage Zone (DL-5 0.46 in 'Data 2' file of Gougeon *et al.* 2025b); and (2) Lewin's Cove shows the low stratigraphical occurrence of *Curvolithus simplex* (LC-B 47.4, LC-B 48.8, LC-C 1.0, LC-C 21.8) and *Psammichnites gigas circularis* (LC-C 3.5, LC-C 4.7, LC-C 5.0, LC-C 9.3, LC-C 11.3, LC-C 15.1, LC-C 27.2, LC-C 36.5) within the *Treptichnus pedum* Ichno-Assemblage Zone (Figs 57, 59B). Furthermore, the lowest occurrence of *Teichichnus rectus*, a horizontal burrow with simple vertically oriented spreiten (Buatois *et al.* 2017), is within Member 2A and is only based on two specimens at Fortune Head and Lewin's Cove (Figs 56, 59B). Moreover, *Didymaulichnus miettensis* is recorded high in Member 2A but with a single occurrence at Fortune Head (Fig. 56), whereas it becomes very common stratigraphically higher in Member 5 both at Fortune North and Grand Bank Head (Figs 57, 59A). Trace fossils typically define monospecific to paucispecific suites. In addition to the typical green heterolithic bedding, Member 2A displays an interval of heterolithic red beds reminiscent of Member 1 at Fortune Head, but bioturbation is mostly absent (Fig. 56).

Trace fossils from Member 2B (heterolithic sandstone and mudstone) do not differ significantly from Member 2A. Large sediment bulldozing trace fossils (*Curvolithus simplex*, *Didymaulichnus miettensis*, *Psammichnites gigas circularis*) are more common and are pervasive on some bed surfaces. Within Member 2B, first stratigraphic appearances are: (1) cf. *Allocotichnus dyeri* at Fortune Head; (2) *Psammichnites* cf. *P. saltensis* at Fortune Head and Grand Bank Head; (3) *Curvolithus* isp. at Fortune Head; (4) *Halopoa imbricata* at Grand Bank Head; and (5) radial probing burrow at Fortune Head and Grand Bank Head (Figs 56, 57). Although rarely recorded in Member 2A (Fig. 56), *Teichichnus rectus* is common (at Fortune Head, Fortune North, and Grand Bank Head) to very abundant (at Point May) within red beds defining the base of Member 2B (Figs 56, 57, 59A, C).

Member 3 (mudstone-dominated) is mostly exposed at Little Dantzic Cove (Fig. 58), with a bias toward exposure of bed tops (Fig. 5). Consequently, trace fossils that are typically recovered from bed bases, such as *Treptichus pedum* or *Didymaulichnus miettensis*, are only rarely or not recorded at all across this interval. The dominant trace fossil observed is *Psammichnites gigas circularis*, reflecting colonisation of large surface areas (BPBI = 4–5). As a result, bed surfaces reworked by *Psammichnites gigas circularis* are typically monospecific. Rare bed tops also display simple horizontal trails (*Cochlichnus anguineus*, *Helminthoidichnites tenuis*, *Helminthopsis tenuis*). Vertical sections and polished samples (Gougeon *et al.* 2018a) show that the sedimentary fabric is characterised by the appearance of mottled intervals overprinted by *Teichichnus rectus* that can rework thick mudstone intervals. *Trichichnus linearis* is also a common trace fossil in Member 3 (Fig. 58).

Member 4 (mudstone-dominated, with limestone beds and calcite nodules) is exposed at Grand Bank Head and Little Dantzic Cove (Figs 57, 58). Trace fossils are more difficult to observe on bed surfaces because of the peculiar weathering of massive mudstone intervals (Fig. 5). Consequently, trace-fossil diversity is low. *Trichichnus linearis* and *Trichichnus* isp. are, however, abundant at Little Dantzic Cove and are easily spotted thanks to their pyritization which improves their color contrasts with the casting rock (Fig. 58). Other intervals at this locality have abundant *Palaeophycus tubularis*, *Psammichnites gigas circularis*, and *Teichichnus rectus*.

Finally, Member 5 shows an important change in sedimentological characteristics between its lower and upper parts, which affects trace-fossil distribution. Lower Member 5 (sandy mudstone-dominated) is only recorded at Little Dantzic Cove and exposes vertical sections with deep pyritized *Trichichnus* isp. (Fig. 58). *Arenicolites* isp., made of paired burrows on bed tops, is inferred to have played a role in the deeper colonisation of the substrate as well (Fig. 58). Other trace fossils are less common and more difficult to observe, namely *Palaeophycus tubularis*, *Teichichnus rectus*, *Trichichnus linearis*, and *Psammichnites gigas circularis*, which are exposed on bed tops. The transition from the lower to upper Member 5 is observed at Little Dantzic Cove. This heterolithic interval shows the appearance of *Rosselia erecta*, a vertical concentrically filled burrow, in association with trace fossils previously found in underlying strata (*Helminthopsis tenuis*, *Palaeophycus tubularis*, *Psammichnites gigas circularis*, *Saerichnites kutscheri*, *Teichichnus rectus*, *Trichichnus* isp.). Upper Member 5 (sandstone-dominated) is present at Fortune North, Grand Bank Head, and Little Dantzic Cove. This interval at Grand Bank Head notably displays well-preserved *Curvolithus simplex*, *Didymaulichnus miettensis,* and *Treptichnus pedum* on bed bases forming paucispecific suites, as well as *Rosselia* isp. in vertical cross-section (Fig. 57). Bed tops at Little Dantzic Cove show the presence of ?*Diplocraterion* isp. (Fig. 58), an inferred vertical U-shaped burrow that suggests colonisation of the deep tier.

Ichnostratigraphy of the Ediacaran–Cambrian boundary interval

Historical aspects

The role that trace fossils could play in delineating the Precambrian–Cambrian boundary was first raised in a mid-fifties pioneer paper by Seilacher (1956). In his ichnostratigraphic scheme (Fig. 60), Seilacher (1956) considered *Helminthoidichnites* cf. *H. spiralis*, *H. spiralis, H. meeki*, *Planolites corrugatus* Walcott, and cf. *Rusophycus* to be typical trace fossils of the Precambrian (all the identifications in this section are from the original sources). This trace-fossil selection was based on material recovered from India and USA (Arizona and Montana). Seilacher (1956) recorded a broader diversity of forms in Cambrian strata, with cf. *Bergaueria*, *Scolithus* (sic), *Dictyodora*, *Diplocraterion*, *Rhizocorallium*, *Teichichnus*, *Phycodes palmatum* (Hall), *Phycodes* isp., and *Phycodes pedum*, among other ichnotaxa, recovered from England, Italy (Sardinia), Pakistan (Salt Range), Sweden, and USA (Grand Canyon). Although Ediacaran forms have dubious taxonomic affinities according to modern standards (for instance, see review in *Helminthoidichnites* section, p. 97), the idea that complex and vertical burrowing developed during the Cambrian was already distinctly stated. The scheme of Seilacher (1956) was commented in the following years (e.g. Goldring 1967; Banks 1970; Young 1972; Osgood 1975; Stanley 1976; Crimes *et al.* 1977) and represented an alternative to the definition of the basal Cambrian using trilobites as index fossils (Wheeler 1947). However, Glaessner (1962) was critical of Seilacher's model and considered that the focus on Cambrian trace fossils should only include early Cambrian ichnotaxa and that Seilacher's selection of Precambrian trace fossils was unclear and needed better described specimens. Nevertheless, Webby (1970) used Seilacher's scheme to consider trace fossils from the Lintiss Vale Formation of New South Wales (Australia) as an intermediate state of behavioural complexity between Seilacher's Precambrian and Cambrian assemblages; Bergström (1970) recovered *Rusophycus parallelum* from the Hardeberga Sandstone of Sweden and argued that this unit was early Cambrian based on Seilacher's work; and Daily (1972) acknowledged the worldwide distribution and the significance of *Diplocraterion*, *Cruziana,* and *Rusophycus* as indicators of lower Cambrian strata, supporting the view of Seilacher.

As a follow-up to a symposium organized by the Working Group on the Precambrian–Cambrian boundary of the Subcommission on Cambrian Stratigraphy held in Montreal in 1972 (Cowie & Glaessner 1975), Alpert (1977) refined the scheme of Seilacher (1956). Alpert's study was based on material collected in the White-Inyo Mountains of California (USA) and was then extended to other stratigraphic units hosting records of the Precambrian–Cambrian boundary interval. Alpert (1977) identified three groups of trace fossils (Fig. 60) (see also Ekdale *et al.* 1984): (1) an assemblage known only from the late Precambrian, comprising *Archaeichnium* Glaessner, *Bunyerichnus* Glaessner, and *Buchholzbrunnichnus* Germs; (2) an assemblage not useful in delineating the basal Cambrian boundary (according to Alpert), comprising *Curvolithus*, *Didymaulichnus*, *Helminthoidichnites*, *Planolites*, *Scolicia*, *Skolithos*, *Torrowangea*, and other forms kept in open nomenclature (the latter are not represented in Fig. 60); and (3) a more diverse assemblage indicative of early Cambrian age, including dwelling burrows (e.g. *Bergaueria*, *Diplocraterion*), feeding burrows (e.g. *Phycodes*, *Teichichnus*), horizontal trails or burrows (e.g. *Cochlichnus*, *Psammichnites*), and arthropod trace fossils (e.g. *Cruziana*, *Rusophycus*). Importantly, Alpert (1977) advocated that the base of the Cambrian should be placed well below the oldest report of trilobites, at the first appearance of arthropod trace fossils. This suggestion followed previous statements by Bergström (1970) and Daily (1972). Byers (1982) argued that, although Alpert's scheme provided a clear picture of trace-fossil diversity and complexity of the basal Cambrian, it did not address the issue of small shelly fossils and their stratigraphic correlation with trace fossils. Nevertheless, Alpert's model gained support, and the use of trace fossils as biostratigraphic markers of the basal Cambrian started to be applied more regularly in other sections worldwide (e.g. Fedonkin 1977, 1981; Nowlan *et al.* 1985; Pacześna 1986). Brasier (1982, fig. 3b) also used Alpert's work to design a curve tracking trace-fossil diversity through the Precambrian–Cambrian boundary interval and to draw more general conclusions on the Cambrian radiation of animals.

In a seminal paper, Crimes (1987) extensively reviewed the literature on Ediacaran and early Cambrian trace fossils recovered below trilobites. Focussing on their first appearance datum, Crimes erected three ichnostratigraphic zones (Fig. 60): (1) an upper Ediacaran Zone I, with mostly horizontal structures (e.g. *Cochlichnus*, *Didymaulichnus*, *Gordia*, *Harlaniella*); (2) a lower Cambrian Zone II, with more complex trace fossils (*Phycodes*, *Teichichnus*, *Treptichnus*) and *Bergaueria*; and (3) a lower Cambrian Zone III, with arthropod trace fossils (*Cruziana*, *Diplichnites*, *Dimorphichnus*,

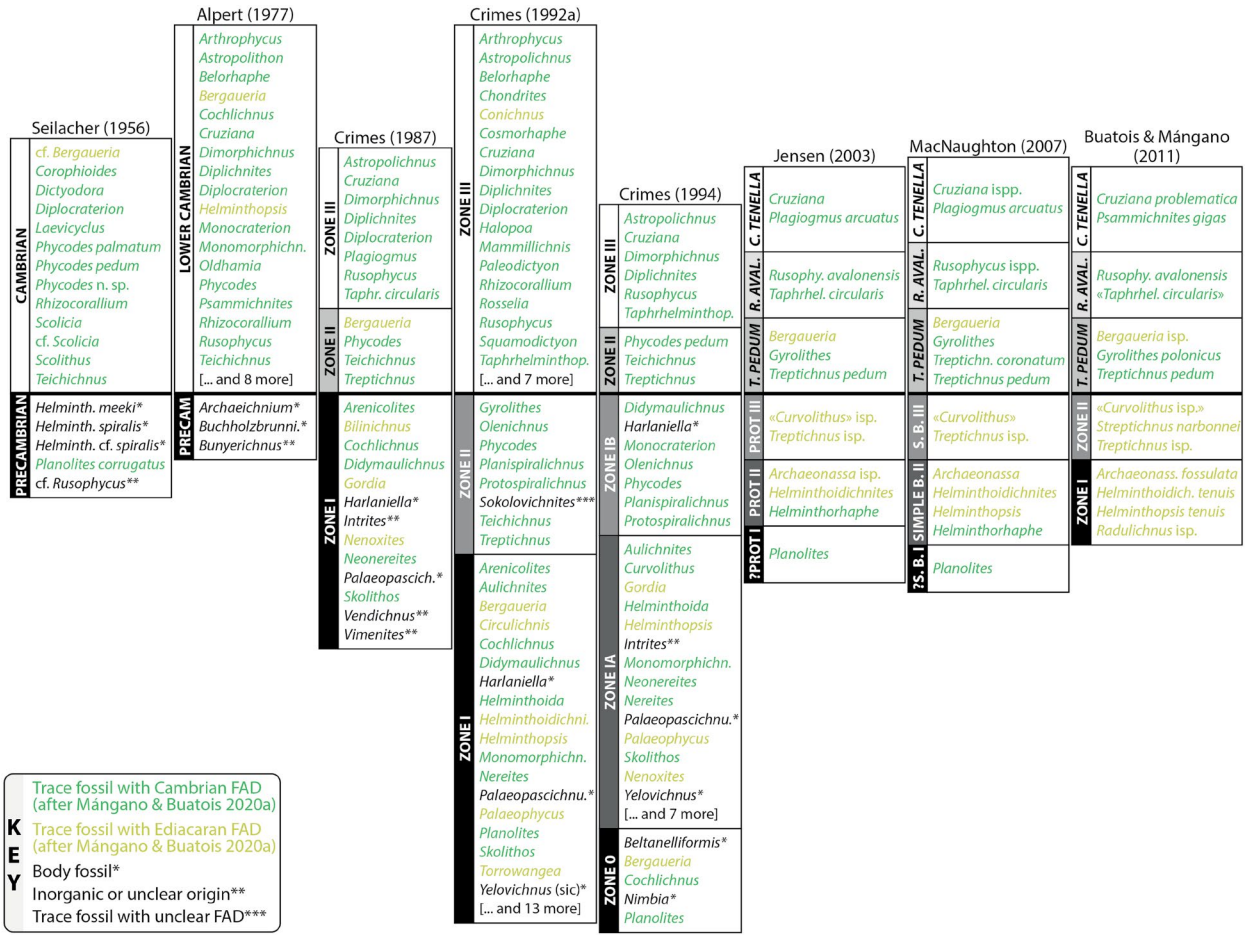

Fig. 60. Summary of trace-fossil biozonation schemes across the Precambrian–Cambrian boundary interval below the oldest record of trilobites that were based on worldwide datasets. Of Alpert (1977) and Crimes (1987, 1992a, 1994), only the most pertinent trace fossils per biozone as mentioned in the text were included here. Other ichnostratigraphic models (e.g. Narbonne *et al.* 1987; Walter *et al.* 1989; MacNaughton & Narbonne 1999; Carbone & Narbonne 2014) are regional rather than global and are not included in this summary, for the sake of simplicity. Abbreviations: FAD, first appearance datum; Precam, Precambrian; s. b./simple b., simple burrows; *Archaeonass.*, *Archaeonassa*; *Buchholzbrunni.*, *Buchholzbrunnichnus*; *C. tenella*, *Cruziana tenella*; *Helminth./Helminthoidich./Helminthoidichni.*, *Helminthoidichnites*; *Monomorphichn.*, *Monomorphichnus*; *Palaeopascich./Palaeopascichnu.*, *Palaeopascichnus*; *R. aval./Rusophy. avalonensis*, *Rusophycus avalonensis*; *Taphrhel./Taphrhelminthop.*, *Taphrhelminthopsis*; and *T. pedum*, *Treptichnus pedum*.

Rusophycus), large horizontal trace fossils (*Plagiogmus* Roedel, *Taphrhelminthopsis*), and vertical forms (*Astropolichnus*, *Diplocraterion*). This trace-fossil scheme aided in the definition of the Cambrian Global Stratotype Section and Point at Fortune Head and was followed in subsequent studies (Narbonne *et al.* 1987; Walter *et al.* 1989; Bergström 1990). Later, Crimes (1989, 1992a, b, 1994) refined his model (Fig. 60). However, Crimes (1992a) placed in his Ediacaran Zone I many trace fossils (*Arenicolites*, *Lockeia* James, *Monocraterion*, *Monomorphichnus*, *Nereites*, *Skolithos*) that are today considered diagnostic of the Cambrian (Mángano & Buatois 2020). In addition, a Zone II in Crimes (1992a) with *Gyrolithes*, *Teichichnus*, and *Treptichnus*, displaying more vertical and complex behaviours, was considered Vendian (i.e. latest Ediacaran) (Fig. 60). In Crimes (1994), the Ediacaran was for the first time subdivided into three ichnozones (Zones 0, IA, IB), and *Phycodes pedum* and *Teichichnus* were placed *de novo* in the lower Cambrian (Fig. 60).

Focussing on datasets from the Mackenzie Mountains (western Canada), MacNaughton & Narbonne (1999) compared their regional trace-fossil biozonation scheme with the type section of the Cambrian at Fortune Head. Notably, they erected a novel *Cruziana tenella* ichnozone following the Fortunian *Rusophycus avalonsensis* ichnozone previously described by Narbonne *et al.* (1987). This work led Jensen (2003) to update and simplify greatly the global ichnostratographic scheme of the Precambrian–Cambrian boundary interval

(Fig. 60). The critical review of Ediacaran fossils by Jensen (2003) aided in the definition of three late Neoproterozoic zones that did not include structures misinterpreted as trace fossils (see also Jensen *et al.* 2006). In addition, Jensen (2003) carefully placed treptichnids as diagnostic features of his Proterozoic zone III, whereas *Treptichnus pedum* was considered diagnostic of the lower Cambrian *T. pedum* zone along with vertical burrows (*Bergaueria*, *Gyrolithes*). This scheme was later slightly refined by MacNaughton (2007), who added a few more typical ichnotaxa in Ediacaran and Cambrian zones (Fig. 60). Finally, the most recent ichnostratigraphic scheme was provided by Buatois & Mángano (2011), who removed the oldest Ediacaran zone and updated some of the typical trace fossils for each zone (Fig. 60) (see also Mángano *et al.* 2012).

Ichnostratigraphy of the Chapel Island Formation

Narbonne *et al.* (1987) proposed an ichnostratigraphic scheme for the Chapel Island Formation mainly based on data recovered from Grand Bank Head, Fortune Head, and Little Dantzic Cove (see also Narbonne & Myrow 1988). This scheme comprises three biozones and broadly agrees with the global ichnostratigraphic model of Crimes (1987). The oldest biozone, the *Harlaniella podolica* Zone, encompasses Member 1 and basal Member 2A (up to 2.4 m) and is composed of *Harlaniella podolica* and *Palaeopascichnus delicatus* of stratigraphic ranges restricted to the Ediacaran, as well as simple trace fossils *Gordia arcuata*, *G. marina*, *Planolites montanus* Richter, and *P. beverleyensis* (identifications from the original source) that were also recovered in younger strata. The earliest Cambrian *Phycodes pedum* Zone is marked by the appearance of plug-shaped burrows (*Conichnus conicus*), elongated vertical trace fossils (*Arenicolites* isp., *Skolithos annulatus*), arthropod scratch imprints (*Monomorphichnus* ispp.), simple horizontal trails (*Helminthopsis tenuis*), large horizontal trace fossils (*Curvolithus* isp.), simple open burrows (*Palaeophycus tubularis*), and complex three-dimensional burrow systems (*Phycodes pedum*). Finally, the *Rusophycus avalonensis* Zone comprises the first appearance of *Taphrhelminthopsis circularis* 133 m above the base of Member 2A, followed by a variety of trace fossils typical of the Cambrian (e.g. *Bergaueria* isp., *Cochlichnus* isp., *Dimorphichnus* isp., *Rusophycus avalonensis*, and *Teichichnus rectus* in the original source). This dataset was later complemented by Landing *et al.* (1988) with detailed sections showing first stratigraphic appearances of trace fossils. This scheme was later used by Brasier (1992) to infer global correlations of strata between Newfoundland, England, eastern Europe, Siberia, and south China. Brasier (1992) erected three additional biozones above the *Rusophycus avalonensis* Zone, namely a *Cruziana* Zone, a *Teichichnus* Zone, and a *Cylindrichnus* Zone, although these have never been supported by detailed evidence and discussion (see also Brasier *et al.* 1992). Finally, MacNaughton & Narbonne (1999) described a *Cruziana tenella* Zone in northwestern Canada that was correlated with strata close to the top of Member 5 in the Chapel Island Formation, although *Cruziana* was not recorded in the succession at the time.

The ichnostratigraphic scheme of Narbonne *et al.* (1987) can be updated following our taxonomic revisions and recent observations in the field (Fig. 61). Overall, the scheme is consistent across sections at Fortune Head, Fortune North, Little Dantzic Cove, and Point May, but shows departures at Grand Bank Head and Lewin's Cove. Based on a composite stratigraphic column of the Chapel Island Formation (see Fig. 61, as well as Fig. 65 for detail on the Ediacaran–Cambrian boundary interval), the Ediacaran *Harlaniella podolica* Zone is composed of simple horizontal trails (*Archaeonassa fossulata*, *Circulichnis montanus*, *Helminthoidichnites tenuis*) and very shallow infaunal burrows (*Palaeophycus* isp., *Torrowangea rosei*, *Treptichnus* indet.). Preservation of *Treptichnus pedum* and *Gyrolithes gyratus* is rare and only limited to the uppermost beds (see also Gougeon *et al.* 2023). The *Treptichnus pedum* Ichno-Assemblage Zone is characterised by a burst in trace-fossil diversity, notably marked by the appearance of distinctive infaunal burrows (*Arenicolites* aff. *A. carbonarius*, *Bergaueria perata*, *B.* cf. *B. radiata*, *Conichnus conicus*, *Gyrolithes scintillus*, *Palaeophycus tubularis*, *Saerichnites kutscheri, Treptichnus coronatum*, *T. pedum*, and *Trichichnus linearis*). At Fortune Head, arthropod scratch imprints are rare and only represented by *Monomorphichnus* indet. (data from Narbonne *et al.* 1987, see Fig. 65) and *Monomorphichnus bilinearis*. The *Rusophycus avalonensis* Ichno-Assemblage Zone demonstrates the appearance of various other arthropod scratch imprints (cf. *Allocotichnus dyeri*, *Dimorphichnus* isp. A, *Dimorphichnus* isp. B, *Monomorphichnus lineatus*, *M. needleiunm*, *Rusophycus avalonensis*, *Rusophycus dabardae*, *Rusophycus* isp.) and trace fossils made by sediment bulldozers (*Curvolithus multiplex*, *C. simplex*, *Curvolithus* isp., *Didymaulichnus miettensis*, *Psammichnites gigas circularis*, *P.* cf. *P. saltensis*). The *Cruziana tenella* Ichno-Assemblage Zone, as described and correlated to the Chapel Island Formation by MacNaughton & Narbonne (1999), has not been recorded in our study (but see below).

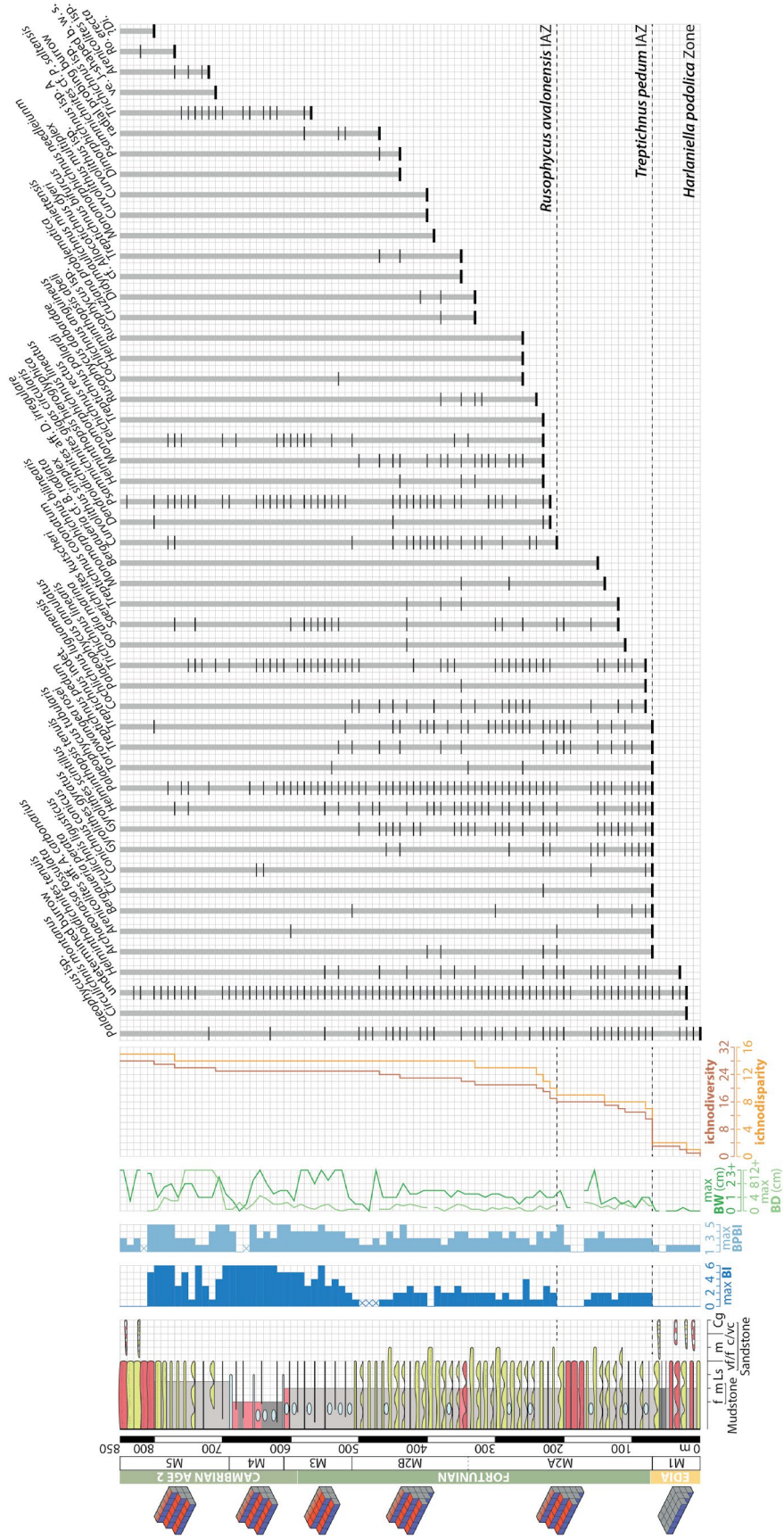

Fig. 61. Ichnostratigraphy and summary of trace-fossil datasets from the Chapel Island Formation. A detail on the Ediacaran–Cambrian boundary interval can be found in Figure 65. Data is based on Grand Bank Head (Member 1), Fortune Head (Members 1 and 2), and Little Dantzic Cove (Members 3–5) sections. From left to right: type of outcrop exposure (provided for every member); age; member; sedimentary log (scale in meters); maximum bioturbation index (BI); maximum bedding plane bioturbation index (BPBI); maximum burrow width (BW); maximum burrow depth (BD); ichnodiversity and ichnodisparity; and stratigraphic position of ichnotaxa. Abbreviations: Edia, Ediacaran; M1 to M5, Members 1 to 5 of the Chapel Island Formation; f and m mudstone, fine and medium mudstone; Ls, limestone; vf/f, m, c/vc sandstone, very fine-/fine-grained, medium-grained, coarse-/very coarse-grained sandstone; Cg, conglomerate; *?Di.*, *?Diplocraterion* isp.; *Ro. erecta*, *Rosselia erecta*; and ve. J-shaped b. w. s., vertical J-shaped burrow with spreiten.

At Grand Bank Head and Lewin's Cove, some inconsistencies exist with the archetypal scheme observed at Fortune Head. The main issue results from the record of *Cruziana problematica* close to the base of the *Rusophycus avalonensis* Ichno-Assemblage Zone. *Cruziana problematica* is a synonym of *C. tenella* (see *Cruziana* section, p. 68) that was used as the index fossil defining the *C. tenella* Ichno-Assemblage Zone (MacNaughton & Narbonne 1999). The presence of *Cruziana problematica* in the *Rusophycus avalonensis* Ichno-Assemblage Zone is not surprising, as arthropod trace fossils become abundant in this stratigraphic interval. *Cruziana problematica* is a simple form of *Cruziana* without some of the complex 'fingerprints' displayed by other *Cruziana* (Seilacher 1970, 1994), and is typically recorded without any scratch imprints preserved at all (e.g. Mángano *et al.* 2002b; Kesidis *et al.* 2019a). Therefore, we suggest that *Cruziana problematica* (or *C. tenella*) is not used as index fossil, but instead that *C. stromnessi* Trewin, the ichnotaxon that was actually used by MacNaughton & Narbonne (1999, fig. 5) to delineate the base of that Ichno-Assemblage Zone and which shows more distinct and complex scratch imprints (Trewin 1976), becomes the name bearer for the *Cruziana stromnessi* Ichno-Assemblage Zone.

Grand Bank Head shows a variety of arthropod scratch imprints (*Monomorphichnus bilinearis*, *M. lineatus*, *Monomorphichnus* isp., and cf. *Dimorphichnus* isp.) on perfectly exposed bed bases within the *Treptichnus pedum* Ichno-Assemblage Zone (Fig. 57). This record would represent the oldest evidence of stem-group euarthropod and is significantly below the second diversification of arthropod trace fossils observed in the *Rusophycus avalonensis* Ichno-Assemblage Zone (see Discussion, p. 166).

Lewin's Cove shows low stratigraphic occurrences of *Curvolithus simplex* and *Psammichnites gigas circularis* below red beds (Fig. 59B) that could be considered coeval strata to intertidal red beds of Fortune Head found within Member 2A (Fig. 56). However, the red beds at Lewin's Cove only show oscillatory-flow and unidirectional current actions (i.e. hummocky cross-stratification and current-ripple cross-lamination, respectively) that do not exactly fit with the tidal origin of supposed red bed equivalents at Fortune Head (see Facies A1, A2, A3 sections, p. 16, and Myrow 1987). In addition, the section at Lewin's Cove is composed of many covered intervals (Fig. 59B and Gougeon *et al.* 2023) that are problematic because the stratal continuity and completeness of the section still remains to be demonstrated. Therefore, the interpretation of ecological and evolutionary implications of the low occurrence of *Curvolithus* and *Psammichnites* at Lewin's Cove are limited.

Evolutionary significance

Palaeoecological implications

In ichnology, tiering corresponds to the vertical partitioning of trace fossils within the substrate because of physical, chemical, and biological factors (Bromley & Ekdale 1986; Bromley 1996). The Chapel Island Formation hosts records of both relict and modern-style seafloors that can be broadly subdivided into three stratigraphic intervals: (1) a matground-dominated ecology of Ediacaran age; (2) a matground/firmground-dominated ecology of Fortunian age; and (3) a mixground-dominated ecology of Cambrian Age 2. These intervals depict a first stage of body-plan diversification at the base of the Fortunian, followed by a second stage of ecological re-structuring around the Fortunian–Cambrian Age 2 transition (Mángano & Buatois 2014, 2020; Gougeon *et al.* 2018a, 2025a).

During the Ediacaran, organism-substrate interactions in the Chapel Island Formation correspond to a matground ecology typifying the *Harlaniella podolica* Zone (Figs 56, 57, 58B, C, 61, 62). Trace fossils are rare and mostly surficial (*Archaeonassa fossulata*, *Circulichnis montanus*, *Helminthoidichnites tenuis*) or of very shallow-tier (*Palaeophycus tubularis*, *Torrowangea rosei*, *Treptichnus* indet.). Vertical bioturbation is negligible (BI = 0–1). Surficial bioturbation is low (BPBI = 1–2) and is restricted to local areas. The small width (0.1–0.2 cm) and negligeable depth of burrows (down to 0.2 cm) concur with low bioturbation intensities. Latest Ediacaran strata at Fortune Head (i.e. basal 2.4 m of Member 2) correspond to a transitional ecological step, with the first instances of distinct vertical disruption of sediment (*Gyrolithes gyratus*, *Treptichnus pedum*) in association with a simple horizontal trail (*Helminthopsis tenuis*) and slight increases in bioturbation intensities (BI =1, BPBI = 1–3). In this interval, overall trace-fossil diversity remains low (n = 3), further supporting the current understanding on trace-fossil biozonation in the Chapel Island Formation (Gougeon *et al.* 2023). Outcrop bias on trace-fossil datasets is negligeable, as both Grand Bank Head and Fortune Head, where most of the Ediacaran strata come from, are stepped sections (*sensu* Shillito & Davies 2020 and Shillito & Gougeon 2023) that display bed bases, bed tops, and vertical sections, with good lateral extensions of beds (Fig. 5; Gougeon *et al.* 2023).

A matground/firmground-dominated ecology was established during most of the Fortunian and has a stratigraphic range from the base of the *Treptichnus pedum* Ichno-Assemblage Zone to *ca.* 20 m below the top of Member 3 (Figs 56–59, 61, 62). This interval is marked by a sharp increase in trace-fossil diversity and the appearance of more complex tiering patterns. Surficial trails (*Archaeonassa fossulata*, *Circulichnis montanus*, *C. ligusticus*, *Cochlichnus anguineus*, *C. luguanensis*, *Gordia marina*, *Helminthoidichnites tenuis*, *Helminthopsis abeli*, *H. hieroglyphica*, and *H. tenuis*) are more diverse and demonstrate the persistence of a matground ecology within the earliest Cambrian (Buatois *et al.* 2014). In addition, scratch imprints (cf. *Allocotichnus dyeri*, *Dimorphichnus* isp. A, *Dimorphichnus* isp. B, *Monomorphichnus bilinearis*, *M. lineatus*, *M. needleiunm*, *Monomorphichnus* isp., *Rusophycus avalonensis*, *Rusophycus dabardae*, and *Rusophycus* isp.) represent surficial to very shallow-tier trace fossils made by arthropods first appearing within the *Treptichnus pedum* Ichno-Assemblage Zone, and later diversifying around the base of the *Rusophycus avalonensis* Ichno-Assemblage Zone (see Discussion, p. 166). In addition to surficial trace fossils, the firmground-dominated interval displays a burst in infaunal behaviours. Shallow-tier (*Bergaueria perata*, *B.* cf. *B. radiata*, *Conichnus conicus*, *Palaeophycus tubularis*) and mid-tier burrows (*Gyrolithes gyratus, G. scintillus*) reflect colonisation deeper into the substrate. Mid-tier *Teichichnus rectus* appears in abundance in red beds of basal Member 2B and is mostly restricted to a *ca.* 10 m interval that can be traced across sections at Fortune Head, Grand Bank Head, and Point May. Although *Trichichnus linearis* was recorded as penetrating as deep as 2.14 m in modern sediments (Weaver & Schultheiss 1983), Chapel Island Formation specimens only range down to 4.1 cm deep and *T. linearis* is therefore considered a mid-tier trace fossil herein. Larger, shallow-tier horizontal burrows (*Curvolithus multiplex*, *C. simplex*, *Curvolithus* isp., *Didymaulichnus miettensis*, *Psammichnites gigas circularis*, and *P.* cf. *P. saltensis*) represent the early settlement of sediment bulldozers mainly responsible for bioturbation of increased sediment volumes (BI = 1–4). Still, the substrate remained firm enough to preserve discrete burrows that did not completely disrupt the sedimentary fabric. Bedding plane bioturbation is highly variable (BPBI = 1–5) and fluctuates depending on environmental conditions (see next section).

A mixground-dominated ecology developed on the seafloor from *ca.* 20 m below the top of Member 3 up to the top of Member 5 (Figs 57, 58, 59A, 61, 62). Large shallow-tier burrows are common (*Curvolithus simplex*, *Didymaulichnus miettensis*, *Psammichnites gigas circularis*) and were made by organisms processing increased volumes of sediment. Hence, bioturbation intensities reach their highest values (BI = 4–6, BPBI = 4–5) suggesting that a modern-style sediment mixed layer was already emplaced (Gougeon *et al.* 2018a, 2025a). Surficial and shallow-tier trace fossils are barely preserved due to taphonomic controls and the soupy nature of the shallowest sediments. Mid-tier burrows emplaced deeper within the transitional layer (Berger *et al.* 1979; Savrda 2007) are discrete (*Teichichnus rectus*), typically overprinting a mottled fabric, and can encompass diagenetic processes that resulted in their pyritization (*Trichichnus linearis*). Finally, deeper tier structures are evidenced by the appearance of vertical structures made by detritus and suspension feeders (*Arenicolites* isp., ?*Diplocraterion* isp., *Rosselia erecta*, and *Rosselia* isp.) in the uppermost strata of Cambrian Age 2.

Environmental versus evolutionary controls

Assessing the influence of environmental controls on trace-fossil distribution across the Ediacaran–Cambrian boundary interval is instrumental to decipher early animal evolution (MacNaughton & Narbonne 1999; Shahkarami *et al.* 2017b; Gougeon *et al.* 2023, 2025a). In this study, we report fourteen sedimentary facies that correspond to deposition across intertidal and shallow-marine environments on the continental shelf. The sedimentary profile of the Chapel Island Formation is therefore composed of several subenvironments that are arranged as follow (Fig. 62, from proximal to distal deposits): (1) intertidal mud-flat (Facies A1); (2) intertidal mixed-flat (Facies A2); (3) intertidal sand-flat (Facies A3); (4) tide-dominated or -influenced embayment (Facies A4); (5) shallow-marine middle shoreface (Facies B1); (6) shallow-marine lower shoreface (Facies B2); (7) shallow-marine offshore transition (Facies C1); (8) shallow-marine upper offshore (Facies C2); (9) shallow-marine lower offshore (Facies C3); and (10) shelf (Facies D1, D2, and D3). In addition, carbonate beds found within Member 4 are less well-constrained spatially and correspond to shallow subtidal (Facies E1) and intertidal (Facies E2) settings. Shallow subtidal sediments are deposited above fair-weather wave base and are the lateral equivalent of the shoreface under wave-dominated conditions (Desjardins *et al.* 2010a, 2012). A time-environment matrix can be built after identification of stratigraphic units that are well-constrained using marker beds and member limits, and represent time intervals (Fig. 62). Due to the presence of offshore deposits in the latest Ediacaran and their importance in understanding the Ediacaran–Cambrian boundary interval, an

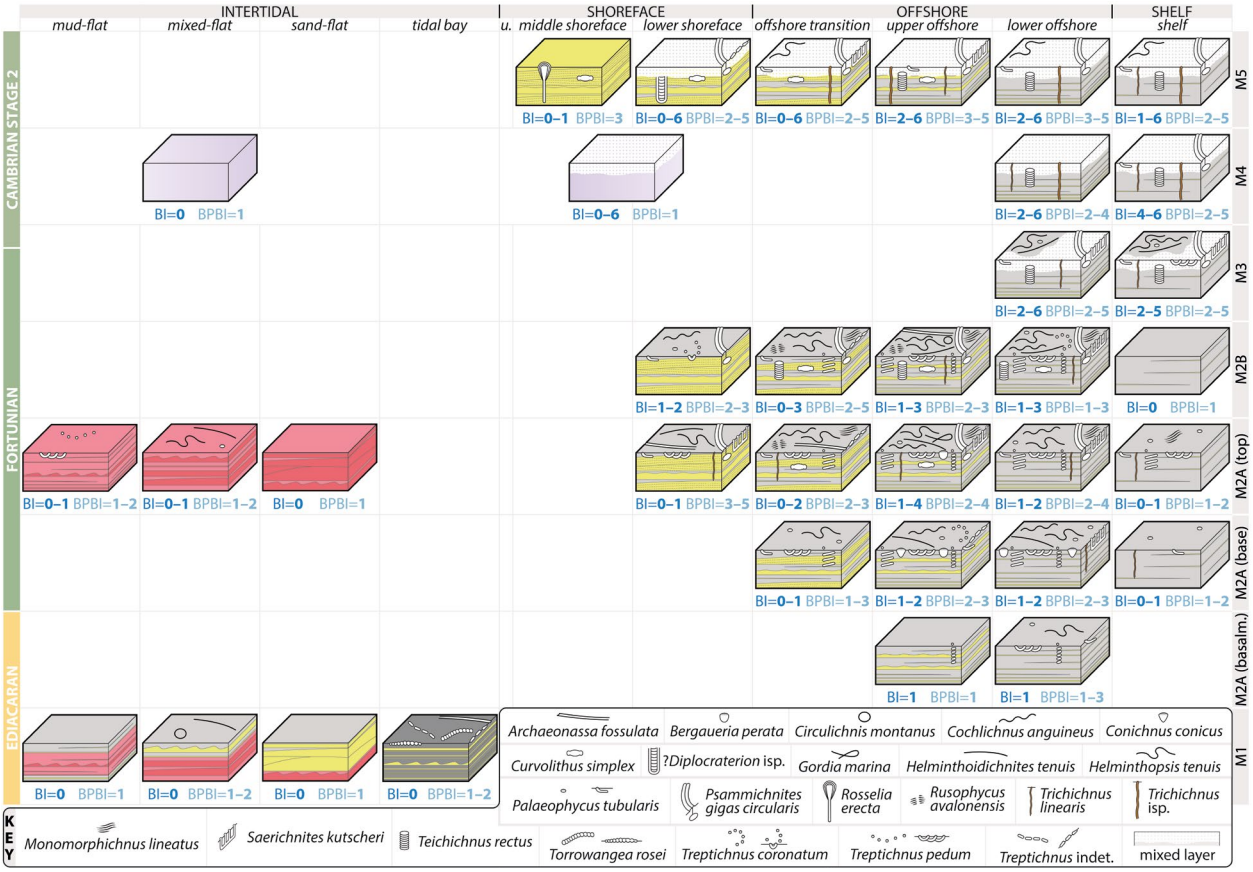

Fig. 62. Environmental controls on trace-fossil distribution, bioturbation intensities, tiering, and mixed layer development. Based on data from Grand Bank Head (lower Member 1), Fortune Head (upper Member 1 and Member 2), and Little Dantzic Cove (Members 3 to 5). For details on the Ediacaran–Cambrian boundary interval (i.e. Member 1 to basal Member 2A), see Figure 65 and figure 6 in Gougeon *et al.* (2023). Abbreviations: basalm., basalmost; BI, bioturbation index; BPBI, bedding plane bioturbation index; M1 to M5, Members 1 to 5 of the Chapel Island Formation; and u., upper shoreface.

additional uppermost Ediacaran time slice is added to the scheme (basal 2.4 m of Member 2 at Fortune Head, Fig. 62). This time-environment matrix allows tracking changes in bioturbation intensities, trace-fossil diversity, and tiering development through time and space (Fig. 62).

Several observations on environmental controls and evolutionary trends can be extracted from the time-environment matrix (Fig. 62). In intertidal settings, data from siliciclastic sedimentology is only available from two time slices but permit comparison between Ediacaran and Fortunian palaeoecology. Bioturbation intensities are in both cases low (BI = 0–1, BPBI = 1–2). Trace-fossil diversity is low as well. The limited colonisation of the intertidal area is explained by the variety of environmental stresses that characterise these settings, notably with salinity fluctuations and subaerial exposures affecting the physiology of soft-bodied organisms (Reise 1985; Mángano *et al.* 2002b). *Treptichnus pedum* is recorded in Fortunian mud-flat, which supports the idea that its tracemaker was euryhaline with a broad environmental tolerance, and it highlights the biostratigraphic soundness of this ichnotaxon (Buatois *et al.* 2013; Buatois 2018; Gougeon *et al.* 2023, 2025a). In shallow-marine environments, the dataset is more complete spatially and through time. Open marine environments are characterised by good oxygenation and food supply and low environmental stresses for organisms and represent ideal settings to track evolutionary changes. The Cambrian Global Stratotype Section and Point is located within a monofacial interval of open marine sedimentary beds without facies breaks, which were prerequisite conditions for its selection (Cowie *et al.* 1986; Remane *et al.* 1996). The base of the Fortunian is characterised by an increase in bioturbation intensities (BI = 0–2, BPBI = 1–3) and trace-fossil diversity in offshore transition to shelf subenvironments, supporting the idea that the birthplace of

behavioural evolutionary innovations is in offshore environments (Mángano & Buatois 2016; Buatois *et al.* 2020). Slightly higher in the Fortunian (i.e. the upper interval in Member 2A), trace fossils of the *Rusophycus avalonensis* Ichno-Assemblage Zone highlight the presence of arthropods (e.g. *Monomorphichnus lineatus*, *Rusophycus avalonensis*) and sediment bulldozers (e.g. *Curvolithus simplex*, *Psammichnites gigas circularis*) in lower shoreface to shelf settings. The time-environment matrix demonstrates that ichnodiversity remained high from the base to the middle of the Fortunian in lower shoreface to offshore environments, while data is scarcer on the shelf. The last major innovation depicted in the matrix (Fig. 62) is the increased seafloor colonisation by the late Fortunian onward, with the appearance of a sediment mixed layer (see next section) and mid- (*Arenicolites* isp., *Rosselia erecta*, *Rosselia* isp., *Teichichnus rectus*) and deep-tier (?*Diplocraterion* isp., *Trichichnus* isp.) trace fossils that are typical component of modern marine ichnocoenoses. The development of a mixed layer is first seen in lower offshore and shelf settings and is then observed landward, up to the lower shoreface (Fig. 62), but this trend may reflect the lack of appropriate facies lower in the succession rather than a true evolutionary signal (see also Gougeon *et al.* 2025a).

Mixed layer development

The sediment mixed layer is a zone of fully homogenized sediment resulting from intense bioturbation (Berger & Heath 1968; Berger *et al.* 1979). As a result of biological churning, burrow outlines are not visible, and sediment becomes softer with an increased water content (Berger *et al.* 1979; Ekdale *et al.* 1984). The mixed layer has been the focus of many studies because the few centimeters below the sediment-water interface host intense micro- and macro-biological interactions affecting the chemistry and physical properties of sediment (e.g. Aller 1978, 1982; Rhoads & Boyer 1982; Jones *et al.* 1994; Solan & Wigham 2005; Mermillod-Blondin & Rosenberg 2006; van de Velde & Meysman 2016; Riemer *et al.* 2023). Below the mixed layer, a zone made of compacted sediment delimits the transition layer (Berger *et al.* 1979; Savrda & Ozalas 1993). In that interval, discrete burrows and elite trace fossils (*sensu* Bromley 1996) form distinctive biogenic structures of maximum color contrast and sharp outlines that are more prone to be preserved in the geological record (Berger *et al.* 1979; Savrda *et al.* 1991). Lower bioturbation intensities in the transition layer result from the higher energetic costs required by organisms to burrow deeper (Jumars & Wheatcroft 1989), or simply from the lower oxygen supply and higher sulfide content characterising those sediments (Diaz & Rosenberg 1995; Glud 2008; D'Hondt *et al.* 2015). Below the reach of the deepest burrowers, the historical layer corresponds to relicts of previously established mixed and transition layers that can cross the fossilization barrier and be preserved in the geological record (Berger *et al.* 1979; Savrda *et al.* 1991; Savrda 2007).

Estimates on the mean depth of the sediment mixed layer (L) are debated and greatly vary depending on environmental and biological controls (Trauth *et al.* 1997; Teal *et al.* 2008; Solan *et al.* 2019; Song *et al.* 2022; Zhang *et al.* 2024; Buatois *et al.* 2025). Boudreau (1994) first suggested that $L = 9.8 \pm 4.5$ cm (with a dataset composed of n = 200+ records), based on tracer data compiled from the literature and covering marginal-, shallow-, and deep-marine sediments (see also Boudreau 1998). Boudreau (1994) notably called the attention on the fact that the mixing depth does not correspond to the maximum depth of an individual burrow, but instead to the thickness of the zone that is most thoroughly mixed biologically. That zone can be difficult to delineate either on tracer profiles or on box core photographs because the contact between mixed and transition layers can be gradual (i.e. with a 'mixed layer transition' interval *sensu* Berger *et al.* 1979 being more developed). In addition, Boudreau (1994) emphasized the limits related to the use of different tracers, with short-lived versus long-lived tracers giving different mixing depth values (see also Teal *et al.* 2008). The mixing depth value calculated by Boudreau (1994) was later contested. Trauth *et al.* (1997) noted that below 2500 m of water depth, the mixed layer depth correlates positively with organic carbon flux (see also Smith 1992 and Smith & Rabouille 2002; but see Miguez-Salas *et al.* 2024). Under eutrophic conditions, organic loading and oxygen stress result in lower abundance, size, and burrowing depth of the macrobenthos (Pearson & Rosenberg 1978; Diaz & Rosenberg 1995; Smith & Rabouille 2002). The species diversity, size of burrowing organisms, and composition of the macrobenthos also have impacts on burrowing intensities and the depth of the mixed layer (Thayer 1983; Smith & Rabouille 2002; Solan *et al.* 2004; Morys *et al.* 2016). Teal *et al.* (2008) also emphasized the role of seasons, water depths, and local, regional, and global disparities on mixed layer depths. Notably, Teal *et al.* (2008) recorded strong discrepancies between their Temperate South America ($L = 6.4 \pm 2.7$ cm) and their Temperate Domain ($L = 0.8 \pm 1.8$ cm). Teal *et al.* (2008) therefore expanded the database of Boudreau and estimated that $L = 5.75 \pm$

5.67 cm (n = 791) in marine environments and noted the lack of data in certain areas and the inconsistency of information provided in the literature (see also Teal *et al.* 2010). Recently, Zhang *et al.* (2024) updated these values and gave a range for *L* of 3.8–9.0 cm for the global ocean (n = 505), with the lower value representing the 25th percentile and the higher value the 75th percentile. These authors noted the similarities in *L* values for shallow- (*L* = 3.6–11.0 cm) and deep-marine (*L* = 3.8–8.0 cm) environments.

Different hypotheses have been proposed regarding the first appearance and thickness variation of the sediment mixed layer in the geological record. A pioneer work by Ausich & Bottjer (1982) tracked infaunal tiering in shallow-marine environments through the Phanerozoic and suggested that from the Cambrian to the Devonian, organisms colonised the first 6 cm of the sediment solely, until several groups of bivalves extended their burrowing depth down to 12 cm from the Devonian to the Permian (see also Bottjer & Ausich 1986). This led to some controversies as other authors recorded dense bioturbation 20 cm deep (Miller & Byers 1984) or deep-tier *Thalassinoides* (Sheehan & Schiefelbein 1984) in lower Palaeozoic strata. These early debates, however, did not deal with the development of the sediment mixed layer *per se*, as they were mostly focussed on the tiering structure and maximum depth of burrows rather than the appearance of biogenically churned sediments. Subsequently, Droser & Bottjer (1988) suggested that a significant increase in the depth of bioturbation took place at the Cambrian Stage 3 in shallow-marine carbonate offshore settings, in conjunction with a diversification of metazoans possessing skeletons (see also Bottjer & Droser 1994 and Droser & Li 1999). Seilacher & Pflüger (1994) proposed that mixgrounds – as opposed to matgrounds of the Ediacaran – first appeared at the beginning of the Cambrian with the advent of infaunal deposit feeding (see also Seilacher 1999). However, neither a definition of what mixground meant (i.e. massively bioturbated beds as suggested in the text, or deeper, local burrowing as suggested by Seilacher & Pflüger 1994, fig. 2), nor an actual thickness of those mixgrounds, were provided. Later, Mángano & Buatois (2014) suggested that maximum bioturbation intensities (i.e. BI = 6) appeared at the base of the Cambrian Stage 2 in offshore settings following a first step in animal behaviour diversification at the start of the Fortunian (see also Mángano & Buatois 2016, 2017, 2020). This conclusion was based on a literature search (60%), on material studied in museum collections (20%), and on direct observations in the field (20%), in a review of 369 stratigraphic units deposited in continental, marginal-, shallow-, and deep-marine settings. Tarhan *et al.* (2015), however, suggested that a sediment mixed layer similar to modern seafloors did not appear at least until the end of the Silurian (see also Tarhan & Droser 2014, Tarhan *et al.* 2014, and Tarhan 2018). This conclusion was based on sedimentological and ichnological field observations of 22 stratigraphic units displaying heterolithic bedding deposited in shallow-marine offshore settings and was focussed on six proxies: (1) bedding thickness; (2) fabric disruption; (3) depth of bioturbation; (4) bioglyph preservation; (5) palaeobiological and palaeoecological complexity; and (6) physical sedimentary structures (see Tarhan *et al.* 2015 for further explanations). However, this latter approach presents conceptual and methodological flaws that were already discussed at length in Mángano & Buatois (2016, 2017, 2020), Gougeon *et al.* (2018a), and Gougeon (2023).

Tracking the mixed layer in deep time should be done on a broad range of depositional settings, at the finest scale possible (i.e. by comparing sub-environments). Modern mixed layers can develop in continental, marginal-marine, shallow-marine, and deep-marine settings, with highly variable mixing depths (Boudreau 1994; Teal *et al.* 2008; Solan *et al.* 2019), and this was also the case in deep time (Mángano & Buatois 2016; Ichaso *et al.* 2022; Ahmad *et al.* 2024). In the Chapel Island Formation, thick and homogeneous intervals of sediment comparable to a mixed layer texture are observed from the uppermost Fortunian to Cambrian Stage 2, first in shelf and lower offshore (Members 3 and 4), and later in upper offshore, offshore transition, and lower shoreface as well (Fig. 62 and Gougeon *et al.* 2025a). Polished samples were presented in Gougeon *et al.* (2018a) and support these conclusions by showing that mid- and deep-tier trace fossils emplaced in a transition layer, notably *Teichichnus rectus*, cross-cut undifferentiated mottling typifying previously buried mixed layers. In addition, thin sections from upper Fortunian and Cambrian Age 2 lower offshore and shelf evidence the poor sorting of fine, medium, and coarse mudstone grains as a result of biomixing (Figs 17, 63). A mixed layer is also evidenced in offshore tempestites of Member 5 (Fig. 64). There, fine-grained sandstone beds commonly display parallel lamination with sharp erosive bases. Their bed tops are diffuse and irregular in shape, and are followed by a thick interval of structureless, homogeneous sandy mudstone sediment. A key feature is the presence of mid-tier *Teichichnus rectus* and shallow-tier *Palaeophycus tubularis* burrows emplaced within the sandstone tempestite, demonstrating that the above homogeneous interval was, at some point in time, fully churned

and soupy. In thin section, thick sandy mudstone intervals are poorly sorted and reminiscent of intervals observed within Members 3 and 4 where mottling was identified from field observations, polished samples, and thin section analyses. In places, sandstone-filled *Palaeophycus tubularis* burrows were also recovered within the upper part of sandy mudstone intervals. These observations closely follow the idea advocated by Savrda (2007) that states that increased color contrast (light-colored fine-grained sandstone versus dark-colored sandy mudstone) demonstrates alternation in sediment deposition preserving shallow mixed layers that are later crosscut by deeper burrows of the transitional layer filled with sediment of a different composition and experiencing different diagenetic histories. These observations provide further support to the appearance of a sediment mixed layer early in the Phanerozoic, close to the base of the Cambrian Stage 2 (Mángano & Buatois 2014, 2016, 2017, 2020; Gougeon *et al.* 2018a, 2025a).

The role of *Psammichnites gigas circularis* and other sediment bulldozers in the improvement in overall sediment mixing was recognised early by Seilacher (1997b). Thayer (1979, 1983) noted that large deposit-feeders occurring in dense populations would have been more prone to process increased volumes of sediment and would have had a negative impact on immobile suspension-feeders. Organisms responsible for sediment bulldozing are recognised in the early Cambrian trace-fossil record as *Curvolithus*, *Didymaulichnus*, and *Psammichnites* (Droser *et al.* 1999; Mángano & Buatois 2017, 2020). In the Chapel Island Formation, the three ichnotaxa appear within the *Rusophycus avalonensis* Ichnoassemblage Zone: (1) *Curvolithus simplex* is first recorded 123.2 m above the base of Member 2 at Fortune Head, first noted in offshore transition and upper offshore and later appearing in lower offshore as well (Fig. 62); (2) *Didymaulichnus miettensis* is first recorded 244.5 m above the base of Member 2 at Fortune Head in offshore transition and upper offshore; and (3) *Psammichnites gigas circularis* is first recorded 152.7 m above the base of Member 2 at Fortune Head, first in lower shoreface, upper

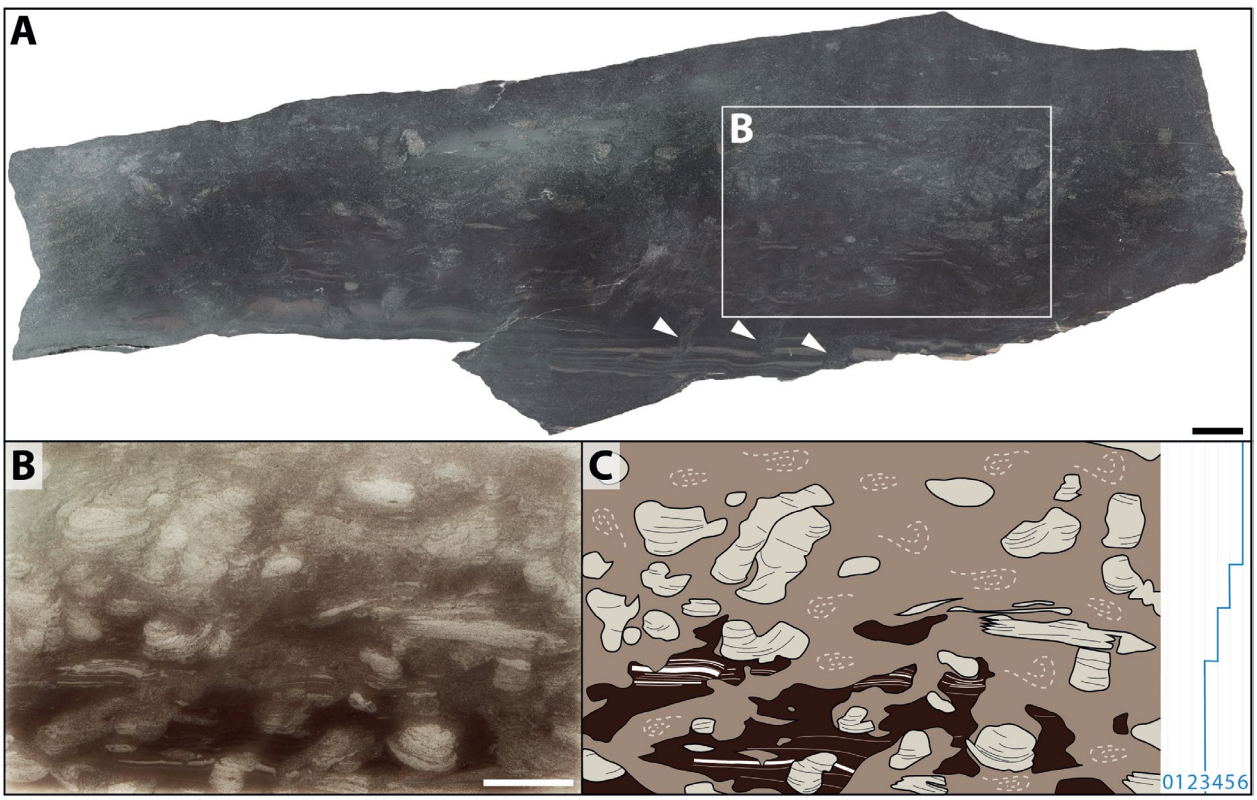

Fig. 63. Mixed layer development in lower offshore of Member 3. Scale bars are 1 cm. **A**, Polished sample from Little Dantzic Cove (LDC 95.7). Note remnant lamination crosscut by burrows with sharp burrow margins (arrows). **B**, Thin section of the same sample. Note abundant *Teichichnus rectus*. **C**, Interpretative sketch of Figure 63B, highlighting: (1) well-preserved patches of undisrupted mudstone at the base (dark red) with remnant lamination, in places crosscut by discrete *Teichichnus rectus* (i.e. transitional layer); and (2) homogenized mudstone and sandstone at center and top (i.e. mixed layer). Bioturbation index is indicated on the right.

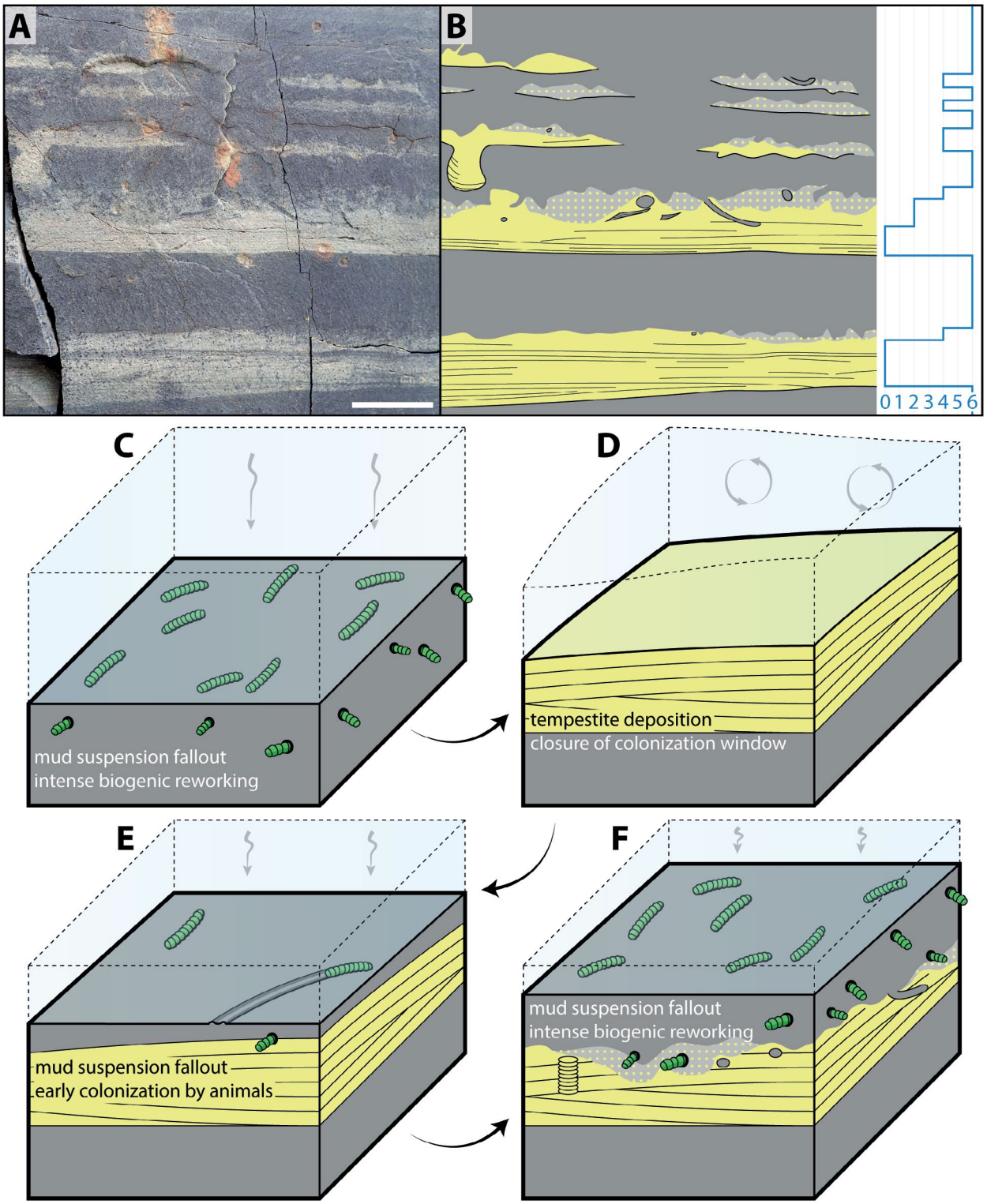

Fig. 64. Mixed layer development in offshore transition of Member 5. Scale bar is 5 cm. **A**, Field photograph of heterolithic fine-grained sandstone (yellow) and sandy mudstone (dark grey). **B**, Interpretative sketch of Figure 64A, highlighting diffuse tops and burrows with sharp margins. Bioturbation index is indicated on the right. **C–F**, Taphonomic pathway explaining Figure 64A. A period of weak energetic conditions allows mud deposition and intense biogenic reworking by deposit feeders, resulting in the development of a homogeneous mixed layer (**C**). A storm deposit (sandy tempestite with hummocky cross-stratification) prevents biogenic activity (**D**). The return to calm conditions provides a window for re-colonization of the seafloor (**E**). With the continuous settlement of mud on the seafloor by suspension fallout highlighting calm conditions, deposit feeders were able to totally disrupt both the shallowest mud blanket and the deeper sand layer (**F**). Note that a shallow mixed layer is capping a deeper transitional layer hosting sharp-walled burrows in **F**.

offshore, and lower offshore, and later expanding into offshore transition and shelf (Fig. 62). *Curvolithus simplex* is 0.5–1.3 cm wide, is moderately common (about 55 specimens were found in the Chapel Island Formation) and is recovered in low abundance on bed surfaces. In Member 5 at Grand Bank Head, however, some bed bases display moderate abundances of *Curvolithus simplex* (BPBI = 3). Therefore, its potential for processing volumetric amounts of sediment went from low to moderate in the succession. *Didymaulichnus miettensis* is 0.2–1.4 cm wide and is moderately recorded (about 60 specimens were found in the Chapel Island Formation). It is first recovered in low abundance in Member 2 but becomes more densely aggregated in Member 5 on bed surfaces at Grand Bank Head and Fortune North (BPBI = 4–5) where lower shoreface conditions dominate. Its potential for sediment processing went from low to moderate in the succession. *Psammichnites gigas circularis* is 0.5–4.5 cm wide and is commonly recorded (about 170 specimens were found in the Chapel Island Formation). It is first noted in low to moderate abundance in Member 2 but becomes very common in Member 3 on bed surfaces at Little Dantzic Cove (BPBI = 4–5). Therefore, *Psammichnites gigas circularis* has a moderate to high potential in sediment reworking in the succession. All three trace fossils appeared during the middle Fortunian, as part of a second phase in animal behaviour diversification (i.e. in the *Rusophycus avalonensis* Ichno-Assemblage Zone). However, only *Psammichnites gigas circularis*, with its overall larger size and increased abundance in the succession, became instrumental in the development of mixgrounds during the late Fortunian. This ichnotaxon is suspected to be one of the main driving forces in the establishment of a mixed layer by Cambrian Age 2, as its producer processed increased volumes of sediment in the shallow-tier, aiding in the development of an infaunal partitioning of the substrate by favoring the formation of mid-tier (*Arenicolites* isp., *Rosselia erecta*, *Rosselia* isp., and *Teichichnus rectus*) and deep-tier (?*Diplocraterion* isp., *Trichichnus* isp.) structures that are commonly found in Phanerozoic and modern ichnofabrics (cf. Berger *et al.* 1979; Ekdale *et al.* 1984; Savrda *et al.* 1991).

Discussion

Revision of the Global Stratotype Section and Point at Fortune Head

Narbonne *et al.* (1987, fig. 5) provided a summary of trace-fossil distribution across the Ediacaran–Cambrian boundary interval at Fortune Head that was instrumental in the decision of the International Union of Geological Sciences and the International Commission on Stratigraphy on the Cambrian Global Stratotype Section and Point. This diagram depicted the appearance of fourteen trace fossils and vendotaenid body fossils along a stratigraphical interval *ca.* 20 m thick. It was frequently reproduced with minor modifications in later papers following the ratification of the Global Stratotype Section and Point at Fortune Head: ?*Gyrolithes* isp. was added in Landing *et al.* (1988); *Sabellidites cambriensis* was added in Brasier *et al.* (1994a); and *Helminthoidichnites tenuis* was added, and *Phycodes pedum* was replaced for *Trichophycus pedum*, in Landing & Westrop (1998). Gehling *et al.* (2001, fig. 1) updated the diagram by adding information from a *ca.* 12 m-thick interval emplaced below the section studied in Narbonne *et al.* (1987), that is separated by a fault. Some ichnotaxonomic revisions were implemented: *Phycodes pedum* was replaced for *Treptichnus (Phycodes) pedum*, and *Gyrolithes polonicus* was recorded. Importantly, *Treptichnus pedum* was found 3.11 and 4.41 m below the Global Stratotype Section and Point, *Skolithos annulatus* and *Gyrolithes polonicus* 2.51 m below the Global Stratotype Section and Point, and *Treptichnus* isp. *ca.* 7, 11, and 13 m below the Global Stratotype Section and Point. More recent diagrams covering this stratigraphic interval (Peng *et al.* 2012, 2020; Babcock *et al.* 2014) mainly resulted from the combination of data coming from Narbonne *et al.* (1987) and Gehling *et al.* (2001). Landing *et al.* (2017, fig. 18) offered an alternative version of the diagram based on work in progress from our research group.

We provide here a revision of sedimentological and ichnological datasets from a 34.1 m interval covering the Global Stratotype Section and Point at Fortune Head (Fig. 65). In addition to the stratigraphic position of trace fossils, the type of outcrop exposure, maximum bioturbation index, maximum bedding plane bioturbation index, maximum burrow width, maximum burrow depth, ichnodiversity, and ichnodisparity are plotted (Fig. 65). Taxonomic revisions are implemented, notably the report of *Harlaniella podolica* and *Palaeopascichnus delicatus* as body fossils which are both restricted to the Ediacaran. Trace-fossil diversity and disparity increase drastically over a 14.0 m interval; contrary to ichnodiversity, the ichnodisparity curve remains mostly stable for the rest of the *Treptichnus pedum* Ichno-Assemblage Zone (see Fig. 56 and Gougeon *et al.* 2023, fig. 3c). Another important element of the revised diagram is the development of slightly higher bioturbation intensities (BI = 2) just above the Global Stratotype Section and Point, which is typical of the Fortunian and coincides with data from other Chapel Island Formation

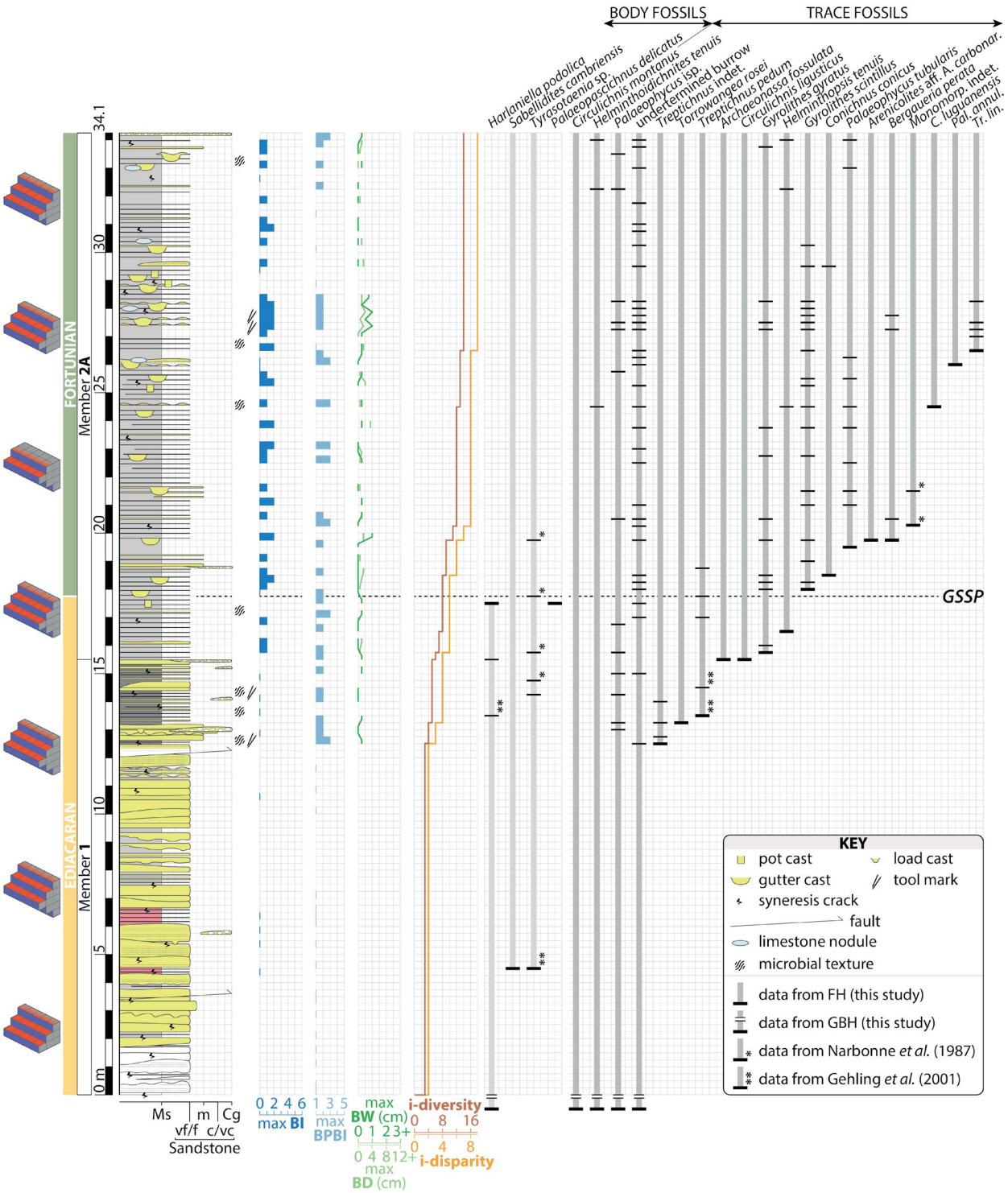

Fig. 65. Detailed distribution of fossils across the Ediacaran–Cambrian boundary interval at Fortune Head. From left to right: type of outcrop exposure (recorded every 5 m); age; member; sedimentary log (in meters); maximum bioturbation index (BI); maximum bedding plane bioturbation index (BPBI); maximum burrow width (BW); maximum burrow depth (BD); ichnodiversity (i-diversity) and ichnodisparity (i-disparity); stratigraphic position of body fossils; and stratigraphic position of trace fossils. Abbreviations: Ms, medium mudstone; vf/f, m, c/vc Sandstone, very fine-/fine-grained, medium-grained, coarse-/very coarse-grained sandstone; Cg, conglomerate; FH, Fortune Head; GBH, Grand Bank Head; *Arenicolites* aff. *A. carbonar.*, *Arenicolites* aff. *A. carbonarius*; *C. luguanensis*, *Cochlichnus luguanensis*; *Monomorp.* indet., *Monomorphichnus* indet.; *Pal. annul.*, *Palaeophycus annulatus*; and *Tr. lin.*, *Trichichnus linearis*.

sections (Gougeon *et al.* 2023). The appearance of novel behavioural strategies just below (*Gyrolithes gyratus*) and above the Global Stratotype Section and Point (*Arenicolites* aff. *A. carbonarius*, *Bergaueria perata*, *Conichnus conicus*, and *G. scintillus*) reflect the onset of vertical bioturbation (maximum depth of 3.5 cm for *G. gyratus*). Below the Global Stratotype Section and Point, trace fossils of the *Harlaniella podolica* Zone are mostly simple (*Archaeonassa fossulata*, *Circulichnis montanus*, *Helminthoidichnites tenuis*, and *Torrowangea rosei*). *Treptichnus pedum* is recorded in the latest Ediacaran and represents a more complex behaviour, and its presence below the Global Stratotype Section and Point can be explained by confidence interval related to first appearance datum (Landing *et al.* 2013; Gougeon *et al.* 2023). *Treptichnus* isp. recorded by Gehling *et al.* (2001) 11 and 13 m below the Global Stratotype Section and Point are in an interval with abundant syneresis cracks. The apparent similarity of *Treptichnus* isp. as figured by these authors and syneresis cracks observed in the field during our study did not support their biogenic affinity. Overall, our analysis reinforces conclusions by previous authors in that this interval records a burst in animal behavioural strategies, which is accompanied by increases in depth and intensity of bioturbation.

Issues related to the Cambrian Global Stratotype Section and Point and relevance of this study

After the decision to use trace fossils as index fossils for the basal Cambrian, concerns were raised among some researchers (Fåhræus 1994; Zhu 1997; Qian *et al.* 2002; Zhu *et al.* 2006, 2019; Peng & Babcock 2011; Babcock *et al.* 2014; Walde *et al.* 2015; Smith *et al.* 2016a; Topper *et al.* 2022). Fåhræus (1994, pp. 5, 6) first criticized the decision and listed ten points of contention: (1) the boundary is based on trace fossils; (2) the biological affinity of *Treptichnus pedum* tracemaker is unknown; (3) *T. pedum* is only morphologically distinctive at ichnogenus or ichnospecies level; (4) *T. pedum* follows the last occurrence datum of *Harlaniella podolica*, a fossil of unknown biological affinity with poor distinctive morphological features; (5) both *H. podolica* and *T. pedum* suffer facies control; (6) *H. podolica* is sensitive to sea level changes; (7) both *H. podolica* and *T. pedum* suffer provincialism; (8) there are major unconformities below and above the Global Stratotype Section and Point; (9) radiometric dating is not possible in the section; and (10) carbon and sulfur isotopes have been altered by heating following rock deposition, and cannot be studied in the section. Fåhræus (1994) also emphasized an additional point that was reiterated by Babcock *et al.* (2014) and Zhu *et al.* (2019), which is that (11) trace fossils and the first appearance datum of *Treptichnus pedum* are diachronic across the Ediacaran–Cambrian boundary interval in successions worldwide. Some of these points still echo strongly among the scientific community (e.g. Babcock *et al.* 2014; Zhu *et al.* 2019; Topper *et al.* 2022). Moreover, Babcock *et al.* (2014) and Zhu *et al.* (2019) suggested additional points of contention: (12) the taxonomic status of *Treptichnus pedum* is unresolved among specialists; (13) *T. pedum* was recovered below the Global Stratotype Section and Point at Fortune Head; (14) the exact definition of the Global Stratotype Section and Point is ambiguous and changed over time; (15) the behaviour associated with *T. pedum* may have arisen multiple times in different groups of organisms; and (16) the exact behaviour involved in *T. pedum* is ambiguous and may not represent true vertical bioturbation. We will demonstrate below that all these arguments are unsound, have been tackled repeatidly over the last decades, and can be updated following recent advances in scientific knowledge.

Fåhræus (1994) indicated that the decision to select a trace fossil as index fossil was problematic because trace fossils depend on ecology, taphonomy, and net rates of rock accumulation. Previous authors (Rozanov 1967; Cowie & Glaessner 1975; Sepkoski & Knoll 1983; Conway Morris 1987; Brasier *et al.* 1994a) overall agreed that the base of the Cambrian and of the Phanerozoic was to be placed in an interval above fossils of the Ediacara Biota and below the oldest trilobites. At the time, two proxies were considered good candidates to help delineate the base of the Cambrian: (1) trace fossils, which are mostly recorded from siliciclastic settings; and (2) small shelly fossils, which are mostly recorded from carbonate settings. Later, other researchers used (3) acritarchs and (4) the Basal Cambrian $\delta^{13}C$ Excursion as secondary proxies in sections lacking good trace fossil or small shelly fossil datasets. Each of these proxies suffer in various ways from facies control, provincialism, taphonomy, or other constraints that have been discussed at length in the literature already (e.g. Brasier 1989; Brasier *et al.* 1994b; Landing *et al.* 2013; Geyer & Landing 2016; Zhu *et al.* 2019; Steiner *et al.* 2020). However, the Precambrian–Cambrian Boundary Working Group of the International Commission on Stratigraphy emphasized that about 70% of the stratigraphic record across the Ediacaran–Cambrian boundary

interval was composed of siliciclastic sedimentary rocks (Rozanov 1984; Cowie 1989, 1992; Brasier *et al.* 1994a). Siliciclastic and mixed carbonate-siliciclastic successions are particularly useful for delineating parasequences, deciphering basin architecture and understanding diachronism in fossil distribution, whereas carbonate successions are subject to develop condensed intervals, complicating the evaluation of facies controls (Buatois 2018; Shahkarami *et al.* 2020). Therefore, trace fossils represent the best candidates to delineate the base of the Cambrian in thick and continuous successions, where high rates of sediment accumulation and vertical repetition of similar sedimentary environments allow the finest understanding of animal evolutionary trends.

Fåhræus (1994) suggested that the origin of the *Treptichnus pedum* tracemaker was unknown at phylum level, and could only be speculated to be a Protostomia coelomate organisms (i.e. clade level) at best (see also Conway Morris 1987 and Babcock *et al.* 2014). Although the identity of the producer is irrelevant for its use in biostratigraphy, there has been significant progress on this front during the last fifteen years. Subsequent studies revealed that priapulid-like scalidophoran worms were most likely producing Cambrian *Treptichnus pedum* (Vannier *et al.* 2010; Kesidis *et al.* 2019b; Turk *et al.* 2024a), which makes it the oldest fossil record of Ecdysozoa (Edgecombe 2020). Priapulid worms are a phylum of nineteen species of deposit-feeders and carnivores, which are common in Cambrian lagerstätten (Vannier 2012; Ma *et al.* 2014; Smith *et al.* 2015). Their circular, longitudinal, and retractor muscles allow the contraction and eversion of a frontal proboscis through peristaltic cycles (Vannier *et al.* 2010; Ma *et al.* 2014). Notably, a characteristic club-shaped inflation favors changes of direction of the organism at every cycle (Vannier *et al.* 2010). The resultant burrow is composed of individual segments repeated one after the other and oriented at 20–40°, forming an overall straight, curved, or looped course, a morphology reminiscent of *Treptichnus bifurcus*, *T. pedum*, and *T. rectangularis* (Vannier *et al.* 2010). Furthermore, modern extent priapulid worms possess longitudinal rows of conical sensory papillae (i.e. scalids) on their proboscis that were demonstrated to finely print the outer surfaces of their burrows (Kesidis *et al.* 2019b). Fine longitudinal and circular striae were also observed on segments of *Treptichnus* burrows (e.g. Turk *et al.* 2024b), matching modern observations on scalidophoran worms (Vannier *et al.* 2010; Kesidis *et al.* 2019b; Turk *et al.* 2024a). Additionally, scalids and teeth of those worms were discovered as small shelly fossils in lower Cambrian strata associated with *Treptichnus* (Kesidis *et al.* 2019b). Furthermore, Babcock *et al.* (2014) added that tracemakers of other trace fossils of the *Treptichnus pedum* Ichno-Assemblage Zone were uncertain. However, there are clear examples where organisms can be confidently assigned to ichnogenera at phylum level: (1) *Bergaueria*, made by cnidarians (Ansell & Trueman 1968; Seilacher-Drexler & Seilacher 1999); (2) *Cochlichnus*, made by nematode worms (Sandstedt *et al.* 1961; Jensen 1996); (3) *Conichnus*, made by cnidarians (Shinn 1968; Gingras *et al.* 2008); and (4) *Dimorphichnus* and *Monomorphichnus*, made by euarthropods (see Discussion, p. 166). Cambrian *Gyrolithes* can also be attributed to enteropneusts (order level; van der Horst 1934; Gingras *et al.* 1999) or annelid worms (phylum level; Hertweck & Reineck 1966; Powell 1977), as crustaceans producing these burrows later in the Phanerozoic (see *Gyrolithes* section, p. 88) were not present in the Fortunian.

Fåhræus (1994) stated that *Treptichnus pedum* was only distinctive at ichnogenus or ichnospecies level. In fact, *Treptichnus pedum* is discriminated from simpler forms identified as *Treptichnus* isp. based on the segment morphology, their orientation and organization, the irregularity in distance between each segment, and the tendency for segments to align (Jensen *et al.* 2000). Therefore, a behavioural continuum is invoked explaining first the appearance of *Treptichnus* isp. in the latest Ediacaran, followed by the appearance of *Treptichnus pedum* (and other *Treptichnus* ichnospecies) in the earliest Cambrian (Jensen 2003; Buatois & Mángano 2011). The distinctive morphology of *Treptichnus pedum* at ichnospecies level is necessary to establish the clear comparison and identification of conspecific materials recorded worldwide and to make it valuable as a robust index fossil.

Harlaniella podolica was considered of unknown origin and having poor morphological features by Fåhræus (1994). The morphology of *Harlaniella podolica*, albeit simple, is however distinctive, with oblique regular segments added along an elongated body, in places displaying dichotomous branching (Kir'yanov 1968; Sokolov 1972; Ivantsov 2013). Due to the peculiar orientation of the segments, Jensen (2003) suggested that *Harlaniella podolica* could not represent a helical trace fossil as it was first suspected (Kir'yanov 1968; Crimes 1987), but that it was a body fossil. Both *Harlaniella podolica* and *H. ingriana* Ivantsov, a second species with longitudinal striae, have restricted stratigraphic ranges within the upper Ediacaran and have been recorded confidently from Canada (Narbonne *et al.* 1987; this study), Norway (Liu & McIlroy 2015; McIlroy & Brasier 2017; Meinhold *et al.* 2022), Russia (Sokolov 1972; Palij *et al.*

1979, 1983; Jensen 2003; Ivantsov 2013) Saudi Arabia (Vickers-Rich *et al.* 2013; Cui *et al.* 2020), and Ukraine (Kir'yanov 1968; Palij 1976; Palij *et al.* 1983; Ivantsov 2013; Ivantsov *et al.* 2015), and possibly from Poland (Pacześna 1985, 1986, 1996, 2010), South Africa (Nelson *et al.* 2022), and Sweden (Moczydlowska *et al.* 2001). A third species, *Harlaniella confusa* Signor, 1994, is a very distinctive tubular fossil reminiscent of body fossils recovered in coeval strata (Corsetti & Hagadorn 2003; Smith *et al.* 2016b) and is unrelated to *H. podolica* or *H. ingriana*. Ivantsov (2013) suggested that *Harlaniella podolica* and *H. ingriana* represented internal casts and impressions of tubes of algal origin. More importantly, *Harlaniella podolica* is recorded in association with *Palaeopascichnus delicatus* just below the Global Stratotype Section and Point at Fortune Head (Fig. 65). Both fossils were also found in association in Ukraine and Norway (Palij 1976; Jensen 2003; McIlroy & Brasier 2017). *Palaeopascichnus* Palij is regarded as an Ediacaran index fossil of worldwide distribution (Jensen *et al.* 2018b; Kolesnikov *et al.* 2018; Xiao & Narbonne 2020; Hawco *et al.* 2021; Kolesnikov & Desiatkin 2022). *Palaeopascichnus* shares strong similarities with modern multichambered xenophyophores (Seilacher *et al.* 2003; Antcliffe *et al.* 2011; Kolesnikov *et al.* 2018; Hawco *et al.* 2021).

Facies control on trace fossils is an argument commonly raised against the current definition of the Cambrian Global Stratotype Section and Point (Fåhræus 1994; Babcock *et al.* 2014; Topper *et al.* 2022; see also Buatois 2018 for discussion). In fact, facies control affects both trace and body fossils (Geyer 2005; Zhu *et al.* 2019; Steiner *et al.* 2020) and is one of the reasons explaining the non-selection of small shelly fossils as index fossils for the basal Cambrian in the 1980's (the other major reason being their provincialism) (Cowie 1989, 1992; Brasier *et al.* 1994a). The type of sedimentary rocks sampled also impacts on geochemical studies and the reliability of the Basal Cambrian $\delta^{13}C$ Excursion (Brasier *et al.* 1992; Steiner *et al.* 2020; Topper *et al.* 2022). In trace-fossil studies, environmental controls can be deciphered through detailed sedimentological work. In fact, ichnological data is typically framed within high-resolution facies information (e.g. Frey & Pemberton 1987; MacEachern & Pemberton 1992; Pemberton *et al.* 1992; Mángano *et al.* 2002b; MacEachern & Gingras 2007; Desjardins *et al.* 2012; Dasgupta *et al.* 2016; Gingras *et al.* 2016; Buatois *et al.* 2019; Paz *et al.* 2019, 2022; Melnyk & Gingras 2020; Gougeon *et al.* 2025a, this study). In this regard, ichnological analysis is particularly suited to discriminate between evolutionary and evolutionary controls, in some cases with the aid of time-environment matrices (Bottjer *et al.* 1988; Droser & Bottjer 1988, 1993; MacNaughton & Narbonne 1999; Shahkarami *et al.* 2017b; Buatois *et al.* 2020; Mángano *et al.* 2021; Gougeon *et al.* 2025a, this study). Therefore, macro-evolutionary trends can be understood by looking at changes in trace-fossil assemblages taking place in stacked parasequences that allow the comparison of recurrent depositional environments in thick and well-exposed successions (Buatois 2018). Broad palaeoecological conclusions on facies versus evolutionary controls are presented herein for the Chapel Island Formation (see Fig. 62 and 'Evolutionary significance' section, p. 152). *Treptichnus pedum* has been shown to be present in marginal-, shallow-marine and possibly deep-marine settings, demonstrating its broad environmental tolerance (Geyer & Uchman 1995; MacNaughton & Narbonne 1999; Buatois *et al.* 2013; Buatois 2018; Gougeon *et al.* 2023, 2025a, this study). Furthermore, Babcock *et al.* (2014) noted that *Treptichnus pedum* was not confidently identified in Russian successions, which are dominantly made of carbonate rocks (see also Topper *et al.* 2022). However, *Treptichnus pedum* has been recorded in mixed carbonate-siliciclastic intervals of the Syhargalakh Formation (lower part of the Kessyusa Group) (Dzik 2005; Grazhdankin *et al.* 2008, 2020a, b; Nagovitsin *et al.* 2015; Rogov *et al.* 2015), in sandy dolostone of the Irkut Formation (Marusin *et al.* 2021) and the Ostrovnoy Formation (Marusin *et al.* 2023), in mudstone-sandstone of the Ust'-Tagul Formation (Marusin *et al.* 2025), and in dolostone-marlstone of the Nokhtuisk Formation (Kolesnikov *et al.* 2023c). Fåhræus (1994) also mentioned a facies control and sensitivity to sea level changes with *Harlaniella podolica*. *Harlaniella podolica* was previously recorded both from marginal-marine (Narbonne *et al.* 1987; this study) and shallow-marine settings (Narbonne *et al.* 1987; Ivantsov 2013; this study), which is an environmental tolerance typically regarded as sufficient for biostratigraphic markers (cf. Cowie 1989; Peng *et al.* 2020). In addition, Kolesnikov & Desiatkin (2022) recently documented the broad marginal-, shallow- and deep-marine environmental tolerance of *Palaeopascichnus*, which is preserved both in siliciclastic and carbonate facies (*contra* Topper *et al.* 2022).

Fåhræus (1994) suggested that both *Harlaniella podolica* and *Treptichnus pedum* suffered provincialism, and Zhu *et al.* (2019) and Topper *et al.* (2022) added that *Palaeopascichnus* had a limited geographic distribution. Both *Harlaniella podolica* (see above) and *Treptichnus pedum* (see *T. pedum* section, p. 135) have worldwide distributions, and *T. pedum* is a common fossil of lower Cambrian strata (Geyer & Uchman 1995; Vannier *et al.* 2010; Sharma *et al.*

2018b). Kolesnikov & Desiatkin (2022) extensively reviewed material of *Palaeopascichnus* and noted that it was recorded from Avalonia, Baltica, Siberia, South China, and Australia, demonstrating its worldwide distribution.

Fåhræus (1994) invoked major unconformities below and above the Global Stratotype Section and Point. In fact, the unconformity below is not located within the Chapel Island Formation, but between the Marystown Group and the Rencontre Formation (Landing 1996a, b; Fig. 3A). The Rencontre Formation is *ca.* 1030 m thick (Smith & Hiscott 1984), which means that this unconformity is located *ca.* 1210 m below the Global Stratotype Section and Point. The major unconformity above the Global Stratotype Section and Point invoked by Fåhræus (1994) is the boundary between the Random and Brigus formations, the latter hosting trilobites, located *ca.* 1005 m above the position of the Cambrian Global Stratotype Section and Point (Hiscott 1982; Myrow 1987; Landing *et al.* 2013, 2022). Therefore, at Burin Peninsula, *ca.* 2215 m of strata spanning the late Ediacaran to early Cambrian are exposed without major break of sedimentation. Babcock *et al.* (2014) further emphasized that a fault was present 6.5 m below the Global Stratotype Section and Point (see also Conway Morris 1987 and Fig. 65). This fault was previously discussed by Gehling *et al.* (2001), who suggested that the displacement along the fault was minor; this is also corroborated by observations and measurements from coeval strata at Grand Bank Head (Myrow 1987). Shahkarami *et al.* (2020) recently demonstrated that minor unconformities are present in most sections spanning the Ediacaran–Cambrian boundary interval worldwide.

Fåhræus (1994) mentioned that radiometric dating was not doable in the Global Stratotype Section and Point section. So far, radiometric dating used to bind the Chapel Island Formation chronostratigraphically are (Fig. 3A): (1) a 552 ± 3 Ma date from volcanic rocks of the Long Harbour Group in direct contact with the Rencontre Formation in northern Fortune Bay (O'Brien *et al.* 1995); (2) a 565 ± 26 Ma date on K-Ar within the Rencontre Formation (King 1982); and (3) a 530.02 ± 1.07 Ma date from volcanic ash (Isachsen *et al.* 1994, later corrected by Schmitz 2012, 2020; see also Compston *et al.* 2008) in a bed from New Brunswick suspected to be coeval with the upper part of Member 5 at Burin Peninsula (Landing *et al.* 2013; but see Barr *et al.* 2023 and 'Regional and stratigraphic framework' section, p. 7). Moreover, several researchers (e.g. Brasier *et al.* 1992; Fåhræus 1994; Babcock *et al.* 2014; Zhu *et al.* 2019) advocated for the need to provide non-biostratigraphic data from the Global Stratotype Section and Point to offer secondary correlation tools. Brasier & Cowie (1989) recorded the presence of low-grade metamorphism in the Chapel Island Formation which is problematic for magnetostratigraphic and geochronometric studies. Brasier *et al.* (1992) provided data on $\delta^{13}C$ and $\delta^{18}O$ from Members 3 and 4 at Little Dantzic Cove. These authors attempted a correlation of the carbon isotope record from Avalonia with the Siberian Platform, as they noted that values of $\delta^{13}C$ remained well within the range of normal marine carbonates and displayed distinct excursions which support their chemostratigraphic significance. However, they emphasized that thermal effects on burial diagenesis, metamorphism, and plutonic intrusion affected $\delta^{18}O$ values which therefore limit their importance. More recently, Hantsoo *et al.* (2018) conducted a chemostratigraphic analysis of carbon and sulfur isotopes in Members 1 to 4 and noted that changes in isotope ratios correlated with increased burrowing and ventilation of seafloor. Topper *et al.* (2022) noted that these data represented organic carbon and not inorganic carbonate carbon isotopes, which are the isotopes used for global correlations. Nevertheless, other major issues related to geochemical proxies (Lucas 2018; Geyer 2019; Steiner *et al.* 2020; Yang & Steiner 2021; Topper *et al.* 2022) affect carbon isotope curves and limit their importance for worldwide correlations.

Fåhræus (1994), Babcock *et al.* (2014), and Zhu *et al.* (2019) claimed that *Treptichnus pedum* first appearance datum may be diachronic across different regions. Notably, Babcock *et al.* (2014, fig. 3) provided a diagram comparing *Treptichnus pedum* first appearance datum from seven worldwide areas, although it is unclear on which grounds the position of the Ediacaran–Cambrian boundary point was then decided to be placed. Five of these areas (Newfoundland, Great Basin, Finmark, South Australia, and Namibia) have *Treptichnus pedum* first appearance datum in proximity to the Ediacaran–Cambrian boundary position, which actually reinforces the current definition of the Global Stratotype Section and Point boundary interval. The first appearance datum from South China, placed in the middle Fortunian, results from dominant carbonate facies and major stratigraphic hiatus in this area (Yang *et al.* 2014; Steiner *et al.* 2020; Yang & Steiner 2021). Recent investigation of the classic Meishucun section of the Yunnan province reveals the presence of *Treptichnus pedum* in the Lower Phosphate (Unit 4) of the Zhongyicun Member (Zhang *et al.* 2025) and reinforces the position of the Ediacaran–Cambrian boundary point in the area as previously established based on the appearance of other trace fossils of the

T. pedum Ichno-Assemblage Zone (Crimes & Jiang 1986). The first appearance datum from Greenland, placed in Cambrian Stage 4, is a consequence of the dearth of studies conducted in this region, and the Ediacaran–Cambrian boundary point has so far not been identified there. Furthermore, Buatois (2018) emphasized that range offset plays a key role in the ecological characteristics of taxa and depends on the stratigraphic architecture of depositional settings. For instance, *Treptichnus pedum* is typically found above sequence boundaries within lowstand systems tracts and within parts of transgressive systems tracts, and is notably lacking in sections demonstrating valley incision (Buatois *et al.* 2013; Buatois 2018; Shahkarami *et al.* 2020). In that respect, the Chapel Island Formation represents a particularly adequate section to host a Global Stratotype Section and Point, as incision by fluvio-estuarine sediment is notably absent (Buatois 2018).

Treptichnus pedum was originally described as *Phycodes pedum* (Seilacher 1955b) and was subsequently referred to as *Trichophycus pedum* (Geyer & Uchman 1995) and *Manykodes pedum* (Dzik 2005). Taxonomy in ichnology is continuously improving thanks to standardization of methods (Bromley 1990, 1996; Bertling *et al.* 2006, 2022; Buatois & Mángano 2011; Rindsberg 2018). After reviews of type materials and using ichnotaxobases (see also Buatois 2018), it can be concluded that: (1) *Phycodes* is a subhorizontal burrow with branches forming bundles (Osgood 1970; Fillion & Pickerill 1990); (2) *Treptichnus* is a three-dimensional burrow with modular segments, pits or projections (Miller 1889; Buatois & Mángano 1993b); and (3) *Trichophycus* is a three-dimensional burrow with U-shaped segments displaying vertical spreiten and delicate striae (Miller & Dyer 1878b; Geyer & Uchman 1995). *Manykodes* was erected by Dzik (2005) to describe a trace fossil based on its supposed producer; this procedure does not follow the International Code of Zoological Nomenclature recommendations and conflicts with the long-standing approach in ichnological systematics (Bertling *et al.* 2006, 2022; Buatois 2018). Consequently, the taxonomic position of *Treptichnus pedum* is sound, and most early Cambrian burrows displaying the morphology suggested by the type material belong to this ichnospecies. Geyer & Uchman (1995) described forms with 'teichichnoid' segments that infer the presence of spreiten and therefore an affinity to *Trichophycus*. These should then be described as *Trichophycus* isp. or as another ichnospecies of *Trichophycus*, but should not be placed in synonymy with *Treptichnus pedum* as the type material from Pakistan (Seilacher 1955b) does not display spreiten.

Treptichnus pedum was recovered 3.31 and 4.41 m below the Global Stratotype Section and Point at Fortune Head by Gehling *et al.* (2001), which led some researchers (Babcock *et al.* 2014; Lucas 2018; Zhu *et al.* 2019) to question the pertinence of the Global Stratotype Section and Point. Our study also agrees with the presence of *Treptichnus pedum* 0.6 m below the Global Stratotype Section and Point (Figs 56, 65; 'Data 1' file in Gougeon *et al.* 2025b), but confident *T. pedum* specimens below that point were not found. First appearance data always underestimate the true range of a species in a section (Geyer 2005; Landing *et al.* 2013). Landing *et al.* (2013) and Gougeon *et al.* (2023) calculated that *Treptichnus pedum* could be recorded as low as 40 and 55.6 m below the Global Stratotype Section and Point, respectively, based on two different datasets. In fact, the International Commission on Stratigraphy explicitly stated that, after the ratification of a Global Stratotype Section and Point, further discoveries of an index fossil below its original position would not necessarily discredit the original position of the Global Stratotype Section and Point, and that the issue could be overcome using other fossils, to correlate assemblages (Cowie 1978; Cowie *et al.* 1986; Remane *et al.* 1996). The lower position of *Treptichnus pedum* first appearance datum at Fortune Head led Landing *et al.* (2013) to re-emphasize the use of other trace fossils of the *T. pedum* Ichno-Assemblage Zone to accurately locate the base of the Fortunian, as well as the use of index fossils *Harlaniella* and *Palaeopascichnus* to constrain the uppermost limit of the Ediacaran. Our current study conforms with that view, and the Cambrian Global Stratotype Section and Point at Fortune Head that contains the first appearance datum of *Treptichnus pedum* also records the first appearances of a multitude of other trace fossils in the section, highlighting a rapid evolutionary event in trace-fossil diversification (see Fig. 65 and previous section; see also Narbonne *et al.* 1987 and Gougeon *et al.* 2023, 2025a). Babcock *et al.* (2014) also added that the definition of the basal Cambrian slightly changed depending on researchers, and that a different emphasis was placed on either the use of *Treptichnus pedum* first appearance datum or the lower boundary of *T. pedum* Ichno-Assemblage Zone. However, both Brasier *et al.* (1994a) and Landing (1994) clearly stated that: (1) the index fossil for the basal Cambrian is *Treptichnus pedum*; (2) the first appearance datum of that coincided with the base of the *T. pedum* Ichno-Assemblage Zone; and (3) the *T. pedum* Ichno-Assemblage Zone started at the uppermost limit of the *Harlaniella podolica* Zone, which comprises simple trace fossils and index fossils of the Ediacaran (i.e. *Harlaniella* and *Palaeopascichnus*). This

definition was and still is in accordance with Global Stratotype Section and Point recommendations by the International Commission on Stratigraphy (Cowie *et al.* 1986; Remane *et al.* 1996).

Finally, Babcock *et al.* (2014) mentioned that the behaviour associated with *Treptichnus pedum* may have arisen more than once in time (i.e. behavioural convergence among different organisms). In fact, *Treptichnus pedum* is known to be produced at least by two groups of animals: scalidophoran priapulid-like worms (Vannier *et al.* 2010; Kesidis *et al.* 2019b; Turk *et al.* 2024a) and insect larvae (Muñiz Guinea *et al.* 2014). However, insect larvae produce *Treptichnus pedum* in continental settings, an environment that was not colonised by animals during the Cambrian. It is possible that other groups of organisms produced *Treptichnus pedum*; however, the question of behavioural convergence with *Treptichnus pedum* has no relevance to the debate on Ediacaran–Cambrian biostratigraphy, as it does not affect the line of reasoning at the origin of the placement of the Ediacaran–Cambrian boundary point (Buatois 2018). Furthermore, Babcock *et al.* (2014) suggested that the behaviour affiliated to *Treptichnus pedum* may correspond to an undermat-mining strategy (following a suggestion by Seilacher 2007), and hence would not be a true testimony of burrowing verticalization. However, in its original description, Seilacher (1955b, fig. 4b) clearly depicted *Treptichnus pedum* as a three-dimensional burrow system made of vertical branches, an interpretation based on observations from the type material. This suggestion is well demonstrated while looking at different preservational variants of *Treptichnus pedum* (e.g. Gougeon *et al.* 2023, fig. 5), and is also strikingly displayed on the specimen selected as first appearance datum for the Global Stratotype Section and Point which shows penetration more than 1.5 cm deep (Narbonne *et al.* 1987, fig. 6D; Hantsoo *et al.* 2018, fig. 2h). Regardless of the trophic type associated with *Treptichnus pedum*, this ichnotaxon typifies a combined vertical and horizontal behaviour associated with deeper colonisation of the substrate (Buatois 2018). The vertical or horizontal configuration of a trace fossil is a property that can be visually appreciated regardless of the suggested interpretation of such morphology.

Oldest fossil evidence of stem-group euarthropod in the Chapel Island Formation

The Chapel Island Formation offers the opportunity to study early arthropod evolution before the advent of trilobites with calcified exoskeletons. In Newfoundland, the oldest report of trilobites is within the Brigus Formation (Cambrian Stage 4), more than 1000 m above the position of the Cambrian Global Stratotype Section and Point (Landing *et al.* 2013). Trilobites of the lower Brigus Formation correspond to eodiscoid forms affiliated to *Serrodiscus* Richter & Richter, *Hebediscus* Whitehouse, and sclerites of ?*Meniscuchus* Öpik and *Calodiscus* Howell that were recovered along Conception and Trinity bays (Hutchinson 1962; Westrop & Landing 2011). Trilobites appeared at the start of the Cambrian Stage 3 worlwide (outside of Avalonia, *ca.* 521 Ma) and represent definite crown-group euarthropods that are abundant in Burgess-Shale type lagerstätten (Daley *et al.* 2018; Edgecombe 2020; Holmes & Budd 2022).

In strata below the Brigus Formation, arthropod trace fossils are commonly recorded in the Chapel Island and Random formations (Crimes & Anderson 1985). In the Chapel Island Formation, their diversification can be interpreted as a two-phase scenario. The first phase corresponds to the appearance of simple and poorly organized scratch imprints. At Fortune Head, this is demonstrated by *Monomorphichnus* indet. a few meters above the Ediacaran–Cambrian boundary point (Fig. 65 and Narbonne *et al.* 1987), while *Monomorphichnus bilinearis* is first recorded *ca.* 70 meters above the boundary (Fig. 56, 'Data 1' file in Gougeon *et al.* 2025b). Both trace fossils are recovered within the *Treptichnus pedum* Ichno-Assemblage Zone. At Grand Bank Head, *Treptichnus pedum* Ichno-Assemblage Zone strata are not as easily accessible compared to Fortune Head (Gougeon *et al.* 2023), but rare large bed bases still display cf. *Dimorphichnus* isp., *Monomorphichnus bilinearis*, *M. lineatus*, and *Monomorphichnus* isp. (Fig. 57). All those scratch imprints were made on the seafloor surface without significantly displacing the sediment. Therefore, their tracemaker(s) did not necessitate a complex musculature nor an extensive sclerotization of their limbs to mark the surface. These scratch imprints, albeit simple, suggest the presence of stem-group euarthropods early in the Fortunian (*ca.* 538–536 Ma), which significantly predates their first record from body-fossil evidence (*ca.* 521 Ma; Daley *et al.* 2018; Holmes & Budd 2022).

At the start of the *Rusophycus avalonensis* Ichno-Assemblage Zone at Fortune Head, Grand Bank Head, and Lewin's Cove, arthropod trace fossils drastically increased in diversity and comprise surficial scratch imprints (cf. *Allocotichnus dyeri*, *Dendroidichnites* aff. *D. irregulare*, *Dimorphichnus* isp. A, *Dimorphichnus* isp. B, *Monomorphichnus needleiunm*) and very-shallow infaunal burrows (*Cruziana problematica*, *Rusophycus avalonensis*, *R. dabardae*, *Rusophycus* isp.).

Arthropod burrows represent the main evolutionary innovation of this second phase, as their formation would require more robust appendages and a powerful musculature to process sediment (Birkenmajer & Bruton 1971; Seilacher 1985; Fortey & Owens 1999). As such, *Rusophycus* is typically regarded as the oldest fossil evidence of crown-group euarthropods because it highlights the bilateral symmetry of a tracemaker that possessed paired jointed appendages with claws (Budd & Jensen 2000; Budd & Telford 2009; Strausfeld *et al.* 2016; Daley *et al.* 2018; Giribet & Edgecombe 2019). This line of reasoning also applies to *Cruziana* and *Dimorphichnus*, and therefore poses the question of whether or not cf. *Dimorphichnus* isp. recorded at Grand Bank Head would represent the oldest evidence of crown-group euarthropods. Nevertheless, the presence of both *Cruziana* and *Rusophycus* within the *Rusophycus avalonensis* Ichno-Assemblage Zone suggests sclerotization of appendages to process the sediment, which would at least argue for arthropodization to have taken place early in those animals. The order of appearance of arthrodization (i.e. sclerotization and jointing of the trunk exoskeleton) versus arthropodization (i.e. sclerotization and jointing of limbs) in arthropods (cf. Liu *et al.* 2011; Fu *et al.* 2022) requires further analyses for the trace-fossil record to provide novel elements to this debate.

Conclusions

A revision of the sedimentology and trace-fossil taxonomy of the Chapel Island Formation of Newfoundland, Canada, permitted the identification of fourteen sedimentary facies and twenty-eight ichnogenera. Sedimentary facies encompass intertidal and shallow-marine environments, covering the tidal flat, tide-dominated or -influenced embayments, and the shoreface, offshore, and shelf. Two limestone beds also provide additional information on intertidal and subtidal settings. Overall, sedimentary facies show recurrence in time across the Ediacaran, Fortunian, and Cambrian Age 2. Trace fossils are recovered from almost all sedimentary facies, and are represented by epifaunal and semi-infaunal trails (*Archaeonassa fossulata, Circulichnis ligusticus*, *C. montanus*, *Cochlichnus anguineus, C. luguanensis, Gordia marina*, *Helminthoidichnites tenuis*, *Helminthopsis abeli*, *H. hieroglyphica*, *H. tenuis*), epifaunal scratch imprints (cf. *Allocotichnus dyeri*, *Dendroidichnites* aff. *D. irregulare*, *Dimorphichnus* isp. A, *Dimorphichnus* isp. B, cf. *Dimorphichnus* isp., *Monomorphichnus bilinearis*, *M. lineatus*, *M. needleiunm*, *Monomorphichnus* isp., *Rusophycus avalonensis*, *Rusophycus dabardae*, *Rusophycus* isp.), shallow infaunal burrows (*Arenicolites* aff. *A. carbonarius*, *Bergaueria perata*, *B.* cf. *B. radiata*, *Conichnus conicus*, *Curvolithus multiplex*, *C. simplex*, *Curvolithus* isp., *Didymaulichnus miettensis*, *Halopoa imbricata*, *Gyrolithes gyratus*, *G. scintillus*, *Palaeophycus annulatus*, *P. tubularis*, *Palaeophycus* isp., *Psammichnites gigas circularis*, *P.* cf. *P. saltensis*, *Saerichnites kutscheri*, *Torrowangea rosei*, *Treptichnus bifurcus*, *T. coronatum*, *T. pedum*, *T. pollardi*, *Trichichnus linearis*), mid infaunal burrows (*Arenicolites* isp., *Rosselia erecta*, *Rosselia* isp., *Teichichnus rectus*), and deep infaunal burrows (?*Diplocraterion* isp., *Trichichnus* isp.).

At Fortune Head, trace fossils show a burst of diversity at the start of the Fortunian, in concomitance with increased vertical burrowing behaviours, increased bioturbation intensities, and increased ichnodisparity. These observations support the view that many trace fossils – not only *Treptichnus pedum*, the index fossil for the Cambrian, but also other vertical burrows such as *Arenicolites* aff. *A. carbonarius* or *Gyrolithes scintillus* – were made by metazoan-grade organisms possessing a bilateral symmetry and a gut system. The current placement of the Ediacaran–Cambrian boundary point at Fortune Head is then reaffirmed as being based on the appearance of trace fossils of the *Treptichnus pedum* Ichno-Assemblage Zone, which also corresponds to the demise of Ediacaran body fossils such as *Harlaniella podolica* and *Palaeopascichnus delicatus*. The Fortunian marks a period of more systematic burrowing, increased vertical bioturbation, and lateral expansion of the seafloor colonisation on dominantly firmground substrates. Arthropod scratch imprints and burrows demonstrate the presence of stem-group euarthropods early in the Fortunian, which correspond to their oldest evidence from the fossil record. The ecology that was typical of the Ediacaran, dominated by matgrounds colonised by simple, surficial or very shallow infaunal grazers, survived in localized areas of the Fortunian. By the end of the Fortunian, vertical partitioning of the substrate became more complex with the advent of mid- and deep-tier burrows colonising the deepest sediments, whereas shallow homogenized sediments resulted from intense churning by animals. This partitioning is significant as it demonstrates the establishment of modern-style seafloors with shallowly emplaced mixed layers and deeper transitional layers. Overall, this study highlights the need for comprehensive and multi-disciplinary approaches to further our understanding of early animal evolution on Earth.

Acknowledgements. - We thank B. Novakovski for help with sample processing, L.-J. Zhang for providing Chinese literature, and K. Zhou for translating parts of those papers into English. P. Myrow is acknowledged for providing his field notes and for discussions on different aspects of the Chapel Island Formation sedimentology. S. Jensen is thanked for providing some literature and for discussion on taxonomic matters. A. Rindsberg and M. Vidal helped us with ichnotaxonomic issues and the use of the code. We are also grateful to R. Thomas for facilitating our work in the Fortune Head Ecological Reserve under a Scientific Research Permit from Parks and Natural Areas, Newfoundland and Labrador. We also thank the people at the inter-library loan system at University of Saskatchewan for their help in finding a large amount of literature otherwise inaccessible to us. This paper was improved thanks to the comments and corrections made by S. Stouge, S. Jensen, and A. Uchman. This research was supported by Natural Sciences and Engineering Research Council (NSERC) Discovery Grants to G. Narbonne, L. Buatois, and M.G. Mángano (2020-06741, 311726-13/422931-20, and 311727-15/20, respectively). M.G. Mángano thanks additional funding by the George J. McLeod Enhancement Chair in Geology. R. Gougeon acknowledges financial supports from the University of Saskatchewan Partial Devolved Scholarship (2016), the University of Saskatchewan Graduate Teaching Fellowship (2017, 2018, 2019), the University of Saskatchewan Dr. Rui Feng Geological Sciences Graduate Studies Award (2018, 2019, 2020), the Geological Society of America Student Geoscience Grant (2018), the International Association of Sedimentologists Postgraduate Grant Scheme (2016), the Palaeontological Society Student Research Grant (2018), and the Society for Sedimentary Geology (SEPM) Student Assistance Grant (2018). B. Laing acknowledges funding by an NSERC Postgraduate Scholarships – Doctoral and a Cotutelle Research Excellence Scholarship from Macquarie University (Australia). S. Stouge died shortly after finishing editing this monograph. We dedicate this work in his memory.

References

Abad, M., Ruiz, F., Pendón, J. G., Tosquella, J. & González-Regalado, M. L. 2006: Estructuras de escape y equilibrio asociadas a *Conichnus conicus* como indicadores de tasas de sedimentación variables en medios litorales tortonienses del SO de España. *Geobios 39*, 1–11. https://doi.org/10.1016/j.geobios.2004.07.001

Abel, O. 1935: *Vorzeitliche Lebensspuren*, G. Fischer, Jena, 644 pp.

Aceñolaza, F. G. 1978: Trazas fósiles de la Formación Patquía en el Bordo Atravesado, Sierra de Famatina, La Rioja. *Acta Geológica Lilloana 15*, 19–29.

Aceñolaza, G. & Aceñolaza, F. G. 2002: Ordovician trace fossils of Argentina. 177–194 *in* Aceñolaza, F. G. (ed): *Aspects of the Ordovician System in Argentina*. INSUGEO, Serie Correlación Geológica, No. 16.

Aceñolaza, G. & Aceñolaza, F. 2007: Insights in the Neoproterozoic–early Cambrian transition of NW Argentina: facies, environments and fossils in the proto-margin of western Gondwana. *Geological Society, London, Special Publications 286*, 1–13. https://doi.org/10.1144/SP286.1

Aceñolaza, F. G. & Buatois, L. A. 1991: Trazas fósiles del Paleozoico superior continental argentino. *Ameghiniana 28*, 89–108.

Aceñolaza, F. G. & Buatois, L. A. 1993: Nonmarine perigondwanic trace fossils from the late Paleozoic of Argentina. *Ichnos 2*, 183–201. https://doi.org/10.1080/10420949309380092

Aceñolaza, F. G. & Durand, F. R. 1973: Trazas fósiles del basamento cristalino del noroeste Argentino. *Boletín de la Asociación Geológica de Córdoba 2*, 45–55.

Aceñolaza, F. G. & Durand, F. R. 1978: Trazas de trilobites en los estratos del Ordovícico basal de la Puna Argentina. *Acta Geológica Lilloana 15*, 5–12.

Aceñolaza, G. F. & Gutiérrez-Marco, J. C. 1999: Icnofósiles del Ordovícico terminal (pizarras Chavera, pizarras de Orea: Hirnantiense) de algunas localidades españolas. *Boletín Geológico y Minero 110-2*, 123–134.

Aceñolaza, G. F. & Milana, J. P. 2005: Remarkable *Cruziana* beds in the lower Ordovician of the Cordillera Oriental, NW Argentina. *Ameghiniana 42*, 633–637.

Aceñolaza, G. F. & Tortello, M. F. 2003: El Alisal: a new locality with trace fossils of the Puncoviscana Formation (late Precambrian-early Cambrian) in Salta Province, Argentina. *Geologica Acta 1*, 95–102.

Aceñolaza, G. F., Germs, G. J. & Aceñolaza, F. G. 2009: Trace fossils and the Agronomic Revolution at the Neoproterozoic-Cambrian transition in southwest Gondwana. *Developments in Precambrian Geology 16*, 339–347. https://doi.org/10.1016/S0166-2635(09)01624-7

Acker, R. 2013: *Sedimentology and Stratigraphy of the Upper Devonian Imperial Formation, Mackenzie Valley, Northwest Territories, Canada*. Unpublished Master Dissertation, University of Calgary, 115 pp.

Adserá, P., Belaústegui, Z. & Uchman, A. 2020: *Estrellichnus jacaensis* from the Eocene Jaca Basin of NE Spain: new locality and new ethological interpretation. *Lethaia 53*, 129–143. https://doi.org/10.1111/let.12346

Ahlbrandt, T. S., Andrews, S. & Gwynne, D. T. 1978: Bioturbation in eolian deposits. *Journal of Sedimentary Petrology 48*, 839–848. https://doi.org/10.1306/212F7586-2B24-11D7-8648000102C1865D

Ahmad, W., Gingras, M. K., Ranger, M. J., MacEachern, J. A. & Zonneveld, J. P. 2024: Depositional setting and trace fossil suites of the early Cambrian (Series 2, Stage 4) Khussak Formation, east-central Salt Range, north-west sub-Himalayas, Pakistan. *Marine and Petroleum Geology 165*, 106858. https://doi.org/10.1016/j.marpetgeo.2024.106858

Ahn, S. Y. & Babcock, L. E. 2012: Microorganism-mediated preservation of *Planolites*, a common trace fossil from the Harkless Formation, Cambrian of Nevada, USA. *Sedimentary Geology 263*, 30–35. https://doi.org/10.1016/j.sedgeo.2011.08.003

Aigner, T. 1982: Calcareous tempestites: storm-dominated stratification in upper Muschelkalk Limestones (middle Trias, SW-Germany). 180–198 *in* Einsele, G. & Seilacher, A. (eds): *Cyclic and Event Stratification*. Springer, Berlin. https://doi.org/10.1007/978-3-642-75829-4_13

Aitken, J. D. 1967: Classification and environmental significance of cryptalgal limestones and dolomites, with illustrations from the Cambrian and Ordovician of southwestern Alberta. *Journal of Sedimentary Petrology 37*, 1163–1178. https://doi.org/10.1306/74D7185C-2B21-11D7-8648000102C1865D

Aitken, J. D. 1989: Uppermost Proterozoic formations in central Mackenzie Mountains, Northwest Territories. *Geological Survey of Canada 368*, 1–26.

Aitken, J. F. & Flint, S. S. 1995: The application of high-resolution sequence stratigraphy to fluvial systems: a case study from the upper Carboniferous Breathitt Group, eastern Kentucky, USA. *Sedimentology 42*, 3–30. https://doi.org/10.1111/j.1365-3091.1995.tb01268.x

Al-Mufti, O. N. & Arnott, R. W. C. 2023: The origin of planar lamination in fine-grained sediment deposited by subaqueous sediment gravity flows. *The Depositional Record 10*, 496–514. https://doi.org/10.1002/dep2.257

Alexander, C. R., DeMaster, D. J. & Nittrouer, C. A. 1991: Sediment accumulation in a modern epicontinental-shelf setting: the Yellow Sea. *Marine Geology 98*, 51–72. https://doi.org/10.1016/0025-3227(91)90035-3

Alexander, H. S. 1932: Pothole erosion. *The Journal of Geology 40*, 305–337. https://doi.org/10.1086/623954

Allen, J. R. L. 1982: *Sedimentary Structures. Their character and physical basis. Volume 2*. Developments in Sedimentology, 30B, Elsevier, 663 pp.

Aller, R. C. 1978: Experimental studies of changes produced by deposit feeders on pore water, sediment, and overlying water chemistry. *American Journal of Science 278*, 1185–1234. https://doi.org/10.2475/ajs.278.9.1185

Aller, R. C. 1982: The effects of macrobenthos on chemical properties of marine sediment and overlying water. 53–102 *in* McCall,

P. L. & Tevez, M. J. S. (eds): *Animal-Sediment Relations*. Plenum Press, New York. https://doi.org/10.1007/978-1-4757-1317-6_2

Aller, R. C. & Yingst, J. Y. 1978: Biogeochemistry of tube dwellings: a study of the sedentary polychaete *Amphitrite ornata* (Leidy). *Journal of Marine Research 36*, 201–254.

Allison, P. A. & Pye, K. 1994: Early diagenetic mineralization and fossil preservation in modern carbonate concretions. *Palaios 9*, 561–575. https://doi.org/10.2307/3515128

Allport, H. A., Davies, N. S., Shillito, A. P., Mitchell, E. G. & Herron, S. T. 2022: Non-palimpsested crowded *Skolithos* ichnofabrics in a Carboniferous tidal rhythmite: disentangling ecological signatures from the spatio-temporal bias of outcrop. *Sedimentology 69*, 1028–1050. https://doi.org/10.1111/sed.12947

Alonso-Muruaga, P. J., Buatois, L. A., Mángano, M. G. & Limarino, C. O. 2012: Ichnology of the late Paleozoic Paganzo and Calingasta-Uspallata Basins of western Argentina. *Ichnology of Latin America, Selected Papers, Monografias da Sociedade Brasileira de Paleontologia 2*, 64–81.

Alpert, S. P. 1973: *Bergaueria* Prantl (Cambrian and Ordovician), a probable actinian trace fossil. *Journal of Paleontology 47*, 919–924.

Alpert, S. P. 1974: Systematic review of the genus *Skolithos*. *Journal of Paleontology 4*, 661–669.

Alpert, S. P. 1976a: Trilobite and star-like trace fossils from the White-Inyo Mountains, California. *Journal of Paleontology 50*, 226–239.

Alpert, S. P. 1976b: Trace fossils of the White-Inyo Mountains. 43–48 *in* Moore, J. N. & Fritsche, A. E. (eds): *Depositional Environments of Lower Paleozoic Rocks in the White–Inyo Mountains, Inyo County, California*. Pacific Coast Paleogeography Field Guides. The Pacific Section, Society of Economic Paleontologists and Mineralogists, Los Angeles.

Alpert, S. P. 1977: Trace fossils and the basal Cambrian boundary. 1–8 *in* Crimes, T. P. & Harper, J. C. (eds): *Trace Fossils 2*. Seel House Press, Liverpool.

Alshuaibi, A., Duane, M. J. & Mahmoud, H. 2012: Microbial-activated sediment traps associated with oncolite formation along a peritidal beach, northern Arabian (Persian) Gulf, Kuwait. *Geomicrobiology Journal 29*, 679–696. https://doi.org/10.1080/01490451.2011.608110

Álvaro, J. J. & Mills, A. 2024: Carbonate production and reef building under ferruginous seawater conditions in the Cambrian rift branches of the Avalon Zone, Newfoundland. *Sedimentology 71*, 1245–1269. https://doi.org/10.1111/sed.13172

Álvaro, J. J. & Vizcaïno, D. 1999: Biostratigraphic significance and environmental setting of the trace fossil *Psammichnites* in the lower Cambrian of the Montagne Noire, France. *Bulletin de la Société Géologique de France 170*, 821–828.

Amos, C. L. 1995: Siliciclastic tidal flats. 273–306 *in* Perillo, G. M. E. (ed): *Developments in Sedimentology 56*, Elsevier. https://doi.org/10.1016/S0070-4571(05)80030-5

Anderson, A. 1976: Fish trails from the early Permian of South Africa. *Palaeontology 19*, 397–409.

Anderson, M. M. 1981: The Random Formation of southeastern Newfoundland: a discussion aimed at establishing its age and relationship to bounding formations. *American Journal of Science 281*, 807–830. https://doi.org/10.2475/ajs.281.6.807

Andrée, K. 1920: Über einige fossile Problematika. I. Ein Problematikum aus dem Paläozoikumvon Battenberg an der Eder und des dasselbe beherbergende Gestein. *Neues Jahrbuch für Mineralogie, Geologie und Paläontologie 1*, 55–88.

Andrews Jr., H. N. 1955: *Index of generic names of fossil plants, 1820–1950*. United States Department of the Interior, Geological Survey Bulletin 1013, 262 pp.

Ansell, A. D. & Trueman, E. R. 1968: The mechanism of burrowing in the anemone, *Peachia hastata* Gosse. *Journal of Experimental Marine Biology and Ecology 2*, 124–134. https://doi.org/10.1016/0022-0981(68)90003-8

Antcliffe, J. B., Gooday, A. J. & Brasier, M. D. 2011: Testing the protozoan hypothesis for Ediacaran fossils: a developmental analysis of *Palaeopascichnus*. *Palaeontology 54*, 1157–1175. https://doi.org/10.1111/j.1475-4983.2011.01058.x

Arai, M. N. & McGugan, A. 1968: A problematical coelenterate (?) from the lower Cambrian, near Moraine Lake, Banff area, Alberta. *Journal of Paleontology 42*, 205–209.

Archer, A. W. 1984: Preservational control of trace-fossil assemblages: middle Mississippian carbonates of south-central Indiana. *Journal of Paleontology 58*, 285–297.

Archer, A. W. & Maples, C. G. 1984: Trace-fossil distribution across a marine-to-nonmarine gradient in the Pennsylvanian of southwestern Indiana. *Journal of Paleontology 58*, 448–466.

Archer, A. W., Calder, J. H., Gibling, M. R., Naylor, R. D., Reid, D. R. & Wightman, W. G. 1995: Invertebrate trace fossils and agglutinated foraminifera as indicators of marine influence within the classic Carboniferous section at Joggins, Nova Scotia, Canada. *Canadian Journal of Earth Sciences 32*, 2027–2039. https://doi.org/10.1139/e95-156

Arnott, R. W. C. 1993: Quasi-planar-laminated sandstone beds of the lower Cretaceous Bootlegger Member, north-central Montana: evidence of combined-flow sedimentation. *Journal of Sedimentary Petrology 63*, 488–494. https://doi.org/10.1306/D4267B31-2B26-11D7-8648000102C1865D

Arnott, R. W. & Southard, J. B. 1990: Exploratory flow-duct experiments on combined-flow bed configurations, and some implications for interpreting storm-event stratification. *Journal of Sedimentary Petrology 60*, 211–219. https://doi.org/10.1306/212F9156-2B24-11D7-8648000102C1865D

Arora, K., Goff, J. A., Wood, L. J., Flood, R. D. & Christensen, B. 2018: Analysis of hummocky bedforms offshore Fire Island, New York, generated by superstorm Sandy. *Continental Shelf Research 163*, 12–22. https://doi.org/10.1016/j.csr.2018.04.010

Ashley, G. M. 1990: Classification of large-scale subaqueous bedforms: a new look at an old problem. *Journal of Sedimentary Petrology 60*, 160–172. https://doi.org/10.2110/jsr.60.160

Assereto, R. L. & Kendall, C. G. S. C. 1977: Nature, origin and classification of peritidal tepee structures and related breccias. *Sedimentology 24*, 153–210. https://doi.org/10.1111/j.1365-3091.1977.tb00254.x

Astibia, H., Rodríguez-Tovar, F. J., Díaz-Martínez, I., Payros, A. & Ortiz, S. 2017: Trace fossils from the middle and upper Eocene (Bartonian–Priabonian) molasse deposits of the Pamplona Basin (Navarre, western Pyrenees): palaeoenvironmental implications. *Geological Journal 52*, 327–349. https://doi.org/10.1002/gj.2763

Ausich, W. I. & Bottjer, D. J. 1982: Tiering in suspension-feeding communities on soft substrata throughout the Phanerozoic. *Science 216*, 173–174. https://doi.org/10.1126/science.216.4542.173

Avanzini, M., Contardi, P., Ronchi, A. & Santi, G. 2011: Ichnosystematics of the lower Permian invertebrate traces from the Collio and Mt. Luco Basins (North Italy). *Ichnos 18*, 95–113. https://doi.org/10.1080/10420940.2011.573604

Awramik, S. M. 1971: Precambrian columnar stromatolite diversity: reflection of metazoan appearance. *Science 174*, 825–827. https://doi.org/10.1126/science.174.4011.825

Awramik, S. M. 1992: The history and significance of stromatolites. 435–449 *in* Schidlowski, M., Golubic, S., Kimberley, M. M., McKirdy, D. M. & Trudinger, P. A. (eds): *Early organic evolution*. Springer, Berlin, Heidelberg. https://doi.org/10.1007/978-3-642-76884-2_34

Ayranci, K., Dashtgard, S. E. & MacEachern, J. A. 2014: A quantitative assessment of the neoichnology and biology of a delta front and prodelta, and implications for delta ichnology. *Palaeogeography, Palaeoclimatology, Palaeoecology 409*, 114–134. https://doi.org/10.1016/j.palaeo.2014.05.013

Babcock, L. E., Peng, S., Zhu, M., Xiao, S. & Ahlberg, P. 2014: Proposed reassessment of the Cambrian GSSP. *Journal of African Earth Sciences 98*, 3–10. https://doi.org/10.1016/j.jafrearsci.2014.06.023

Badve, R. M. 1987: A reassessment of stratigraphy of Bagh Beds, Barwah area, Madhya Pradesh, with description of trace fossils. *Journal Geological Society of India 30*, 106–120. https://doi.org/10.17491/jgsi/1987/300201

Badve, R. M. & Ghare, M. A. 1978: Jurassic ichnofauna of Kutch-I. *Biovigyanam 4*, 125–140.

Badve, R. M. & Ghare, M. A. 1980: Ichnofauna of Bagh Beds from Deva River valley, south of Narmada. *Biovigyanam 6*, 121–130.

Baghiyan-Yazd, M. H. 1998: *Palaeoichnology of the terminal Proterozoic-Early Cambrian transition in central Australia: interregional correlation and palaeoecology*. Unpublished Doctoral Dissertation, University of Adelaide, 244 pp.

Bai, Z., Lü, X., Liu, X., Xie, Q., Li, J. & Wu, J. 2012: Trace fossils from lower Cambrian Wusongger Formation in Xiaoerbulake outcrop, Kalpin Area, Xinjiang. *Acta Geologica Sinica (English Edition) 86*, 313–319. https://doi.org/10.1111/j.1755-6724.2012.00661.x

Baird, G. C. & Brett, C. E. 1986: Erosion on an anaerobic seafloor: significance of reworked pyrite deposits from the Devonian of New York State. *Palaeogeography, Palaeoclimatology, Palaeoecology 57*, 157–193. https://doi.org/10.1016/0031-0182(86)90012-X

Bajard, J. 1966: Figures et structures sédimentaires dans la zone intertidale de la partie orientale de la Baie du Mont Saint-Michel. *Revue de géologie dynamique et de géographie physique 8*, 39–111.

Baldwin, C. T. 1977a: Internal structures of trilobite trace fossils indicative of an open surface furrow origin. *Palaeogeography, Palaeoclimatology, Palaeoecology 21*, 273–284. https://doi.org/10.1016/0031-0182(77)90039-6

Baldwin, C. T. 1977b: The stratigraphy and facies associations of trace fossils in some Cambrian and Ordovician rocks of north western Spain. 9–40 *in* Crimes, T. P. & Harper, J. C. (eds): *Trace Fossils 2*. Seel House Press, Liverpool.

Baldwin, C. T. 1978: A comparison of the stratigraphy and depositional processes in the Cambro-Ordovician rocks of the Cantabrian and west Asturian-Leonese zones, NW Spain. 43–70 *in* Anthonioz, D. M. (ed): *Geología de la parte Norte del Macizo Ibérico*. Castro, La Coruña.

Baldwin, C. T. & McCave, I. N. 1999: Bioturbation in an active deep-sea area: implications for models of trace fossil tiering. *Palaios 14*, 375–388. https://doi.org/10.2307/3515463

Baldwin, C. T., Strother, P. K., Beck, J. H. & Rose, E. 2004: Palaeoecology of the Bright Angel Shale in the eastern Grand Canyon, Arizona, USA, incorporating sedimentological, ichnological and palynological data. *Geological Society, London, Special Publications 228*, 213–236. https://doi.org/10.1144/GSL.SP.2004.228.01.11

Baliński, A., Sun, Y. & Dzik, J. 2013: Traces of marine nematodes from 470 million years old Early Ordovician rocks in China. *Nematology 15*, 567–574. https://doi.org/10.1163/15685411-00002702

Balistieri, P., Netto, R. G. & Lavina, E. L. C. 2002: Ichnofauna from the upper Carboniferous-lower Permian rhythmites from Mafra, Santa Catarina State, Brazil: ichnotaxonomy. *Revista Brasileira de Paleontologia 4*, 13–26.

Bandel, K. 1967: Trace fossils from two upper Pennsylvanian sandstones in Kansas. *The University of Kansas Paleontological Contributions 18*, 1–13.

Banerjee, S., Sarkar, S., Eriksson, P. G. & Samanta, P. 2010: Microbially related structures in siliciclastic sediment resembling Ediacaran fossils: examples from India, ancient and modern. 109–129 *in* Seckbach, J. & Oren, A. (eds): *Microbial Mats: Modern and Ancient Microorganisms in Stratified Systems*. Springer, Dordrecht. https://doi.org/10.1007/978-90-481-3799-2_6

Banks, N. L. 1970: Trace fossils from the late Precambrian and lower Cambrian of Finnmark, Norway. 19–34 *in* Crimes, T. P. & Harper, J. C. (eds): *Trace Fossils*. Seel House Press, Liverpool.

Banks, N. L. 1973: Tide-dominated offshore sedimentation, lower Cambrian, north Norway. *Sedimentology 20*, 213–228. https://doi.org/10.1111/j.1365-3091.1973.tb02046.x

Bann, K. 1998: *Ichnology and sequence stratigraphy of the early Permian Pebbley Beach Formation and Snapper Point Formation in the southern Sydney basin*. Unpublished Doctoral Dissertation, University of Wollongong, 215 pp.

Bann, K. L., Fielding, C. R., MacEachern, J. A. & Tye, S. C. 2004: Differentiation of estuarine and offshore marine deposits using integrated ichnology and sedimentology: Permian Pebbley Beach Formation, Sydney Basin, Australia. *Geological Society, London, Special Publications 228*, 179–211. https://doi.org/10.1144/GSL.SP.2004.228.01.10

Barbour, I. H. 1892: Notice of new gigantic fossils. *Science 19*, 99–100. https://doi.org/10.1126/science.ns-19.472.99

Barr, S. M., White, C. E., Jensen, S., Palacios, T. & van Rooyen, D. 2020: Ediacaran and Cambrian rocks on Scatarie Island, Avalonian Mira Terrane, Cape Breton Island, Nova Scotia, Canada. *Atlantic Geology 56*, 257–279. https://doi.org/10.4138/atlgeol.2020.011

Barr, S. M., White, C. E., Palacios, T., Jensen, S., van Rooyen, D. & Crowley, J. L. 2023: The Terreneuvian MacCodrum Brook section, Mira terrane, Cape Breton Island, Nova Scotia, Canada: age constraints from ash layers, organic-walled microfossils, and trace fossils. *Canadian Journal of Earth Sciences 60*, 307–332. https://doi.org/10.1139/cjes-2022-0044

Barreto, A. M. F., Oliveira, E. V., Cassab, R. C. T., Duque, R. R. C., Sucerquia, P. & de Lira Mota, M. A. 2014: Catálogo do material-tipo da Coleção Paleontológica do Departamento de geologia, Centro de Tecnologia e Geociências da Universidade Federal de Pernambuco. *Estudos Geológicos 24*, 3–53. https://doi.org/10.18190/1980-8208/estudosgeologicos.v24n3p3-53

Bartley, J. K., Pope, M., Knoll, A. H., Semikhatov, M. A. & Petrov, P. Y. 1998: A Vendian–Cambrian boundary succession from the northwestern margin of the Siberian Platform: stratigraphy, palaeontology, chemostratigraphy and correlation. *Geological Magazine 135*, 473–494. https://doi.org/10.1017/S0016756898008772

Basilici, G., de Luca, P. H. V. & Poiré, D. G. 2012: Hummocky cross-stratification-like structures and combined-flow ripples in the Punta Negra Formation (lower-middle Devonian, Argentine Precordillera): a turbiditic deep-water or storm-dominated prodelta inner-shelf system? *Sedimentary Geology 267*, 73–92. https://doi.org/10.1016/j.sedgeo.2012.05.012

Bather, F. A. 1925: U-shaped burrows near Blea Wyke. *Proceedings of the Yorkshire Geological Society 20*, 185–199. https://doi.org/10.1144/pygs.20.2.185

Baucon, A. & Felletti, F. 2013: Neoichnology of a barrier-island system: the Mula di Muggia (Grado lagoon, Italy). *Palaeogeography, Palaeoclimatology, Palaeoecology 375*, 112–124. https://doi.org/10.1016/j.palaeo.2013.02.011

Baucon, A., Bordy, E., Brustur, T., Buatois, L. A., Cunningham, T., De, C., Duffin, C., Felletti, F., Gaillard, C., Hu, B., Hu, L., Jensen, S., Knaust, D., Lockley, M., Lowe, P., Mayor, A., Mayoral, E., Mikuláš, R., Muttoni, G., Neto de Carvalho, C., Pemberton, S. G., Pollard, J., Rindsberg, A. K., Santos, A., Seike, K., Song, H.-B., Turner, S., Uchman, A., Wang, Y.-Y., Gong, Y.-M., Zhang, L. & Zhang, W.-T. 2012: A history of ideas in ichnology. 3–43 *in* Knaust, D. & Bromley, R. G. (eds): *Trace Fossils as Indicators of Sedimentary Environments*. Developments in Sedimentology *64*, Elsevier. https://doi.org/10.1016/B978-0-444-53813-0.00001-0

Bayet-Goll, A., Neto De Carvalho, C., Moussavi-Harami, R., Mahboubi, A. & Nasiri, Y. 2014: Depositional environments and ichnology of the deep-marine succession of the Amiran Formation (upper Maastrichtian–paleocene), Lurestan Province, Zagros Fold–thrust Belt, Iran. *Palaeogeography, Palaeoclimatology, Palaeoecology 401*, 13–42. https://doi.org/10.1016/j.palaeo.2014.02.019

Bayet-Goll, A., Neto De Carvalho, C., Mahmudy-Gharaei, M. H. & Nadaf, R. 2015: Ichnology and sedimentology of a shallow marine upper Cretaceous depositional system (Neyzar Formation, Kopet-Dagh, Iran): palaeoceanographic influence

on ichnodiversity. *Cretaceous Research 56*, 628–646. https://doi.org/10.1016/j.cretres.2015.07.008

Bayet-Goll, A., Uchman, A., Daraei, M. & Neto de Carvalho, C. 2020: Crowded *Trichophycus* ichnofabrics in the Early Ordovician successions of central Iran: insight into the Ordovician radiation. *Lethaia 54*, 314–329. https://doi.org/10.1111/let.12404

Bekker, J. R. 2013: Ichnofossils – a new paleontological object in the Late Precambrian stratotype of the Urals. *Litosfera 1*, 52–80.

Bel Haouz, W., Lagnaoui, A. & Silantiev, V. V. 2020: A new possible bivalve burrow *Oblongichnus solodukhoi* from the late Kazanian (middle Permian) stratotype section in Russia. *Palaeoworld 29*, 96–107. https://doi.org/10.1016/j.palwor.2019.05.013

Belaústegui, Z. & de Gibert, J. M. 2013: Bow-shaped, concentrically laminated polychaete burrows: a *Cylindrichnus concentricus* ichnofabric from the Miocene of Tarragona, NE Spain. *Palaeogeography, Palaeoclimatology, Palaeoecology 381-382*, 119–127. https://doi.org/10.1016/j.palaeo.2013.04.021

Belaústegui, Z. & Muñiz, F. 2016: Ichnology of the Lepe area (Huelva, SW Spain): trace fossils at the Pliocene 'Arroyo Valleforero' section and modern traces at the Piedras Estuary. *Comunicaçõe Geológicas 103*, 131–142.

Bellaiche, G. & Blanpied, C. 1979: La bioturbation en tant que critère paléoclimatique. *Géologie Méditerranéenne 6*, 297–303.

Bengtson, S. & Fletcher, T. P. 1981: The succession of skeletal fossils in the basal lower Cambrian of southeastern Newfoundland. p. 18 *in* Taylor, M. E. (ed): *Short Papers for the Second International Symposium on the Cambrian System*. Open-File Report 81-743, United States Geological Survey.

Bengtson, S. & Fletcher, T. P. 1983: The oldest sequence of skeletal fossils in the lower Cambrian of southeastern Newfoundland. *Canadian Journal of Earth Sciences 20*, 525–536. https://doi.org/10.1139/e83-050

Benton, M. J. 1982a: Trace fossils from Lower Palaeozoic ocean-floor sediments of the Southern Uplands of Scotland. *Transactions of The Royal Society of Edinburgh: Earth Sciences 73*, 67–87. https://doi.org/10.1017/S0263593300009627

Benton, M. J. 1982b: *Dictyodora* and associated trace fossils from the Palaeozoic of Thuringia. *Lethaia 15*, 115–132. https://doi.org/10.1111/j.1502-3931.1982.tb01984.x

Benton, M. J. & Trewin, N. H. 1978: Catalogue of the type and figured material in the Palaeontology Collection, University of Aberdeen, with notes on the H. A. Nicholson collection. *Publications of the Department of Geology and Mineralogy, University of Aberdeen 2*, 1–28.

Beraldi-Campesi, H., Cuen-Romero, F. & Buitrón-Sánchez, B. E. 2018: Cambrian oncolites from San José de Gracia, Sonora, Mexico. *Paleontología Mexicana 7*, 23–56. https://doi.org/10.22201/igl.05437652e.2018.7.1.217

Berger, W. 1957: Eine spiralförmige Lebensspur aus dem Rupel der bayrischen Beckenmolasse. *Neues Jahrbuch für Geologie und Paläontologie Monatshefte 1957*, 538–540.

Berger, W. H. & Heath, G. R. 1968: Vertical mixing in pelagic sediments. *Journal of Marine Research 26*, 134–143.

Berger, W. H., Ekdale, A. A. & Bryant, P. P. 1979: Selective preservation of burrows in deep-sea carbonates. *Marine Geology 32*, 205–230. https://doi.org/10.1016/0025-3227(79)90065-3

Bergström, J. 1970: *Rusophycus* as an indication of early Cambrian age. 35–42 *in* Crimes, T.P. & Harper, J.C. (eds): *Trace Fossils*. Seel House Press, Liverpool.

Bergström, J. 1973: Organization, life, and systematics of trilobites. *Fossils and Strata 2*, 1–69. https://doi.org/10.18261/82000 93301-1973-01

Bergström, J. 1976: Lower Palaeozoic trace fossils from eastern Newfoundland. *Canadian Journal of Earth Sciences 13*, 1613–1633. https://doi.org/10.1139/e76-169

Bergström, J. 1990: Precambrian trace fossils and the rise of bilaterian animals. *Ichnos 1*, 3–13. https://doi.org/10.1080/10420949009386326

Berner, R. A. 1968: Calcium carbonate concretions formed by the decomposition of organic matter. *Science 159*, 195–197. https://doi.org/10.1126/science.159.3811.195

Bertling, M., Braddy, S. J., Bromley, R. G., Demathieu, G. R., Genise, J., Mikuláš, R., Nielsen, J. K., Nielsen, K. S. S., Rindsberg, A. K., Schlirf, M. & Uchman, A. 2006: Names for trace fossils: a uniform approach. *Lethaia 39*, 265–286. https://doi.org/10.1080/00241160600787890

Bertling, M., Buatois, L. A., Knaust, D., Laing, B., Mángano, M. G., Meyer, N., Mikuláš, R., Minter, N .J., Neumann, C., Rindsberg, A. K., Uchman, A. & Wisshak, M. 2022: Names for trace fossils 2.0: theory and practice in ichnotaxonomy. *Lethaia 55*, 1–19. https://doi.org/10.18261/let.55.3.3

Beynon, B. M. & Pemberton, S. G. 1992: Ichnological signature of a brackish water deposit: an example from the lower Cretaceous Grand Rapids Formation, Cold Lake oil sands area, Alberta. 199–221 *in* Pemberton, S. G. (ed): *Applications of ichnology to petroleum exploration: A core workshop*. Society for Sedimentary Geology Core Workshop, Vol. 17. https://doi.org/10.2110/cor.92.01.0199

Beynon, B. M., Pemberton, S. G., Bell, D. D. & Logan, C. A. 1988: Environmental implications of ichnofossils from the lower Cretaceous Grand Rapids Formation, Cold Lake oil sands deposit. 275–290 *in* James, D. P. & Leckie, D. A. (eds): *Sequences, Stratigraphy, Sedimentology: Surface and Subsurface*. Canadian Society of Petroleum Geologists, Memoir 15.

Bhattacharya, J. P. & MacEachern, J. A. 2009: Hyperpycnal rivers and prodeltaic shelves in the Cretaceous seaway of North America. *Journal of Sedimentary Research 79*, 184–209. https://doi.org/10.2110/jsr.2009.026

Billings, E. 1866: *Catalogues of the Silurian Fossils of the island of Anticosti, with descriptions and some new genera and species*. Geological Survey of Canada, Dawson Brothers, Montreal, 93 pp.

Billings, E. 1872: On some fossils from the primordial rocks of Newfoundland. *The Canadian Naturalist 6*, 465–479.

Binney, E. W. 1852: On some trails and holes found in rocks of the Carboniferous strata, with remarks on the Microconchus carbonarius. *Memoirs and proceedings of the Manchester Literary and Philosophical Society 10*, 181–201.

Birgenheier, L. P., Horton, B., McCauley, A. D., Johnson, C. L. & Kennedy, A. 2017: A depositional model for offshore deposits of the lower Blue Gate Member, Mancos Shale, Uinta Basin, Utah, USA. *Sedimentology 64*, 1402–1438. https://doi.org/10.1111/sed.12359

Birkenmajer, K. 1959: *Fucusopsis angulatus* Palibin (Problematica) z warstw pstrych (dan-paleocen) osłony Pienińskiego Pasa Skałkowego. *Annales de la Société Géologique de Pologne 29*, 227–232.

Birkenmajer, K. & Bruton, D. L. 1971: Some trilobite resting and crawling traces. *Lethaia 4*, 303–319. https://doi.org/10.1111/j.1502-3931.1971.tb01926.x

Bjerstedt, T. W. 1987: Latest Devonian–earliest Mississippian nearshore trace-fossil assemblages from west Virginia, Pennsylvania, and Maryland. *Journal of Paleontology 61*, 865–889. https://doi.org/10.1017/S0022336000029279

Bjerstedt, T. W. 1988: Trace fossils from the early Mississippian price delta, southeast west Virginia. *Journal of Paleontology 62*, 506–519.

Blaise, J. & Bouyx, E. 1980: Les séries Cambro-ordoviciennes à Cruziana et le problème de l'extension septentrionale des plateformes « périgondwaniennes » durant le Paléozoïque inférieur. *Comptes Rendus Hebdomadaires des Séances de l'Académie des Sciences 291*, 793–796.

Blanckenhorn, M. 1916: Organische Reste im Mittleren Buntsandstein Hessens. *Sitzungsberichte der Gesellschaft zur Beförderung der gesamten Naturwissenschaften zu Marburg 1916*, 21–43.

Bland, B. H. & Goldring, R. 1995: *Teichichnus* Seilacher 1955 and other trace fossils (Cambrian?) from the Charnian of Central England. *Neues Jahrbuch fur Geologie und Palaontologie Abhandlungen 195*, 5–24. https://doi.org/10.1127/njgpa/195/1995/5

Blanpied, C. & Bellaiche, G. 1981: Bioturbation on the Pelagian platform: ichnofacies variations as paleoclimatic

indicator. *Marine Geology 43*, M49–M57. https://doi.org/10.1016/0025-3227(81)90175-4
Blodgett, R. H., Crabaugh, J. P. & McBride, E. F. 1993: The color of red beds—a geologic perspective. *Soil Color 31*, 127–159. https://doi.org/10.2136/sssaspecpub31.c8
Bokr, P., Mikuláš, R., Budil, P. & Kraft, P. 2021: Early complex tiering pattern: upper Ordovician, Barrandian area, the Czech Republic. *Fossil Imprint 77*, 17–35. https://doi.org/10.37520/fi.2021.003
Bolton, T. E. 1961: *Ordovician and Silurian formations of Anticosti Island, Quebec*. Geological Survey of Canada, Department of Mines and Technical Surveys, Paper 61-26, 18 pp.
Bordonaro, O., Aceñolaza, G. & Pereyra, M. E. 1992: Primeras trazas fósiles de la sierra de Pie de Palo, San Juan, Argentina. *Ciencias 1*, 7–14.
Bordy, E. M., Linkermann, S. & Prevec, R. 2011: Palaeoecological aspects of some invertebrate trace fossils from the mid-to upper Permian Middleton Formation (Adelaide Subgroup, Beaufort Group, Karoo Supergroup), eastern Cape, South Africa. *Journal of African Earth Sciences 61*, 238–244. https://doi.org/10.1016/j.jafrearsci.2011.06.002
Borrello, A. V. 1966: *Paleontografia bonaerense. Fasciculo v. trazas, restos tubiformes y cuerpos fosiles problematicos de la Formacion La Tinta Sierras septentrionales – provincia de Buenos Aires*. Comision de Investigation Cientifica, Provincia de Buenos Aires Gobernacion, 42 pp.
Bottjer, D. J. 1981: Trace fossils from an upper Cretaceous deep-sea fan, Simi Hills, California. 59–62 *in* Link, M. H., Squires, R. L. & Colburn, I. P. (eds): *Simi Hills Cretaceous Turbidites, Southern California, Southern California, Pacific Section, Society Economic Paleontologists and Mineralogists*. Fall Field Trip Guidebook.
Bottjer, D. J. & Ausich, W. I. 1986: Phanerozoic development of tiering in soft substrata suspension-feeding communities. *Paleobiology 12*, 400–420. https://doi.org/10.1017/S0094837300003134
Bottjer, D. J. & Droser, M. L. 1994: The history of Phanerozoic bioturbation. 155–176 *in* Donovan, S. K. (ed): *The Palaeobiology of Trace Fossils*. Johns Hopkins University Press, Baltimore.
Bottjer, D. J., Droser, M. L. & Jablonski, D. 1988: Palaeoenvironmental trends in the history of trace fossils. *Nature 333*, 252–255. https://doi.org/10.1038/333252a0
Boudreau, B. P. 1994: Is burial velocity a master parameter for bioturbation? *Geochimica et Cosmochimica Acta 58*, 1243–1249. https://doi.org/10.1016/0016-7037(94)90378-6
Boudreau, B. P. 1998: Mean mixed depth of sediments: the wherefore and the why. *Limnology and Oceanography 43*, 524–526. https://doi.org/10.4319/lo.1998.43.3.0524
Bouougri, E. & Porada, H. 2002: Mat-related sedimentary structures in Neoproterozoic peritidal passive margin deposits of the West African Craton (Anti-Atlas, Morocco). *Sedimentary Geology 153*, 85–106. https://doi.org/10.1016/S0037-0738(02)00103-3
Bown, T. M. & Kraus, M. J. 1983: Ichnofossils of the alluvial Willwood Formation (lower Eocene), Bighorn Basin, northwest Wyoming, U.S.A. *Palaeogeography, Palaeoclimatology, Palaeoecology 43*, 95–128. https://doi.org/10.1016/0031-0182(83)90050-0
Boyd, C. & McIlroy, D. 2016: Three-dimensional morphology and palaeobiology of the trace fossil *Dactyloidites jordii* nov. isp. from the Carboniferous of England. *Geobios 49*, 257–264. https://doi.org/10.1016/j.geobios.2016.05.004
Boyd, R. 2010: Transgressive wave-dominated coasts. 265–294 *in* James, N. P. & Dalrymple, R. W. (eds): *Facies models 4*. The Geological Association of Canada, St John's.
Boyd, R., Dalrymple, R. & Zaitlin, B. A. 1992: Classification of clastic coastal depositional environments. *Sedimentary Geology 80*, 139–150. https://doi.org/10.1016/0037-0738(92)90037-R
Braddy, S. J. 1998: An overview of the invertebrate ichnotaxa from the Robledo Mountains ichnofauna (lower Permian), southern New Mexico. 93–98 *in* Lucas, S. G., Estep, J. W. & Hoffer, J. M. (eds): *Permian Stratigraphy and Paleontology of the Robledo Mountains, New Mexico*. New Mexico Museum of Natural History and Science, Albuquerque, Bulletin 12.
Braddy, S. J. & Briggs, D. E. 2002: New lower Permian nonmarine arthropod trace fossils from New Mexico and South Africa. *Journal of Paleontology 76*, 546–557. https://doi.org/10.1666/0022-3360(2002)076<0546:NLPNAT>2.0.CO;2
Bradshaw, M. A. 1981: Paleoenvironmental interpretations and systematics of Devonian trace fossils from the Taylor Group (lower Beacon Supergroup), Antarctica. *New Zealand Journal of Geology and Geophysics 24*, 615–652. https://doi.org/10.1080/00288306.1981.10421537
Bradshaw, M. A. 2010: Devonian trace fossils of the Horlick Formation, Ohio Range, Antarctica: systematic description and palaeoenvironmental interpretation. *Ichnos 17*, 58–114. https://doi.org/10.1080/10420941003659329
Brady, L. F. 1947: Invertebrate tracks from the Coconino Sandstone of northern Arizona. *Journal of Paleontology 21*, 466–472.
Brandt, A., Chen, C., Tandberg, A. H. S., Miguez-Salas, O. & Sigwart, J. D. 2023: Complex sublinear burrows in the deep sea may be constructed by amphipods. *Ecology and Evolution 13*, e9867. https://doi.org/10.1002/ece3.9867
Brasier, M. D. 1982: Sea-level changes, facies changes and the late Precambrian—early Cambrian evolutionary explosion. *Precambrian Research 17*, 105–123. https://doi.org/10.1016/0301-9268(82)90050-X
Brasier, M. D. 1989: Towards a biostratigraphy of the earliest skeletal biotas. 117–165 *in* Cowie, J. W. & Brasier M. D. (eds): *The Precambrian-Cambrian boundary*, Clarendon Press, Oxford.
Brasier, M. D. 1992: Background to the Cambrian explosion. *Journal of the Geological Society, London 149*, 585–587. https://doi.org/10.1144/gsjgs.149.4.0585
Brasier, M. D. & Cowie, J. W. 1989: Concluding remarks. 205–209 *in* Cowie, J. W. & Brasier M. D. (eds): *The Precambrian-Cambrian boundary*. Clarendon Press, Oxford.
Brasier, M. D. & Hewitt, R. A. 1979: Environmental setting of fossiliferous rocks from the uppermost Proterozoic–lower Cambrian of central England. *Palaeogeography, Palaeoclimatology, Palaeoecology 27*, 35–57. https://doi.org/10.1016/0031-0182(79)90092-0
Brasier, M. D., Perejón, A. & de San José, M. A. 1979: Discovery of an important fossiliferous Precambrian-Cambrian sequence in Spain. *Estudios Geológicos 35*, 379–383.
Brasier, M. D., Anderson, M. M. & Corfield, R. M. 1992: Oxygen and carbon isotope stratigraphy of early Cambrian carbonates in southeastern Newfoundland and England. *Geological Magazine 129*, 265–279. https://doi.org/10.1017/S001675680001921X
Brasier, M., Cowie, J. & Taylor, M. 1994a: Decision on the Precambrian-Cambrian boundary stratotype. *Episodes 17*, 3–8. https://doi.org/10.18814/epiiugs/1994/v17i1.2/002
Brasier, M. D., Rozanov, A. Y., Zhuravlev, A. Y., Corfield, R. M. & Derry, L. A. 1994b: A carbon isotope reference scale for the lower Cambrian succession in Siberia: report of IGCP Project 303. *Geological Magazine 131*, 767–783. https://doi.org/10.1017/S0016756800012851
Brenchley, P. J., Pickerill, R. K. & Stromberg, S. G. 1993: The role of wave reworking on the architecture of storm sandstone facies, Bell Island Group (Lower Ordovician), eastern Newfoundland. *Sedimentology 40*, 359–382. https://doi.org/10.1111/j.1365-3091.1993.tb01341.x
Brett, C. E., Baarli, B. G., Chowns, T., Cotter, E., Driese, S., Goodman, W. & Johnson, M. E. 1998: Early Silurian condensed intervals, ironstones, and sequence stratigraphy in the Appalachian foreland basin. *New York State Museum Bulletin 491*, 89–143.
Briggs, D. E. 2015: The Cambrian explosion. *Current Biology 25*, R864–R868. https://doi.org/10.1016/j.cub.2015.04.047
Bromley, R. G. 1990: *Trace fossils. Biology and taphonomy*. Unwin Hyman, London, 280 pp.

Bromley, R. G. 1996: *Trace fossils. Biology, taphonomy and applications*. Chapman and Hall, London, 361 pp.

Bromley, R. G. & Asgaard, U. 1972: Freshwater *Cruziana* from the upper Triassic of Jameson Land, east Greenland. *Rapport Grønlands Geologiske Undersøgelse 49*, 7–13. https://doi.org/10.34194/rapggu.v49.7317

Bromley, R. G. & Asgaard, U. 1979: Triassic freshwater ichnocoenoses from Carlsberg Fjord, east Greenland. *Palaeogeography, Palaeoclimatology, Palaeoecology 28*, 39–80. https://doi.org/10.1016/0031-0182(79)90112-3

Bromley, R. G. & Asgaard, U. 1991: Ichnofacies: a mixture of taphofacies and biofacies. *Lethaia 24*, 153–163. https://doi.org/10.1111/j.1502-3931.1991.tb01463.x

Bromley, R. G. & Ekdale, A. A. 1986: Composite ichnofabrics and tiering of burrows. *Geological Magazine 123*, 59–65. https://doi.org/10.1017/S0016756800026534

Bromley, R. G. & Frey, R. W. 1974: Redescription of the trace fossil *Gyrolithes* and taxonomic evaluation of *Thalassinoides*, *Ophiomorpha* and *Spongeliomorpha*. *Bulletin of the Geological Society of Denmark 23*, 311–335.

Bromley, R. G. & Hanken, N.-M. 1991: The growth vector in trace fossils: examples from the lower Cambrian of Norway. *Ichnos 1*, 261–276. https://doi.org/10.1080/10420949109386361

Bryant, I. D. & Pickerill, R. K. 1990: Lower Cambrian trace fossils from the Buen Formation of central North Greenland: preliminary observations. *Rapport Grønlands Geologiske Undersøgelse 147*, 44–62. https://doi.org/10.34194/rapggu.v147.8106

Buatois, L. A. 2018: *Treptichnus pedum* and the Ediacaran–Cambrian boundary: significance and caveats. *Geological Magazine 155*, 174–180. https://doi.org/10.1017/S0016756817000656

Buatois, L. A., Jalfin, G. & Aceñolaza, F. G. 1997: Permian nonmarine invertebrate trace fossils from southern Patagonia, Argentina: ichnologic signatures of substrate consolidation and colonization sequences. *Journal of Paleontology 71*, 324–336. https://doi.org/10.1017/S0022336000039238

Buatois, L. A. & Mángano, M. G. 1992: La oxigenación como factor de control en la distribución de asociaciones de trazas fósiles. Formación Kotich Point, Cretácico de Antártida. *Ameghiniana 29*, 69–84.

Buatois, L. A. & Mángano, M. G. 1993a: Trace fossils from a Carboniferous turbiditic lake: implications for the recognition of additional nonmarine ichnofacies. *Ichnos 2*, 237–258. https://doi.org/10.1080/10420949309380098

Buatois, L. A. & Mángano, M. G. 1993b: The ichnotaxonomic status of *Plangtichnus* and *Treptichnus*. *Ichnos 2*, 217–224. https://doi.org/10.1080/10420949309380095

Buatois, L. A. & Mángano, M. G. 1995: Post glacial lacustrine event sedimentation in an ancient mountain setting: Carboniferous Lake Malanzán (western Argentina). *Journal of Paleolimnology 14*, 1–22. https://doi.org/10.1007/BF00682591

Buatois, L. A., & Mángano, M. G. 1998: Trace fossil analysis of lacustrine facies and basins. *Palaeogeography, Palaeoclimatology, Palaeoecology 140*, 367–382. https://doi.org/10.1016/S0031-0182(98)00020-0

Buatois, L. A. & Mángano, M. G. 2002: Trace fossils from Carboniferous floodplain deposits in western Argentina: implications for ichnofacies models of continental environments. *Palaeogeography, Palaeoclimatology, Palaeoecology 183*, 71–86. https://doi.org/10.1016/S0031-0182(01)00459-X

Buatois, L. A. & Mángano, M. G. 2003a: Sedimentary facies, depositional evolution of the upper Cambrian–lower Ordovician Santa Rosita Formation in northwest Argentina. *Journal of South American Earth Sciences 16*, 343–363. https://doi.org/10.1016/S0895-9811(03)00097-X

Buatois, L. A. & Mángano, M. G. 2003b: La icnofauna de la Formación Puncoviscana en el noroeste Argentino : la colonización de fondos oceánicos y reconstrucción de paleoambientes y paleoecosistemas de la transición precámbrica-cámbrica. *Ameghiniana 40*, 53–70.

Buatois, L. A. & Mángano, M. G. 2003c: Early colonization of the deep sea: ichnologic evidence of deep-marine benthic ecology from the early Cambrian of northwest Argentina. *Palaios 18*, 572–581. https://doi.org/10.1669/0883-1351(2003)018<0572:ECOTDS>2.0.CO;2

Buatois, L. A. & Mángano, M. G. 2003d: Caracterización icnológica y paleoambiental de la localidad tipo de *Orchesteropus atavus* Frenguelli, Huerta de Huachi, provincia de San Juan, Argentina. *Ameghiniana 40*, 103–117.

Buatois, L. A. & Mángano, M. G. 2004a: Terminal Proterozoic–early Cambrian ecosystems: ichnology of the Puncoviscana Formation, northwest Argentina. *Fossils and Strata 51*, 1–16. https://doi.org/10.18261/9781405169851-2004-01

Buatois, L. A. & Mángano, M. G. 2004b: Animal-substrate interactions in freshwater environments: applications of ichnology in facies and sequence stratigraphic analysis of fluvio-lacustrine successions. *Geological Society, London, Special Publications 228*, 311–333. https://doi.org/10.1144/GSL.SP.2004.228.01.14

Buatois, L. A. & Mángano, M. G. 2009: Applications of ichnology in lacustrine sequence stratigraphy: potential and limitations. *Palaeogeography, Palaeoclimatology, Palaeoecology 272*, 127–142. https://doi.org/10.1016/j.palaeo.2008.10.012

Buatois, L. A. & Mángano, M. G. 2011: *Ichnology. Organism-substrate interactions in space and time*. Cambridge University Press, 358 pp.

Buatois, L. A. & Mángano, M. G. 2012a: An early Cambrian shallow-marine ichnofauna from the Puncoviscana Formation of northwest Argentina: the interplay between sophisticated feeding behaviors, matgrounds and sea-level changes. *Journal of Paleontology 86*, 7–18. https://doi.org/10.1666/11-001.1

Buatois, L. A. & Mángano, M. G. 2012b: Ichnology of the Ediacaran-Cambrian Puncoviscana Formation of northwestern Argentina: recent progress in understanding its potential in paleoecology and macroevolution. *Ichnology of Latin America, Selected Papers, Monografias da Sociedade Brasileira de Paleontologia 2*, 27–36.

Buatois, L. A. & Mángano, M. G. 2016: Ediacaran ecosystems and the dawn of animals. 27–72 *in* Mángano, M. G. & Buatois, L. A. (eds): *The Trace Fossil Record of Major Evolutionary Events Volume 1, Precambrian and Paleozoic*. Topics in Geobiology, Springer. https://doi.org/10.1007/978-94-017-9600-2_2

Buatois, L. A., Mangano, M. G., Wu, X. & Zhang, G. 1995: *Vagorichnus*, a new ichnogenus for feeding burrow systems and its occurrence as discrete and compound ichnotaxa in Jurassic lacustrine turbidites of central China. *Ichnos 3*, 265–272.

Buatois, L. A., Mángano, M. G., Wu, X. & Zhang, G. 1996: Trace fossils from Jurassic lacustrine turbidites of the Anyao Formation (central China) and their environmental and evolutionary significance. *Ichnos 4*, 287–303. https://doi.org/10.1080/10420949509386396

Buatois, L. A., Mangano, M. G., Maples, C. G. & Lanier, W. P. 1998a: Ichnology of an upper Carboniferous fluvio-estuarine paleovalley: the Tonganoxie sandstone, Buildex quarry, eastern Kansas, USA. *Journal of Paleontology 72*, 152–180. https://doi.org/10.1017/S0022336000024094

Buatois, L. A., Mángano, M. G., Maples, C. G. & Lanier, W. P. 1998b: Taxonomic reassessment of the ichnogenus *Beaconichnus* and additional examples from the Carboniferous of Kansas, USA. *Ichnos 5*, 287–302. https://doi.org/10.1080/10420949809386427

Buatois, L. A., Mangano, M. G., Mikuláš, R. & Maples, C. G. 1998c: The ichnogenus *Curvolithus* revisited. *Journal of Paleontology 72*, 758–769. https://doi.org/10.1017/S0022336000040452

Buatois, L. A., Mángano, M. G., Maples, C. G. & Lanier, W. P. 1998d: Allostratigraphic and sedimentologic applications of trace fossils to the study of incised estuarine valleys: an example from the Virgilian Tonganoxie Sandstone Member of eastern Kansas. *Current Research in Earth Sciences, Kansas Geological Survey 241*, 1–27. https://doi.org/10.17161/cres.v0i241.11782

Buatois, L. A., Mángano, M. G., Fregenal-Martínez, M. A. & de Gibert, J. M. 2000: Short-term colonization trace-fossil assemblages in a carbonate lacustrine Konservat-Lagerstätte (Las Hoyas fossil site, Lower Cretaceous, Cuenca, Central Spain). *Facies 43*, 145–156. https://doi.org/10.1007/BF02536988

Buatois, L. A., Gingras, M. K., MacEachern, J., Mángano, M. G., Zonneveld, J. P., Pemberton, S. G., Netto, R. G. & Martin, A. 2005: Colonization of brackish-water systems through time: evidence from the trace-fossil record. *Palaios 20*, 321–347. https://doi.org/10.2110/palo.2004.p04-32

Buatois, L. A., Netto, R. G., Mángano, M. G. & Balistieri, P. R. 2006: Extreme freshwater release during the late Paleozoic Gondwana deglaciation and its impact on coastal ecosystems. *Geology 34*, 1021–1024. https://doi.org/10.1130/G22994A.1

Buatois, L. A., Mángano, M. G., Brussa, E. D., Benedetto, J. L. & Pompei, J. F. 2009: The changing face of the deep: colonization of the early Ordovician deep-sea floor, Puna, northwest Argentina. *Palaeogeography, Palaeoclimatology, Palaeoecology 280*, 291–299. https://doi.org/10.1016/j.palaeo.2009.06.014

Buatois, L. A. Almond, J. & Germs, G. J. 2013: Environmental tolerance and range offset of *Treptichnus pedum*: implications for the recognition of the Ediacaran-Cambrian boundary. *Geology 41*, 519–522. https://doi.org/10.1130/G33938.1

Buatois, L. A., Narbonne, G. M., Mángano, M. G., Carmona, N. B. & Myrow, P. 2014: Ediacaran matground ecology persisted into the earliest Cambrian. *Nature Communications 5*, 3544. https://doi.org/10.1038/ncomms4544

Buatois, L. A., Mángano, M. G., Olea, R. A. & Wilson, M.A. 2016a: Decoupled evolution of soft and hard substrate communities during the Cambrian Explosion and Great Ordovician Biodiversification Event. *Proceedings of the National Academy of Sciences 113*, 6945–6948. https://doi.org/10.1073/pnas.1523087113

Buatois, L. A., García-Ramos, J. C., Piñuela, L., Mángano, M. G. & Rodríguez-Tovar, F. J. 2016b: *Rosselia socialis* from the Ordovician of Asturias (northern Spain) and the early evolution of equilibrium behavior in polychaetes. *Ichnos 23*, 147–155. https://doi.org/10.1080/10420940.2015.1132213

Buatois, L. A., Wisshak, M., Wilson, M. A. & Mángano, M. G. 2017: Categories of architectural designs in trace fossils: a measure of ichnodisparity. *Earth-Science Reviews 164*, 102–181. https://doi.org/10.1016/j.earscirev.2016.08.009

Buatois, L. A., Almond, J., Mángano, M. G., Jensen, S. & Germs, G. J. B. 2018: Sediment disturbance by Ediacaran bulldozers and the roots of the Cambrian explosion. *Scientific Reports 8*, 4514. https://doi.org/10.1038/s41598-018-22859-9

Buatois, L. A., Mángano, M. G. & Pattison, S. A. J. 2019: Ichnology of prodeltaic hyperpycnite–turbidite channel complexes and lobes from the upper Cretaceous Prairie Canyon Member of the Mancos Shale, Book Cliffs, Utah, USA. *Sedimentology 66*, 1825–1860. https://doi.org/10.1111/sed.12560

Buatois, L. A., Mángano, M. G., Minter, N. J., Zhou, K., Wisshak, M., Wilson, M. A. & Olea, R. A. 2020: Quantifying ecospace utilization and ecosystem engineering during the early Phanerozoic—the role of bioturbation and bioerosion. *Science Advances 6*, eabb0618. https://doi.org/10.1126/sciadv.abb0618

Buatois, L. A., Mángano, M. G. & Carmona, N. B. 2023: *Scolicia*, ichnotaxonomic practices, and the limits of behavioural convergence. *Ichnos 30*, 338–361. https://doi.org/10.1080/10420940.2024.2325468

Buatois, L. A., Mángano, M. G., Gougeon, R., Gilbert, F., Cabrera De Leo, F., Godbold, J. A. & Solan, M. 2025b: Biogenic sediment mixing: bridging the gap between the modern and the ancient. Palaios 40, 248–257. https://doi.org/10.2110/palo.2025.011

Buatois, L. A., Mángano, M. G., Paz, M., Minter, N. J. & Zhou, K. 2025a: Early colonization of the deep-sea bottom—the protracted build-up of an ecosystem. *Proceedings of the National Academy of Sciences 122,* e2414752122. https://doi.org/10.1073/pnas.2414752122

Buchanan, J. B. & Hedley, R. H. 1960: A contribution to the biology of *Astrorhiza limicola* (Foraminifera). *Journal of the Marine Biological Association of the United Kingdom 39*, 549–560. https://doi.org/10.1017/S0025315400013540

Buck, S. G. & Goldring, R. 2003: Conical sedimentary structures, trace fossils or not? Observations, experiments, and review. *Journal of Sedimentary Research 73*, 338–353. https://doi.org/10.1306/091602730338

Buckman, J. O. 1992: *Lower Carboniferous trace fossils from northwest Ireland*. Unpublished Doctoral Dissertation, Aston University, 335 pp.

Buckman, J. O. 1994a: *Archaeonassa* Fenton and Fenton 1937 reviewed. *Ichnos 3*, 185–192. https://doi.org/10.1080/10420949409386387

Buckman, J. O. 1994b: *Rhizocorallium* Zenker 1836 not *Teichichnus repandus* Chamberlain 1977. *Ichnos 3*, 135–136. https://doi.org/10.1080/10420949409386381

Buckman, J. O. 1995: A comment on annulate forms of *Palaeophycus* Hall 1847: with particular reference to *P.'annulatus' sensu* Pemberton and Frey 1982, and the erection of *P. crenulatus* ichnosp. nov. *Ichnos 4*, 131–140. https://doi.org/10.1080/10420949509380120

Buckman, J. O. 1996: *Heimdallia* from the lower Carboniferous of Ireland: *H. mullaghmori* a new ichnospecies, and re-evaluation of the three-dimensional format of the ichnogenus. *Ichnos 5*, 43–51. https://doi.org/10.1080/10420949609386405

Budd, G. E. & Jensen, S. 2000: A critical reappraisal of the fossil record of the bilaterian phyla. *Biological Reviews 75*, 253–295. https://doi.org/10.1111/j.1469-185X.1999.tb00046.x

Budd, G. E. & Jensen, S. 2017: The origin of the animals and a 'Savannah' hypothesis for early bilaterian evolution. *Biological Reviews 92*, 446–473. https://doi.org/10.1111/brv.12239

Budd, G. E. & Telford, M. J. 2009: The origin and evolution of arthropods. *Nature 457*, 812–817. https://doi.org/10.1038/nature07890

Bureau, E. 1886: Sur la formation de bilobites à l'époque actuelle. *Compte Rendu Hebdomadaires des Séances de l'Académie des Sciences 103*, 1164–1167.

Burri, P., du Dresnay, R. & Wagner, C. W. 1973: Tepee structures and associated diagenetic features in intertidal carbonate sands (lower Jurassic, Morocco). *Sedimentary Geology 9*, 221–228. https://doi.org/10.1016/0037-0738(73)90046-8

Butterfield, N. 2018: Oxygen, animals and aquatic bioturbation: an updated account. *Geobiology 16*, 3–16. https://doi.org/10.1111/gbi.12267

Byers, C. W. 1982: Geological significance of marine biogenic sedimentary structures. 221–256 *in* McCall, P. L. & Tevesz, M. J. S. (eds): *Animal-Sediment Relations. The Biogenic Alteration of Sediments*. Topics in Geobiology, 100, Springer. https://doi.org/10.1007/978-1-4757-1317-6_5

Callow, R. H., McIlroy, D. & Brasier, M. D. 2011: John Salter and the Ediacara fauna of the Longmyndian Supergroup. *Ichnos 18*, 176–187. https://doi.org/10.1080/10420940.2011.606516

Campbell, K. S. W. 1975: The functional morphology of *Cryptolithus*. *Fossils and Strata 4*, 65–86. https://doi.org/10.18261/8200049639-1975-04

Carbone, C. & Narbonne, G. M. 2014: When life got smart: the evolution of behavioral complexity through the Ediacaran and early Cambrian of NW Canada. *Journal of Paleontology 88*, 309–330. https://doi.org/10.1666/13-066

Carmona, N. B., Mángano, M. G., Buatois, L. A. & Ponce, J. J. 2010: Taphonomy and paleoecology of the bivalve trace fossil *Protovirgularia* in deltaic heterolithic facies of the Miocene Chenque Formation, Patagonia, Argentina. *Journal of Paleontology 84*, 730–738. https://doi.org/10.1666/09-119.1

Carroll, S. & Trewin, N. H. 1995: *Cornulatichnus*: a new trace fossil from the Old Red Sandstone of Orkney. *Scottish Journal of Geology 31*, 37–41. https://doi.org/10.1144/sjg31010037

Caruso, C., Cianflone, G., Dominici, R., Sonnino, M. & Veltri, M. 2013: Continental to marine deposits of the Stilo-Capo d'Orlando Formation (Oligo-Miocene) in the area of Agnana Calabra (southern Ionian Calabria, Italy); inferred from sedimentological and ichnological data. *Journal of Mediterranean Earth Sciences Special Issue*, 27–29.

Cattaneo, A., Correggiari, A., Langone, L. & Trincardi, F. 2003: The late-Holocene Gargano subaqueous delta, Adriatic shelf: sediment pathways and supply fluctuations. *Marine Geology 193*, 61–91. https://doi.org/10.1016/S0025-3227(02)00614-X

Chafetz, H. S. 1978: A trough cross-stratified glaucarenite: a Cambrian tidal inlet accumulation. *Sedimentology 25*, 545–559. https://doi.org/10.1111/j.1365-3091.1978.tb02079.x

Chafetz, H. S. 1979: Petrology of carbonate nodules from a Cambrian tidal inlet accumulation, central Texas. *Journal of Sedimentary Petrology 49*, 215–222. https://doi.org/10.1306/212F76F8-2B24-11D7-8648000102C1865D

Chamberlain, C. K. 1971: Morphology and ethology of trace fossils from the Ouachita Mountains, southeast Oklahoma. *Journal of Paleontology 45*, 212–246.

Chamberlain, C. K. 1975: Recent lebensspuren in nonmarine aquatic environments. 431–458 *in* Frey, R. W. (ed): *The Study of Trace Fossils. A Synthesis of Principles, Problems, and Procedures in Ichnology*. Springer-Verlag, Berlin. https://doi.org/10.1007/978-3-642-65923-2_19

Chamberlain, C. K. 1977: Ordovician and Devonian trace fossils from Nevada. *Nevada Bureau of Mines and Geology Bulletin 90*, 4–24.

Chamberlain, C.K. 1978: Recognition of trace fossils in cores. 133–183 *in* Basan, P. B. (ed): *Trace Fossil Concepts*. SEPM Short Course 5. https://doi.org/10.2110/scn.77.01.0133

Chamberlain, C. K. & Clark, D. L. 1973: Trace fossils and conodonts as evidence for deep-water deposits in the Oquirrh Basin of central Utah. *Journal of Paleontology 47*, 663–682.

Chapman, F. 1928: On some remarkable annelid remains from Arthur River, NW Tasmania. *Royal Society of Tasmania, Papers and Proceedings for 1928*, 1–5.

Cheel, R.J. & Leckie, D.A. 1993: Hummocky cross-stratification. 103–122 *in* Wright, V. P. (ed): *Sedimentology review 1*. Blackwell Scientific Publications. https://doi.org/10.1002/9781444304534.ch7

Chen, J. & Lee, H. S. 2013: Soft-sediment deformation structures in Cambrian siliciclastic and carbonate storm deposits (Shandong Province, China): differential liquefaction and fluidization triggered by storm-wave loading. *Sedimentary Geology 288*, 81–94. https://doi.org/10.1016/j.sedgeo.2013.02.001

Chen, S., Steel, R. J. & Olariu, C. 2015: Palaeo-Orinoco (Pliocene) channels on the tide-dominated Morne L'Enfer delta lobes and estuaries, SW Trinidad. 227–281 *in* Ashworth, P .J., Best, J .L. & Parsons, D. R. (eds): *Developments in Sedimentology*. Elsevier, Volume 68. https://doi.org/10.1016/B978-0-444-63529-7.00010-9

Chen, Z. & Liu, Y. 2025: Advent of three-dimensional sediment exploration reveals Ediacaran-Cambrian ecosystem transition. *Science Advances 11*, eadx9449. https://doi.org/10.1126/sciadv.adx9449

Chen, Z.-Q., Tong, J. & Fraiser, M. L. 2011: Trace fossil evidence for restoration of marine ecosystems following the end-Permian mass extinction in the Lower Yangtze region, South China. *Palaeogeography, Palaeoclimatology, Palaeoecology 299*, 449–474. https://doi.org/10.1016/j.palaeo.2010.11.023

Cherif, A., Naimi, M. N., & Belaid, M. 2022: Oxfordian plug-shaped trace fossils from northwestern Algeria. *Proceedings of the Geologists' Association 133*, 518–525. https://doi.org/10.1016/j.pgeola.2022.06.006

Cheriton, O. M., McPhee-Shaw, E. E., Shaw, W. J., Stanton, T. P., Bellingham, J. G. & Storlazzi, C. D. 2014: Suspended particulate layers and internal waves over the southern Monterey Bay continental shelf: an important control on shelf mud belts? *Journal of Geophysical Research: Oceans 119*, 428–444. https://doi.org/10.1002/2013JC009360

Chisholm, J. I. 1970: *Teichichnus* and related trace-fossils in the lower Carboniferous at St. Monance, Scotland. *Bulletin of the Geological Survey of Great Britain 32*, 21–51.

Choi, K. 2011: Tidal rhythmites in a mixed-energy, macrotidal estuarine channel, Gomso Bay, west coast of Korea. *Marine Geology 280*, 105–115. https://doi.org/10.1016/j.margeo.2010.12.004

Chu, Q. 1988: Trace fossils from the Xuzhuang Formation (Middle Cambrian) of Liujiang Basin (Funing, Hebei Prov.) and their depositional environments. *Acta Scientiarum Naturalium 24*, 220–234.

Clark, R. B. 1964: *Dynamics of Metazoan Evolution: The Origin of the Coelom and Segments*. Clarendon Press, Oxford, 313 pp.

Clarke, J. M. & Swartz, C. K. 1913: Systematic paleontology of the upper Devonian deposits of Maryland. 535–701 *in*: *Maryland Geological Survey. Middle and upper Devonian*. The John Hopkins Press, Baltimore.

Clausen, C. K. & Vilhjálmsson, M. 1986: Substrate control of lower Cambrian trace fossils from Bornholm, Denmark. *Palaeogeography, Palaeoclimatology, Palaeoecology 56*, 51–68. https://doi.org/10.1016/0031-0182(86)90107-0

Clifton, H. E. 1981: Progradational sequences in Miocene shoreline deposits, southeastern Caliente Range, California. *Journal of Sedimentary Petrology 51*, 165–184. https://doi.org/10.1306/212F7C39-2B24-11D7-8648000102C1865D

Clifton, H. E. & Thompson, J. K. 1978: *Macaronichnus segregatis*: a feeding structure of shallow marine polychaetes. *Journal of Sedimentary Petrology 48*, 1293–1302. https://doi.org/10.1306/212F7667-2B24-11D7-8648000102C1865D

Clifton, H. E., Hunter, R. E. & Phillips, R. L. 1971: Depositional structures and processes in the non-barred high-energy nearshore. *Journal of Sedimentary Petrology 41*, 651–670. https://doi.org/10.1306/74D7231A-2B21-11D7-8648000102C1865D

Cloud Jr., P. E. 1968: Pre-metazoan evolution and the origins of the Metazoa. 1–72 *in* Drake, E. T. (ed): *Evolution and environment*. Yale University Press, New Haven.

Cloud Jr., P. E. & Nelson, C. A. 1966: Phanerozoic-Cryptozoic and related transitions: new evidence. *Science 154*, 766–770. https://doi.org/10.1126/science.154.3750.766

Coleman, M. L. 1993: Microbial processes: controls on the shape and composition of carbonate concretions. *Marine Geology 113*, 127–140. https://doi.org/10.1016/0025-3227(93)90154-N

Collette, J. H., Hagadorn, J. W. & Lacelle, M. A. 2010: Dead in their tracks—Cambrian arthropods and their traces from intertidal sandstones of Quebec and Wisconsin. *Palaios 25*, 475–486. https://doi.org/10.2110/palo.2009.p09-134r

Collette, J. H., Getty, P. R. & Hagadorn, J. W. 2011: Insights into an early Jurassic dinosaur habitat: ichnofacies and enigmatic structures from the Portland Formation, Hoover Quarry, Massachusetts, USA. *Atlantic Geology 47*, 81–98. https://doi.org/10.4138/atlgeol.2011.003

Collins, A. G., Lipps, J. H. & Valentine, J. W. 2000: Modern muco-ciliary creeping trails and the bodyplans of Neoproterozoic trace-makers. *Paleobiology 26*, 47–55. https://doi.org/10.1666/0094-8373(2000)026<0047:MMCTAT>2.0.CO;2

Compston, W., Zhang, Z., Cooper, J. A., Ma, G. & Jenkins, R. J. F. 2008: Further SHRIMP geochronology on the early Cambrian of South China. *American Journal of Science 308*, 399–420. https://doi.org/10.2475/04.2008.01

Cónsole-Gonella, C. & Aceñolaza, F. G. 2013: *Meanderovaleichnus huenickeni* ichnogen. et ichnosp. nov. from the Bajo de Vélez Formation (upper Carboniferous-Permian), Argentina: a new case of worm-type burrowing. *Spanish Journal of Palaeontology 29*, 51–60. https://doi.org/10.7203/sjp.29.1.17488

Conti, S. & Serventi, P. 2023: Paleoecology of a new Gyrolithes ichnospecies as a component of a compound trace fossil from the Middle Miocene Marnoso-arenacea Formation (northern Apennines, Italy). *Bollettino Della Società Paleontologica Italiana 62,* 85–103. https://dx.doi.org/10.4435/BSPI.2023.04

Conway Morris, S. 1987: The search for the Precambrian-Cambrian boundary. *American Scientist 75*, 156–167.

Conway Morris, S. 1989: South-eastern Newfoundland and adjacent areas (Avalon Zone). 7–39 *in* Cowie, J.W. & Brasier M.D. (eds): *The Precambrian-Cambrian boundary*. Clarendon Press, Oxford.

Cooper, M. R. 1984: *Cruziana acacencis*–the first Silurian index-trace fossil from South Africa. Discussion. *Transactions of the Geological Society of South Africa 87*, 53–54.

Cope, J. C. W. 1982: Precambrian fossils of the Carmarthen area, Dyfed. *Nature in Wales 1*, 11–16.

Corner, G. D. & Fjalstad, A. 1993: Spreite trace fossils (*Teichichnus*) in a raised Holocene fjord-delta, Breidvikeidet, Norway. *Ichnos 2*, 155–164. https://doi.org/10.1080/10420949309380085

Cornish, F. G. 1986: The trace-fossil *Diplocraterion*: evidence of animal-sediment interactions in Cambrian tidal deposits. *Palaios 1*, 478–491. https://doi.org/10.2307/3514630

Corrêa, L. M. S. A. & Fernandes, A. C. S. 2002: *Cochlichnus lagartensis* Muniz, 1980: um caso de gretas de contração senoidais. *Boletim do Museu Nacional, Nova Série, Geologia 66*, 1–12.

Corsetti, F. A. & Hagadorn, J. W. 2003: The Precambrian-Cambrian transition in the southern Great Basin, USA. *The Sedimentary Record 1*, 4–8. https://doi.org/10.2110/sedred.2003.1.4

Cotter, E. 1977: The evolution of fluvial style, with special reference to the central Appalachian Paleozoic. 361–383 *in* Miall, A.D. (ed): *Fluvial Sedimentology*. Canadian Society of Petroleum Geologists Memoir, vol. 5.

Counts, J. W., Rarity, F., Ainsworth, R. B., Amos, K. J., Lane, T., Morón, S., Trainor, J., Valenti, C. & Nanson, R. 2016: Sedimentological interpretation of an Ediacaran delta: Bonney Sandstone, south Australia. *Australian Journal of Earth Sciences 63*, 257–273. https://doi.org/10.1080/08120099.2016.1180322

Coutret, B., Néraudeau, D., Gendry, D., Loi, A. & Poujol, M. 2024: The Lower Cambrian deposits of the Le Rozel Formation (Normandy, NW France): insight into a newly described ichnofossil assemblage. *Palaeogeography, Palaeoclimatology, Palaeoecology 641*, 112126. https://doi.org/10.1016/j.palaeo.2024.112126

Cowie, J. W. 1978: IUGS/IGCP Project 29 Precambrian–Cambrian boundary working group in Cambridge, 1978. *Geological Magazine 115*, 151–152. https://doi.org/10.1017/S0016756800041212

Cowie, J. W. 1989: Introduction. 3–6 *in* Cowie, J. . & Brasier, M. D. (eds): *The Precambrian-Cambrian Boundary*. Clarendon Press, Oxford.

Cowie, J. W. 1992: Two decades of research on the Proterozoic-Phanerozoic transition: 1972-1991. *Journal of the Geological Society, London 149*, 589–592. https://doi.org/10.1144/gsjgs.149.4.0589

Cowie, J. W. & Glaessner, M. F. 1975: The Precambrian-Cambrian boundary: a symposium. *Earth-Science Reviews 11*, 209–251. https://doi.org/10.1016/0012-8252(75)90120-8

Cowie, J. W. & Spencer, A. M. 1970: Trace fossils from the late Precambrian/lower Cambrian of east Greenland. 91–100 *in* Crimes, T .P. & Harper, J. C. (eds): *Trace Fossils*. Seel House Press, Liverpool.

Cowie, J. W., Ziegler, W., Boucot, A. J., Bassett, M. G. & Remane, J. 1986: Guidelines and statutes of the International Commission on Stratigraphy (ICS). *Courier Forschungsinstitut Senckenberg 83*, 1–14.

Coysh, A. W. 1931: U-shaped burrows in the lower Lias of Somerset and Dorset. *Geological Magazine 68*, 13–15. https://doi.org/10.1017/S0016756800002806

Craig, G. Y. & Walton, E. K. 1962: Sedimentary structures and palaeocurrent directions from the Silurian rocks of Kirkcudbright. *Transactions of the Edinburgh Geological Society 19*, 100–119. https://doi.org/10.1144/transed.19.1.100

Cribb, A. T., Kenchington, C. G., Koester, B., Gibson, B. M., Boag, T. H., Racicot, R. A., Mocke, H., Laflamme, M. & Darroch, S. A. F. 2019: Increase in metazoan ecosystem engineering prior to the Ediacaran–Cambrian boundary in the Nama Group, Namibia. *Royal Society Open Science 6*, 190548. https://doi.org/10.1098/rsos.190548

Crimes, T. P. 1968: *Cruziana*: a stratigraphically useful trace fossil. *Geological Magazine 105*, 360–364. https://doi.org/10.1017/S001675680005439X

Crimes, T. P. 1969: Trace fossils from the Cambro-Ordovician rocks of north Wales and their stratigraphic significance. *Geological Journal 6*, 333–338. https://doi.org/10.1002/gj.3350060214

Crimes, T. P. 1970: Trilobite tracks and other trace fossils from the upper Cambrian of north Wales. *Geological Journal 7*, 47–68. https://doi.org/10.1002/gj.3350070104

Crimes, T. P. 1975a: Trilobite traces from the lower Tremadoc of Tortworth. *Geological Magazine 112*, 33–46. https://doi.org/10.1017/S0016756800045568

Crimes, T. P. 1975b: The production and preservation of trilobite resting and furrowing traces. *Lethaia 8*, 35–48. https://doi.org/10.1111/j.1502-3931.1975.tb00914.x

Crimes, T. P. 1977: Trace fossils of an Eocene deep-sea sand fan, northern Spain. 71–90 *in* Crimes, T. P. & Harper, J. C. (eds): *Trace Fossils 2*. Seel House Press, Liverpool.

Crimes, T. P. 1981: Lower Palaeozoic trace fossils of Africa. 189–198 *in* Holland, C. H. (ed): *Lower Palaeozoic of the Middle East, Eastern and Southern Africa, and Antarctica*. John Wiley and Sons.

Crimes, T. P. 1987: Trace fossils and correlation of late Precambrian and early Cambrian strata. *Geological Magazine 124*, 97–119. https://doi.org/10.1017/S0016756800015922

Crimes, T. P. 1989: Trace fossils. 166–185 *in* Cowie, J. W. & Brasier M. D. (eds): *The Precambrian-Cambrian boundary*. Clarendon Press, Oxford.

Crimes, T. P. 1992a: Changes in the trace fossil biota across the Proterozoic-Phanerozoic boundary. *Journal of the Geological Society, London 149*, 637–646. https://doi.org/10.1144/gsjgs.149.4.0637

Crimes, T. P. 1992b: The record of trace fossils across the Proterozoic—Cambrian boundary. 177–202 *in* Lipps, J.H. & Signor, P.W. (eds): *Origin and Early Evolution of the Metazoa*. Topics in Geobiology, 10, Springer. https://doi.org/10.1007/978-1-4899-2427-8_6

Crimes, T. P. 1994: The period of early evolutionary failure and the dawn of evolutionary success: the record of biotic changes across the Precambrian-Cambrian boundary. 105–133 *in* Donovan, S. K. (ed): *The Palaeobiology of Trace Fossils*. Johns Hopkins University Press, Baltimore.

Crimes, T. P. & Anderson, M. M. 1985: Trace fossils from late Precambrian-early Cambrian strata of southeastern Newfoundland (Canada): temporal and environmental implications. *Journal of Paleontology 59*, 310–343. https://doi.org/10.1017/S0016756800015922

Crimes, T. P. & Crossley, J. D. 1991: A diverse ichnofauna from Silurian flysch of the Aberystwyth Grits Formation, Wales. *Geological Journal 26*, 27–64. https://doi.org/10.1002/gj.3350260104

Crimes, T. P. & Fedonkin, M. A. 1994: Evolution and dispersal of deepsea traces. *Palaios 9*, 74–83. https://doi.org/10.2307/3515080

Crimes, T. P. & Germs, G. J. 1982: Trace fossils from the Nama Group (Precambrian-Cambrian) of southwest Africa (Namibia). *Journal of Paleontology 4*, 890–907.

Crimes, T. P. & Jiang, Z. 1986: Trace fossils from the Precambrian–Cambrian boundary candidate at Meishucun, Jinning, Yunnan, China. *Geological Magazine 123*, 641–649. https://doi.org/10.1017/S0016756800024158

Crimes, T. P., Goldring, R., Homewood, P., van Stuijvenberg, J. & Winkler, W. 1981: Trace fossil assemblages of deep-sea fan deposits, Gurnigel and Schlieren flysch (Cretaceous-Eocene), Switzerland. *Eclogae Geologicae Helvetiae 74*, 953–995. https://doi.org/10.5169/seals-165136

Crimes, T. P., Legg, I., Marcos, A. & Arboleya, M. 1977: ?Late Precambrian–low lower Cambrian trace fossils from Spain. 91–138 *in* Crimes, T. P. and Harper, J. C. (eds): *Trace Fossils 2*. Seel House Press, Liverpool.

Crimes, T. P., Garcia Hidalgo, J. F. & Poire, D. G. 1992: Trace fossils from Arenig flysch sediments of Eire and their bearing on the early colonisation of the deep seas. *Ichnos 2*, 61–77. https://doi.org/10.1080/10420949209380076

Crimes, T. P. & McCall, G. J. H. 1995: A diverse ichnofauna from Eocene-Miocene rocks of the Makran Range (SE Iran). *Ichnos 3*, 231–258. https://doi.org/10.1080/10420949509386394

Cui, H., Kaufman, A. J., Zou, H., Kattan, F. H., Trusler, P., Smith, J., Ivantsov, A. Y., Rich, T. H., Al Qubsani, A., Yazedi, A., Liu, X.-M., Johnson, P., Goderis, S., Claeys, P. & Vickers-Rich, P. 2020: Primary or secondary? A dichotomy of the strontium isotope anomalies in the Ediacaran carbonates of Saudi Arabia. *Precambrian Research 343*, 105720. https://doi.org/10.1016/j.precamres.2020.105720

Cui, Y., Lang, X., Li, F., Huang, K., Ma, H., Li, C., Pei, H., Li, C., Zhou, C. & Shen, B. 2019: Germanium/silica ratio and rare

earth element composition of silica-filling in sheet cracks of the Doushantuo cap carbonates, South China: constraining hydrothermal activity during the Marinoan snowball Earth glaciation. *Precambrian Research 332*, 105407. https://doi.org/10.1016/j.precamres.2019.105407

Cullen, D. J. 1973: Bioturbation of superficial marine sediments by interstitial meiobenthos. *Nature 242*, 323–324. https://doi.org/10.1038/242323a0

Cummings, J. P. & Hodgson, D. M. 2011: Assessing controls on the distribution of ichnotaxa in submarine fan environments, the Basque Basin, northern Spain. *Sedimentary Geology 239*, 162–187. https://doi.org/10.1016/j.sedgeo.2011.06.009

Curran, H. A. & Frey, R. W. 1977: Pleistocene trace fossils from North Carolina (U.S.A.), and their Holocene analogues. 139–162 *in* Crimes, T. P. & Harper, J. C. (eds): *Trace Fossils 2*. Seel House Press, Liverpool.

Czarnocki, J. 1927: Kambr i jego fauna w środkowej części Gór Świętokrzyskich (Komunikat tymczasowy). *Sprawozdania Polskiego Instytutu Geologicznego 4*, 189–207.

D'Alessandro, A., Ekdale, A. A. & Sonnino, M. 1986: Sedimentologic significance of turbidite ichnofacies in the Saraceno Formation (Eocene), southern Italy. *Journal of Sedimentary Petrology 56*, 294–306. https://doi.org/10.1306/212F88EB-2B24-11D7-8648000102C1865D

D'Hondt, S., Inagaki, F., Zarikian, C. A., Abrams, L. J., Dubois, N., *et al.* 2015: Presence of oxygen and aerobic communities from sea floor to basement in deep-sea sediments. *Nature Geoscience 8*, 299–304. https://doi.org/10.1038/ngeo2387

d'Orbigny, A. 1842: *Voyage dans l'Amérique Méridionale. Tome troisième, Géologie*. P. Bertrand, Paris, V. Levrault, Strasbourg, 188 pp.

d'Orbigny, A. 1846: *Voyage dans l'Amérique Méridionale. Tome huitième, Atlas Historique, Géologique, Paléontologique et Botanique*. P. Bertrand, Paris, V. Levrault, Strasbourg.

D'souza, R., Dasgupta, S., Das, M., Natarajan, A. & Rajkhowa, D. 2024: Morphology and ethology of *Rosselia erecta* in Eocene lignitic mudstone. *Ichnos 31*, 257–274. https://doi.org/10.1080/10420940.2024.2401329

da Silva, R. C., Fernandes, A. C. S. & Sedor, F. A. 2003: Ocorrência de icnofósseis de invertebrados na Formação Irati (Permiano superior da Bacia do Paraná, Brasil). *Arquivos do Museu Nacional, Rio de Janeiro 61*, 261–266.

Dahanayake, K., Gerdes, G. & Krumbein, W. E. 1985: Stromatolites, oncolites and oolites biogenically formed in situ. *Naturwissenschaften 72*, 513–518. https://doi.org/10.1007/BF00367596

Dahmer, G. 1937: Lebensspuren aus dem Taunusquarzit und den Siegener Schichten (Unterdevon). *Jahrbuch der Preussischen Geologischen Landesanstalt zu Berlin 57*, 523–539.

Daily, B. 1972: The base of the Cambrian and the first Cambrian faunas. *Center for Precambrian Research, University of Adelaide, South Australia, Special Paper 1*, 13–37.

Dale, N. C. 1927: Pre-Cambrian and Paleozoic geology of Fortune Bay, Newfoundland. *Bulletin of the Geological Society of America 38*, 411–430. https://doi.org/10.1130/GSAB-38-411

Daley, A. C., Antcliffe, J. B., Drage, H. B. & Pates, S. 2018: Early fossil record of Euarthropoda and the Cambrian Explosion. *Proceedings of the National Academy of Sciences 115*, 5323–5331. https://doi.org/10.1073/pnas.1719962115

Dalrymple, R. W. 1979: Wave-induced liquefaction: a modern example from the Bay of Fundy. *Sedimentology 26*, 835–844. https://doi.org/10.1111/j.1365-3091.1979.tb00976.x

Dalrymple, R. W. 2006: Incised valleys in time and space: an introduction to the volume and an examination of the controls on valley formation and filling. 5–12 *in* Dalrymple, R. W., Leckie, D. A. & Tillman, R. W. (eds): *Incised Valleys in Time and Space*. SEPM Special Publication, Volume 85. https://doi.org/10.2110/pec.06.85.0005

Dalrymple, R. W. 2010: Tidal depositional systems. 201–231 *in* James, N. P. & Dalrymple, R. W. (eds): *Facies models 4*. The Geological Association of Canada, St John's.

Dalrymple, R. W. & Choi, K. 2007: Morphologic and facies trends through the fluvial–marine transition in tide-dominated depositional systems: a schematic framework for environmental and sequence-stratigraphic interpretation. *Earth-Science Reviews 81*, 135–174. https://doi.org/10.1016/j.earscirev.2006.10.002

Dalrymple, R. W., Zaitlin, B. A. & Boyd, R. 1992: Estuarine facies models: conceptual basis and stratigraphic implications. *Journal of Sedimentary Petrology 62*, 1130–1146. https://doi.org/10.1306/D4267A69-2B26-11D7-8648000102C1865D

Dam, G. 1990: Taxonomy of trace fossils from the shallow marine lower Jurassic Neill Klinter Formation, east Greenland. *Bulletin of the Geological Society of Denmark 38*, 119–144. https://doi.org/10.37570/bgsd-1990-38-12

Darngawn, J. L., Patel, S. J., Joseph, J. K. & Shitole, A. D. 2018: Palaeoecological significance of trace fossils of Chorar Island, eastern Kachchh Basin, western India. *Journal of the Palaeontological Society of India 63*, 169–180. https://doi.org/10.1177/0971102320180204

Darroch, S. A. F., Boag, T. H., Racicot, R. A., Tweedt, S., Mason, S. J., Erwin, D. H. & Laflamme, M. 2016: A mixed Ediacaran-metazoan assemblage from the Zaris Sub-basin, Namibia. *Palaeogeography, Palaeoclimatology, Palaeoecology 459*, 198–208. https://doi.org/10.1016/j.palaeo.2016.07.003

Darroch, S. A. F., Cribb, A. T., Buatois, L. A., Germs, G. J. B., Kenchington, C. G., Smith, E. F., Mocke, H., O'Neil, G. R., Schiffbauer, J. D., Maloney, K. M., Racicot, R. A., Turk, K. A., Gibson, B. M., Almond, J., Koester, B., Boag, T. H., Tweedt, S. M. & Laflamme, M. 2021: The trace fossil record of the Nama Group, Namibia: exploring the terminal Ediacaran roots of the Cambrian explosion. *Earth-Science Reviews 212*, 103435. https://doi.org/10.1016/j.earscirev.2020.103435

Dasgupta, S., Buatois, L. A. & Mángano, M. G. 2016: Living on the edge: evaluating the impact of stress factors on animal–sediment interactions in subenvironments of a shelf-margin delta, the Mayaro Formation, Trinidad. *Journal of Sedimentary Research 86*, 1034–1066. https://doi.org/10.2110/jsr.2016.47

Dashtgard, S. E. 2011: Neoichnology of the lower delta plain: Fraser River Delta, British Columbia, Canada: implications for the ichnology of deltas. *Palaeogeography, Palaeoclimatology, Palaeoecology 307*, 98–108. https://doi.org/10.1016/j.palaeo.2011.05.001

Dashtgard, S. E. & Gingras, M. K. 2012: Marine invertebrate neoichnology. 273–295 *in* Knaust, D. & Bromley, R. G. (eds): *Developments in Sedimentology*. Elsevier, Vol. 64. https://doi.org/10.1016/B978-0-444-53813-0.00010-1

Dashtgard, S. E., Gingras, M. K. & Pemberton, S. G. 2008: Grain-size controls on the occurrence of bioturbation. *Palaeogeography, Palaeoclimatology, Palaeoecology 257*, 224–243. https://doi.org/10.1016/j.palaeo.2007.10.024

Dashtgard, S. E., MacEachern, J. A., Frey, S. E. & Gingras, M. K. 2012: Tidal effects on the shoreface: towards a conceptual framework. *Sedimentary Geology 279*, 42–61. https://doi.org/10.1016/j.sedgeo.2010.09.006

Dashtgard, S. E., Ainsworth, R.B. & MacEachern, J. A. 2017: Preferential orientation of shrimp-generated *Diplocraterion Parallelum* and their reliability as paleocurrent indicators. *Palaios 32*, 429–438. https://doi.org/10.2110/palo.2016.099

Dashtgard, S. E., Vaucher, R., Yang, B. & Dalrymple, R. W. 2021: Wave-dominated to tide-dominated coastal systems: a unifying model for tidal shorefaces and refinement of the coastal-environments classification scheme. *Geoscience Canada 48*, 5–22. https://doi.org/10.12789/geocanj.2021.48.171

Davies, N. S. & Gibling, M. R. 2010: Cambrian to Devonian evolution of alluvial systems: the sedimentological impact of the earliest land plants. *Earth-Science Reviews 98*, 171–200. https://doi.org/10.1016/j.earscirev.2009.11.002

Davies, N. S., Herringshaw, L. G. & Raine, R. J. 2009: Controls on trace fossil diversity in an early Cambrian epeiric sea: new perspectives from northwest Scotland. *Lethaia 42*, 17–30. https://doi.org/10.1111/j.1502-3931.2008.00130.x

Davies, N. S., Rygel, M. C. & Gibling, M. R. 2010: Marine influence in the upper Ordovician Juniata Formation (Potters Mills, Pennsylvania): implications for the history of life on

land. *Palaios 25*, 527–539. https://doi.org/10.2110/palo.2010.p10-025r

Davies, N. S., Liu, A. G., Gibling, M. R. & Miller, R. F. 2016: Resolving MISS conceptions and misconceptions: a geological approach to sedimentary surface textures generated by microbial and abiotic processes. *Earth-Science Reviews 154*, 210–246. https://doi.org/10.1016/j.earscirev.2016.01.005

Davis, R. B., Minter, N. J. & Braddy, S. J. 2007: The neoichnology of terrestrial arthropods. *Palaeogeography, Palaeoclimatology, Palaeoecology 255*, 284–307. https://doi.org/10.1016/j.palaeo.2007.07.013

Davison, J. E. & MacEachern, J. A. 2007: Ichnological variations in brackish-water central-basin complexes of wave-dominated estuarine incised-valley fills, lower Cretaceous Viking Formation, central Alberta. 273–289 *in* MacEachern, J. A., Bann, K. L., Gingras, M. K. & Pemberton, S .G. (eds): *Applied Ichnology*. SEPM Short Course 52. https://doi.org/10.2110/pec.07.52.0273

Dawson, J. W. 1864: On the fossils of the genus *Rusophycus*. *The Canadian Naturalist 1*, 363–367.

Dawson, J. W. 1873: Impressions and footprints of aquatic animals and imitative markings on Carboniferous rocks. *American Journal of Science 3*, 16–24.

Dawson, J. W. 1890: On burrows and tracks of invertebrate animals in Palaeozoic rocks, and other markings. *Quarterly Journal of the Geological Society 46*, 595–618.

de Gibert Atienza, J. M. 1996: *Icnologia de les conques marines pliocenes del marge Nord-Occidental de la Mediterrània*. Unpublished Doctoral Dissertation, Universidad de Barcelona, 75 pp.

de Gibert, J. M. & Ekdale, A. A. 2002: Ichnology of a restricted epicontinental sea, Arapien Shale, middle Jurassic, Utah, USA. *Palaeogeography, Palaeoclimatology, Palaeoecology 183*, 275–286. https://doi.org/10.1016/S0031-0182(01)00491-6

de Gibert, J. M. & Sáez, A. 2009: Paleohydrological significance of trace fossil distribution in Oligocene fluvial-fan-to-lacustrine systems of the Ebro Basin, Spain. *Palaeogeography, Palaeoclimatology, Palaeoecology 272*, 162–175. https://doi.org/10.1016/j.palaeo.2008.10.030

de Gibert, J. M., Jeong, K. & Martinell, J. 1999a: Ethologic and ontogenic significance of the Pliocene trace fossil *Sinusichnus sinuosus* from the northwestern Mediterranean. *Lethaia 32*, 31–40. https://doi.org/10.1111/j.1502-3931.1999.tb00578.x

de Gibert, J. M., Buatois, L. A., Fregenal-Martínez, M. A., Mángano, M. G., Ortega, F., Poyato-Ariza, F. J. & Wenz, S. 1999b: The fish trace fossil *Undichna* from the Cretaceous of Spain. *Palaeontology 42*, 409–427. https://doi.org/10.1111/1475-4983.00079

de Gibert, J. M., Fregenal-Martínez, M. A., Buatois, L. A. & Mángano, M. G. 2000: Trace fossils and their palaeoecological significance in lower Cretaceous lacustrine conservation deposits, El Montsec, Spain. *Palaeogeography, Palaeoclimatology, Palaeoecology 156*, 89–101. https://doi.org/10.1016/S0031-0182(99)00133-9

de Gibert, J. M., Mas, G. & Ekdale, A. A. 2012: Architectural complexity of marine crustacean burrows: unusual helical trace fossils from the Miocene of Mallorca, Spain. *Lethaia 45*, 574–585. https://doi.org/10.1111/j.1502-3931.2012.00318.x

de la Sicotière, L. 1866: Séance du 31 janvier 1866. *Bulletin de la Société Linnéenne de Normandie 1*, 83–91.

de Quatrefages, A. 1849: Note sur la *Scolicia prisca* (A. de Q.), annélide fossile de la craie. *Annales des Sciences Naturelles, Troisième Série, Zoologie*, 265–266.

de Raaf, J. F. M. & Boersma, J. R. 1971: Tidal deposits and their sedimentary structures (seven examples from western Europe). *Geologie en Mijnbouw 50*, 479–504.

De Renzi, M. & Mayoral, E. 2024: Understanding behaviour through theoretical morphology: the case of helical-shaped burrows. *Journal of Iberian Geology 50*, 549–566. https://doi.org/10.1007/s41513-024-00249-7

De Renzi, M., Palmqvist, P. & Mayoral, E. 2017: *Theoretical morphology and ichnofossils:* Gyrolithes *as a case study*. Presented at the Jornadas de Paleontología, Sociedad Española de Paleontología, Cádiz, Spain, 45–48.

de Saporta, G. 1872: *Paléontologie Française ou description des fossiles de la France continuée par une réunion de paléontologistes sous la direction d'un comité régional. 2e Série. Végétaux. Plantes Jurassiques. Tome I. Algues, équisétacées, characées, fougères*. G. Masson, Paris, 506 pp.

de Saporta, G. 1882: *A propos des Algues Fossiles*. G. Masson, Paris, 82 pp.

de Saporta, G. 1884: *Les organismes problématiques des anciennes mers*. G. Masson, Paris, 102 pp.

de Saporta, G. 1887: Nouveaux documents relatifs aux organismes problématiques des anciennes mers. *Bulletin de la Société Géologique de France 15*, 286–302.

de Saporta, G. & Marion, A.-F. 1881: *L'Évolution du Règne Végétal. Les Cryptogames*. G. Baillière et cie, Paris, 238 pp.

de Saporta, G. & Marion, A. F. 1883: *Die Paläontologische Entwickelung des Pflanzenreichs. Die Kryptogamen*. Internationale Wissenschaftliche Bibliothek, Vol. 54, F.A. Brockhaus, Leipzig, 250 pp.

de Serres, M. 1840: Description de quelques mollusques fossiles nouveaux des terrains infra-jurassiques et de la craie compacte inférieure du midi de la France. *Annales des Sciences Naturelles, Partie Zoologique 14*, 5–25.

de Tromelin, G. G. & Lebesconte, P. 1876: Essai d'un catalogue raisonné des fossiles Siluriens des départements de Maine-et-Loire, de la Loire-Inférieure et du Morbihan, avec des observations sur les terrains Paléozoiques de l'ouest de la France. *Association Française pour l'Avancement des Sciences 4*, 601–661.

Dean, W. E. & Eggleston, J. R. 1984: Freshwater oncolites created by industrial pollution, Onondaga Lake, New York. *Sedimentary Geology 40*, 217–232. https://doi.org/10.1016/0037-0738(84)90009-5

Dec, T., O'Brien, S. J. & Knight, I. 1992: Late Precambrian volcaniclastic deposits of the Avalonian Eastport Basin (Newfoundland Appalachians): petrofacies, detrital clinopyroxene geochemistry and palaeotectonic implications. *Precambrian Research 59*, 243–262. https://doi.org/10.1016/0301-9268(92)90059-W

DeCelles, P. G. & Cavazza, W. 1992: Constraints on the formation of Pliocene hummocky cross-stratification in Calabria (southern Italy) from consideration of hydraulic and dispersive equivalence, grain-flow theory, and suspended-load fallout rate. *Journal of Sedimentary Petrology 62*, 555–568. https://doi.org/10.1306/D426795B-2B26-11D7-8648000102C1865D

Dekay, J. E. 1824: Note on the organic remains termed *Bilobites* from the Catskill Mountains. *Annals of the Lyceum of Natural History of New York 1*, 45–49.

Delgado, J. F. N. 1886: *Etude sur les bilobites et autres fossiles des quartzites de la base du Système Silurique du Portugal*. Imprimerie de l'académie royale des sciences, Lisbonne, 113 pp.

Demathieu, G., Gand, G. & Toutin-Morin, N. 1992: La palichnofaune des bassins permiens provençaux. *Geobios 25*, 19–54. https://doi.org/10.1016/S0016-6995(09)90036-5

Demircan, H. & Uchman, A. 2010: Kiss of death of a hunting fish: trace fossil *Osculichnus labialis* igen. et isp. nov. from late Eocene – early Oligocene prodelta sediments of the Mezardere Formation, Thrace Basin, NW Turkey. *Acta Geologica Polonica 60*, 29–38.

Demircan, H. & Uchman, A. 2016: Ichnology of prodelta deposits of the Mezardere Formation (late Eocene–early Oligocene) in the Gökçeada island, western Turkey. *Geodinamica Acta 28*, 86–100. https://doi.org/10.1080/09853111.2015.1113720

Denommee, K. C., Bentley, S. J., Harazim, D. & Macquaker, J. H. S. 2016: Hydrodynamic controls on muddy sedimentary-fabric development on the southwest Louisiana subaqueous delta. *Marine Geology 382*, 162–175. https://doi.org/10.1016/j.margeo.2016.09.013

Desai, B. G. 2010: Biogenic sedimentary structures produced by *Architectonica laevigata* (Gastropod: Architectonicidae),

Mandvi intertidal zone, Gulf of Kachchh, western India. *Earth Science India 3*, 242–247.

Desai, B. G. & Saklani, R. D. 2015: Palaeocommunity dynamics and behavioral analysis of *Conichnus*: Bhuj Formation (lower Cretaceous), Kachchh-India. *Ichnos 22*, 43–55. https://doi.org/10.1080/10420940.2014.995377

Desio, A. 1940: Vestigia problematiche paleozoiche della Libia. *Annali del Museo Libico di Storia Naturale 2*, 47–92.

Desjardins, P. R., Buatois, L. A., Pratt, B. R. & Mángano, M. G. 2010a: Stratigraphy and sedimentary environments of the lower Cambrian Gog Group in the southern Rocky Mountains of western Canada: transgressive sandstones on a broad continental margin. *Bulletin of Canadian Petroleum Geology 58*, 403–439. https://doi.org/10.2113/gscpgbull.58.4.403

Desjardins, P. R., Buatois, L. A., Mángano, M. G. & Limarino, C. O. 2010b: Ichnology of the latest Carboniferous–earliest Permian transgression in the Paganzo Basin of western Argentina: the interplay of ecology, sea-level rise, and paleogeography during postglacial times in Gondwana. 175–192 *in* López-Gamundí, O. R. & Buatois, L. A. (eds): *Late Paleozoic Glacial Events and Postglacial Transgressions in Gondwana*. Geological Society of America Special Paper 468. https://doi.org/10.1130/2010.2468(08)

Desjardins, P. R., Mángano, M. G., Buatois, L. A. & Pratt, B. R. 2010c: *Skolithos* pipe rock and associated ichnofabrics from the southern Rocky Mountains, Canada: colonization trends and environmental controls in an early Cambrian sand-sheet complex. *Lethaia 43*, 507–528. https://doi.org/10.1111/j.1502-3931.2009.00214.x

Desjardins, P. R., Buatois, L. A., Pratt, B. R. & Mángano, M. G. 2012: Forced regressive tidal flats: response to falling sea level in tide-dominated settings. *Journal of Sedimentary Research 82*, 149–162. https://doi.org/10.2110/jsr.2012.18

Deslongchamps, E. 1856: Notice sur des empreintes ou traces d'animaux existant à la surface d'une roche de grès, au lieu dit les Vaux-d'Aubin, près Argentan, département de l'Orne, et connus dans le pays sous le nom de pas de boeufs. *Mémoires de la Société Linnéenne de Normandie 10*, 19–44.

Devaere, L., Clausen, S., Steiner, M., Álvaro, J. J. & Vachard, D. 2013: Chronostratigraphic and palaeogeographic significance of an early Cambrian microfauna from the Heraultia Limestone, northern Montagne Noire, France. *Palaeontologia Electronica 16*, 17A–91. https://doi.org/10.26879/366

Devaere, L., Korn, D., Ghaderi, A., Struck, U. & Bavandpur, A. K. 2021: New and revised small shelly fossil record from the lower Cambrian of northern Iran. *Papers in Palaeontology 7*, 2141–2181. https://doi.org/10.1002/spp2.1391

Devera, J. A. 1989: Ichnofossil assemblages and associated lithofacies of the lower Pennsylvanian (Caseyville and Tradewater formations), southern Illinois. *Geology of the Lower Pennsylvanian in Kentucky, Indiana, and Illinois. Illinois Basin Studies 1*, 57–83.

Dias Da Silva, Í., Jensen, S. & González-Clavijo, E. 2014: Trace fossils from the Desejosa Formation (Schist and Greywacke Complex, Douro Group, NE Portugal): new Cambrian age constraints. *Geologica Acta 12*, 109–120. https://doi.org/10.1344/105.000002080

Diaz, R. J. & Rosenberg, R. 1995: Marine benthic hypoxia: a review of its ecological effects and the behavioural responses of benthic macrofauna. *Oceanography and Marine Biology: an Annual Review 33*, 245–303.

Dill, R. F., Shinn, E. A., Jones, A. T., Kelly, K. & Steinen, R. P. 1986: Giant subtidal stromatolites forming in normal salinity waters. *Nature 324*, 55–58. https://doi.org/10.1038/324055a0

Ding, Y., Liu, J. & Chen, F. 2020: Ichnology, palaeoenvironment, and ecosystem dynamics of the early Cambrian (stage 4, series 2) Guanshan Biota, South China. *Geological Journal 55*, 77–94. https://doi.org/10.1002/gj.3360

Dionne, J.-C. & Pérez Alberti, A. 2000: Structures cylindriques verticales dans un dépôt meuble Quaternaire, en Galice (Espagne). *Géographie physique et Quaternaire 54*, 343–349. https://doi.org/10.7202/005640ar

Dornbos, S. Q., Noffke, N. & Hagadorn, J. W. 2007: Mat-decay features. 106–110 *in* Schieber, J., Bose, P. K., Eriksson, P. G., Banerjee, S., Sarkar, S., Altermann, W. & Catuneanu, O. (eds): *Atlas of microbial mat features preserved within the siliciclastic rock record*. Atlases in Geosciences 2, Elsevier.

Dott Jr., R. H. & Bourgeois, J. 1982: Hummocky stratification: significance of its variable bedding sequences. *Geological Society of America Bulletin 93*, 663–680. https://doi.org/10.1130/0016-7606(1982)93<663:HSSOIV>2.0.CO;2

Downie, C. 1982: Lower Cambrian acritarchs from Scotland, Norway, Greenland and Canada. *Transactions of The Royal Society of Edinburgh: Earth Sciences 72*, 257–285. https://doi.org/10.1017/S0263593300010051

Draper, J. J. 1980: *Rusophycus* (early Ordovician ichnofossil) from the Mithaka Formation, Georgina Basin. *BMR Journal of Australian Geology and Geophysics 5*, 57–61.

Dravis, J. J. 1983: Hardened subtidal stromatolites, Bahamas. *Science 219*, 385–386. https://doi.org/10.1126/science.219.4583.385

Driese, S. G., Byers, C. W. & Dott Jr., R. H. 1981: Tidal deposition in the basal upper Cambrian Mt. Simon formation in Wisconsin. *Journal of Sedimentary Petrology 51*, 367–381. https://doi.org/10.1306/212F7C84-2B24-11D7-8648000102C1865D

Droser, M. L. & Bottjer, D. J. 1988: Trends in depth and extent of bioturbation in Cambrian carbonate marine environments, western United States. *Geology 16*, 233–236. https://doi.org/10.1130/0091-7613(1988)016<0233:TIDAEO>2.3.CO;2

Droser, M. L. & Bottjer, D. J. 1993: Trends and patterns of Phanerozoic ichnofabrics. *Annual Review of Earth and Planetary Sciences 21*, 205–225. https://doi.org/10.1146/annurev.ea.21.050193.001225

Droser, M. L. & Li, X. 1999: The Cambrian radiation and the diversification of sedimentary fabrics. 137–170 *in* Zhuravlev, A. & Riding, R. (eds): *Ecology of the Cambrian Radiation*. Columbia University Press, New York. https://doi.org/10.7312/zhur10612-007

Droser, M. L., Hughes, N. C. & Jell, P. A. 1994: Infaunal communities and tiering in early Palaeozoic nearshore clastic environments: trace-fossil evidence from the Cambro-Ordovician of New South Wales. *Lethaia 27*, 273–283. https://doi.org/10.1111/j.1502-3931.1994.tb01574.x

Droser, M. L., Gehling, J. G. & Jensen, S. 1999: When the worm turned: concordance of early Cambrian ichnofabric and trace-fossil record in siliciclastic rocks of south Australia. *Geology 27*, 625–628. https://doi.org/10.1130/0091-7613(1999)027<0625:WTWTCO>2.3.CO;2

Droser, M. L., Jensen, S., Gehling, J. G., Myrow, P. M. & Narbonne, G. M. 2002: Lowermost Cambrian ichnofabrics from the Chapel Island Formation, Newfoundland: implications for Cambrian substrates. *Palaios 17*, 3–15. https://doi.org/10.1669/0883-1351(2002)017<0003:LCIFTC>2.0.CO;2

Droser, M. L., Gehling, J. G. & Jensen, S. 2005: Ediacaran trace fossils: true and false. 125–138 *in* Briggs, D. E. G. (ed): *Evolving Form and Function: Fossils and Development*. Peabody Museum of Natural History, Yale University, New Haven.

Droser, M. L., Gehling, J. G. & Jensen, S. R. 2006: Assemblage palaeoecology of the Ediacara biota: the unabridged edition? *Palaeogeography, Palaeoclimatology, Palaeoecology 232*, 131–147. https://doi.org/10.1016/j.palaeo.2005.12.015

Droser, M. L., Tarhan, L. G. & Gehling, J. G. 2017: The rise of animals in a changing environment: global ecological innovation in the late Ediacaran. *Annual Review of Earth and Planetary Sciences 45*, 593–617. https://doi.org/10.1146/annurev-earth-063016-015645

Du, R., Tian, L. & Li, H. 1986: Discovery of megafossils in the Gaoyuzhang Formation of the Changchengian System, Jixian. *Acta Geologica Sinica 60*, 115–120.

Duke, W. L. 1985: Hummocky cross-stratification, tropical hurricanes, and intense winter storms. *Sedimentology 32*, 167–194. https://doi.org/10.1111/j.1365-3091.1985.tb00502.x

Dumas, S. & Arnott, R. W. C. 2006: Origin of hummocky and swaley cross-stratification—the controlling influence of unidirectional current strength and aggradation rate. *Geology 34*, 1073–1076. https://doi.org/10.1130/G22930A.1

Dumas, S., Arnott, R. W. C. & Southard, J. B. 2005: Experiments on oscillatory-flow and combined-flow bed forms: implications for interpreting parts of the shallow-marine sedimentary record. *Journal of Sedimentary Research 75*, 501–513. https://doi.org/10.2110/jsr.2005.039

Dunn, F. S. & Liu, A. G. 2019: Viewing the Ediacaran biota as a failed experiment is unhelpful. *Nature Ecology and Evolution 3*, 512–514. https://doi.org/10.1038/s41559-019-0815-4

Durand, F. R. & Aceñolaza, F. G. 1990: Caracteres biofaunísticos, paleoecológicos y paleogeográficos de la Formación Puncoviscana (Precámbrico superior-Cámbrico inferior) del noroeste Argentino. 71–112 *in* Aceñolaza, F., Miller, H. & Toselli, A.J. (eds): *El Ciclo Pampeano en el Noroeste Argentino*. Serie de Correlación Geológica No 4.

Durand, J. 1985: *Le Grès Armoricain. Sédimentologie – Traces fossils. Milieux de dépôt*. Mémoires et documents du Centre Armoricain d'étude structure des socles, Rennes, No. 3, 150 pp.

Durbano, A. M., Pratt, B. R., Hadlari, T. & Dewing, K. 2015: Sedimentology of an early Cambrian tide-dominated embayment: Quyuk Formation, Victoria Island, Arctic Canada. *Sedimentary Geology 320*, 1–18. https://doi.org/10.1016/j.sedgeo.2015.02.004

Duval, X. 1838: Séance du 5 Mars 1838. *Bulletin de la Société Géologique de France 9*, 199–200.

Dworschak, P. C. & Rodrigues, S. A. 1997: A modern analogue for the trace fossil *Gyrolithes*: burrows of the thalassinidean shrimp *Axianassa australis*. *Lethaia 30*, 41–52. https://doi.org/10.1111/j.1502-3931.1997.tb00443.x

Dzik, J. 2005: Behavioral and anatomical unity of the earliest burrowing animals and the cause of the "Cambrian Explosion". *Paleobiology 31*, 503–521. https://doi.org/10.1666/0094-8373(2005)031[0503:BAAUOT]2.0.CO;2

Dzik, J. 2007: The Verdun syndrome: simultaneous origin of protective armour and infaunal shelters at the Precambrian–Cambrian transition. *Geological Society, London, Special Publications 286*, 405–414. https://doi.org/10.1144/SP286.30

Dzik, J. & Mazurek, D. 2013: Affinities of the alleged earliest Cambrian gastropod *Aldanella*. *Canadian Journal of Zoology 91*, 914–923. https://doi.org/10.1139/cjz-2013-0119

Dżułyński, S. & Walton, E. K. 1965: *Sedimentary features of flysch and greywackes*. Developments in sedimentology 7, Elsevier, 274 pp.

Eagar, R .M. C., Baines, J. G., Collinson, J. D., Hardy, P. G., Okolo, S. A. & Pollard, J. E. 1985: Trace fossil assemblages and their occurrence in Silesian (mid-Carboniferous) deltaic sediments of the central Pennine Basin, England. 99–149 *in* Curran, H. A. (ed): *Biogenic structures: their use in interpreting depositional environments*. SEPM Special Publication, Vol. 35. https://doi.org/10.2110/pec.85.35.0099

Ebbestad, J. O. R., Hybertsen, F., Högström, A. E., Jensen, S., Palacios, T., Taylor, W. L., Agić, H., Høyberget, M. & Meinhold, G. 2022: Distribution and correlation of *Sabellidites cambriensis* (Annelida?) in the basal Cambrian on Baltica. *Geological Magazine 159*, 1262–1283. https://doi.org/10.1017/S0016756821001187

Edgecombe, G. D. 2020: Arthropod origins: integrating paleontological and molecular evidence. *Annual Review of Ecology, Evolution, and Systematics 51*, 1–25. https://doi.org/10.1146/annurev-ecolsys-011720-124437

Egenhoff, S. O., Weber, B., Lehnert, O. & Maletz, J. 2007: Biostratigraphic precision of the *Cruziana rugosa* group: a study from the Ordovician succession of southern and central Bolivia. *Geological Magazine 144*, 289–303. https://doi.org/10.1017/S0016756807003093

Eichwald, E. 1860: *Lethaea rossica ou paléontologie de la Russie, décrite et figurée. Premier volume. Ancienne période en deux sections*. E. Schweizerbart, Stuttgart, 1657 pp.

Eide, C. H., Howell, J. A. & Buckley, S. J. 2015: Sedimentology and reservoir properties of tabular and erosive offshore transition deposits in wave-dominated, shallow-marine strata: Book Cliffs, USA. *Petroleum Geoscience 21*, 55–73. https://doi.org/10.1144/petgeo2014-015

Ekdale, A. A. 1977: Abyssal trace fossils in worldwide deep sea drilling project cores. 163–182 *in* Crimes, T. P. & Harper, J. C. (eds): *Trace Fossils 2*. Seel House Press, Liverpool.

Ekdale, A. A. & Berger, W. H. 1978: Deep-sea ichnofacies: modern organism traces on and in pelagic carbonates of the western equatorial Pacific. *Palaeogeography, Palaeoclimatology, Palaeoecology 23*, 263–278. https://doi.org/10.1016/0031-0182(78)90096-2

Ekdale, A. A. & Harding, S. C. 2015: *Cylindrichnus concentricus* Toots in Howard, 1966 (trace fossil) in its type locality, Upper Cretaceous, Wyoming. *Annales Societatis Geologorum Poloniae 85*, 427–432. https://doi.org/10.14241/asgp.2015.018

Ekdale, A. A. & Lewis, D. W. 1991: Trace fossils and paleoenvironmental control of ichnofacies in a late Quaternary gravel and loess fan delta complex, New Zealand. *Palaeogeography, Palaeoclimatology, Palaeoecology 81*, 253–279. https://doi.org/10.1016/0031-0182(91)90150-P

Ekdale, A. A., Bromley, R. G. & Pemberton, S. G. 1984: *Ichnology. The Use of Trace Fossils in Sedimentology and Stratigraphy*. Society of Economic Paleontologists and Mineralogists Short Course No. 15, Tulsa, 317 pp.

El-Khayal, A. A. & Romano, M. 1988: A revision of the upper part of the Saq Formation and Hanadir Shale (lower Ordovician) of Saudi Arabia. *Geological Magazine 125*, 161–174. https://doi.org/10.1017/S0016756800009560

Elder, H. Y. 1973: Direct peristaltic progression and the functional significance of the dermal connective tissues during burrowing in the polychaete *Polyphysia crassa* (Oersted). *Journal of Experimental Biology 58*, 637–655. https://doi.org/10.1242/jeb.58.3.637

Elicki, O. & Altumi, M. M. 2019: Cambrian trace fossils from north Africa and their contribution to Gondwana's paleobiogeography and depositional history. *Journal of African Earth Sciences 158*, 103556. https://doi.org/10.1016/j.jafrearsci.2019.103556

Elicki, O. & Magnus, M. 2021: First report of *Cruziana rouaulti* Lebesconte, 1883 from the Ordovician of Algeria and its stratigraphic and palaeogeographic significance. *Freiberger Forschungshefte C 559*, 63–76.

Elicki, O., Khalifa, M. A. G. & Farouk, S. M. 2013: Cambrian ichnofossils from northeastern Egypt. *Neues Jahrbuch für Geologie und Paläontologie Abhandlungen 270*, 129–149. https://doi.org/10.1127/0077-7749/2013/0358

Elliott, R. E. 1985: An interpretation of the trace fossil *Cochlichnus kochi* (Ludwig) from the east Pennine Coalfield of Britain. *Proceedings of the Yorkshire Geological Society 45*, 183–187. https://doi.org/10.1144/pygs.45.3.183

Emmons, E. 1844: *The Taconic System; based on observations in New-York, Massachusetts, Maine, Vermont and Rhode-Island*. Carroll and Cook, Printers, Albany, 65 pp.

Eriksson, P. G., Reczko, B .F., Boshoff, A. J., Schreiber, U. M., Van der Neut, M. & Snyman, C. P. 1995: Architectural elements from lower Proterozoic braid-delta and high-energy tidal flat deposits in the Magaliesberg Formation, Transvaal Supergroup, South Africa. *Sedimentary Geology 97*, 99–117. https://doi.org/10.1016/0037-0738(95)00004-R

Eriksson, P. G., Porada, H., Banerjee, S., Bouougri, E., Sarkar, S. & Bumby, A. J. 2007: Mat-destruction features. 76–105 *in* Schieber, J., Bose, P. K., Eriksson, P. G., Banerjee, S., Sarkar, S., Altermann, W. & Catuneanu, O. (eds): *Atlas of Microbial Mat Features Preserved within the Siliciclastic Rock Record*. Atlases in Geoscience 2, Elsevier.

Ershova, V. B., Fedorov, P. V. & Mikuláš, R. 2006: Trace fossils on and above the transgressive surface: substrate consistency and phosphogenesis (lower Ordovician, St Petersburg region, Russia). *Geologica Carpathica 57*, 415–422.

Erwin, D. H. 1999: The origin of bodyplans. *American Zoologist 39*, 617–629.

Erwin, D. H. 2020: The origin of animal body plans: a view from fossil evidence and the regulatory genome. *Development 147*, dev182899. https://doi.org/10.1242/dev.182899

Erwin, D. H. & Valentine, J. W. 2013: *The Cambrian explosion: the construction of animal biodiversity*. Greenwood Village, Colorado, Roberts, 406 pp.

Evans, S. D., Hughes, I. V., Gehling, J. G. & Droser, M. L. 2020: Discovery of the oldest bilaterian from the Ediacaran of South Australia. *Proceedings of the National Academy of Sciences 117*, 7845–7850. https://doi.org/10.1073/pnas.2001045117

Ewing, M. & Davis, R. A. 1967: Lebensspuren photographed on the ocean floor. 259–294 *in* Hersey, J. B. (ed.): *Deep-sea photography*. The John Hopkins Press, Baltimore.

Fåhræus, L. E. 1994: The Precambrian-Cambrian boundary–victim of parochialism. *Newsletters on Stratigraphy 31*, 1–19. https://doi.org/10.1127/nos/31/1994/1

Fan, D. 2013: Classifications, sedimentary features and facies associations of tidal flats. *Journal of Palaeogeography 2*, 66–80. https://doi.org/10.3724/SP.J.1261.2013.00018

Fan, R.-Y., Gong, Y.-M. & Uchman, A. 2018: Topological analysis of graphoglyptid trace fossils, a study of macrobenthic solitary and collective animal behaviors in the deep-sea environment. *Paleobiology 44*, 306–325. https://doi.org/10.1017/pab.2018.1

Fan, R.-Y., Zong, R.-W. & Gong, Y.-M. 2021: Deep-time geometricians and hints on motor control evolution of marine invertebrates. *Palaeogeography, Palaeoclimatology, Palaeoecology 567*, 110255. https://doi.org/10.1016/j.palaeo.2021.110255

Farrow, G. E. 1967: *The morphology, ethology and palaeoecology of certain trace fossils from the Jurassic rocks of England*. Unpublished Doctoral Dissertation, Durham University, 369 pp.

Farrow, G. E. 1971: Back-reef and lagoonal environments of Aldabra Atoll distinguished by their crustacea burrows. *Symposium Zoological Society London 28*, 455–500.

Fedo, C. M. & Cooper, J. D. 2001: Sedimentology and sequence stratigraphy of Neoproterozoic and Cambrian units across a craton-margin hinge zone, southeastern California, and implications for the early evolution of the Cordilleran margin. *Sedimentary Geology 141–142*, 501–522. https://doi.org/10.1016/S0037-0738(01)00088-4

Fedonkin, M. A. 1977: Precambrian-Cambrian ichnocoenoses of the east European platform. 183–194 *in* Crimes, T. P. & Harper, J. C. (eds): *Trace Fossils 2*. Seel House Press, Liverpool.

Fedonkin, M. A. 1981: *Belomorskaya biota Venda (dokembriyskaia besskeletnaya fauna severa Russkoy platformi)*. Nauka, Moskow, 99 pp.

Fedonkin, M. A. 1985: Paleoikhnologiya vendskikh Metazoa. 112–117 *in* Sokolov, B.S. & Ivanovskij, A.B. (eds): *Vendskaya Sistema l. Paleontologiya*. Nauka, Moskva.

Fedonkin, M. A. 1990: Paleoichnology of Vendian metazoa. 132–341 *in* Sokolov, B. S. & Iwanoski, A. B. (eds): *The Vendian System 1: Paleontology*. Berlin, Springer.

Fedonkin, M. A. & Vickers-Rich, P. 2007: First trace of motion. 205–217 *in* Fedonkin, M. A., Gehling, J. G., Grey, K., Narbonne, G. M. & Vickers-Rich, P. (eds): *The Rise of Animals. Evolution and Diversification of the Kingdom Animalia*. Baltimore, The John Hopkins University Press.

Fedonkin, M., Liñán, E. & Perejón, A. 1983: Icnofósiles de las rocas Precámbrico-Cámbricas de la Sierra de Córdoba. España. *Boletín de la Real Sociedad Española de Historia Natural (Sección Geológica) 81*, 125–138.

Feibel, C. S. 1987: Fossil fish nests from the Koobi Fora Formation (Plio-Pleistocene) of northern Kenya. *Journal of Paleontology 61*, 130–134.

Felder, D. L. 2001: Diversity and ecological significance of deep-burrowing macrocrustaceans in coastal tropical waters of the Americas (Decapoda: Thalassinidea). *Interciencia 26*, 440–449.

Feldmann, M. & McKenzie, J. A. 1998: Stromatolite-thrombolite associations in a modern environment, Lee Stocking Island, Bahamas. *Palaios 13*, 201–212. https://doi.org/10.2307/3515490

Feng, X., Chen, Z.-Q., Woods, A. & Fang, Y. 2017: A Smithian (early Triassic) ichnoassemblage from Lichuan, Hubei Province, South China: implications for biotic recovery after the latest Permian mass extinction. *Palaeogeography, Palaeoclimatology, Palaeoecology 486*, 123–141. https://doi.org/10.1016/j.palaeo.2017.03.003

Feng, X., Chen, Z.-Q., Benton, M.J., Wu, S., Bottjer, D. J. & Thompson, J .R. 2019: A diverse trackway-dominated marine ichnoassemblage from the lower Triassic in the northern Paleotethys: ichnology and implications for biotic recovery. *Palaeogeography, Palaeoclimatology, Palaeoecology 519*, 124–140. https://doi.org/10.1016/j.palaeo.2017.11.059

Fenton, C. L. & Fenton, M. A. 1931: Apparent gastropod trails in the lower Cambrian. *American Midland Naturalist 12*, 401–405. https://doi.org/10.2307/2420139

Fenton, C. L. & Fenton, M. A. 1937a: Archaeonassa: Cambrian snail trails and burrows. *American Midland Naturalist 18*, 454–456. https://doi.org/10.2307/2420587

Fenton, C. L. & Fenton, M. A. 1937b: Olivellites, a Pennsylvanian snail burrow. *American Midland Naturalist 18*, 452–453.

Ferguson, S. A. 2017: *Late Neoproterozoic epithermal-style Au mineralization of the Burin Peninsula, Newfoundland: U-Pb geochronology and deposit characteristics*. Unpublished Master Dissertation, Memorial University of Newfoundland, St John's, 368 pp.

Fernandes, A. C. S. & Carvalho, I. S. 2006: Invertebrate ichnofossils from the Adamantina Formation (Bauru Basin, late Cretaceous), Brazil. *Revista Brasileira de Paleontologia 9*, 211–220. https://doi.org/10.4072/rbp.2006.2.05

Fernandes, A. C. S., Borghi, L., Carvalho, I. S. & Abreu, C. J. 2002: *Guia dos Icnofósseis de Invertebrados do Brasil*. Interciência, Rio de Janeiro, 260 pp.

Fernández, D. E. & Pazos, P. J. 2012: Ichnology of marginal marine facies of the Agrio Formation (lower Cretaceous, Neuquén Basin, Argentina) at its type locality. *Ameghiniana 49*, 505–524. https://doi.org/10.5710/AMGH.23.7.2012.439

Fillion, D. & Pickerill, R. K. 1984a: On *Arthraria antiquata* Billings, 1872 and its relationship to *Diplocraterion* Torell, 1870 and *Bifungites* Desio, 1940. *Journal of Paleontology 58*, 683–696.

Fillion, D. & Pickerill, R. 1984b: Systematic ichnology of the middle Ordovician Trenton Group, St Lawrence Lowland, eastern Canada. *Maritime Sediments and Atlantic Geology 20*, 1–41. https://doi.org/10.4138/1572

Fillion, D. & Pickerill, R. K. 1990: Ichnology of the upper Cambrian? to lower Ordovician Bell Island and Wabana groups of eastern Newfoundland, Canada. *Palaeontographica Canadiana 7*, 1–119.

Fillmore, D. L., Szajna, M. J., Lucas, S. G., Hartline, B. W. & Simpson, E. L. 2017: Ichnology of a late Triassic lake margin: the Lockatong Formation, Newark Basin, Pennsylvania. *New Mexico Museum of Natural History and Science 76*, 1–107.

Fischer, P. & Paulus, B. 1969: Spurenfossilien aus den Oberen Nohn-Schichten der Blankenheimer Mulde (Eifelium, Eifel). *Senckenbergiana lethaea 50*, 81–101.

Fischer, W. A. 1978: The habitat of the early vertebrates: trace and body fossil evidence from the Harding Formation (middle Ordovician), Colorado. *Mountain Geologist 15*, 1–26.

Fisher, W. K. & MacGinitie, G. E. 1928: The natural history of an echiuroid worm. *Annals and Magazine of Natural History 1*, 204–213. https://doi.org/10.1080/00222932808672765

Fitch, A. 1850: A historical, topographical and agricultural survey of the County of Washington. Part 2-5. *Transactions of the New York Agricultural Society 9*, 753–944.

Fleming, C. A. 1973: "Fossil cuff-links": a new Miocene trace fossil of the genus *Diplocraterion* from New Zeland. *Tohoku University, Science Reports, 2nd Series (Geology), Special Volume 6*, 415–418.

Flemming, B. W. & Ziegler, K. 1995: High-resolution grain size distribution patterns and textural trends in the backbarrier environment of Spiekeroog Island (Southern North Sea). *Senckenbergiana Maritima 26*, 1–24.

Flügel, E. 2010: *Microfacies of Carbonate Rocks. Analysis, Interpretation and Application. 2nd Edition*. Springer, Dordrecht, 984 pp.

Föllmi, K. B. & Grimm, K. A. 1990: Doomed pioneers: gravity-flow deposition and bioturbation in marine oxygen-deficient environments. *Geology 18*, 1069–1072. https://doi.org/10.1130/0091-7613(1990)018<1069:DPGFDA>2.3.CO;2

Fortey, R. A. & Owens, R. M. 1999: Feeding habits in trilobites. *Palaeontology 42*, 429–465. https://doi.org/10.1111/1475-4983.00080

Fortey, R. A. & Seilacher, A. 1997: The trace fossil *Cruziana semiplicata* and the trilobite that made it. *Lethaia 30*, 105–112. https://doi.org/10.1111/j.1502-3931.1997.tb00450.x

Foster, G. & Carter, L. 1997: Mud sedimentation on the continental shelf at an accretionary margin—Poverty Bay, New Zealand. *New Zealand Journal of Geology and Geophysics 40*, 157–173. https://doi.org/10.1080/00288306.1997.9514750

Fournier, J. A., Pemberton, S. G. & Risk, M. J. 1980: *Polycylindrichnus*: possible Silurian tunicate burrows from southern Ontario. *Canadian Journal of Earth Sciences 17*, 738–743. https://doi.org/10.1139/e80-070

Frey, R. W. 1970: *Trace fossils of Fort Hays Limestone Member of Niobrara Chalk (Upper Cretaceous), west-central Kansas*. The University of Kansas. Paleontological contributions. Article 53 (Cretaceous 2), 41 pp.

Frey, R. W. 1975: The realm of ichnology, its strengths and limitations. 13–38 *in* Frey, R. W. (ed): *The study of trace fossils. A synthesis of Principles, Problems, and Procedures in Ichnology*. Springer-Verlag, Berlin. https://doi.org/10.1007/978-3-642-65923-2_2

Frey, R. W. & Bromley, R. G. 1985: Ichnology of American chalks: the Selma Group (upper Cretaceous), western Alabama. *Canadian Journal of Earth Sciences 22*, 801–828. https://doi.org/10.1139/e85-087

Frey, R. W. & Chowns, T. M. 1972: Trace fossils from the Ringgold road cut (Ordovician and Silurian), Georgia. *Sedimentary environments in the Paleozoic rocks of northwest Georgia 11*, 25–55.

Frey, R. W. & Howard, J. D. 1981: *Conichnus* and *Schaubcylindrichnus*: redefined trace fossils from the upper Cretaceous of the Western Interior. *Journal of Paleontology 55*, 800–804.

Frey, R. W. & Howard, J. D. 1985: Trace fossils from the Panther Member, Star Point Formation (upper Cretaceous), Coal Creek Canyon, Utah. *Journal of Paleontology 59*, 370–404.

Frey, R. W. & Pemberton, S. G. 1987: The *Psilonichnus* ichnocoenose, and its relationship to adjacent marine and nonmarine ichnocoenoses along the Georgia coast. *Bulletin of Canadian Petroleum Geology 35*, 333–357. https://doi.org/10.35767/gscpgbull.35.3.333

Frey, R. W., Howard, J. D., Han, S. J. & Park, B. K. 1989: Sediments and sedimentary sequences on a modern macrotidal flat, Inchon, Korea. *Journal of Sedimentary Petrology 59*, 28–44. https://doi.org/10.1306/212F8F0D-2B24-11D7-8648000102C1865D

Fritsch, A. 1908: *Problematica Silurica. Systême Silurien du Centre de la Bohême par Joachim Barrande Suite éditée aux frais du Barrande Fonds*. Prague, 24 pp.

Fritz, W. H. & Crimes, T. P. 1985: Lithology, trace fossils, and correlation of Precambrian-Cambrian boundary beds, Cassiar Mountains, north-central British Columbia. *Geological Survey of Canada Paper 83-13*, 1–24. https://doi.org/10.4095/120142

Fu, D., Legg, D. A., Daley, A. C., Budd, G. E., Wu, Y. & Zhang, X. 2022: The evolution of biramous appendages revealed by a carapace-bearing Cambrian arthropod. *Philosophical Transactions of the Royal Society B 377*, 20210034. https://doi.org/10.1098/rstb.2021.0034

Fu, S. & Werner, F. 1994: Distribution and composition of biogenic structures on the Iceland-Faeroe ridge: relation to different environments. *Palaios 9*, 92–101. https://doi.org/10.2307/3515082

Fuchs, T. 1895: Studien über Fucoiden und Hieroglyphen. *Denkschriften der Kaiserlichen Akademie der Wissenschaften, Mathematisch-Naturwissenschaftliche Classe 62*, 369–448.

Fürsich, F. T. 1974a: Corallian (upper Jurassic) trace fossils from England and Normandy. *Stuttgarter Beiträge zur Naturkunde Serie B 13*, 1–52.

Fürsich, F. T. 1974b: On *Diplocraterion* Torell 1870 and the significance of morphological features in vertical, spreiten-bearing, U-shaped trace fossils. *Journal of Paleontology 48*, 952–962.

Fürsich, F. T. 1975: Trace fossils as environmental indicators in the Corallian of England and Normandy. *Lethaia 8*, 151–172. https://doi.org/10.1111/j.1502-3931.1975.tb01309.x

Fürsich, F. T. & Heinberg, C. 1983: Sedimentology, biostratinomy, and palaeoecology of an upper Jurassic offshore sand bar complex. *Bulletin of the Geological Society of Denmark 32*, 67–95. https://doi.org/10.37570/bgsd-1983-32-04

Fürsich, F. T., Oschmann, W., Singh, I. B. & Jaitly, A. K. 1992: Hardgrounds, reworked concretion levels and condensed horizons in the Jurassic of western India: their significance for basin analysis. *Journal of the Geological Society, London 149*, 313–331. https://doi.org/10.1144/gsjgs.149.3.0313

Fürsich, F. T., Pandey, D. K., Kashyab, D. & Wilmsen, M. 2006: The trace fossil *Ctenopholeus* Seilacher and Hemleben, 1966 from the Jurassic of India and Iran: distinction from related ichnogenera. *Neues Jahrbuch für Geologie und Paläontologie Monatshefte 11*, 641–654. https://doi.org/10.1127/njgpm/2006/2006/641

Gaigalas, A. & Uchman, A. 2004: Trace fossils from upper Pleistocene varved clays S of Kaunas, Lithuania. *Geologija 45*, 16–26.

Gaillard, C. 1980: *Megagyrolithes ardescensis* n. gen, n. sp., trace fossile nouvelle du Valanginien d'Ardeche (France). *Géobios 13*, 465–471. https://doi.org/10.1016/S0016-6995(80)80083-0

Gaillard, C. & Olivero, D. 2009: The ichnofossil *Halimedides* in Cretaceous pelagic deposits from the Alps: environmental and ethological significance. *Palaios 24*, 257–270. https://doi.org/10.2110/palo.2008.p08-055r

Gaillard, C. & Racheboeuf, P. R. 2006: Trace fossils from nearshore to offshore environments: lower Devonian of Bolivia. *Journal of Paleontology 80*, 1205–1226. https://doi.org/10.1666/0022-3360(2006)80[1205:TFFNTO]2.0.CO;2

Gaines, R. R. & Vorhies, J. S. 2016: Growth mechanisms and geochemistry of carbonate concretions from the Cambrian Wheeler Formation (Utah, USA). *Sedimentology 63*, 662–698. https://doi.org/10.1111/sed.12234

Gámez-Vintaned, J. A. 1995: Los materiales prehercínicos de la Sierra del Moncayo (Cadena Ibérica Oriental, España) y su contenido paleoicnológico. *Boletín de la Real Sociedad Española de Historia Natural (Sección Geológica) 90*, 21–50.

Gámez-Vintaned, J. A. & Liñán, E. 1993: Paléoichnologie. 19–26 *in* Amerom, H. W. J. (ed): *Les flores du Permien basal et la paléoichnologie de la fosse de Fombuena (province de Zaragoza, Espagne)*. Mededelingen Rijks Geologische Dienst, Haarlem, Nr. 48.

Gámez Vintaned, J. A., Liñán, E., Mayoral, E., Dies, M. E., Gozalo, R. & Muñiz, F. 2006: Trace and soft body fossils from the Pedroche Formation (Ovetian, lower Cambrian of the Sierra de Córdoba, S Spain) and their relation to the Pedroche event. *Geobios 39*, 443–468. https://doi.org/10.1016/j.geobios.2005.04.004

Gand, G., Garric, J., Schneider, J., Walter, H., Lapeyrie, J., Martin, C. & Thiery, A. 2008: Notostraca trackways in Permian playa environments of the Lodève basin (France). *Journal of Iberian Geology 34*, 73–108.

Gao, S. 2019: Geomorphology and sedimentology of tidal flats. 359–381 *in* Perillo, G. M. E., Wolanski, E., Cahoon D. R. & Hopkinson C. S. (eds): *Coastal wetlands: an integrated ecosystem approach*. Elsevier, Netherlands. https://doi.org/10.1016/B978-0-444-63893-9.00010-1

García-Hidalgo, J. F. 1993: Las pistas fósiles de los anticlinales de Alcudia y Abenójar (Zona Centroibérica). Edad de las series. *Geogaceta 14*, 57–59.

Garcia-Pichel, F., Al-Horani, F. A., Farmer, J. D., Ludwig, R. & Wade, B. D. 2004: Balance between microbial calcification and metazoan bioerosion in modern stromatolitic oncolites. *Geobiology 2*, 49–57. https://doi.org/10.1111/j.1472-4669.2004.00017.x

Garcia-Ramos, J. C. M. 1976: Morfología de trazas fósiles en dos afloramientos de "Arenisca del Naranco" (Devónico medio) de Asturias (NW de España). *Trabajos de Geología 8*, 131–173. https://doi.org/10.17811/tdg.8.1976.131-173

Garvey, J. M. & Hasiotis, S. T. 2008: An ichnofossil assemblage from the lower Carboniferous Snowy Plains Formation, Mansfield Basin, Australia. *Palaeogeography, Palaeoclimatology, Palaeoecology 258*, 257–276. https://doi.org/10.1016/j.palaeo.2007.11.002

Gehling, J. G. 2000: Environmental interpretation and a sequence stratigraphic framework for the terminal Proterozoic Ediacara Member within the Rawnsley Quartzite, south Australia. *Precambrian Research 100*, 65–95. https://doi.org/10.1016/S0301-9268(99)00069-8

Gehling, J. G. & Droser, M. L. 2009: Textured organic surfaces associated with the Ediacara biota in south Australia. *Earth-Science Reviews 96*, 196–206. https://doi.org/10.1016/j.earscirev.2009.03.002

Gehling, J. G. & Droser, M. L. 2018: Ediacaran scavenging as a prelude to predation. *Emerging Topics in Life Sciences 2*, 213–222. https://doi.org/10.1042/ETLS20170166

Gehling, J. G., Jensen, S., Droser, M. L., Myrow, P. M. & Narbonne, G. M. 2001: Burrowing below the basal Cambrian GSSP, Fortune Head, Newfoundland. *Geological Magazine 138*, 213–218. https://doi.org/10.1017/S001675680100509X

Gehling, J. G., Runnegar, B. N. & Droser, M. L. 2014: Scratch traces of large Ediacara bilaterian animals. *Journal of Paleontology 88*, 284–298. https://doi.org/10.1666/13-054

Gehling, J. G., García-Bellido, D. C., Droser, M. L., Tarhan, M. L. & Runnegar, B. 2019: The Ediacaran–Cambrian transition: sedimentary facies versus extinction. *Estudios Geológicos 75*, e099. https://doi.org/10.3989/egeol.43601.554

Geinitz, H. B. 1871: Die Seeschwämme des unteren Quaders. 3–41 *in* Geinitz, H. B. (ed): *Das Elbthagebirge in Sachsen. Erster Theil. Der untere Quader*. T. Fischer, Cassel.

Genise, J. F., Melchor, R. N., Bellosi, E. S. & Verde, M. 2010: Invertebrate and vertebrate trace fossils from continental carbonates. *Developments in Sedimentology 61*, 319–369. https://doi.org/10.1016/S0070-4571(09)06107-X

Germs, G. J. B. 1972: Trace fossils from the Nama Group, southwest Africa. *Journal of Paleontology 46*, 864–870.

Gernant, R. E. 1972: The paleoenvironmental significance of *Gyrolithes* (Lebensspur). *Journal of Paleontology 46*, 735–741.

Getty, P. R. & Bush, A. M. 2017: On the ichnotaxonomic status of *Haplotichnus indianensis* (Miller, 1889). *Ichnos 24*, 234–238. https://doi.org/10.1080/10420940.2016.1270210

Getty, P. R. & Goldstein, D. H. 2022: A redescription and reassessment of the fossil trail *Trisulcus laqueatus* Hitchcock, 1865 from the early Jurassic of Massachusetts. *Palaeodiversity 15*, 61–71. https://doi.org/10.18476/pale.v15.a4

Getty, P. R., McCarthy, T. D., Hsieh, S. & Bush, A. M. 2016: A new reconstruction of continental *Treptichnus* based on exceptionally preserved material from the Jurassic of Massachusetts. *Journal of Paleontology 90*, 269–278. https://doi.org/10.1017/jpa.2016.20

Getty, P. R., Sproule, R., Stimson, M. R. & Lyons, P. C. 2017: Invertebrate trace fossils from the Pennsylvanian Rhode Island formation of Massachusetts, USA. *Atlantic Geology 53*, 185–206. https://doi.org/10.4138/atlgeol.2017.007

Gevirtzman, D. A. & Mount, J. F. 1986: Paleoenvironments of an earliest Cambrian (Tommotian) shelly fauna in the southwestern Great Basin, USA. *Journal of Sedimentary Petrology 56*, 412–421. https://doi.org/10.1306/212F8931-2B24-11D7-8648000102C1865D

Geyer, G. 2005: The Fish River Subgroup in Namibia: stratigraphy, depositional environments and the Proterozoic–Cambrian boundary problem revisited. *Geological Magazine 142*, 465–498. https://doi.org/10.1017/S0016756805000956

Geyer, G. 2019: A comprehensive Cambrian correlation chart. *Episodes 42*, 321–332. https://doi.org/10.18814/epiiugs/2019/019026

Geyer, G. & Landing, E. 2016: The Precambrian-Phanerozoic and Ediacaran-Cambrian boundaries: a historical approach to a dilemma. *Geological Society, London, Special Publications 448*, 311–349. https://doi.org/10.1144/SP448.10

Geyer, G. & Uchman, A. 1995: Ichnofossil assemblages from the Nama Group (Neoproterozoic–lower Cambrian) in Namibia and the Proterozoic–Cambrian boundary problem revisited. *Beringeria Special Issue 2*, 175–202.

Ghare, M. A. & Kulkarni, K. G. 1986: Jurassic ichnofauna of Kutch–II. Wagad region. *Biovigyanam 12*, 44–62.

Ghienne, J.-F., Boumendjel, K., Paris, F., Videt, B., Racheboeuf, P. & Salem, H. A. 2007: The Cambrian-Ordovician succession in the Ougarta Range (western Algeria, north Africa) and interference of the late Ordovician glaciation on the development of the lower Palaeozoic transgression on northern Gondwana. *Bulletin of Geosciences 82*, 183–214. https://doi.org/10.3140/bull.geosci.2007.03.183

Ghienne, J.-F., Monod, O., Kozlu, H. & Dean, W. T. 2010: Cambrian–Ordovician depositional sequences in the Middle East: a perspective from Turkey. *Earth-Science Reviews 101*, 101–146. https://doi.org/10.1016/j.earscirev.2010.04.004

Gibb, S., Chatterton, B. D. E. & Pemberton, S. G. 2009: Arthropod ichnofossils from the Ordovician Stairway Sandstone of central Australia. *Memoirs of the Association of Australasian Palaeontologists 37*, 695–716.

Gibb, S., Chatterton, B. D. E. & Gingras, M. K. 2010: *Rusophycus carleyi* (James, 1885), trace fossils from the lower Ordovician of southern Morocco, and the trilobites that made them. *Ichnos 17*, 271–283. https://doi.org/10.1080/10420940.2010.535452

Gibb, S., Pemberton, S. G. & Chatterton, B. D. 2017: Arthropod trace fossils of the upper lower Cambrian Gog Group, southern Rocky Mountains of Canada. *Ichnos 24*, 91–123. https://doi.org/10.1080/10420940.2016.1216845

Gibbard, P. L. & Stuart, A. J. 1974: Trace fossils from proglacial lake sediments. *Boreas 3*, 69–74. https://doi.org/10.1111/j.1502-3885.1974.tb00829.x

Gibson, G. G. 1989: Trace fossils from late Precambrian Carolina slate belt, south-central North Carolina. *Journal of Paleontology 63*, 1–10. https://doi.org/10.1017/S0022336000040889

Gingras, M. K. & Zonneveld, J. P. 2015: Tubular tidalites: a biogenic sedimentary structure indicative of tidally influenced sedimentation. *Journal of Sedimentary Research 85*, 845–854. https://doi.org/10.2110/jsr.2015.54

Gillette, L., Pemberton, S. G. & Sarjeant, W. A. S. 2003: A late Triassic invertebrate ichnofauna from Ghost Ranch, New Mexico. *Ichnos 10*, 141–151. https://doi.org/10.1080/10420940390255493

Gingras, M. K., Pemberton, S. G., Saunders, T. & Clifton, H. E. 1999: The ichnology of modern and Pleistocene brackish-water deposits at Willapa Bay, Washington: variability in estuarine settings. *Palaios 14*, 352–374. https://doi.org/10.2307/3515462

Gingras, M. K., Pemberton, S. G. & Saunders, T. 2001: Bathymetry, sediment texture, and substrate cohesiveness; their impact on modern *Glossifungites* trace assemblages at Willapa Bay, Washington. *Palaeogeography, Palaeoclimatology, Palaeoecology 169*, 1–21. https://doi.org/10.1016/S0031-0182(01)00212-7

Gingras, M. K., Pickerill, R. & Pemberton, S. G. 2002: Resin cast of modern burrows provides analogs for composite trace fossils. *Palaios 17*, 206–211. https://doi.org/10.1669/0883-1351(2002)017<0206:RCOMBP>2.0.CO;2

Gingras, M. K., Dashtgard, S. E., MacEachern, J. A. & Pemberton, S. G. 2008: Biology of shallow marine ichnology: a modern perspective. *Aquatic Biology 2*, 255–268. https://doi.org/10.3354/ab00055

Gingras, M. K., Waldron, J. W., White, C. E. & Barr, S. M. 2011: The evolutionary significance of a lower Cambrian trace-fossil assemblage from the Meguma Terrane, Nova Scotia. *Canadian Journal of Earth Sciences 48*, 71–85. https://doi.org/10.1139/E10-086

Gingras, M. K., MacEachern, J. A., Dashtgard, S. E., Ranger, M. J. & Pemberton, S. G. 2016: The significance of trace fossils in the

McMurray Formation, Alberta, Canada. *Bulletin of Canadian Petroleum Geology 64*, 233–250. https://doi.org/10.2113/gscpgbull.64.2.233

Giribet, G. & Edgecombe, G. D. 2019: The phylogeny and evolutionary history of arthropods. *Current Biology 29*, R592–R602. https://doi.org/10.1016/j.cub.2019.04.057

Glaessner, M. F. 1957: Palaeozoic arthropod trails from Australia. *Paläontologische Zeitschrift 31*, 103–108. https://doi.org/10.1007/BF02988968

Glaessner, M. F. 1962: Pre-Cambrian fossils. *Biological Reviews 37*, 467–493. https://doi.org/10.1111/j.1469-185X.1962.tb01331.x

Glaessner, M. F. 1969: Trace fossils from the Precambrian and basal Cambrian. *Lethaia 2*, 369–393. https://doi.org/10.1111/j.1502-3931.1969.tb01258.x

Glud, R. N. 2008: Oxygen dynamics of marine sediments. *Marine Biology Research 4*, 243–289. https://doi.org/10.1080/17451000801888726

Głuszek, A. 1995: Invertebrate trace fossils in the continental deposits of an upper Carboniferous coal-bearing succession, upper Silesia, Poland. *Studia Geologica Polonica 108*, 171–202.

Głuszek, A. 1998: Trace fossils from late Carboniferous storm deposits, upper Silesia Coal Basin, Poland. *Acta Palaeontologica Polonica 43*, 517–546.

Goldring, R. 1962: The trace fossils of the Baggy Beds (upper Devonian) of north Devon, England. *Paläontologische Zeitschrift 36*, 232–251. https://doi.org/10.1007/BF02986976

Goldring, R. 1967: The significance of certain trace-fossil ranges. *Geological Society, London, Special Publications 2*, 37–39. https://doi.org/10.1144/GSL.SP.1967.002.01.05

Goldring, R. 1985: The formation of the trace fossil *Cruziana*. *Geological Magazine 122*, 65–72. https://doi.org/10.1017/S0016756800034099

Goldring, R. & Jensen, S. 1996: Trace fossils and biofabrics at the Precambrian–Cambrian boundary interval in western Mongolia. *Geological Magazine 133*, 403–415. https://doi.org/10.1017/S0016756800007573

Goldring, R., Pollard, J. E. & Radley, J. D. 2005: Trace fossils and pseudofossils from the Wealden strata (non-marine lower Cretaceous) of southern England. *Cretaceous Research 26*, 665–685. https://doi.org/10.1016/j.cretres.2005.03.001

Goldstein, D. H., Getty, P. R. & Bush, A. M. 2017: Hitchcock's treptichnid trace fossils (Jurassic, Massachusetts, USA): conflicting interpretations in the "Age of Fucoids". *Bollettino della Società Paleontologica Italiana 56*, 109–116. https://doi.org/10.4435/BSPI.2017.11

Golubic, S. & Focke, J. W. 1978: *Phormidium hendersonii* Howe: identity and significance of a modern stromatolite building microorganism. *Journal of Sedimentary Petrology 48*, 751–764. https://doi.org/10.1306/212F7559-2B24-11D7-8648000102C1865D

Gomez de Llarena, J. 1946: Revisión de algunos datos paleontológicos del flysch Cretáceo y nummulítico de Guipúzcoa. *Notas y Comunicaciones des Instituto Geológico y Minero de España 15*, 113–165.

Gong, Y. & Droser, M. L. 2001: Periodic anoxic shelf in the early-middle Ordovician transition: ichnosedimentologic evidence from west-central Utah, USA. *Science in China (Series D) 44*, 979–989. https://doi.org/10.1007/BF02875391

Goodwin, P. W. & Anderson, E. J. 1974: Associated physical and biogenic structures in environmental subdivision of a Cambrian tidal sand body. *Journal of Geology 82*, 779–794. https://doi.org/10.1086/628029

Gougeon, R. 2023: *The Chapel Island Formation of Newfoundland (Canada) revisited: integrating ichnologic and sedimentologic datasets to unravel early metazoan evolution*. Unpublished Doctoral Dissertation, University of Saskatchewan, 648 pp.

Gougeon, R. C., Mángano, M. G., Buatois, L. A., Narbonne, G. M. & Laing, B. A. 2018a: Early Cambrian origin of the shelf sediment mixed layer. *Nature Communications 9*, 1909. https://doi.org/10.1038/s41467-018-04311-8

Gougeon, R., Néraudeau, D., Dabard, M.-P., Pierson-Wickmann, A.-C., Polette, F., Poujol, M. & Saint-Martin, J.-P. 2018b: Trace fossils from the Brioverian (Ediacaran–Fortunian) in Brittany (NW France). *Ichnos 25*, 11–24. https://doi.org/10.1080/10420940.2017.1308865

Gougeon, R., Néraudeau, D., Loi, A. & Poujol, M. 2022: New insights into the early evolution of horizontal spiral trace fossils and the age of the Brioverian series (Ediacaran–Cambrian) in Brittany, NW France. *Geological Magazine 159*, 1284–1294. https://doi.org/10.1017/S0016756820001430

Gougeon, R., Mángano, M. G., Buatois, L. A., Narbonne, G. M., Laing, B. A. & Paz, M. 2023: The Ediacaran–Cambrian Chapel Island Formation of Newfoundland, Canada: evaluating the impact of outcrop quality on trace-fossil data sets at the Cambrian GSSP and less-explored sections. *Canadian Journal of Earth Sciences 60*, 897–911. https://doi.org/10.1139/cjes-2022-0060

Gougeon, R., Buatois, L. A., Mángano, M. G., Narbonne, G. M., Laing, B. A., Paz, M. & Minter, N. J. 2025a: Environmental and evolutionary controls in animal-sediment interactions at the onset of the Cambrian explosion. *Current Biology 35*, P249–264. E4. https://doi.org/10.1016/j.cub.2024.11.028

Gougeon, R., Mángano, M. G., Buatois, L. A., Narbonne, G. M., Laing, B. A. & Paz, M. 2025b: Ichnologic and sedimentologic datasets from the Ediacaran–Cambrian Chapel Island Formation, Newfoundland, Canada. *Data in Brief 58*, 111258. https://doi.org/10.1016/j.dib.2024.111258

Gougeon, R., Mángano, M. G., Buatois, L. A., Narbonne, G. & Rindsberg, A. In press: Case 3914 – *Rusophycus avalonensis* Crimes & Anderson, 1985 (trace fossil): proposed conservation of current usage by designation of a neotype. *Bulletin of the Zoological Nomenclature*.

Gougeon, R., Vidal, M. & Michaud, E. 2025c: *Bifungites* from the Ordovician of Crozon Peninsula (Kermeur Formation, Brittany, France): environmental tolerance and evolutionary trajectory of an extinct animal behaviour. *Geological Society, London, Special Publications 556*, SP556-2025. https://doi.org/10.1144/SP556-2025-2

Gradziński, R. & Uchman, A. 1994: Trace fossils from interdune deposits—an example from the lower Triassic aeolian Tumlin Sandstone, central Poland. *Palaeogeography, Palaeoclimatology, Palaeoecology 108*, 121–138. https://doi.org/10.1016/0031-0182(94)90025-6

Graulich, J.-M. 1961: Description et occurrence de *Arenicolites fourmarieri* nov. sp. *Bulletin de la Société Belge de Géologie, de Paléontologie et d'Hydrologie 70*, 6–14.

Gray, J. & Lissmann, H. W. 1964: The locomotion of nematodes. *Journal of Experimental Biology 41*, 135–154. https://doi.org/10.1242/jeb.41.1.135

Grazhdankin, D. V. & Gerdes, G. 2007: Ediacaran microbial colonies. *Lethaia 40*, 201–210. https://doi.org/10.1111/j.1502-3931.2007.00025.x

Grazhdankin, D. V. & Krayushkin, A. V. 2007: Trace fossils and the upper Vendian boundary in the southeastern White Sea region. *Doklady Earth Sciences 416*, 1027–1031. https://doi.org/10.1134/S1028334X07070100

Grazhdankin, D. V., Balthasar, U., Nagovitsin, K. E. & Kochnev, B. B. 2008: Carbonate-hosted Avalon-type fossils in arctic Siberia. *Geology 36*, 803–806. https://doi.org/10.1130/G24946A.1

Grazhdankin, D. V., Marusin, V. V., Izokh, O. P., Karlova, G. A., Kochnev, B. B., Markov, G. E., Nagovitsin, K. E., Sarsembaev, Z., Peek, S., Cui, H. & Kaufman, A. J. 2020a: Quo vadis, Tommotian? *Geological Magazine 157*, 22–34. https://doi.org/10.1017/S0016756819001286

Grazhdankin, D., Nagovitsin, K., Golubkova, E., Karlova, G., Kochnev, B., Rogov, V. & Marusin, V. 2020b: Doushantuo-Pertatataka–type acanthomorphs and Ediacaran ecosystem stability. *Geology 48*, 708–712. https://doi.org/10.1130/G47467.1

Greb, S. F. & Archer, A. W. 1995: Rhythmic sedimentation in a mixed tide and wave deposit, Hazel Patch Sandstone (Pennsylvanian), eastern Kentucky coal field. *Journal of Sedimentary Research 65*, 96–106. https://doi.org/10.1306/D42681EE-2B26-11D7-8648000102C1865D

Greb, S. F. & Chesnut Jr., D. R. 1994: Paleoecology of an estuarine sequence in the Breathitt Formation (Pennsylvanian), central Appalachian Basin. *Palaios 9*, 388-402. https://doi.org/10.2307/3515057

Greene, B. & Williams, H. 1974: New fossil localities and the base of the Cambrian in southeastern Newfoundland. *Canadian Journal of Earth Sciences 11*, 319–323. https://doi.org/10.1139/e74-027

Gregory, M. R. 1991: New trace fossils from the Miocene of Northland, New Zealand: *Rorschachichnus amoeba* and *Piscichnus waitemata*. *Ichnos 1*, 195–205. https://doi.org/10.1080/10420949109386352

Grice, K., Holman, A. I., Plet, C. & Tripp, M. 2019: Fossilised biomolecules and biomarkers in carbonate concretions from Konservat-Lagerstätten. *Minerals 9*, 158. https://doi.org/10.3390/min9030158

Grimm, K. A. & Föllmi, K. B. 1994: Doomed pioneers: allochthonous crustacean tracemakers in anaerobic basinal strata, Oligo-Miocene San Gregorio Formation, Baja California Sur, Mexico. *Palaios 9*, 313–334. https://doi.org/10.2307/3515054

Grotzinger, J. P. & James, N. P. 2000: Precambrian carbonates: evolution of understanding. 3–20 *in* Grotzinger, J. P. & James, N. P. (eds): *Carbonate Sedimentation and Diagenesis in the Evolving Precambrian World*. SEPM Special Publication 67.

Grundvåg, S.-A., Jelby, M. E., Olaussen, S. & Śliwińska, K. K. 2021: The role of shelf morphology on storm-bed variability and stratigraphic architecture, lower Cretaceous, Svalbard. *Sedimentology 68*, 196–237. https://doi.org/10.1111/sed.12791

Grytsenko, V. 2016: A new discovery of metazoa imprints and ichnofossils in the Vendian Mohyliv suite from the Bernashivka quarry. *Proceedings of the National Museum of Natural History (Kyiv) 14*, 23–34. https://doi.org/10.15407/vnm.2016.14.023

Gugliotta, M., Saito, Y., Nguyen, V. L., Ta, T. K. O., Tamura, T. & Fukuda, S. 2018: Tide-and river-generated mud pebbles from the fluvial to marine transition zone of the Mekong River delta, Vietnam. *Journal of Sedimentary Research 88*, 981–990. https://doi.org/10.2110/jsr.2018.54

Gutschick, R. C. & Rodriguez, J. 1977: Late Devonian-early Mississippian trace fossils and environments along the Cordilleran Miogeocline, western United States. 195–208 *in* Crimes, T.P. & Harper, J.C. (eds): *Trace Fossils 2*. Seel House Press, Liverpool.

Hagadorn, J. W. & Mcdowell, C. 2012: Microbial influence on erosion, grain transport and bedform genesis in sandy substrates under unidirectional flow. *Sedimentology 59*, 795–808. https://doi.org/10.1111/j.1365-3091.2011.01278.x

Hagadorn, J. W., Schellenberg, S. A. & Bottjer, D. J. 2000: Paleoecology of a large early Cambrian bioturbator. *Lethaia 33*, 142–156. https://doi.org/10.1080/00241160025100026

Hagadorn, J. W. & Waggoner, B. 2000: Ediacaran fossils from the southwestern Great Basin, United States. *Journal of Paleontology 74*, 349–359. https://doi.org/10.1666/0022-3360(2000)074<0349:EFFTSG>2.0.CO;2

Hagdorn, H. 2014: Spurenfossilien aus dem Lettenkeuper. 267–281 *in* Hagdorn, H., Schoch, R. & Schweigert, G. (eds): *Der Lettenkeuper-ein Fenster in die Zeit vor den Dinosauriern*. Palaeodiversity Sonderband, Special Issue, Staatliches Museum für Naturkunde Stuttgart.

Hageman, S. J. & Miller III, W. 2016: New fossil discoveries in the Chilhowee Group (southern Appalachians, USA): evidence for the Ediacaran-Cambrian transition, 'Cambrian Agronomic Revolution', and earliest trilobites at the southern margin of Laurentia. *Neues Jahrbuch für Geologie und Paläontologie Abhandlungen 281*, 135–154. https://doi.org/10.1127/njgpa/2016/0592

Hakes, W. G. 1976: Trace fossils and depositional environment of four clastic units, upper Pennsylvanian megacyclothems, northeast Kansas. *The University of Kansas Paleontological Contributions 63*, 1–46.

Hakes, W. G. 1977: Trace fossils in late Pennsylvanian cyclothems, Kansas. 209–226 *in* Crimes, T. P. & Harper, J. C. (eds): *Trace Fossils 2*. Seel House Press, Liverpool.

Hakes, W. G. 1985: Trace fossils from brackish-marine shales, upper Pennsylvanian of Kansas, U.S.A. 21–35 *in* Curran, H. A. (ed): *Biogenic structures: their use in interpreting depositional environments*. SEPM Special Publication, Vol. 35. https://doi.org/10.2110/pec.85.35.0021

Haldeman, S. S. 1840: *Supplement to Number One of "A Monograph of the Limniades, or Freshwater Univalve Shells of North America", Descriptions of Apparently New Animals in Different Classes, and the Names and Characters of the Subgenera in Paludina and Anculosa*. J. Dobson, Philadelphia, 3 pp.

Hall, J. 1847: *Palaeontology of New-York. Volume I. Containing descriptions of the organic remains of the lower division of the New-York System*. Van Benthuysen, Albany, 338 pp.

Hall, J. 1852: *Palaeontology of New-York. Volume II. Containing descriptions of the organic remains of the lower middle division of the New-York System*. Van Benthuysen, Albany, 362 pp.

Hall, J. 1886: Note on some obscure organisms in the roofing slate of Washington County, New York. *New York State Museum of Natural History, Annual Report 39*, 160.

Hallam, A. 1960: *Kulindrichnus langi*, a new trace-fossil from the Lias. *Palaeontology 3*, 64–68.

Halley, R. B. 1975: Peritidal lithologies of Cambrian carbonate islands, Carrara Formation, southern Great Basin. 279–288 *in* Ginsburg, R. N. (ed): *Tidal Deposits*. Springer, Berlin. https://doi.org/10.1007/978-3-642-88494-8_32

Halley, R. B. & Evans, C. C. 1983: *The Miami Limestone, A Guide to Selected Outcrops and Their Interpretation*. Miami Geological Society, 67 pp.

Hamilton, M. A., Álvaro, J. J., Barr, S. M., Jensen, S., Johnson, S. C., Palacios, T., van Rooyen, D. & White, C. E. 2024: U-Pb zircon ages from tuffaceous beds in the Terreneuvian to Cambrian Series 2 sections of Avalonian southern New Brunswick, Canada: new constraints on chronostratigraphic correlations and the Cambrian time scale. *Geological Society, London, Special Publications 542*, SP542-2022. https://doi.org/10.1144/SP542-2022-11

Hammersburg, S. R., Hasiotis, S. T. & Robison, R. A. 2018: Ichnotaxonomy of the Cambrian Spence Shale Member of the Langston Formation, Wellsville Mountains, northern Utah, USA. *Paleontological Contributions 2018*, 1–66. https://doi.org/10.17161/1808.26428

Han, Y. & Pickerill, R. K. 1994a: Taxonomic reassessment of *Protovirgularia* M'Coy 1850 with new examples from the Paleozoic of New Brunswick, eastern Canada. *Ichnos 3*, 203–212. https://doi.org/10.1080/10420949409386389

Han, Y. & Pickerill, R. K. 1994b: Palichnology of the lower Devonian Wapske Formation, Perth-Andover-Mount Carleton region, northwestern New Brunswick, eastern Canada. *Atlantic Geology 30*, 217–245. https://doi.org/10.4138/2131

Han, Y. & Pickerill, R. K. 1995: Taxonomic review of the ichnogenus *Helminthopsis* Heer 1877 with a statistical analysis of selected ichnospecies. *Ichnos 4*, 83–118. https://doi.org/10.1080/10420949509380118

Hanebuth, T. J. J., Lantzsch, H. & Nizou, J. 2015: Mud depocenters on continental shelves—appearance, initiation times, and growth dynamics. *Geo-Marine Letters 35*, 487–503. https://doi.org/10.1007/s00367-015-0422-6

Hanken, N.-M., Uchman, A., Nielsen, J. K., Olaussen, S., Eggebø, T. & Steinsland, R. 2016: Late Ordovician trace fossils from offshore to shallow water mixed siliciclastic and carbonate facies in the Ringerike Area, Oslo Region, Norway. *Ichnos 23*, 189–221. https://doi.org/10.1080/10420940.2016.1199427

Hantsoo, K. G., Kaufman, A. J., Cui, H., Plummer, R. E. & Narbonne, G. M. 2018: Effects of bioturbation on carbon and sulfur cycling across the Ediacaran–Cambrian transition at the GSSP in Newfoundland. *Canadian Journal of Earth Sciences 55*, 1240–1252. https://doi.org/10.1139/cjes-2017-0274

Häntzschel, W. 1934: Schraubenförmige und spiralige Grabgänge in turonen Sandsteinen des Zittauer Gebirges. *Senckenbergiana 16*, 313–324.

Häntzschel, W. 1962: Trace fossils and Problematica. 177–245 *in* Moore, R.C. (ed): *Treatise on Invertebrate Paleontology, Part W, Miscellanea*. Geological Society of America and University of Kansas Press, Boulder, Colorado.

Häntzschel, W. 1975: Trace fossils and Problematica. 1–269 *in* Teichert, C. (ed): *Treatise on Invertebrate Paleontology, Part W, Miscellanea, Supplement 1*. Geological Society of America and University of Kansas Press, Boulder, Colorado and Lawrence, Kansas.

Hauck, T. E., Dashtgard, S. E., Pemberton, S. G. & Gingras, M. K. 2009: Brackish-water ichnological trends in a microtidal barrier island–embayment system, Kouchibouguac National Park, New Brunswick, Canada. *Palaios 24*, 478–496. https://doi.org/10.2110/palo.2008.p08-056r

Hawco, J. B., Kenchington, C. G. & McIlroy, D. 2021: A quantitative and statistical discrimination of morphotaxa within the Ediacaran genus *Palaeopascichnus*. *Papers in Palaeontology 7*, 657–673. https://doi.org/10.1002/spp2.1290

Hawkins, T. R. W. & Jones, F. G. 1981: Fold and cleavage development within Cambrian metasediments of the Vale of Ffestiniog, north Wales. *Geological Journal 16*, 65–84. https://doi.org/10.1002/gj.3350160107

Hayes, M. O. 1967: Hurricanes as geological agents, south Texas coast. *AAPG Bulletin 51*, 937–942. https://doi.org/10.1306/5D25C0FF-16C1-11D7-8645000102C1865D

Hecker, R. F., Osipova, A. I. & Belskaya, T. N. 1962: *Ferganskiy zaliv paleogenovogo morya Sredney Azyi, ego istoria, osadki i fauna, flora, uslovia ih obitanya i razvitya. Kniga 2*. Izvestiia Akademii nauk SSSR, Moscow, 312 pp.

Heer, O. 1865: *Die Urwelt der Schweiz*. Friedrich Schultez, Zürich, 622 pp.

Heer, O. 1877: *Flora Fossilis Helvetiae. Die Vorweltliche Flora der Schweiz*. J. Wurster and Comp., Zürich, 182 pp.

Heezen, B. C. & Hollister, C. D. 1971: *The face of the deep*. Oxford University Press, New York, 659 pp.

Heinberg, C. 1970: Some Jurassic trace fossils from Jameson Land (east Greenland). 227–234 *in* Crimes, T. P. & Harper, J. C. (eds): *Trace Fossils*. Seel House Press, Liverpool.

Heinberg, C. 1973: The internal structure of the trace fossils *Gyrochorte* and *Curvolithus*. *Lethaia 6*, 227–238. https://doi.org/10.1111/j.1502-3931.1973.tb01196.x

Heinberg, C. & Birkelund, T. 1984: Trace-fossil assemblages and basin evolution of the Vardekløft Formation (middle Jurassic, central east Greenland). *Journal of Paleontology 58*, 362–397.

Hembree, D. I. & Hasiotis, S. T. 2007: Paleosols and ichnofossils of the White River Formation of Colorado: insight into soil ecosystems of the North American Midcontinent during the Eocene-Oligocene transition. *Palaios 22*, 123–142. https://doi.org/10.2110/palo.2005.p05-119r

Herbers, D. S., MacNaughton, R. B., Timmer, E. R. & Gingras, M. K. 2016: Sedimentology and ichnology of an early-middle Cambrian storm-influenced barred shoreface succession, Colville Hills, Northwest Territories. *Bulletin of Canadian Petroleum Geology 64*, 538–554. https://doi.org/10.2113/gscpgbull.64.4.538

Herringshaw, L. G., Callow, R. H. & McIlroy, D. 2017: Engineering the Cambrian explosion: the earliest bioturbators as ecosystem engineers. *Geological Society, London, Special Publications 448*, 369–382. https://doi.org/10.1144/SP448.18

Hertweck, G. & Reineck, H.-E. 1966: Untersuchungsmethoden von Gangbauten und anderen Wühlgefügen mariner Bodentiere. *Natur und Museum 96*, 429–437.

Hertweck, G., Wehrmann, A., Liebezeit, G. & Steffens, M. 2005: Ichnofabric zonation in modern tidal flats: palaeoenvironmental and palaeotrophic implications. *Senckenbergiana Maritima 35*, 189–201. https://doi.org/10.1007/BF03043685

Heward, A. P., Booth, G. A., Fortey, R. A., Miller, C. G. & Sansom, I. J. 2018: Darriwilian shallow-marine deposits from the Sultanate of Oman, a poorly known portion of the Arabian margin of Gondwana. *Geological Magazine 155*, 59–84. https://doi.org/10.1017/S0016756816000819

Higgs, K. T. & Higgs, B. M. 2015: New discoveries of *Diplocraterion* and tidal rhythmites in the upper Devonian rocks of Grab-All Bay, Cork Harbour: palaeoenvironmental implications. *Irish Journal of Earth Sciences 33*, 35–54. https://doi.org/10.1353/ijes.2015.0003

Hinga, K. R. 1981: The distribution of linear rows of holes in the sea floor. *Biological Oceanography 1*, 205–210. https://doi.org/10.1080/01965581.1981.10749439

Hitchcock, E. 1858: *Ichnology of New England. A report on the sandstone of the Connecticut Valley, especially its fossil footmarks, made to the government of the Commonwealth of Massachusetts*. W. White, Boston, 220 pp.

Hitchcock, E. 1865: *Supplement to the Ichnology of New England*. Wright and Potter, Boston, 96 pp.

Hiscott, R. N. 1982: Tidal deposits of the lower Cambrian Random Formation, eastern Newfoundland: facies and paleoenvironments. *Canadian Journal of Earth Sciences 19*, 2028–2042. https://doi.org/10.1139/e82-180

Hiscott, R. N., James, N .P. & Pemberton, S. G. 1984: Sedimentology and ichnology of the lower Cambrian Bradore Formation, coastal Labrador: fluvial to shallow-marine transgressive sequence. *Bulletin of Canadian Petroleum Geology 32*, 11–26. https://doi.org/10.35767/gscpgbull.32.1.011

Hoffman, P. F. & Macdonald, F. A. 2010: Sheet-crack cements and early regression in Marinoan (635 Ma) cap dolostones: regional benchmarks of vanishing ice-sheets? *Earth and Planetary Science Letters 300*, 374–384. https://doi.org/10.1016/j.epsl.2010.10.027

Hoffmann, R. & Grimmberger, G. 2011: Kegelförmige organische und anorganische Strukturen in unter-kambrischen Sandsteingeschieben Norddeutschlands. *Archiv für Geschiebekunde 6*, 73–152.

Hofmann, H. J. 1971: Precambrian fossils, pseudofossils, and problematica in Canada. *Geological Survey of Canada Bulletin 189*, 1–146. https://doi.org/10.4095/123948

Hofmann, H. J. 1979: Chazy (middle Ordovician) trace fossils in the Ottawa – St. Lawrence Lowlands. *Geological Survey of Canada Bulletin 321*, 27–59. https://doi.org/10.4095/106172

Hofmann, H. J. 1981: First record of a late Proterozoic faunal assemblage in the North American Cordillera. *Lethaia 14*, 303–310. https://doi.org/10.1111/j.1502-3931.1981.tb01103.x

Hofmann, H. J. 1983: Early Cambrian problematic fossils near June Lake, Mackenzie Mountains, N.W.T. *Canadian Journal of Earth Sciences 20*, 1513–1520. https://doi.org/10.1139/e83-140

Hofmann, H. J. 1990: Computer simulation of trace fossils with random patterns, and the use of goniograms. *Ichnos 1*, 15–22. https://doi.org/10.1080/10420949009386327

Hofmann, H. J. & Chen, J. 1981: Carbonaceous megafossils from the Precambrian (1800 Ma) near Jixian, northern China. *Canadian Journal of Earth Sciences 18*, 443–447. https://doi.org/10.1139/e81-038

Hofmann, H. J. & Mountjoy, E. W. 2010: Ediacaran body and trace fossils in Miette Group (Windermere Supergroup) near Salient Mountain, British Columbia, Canada. *Canadian Journal of Earth Sciences 47*, 1305–1325. https://doi.org/10.1139/E10-070

Hofmann, H. J. & Patel, I. M. 1989: Trace fossils from the type 'Etcheminian Series' (lower Cambrian Ratcliffe Brook Formation), Saint John area, New Brunswick, Canada. *Geological Magazine 126*, 139–157. https://doi.org/10.1017/S0016756800006294

Hofmann, H. J., Cecile, M. P. & Lane, L. S. 1994: New occurrences of *Oldhamia* and other trace fossils in the Cambrian of the Yukon and Ellesmere Island, arctic Canada. *Canadian Journal of Earth Sciences 31*, 767–782. https://doi.org/10.1139/e94-070

Hofmann, R., Mángano, M. G., Elicki, O. & Shinaq, R. 2012: Paleoecologic and biostratigraphic significance of trace fossils from shallow-to marginal-marine environments from the middle Cambrian (Stage 5) of Jordan. *Journal of Paleontology 86*, 931–955. https://doi.org/10.1666/11-129R1.1

Högström, A. E. S., Jensen, S., Palacios, T. & Ebbestad, J. O. R. 2013: New information on the Ediacaran-Cambrian transition in the Vestertana Group, Finnmark, northern Norway, from trace fossils and organic-walled microfossils. *Norwegian Journal of Geology 93*, 95–106.

Hogue, J. D. 2018: *Ichnotaxonomy of the Eocene Green River Formation, Soldier Summit and Spanish Fork Canyon, Uinta Basin, Utah: Interpreting behaviors, lifestyles, and erecting the Cochlichnus Ichnofacies*. Unpublished Master Dissertation, University of Kansas, 171 pp.

Holmes, J. D. & Budd, G. E. 2022: Reassessing a cryptic history of early trilobite evolution. *Communications Biology 5*, 1177. https://doi.org/10.1038/s42003-022-04146-6

Holub, V. & Kozur, H. 1981: Arthropodenfährten aus dem Rotliegenden der CSSR. *Geologisch-Paläontologische Mitteilungen Innsbruck 11*, 95–148.

Hoşgör, İ. & Yılmaz, İ. Ö. 2018: Occurrence of the lower Cambrian anemone-style trace fossils in the Zabuk Formation (Mardin–Derik, SE Turkey). *Comptes Rendus Palevol 17*, 495–503. https://doi.org/10.1016/j.crpv.2018.02.004

Hovikoski, J., Virtasalo, J. J., Wetzel, A., Muthre, M., Strasser, M., Proust, J.-N. & Ikehara, K. 2025: Bioturbation in the hadal zone. *Nature Communications 16,* 1401. https://doi.org/10.1038/s41467-025-56627-x

Howard, J. D. 1966: Characteristic trace fossils in upper Cretaceous sandstones of the Book Cliffs. *Utah Geological and Mineralogical Survey Bulletin 80*, 35–53.

Howard, J. D. & Dörjes, J. 1972: Animal-sediment relationships in two beach-related tidal flats; Sapelo Island, Georgia. *Journal of Sedimentary Petrology 42*, 608–623. https://doi.org/10.1306/74D725DB-2B21-11D7-8648000102C1865D

Howard, J. D. & Frey, R. W. 1975: Estuaries of the Georgia coast, U.S.A.: sedimentology and biology. II. Regional animal-sediment characteristics of Georgia estuaries. *Senckenbergiana Maritima 7*, 33–103.

Howard, J. D. & Frey, R. W. 1984: Characteristic trace fossils in nearshore to offshore sequences, upper Cretaceous of east-central Utah. *Canadian Journal of Earth Sciences 21*, 200–219. https://doi.org/10.1139/e84-022

Howard, J. D. & Reineck, H.-E. 1981: Depositional facies of high-energy beach-to-offshore sequence: comparison with low-energy sequence. *AAPG Bulletin 65*, 807–830. https://doi.org/10.1306/2F919B0C-16CE-11D7-8645000102C1865D

Howell, B. F. 1957: *Stipsellus annulatus*, a *Skolithos*-like Cambrian fossil from Arizona. *Wagner Free Institute of Science Bulletin 32*, 17–20.

Hsieh, S. & Plotnick, R. E. 2020: The representation of animal behaviour in the fossil record. *Animal Behaviour 169*, 65–80. https://doi.org/10.1016/j.anbehav.2020.09.010

Hu, J., Meng, Q., Zhang, W. & Wang, Z. 1991: Trace fossils from the Changcheng System of western Henan and their significance. *Geological Review 37*, 437–444.

Hu, Y. 1991: The sequence of ichnofacies in middle Silurian to early Devonian of the west Qinling mountains. *Bulletin of the Xi'an Institute of Geology and Mineral Ressources, the Chinese Academy of Sciences 31*, 92–96.

Hu, X., Scott, R. W., Cai, Y., Wang, C. & Melinte-Dobrinescu, M. C. 2012: Cretaceous oceanic red beds (CORBs): different time scales and models of origin. *Earth-Science Reviews 115*, 217–248. https://doi.org/10.1016/j.earscirev.2012.09.007

Hu, X., Wang, C., Li, X. & Luba, J. 2006: Upper Cretaceous oceanic red beds in southern Tibet: lithofacies, environments and colour origin. *Science in China: Series D Earth Sciences 49*, 785–795. https://doi.org/10.1007/s11430-006-0785-7

Hubbard, S. M. & Shultz, M. R. 2008: Deep burrows in submarine fan-channel deposits of the Cerro Toro Formation (Cretaceous), Chilean Patagonia: implications for firmground development and colonization in the deep sea. *Palaios 23*, 223–232. https://doi.org/10.2110/palo.2006.p06-127r

Hughes, N. C., Sell, B. K., English, L. T., Myrow, P. M. & Singh, B. P. 2013: Cambrian trace fossils from the Parahio Formation (Tethyan Himalaya) in its type section and elsewhere. *Journal of the Palaeontological Society of India 58*, 175–193.

Hundt, R. 1928: *Das Untersilur Thüringens mit besonderer Berücksichtigung des nördlichen Ostthüringens*. Kanitzsch, Gera, 48 pp.

Hundt, R. 1931: Neues von Phycodes circinnatum Richt., Dictodora Zimmermanni Hundt und einem neuen Problematikum aus dem untersten Silur Ostthüringens. *Centralblatt für Mineralogie, Geologie und Paläontologie 1931*, 181–186.

Hunter, R. E. & Clifton, H. E. 1982: Cyclic deposits and hummocky cross-stratification of probable storm origin in upper Cretaceous rocks of the Cape Sebastian area, southwestern Oregon. *Journal of Sedimentary Petrology 52*, 127–143. https://doi.org/10.1306/212F7EF5-2B24-11D7-8648000102C1865D

Hutchinson, R. D. 1962: *Cambrian stratigraphy and trilobite faunas of southeastern Newfoundland*. Geological Survey of Canada, Department of Mines and Technical Surveys, Bulletin 88. https://doi.org/10.4095/123902

Hutsky, A .J. & Fielding, C. R. 2016: The offshore bar revisited: a new depositional model for isolated shallow marine sandstones in the Cretaceous Frontier Formation of the northern Uinta Basin, Utah, USA. *Journal of Sedimentary Research 86*, 38–58. https://doi.org/10.2110/jsr.2015.101

Ichaso, A. A. & Dalrymple, R. W. 2009: Tide-and wave-generated fluid mud deposits in the Tilje Formation (Jurassic), offshore Norway. *Geology 37*, 539–542. https://doi.org/10.1130/G25481A.1

Ichaso, A. A., Buatois, L. A., Mángano, M. G., Thomas, P. & Marion, D. 2022: Assessing the expansion of the Cambrian Agronomic Revolution into fan-delta environments. *Scientific Reports 12*, 14431. https://doi.org/10.1038/s41598-022-18199-4

Ielpi, A., Lapôtre, M. G., Gibling, M. R. & Boyce, C. K. 2022: The impact of vegetation on meandering rivers. *Nature Reviews Earth and Environment 3*, 165–178. https://doi.org/10.1038/s43017-021-00249-6

Ineson, J. R. 1987: Trace fossils from a submarine fan-slope complex in the Cretaceous of James Ross Island, Antarctica. *British Antarctic Survey Bulletin 74*, 1–16.

Isachsen, C. E., Bowring, S. A., Landing, E. & Samson, S. D. 1994: New constraint on the division of Cambrian time. *Geology 22*, 496–498. https://doi.org/10.1130/0091-7613(1994)022<0496:NCOTDO>2.3.CO;2

Ivantsov, A. Y. 1990: New data on the ultrastructure of sabelliditids (Pogonophora?). *Paleontologicheskii Zhurnal 24*, 125–128.

Ivantsov, A. Y. 2013: New data on late Vendian problematic fossils from the genus *Harlaniella*. *Stratigraphy and Geological Correlation 21*, 592–600. https://doi.org/10.1134/S0869593813060051

Ivantsov, A. Y., Gritsenko, V. P., Paliy, V. M., Velikanov, V. A., Konstantinenko, L. I., Menasova, A. S., Fedonkin, M. A., Zakrevskaya, M. A. & Serezhnikova, E. A. 2015: *Upper Vendian macrofossils of Eastern Europe. Middle Dniester area and Volhynia*. Borissiak Paleontological Institute, Russian Academy of Sciences, Moscow, 144 pp.

Jacquet, S. M., Brougham, T., Skovsted, C. B., Jago, J. B., Laurie, J. R., Betts, M. J., Topper, T. P. & Brock, G. A. 2017: *Watsonella crosbyi* from the lower Cambrian (Terreneuvian, Stage 2) Normanville Group in South Australia. *Geological Magazine 154*, 1088–1104. https://doi.org/10.1017/S0016756816000704

Jago, J. B. & Gatehouse, C. G. 2007: Early Cambrian trace fossils from the Kanmantoo Group at Red Creek, South Australia, and their stratigraphic significance. *Australian Journal of Earth Sciences 54*, 531–540. https://doi.org/10.1080/08120090601078370

Jago, J. B. & Gatehouse, C. G. 2014: A small trace fossil assemblage from the ?middle Cambrian Pantapinna Sandstone, Flinders Ranges, south Australia and its paleoenvironmental significance. *Australian Journal of Earth Sciences 61*, 837–841. https://doi.org/10.1080/08120099.2014.940607

James, J. F. 1885: Fucoids of the Cincinnati Group. *Journal of the Cincinnati Society of Natural History 7*, 151–166.

James, J. F. 1892: Studies in problematic organisms–the genus *Scolithus*. *Geological Society of America Bulletin 3*, 32–44.

Jansa, L. F. 1974: Trace fossils from the Cambro-Ordovician Cow Head Group, Newfoundland, and their paleobathymetric implication. *Palaeogeography, Palaeoclimatology, Palaeoecology 15*, 233–244. https://doi.org/10.1016/0031-0182(74)90001-7

Jelby, M. E., Grundvåg, S. A., Helland-Hansen, W., Olaussen, S. & Stemmerik, L. 2020: Tempestite facies variability and storm-depositional processes across a wide ramp: towards a polygenetic model for hummocky cross-stratification. *Sedimentology 67*, 742–781. https://doi.org/10.1111/sed.12671

Jenkins, R. J. F. 1981: The concept of an 'Ediacaran Period' and its stratigraphic significance in Australia. *Transactions of the Royal Society of South Australia 105*, 179–194.

Jenkins, R. J. F. 1995: The problems and potential of using animal fossils and trace fossils in terminal Proterozoic biostratigraphy. *Precambrian Research 73*, 51–69. https://doi.org/10.1016/0301-9268(94)00071-X

Jenkins, R. J. F., Ford, C. H. & Gehling, J. G. 1983: The Ediacara member of the Rawnsley Quartzite: the context of the Ediacara assemblage (late Precambrian, Flinders Ranges). *Journal of the Geological Society of Australia 30*, 101–119. https://doi.org/10.1080/00167618308729240

Jensen, P. 1996: Burrows of marine nematodes as centres for microbial growth. *Nematologica 42*, 320–329. https://doi.org/10.1163/004425996X00056

Jensen, S. 1990: Predation by early Cambrian trilobites on infaunal worms-evidence from the Swedish Mickwitzia Sandstone. *Lethaia 23*, 29–42. https://doi.org/10.1111/j.1502-3931.1990.tb01779.x

Jensen, S. 1997: Trace fossils from the lower Cambrian Mickwitzia sandstone, south-central Sweden. *Fossils and Strata 42*, 1–111.

Jensen, S. 2003: The Proterozoic and earliest Cambrian trace fossil record; patterns, problems and perspectives. *Integrative and Comparative Biology 43*, 219–228. https://doi.org/10.1093/icb/43.1.219

Jensen, S. & Bergström, J. 2000: *Cheiichnus gothicus* igen. et isp. n., a new *Bergaueria*-like arthropod trace fossil from the lower Cambrian of Västergötland, Sweden. *GFF 122*, 293–296. https://doi.org/10.1080/11035890001223293

Jensen, S. & Grant, S. W. F. 1992: *Stratigraphy and paleobiology of Kullingia and trace fossils from the late Neoproterozoic to Cambrian of northern Sweden*. Geological Society of America Annual Meeting, Abstracts with Programs, Vol. 24, p. A114.

Jensen, S. & Grant, S. W. F. 1993: Implications from trace fossils for the Vendian-Cambrian boundary in the Torneträsk Formation, northern Sweden. p. 15 *in* Siverson, M. (ed): *Lundadagarna I Historisk Geologi och Paleontologi*. Lund Publications in Geology, Abstracts, 109.

Jensen, S. & Grant, S. W. F. 1998: Trace fossils from the Dividalen Group, northern Sweden: implications for early Cambrian biostratigraphy of Baltica. *Norsk Geologisk Tidsskrift 78*, 305–317.

Jensen, S. & Mens, K. 1999: A lower Cambrian shallow-water occurrence of the branching 'deep-water' type trace fossil *Dendrorhaphe* from the Lontova Formation, eastern Latvia. *Paläontologische Zeitschrift 73*, 187–193. https://doi.org/10.1007/BF02987992

Jensen, S. & Mens, K. 2001: Trace fossils *Didymaulichnus* cf. *tirasensis* and *Monomorphichnus* isp. from the Estonian lower Cambrian, with a discussion on the early Cambrian ichnocoenoses of Baltica. *Proceedings of the Estonian Academy of Sciences, Geology 50*, 75–85. https://doi.org/10.3176/geol.2001.2.01

Jensen, J. P. & Miller, J. 1990: Vertical cylindrical structures in Danish Quaternary (Weichselian) glaciofluvial deposits: their description and genesis. *Bulletin of the Geological Society of Denmark 38*, 59–67. https://doi.org/10.37570/bgsd-1990-38-06

Jensen, S. & Palacios, T. 2016: The Ediacaran-Cambrian trace fossil record in the Central Iberian Zone, Iberian Peninsula. *Comunicaçõe Geológicas 103*, 83–92.

Jensen, S. & Runnegar, B. N. 2005: A complex trace fossil from the Spitskop Member (terminal Ediacaran–?lower Cambrian) of southern Namibia. *Geological Magazine 142*, 561–569. https://doi.org/10.1017/S0016756805000853

Jensen, S., Gehling, J. G. & Droser, M. L. 1998: Ediacara-type fossils in Cambrian sediments. *Nature 393*, 567–569. https://doi.org/10.1038/31215

Jensen, S., Saylor, B. Z., Gehling, J. G. & Germs, G. J. B. 2000: Complex trace fossils from the terminal Proterozoic of Namibia. *Geology 28*, 143–146. https://doi.org/10.1130/0091-7613(2000)028<0143:CTFFTT>2.3.CO;2

Jensen, S., Gehling, J. G., Droser, M. L. & Grant, S. W. 2002a: A scratch circle origin for the medusoid fossil *Kullingia*. *Lethaia 35*, 291–299. https://doi.org/10.1080/002411602320790616

Jensen, S., Droser, M. L. & Heim, N. A. 2002b: Trace fossils and ichnofabrics of the lower Cambrian Wood Canyon Formation, southwest Death Valley area. 123–135 *in* Corsetti, F. A. (ed): *Proterozoic-Cambrian of the Great Basin and beyond*. Field trip guidebook and volume prepared for the annual Pacific Section SEPM fall field trip, Shoshone, California, Book 93.

Jensen, S., Droser, M. L. & Gehling, J. G. 2005: Trace fossil preservation and the early evolution of animals. *Palaeogeography, Palaeoclimatology, Palaeoecology 220*, 19–29. https://doi.org/10.1016/j.palaeo.2003.09.035

Jensen, S., Droser, M. L. & Gehling, J. G. 2006: A critical look at the Ediacaran trace fossil record. *In* Xiao, S. & Kaufman, A. J. (eds): *Neoproterozoic Geobiology and Paleobiology*, 115–157. Springer, Dordrecht. https://doi.org/10.1007/1-4020-5202-2_5

Jensen, S., Palacios, T. & Martí Mus, M. 2010: Revised biochronology of the lower Cambrian of the Central Iberian Zone, southern Iberian massif, Spain. *Geological Magazine 147*, 690–703. https://doi.org/10.1017/S0016756809990677

Jensen, S., Bogolepova, O. K. & Gubanov, A. P. 2011: *Cruziana semiplicata* from the Furongian (late Cambrian) of Severnaya Zemlya Archipelago, Arctic Russia, with a review of the spatial and temporal distribution of this ichnospecies. *Geological Journal 46*, 26–33. https://doi.org/10.1002/gj.1248

Jensen, S., Buatois, L. A. & Mángano, M. G. 2013: Testing for palaeogeographical patterns in the distribution of Cambrian trace fossils. *Geological Society, London, Memoirs 38*, 45–58. https://doi.org/10.1144/M38.5

Jensen, S., Harper, D. A. T. & Stouge, S. 2016: Trace fossils from the lower Cambrian Kløftelv Formation, Ella Ø, north-east Greenland. *GFF 138*, 369–376. https://doi.org/10.1080/11035897.2015.1076029

Jensen, S., Högström, A. E. S., Almond, J., Taylor, W. L., Meinhold, G., Høyberget, M., Ebbestad, J. O. R., Agić, H. & Palacios, T. 2018a: Scratch circles from the Ediacaran and Cambrian of Arctic Norway and southern Africa, with a review of scratch circle ocurrences. *Bulletin of Geosciences 93*, 287–304. https://doi.org/10.3140/bull.geosci.1685

Jensen, S., Högström, A. E. S., Høyberget, M., Meinhold, G., McIlroy, D., Ebbestad, J. O. R., Taylor, W. L., Agić, H. & Palacios, T. 2018b: New occurrences of *Palaeopascichnus* from the Stáhpogieddi Formation, Arctic Norway, and their bearing on the age of the Varanger Ice Age. *Canadian Journal of Earth Sciences 55*, 1253–1261. https://doi.org/10.1139/cjes-2018-0035

Jiang, G., Shi, X., Zhang, S., Wang, Y. & Xiao, S. 2011: Stratigraphy and paleogeography of the Ediacaran Doushantuo Formation (ca. 635–551 Ma) in south China. *Gondwana Research 19*, 831–849. https://doi.org/10.1016/j.gr.2011.01.006

Jiang, Y., Yue, W. & Ye, Z. 1998: Oncolites of the lower Permian Chuanshan Formation in South China and their geological and economic significance. *Acta Geologica Sinica (English Edition) 72*, 441–454. https://doi.org/10.1111/j.1755-6724.1998.tb00422.x

Jiang, Z., Luo, H. & Zhang, S. 1982: Trace fossils of the Meishucun Stage (lowermost Cambrian) from the Meishucun section in China. *Geological Review 28*, 7–13.

Johnson, M. E., Tesakov, Y. I., Predtetchensky, N. N. & Baarli, B. G. 1997: Comparison of lower Silurian shores and shelves in North America and Siberia. *Geological Society of America Special Papers 321*, 23–46. https://doi.org/10.1130/0-8137-2321-3.23

Jones, B. 2010: Warm-water neritic carbonates. 341–370 *in* James, N. P. & Dalrymple, R. W. (eds): *Facies models 4*. The Geological Association of Canada, St John's.

Jones, B. & Goodbody, Q. H. 1985: Oncolites from a shallow lagoon, Grand Cayman Island. *Bulletin of Canadian Petroleum Geology 33*, 254–260. https://doi.org/10.35767/gscpgbull.33.2.254

Jones, C. G., Lawton, J .H. & Shachak, M. 1994: Organisms as ecosystem engineers. *Oikos 69*, 373–386. https://doi.org/10.2307/3545850

Jordan, D. W. 1985: Trace fossils and depositional environments of upper Devonian black shales, east-central Kentucky, USA. 279–298 *in* Curran, H. A. (ed): *Biogenic structures: their use in interpreting depositional environments*. SEPM Special Publication, Vol. 35. https://doi.org/10.2110/pec.85.35.0279

Jørgensen, P., Erlenkeuser, H., Lange, H., Nagy, J., Rumohr, J. & Werner, F. 1981: Sedimentological and stratigraphical studies of two cores from the Skagerrak. 397–414 *in* Nio, S.-D., Shüttenhelm, R. T. E. & van Weering, T. C. E. (eds): *Holocene Marine Sedimentation in the North Sea Basin*. The International Association of Sedimentologists, Special Publication 5. https://doi.org/10.1002/9781444303759.ch28

Jumars, P. A. & Wheatcroft, R. A. 1989: Responses of benthos to changing food quality and quantity, with a focus on deposit feeding and bioturbation. 235–253 *in* Berger, W. H., Smetacek, V. S. & Wefer, G. (eds): *Productivity of the ocean: Present and past*. John Wiley and Sons.

Kamola, D. L. 1984: Trace fossils from marginal-marine facies of the Spring Canyon Member, Blackhawk Formation (upper Cretaceous), east-central Utah. *Journal of Paleontology 58*, 529–541.

Karcz, I., Enos, P. & Langille, G. 1974: Structures generated in fluid stressing of freshly deposited clays resemble ichnofossils. *Geology 2*, 289–290. https://doi.org/10.1130/0091-7613(1974)2<289:SGIFSO>2.0.CO;2

Kaur, R., Singh, B. P., Bhargava, O. N., Mikuláš, R., Singla, G., Prasad, S. K. & Stopden, S. 2021: Ichnology and biostratigraphic significance of Cambrian trace fossils from the lowest stratigraphic level of Kunzam La Formation, Chandra Valley, Lahaul and Spiti, India. *Ichnos 28*, 176–207. https://doi.org/10.1080/10420940.2021.1932490

Kędzierski, M., Uchman, A., Sawlowicz, Z. & Briguglio, A. 2015: Fossilized bioelectric wire–the trace fossil *Trichichnus*. *Biogeosciences 12*, 2301–2309. https://doi.org/10.5194/bg-12-2301-2015

Keighley, D. G. & Pickerill, R. K. 1995: The ichnotaxa *Palaeophycus* and *Planolites*: historical perspectives and recommendations. *Ichnos 3*, 301–309. https://doi.org/10.1080/10420949509386400

Keighley, D. G. & Pickerill, R. K. 1996: Small *Cruziana*, *Rusophycus*, and related ichnotaxa from eastern Canada: the nomenclatural debate and systematic ichnology. *Ichnos 4*, 261–285. https://doi.org/10.1080/10420949609380136

Keighley, D. & Pickerill, R. 1997: Systematic ichnology of the Mabou and Cumberland groups (Carboniferous) of western Cape Breton Island, eastern Canada, 1: burrows, pits, trails, and coprolites. *Atlantic Geology 33*, 181–215. https://doi.org/10.4138/2068

Keighley, D. & Pickerill, R. 1998: Systematic ichnology of the Mabou and Cumberland groups (Carboniferous) of western Cape Breton Island, eastern Canada, 2: surface markings. *Atlantic Geology 34*, 83–112. https://doi.org/10.4138/2041

Keij, A. J. 1965: Miocene trace fossils from Borneo. *Paläontologische Zeitschrift 39*, 220–228. https://doi.org/10.1007/BF02990166

Kendall, C. G. S. C. & Warren, J. 1987: A review of the origin and setting of tepees and their associated fabrics. *Sedimentology 34*, 1007–1027. https://doi.org/10.1111/j.1365-3091.1987.tb00590.x

Kennedy, M. J. & Droser, M. L. 2011: Early Cambrian metazoans in fluvial environments, evidence of the non-marine Cambrian radiation. *Geology 39*, 583–586. https://doi.org/10.1130/G32002.1

Keppie, J. D., Nance, R. D., Murphy, J. B. & Dostal, J. 2003: Tethyan, Mediterranean, and Pacific analogues for the Neoproterozoic–Paleozoic birth and development of peri-Gondwanan terranes and their transfer to Laurentia and Laurussia. *Tectonophysics 365*, 195–219. https://doi.org/10.1016/S0040-1951(03)00037-4

Keppie, J. D., Keppie, D. F. & Dostal, J. 2021: The northern Appalachian terrane wreck model. *Canadian Journal of Earth Sciences 58*, 542–553. https://doi.org/10.1139/cjes-2020-0114

Kesidis, G., Budd, G. E. & Jensen, S. 2019a: An intermittent mode of formation for the trace fossil *Cruziana* as a serial repetition of *Rusophycus*: the case of *Cruziana tenella* (Linnarsson). *Lethaia 52*, 133–148. https://doi.org/10.1111/let.12303

Kesidis, G., Slater, B. J., Jensen, S. & Budd, G. E. 2019b: Caught in the act: priapulid burrowers in early Cambrian substrates. *Proceedings of the Royal Society 286*, 20182505. https://doi.org/10.1098/rspb.2018.2505

Kilibarda, Z. & Schassburger, A. 2018: A diverse deep-sea trace fossil assemblage from the Adriatic Flysch Formation (middle Eocene–middle Miocene), Montenegro (central Mediterranean). *Palaeogeography, Palaeoclimatology, Palaeoecology 506*, 112–127. https://doi.org/10.1016/j.palaeo.2018.06.023

Kim, J. Y., Kim, K.-S. & Pickerill, R. K. 2003: Cretaceous nonmarine trace fossils from the Hasandong and Jinju formations of the Namhae Area, Kyongsangnamdo, southeast Korea. *Ichnos 9*, 41–60. https://doi.org/10.1080/10420940190034076

Kim, J.-Y. & Paik, I. S. 1997: Nonmarine *Diplocraterion luniforme* (Blanckenhorn 1916) from the Hasandong Formation (Cretaceous) of the Jinju area, Korea. *Ichnos 5*, 131–138. https://doi.org/10.1080/10420949709386412

Kim, J. Y., Pickerill, R. K. & Wilson, R. A. 2000: *Palaeophycus bolbitermilus* isp. nov. from the lower Silurian Upsalquitch Formation of New Brunswick, eastern Canada. *Atlantic Geology 36*, 131–137. https://doi.org/10.4138/2016

King, A. F. 1982: *Field Guide for Avalon and Meguma Zones. The Caledonide Orogen IGCP Project 27, NATO Advanced Study Institute, Atlantic Canada, August 1982*. Department of Earth Sciences, Memorial University, St John's.

Kir'yanov, V. V. 1968: Paleontologicheskie ostatki i stratigrafiya otlozhenij baltijskoj serii Volyno-Podolii. 5–25 *in* Krandievskij, V. S., Ishchenko, T. A. & Kir'yanov, V. V. (eds): *Paleontologiya I stratigrafiya nizhnegopaleozoya Volyno-Podolii*. Naukova Dumka, Kiev.

Kitchell, J. A. & Clark, D. L. 1979: A multivariate approach to biofacies analysis of deep-sea traces from the central Arctic. *Journal of Paleontology 53*, 1045–1067.

Kitchell, J. A., Kitchell, J. F., Johnson, G. L. & Hunkins, K. L. 1978: Abyssal traces and megafauna: comparison of productivity, diversity and density in the Arctic and Antarctic. *Paleobiology 4*, 171–180. https://doi.org/10.1017/S0094837300005844

Klein, G. D. 1963: Bay of Fundy intertidal zone sediments. *Journal of Sedimentary Petrology 33*, 844–854. https://doi.org/10.1306/74D70F5B-2B21-11D7-8648000102C1865D

Klein, G. D. 1970: Depositional and dispersal dynamics of intertidal sandbars. *Journal of Sedimentary Petrology 40*, 1095–1127. https://doi.org/10.1306/74D72144-2B21-11D7-8648000102C1865D

Klein, G. D. 1977: *Clastic tidal facies*. Continuing Education Publication Co, Champaign, IL, 149 pp.

Klug, C. & Hoffmann, R. 2018: Early Devonian actiniarian trace fossils (*Conichnus conicus*) from the Anti-Atlas of Morocco. *Neues Jahrbuch für Geologie und Paläontologie Abhandlungen 290*, 65–74. https://doi.org/10.1127/njgpa/2018/0767

Knaust, D. 2004: Cambro–Ordovician trace fossils from the SW-Norwegian Caledonides. *Geological Journal 39*, 1–24. https://doi.org/10.1002/gj.941

Knaust, D. 2007: Invertebrate trace fossils and ichnodiversity in shallow-marine carbonates of the German Middle Triassic (Muschelkalk). 223–240 *in* Bromley, R. G., Buatois, L. A., Mángano, G., Genise, J. F. & Melchor R. N. (eds):

Sediment-organism interactions: a multifaceted ichnology. SEPM Special Publication, vol. 88. https://doi.org/10.2110/pec.07.88.0223

Knaust, D. 2010: Remarkably preserved benthic organisms and their traces from a middle Triassic (Muschelkalk) mud flat. *Lethaia 43*, 344–356. https://doi.org/10.1111/j.1502-3931.2009.00196.x

Knaust, D. 2013: The ichnogenus *Rhizocorallium*: classification, trace makers, palaeoenvironments and evolution. *Earth-Science Reviews 126*, 1–47. https://doi.org/10.1016/j.earscirev.2013.04.007

Knaust, D. 2017: *Atlas of trace fossils in well core: appearance, taxonomy and interpretation*. Springer, 209 pp.

Knaust, D. 2018a: The ichnogenus *Teichichnus* Seilacher, 1955. *Earth-Science Reviews 177*, 386–403. https://doi.org/10.1016/j.earscirev.2017.11.023

Knaust, D. 2018b: *Teichichnus zigzag* Frey and Bromley, 1985: a probable echiuran or holothurian burrow from the Jurassic offshore Norway. *PalZ 92*, 617–632. https://doi.org/10.1007/s12542-018-0413-9

Knaust, D. 2019: The enigmatic trace fossil *Tisoa* de Serres, 1840. *Earth-Science Reviews 188*, 123–147. https://doi.org/10.1016/j.earscirev.2018.11.001

Knaust, D. 2020: Invertebrate coprolites and cololites revised. *Papers in Palaeontology 6*, 385–423. https://doi.org/10.1002/spp2.1297

Knaust, D. 2021: Rosselichnidae ifam. nov.: burrows with concentric, spiral or eccentric lamination. *Papers in Palaeontology 7*, 1847–1875. https://doi.org/10.1002/spp2.1367

Knaust, D. 2023: The multifaceted ichnogenus *Protovirgularia* M'Coy, 1850: taxonomy, producers and environments. *Earth-Science Reviews 244*, 104511. https://doi.org/10.1016/j.earscirev.2023.104511

Knaust, D. & Desrochers, A. 2019: Exceptionally preserved soft-bodied assemblage in Ordovician carbonates of Anticosti Island, eastern Canada. *Gondwana Research 71*, 117–128. https://doi.org/10.1016/j.gr.2019.01.016

Knaust, D. & Langbein, R. 1995: Pot casts in the upper Muschelkalk (middle Triassic) of Weimar/Thuringia—composition, microfabrics and diagnesis. *Facies 33*, 151–166. https://doi.org/10.1007/BF02537449

Knaust, D., Warchoł, M. & Kane, I. A. 2014: Ichnodiversity and ichnoabundance: revealing depositional trends in a confined turbidite system. *Sedimentology 61*, 2218–2267. https://doi.org/10.1111/sed.12134

Knaust, D., Thomas, R. D. & Curran, H. A. 2018: *Skolithos linearis* Haldeman, 1840 at its early Cambrian type locality, Chickies Rock, Pennsylvania: analysis and designation of a neotype. *Earth-Science Reviews 185*, 15–31. https://doi.org/10.1016/j.earscirev.2018.05.009

Knight, I. & O'Brien, S. J. 1988: Stratigraphy and sedimentology of the Connecting Point Group, Newfoundland: an example of a late Precambrian Avalonian basin. *Current Research, Newfoundland Department of Mines, Mineral Resources Division 88-1*, 207–228.

Knoll, A. H. & Nowak, M. A. 2017: The timetable of evolution. *Science Advances 3*, e1603076. https://doi.org/10.1126/sciadv.1603076

Knox, L. W. & Miller, M. F. 1985: Environmental control of trace fossil morphology. 167–176 *in* Curran, H. A. (ed): *Biogenic structures: their use in interpreting depositional environments*. Society of Economic Petrologists and Mineralogists, Special Publication 35. https://doi.org/10.2110/pec.85.35.0167

Knox, R. W. O. 1973: Ichnogenus *Corophioides*. *Lethaia 6*, 133–146. https://doi.org/10.1111/j.1502-3931.1973.tb01187.x

Kolb, S. & Wolf, R. 1979: Distribution of *Cruziana* in the lower Ordovician sequence of Celtiberia (NE Spain) with a revision of the *Cruziana rugosa*-group. *Neues Jahrbuch für Geologie une Paläontologie Monatshefte 1979*, 457–474.

Kolesch, K. 1922: Beitrag zur Stratigraphie des mittleren Bundsandsteinsim Gebiet des Blattes Kahla (S.-A.). *Jahrbuch der Preussischen Geologischen Landesanstalt 40*, 307–382.

Kolesnikov, A. V. & Bobkov, N. I. 2019: Revisiting the age of the Asha Group in the south Urals. *Estudios Geológicos 75*, e103. https://doi.org/10.3989/egeol.43590.558

Kolesnikov, A. & Desiatkin, V. 2022: Taxonomy and palaeoenvironmental distribution of palaeopascichnids. *Geological Magazine 159*, 1175–1191. https://doi.org/10.1017/S0016756822000437

Kolesnikov, A. V., Marusin, V. V., Nagovitsin, K. E., Maslov, A. V. & Grazhdankin, D. V. 2015: Ediacaran biota in the aftermath of the Kotlinian Crisis: Asha Group of the south Urals. *Precambrian Research 263*, 59–78. https://doi.org/10.1016/j.precamres.2015.03.011

Kolesnikov, A. V., Rogov, V. I., Bykova, N. V., Danelian, T., Clausen, S., Maslov, A. V. & Grazhdankin, D. V. 2018: The oldest skeletal macroscopic organism *Palaeopascichnus linearis*. *Precambrian Research 316*, 24–37. https://doi.org/10.1016/j.precamres.2018.07.017

Korovnikov, I. V., Marusin, V. V., Tokarev, D. A. & Obut, O. T. 2019: Trace Fossils from the Vendian-Cambrian transitional strata of the Igarka Uplift (northwestern Siberian Platform). *Paleontological Journal 53*, 566–574. https://doi.org/10.1134/S0031030119060030

Kolesnikov, A. V., Latysheva, I. V., Shatsillo, A. V., Kuznetsov, N. B., Kolesnikov, A. S., Desiatkin, V. D. & Romanyuk, T. V. 2023a: Ediacara-type biota in the upper Precambrian of the Timan Range (Dzhezhim-Parma Hill, Komi Republic). *Doklady Earth Sciences 510*, 289–292. https://doi.org/10.1134/S1028334X23600032

Kolesnikov, A. V., Desuatkin, V. D., Terekhova, V. A., Pan'kov, V. N. & Maslov, A. V. 2023b: The oldest trace fossils in association with an Ediacara-type biota in the upper Vendian of the South Urals. *Doklady Earth Sciences 512*, 1032–1038. https://doi.org/10.1134/S1028334X23601487

Kolesnikov, A. V., Marusin, V. V., Rud'ko, S. V. & Pokrovsky, B. G. 2023c: Shadows of the past: an Ediacara-style taphonomic window in advent of Cambrian bioturbators. *Precambrian Research 399*, 107238. https://doi.org/10.1016/j.precamres.2023.107238

Kozur, H. W. & Lemone, D. V. 1995: New terrestrial arthropod trackways from the Abo Member (Sterlitamakian, late Sakmarian, late Wolfcampian) of the Shalem Colony Section, Robledo Mountains, New Mexico. *New Mexico Museum of Natural History and Science Bulletin 6*, 107–113.

Krapovickas, V., Ciccioli, P. L., Mángano, M. G., Marsicano, C. A. & Limarino, C. O. 2009: Paleobiology and paleoecology of an arid–semiarid Miocene South American ichnofauna in anastomosed fluvial deposits. *Palaeogeography, Palaeoclimatology, Palaeoecology 284*, 129–152. https://doi.org/10.1016/j.palaeo.2009.09.015

Krobicki, M. & Uchman, A. 2003: Trace fossil *Curvolithus* from the middle Jurassic crinoidal limestones of the Pieniny Klippen Belt (Carpathians, Poland). *Geologica Carpathica 54*, 175–180.

Krogh, T. E., Strong, D. F., O'Brien, S. J. & Papezik, V. S. 1988: Precise U–Pb zircon dates from the Avalon Terrane in Newfoundland. *Canadian Journal of Earth Sciences 25*, 442–453. https://doi.org/10.1139/e88-045

Książkiewicz, M. 1968: O niektórych problematykach z fliszu Karpat Polskich (Część III). *Annales de la Société Géologique de Pologne 38*, 3–17.

Książkiewicz, M. 1970: Observations on the ichnofauna of the Polish Carpathians. 283–322 *in* Crimes, T. P. & Harper, C. (eds): *Trace fossils*. Seel House Press, Liverpool.

Książkiewicz, M. 1977: Trace fossils in the flysch of the Polish Carpathians. *Palaeontologica Polonica 36*, 1–208.

Kulkarni, K. G. & Borkar, V. D. 1996: Occurrence of *Cochlichnus* Hitchcock in the Vindhyan Supergroup (Proterozoic) of Madhya Pradesh. *Journal Geological Society of India 47*, 725–729. https://doi.org/10.17491/jgsi/1996/470608

Kulkarni, K. G. & Borkar, V. D. 1997a: On occurrence of *Cochlichnus* in the Proterozoic rocks of Kaladgi Basin. *Gondwana Geological Magazine 12*, 55–59.

Kulkarni, K. G. & Borkar, V. D. 1997b: Ichnogenus *Palaeophycus* Hall from the Bagalkot Group, Karnataka State. *Journal*

Geological Society of India 49, 215–220. https://doi.org/10.17491/jgsi/1997/490213
Kulkarni, K. G., Borkar, V. D. & Petare, T. J. 2008: Ichnofossils from the Fort Member (middle Jurassic), Jaisalmer Formation, Rajasthan. *Journal Geological Society of India 71*, 731–738.
Kumar, N. & Sanders, J. E. 1976: Characteristics of shoreface storm deposits: modern and ancient examples. *Journal of Sedimentary Petrology 46*, 145–162. https://doi.org/10.1306/212F6EDD-2B24-11D7-8648000102C1865D
Kumar, G., Raina, B. K., Bhargava, O. N., Maithy, P.K. & Babu, R. 1984: The Precambrian–Cambrian boundary problem and its prospects, northwest Himalaya, India. *Geological Magazine 121*, 211–219. https://doi.org/10.1017/S0016756800028272
Kumpulainen, R. A., Uchman, A., Woldehaimanot, B., Kreuser, T. & Ghirmay, S. 2006: Trace fossil evidence from the Adigrat Sandstone for an Ordovician glaciation in Eritrea, NE Africa. *Journal of African Earth Sciences 45*, 408–420. https://doi.org/10.1016/j.jafrearsci.2006.03.011
Kvale, E. P. 2012: Tidal constituents of modern and ancient tidal rhythmites: criteria for recognition and analyses. 1–17 *in* Davis, R. A. & Dalrymple, R. W. (eds): *Principles of tidal sedimentology*. Springer, Dordrecht. https://doi.org/10.1007/978-94-007-0123-6_1
Łabaj, M. A. & Pratt, B. R. 2016: Depositional dynamics in a mixed carbonate–siliciclastic system: middle–upper Cambrian Abrigo Formation, southeastern Arizona, USA. *Journal of Sedimentary Research 86*, 11–37. https://doi.org/10.2110/jsr.2015.96
Laing, B. A., Buatois, L. A., Mángano, M. G., Narbonne, G. M. & Gougeon, R. C. 2018: *Gyrolithes* from the Ediacaran-Cambrian boundary section in Fortune Head, Newfoundland, Canada: exploring the onset of complex burrowing. *Palaeogeography, Palaeoclimatology, Palaeoecology 495*, 171–185. https://doi.org/10.1016/j.palaeo.2018.01.010
Laing, B. A., Mángano, M. G., Buatois, L. A., Narbonne, G. M. & Gougeon, R. C. 2019: A protracted Ediacaran–Cambrian transition: an ichnologic ecospace analysis of the Fortunian in Newfoundland. *Geological Magazine 156*, 1623–1630. https://doi.org/10.1017/S0016756819000141
Lamb, M. P., Myrow, P. M., Lukens, C., Houck, K. & Strauss, J. 2008: Deposits from wave-influenced turbidity currents: Pennsylvanian Minturn Formation, Colorado, USA. *Journal of Sedimentary Research 78*, 480–498. https://doi.org/10.2110/jsr.2008.052
Lan, Z., Zhang, S., Chen, Z.-Q. & Mitchell, R. N. 2021: Locomotion and feeding trails produced by crabs. *Geological Journal 56*, 6288–6293. https://doi.org/10.1002/gj.4190
Landing, E. 1993: In situ earliest Cambrian tube worms and the oldest metazoan-constructed biostrome (Placentian series, southeastern Newfoundland). *Journal of Paleontology 67*, 333–342. https://doi.org/10.1017/S0022336000036817
Landing, E. 1994: Precambrian-Cambrian boundary global stratotype ratified and a new perspective of Cambrian time. *Geology 22*, 179–182. https://doi.org/10.1130/0091-7613(1994)022<0179:PCBGSR>2.3.CO;2
Landing, E. 1996a: Avalon: insular continent by the latest Precambrian. *Geological Society of America Special Papers 304*, 29–63. https://doi.org/10.1130/0-8137-2304-3.29
Landing, E. 1996b: Reconstructing the Avalon continent: marginal to inner platform transition in the Cambrian of southern New Brunswick. *Canadian Journal of Earth Sciences 33*, 1185–1192. https://doi.org/10.1139/e96-089
Landing, E. 2004: Precambrian–Cambrian boundary interval deposition and the marginal platform of the Avalon microcontinent. *Journal of Geodynamics 37*, 411–435. https://doi.org/10.1016/j.jog.2004.02.014
Landing, E. & Kruse, P. D. 2017: Integrated stratigraphic, geochemical, and paleontological late Ediacaran to early Cambrian records from southwestern Mongolia: comment. *Geological Society of America Bulletin 129*, 1012–1015. https://doi.org/10.1130/B31640.1
Landing, E. & Westrop, S. R. 1998: Avalon 1997—the Cambrian standard. *New York State Museum Bulletin 492*, 1–92.
Landing, E. & Westrop, S. R. 2004: Environmental patterns in the origin and diversification loci of early Cambrian skeletalized Metazoa: evidence from the Avalon microcontinent. *The Paleontological Society Papers 10*, 93–106. https://doi.org/10.1017/S1089332600002369
Landing, E., Narbonne, G. M., Myrow, P., Benus, A. P. & Anderson, M. M. 1988: Faunas and depositional environments of the upper Precambrian through lower Cambrian, southeastern Newfoundland. *New York State Museum Bulletin 463*, 8–52.
Landing, E., Myrow, P., Benus, A. P. & Narbonne, G. M. 1989: The Placentian series: appearance of the oldest skeletalized faunas in southeastern Newfoundland. *Journal of Paleontology 63*, 739–769. https://doi.org/10.1017/S0022336000036465
Landing, E., Geyer, G., Brasier, M. D. & Bowring, S. A. 2013: Cambrian evolutionary radiation: context, correlation, and chronostratigraphy—overcoming deficiencies of the first appearance datum (FAD) concept. *Earth-Science Reviews 123*, 133–172. https://doi.org/10.1016/j.earscirev.2013.03.008
Landing, E., Myrow, P. M., Narbonne, G. M., Geyer, G., Buatois, L. A., Mángano, M. G., Kauffman, A., Westrop, S. R., Kröger, B., Laing, B. & Gougeon, R. 2017: *Ediacaran–Cambrian of Avalonian Eastern Newfoundland (Avalon, Burin, and Bonavista Peninsulas)*. International Symposium on the Ediacaran–Cambrian Transition, Field Trip, Vol. 4, 169 pp.
Landing, E., Keppie, J. D., Keppie, D. F., Geyer, G. & Westrop, S. R. 2022: Greater Avalonia—latest Ediacaran–Ordovician "peribaltic" terrane bounded by continental margin prisms ("Ganderia", Harlech Dome, Meguma): review, tectonic implications, and paleogeography. *Earth-Science Reviews 224*, 103863. https://doi.org/10.1016/j.earscirev.2021.103863
Lane, A. A., Braddy, S. J., Briggs, D. E. G. & Elliott, D. K. 2003: A new trace fossil from the middle Cambrian of the Grand Canyon, Arizona, USA. *Palaeontology 46*, 987–997. https://doi.org/10.1111/1475-4983.00329
Lanés, S., Manceñido, M. & Damborenea, S. 2007: *Lapispira*: a double helicoidal burrow from Jurassic marine nearshore environments. 59–77 *in* Bromley, R. G., Buatois, L. A., Mángano, G., Genise, J. F. & Melchor R. N. (eds): *Sediment-organism interactions: a multifaceted ichnology*. SEPM Special Publication, vol. 88. https://doi.org/10.2110/pec.07.88.0059
Lange, F. W. 1942: Restos vermiformes do Arenito das Furnas. *Arquivos do Museu Paranaense 2*, 3–8.
Lange, W. 1932: Über spirale Wohngänge, *Lapispira bispiralis* gen. nov. spec. nov., ein Leitfossil aus der Schlotheimienstufe des Lias Norddeutschlands. *Zeitschrift der Deutsche Geologischen Gesellschaft 84*, 537–543. https://doi.org/10.1127/zdgg/84/1932/537a
Lantzsch, H., Hanebuth, T. J. J. & Bender, V. B. 2009: Holocene evolution of mud depocentres on a high-energy, low-accumulation shelf (NW Iberia). *Quaternary Research 72*, 325–336. https://doi.org/10.1016/j.yqres.2009.07.009
Lawfield, A. M. W. & Pickerill, R. K. 2006: A novel contemporary fluvial ichnocoenose: unionid bivalves and the *Scoyenia–Mermia* ichnofacies transition. *Palaios 21*, 391–396. https://doi.org/10.2110/palo.2006.P06-08
Lazar, O. R., Bohacs, K. M., Macquaker, J. H. S., Schieber, J. & Demko, T .M. 2015: Capturing key attributes of fine-grained sedimentary rocks in outcrops, cores, and thin sections: nomenclature and description guidelines. *Journal of Sedimentary Research 85*, 230–246. https://doi.org/10.2110/jsr.2015.11
Lebesconte, P. 1883: Présentation à la société géologique des œuvres posthumes de Marie Rouault. *Bulletin de la Société Géologique de France 11*, 466–472.
Lebesconte, P. 1886: Constitution générale du massif breton comparée à celle du Finistère. *Bulletin de la Société Géologique de France 17*, 776–811.
Leckie, D. A. & Krystinik, L. F. 1989: Is there evidence for geostrophic currents preserved in the sedimentary record of inner to middle-shelf deposits. *Journal*

of Sedimentary Petrology 59, 862–870. https://doi.org/10.1306/212F9093-2B24-11D7-8648000102C1865D

Leckie, D. A. & Walker, R. G. 1982: Storm-and tide-dominated shorelines in Cretaceous Moosebar-Lower Gates interval—outcrop equivalents of deep basin gas trap in western Canada. *AAPG Bulletin 66*, 138–157. https://doi.org/10.1306/03B59A53-16D1-11D7-8645000102C1865D

Lee, H. J. 2015: A review on the Holocene evolution of an inner-shelf mud deposit in the southeastern Yellow Sea: the Huksan Mud Belt. *Ocean Science Journal 50*, 615–621. https://doi.org/10.1007/s12601-015-0056-7

Lee, H. J. & Chu, Y. S. 2001: Origin of inner-shelf mud deposit in the southeastern Yellow Sea: Huksan Mud Belt. *Journal of Sedimentary Research 71*, 144–154. https://doi.org/10.1306/040700710144

Lee, H. J., Jo, H. R., Chu, Y. S. & Bahk, K. S. 2004: Sediment transport on macrotidal flats in Garolim Bay, west coast of Korea: significance of wind waves and asymmetry of tidal currents. *Continental Shelf Research 24*, 821–832. https://doi.org/10.1016/j.csr.2004.01.005

Legg, I. C. 1985: Trace fossils from a middle Cambrian deltaic sequence, north Spain. 151–165 *in* Curran, H. A. (ed): *Biogenic structures: their use in interpreting depositional environments*. SEPM Special Publication, Vol. 35. https://doi.org/10.2110/pec.85.35.0151

Lehane, J. R. & Ekdale, A. A. 2016: Morphometric analysis of graphoglyptid trace fossils in two dimensions: implications for behavioral evolution in the deep sea. *Paleobiology 42*, 317–334. https://doi.org/10.1017/pab.2015.52

Leithold, E. L. 1993: Preservation of laminated shale in ancient clinoforms; comparison to modern subaqueous deltas. *Geology 21*, 359–362. https://doi.org/10.1130/0091-7613(1993)021<0359:POLSIA>2.3.CO;2

Lemche, H., Hansen, B., Madsen, F. J., Tendal, O. S. & Wolff, T. 1976: Hadal life as analyzed from photographs. *Videnskabelige Meddelelser fra Dansk naturhistorisk Forening i Kjøbenhavn 139*, 263–336.

Leonowicz, P. 2015: Ichnofabrics of shallow-marine mudstone, the result of changing environmental conditions: an example from the middle Jurassic ore-bearing clay from southern Poland. *Facies 61*, 11. https://doi.org/10.1007/s10347-015-0438-4

Lerner, A. J., Love, D. W., Lucas, S. G. & Morgan, G. S. 2007: First report of invertebrate trace fossils from the Pliocene Ceja Formation of central New Mexico. 53–58 *in* Lucas, S. G., Spielmann, J. A. & Lockley, M. G. (eds): *Cenozoic Vertebrate Tracks and Traces*. New Mexico Museum of Natural History and Science, Bulletin 42.

Lerner, A. J. & Lucas, S. G. 2015: A *Selenichnites* ichnoassociation from early Permian tidal flats of the Prehistoric Trackways National Monument of south-central New Mexico. *New Mexico Museum of Natural History Bulletin 65*, 141–152.

Lesquereux, L. 1876: Species of fossil marine plants from the Carboniferous measures. *Indiana Geological Survey Annual Report 7*, 134–145.

Lessertisseur, J. 1955: Traces fossiles d'activité animale et leur signification paléobiologique. *Mémoires de la Société Géologique de France, Nouvelle Série 74*, 1–150.

Lesueur, P., Jouanneau, J.-M., Boust, D., Tastet, J.-P. & Weber, O. 2001: Sedimentation rates and fluxes in the continental shelf mud fields in the Bay of Biscay (France). *Continental Shelf Research 21*, 1383–1401. https://doi.org/10.1016/S0278-4343(01)00004-8

Leszczyński, S. 2004: Bioturbation structures of the Kropivnik Fucoid Marls (Campanian-lower Maastrichtian) of the Huwniki–Rybotycze area (Polish Carpathians). *Geological Quarterly 48*, 35–60.

Leszczynski, S., Uchman, A. & Bromley, R. G. 1996: Trace fossils indicating bottom aeration changes: Folusz Limestone, Oligocene, Outer Carpathians, Poland. *Palaeogeography, Palaeoclimatology, Palaeoecology 121*, 79–87. https://doi.org/10.1016/0031-0182(95)00052-6

Li, D. 2014: *Ichnofabrics from the Mantou Formation (Cambrian Series 2, 3) in Western Henan Province*. Unpublished Doctoral Dissertation, Henan University of Technology, 157 pp.

Li, G., Zhao, X., Gubanov, A., Zhu, M. & Na, L. 2011: Early Cambrian mollusc *Watsonella crosbyi*: a potential GSSP index fossil for the base of the Cambrian Stage 2. *Acta Geologica Sinica (English Edition) 85*, 309–319. https://doi.org/10.1111/j.1755-6724.2011.00400.x

Li, M., Song, H., Wignall, P. B., She, Z., Dai, X., Song, H. & Xiao, Q. 2019: Early Triassic oceanic red beds coupled with deep sea oxidation in South Tethys. *Sedimentary Geology 391*, 105519. https://doi.org/10.1016/j.sedgeo.2019.105519

Lim, D. I., Choi, J. Y., Jung, H. S., Rho, K. C. & Ahn, K. S. 2007: Recent sediment accumulation and origin of shelf mud deposits in the Yellow and East China Seas. *Progress in Oceanography 73*, 145–159. https://doi.org/10.1016/j.pocean.2007.02.004

Lima, J. H. D., Minter, N. J. & Netto, R. G. 2017: Insights from functional morphology and neoichnology for determining tracemakers: a case study of the reconstruction of an ancient glacial arthropod-dominated fauna. *Lethaia 50*, 576–590. https://doi.org/10.1111/let.12214

Lima, J. H. D. & Netto, R. G. 2012: Trace fossils from the Permian Teresina Formation at Cerro Caveiras (S Brazil). *Revista Brasileira de Paleontologia 15*, 5–22. https://doi.org/10.4072/rbp.2012.1.01

Lin, S., Zhang, Y. & Zhang, L. 1986: Body and trace fossils of Metazoa and algal macrofossils from the upper Sinian Gaojiashan Formation in southern Shaanxi. *Geology of Shaanxi 6*, 9–17.

Lin, W. & Bhattacharya, J. P. 2021: Storm-flood-dominated delta: a new type of delta in stormy oceans. *Sedimentology 68*, 1109–1136. https://doi.org/10.1111/sed.12819

Liñán, E. 1984: Los icnofósiles de la Formación Torrearboles (¿Precámbrico?-Cámbrico inferior) en los alrededores de fuente de Cantos, Badajoz. *Caudernos do Laboratoria Xeologico de Laxe 8*, 47–74.

Liñán, E. & Palacios, T. 1987: Asociaciones de pistas fósiles y microorganismos de pared orgánica del Proterozoico, en las facias esquisto-grauváquicas del norte de Cáceres. Consecuencias regionales. *Boletín de la Real Sociedad Española de Historia Natural (Sección Geológica) 82*, 211–232.

Liñán, E. & Tejero, R. 1988: Las formaciones precámbricas del antiforme de Paracuellos (Cadenas ibéricas). *Boletín de la Real Sociedad Española de Historia Natural (Sección Geológica) 84*, 39–49.

Linck, O. 1942: Die Spur *Isopodichnus*. *Senckenbergiana 25*, 232–255.

Linnarsson, J. G. O. 1869: On some fossils found in the Eophyton Sandstone, at Lugnås, in Sweden. *Geological Magazine 6*, 393–406. https://doi.org/10.1017/S0016756800162910

Linnarsson, J. G. O. 1871: Geognostiska och palaeontologiska iakttagelser öfver Eophytonsandstenen i Vestergötland. *Kongliga Svenska Vetenskaps-Akademiens Handlingar 9*, 1–19.

Liou, Y.-H., Löwemark, L., Wang, P.-L. & Dashtgard, S. 2022: Geochemical signatures of sedimentary and diagenetic processes in the trace fossil *Rosselia* from the Pliocene in Taiwan. *Scientific Reports 12*, 22316. https://doi.org/10.1038/s41598-022-26772-0

Lissón, C. I. 1904: Los Tigillites del Salto del Fraile y algunas Sonneratia del Morro Solar. *Cuerpo de Ingenieros de Minas del Peru 15*, 11–64.

Liu, A. G. & McIlroy, D. 2015: Horizontal surface traces from the Fermeuse Formation, Ferryland (Newfoundland, Canada), and their place within the late Ediacaran ichnological revolution. 141–156 *in* McIlroy, D. (ed): *Ichnology: Papers from ICHNIA III*. Geological Association of Canada, Miscellaneous Publication, 9.

Liu, B., Li, D., Wang, M., Dai, M., He, W., Li, J. & Qi, Y. 2022: Piperock ichnofabrics from western Henan, China: spatial

distribution pattern and environmental controls on middle Cambrian carbonates. *International Journal of Earth Sciences 111*, 1609–1630. https://doi.org/10.1007/s00531-022-02195-0

Liu, J. T., Hsu, R. T., Yang, R. J., Wang, Y. P., Wu, H., Du, X., Li, A., Chien, S. C., Lee, J., Yang, S., Zhu, J., Su C.-C., Chang, Y. & Huh, C.-A. 2018: A comprehensive sediment dynamics study of a major mud belt system on the inner shelf along an energetic coast. *Scientific Reports 8*, 4229. https://doi.org/10.1038/s41598-018-22696-w

Liu, J., Steiner, M., Dunlop, J. A., Keupp, H., Shu, D., Ou, Q., Han, J., Zhang, Z. & Zhang, X. 2011: An armoured Cambrian lobopodian from China with arthropod-like appendages. *Nature 470*, 526–530. https://doi.org/10.1038/nature09704

Liu, Y., Gao, S., Wang, Y. P., Yang, Y., Long, J., Zhang, Y. & Wu, X. 2014: Distal mud deposits associated with the Pearl River over the northwestern continental shelf of the South China Sea. *Marine Geology 347*, 43–57. https://doi.org/10.1016/j.margeo.2013.10.012

Locklair, R. E. & Savrda, C. E. 1998: Ichnology of rhythmically bedded Demopolis Chalk (upper Cretaceous, Alabama): implications for paleoenvironment, depositional cycle origins, and tracemaker behavior. *Palaios 13*, 423–438. https://doi.org/10.2307/3515472

Lockley, M. G., Rindsberg, A. K. & Zeiler, R. M. 1987: The paleoenvironmental significance of the nearshore *Curvolithus* ichnofacies. *Palaios 2*, 255–262. https://doi.org/10.2307/3514675

Lokho, K. & Singh, B. P. 2013: Ichnofossils from the Miocene middle Bhuban Formation, Mizoram, northeast India and their paleoenvironmental significance. *Acta Geologica Sinica (English Edition) 87*, 1460–1471. https://doi.org/10.1111/1755-6724.12142

Lokho, K., Singh, B. P., Whiso, K. & Ezung, O. C. 2018: Ichnology of the Laisong Formation (late Eocene-early Oligocene) of the Naga Hills, Indo-Burma range (IBR): paleoenvironmental significance. *Journal of Asian Earth Sciences 162*, 13–24. https://doi.org/10.1016/j.jseaes.2017.12.019

Long, D. G. F. 2004: Precambrian Rivers. 660–663 *in* Eriksson, P. G., Altermann, W., Nelson, D. R., Mueller, W. U. & Catuneanu, O. (eds): *The Precambrian Earth: Tempos and Events*. Developments in Precambrian Geology, Vol. 12.

Long, D. G. F. & Copper, P. 1987: Stratigraphy of the upper Ordovician upper Vaureal and Ellis Bay formations, eastern Anticosti Island, Quebec. *Canadian Journal of Earth Sciences 24*, 1807–1820. https://doi.org/10.1139/e87-172

López Cabrera, M. I., Mángano, M. G., Buatois, L. A., Olivero, E. B. & Maples, C. G. 2019: Bivalves on the move: the interplay of extrinsic and intrinsic factors on the morphology of the trace fossil *Protovirgularia*. *Palaios 34*, 349–363. https://doi.org/10.2110/palo.2019.004

Lorenz von Liburnau, J. R. 1902: Ergänzung zur Beschreibung der fossilen *Halimeda fuggeri*. *Sitzungsberichte der kaiserlich-königlichen Akademie der Wissemschaften, Mathematisch-Naturwissenschaftliche Klasse 111*, 685–712.

Loughlin, N. J. D. & Hillier, R. D. 2010: Early Cambrian *Teichichnus*-dominated ichnofabrics and palaeoenvironmental analysis of the Caerfai Group, southwest Wales, UK. *Palaeogeography, Palaeoclimatology, Palaeoecology 297*, 239–251. https://doi.org/10.1016/j.palaeo.2010.07.030

Lowe, D. G. & Arnott, R. W. C. 2016: Composition and architecture of braided and sheetflood-dominated ephemeral fluvial strata in the Cambrian–Ordovician Potsdam Group: a case example of the morphodynamics of early Phanerozoic fluvial systems and climate change. *Journal of Sedimentary Research 86*, 587–612. https://doi.org/10.2110/jsr.2016.39

Löwemark, L. 2003: Automatic image analysis of X-ray radiographs: a new method for ichnofabric evaluation. *Deep Sea Research I 50*, 815–827. https://doi.org/10.1016/S0967-0637(03)00062-1

Löwemark, L. 2007: Importance and usefulness of trace fossils and bioturbation in paleoceanography. 413–427 *in* Miller III, W. (ed): *Trace Fossils. Concepts, Problems, Prospects*. Elsevier. https://doi.org/10.1016/B978-044452949-7/50150-9

Lucas, S. G. 2018: The GSSP method of chronostratigraphy: a critical review. *Frontiers in Earth Science 6*, 191. https://doi.org/10.3389/feart.2018.00191

Lucas, S. G. & Lerner, A. J. 2004: Extensive ichnofossil assemblage at the base of the Permian Abo Formation, Carrizo Arroyo, New Mexico. 285–289 *in* Lucas, S. G. & Zeigler, K. E. (eds): *Carboniferous-Permian Transition at Carrizo Arroyo, Central New Mexico*. New Mexico Museum of Natural History and Science, Bulletin 25, Albuquerque.

Lucas, S. G. & Lerner, A. J. 2005: Lower Pennsylvanian invertebrate ichnofossils from the Union Chapel Mine, Alabama: a preliminary assessment. 147–152 *in* Buta, R. J., Rindsberg, A. K. & Kopaska-Merkel, D. C. (eds): *Pennsylvanian Footprints in the Black Warrior Basin of Alabama*. Alabama Paleontological Society Monograph no. 1.

Lucas, S. G. & Lerner, A. J. 2010: Pennsylvanian lake-margin ichnoassemblage from Cañon del Cobre, Rio Arriba County, New Mexico. 37–47 *in* Lucas, S. G., Schneider, J. W. & Spielmann, J. A. (eds): *Carboniferous-Permian transition in Cañon del Cobre, northern New Mexico*. New Mexico Museum of Natural History and Science, Albuquerque, Bulletin 49.

Lucas, S. G. & Stimson, M. 2013: Re-evaluation of *Arenicolites* and *Treptichnus* ichnospecies from the Pennsylvanian Pottsville Formation, Union Chapel Mine, Alabama. 240–243 *in* Lucas, S. G., Nelson, W. J., DiMichele, W. A., Spielmann, J. A., Krainer, K., Barrick, J. A., Elrick, S. D. & Voigt, S. (eds): *The Carboniferous-Permian Transition*. New Mexico Museum of Natural History and Science, Albuquerque, Bulletin 60.

Lucas, S. G., Lerner, A. J., Bruner, M. & Shipman, P. 2004: Middle Pennsylvanian ichnofauna from eastern Oklahoma, USA. *Ichnos 11*, 45–55. https://doi.org/10.1080/10420940490442322

Lucas, S. G., Minter, N .J., Spielmann, J. A., Smith, J. A., Braddy, S. J. & Zeigler, K. E. 2005a: Early Permian ichnofossils from the northern Caballo Mountains, Sierra County, New Mexico. 151–162 *in* Lucas, S. G., Zeigler, K. E. & Spielmann, J. A. (eds): *The Permian of Central New Mexico*. New Mexico Museum of Natural History and Science, Albuquerque, Bulletin 31.

Lucas, S. G., Minter, N .J., Spielmann, J. A., Hunt, A. P. & Braddy, S. J. 2005b: Early Permian ichnofossil assemblage from the Fra Cristobal Mountains, southern New Mexico. 140–150 *in* Lucas, S. G., Zeigler, K. E. & Spielmann, J. A. (eds): *The Permian of Central New Mexico*. New Mexico Museum of Natural History and Science, Albuquerque, Bulletin 31.

Luo, H. 1993: Early Ordovician trace fossils from Ercun, Kunming, Yunnan. *Journal of Chengdu College of Geology 20*, 64–68.

Luo, H.-L., Tao, Y.-H. & Gao, S.-M 1994: Early Cambrian trace fossils near Kunming, Yunnan. *Acta Palaeontologica Sinica 33*, 676–685.

Luo, M., George, A. D. & Chen, Z.-Q. 2016: Sedimentology and ichnology of two lower Triassic sections in South China: implications for the biotic recovery following the end-Permian mass extinction. *Global and Planetary Change 144*, 198–212. https://doi.org/10.1016/j.gloplacha.2016.07.007

Luo, M., Shi, G. R., Lee, S. & Yang, B. 2017: A new trace fossil assemblage from the middle Permian Broughton Formation, southern Sydney Basin (southeastern Australia): ichnology and palaeoenvironmental significance. *Palaeogeography, Palaeoclimatology, Palaeoecology 485*, 455–465. https://doi.org/10.1016/j.palaeo.2017.06.033

M'Coy, F. 1850: On some genera and species of Silurian Radiata in the collection of the University of Cambridge. *Annals and Magazine of Natural History 6*, 270–290.

Ma, X., Aldridge, R. J., Siveter, D. J., Siveter, D. J., Hou, X. & Edgecombe, G. D. 2014: A new exceptionally preserved Cambrian priapulid from the Chengjiang Lagerstätte. *Journal of Paleontology 88*, 371–384. https://doi.org/10.1666/13-082

MacEachern, J. A. & Bann, K. L. 2020: The *Phycosiphon* Ichnofacies and the *Rosselia* Ichnofacies: two new ichnofacies for marine deltaic environments. *Journal of Sedimentary Research 90*, 855–886. https://doi.org/10.2110/jsr.2020.41

MacEachern, J. A. & Gingras, M. K. 2007: Recognition of brackish-water trace-fossil suites in the Cretaceous western interior seaway of Alberta, Canada. 149–193 *in* Bromley, R. G., Buatois, L. A., Mángano, G., Genise, J. F. & Melchor R. N. (eds): *Sediment-organism interactions: a multifaceted ichnology*. SEPM Special Publication, vol. 88. https://doi.org/10.2110/pec.07.88.0149

MacEachern, J. A. & Hobbs, T. W. 2004: The ichnological expression of marine and marginal marine conglomerates and conglomeratic intervals, Cretaceous Western Interior Seaway, Alberta and northeastern British Columbia. *Bulletin of Canadian Petroleum Geology 52*, 77–104. https://doi.org/10.2113/52.1.77

MacEachern, J. A. & Pemberton, S. G. 1992: Ichnological aspects of Cretaceous shoreface successions and shoreface variability in the western interior seaway of North America. 57–84 *in* Pemberton, S. G. (ed): *Applications of ichnology to petroleum exploration: a core workshop*. SEPM Core Workshop Notes, vol. 17. https://doi.org/10.2110/cor.92.01.0057

MacEachern, J. A., Zaitlin, B. A. & Pemberton, S. G. 1999: A sharp-based sandstone of the Viking Formation, Joffre field, Alberta, Canada: criteria for recognition of transgressively incised shoreface complexes. *Journal of Sedimentary Research 69*, 876–892. https://doi.org/10.2110/jsr.69.876

MacEachern, J. A., Pemberton, S. G., Gingras, M. K., Bann, K. L. & Dafoe, L. T. 2007: Uses of trace fossils in genetic stratigraphy. 110–134 *in* Miller III, W. (ed): *Trace Fossils. Concepts, Problems, Prospects*. Elsevier. https://doi.org/10.1016/B978-044452949-7/50133-9

Machhour, L., Philip, J. & Oudin, J. L. 1994: Formation of laminite deposits in anaerobic-dysaerobic marine environments. *Marine Geology 117*, 287–302. https://doi.org/10.1016/0025-3227(94)90021-3

MacNaughton, R. B. 2007: The application of trace fossils to biostratigraphy. 135–148 *in* Miller III, W. (ed): *Trace Fossils. Concepts, Problems, Prospects*. Elsevier. https://doi.org/10.1016/B978-044452949-7/50134-0

MacNaughton, R. B. & Narbonne, G. M. 1999: Evolution and ecology of Neoproterozoic-lower Cambrian trace fossils. *Palaios 14*, 97–115. https://doi.org/10.2307/3515367

MacNaughton, R. B. & Pickerill, R. K. 1995: Invertebrate ichnology of the nonmarine Lepreau Formation (Triassic), southern New Brunswick, eastern Canada. *Journal of Paleontology 69*, 160–171. https://doi.org/10.1017/S0022336000027001

MacNaughton, R. B., Dalrymple, R. W. & Narbonne, G. M. 1997: Early Cambrian braid-delta deposits, MacKenzie Mountains, north-western Canada. *Sedimentology 44*, 587–609. https://doi.org/10.1046/j.1365-3091.1997.d01-41.x

MacNaughton, R. B., Narbonne, G. M. & Dalrymple, R. W. 2000: Neoproterozoic slope deposits, Mackenzie Mountains, northwestern Canada: implications for passive-margin development and Ediacaran faunal ecology. *Canadian Journal of Earth Sciences 37*, 997–1020. https://doi.org/10.1139/e00-012

MacNaughton, R. B., Hagadorn, J. W. & Dott Jr., R. H. 2019: Cambrian wave-dominated tidal-flat deposits, central Wisconsin, USA. *Sedimentology 66*, 1643–1672. https://doi.org/10.1111/sed.12546

MacNaughton, R. B., Fallas, K .M. & Finley, T. D. 2021: *Psammichnites gigas* from the lower Cambrian of the Mackenzie Mountains, northwest Canada, and their biostratigraphic implications. *Ichnos 28*, 164–175. https://doi.org/10.1080/10420940.2021.1932491

Macquaker, J. H. S., Bentley, S .J. & Bohacs, K. M. 2010: Wave-enhanced sediment-gravity flows and mud dispersal across continental shelves: reappraising sediment transport processes operating in ancient mudstone successions. *Geology 38*, 947–950. https://doi.org/10.1130/G31093.1

Macsotay, O. 1967: Huellas problematicas y su valor paleoecologico en Venezuela. *Geos 16*, 7–79.

Madon, M. 2021: Deep-sea trace fossils in the West Crocker Formation, Sabah (Malaysia), and their palaeoenvironmental significance. *Bulletin of the Geological Society of Malaysia 71*, 23–46. https://doi.org/10.7186/bgsm71202103

Magwood, J. P. A. & Pemberton, S. G. 1990: Stratigraphic significance of *Cruziana*: new data concerning the Cambrian-Ordovician ichnostratigraphic paradigm. *Geology 18*, 729–732. https://doi.org/10.1130/0091-7613(1990)018<0729:SSOCND>2.3.CO;2

Maillard, G. 1887: Considérations sur les fossiles décrits comme algues. *Mémoires de la Société Paléontologique Suisse 14*, 3–40.

Manca, N. V. 1986: Caracteres icnológicos de la Formación Campanario (Cámbrico superior) en Salta y Jujuy. *Ameghiniana 23*, 75–87.

Mángano, M. G. 2011: Trace-fossil assemblages in a Burgess Shale-type deposit from the Stephen Formation at Stanley Glacier, Canadian Rocky Mountains: unraveling ecologic and evolutionary controls. 89–108 *in* Johnston, P. A. & Johnston, K. J. (eds): *International Conference on the Cambrian Explosion, Proceedings*. Palaeontographica Canadiana No. 31.

Mángano, M. G. & Buatois, L. A. 2003a: Trace fossils. 507–553 *in* Benedetto, J. L. (ed): *Ordovician Fossils of Argentina*. Secretaría de Ciencia y Tecnología, Universidad Nacional de Córdoba, Argentina.

Mángano, M. G. & Buatois, L. A. 2003b: *Rusophycus leiferikssoni* en la Formación Campanario: implicancias paleobiológicas, paleoecológicas y paleoambientales. *Asociación Paleontológica Argentina, Publicación Especial 9*, 65–84.

Mángano, M. G. & Buatois, L. A. 2004a: Reconstructing early Phanerozoic intertidal ecosystems: ichnology of the Cambrian Campanario Formation in northwest Argentina. *Fossils and Strata 51*, 17–38. https://doi.org/10.18261/9781405169851-2004-02

Mángano, M. G. & Buatois, L. A. 2004b: Ichnology of Carboniferous tide-influenced environments and tidal flat variability in the North American Midcontinent. *Geological Society, London, Special Publications 228*, 157–178. https://doi.org/10.1144/GSL.SP.2004.228.01.09

Mángano, M. G. & Buatois, L. A. 2014: Decoupling of body-plan diversification and ecological structuring during the Ediacaran–Cambrian transition: evolutionary and geobiological feedbacks. *Proceedings of the Royal Society B 281*, 20140038. https://doi.org/10.1098/rspb.2014.0038

Mángano, M. G. & Buatois, L. A. 2016: The Cambrian Explosion. 73–126 *in* Mángano, M. G. & Buatois, L. A. (eds): *The Trace Fossil Record of Major Evolutionary Events Volume 1, Precambrian and Paleozoic*. Topics in Geobiology, Springer. https://doi.org/10.1007/978-94-017-9600-2_3

Mángano, M. G. & Buatois, L. A. 2017: The Cambrian revolutions: trace-fossil record, timing, links and geobiological impact. *Earth-Science Reviews 173*, 96–108. https://doi.org/10.1016/j.earscirev.2017.08.009

Mángano, M. G. & Buatois, L. A. 2020: The rise and early evolution of animals: where do we stand from a trace-fossil perspective? *Interface Focus 10*, 20190103. https://doi.org/10.1098/rsfs.2019.0103

Mángano, M. G. & Buatois, L. A. 2021: Cambrian Explosion. 583–602 *in* Alderton, D. & Elias, S. A. (eds): *Encyclopedia of Geology*. Academic Press, Elsevier. https://doi.org/10.1016/B978-0-08-102908-4.00142-9

Mángano, M. G., Buatois, L. A. & Aceñolaza, G. F. 1996a: Trace fossils and sedimentary facies from a late Cambrian-early Ordovician tide-dominated shelf (Santa Rosita Formation, northwest Argentina): implications for ichnofacies models of shallow marine successions. *Ichnos 5*, 53–88. https://doi.org/10.1080/10420949609386406

Mángano, M. G., Buatois, L. A. & Claps, G. L. 1996b: Grazing trails formed by soldier fly larvae (Diptera: Stratiomyidae) and their paleoenvironmental and paleoecological implications for the fossil record. *Ichnos 4*, 163–167. https://doi.org/10.1080/10420949609380124

Mángano, M. G., Buatois, L. A. & Aceñolaza, F. G. 1996c: Icnología de ambientes marinos afectados por vulcanismo: la Formación Suri, Ordovícico del extremo norte de la sierra de Narváez,

Sistema del Famatina. *Asociación Paleontológica Argentina, Publicación Especial 4*, 69–88.

Mángano, M. G., Buatois, L. A., West, R. R. & Maples, C. G. 1998: Contrasting behavioral and feeding strategies recorded by tidal-flat bivalve trace fossils from the upper Carboniferous of eastern Kansas. *Palaios 13*, 335–351. https://doi.org/10.2307/3515322

Mangano, M. G., Buatois, L. A., Maples, C. G. & West, R. R. 2000: A new ichnospecies of *Nereites* from Carboniferous tidal-flat facies of eastern Kansas, USA: implications for the *Nereites-Neonereites* debate. *Journal of Paleontology 74*, 149–157. https://doi.org/10.1017/S0022336000031322

Mángano, M. G., Buatois, L. A. & Moya, M. C. 2001: Trazas fósiles de trilobites de la Formación Mojotoro (Ordovícico Inferior-Medio de Salta, Argentina): implicancias paleoecológicas, paleobiológicas y bioestratigráficas. *Spanish Journal of Palaeontology 16*, 9–28. https://doi.org/10.7203/sjp.16.1.21577

Mángano, M. G., Buatois, L. A. & Rindsberg, A. 2002a: Carboniferous *Psammichnites*: systematic re-evaluation, taphonomy and autecology. *Ichnos 9*, 1–22. https://doi.org/10.1080/10420940216409

Mángano, M. G., Buatois, L. A., West, R. R. & Maples, C. G. 2002b: *Ichnology of a Pennsylvanian equatorial tidal flat: the Stull Shale Member at Waverly, eastern Kansas*. Kansas Geological Survey, Bulletin 245, 133 pp.

Mángano, M. G., Buatois, L. A. & Muñiz Guinea, F. 2005a: Ichnology of the Alfarcito Member (Santa Rosita Formation) of northwestern Argentina: animal-substrate interactions in a lower Paleozoic wave-dominated shallow sea. *Ameghiniana 42*, 641–668.

Mángano, M. G., Carmona, N. B., Buatois, L. A. & Muñiz Guinea, F. 2005b: A new ichnospecies of *Arthrophycus* from the upper Cambrian-lower Tremadocian of northwest Argentina: implications for the arthrophycid lineage and potential in ichnostratigraphy. *Ichnos 12*, 179–190. https://doi.org/10.1080/10420940591009132

Mángano, M. G., Buatois, L. A. & MacNaughton, R. B. 2012: Ichnostratigraphy. 195–212 *in* Knaust, D. & Bromley, R. G. (eds): *Trace Fossils as Indicators of Sedimentary Environments*. Developments in Sedimentology, Vol. 64, Elsevier. https://doi.org/10.1016/B978-0-444-53813-0.00007-1

Mángano, M. G., Buatois, L. A., Hofmann, R., Elicki, O. & Shinaq, R. 2013: Exploring the aftermath of the Cambrian Explosion: the evolutionary significance of marginal-to shallow-marine ichnofaunas of Jordan. *Palaeogeography, Palaeoclimatology, Palaeoecology 374*, 1–15. https://doi.org/10.1016/j.palaeo.2012.05.029

Mángano, M. G., Buatois, L. A., Astini, R. & Rindsberg, A. K. 2014: Trilobites in early Cambrian tidal flats and the landward expansion of the Cambrian Explosion. *Geology 42*, 143–146. https://doi.org/10.1130/G34980.1

Mángano, M. G., Hawkes, C. D. & Caron, J.-B. 2019: Trace fossils associated with Burgess Shale non-biomineralized carapaces: bringing taphonomic and ecological controls into focus. *Royal Society Open Science 6*, 172074. https://doi.org/10.1098/rsos.172074

Mángano, M. G., Buatois, L. A., Waisfeld, B. G., Muñoz, D. F., Vaccari, N. E. & Astini, R. A. 2021: Were all trilobites fully marine? Trilobite expansion into brackish water during the early Palaeozoic. *Proceedings of the Royal Society B 288*, 20202263. https://doi.org/10.1098/rspb.2020.2263

Mángano, M. G., Buatois, L. A., MacNaughton, R. B., Jensen, S., Gougeon, R., Marcos, A., Meek, D., Piñuela, L. & García-Ramos, J. C. 2022: The *Psammichnites-Taphrhelminthopsis* conundrum: implications for calibrating the Cambrian Explosion. *Earth-Science Reviews 227*, 103971. https://doi.org/10.1016/j.earscirev.2022.103971

Mangum, D. C. 1970: Burrowing behavior of the sea anemone *Phyllactis*. *The Biological Bulletin 138*, 316–325. https://doi.org/10.2307/1540215

Männil, R. 1966: O vertikalnykh norkakh zaryvaniya v Ordovikskikh izvestnyakakh Pribaltiki. 200–207 *in* Hecker, R. F. (ed): *Organizm i sreda v geologischeskom proshlom*. Akademiya Nauk SSSR, Paleontologicheskij Institut.

Mansfield, W. C. 1927: Some peculiar fossil forms from Maryland. *Proceedings of the United States National Museum 71*, 1–9. https://doi.org/10.5479/si.00963801.71-2688.1

Mansfield, W. C. 1930: Some peculiar spiral fossil forms from California and Mexico. *Proceedings of the United States National Museum 77*, 1–3. https://doi.org/10.5479/si.00963801.77-2836.1

Maples, C.G. & Archer, A.W. 1987: Redescription of early Pennsylvanian trace-fossil holotypes from the nonmarine Hindostan Whetstone Beds of Indiana. *Journal of Paleontology 61*, 890–897. https://doi.org/10.1017/S0022336000029280

Maples, C. G. & Archer, A. W. 1989: The potential of Paleozoic nonmarine trace fossils for paleoecological interpretations. *Palaeogeography, Palaeoclimatology, Palaeoecology 73*, 185–195. https://doi.org/10.1016/0031-0182(89)90003-5

Maples, C. G. & Suttner, L. J. 1990: Trace fossils and marine-nonmarine cyclicity in the Fountain Formation (Pennsylvanian: Morrowan/Atokan) near Manitou springs, Colorado. *Journal of Paleontology 64*, 859–880. https://doi.org/10.1017/S002233600001996X

Marchetti, L., Ronchi, A., Santi, G. & Voigt, S. 2015: The Gerola Valley site (Orobic Basin, northern Italy): a key for understanding late early Permian tetrapod ichnofaunas. *Palaeogeography, Palaeoclimatology, Palaeoecology 439*, 97–116. https://doi.org/10.1016/j.palaeo.2015.02.032

Mariotti, G., Pruss, S. B., Ai, X., Perron, J. T. & Bosak, T. 2016: Microbial origin of early animal trace fossils? *Journal of Sedimentary Research 86*, 287–293. https://doi.org/10.2110/jsr.2016.19

Marshall, J. D. & Pirrie, D. 2013: Carbonate concretions—explained. *Geology Today 29*, 53–62. https://doi.org/10.1111/gto.12002

Martin, A. J. 2009: Neoichnology of an Arctic fluvial point bar, North Slope, Alaska (USA). *Geological Quarterly 53*, 383–396.

Martino, R. L. 1989: Trace fossils from marginal marine facies of the Kanawha Formation (middle Pennsylvanian), west Virginia. *Journal of Paleontology 63*, 389–403. https://doi.org/10.1017/S0022336000019648

Martinsson, A. 1965: Aspects of a middle Cambrian thanatotope on Öland. *Geologiska Foereningen i Stockholm Foerhandlingar 87*, 181–230. https://doi.org/10.1080/11035896509448903

Marusin, V. V. & Kuper, K. E. 2020: Complex tunnel systems of early Fortunian macroscopic endobenthos in the Ediacaran-Cambrian transitional strata of the Olenek Uplift (NE Siberian Platform). *Precambrian Research 340*, 105627. https://doi.org/10.1016/j.precamres.2020.105627

Marusin, V. V., Kolesnikova, A. A., Kochnev, B. B., Kuznetsov, N. B., Pokrovsky, B. G., Romanyuk, T. V., Karlova, G. A., Rud'ko, S. V., Shatsillo, A. V., Dubenskiy, A. S., Sheshukov, V. S. & Lyapunov, S. M. 2021: Detrital zircon age and biostratigraphic and chemostratigraphic constraints on the Ediacaran–Cambrian transitional interval in the Irkutsk Cis–Sayans Uplift, southwestern Siberian Platform. *Geological Magazine 158*, 1156–1172. https://doi.org/10.1017/S0016756820001132

Marusin, V. V., Kochnev, B. B., Karlova, G. A. & Proshenkin, A. I. 2023: Age constraints and source areas for the Precambrian to Cambrian strata of the southern Yenisei Ridge (Redkolesnaya and Ostrovnoy formations). *Geodynamics & Tectonophysics 14*, 0700. https://doi.org/10.5800/GT-2023-14-3-0700

Marusin, V. V., Kochnev, B. B., Pokrovsky, B. G. & Metelkin, D. V. 2025: Precambrian–Cambrian transition in the Biryusa Cis-Sayans Uplift (southwestern Siberian Platform). *Doklady Earth Sciences 521,* 19. https://doi.org/10.1134/S1028334X24605820

Mason, T. R. & Christie, A. D. M. 1986: Palaeoevironmental significance of ichnogenus *Diplocraterion* Torell from the Permian Vryheid Formation of the Karoo Supergroup, South Africa.

Palaeogeography, Palaeoclimatology, Palaeoecology 52, 249–265. https://doi.org/10.1016/0031-0182(86)90050-7

Massari, F. & Dieni, I. 1983: Pelagic oncoids and ooids in the middle-upper Jurassic of eastern Sardinia. 367–376 *in* Peryt, T. M. (ed): *Coated Grains*. Springer, Berlin. https://doi.org/10.1007/978-3-642-68869-0_31

Mata, S. A., Corsetti, C. L., Corsetti, F. A., Awramik, S .M. & Bottjer, D. J. 2012: Lower Cambrian anemone burrows from the upper member of the Wood Canyon Formation, Death Valley region, United States: paleoecological and paleoenvironmental significance. *Palaios 27*, 594–606. https://doi.org/10.2110/palo.2012.p12-016r

Mathieu, G. 1949: Contribution à l'étude des Monts Troglodytes dans l'extrême sud-Tunisien. Géologie régionale des environs de Matmata Medenine et Foum-Tatahouine. *Annales des Mines et de la Géologie 4*, 1–82.

Mathieu, R. 1966: Structures sédimentaires des dépôts de la zone intertidale dans la partie occidentale de la baie du Mont-Saint-Michel. *Revue de géographie physique et de géologie dynamique 8*, 113–122.

Matthew, G. F. 1888: On Psammichnites and the early trilobites of the Cambrian rocks in eastern Canada. *The American Geologist 2*, 1–9.

Matthew, G. F. 1890: On Cambrian organisms in Acadia. *Transactions of the Royal Society of Canada 7*, 135–162.

Matthew, G. F. 1891: Illustrations of the fauna of the St. John Group, no. V. *Transactions of the Royal Society of Canada 8*, 123–166.

Matthew, G. F. 1899: Studies on Cambrian faunas, no. 4. –Fragments of the Cambrian faunas of Newfoundland. *Proceedings and Transactions of the Royal Society of Canada 5*, 67–95.

Matz, M. V., Frank, T. M., Marshall, N. J., Widder, E. A. & Johnsen, S. 2008: Giant deep-sea protist produces bilaterian-like traces. *Current Biology 18*, 1849–1854. https://doi.org/10.1016/j.cub.2008.10.028

Mayoral, E. 1986: Gyrolithes vidali nov. icnoesp. (Plioceno marino) en el sector suroccidental de la Cuenca del Guadalquivir (área de Palos de la Frontera, Huelva, España). *Estudios Geológicos 42*, 211–223. https://doi.org/10.3989/egeol.86422-3749

Mayoral, E. & Muñiz, F. 1995: Nueva icnoespecie de *Gyrolithes* del Mioceno superior de la Cuenca del Guadalquivir (Lepe, Huelva). *Spanish Journal of Palaeontology 10*, 190–201. https://doi.org/10.7203/sjp.24136

Mayoral, E. & Muñiz, F. 1998: Nuevos datos icnotaxonomicos sobre *Gyrolithes* del Plioceno inferior de la Cuenca del Guadalquivir (Lepe, Huelva, España). *Spanish Journal of Palaeontology 13*, 61–69. https://doi.org/10.7203/sjp.24000

Mayoral, E., Ledesma-Vazquez, J., Baarli, B. G., Santos, A., Ramalho, R., Cachão, M., da Silva, C. M. & Johnson, M. E. 2013: Ichnology in oceanic islands; case studies from the Cape Verde Archipelago. *Palaeogeography, Palaeoclimatology, Palaeoecology 381*, 47–66. https://doi.org/10.1016/j.palaeo.2013.04.014

Mazumder, R. & Arima, M. 2005: Tidal rhythmites and their implications. *Earth-Science Reviews 69*, 79–95. https://doi.org/10.1016/j.earscirev.2004.07.004

McBride, E. F. & Picard, M. D. 1991: Facies implications of *Trichichnus* and *Chondrites* in turbidites and hemipelagites, Marnoso-arenacea Formation (Miocene), northern Apennines, Italy. *Palaios 6*, 281–290. https://doi.org/10.2307/3514908

McCann, T. 1993: A *Nereites* ichnofacies from the Ordovician-Silurian Welsh Basin. *Ichnos 3*, 39–56. https://doi.org/10.1080/10420949309386372

McCann, T. & Pickerill, R. K. 1988: Flysch trace fossils from the Cretaceous Kodiak Formation of Alaska. *Journal of Paleontology 62*, 330–348. https://doi.org/10.1017/S0022336000059138

McCarthy, B. 1979: Trace fossils from a Permian shoreface-foreshore environment, eastern Australia. *Journal of Paleontology 53*, 345–366.

McIlroy, D. 1999: Additional ichnotaxa from the flysch-type deposits of the Arenig Ribband Group, Co. Wexford, Ireland. *Irish Journal of Earth Sciences 17*, 103–113.

McIlroy, D. & Brasier, M. D. 2017: Ichnological evidence for the Cambrian explosion in the Ediacaran to Cambrian succession of Tanafjord, Finnmark, northern Norway. *Geological Society, London, Special Publications 448*, 351–368. https://doi.org/10.1144/SP448.7

McIlroy, D. & Heys, G. R. 1997: Palaeobiological significance of *Plagiogmus arcuatus* from the lower Cambrian of central Australia. *Alcheringa 21*, 161–178. https://doi.org/10.1080/03115519708619171

McIlroy, D. & Logan, G. A. 1999: The impact of bioturbation on infaunal ecology and evolution during the Proterozoic-Cambrian transition. *Palaios 14*, 58–72. https://doi.org/10.2307/3515361

McIlroy, D., Green, O. R. & Brasier, M. D. 2001: Palaeobiology and evolution of the earliest agglutinated foraminifera: *Platysolenites*, *Spirosolenites* and related forms. *Lethaia 34*, 13–29. https://doi.org/10.1080/002411601300068170

McIlroy, D., Crimes, T. P. & Pauley, J. C. 2005: Fossils and matgrounds from the Neoproterozoic Longmyndian Supergroup, Shropshire, UK. *Geological Magazine 142*, 441–455. https://doi.org/10.1017/S0016756805000555

McKay, J. L. & Longstaffe, F. J. 2003: Sulphur isotope geochemistry of pyrite from the upper Cretaceous Marshybank Formation, Western Interior Basin. *Sedimentary Geology 157*, 175–195. https://doi.org/10.1016/S0037-0738(02)00233-6

McLachlan, A. J. & Cantrell, M. A. 1976: Sediment development and its influence on the distribution and tube structure of *Chironomus plumosus* L. (Chironomidae, Diptera) in a new impoundment. *Freshwater Biology 6*, 437–443. https://doi.org/10.1111/j.1365-2427.1976.tb01632.x

McLoughlin, S., Vajda, V., Topper, T. P., Crowley, J. L., Liu, F., Johansson, O. & Skovsted, C. B. 2021: Trace fossils, algae, invertebrate remains and new U-Pb detrital zircon geochronology from the lower Cambrian Torneträsk Formation, northern Sweden. *GFF 143*, 103–133. https://doi.org/10.1080/11035897.2021.1939775

McMahon, W. J., Davies, N. S. & Went, D. J. 2017: Negligible microbial matground influence on pre-vegetation river functioning: evidence from the Ediacaran-lower Cambrian Series Rouge, France. *Precambrian Research 292*, 13–34. https://doi.org/10.1016/j.precamres.2017.01.020

Meinhold, G., Willbold, M., Karius, V., Jensen, S., Agić, H., Ebbestad, J. O. R., Palacios, T., Högström, A. E. S., Høyberget, M. & Taylor, W. L. 2022: Rare earth elements and neodymium and strontium isotopic constraints on provenance switch and post-depositional alteration of fossiliferous Ediacaran and lowermost Cambrian strata from Artic Norway. *Precambrian Research 381*, 106845. https://doi.org/10.1016/j.precamres.2022.106845

Meischner, T., Elicki, O., Masri, A., Moumani, K. A. & Hussein, M. A. A. 2020: Ordovician trace fossils from southern Jordan with particular consideration to the *Cruziana rugosa* group: taxonomy, stratigraphy and trans-regional correlation throughout the Middle East and northern Africa. *Journal of African Earth Sciences 164*, 103595. https://doi.org/10.1016/j.jafrearsci.2019.103595

Melchor, R. N. & Cardonatto, M. C. 2014: Insights on the behavior of late Paleozoic aquatic crustaceans (Pygocephalomorpha?): compound trace fossils from western Argentina. *Ichnos 21*, 76–99. https://doi.org/10.1080/10420940.2013.879868

Melchor, R. N., Bellosi, E. S. & Genise, J. F. 2003: Invertebrate and vertebrate trace fossils from a Triassic lacustrine delta: the Los Rastros Formation, Ischigualasto Provincial Park, San Juan, Argentina. *Asociación Paleontológica Argentina 9*, 17–23.

Mello, A. B., Netto, R. G., Aquino, C. D. & Dasgupta, S. 2021: Crowded *Rosselia* ichnofabric in estuarine settings recording early transgressions in lowermost Permian post-glacial Gondwana (Rio Bonito Formation, Paraná Basin, S Brazil). *Journal of South American Earth Sciences 110*, 103372. https://doi.org/10.1016/j.jsames.2021.103372

Melnyk, S. & Gingras, M. K. 2020: Using ichnological relationships to interpret heterolithic fabrics in fluvio-tidal settings. *Sedimentology 67*, 1069–1083. https://doi.org/10.1111/sed.12674

Memória, S. C., Netto, R. G. & Sedorko, D. 2023: A new model for Early Paleozoic ichnostratigraphy based on trace fossil

assemblages from Brazil. *Evolving Earth 1*, 100026. https://doi.org/10.1016/j.eve.2023.100026

Mendiola, J., Martínez, J., Blasco, J. & López, A. 1998: *Gyrolithes valeroi* nueva icnospecie del Plioceno inferior de Guardamar-España (Cuenca del Bajo Segura, Cordilliera Bética Oriental). *Revista de la Societat Paleontologica d'Elx, Secció Paleontológica 4*, 1–49.

Menon, L. R., McIlroy, D. & Brasier, M. D. 2013: Evidence for Cnidaria-like behavior in ca. 560 Ma Ediacaran *Aspidella*. *Geology 41*, 895–898. https://doi.org/10.1130/G34424.1

Menon, L. R., McIlroy, D. & Brasier, M. D. 2017: '*Intrites*' from the Ediacaran Longmyndian Supergroup, UK: a new form of microbially-induced sedimentary structure (MISS). *Geological Society, London, Special Publications 448*, 271–283. https://doi.org/10.1144/SP448.12

Menon, L. R., McIlroy, D., Liu, A. G. & Brasier, M. D. 2016: The dynamic influence of microbial mats on sediments: fluid escape and pseudofossil formation in the Ediacaran Longmyndian Supergroup, UK. *Journal of the Geological Society 173*, 177–185. https://doi.org/10.1144/jgs2015-036

Mermillod-Blondin, F. & Rosenberg, R. 2006: Ecosystem engineering: the impact of bioturbation on biogeochemical processes in marine and freshwater benthic habitats. *Aquatic Sciences 68*, 434–442. https://doi.org/10.1007/s00027-006-0858-x

Metz, R. 1987a: Insect traces from nonmarine ephemeral puddles. *Boreas 16*, 189–195. https://doi.org/10.1111/j.1502-3885.1987.tb00770.x

Metz, R. 1987b: Sinusoidal trail formed by a recent biting midge (Family Ceratopogonidae): trace fossil implications. *Journal of Paleontology 61*, 312–314. https://doi.org/10.1017/S0022336000028481

Metz, R. 1998: Nematode trails from the late Triassic of Pennsylvania. *Ichnos 5*, 303–308. https://doi.org/10.1080/10420949809386428

Metz, R. 2000: Triassic trace fossils from lacustrine shoreline deposits of the Passaic Formation, Douglassville, Pennsylvania. *Ichnos 7*, 253–266. https://doi.org/10.1080/10420940009380165

Metz, R. 2009: Trace fossils from the Mahantango Formation (upper middle Devonian) Pike County, Pennsylvania. *Bulletin New Jersey Academy of Science 54*, 9–17.

Metz, R. 2022: *Cruziana* and *Helminthopsis* in fluvial deposits of the uppermost Stockton Formation (late Triassic), west-central New Jersey. *Ichnos 29*, 76–83. https://doi.org/10.1080/10420940.2022.2056168

Middleton, G.V. & Hampton, M.A. 1973: Sediment gravity flows: mechanics of flow and deposition. 1–38 *in* Middleton, G. V. & Bouma, A. H. (eds): *Turbidites and Deep Water Sedimentation*. SEPM, Pacific Session, Los Angeles, CA.

Midtgaard, H. H. 1996: Inner-shelf to lower-shoreface hummocky sandstone bodies with evidence for geostrophic influenced combined flow, lower Cretaceous, west Greenland. *Journal of Sedimentary Research 66*, 343–353. https://doi.org/10.1306/D4268342-2B26-11D7-8648000102C1865D

Miguez-Salas, O., Saeedi, H., Brandt, A. & Riehl, T. 2024: Seafloor bioturbation intensity on the deep sea: more complex than organic matter. *Limnology and Oceanography 69*, 1857–1869. https://doi.org/10.1002/lno.12632

Mikuláš, R. 1990: Trace fossils from the Zahořany Formation (upper Ordovician, Bohemia). *Acta Universitatis Carolina 3*, 307–335.

Mikuláš, R. 1992: Trace fossils from the Kosov Formation of the Bohemian Upper Ordovician. *Sborník Geologických věd, Paleontologie 32*, 9–54.

Mikuláš, R. 1993: New information on trace fossils of the early Ordovician of Prague Basin (Barrandian area, Czech Republic). *Journal of the Czech Geological Society 38*, 171–182.

Mikuláš, R. 1995: Trace fossils from the Paseky Shale (early Cambrian, Czech Republic). *Journal of the Czech Geological Society 40*, 37–44.

Mikuláš, R. & Lehotský, T. 2002: Ichnofosilie *Cruziana problematica* ve svrchním Karbonu Hornoslezské Pánve. *Geologické Výzkumy na Moravě a ve Slezsku 9*, 55–56.

Mikuláš, R. & Pek, I. 1994: Spirocircus cycloides, a new ichnofossil from the upper Cretaceous in northern Moravia. *Věstník Českého Geologickéo Ústavu 69*, 75–77.

Miller, M. F. & Byers, C. W. 1984: Abundant and diverse early Paleozoic infauna indicated by the stratigraphic record. *Geology 12*, 40–43. https://doi.org/10.1130/0091-7613(1984)12<40:AADEPI>2.0.CO;2

Miller, M. F. & Knox, L. W. 1985: Biogenic structures and depositional environments of a lower Pennsylvanian coal-bearing sequence, northern Cumberland Plateau, Tennessee, USA. 67–97 *in* Curran, H. A. (ed): *Biogenic structures: their use in interpreting depositional environments*. Society for Sedimentary Geology Special Publication, Vol. 35. https://doi.org/10.2110/pec.85.35.0067

Miller, M. F. & Smail, S. E. 1997: A semiquantitative field method for evaluating bioturbation on bedding planes. *Palaios 12*, 391–396. https://doi.org/10.2307/3515338

Miller, S. A. 1875: Some new species of fossils from the Cincinnati group and remarks upon some described forms. *The Cincinnati Quarterly Journal of Science 2*, 349–355.

Miller, S. A. 1880: Silurian ichnolites, with definitions of new genera and species. *Journal of the Cincinnati Society of Natural History 2*, 217–222.

Miller, S. A. 1889: *North American Geology and Palaeontology for the use of amateurs, students and scientists*. Western Methodist Book Concern, Cincinnati, Ohio, 664 pp.

Miller, S. A. & Dyer, C. B. 1878a: *Contributions to Palaeontology. No. 2*. J. Barclay, Cincinnati, 11 pp.

Miller, S. A. & Dyer, C. B. 1878b: Contributions to palaeontology. *Journal of the Cincinnati Society of Natural History 1*, 24–40.

Miller III, W. 1997: Trail-producing behavior of *Oliva sayana* (Gastropoda) in the lower foreshore at Bogue Banks, North Carolina. *Tulane Studies in Geology and Paleontology 30*, 109–116.

Miller III, W., Webb Jr., F. & Raymond, L. A. 2009: "*Pteridichnites*" (= *Psammichnites*) from the upper Devonian Brallier Formation of southwestern Virginia, USA: ichnotaxonomic status, constructional morphology, and paleoecology. *Southeastern Geology 46*, 187–199.

Mills, A. & Sandeman, H. 2021: Lithostratigraphy and lithogeochemistry of Ediacaran alkaline basaltic rocks of the Musgravetown Group, Bonavista Peninsula, northeastern Newfoundland, Canada: an extensional volcanogenic basin in the type-Avalon terrane. *Atlantic Geology 57*, 207–234. https://doi.org/10.4138/atlgeol.2021.010

Mills, A. J., Dunning, G. R. & Langille, A. 2016: New geochronological constraints on the Connecting Point Group, Bonavista Peninsula, Avalon Zone, Newfoundland. *Current Research, Newfoundland and Labrador Department of Natural Resources, Geological Survey 16-1*, 153–171.

Mills, A. J., Dunning, G. R. & Sandeman, H. A. 2021: Lithogeochemical, isotopic, and U–Pb (zircon) age constraints on arc to rift magmatism, northwestern and central Avalon Terrane, Newfoundland, Canada: implications for local lithostratigraphy. *Canadian Journal of Earth Sciences 58*, 332–354. https://doi.org/10.1139/cjes-2019-0196

Mills, P. C. 1983: Genesis and diagnostic value of soft-sediment deformation structures—a review. *Sedimentary Geology 35*, 83–104. https://doi.org/10.1016/0037-0738(83)90046-5

Minter, N. J. & Braddy, S. J. 2009: Ichnology of an early Permian intertidal flat: the Robledo Mountains Formation of southern New Mexico, USA. *Special Papers in Palaeontology 82*, 1–107.

Minter, N. J. & Lucas, S. G. 2009: The arthropod trace fossil *Cruziana* and associated ichnotaxa from the lower Permian Abo Formation, Socorro County, New Mexico. *New Mexico Geological Society Guidebook, 60th Field Conference, Geology of the Chupadera Mesa Region 60*, 291–298. https://doi.org/10.56577/FFC-60.291

Minter, N. J., Braddy, S. J. & Davis, R. B. 2007: Between a rock and a hard place: arthropod trackways and ichnotaxonomy. *Lethaia 40*, 365–375. https://doi.org/10.1111/j.1502-3931.2007.00035.x

Minter, N. J., Buatois, L. A., Mángano, M. G., Davies, N. S., Gibling, M. R. & Labandeira, C. 2016: The establishment of continental ecosystems. 205–324 *in* Mángano, M. G. & Buatois, L. A. (eds): *The Trace Fossil Record of Major Evolutionary Events Volume 1, Precambrian and Paleozoic*. Topics in Geobiology, Springer. https://doi.org/10.1007/978-94-017-9600-2_6

Minter, N. J., Lucas, S. G., Lerner, A. J. & Braddy, S. J. 2008: *Augerinoichnus helicoidalis*, a new helical trace fossil from the nonmarine Permian of New Mexico. *Journal of Paleontology 82*, 1201–1206. https://doi.org/10.1666/07-129.1

Mochizuki, T., Oji, T., Zhao, Y., Peng, J., Yang, X. & Gonchigdorj, S. 2014: Diachronous increase in early Cambrian ichnofossil size and benthic faunal activity in different climatic regions. *Journal of Paleontology 88*, 331–338. https://doi.org/10.1666/13-056

Moczydłowska, M., Jensen, S., Ebbestad, J. O. R., Budd, G. E. & Martí-Mus, M. 2001: Biochronology of the autochthonous lower Cambrian in the Laisvall–Storuman area, Swedish Caledonides. *Geological Magazine 138*, 435–453. https://doi.org/10.1017/S0016756801005416

Moczydłowska, M., Westall, F. & Foucher, F. 2014: Microstructure and biogeochemistry of the organically preserved Ediacaran metazoan *Sabellidites*. *Journal of Paleontology 88*, 224–239. https://doi.org/10.1666/13-003

Moghadam, H. V. & Paul, C. R. C. 2000: Trace fossils of the Jurassic, Blue Lias, Lyme Regis, southern England. *Ichnos 7*, 283–306. https://doi.org/10.1080/10420940009380167

Molina, J. M., Alfaro, P., Moretti, M. & Soria, J. M. 1998: Soft-sediment deformation structures induced by cyclic stress of storm waves in tempestites (Miocene, Guadalquivir Basin, Spain). *Terra Nova 10*, 145–150. https://doi.org/10.1046/j.1365-3121.1998.00183.x

Monaco, P. 2014: Taphonomic aspects of the radial backfill of asterosomids in Oligo-Miocene turbidites of central Italy (northern Apennines). *Rivista Italiana di Paleontologia e Stratigrafia 120*, 215–224. https://doi.org/10.13130/2039-4942/6061

Monaco, P. & Checconi, A. 2010: Taphonomy of the graphoglyptid trace fossil *Desmograpton* Fuchs 1895 at the sole of Miocene thin-bedded turbidites, northern Apennines. *Bollettino della Società Paleontologica Italiana 49*, 163–172. https://doi.org/10.13140/2.1.4958.2405

Monaco, P. & Trecci, T. 2014: Ichnocoenoses in the Macigno turbidite basin system, lower Miocene, Trasimeno (Umbrian Apennines, Italy). *Italian Journal of Geosciences 133*, 116–130. https://doi.org/10.3301/IJG.2013.18

Monaco, P. & Uchman, A. 1999: Deep-sea ichnoassemblages and ichnofabrics of the Eocene Scisti varicolori beds in the Trasimeno area, western Umbria, Italy. 39–52 *in* Farinacci, A. & Lord, A. R. (eds): *Depositional Episodes and Bioevents*. Palaeopelagos Special Publication No 2. https://doi.org/10.13140/2.1.3156.0002

Monaco, P., Milighetti, M. & Checconi, A. 2010: Ichnocoenoses in the Oligocene to Miocene foredeep basins (northern Apennines, central Italy) and their relation to turbidite deposition. *Acta Geologica Polonica 60*, 53–70.

Monaco, P., Rodríguez-Tovar, F. J. & Uchman, A. 2012: Ichnological analysis of lateral environmental heterogeneity within the Bonarelli Level (uppermost Cenomanian) in the classical localities near Gubbio, central Apennines, Italy. *Palaios 27*, 48–54. https://doi.org/10.2110/palo.2011.p11-018r

Morgan, R. F. 2019: A new ichnospecies of *Gyrolithes* from the Austin Chalk, upper Cretaceous, Texas, USA. *Ichnos 26*, 1–7. https://doi.org/10.1080/10420940.2016.1244056

Morgan, R. F., Juntunen, K. L., Scott, A. & Landreth, M. 2023: *Circulichnis leomonti*, a new ring-like ichnospecies (trace fossil) from the late Cambrian Lion Mountain member, Riley Formation, Burnet County, Texas. *Texas Journal of Science 75*, article 1. https://doi.org/10.32011/txjsci_75_1_Article1

Morière, M. 1878: Note sur le grès de Bagnoles (Orne). *Bulletin de la Société Linnéenne de Normandie 2*, 20–33.

Morsilli, M. & Pomar, L. 2012: Internal waves vs. surface storm waves: a review on the origin of hummocky cross-stratification. *Terra Nova 24*, 273–282. https://doi.org/10.1111/j.1365-3121.2012.01070.x

Morys, C., Forster, S. & Graf, G. 2016: Variability of bioturbation in various sediment types and on different spatial scales in the southwestern Baltic Sea. *Marine Ecology Progress Series 557*, 31–49. https://doi.org/10.3354/meps11837

Moslow, T. F. & Pemberton, S. G. 1988: An integrated approach to the sedimentological analysis of some lower Cretaceous shoreface and delta front sandstone sequences. 373–386 *in* James, D. P. & Leckie, D. A. (eds): *Sequences, Stratigraphy, Sedimentology: Surface and Subsurface*. Canadian Society of Petroleum Geologists, Memoir 15.

Mount, J. 1993: Appendix B: Uratanna Formation and the base of the Cambrian System, Angepena Syncline. 86–90 *in* Jenkins, R .J. F., Lindsay, J. F. & Walter, M. R. (eds): *Field Guide to the Adelaide Geosyncline and Amadeus Basin, Australia*. Australian Geological Survey Organisation, Record No 1993/35.

Mount, J. F. & McDonald, C. 1992: Influence of changes in climate, sea level, and depositional systems on the fossil record of the Neoproterozoic-early Cambrian metazoan radiation, Australia. *Geology 20*, 1031–1034. https://doi.org/10.1130/0091-7613(1992)020<1031:IOCICS>2.3.CO;2

Moussa, M. T. 1970: Nematode fossil trails from the Green River Formation (Eocene) in the Uinta basin, Utah. *Journal of Paleontology 44*, 304–307.

Mulder, T. & Alexander, J. 2001: The physical character of subaqueous sedimentary density flows and their deposits. *Sedimentology 48*, 269–299. https://doi.org/10.1046/j.1365-3091.2001.00360.x

Mulder, T., Syvitski, J. P. M., Migeon, S., Faugères, J.-C. & Savoye, B. 2003: Marine hyperpycnal flows: initiation, behavior and related deposits. A review. *Marine and Petroleum Geology 20*, 861–882. https://doi.org/10.1016/j.marpetgeo.2003.01.003

Mulder, T., Razin, P. & Faugeres, J.-C. 2009: Hummocky cross-stratification-like structures in deep-sea turbidites: upper Cretaceous Basque basins (western Pyrenees, France). *Sedimentology 56*, 997–1015. https://doi.org/10.1111/j.1365-3091.2008.01014.x

Muñiz, F. & Belaústegui, Z. 2019: Helical crustacean burrows: *Gyrolithes* ichnofabrics from the Pliocene of Lepe (Huelva, SW Spain). *Palaios 34*, 1–14. https://doi.org/10.2110/palo.2018.084

Muñiz, F. & Gámez Vintaned, J. A. 2008: *Avian incipient "Monomorphichnus" in modern dune and ephemeral pond environments*. 2008 Joint Annual Meeting, ASA, CSSA, and SSSA, Abstract 249-31.

Muñiz, F., Belaústegui, Z., Cárcamo, C., Domènech, R. & Martinell, J. 2015: *Cruziana*- and *Rusophycus*-like traces of recent Sparidae fish in the estuary of the Piedras River (Lepe, Huelva, SW Spain). *Palaeogeography, Palaeoclimatology, Palaeoecology 439*, 176–183. https://doi.org/10.1016/j.palaeo.2015.03.017

Muniz, G. C. B. 1980: Cochlichnus lagartensis ichnosp. nov., ichnofóssil da Formação Lagarto, Grupo Estância, no Estado de Sergipe. *Anais do XXXI Congresso Brasileiro de Geologia, Baleario de Camboriú, Santa Catarina 5*, 3101–3105.

Muniz, G. C. B. 1985: *Cochlichnus sousensis*, icnospécie da Formação Sousa, Grupo Rio do Peixe, no Estado da Paraíba. 239–241 *in*: *Coletânea de trabalhos paleontológicos*. Trabahos apresentados no VIII congresso Brasileiro de paleontologia, 1983, Ministério das Minas e Energia, Departmento Nacional da Produção Mineral.

Muñiz Guinea, F., Mángano, M. G., Buatois, L. A., Podeniene, V., Gámez Vintaned, J. A. & Mayoral Alfaro, E. 2014: Compound biogenic structures resulting from ontogenetic variation: an example from a modern dipteran. *Spanish Journal of Palaeontology 29*, 83–94. https://doi.org/10.7203/sjp.29.1.17491

Muñoz, D. F., Mángano, M. G. & Buatois, L. A. 2019: Unravelling Phanerozoic evolution of radial to rosette trace fossils. *Lethaia 52*, 350–369. https://doi.org/10.1111/let.12317

Murchison, R. I. 1839: *The Silurian System, founded on Geological Researches in the counties of Salop, Hereford, Radnor, Montgomery, Caermarthen, Brecon, Pembroke, Monmouth, Gloucester, Worcester, and Stafford; with descriptions of the*

coal-fields and overlying formations. Part II. J. Murray, London, 768 pp.

Murphy, J. B. & Nance, R. D. 1989: Model for the evolution of the Avalonian-Cadomian belt. *Geology 17*, 735–738. https://doi.org/10.1130/0091-7613(1989)017<0735:MFTEOT>2.3.CO;2

Murphy, J. B., McCausland, P. J., O'Brien, S. J., Pisarevsky, S. & Hamilton, M. A. 2008: Age, geochemistry and Sm–Nd isotopic signature of the 0.76 Ga Burin Group: compositional equivalent of Avalonian basement? *Precambrian Research 165*, 37–48. https://doi.org/10.1016/j.precamres.2008.05.006

Murphy, J. B., Nance, R. D., Keppie, J. D. & Dostal, J. 2019: Role of Avalonia in the development of tectonic paradigms. *Geological Society, London, Special Publications 470*, 265–287. https://doi.org/10.1144/SP470.12

Murphy, J. B., Nance, R. D. & Wu, L. 2023: The provenance of Avalonia and its tectonic implications: a critical reappraisal. *Geological Society, London, Special Publications 531*, SP531-2022-176. https://doi.org/10.1144/SP531-2022-176

Murray, J., MacGabhann, B. A., Doyle, E., Mángano, M. G., Tyrrell, S. & Harper, D. A. 2024: An enigmatic large discoidal fossil from the Pennsylvanian of County Clare, Ireland. *Palaeoworld 33*, 105–118. https://doi.org/10.1016/j.palwor.2023.01.008

Musial, G., Reynaud, J.-Y., Gingras, M. K., Féniès, H., Labourdette, R. & Parize, O. 2012: Subsurface and outcrop characterization of large tidally influenced point bars of the Cretaceous McMurray Formation (Alberta, Canada). *Sedimentary Geology 279*, 156–172. https://doi.org/10.1016/j.sedgeo.2011.04.020

Muszer, J. 2020: First discovery of Mississippian trace fossils in the Świebodzice Unit from the Witoszów region (SW Poland). *Geological Quarterly 64*, 838–860. https://doi.org/10.7306/gq.1558

Myint, M. H. & Noda, H. 2000: First discovery of *Gylorithes* (spirally coiled burrow; trace fossil) from the Pleistocene Haneji Formation in the central part of Okinawa-jima, Okinawa prefecture, southwest Japan. *Annual Report of the Institute of Geoscience, University of Tsukuba 26*, 65–68.

Myrow, P. M. 1987: *Sedimentology and depositional history of the Chapel Island formation (late Precambrian to early Cambrian), southeast Newfoundland*. Unpublished Doctoral Dissertation, Memorial University of Newfoundland, St. John's, 511 pp.

Myrow, P. M. 1992a: Pot and gutter casts from the Chapel Island Formation, southeast Newfoundland. *Journal of Sedimentary Petrology 62*, 992–1007. https://doi.org/10.2110/jsr.62.992

Myrow, P. M. 1992b: Bypass-zone tempestite facies model and proximality trends for an ancient muddy shoreline and shelf. *Journal of Sedimentary Petrology 62*, 99–115. https://doi.org/10.1306/D426789D-2B26-11D7-8648000102C1865D

Myrow, P. M. 1994: Pot and gutter casts from the Chapel Island Formation, southeast Newfoundland–reply. *Journal of Sedimentary Research A64*, 708–709. https://doi.org/10.1306/D4267E92-2B26-11D7-8648000102C1865D

Myrow, P. M. & Coniglio, M. 1991: Origin and diagenesis of cryptobiontic *Frutexites* in the Chapel Island Formation (Vendian to early Cambrian) of southeast Newfoundland, Canada. *Palaios 6*, 572–585. https://doi.org/10.2307/3514920

Myrow, P. M. & Hiscott, R. N. 1991: Shallow-water gravity-flow deposits, Chapel Island Formation, southeast Newfoundland. *Sedimentology* 38, 935–959. https://doi.org/10.1111/j.1365-3091.1991.tb01880.x

Myrow, P. M. & Hiscott, R. N. 1993: Depositional history and sequence stratigraphy of the Precambrian-Cambrian boundary stratotype section, Chapel Island Formation, southeast Newfoundland. *Palaeogeography, Palaeoclimatology, Palaeoecology 104*, 13–35. https://doi.org/10.1016/0031-0182(93)90117-2

Myrow, P. M. & Landing, E. 1992: Mixed siliciclastic-carbonate deposition in an early Cambrian oxygen-stratified basin, Chapel Island Formation, southeastern Newfoundland. *Journal of Sedimentary Petrology 62*, 455–473. https://doi.org/10.1306/D4267924-2B26-11D7-8648000102C1865D

Myrow, P. M. & Southard, J. B. 1996: Tempestite deposition. *Journal of Sedimentary Research 66*, 875–887. https://doi.org/10.1306/D426842D-2B26-11D7-8648000102C1865D

Myrow, P. M., Fischer, W. & Goodge, J. W. 2002: Wave-modified turbidites: combined-flow shoreline and shelf deposits, Cambrian, Antarctica. *Journal of Sedimentary Research 72*, 641–656. https://doi.org/10.1306/022102720641

Myrow, P. M., Tice, L., Archuleta, B., Clark, B., Taylor, J. F. & Ripperdan, R. L. 2004: Flat-pebble conglomerate: its multiple origins and relationship to metre-scale depositional cycles. *Sedimentology 51*, 973–996. https://doi.org/10.1111/j.1365-3091.2004.00657.x

Myrow, P. M., Thompson, K. R., Hughes, N. C., Paulsen, T. S., Sell, B. K. & Parcha, S. K. 2006a: Cambrian stratigraphy and depositional history of the northern Indian Himalaya, Spiti Valley, north-central India. *Geological Society of America Bulletin 118*, 491–510. https://doi.org/10.1130/B25828.1

Myrow, P. M., Snell, K. E., Hughes, N. C., Paulsen, T. S., Heim, N. A. & Parcha, S. K. 2006b: Cambrian depositional history of the Zanskar Valley region of the Indian Himalaya: tectonic implications. *Journal of Sedimentary Research 76*, 364–381. https://doi.org/10.2110/jsr.2006.020

Nagovitsin, K. E., Rogov, V. I., Marusin, V. V., Karlova, G. A., Kolesnikov, A. V., Bykova, N. V. & Grazhdankin, D. V. 2015: Revised Neoproterozoic and Terreneuvian stratigraphy of the Lena-Anabar Basin and north-western slope of the Olenek Uplift, Siberian Platform. *Precambrian Research 270*, 226–245. https://doi.org/10.1016/j.precamres.2015.09.012

Nance, R. D., Murphy, J. B. & Keppie, J. D. 2002: A Cordilleran model for the evolution of Avalonia. *Tectonophysics 352*, 11–31. https://doi.org/10.1016/S0040-1951(02)00187-7

Nara, M. 1995: *Rosselia socialis*: a dwelling structure of a probable terebellid polychaete. *Lethaia 28*, 171–178. https://doi.org/10.1111/j.1502-3931.1995.tb01610.x

Nara, M. & Haga, M. 2007: The youngest record of trace fossil *Rosselia socialis*: occurrence in the Holocene shallow marine deposits of Japan. *Paleontological Research 11*, 21–27. https://doi.org/10.2517/1342-8144(2007)11[21:TYROTF]2.0.CO;2

Nara, M., Schlirf, M. & Uchman, A. 2004: Type locality of *Rosselia socialis* Dahmer, 1937 revisited: probable tidal flat deposits of the lower Devonian Taunus Quartzite in Rossel, west of Rudesheim Germany. *Fossils 72*, 1–2.

Narbonne, G. M. 1984: Trace fossils in upper Silurian tidal flat to basin slope carbonates of Arctic Canada. *Journal of Paleontology 58*, 398–415.

Narbonne, G. M. 2005: The Ediacara Biota: Neoproterozoic origin of animals and their ecosystems. *Annual Review of Earth and Planetary Sciences 33*, 421–442. https://doi.org/10.1146/annurev.earth.33.092203.122519

Narbonne, G. M. & Aitken, J. D. 1990: Ediacaran fossils from the Sekwi Brook Area, Mackenzie Mountains, northwestern Canada. *Palaeontology 33*, 945–980.

Narbonne, G. M. & Aitken, J. D. 1995: Neoproterozoic of the Mackenzie Mountains, northwestern Canada. *Precambrian Research 73*, 101–121. https://doi.org/10.1016/0301-9268(94)00073-Z

Narbonne, G. M. & Hofmann, H. J. 1987: Ediacaran biota of the Wernecke Mountains, Yukon, Canada. *Palaeontology 30*, 647–676.

Narbonne, G. M. & Myrow, P. 1988: Trace fossil biostratigraphy in the Precambrian–Cambrian boundary interval. *New York State Museum Bulletin 463*, 72–76.

Narbonne, G. M., Myrow, P. M., Landing, E. & Anderson, M. M. 1987: A candidate stratotype for the Precambrian–Cambrian boundary, Fortune Head, Burin Peninsula, southeastern Newfoundland. *Canadian Journal of Earth Sciences 24*, 1277–1293. https://doi.org/10.1139/e87-124

Narbonne, G. M., Myrow, P., Landing, E. & Anderson, M. M. 1991: A chondrophorine (medusoid hydrozoan) from the basal Cambrian (Placentian) of Newfoundland. *Journal of Paleontology 65*, 186–191. https://doi.org/10.1017/S0022336000020412

Nathorst, A. G. 1881: Om spår av några evertebrerade djur m.m. och deras paleontologiska betydelse. *Kongliga Svenska Vetenskaps-Akademiens Handlingar 18*, 1–59. https://doi.org/10.1080/11035898209455544

Nathorst, A. G. 1883: On the so-called "plant fossils" from the Silurian of central Wales. *Geological Magazine 10*, 33–34. https://doi.org/10.1017/S0016756800159710

Nathorst, A.-G. 1886: *Nouvelles Observations sur des Traces d'Animaux et autres Phénomènes d'origine purement Mécanique décrits comme « Algues Fossiles »*. P.A. Norstedt and Söner, Stockholm and Librairie F. Savy, Paris, 58 pp.

Nayak, K. K. 2000: Additional trace fossils from the Nimar Sandstone, Bagh Group, Jhabua District, Madhya Pradesh. *Bulletin Oil and Natural Gas Commission India 37*, 189–197.

Neef, G. 2004: Non-marine ?late Silurian-early Devonian trace fossils, Darling Basin, western New South Wales. *Alcheringa 28*, 389–399. https://doi.org/10.1080/03115510408619288

Nelson, L. L., Ramezani, J., Almond, J. E., Darroch, S. A. F., Taylor, W. L., Brenner, D. C., Furey, R.P., Turner, M. & Smith, E. F. 2022: Pushing the boundary: a calibrated Ediacaran-Cambrian stratigraphic record from the Nama Group in northwestern Republic of South Africa. *Earth and Planetary Science Letters 580*, 117396. https://doi.org/10.1016/j.epsl.2022.117396

Netto, R. G. 2007: *Skolithos*-dominated piperock in nonmarine environments: an example from the Triassic Caturrita Formation, southern Brazil. 109–121 *in* Bromley, R. G., Buatois, L. A. Mángano, G., Genise, J. F. & Melchor, R. N. (eds): *Sediment-Organism Interactions: A Multifaceted Ichnology*. SEPM Special Publication No. 88. https://doi.org/10.2110/pec.07.88.0107

Neto de Carvalho, C. 2008: Mais recente e mais profundo: *Treptichnus (Phycodes) pedum* (Seilacher) no Devónico inferior de Barrancos, Zona de Ossa Morena (Portugal). *Comunicaçoes Geológicas 95*, 167–171.

Netto, R. G., Balistieri, P. R. M. N., Lavina, E. C. L. & Silveira, D. M. 2009: Ichnological signatures of shallow freshwater lakes in the glacial Itararé group (Mafra Formation, upper Carboniferous–lower Permian of Paraná Basin, S Brazil). *Palaeogeography, Palaeoclimatology, Palaeoecology 272*, 240–255. https://doi.org/10.1016/j.palaeo.2008.10.028

Netto, R. G., Benner, J. S., Buatois, L. A., Uchman, A., Mángano, M. G., Ridge, J. C., Kazakauskas, V. & Gaigalas, A. 2012: Glacial environments. *Developments in Sedimentology 64*, 299–327. https://doi.org/10.1016/B978-0-444-53813-0.00011-3

Netto, R. G., Tognoli, F. M. W., Assine, M. L. & Nara, M. 2014: Crowded *Rosselia* ichnofabric in the early Devonian of Brazil: an example of strategic behavior. *Palaeogeography, Palaeoclimatology, Palaeoecology 395*, 107–113. https://doi.org/10.1016/j.palaeo.2013.12.032

Neto de Carvalho, C., Couto, H., Figueiredo, M. V. & Baucon, A. 2016a: Microbial-related biogenic structures from the middle Ordovician slates of Canelas (northern Portugal). *Comunicaçõe Geológicas 103*, 23–37.

Neto de Carvalho, C., Pereira, B., Klompmaker, A., Baucon, A., Moita, J. A., Pereira, P., Machado, S., Belo, J., Carvalho, J. & Mergulhão, L. 2016b: Running crabs, walking crinoids, grazing gastropods: behavioral diversity and evolutionary implications in the Cabeço da Ladeira lagerstätte (middle Jurassic, Portugal). *Comunicações Geológicas 103*, 39–54.

Nichols, G. 2009: *Sedimentology and Stratigraphy. Second Edition*. Wiley-Blackwell, Chichester, 419 pp.

Nicholson, H. A. 1873: Contributions to the study of the errant annelides of the older Palaeozoic rocks. *Proceedings of the Royal Society of London 21*, 288–290. https://doi.org/10.1098/rspl.1872.0061

Niebuhr, B. & Wilmsen, M. 2016: Ichnofossilien. *Geologica Saxonica 62*, 181–238.

Niedoroda, A. W., Swift, D. J. P., Hopkins, T. S. & Ma, C.-M. 1984: Shoreface morphodynamics on wave-dominated coasts. *Marine Geology 60*, 331–354. https://doi.org/10.1016/0025-3227(84)90156-7

Niedoroda, A. W., Swift, D. J. P. & Hopkins, T. S. 1985: The Shoreface. 533–624 *in* Davis Jr., R. A. (ed): *Coastal Sedimentary Environments*. Springer, New York. https://doi.org/10.1007/978-1-4612-5078-4_8

Nielsen, J. K., Hansen, K. S. & Simonsen, L. 1996: Sedimentology and ichnology of the Robbedale Formation (lower Cretaceous), Bornholm, Denmark. *Bulletin of the Geological Society of Denmark 43*, 115–131. https://doi.org/10.37570/bgsd-1996-43-12

Nio, S. D. & Yang, C. S. 1991: Diagnostic attributes of clastic tidal deposits: a review. 3–28 *in* Smith, D. G., Reinson, G. E., Zaitlin, B. A. & Rahmani, R. A. (eds): *Clastic Tidal Sedimentology*. Canadian Society of Petroleum Geologists, Memoir 16.

Niu, S. 1998: Confirmation of the genus *Grypania* (megascopic alga) in Gaoyuzhuang Formation (1434Ma) in Jixian (Tianjin) and its significance. *North China Geology 21*, 36–46. https://doi.org/10.3969/j.issn.1672-4135.1998.04.005

Noffke, N., Eriksson, K. A., Hazen, R. M. & Simpson, E. L. 2006: A new window into early Archean life: microbial mats in Earth's oldest siliciclastic tidal deposits (3.2 Ga Moodies Group, South Africa). *Geology 34*, 253–256. https://doi.org/10.1130/G22246.1

Noffke, N., Mángano, M. G. & Buatois, L. A. 2022: Biofilm harvesters in coastal settings of the early Palaeozoic. *Lethaia 55*, 1–18. https://doi.org/10.1111/let.12453

Novis, L. K., Jensen, S., Høyberget, M. & Högström, A. E. S. 2022: Trace fossils from the upper Member of the Duolbagáisá Formation (Cambrian Series 2-Miaolingian), northern Norway, with the first diverse Cambrian record of *Halimedides*. *Norwegian Journal of Geology 102*, 1–18. https://doi.org/10.17850/njg102-4-1

Nowlan, G. S., Narbonne, G. M. & Fritz, W. H. 1985: Small shelly fossils and trace fossils near the Precambrian-Cambrian boundary in the Yukon Territory, Canada. *Lethaia 18*, 233–256. https://doi.org/10.1111/j.1502-3931.1985.tb00701.x

O'Brien, S. J. 1979: *Volcanic stratigraphy, petrology and geochemistry of the Marystown Group; Burin Peninsula, Newfoundland*. Unpublished Doctoral Dissertation, Memorial University of Newfoundland, St John's, 261 pp.

O'Brien, S .J. F., Strong, D. F., Taylor, S. W. & Wilton, D. H. 1976: *Geology of the Marystown - St Lawrence area*. Newfoundland Department of Mines and Energy.

O'Brien, S. J., Strong, P. G. & Evans, J. L. 1977: *Geology of the Grand Bank (1M/4) and Lamaline (1L/13) map areas*. Newfoundland Department of Mines and Energy.

O'Brien, S. J., O'Driscoll, C. F., Greene, B. A. & Tucker, R. D. 1995: Pre-Carboniferous geology of the Connaigre Peninsula and the adjacent coast of Fortune Bay, southern Newfoundland. *Current Research, Newfoundland Department of Natural Resources, Geological Survey Report 95-1*, 267–297.

O'Brien, S. J., O'Brien, B. H., Dunning, G. R. & Tucker, R. D. 1996: Late Neoproterozoic Avalonian and related peri-Gondwanan rocks of the Newfoundland Appalachians. 9–28 *in* Nance, R .D. & Thompson, M. D. (eds): *Avalonian and Related Peri-Gondwanan Terranes of the Circum–North Atlantic*. Geological Society of America Special Paper 304, Boulder, Colorado. https://doi.org/10.1130/0-8137-2304-3.9

O'Brien, S. J., Dubé, B. & O'Driscoll, C. F. 1999: High-sulphidation, epithermal-style hydrothermal systems in late Neoproterozoic Avalonian rocks on the Burin Peninsula, Newfoundland: implications for gold exploration. *Current Research, Newfoundland and Labrador Department of Natural Resources, Geological Survey 99-1*, 275–296.

O'Driscoll, C. F., Dean, M. T., Wilton, D. H. C. & Hinchley, J. G. 2001: The Burin Group: a late Neoproterozoic ophiolite containing shear-zone hosted mesothermal-style gold mineralization in the Avalon Zone. *Current Research, Newfoundland Department of Mines and Energy, Geological Survey 2001-1*, 229–246.

Oji, T., Dornbos, S. Q., Yada, K., Hasegawa, H., Gonchigdorj, S., Mochizuki, T., Takayanagi, H. & Iryu, Y. 2018: Penetrative trace fossils from the late Ediacaran of Mongolia: early onset of the Agronomic Revolution. *Royal Society Open Science 5*, 172250. https://doi.org/10.1098/rsos.172250

Oligmueller, A. R. & Hasiotis, S. T. 2024: An ichnotaxonomic assessment of the Cretaceous Dakota Group, Front Range, Colorado, USA, and its comparison to other Western Interior Seaway deposits. *Paleontological Contributions 23*, 1–87. https://doi.org/10.17161/pc.vi23.22542

Oliver, J., Hammerstrom, K., McPhee-Shaw, E., Slattery, P., Oakden, J., Kim, S. & Hartwell, S. I. 2011: High species density patterns in macrofaunal invertebrate communities in the marine benthos. *Marine Ecology 32*, 278–288. https://doi.org/10.1111/j.1439-0485.2011.00461.x

Olivero, E. B. & López Cabrera, M. I. 2023: *Helminthopsis* and *Cylindrichnus* ichnoguilds from Miocene thin-bedded turbidites, Tierra del Fuego, Argentina. *Palaios 38*, 371–393. https://doi.org/10.2110/palo.2022.058

Olivero, E. B., Buatois, L. A. & Scasso, R. A. 2004: *Paradictyodora antarctica*: a new complex vertical spreite trace fossil from the upper Cretaceous-Paleogene of Antarctica and Tierra del Fuego, Argentina. *Journal of Paleontology 78*, 783–789. https://doi.org/10.1666/0022-3360(2004)078<0783:PAANCV>2.0.CO;2

Olivero, E. B., Lopez Cabrera, M. I., Ercolano, B., Pittaluga, S. & Lizarralde, Z. 2012: Caught in fraganti: actual and Holocene, crowded *Rosselia*-like mud-lined tubes produced by spionid polychaetes. *Ameghiniana 49*, R152.

Olszewski, T. 1996: Sequence stratigraphy of an upper Pennsylvanian, midcontinent cyclothem from North America (Iola Limestone, Kansas and Missouri, USA). *Facies 35*, 81–103. https://doi.org/10.1007/BF02536958

Omori, M., Ishida, Y. & Adachi, H. 1992: On the *Gyrolithes chosiensis* n. sp. from the Kimigahama Formation (lower Cretaceous) in the district of Chosi City, Chiba Prefecture, Japan. *Journal of the Faculty of General Education, Azubu University 25*, 113–119.

Öpik, A. 1929: Studien über das Estnische Unterkambrium (Estonium) I-IV. *Acta et Commentationes Universitatis Tartuensis (Dorpatensis) 15*, 1–56.

Orłowski, S. 1968: Kambr antykliny łysogórskiej Gór Świętokrzyskich. *Biuletyn Geologiczny 10*, 153–219.

Orłowski, S. 1989: Trace fossils in the lower Cambrian sequence in the Świętokrzyskie Mountains, central Poland. *Acta Palaeontologica Polonica 34*, 211–231.

Orłowski, S. 1992: Trilobite trace fossils and their stratigraphical significance in the Cambrian sequence of the Holy Cross Mountains, Poland. *Geological Journal 27*, 15–34. https://doi.org/10.1002/gj.3350270104

Orłowski, S. & Żylińska, A. 1996: Non-arthropod burrows from the middle and late Cambrian of the Holy Cross Mountains, Poland. *Acta Palaeontologica Polonica 41*, 385–409.

Orłowski, S. & Żylińska, A. 2002: Lower Cambrian trace fossils from the Holy Cross Mountains, Poland. *Geological Quarterly 46*, 135–146.

Ornia, M., Buatois, L. A., Mángano, M. G., Thue, K., Fernández-Martínez, J. & Marcos, A. 2024: Trazas fósiles marinas someras de la Formación Furada, Silúrico-Devónico de Asturias, España. *Spanish Journal of Palaeontology 39*, 163–194. https://doi.org/10.7203/sjp.29180

Orr, P. J. & Pickerill, R. K. 1995: Trace fossils from early Silurian flysch of the Waterville Formation, Maine, USA. *Northeastern Geology and Environmental Sciences 17*, 394–414.

Ortolam, D. 1967: Fossile Böden als Leithorizonte für die Gliederung des Höheren Buntsandsteins im nördlichen Schwarzwald und südlichen Odenwald. *Geologisches Jahrbuch der BGR 84*, 485–590.

Osgood Jr., R. G. 1970: Trace fossils of the Cincinnati area. *Palaeontographica Americana 41*, 281–444.

Osgood Jr., R. G. 1975: The paleontological significance of trace fossils. 87–108 *in* Frey, R. W. (ed): *The Study of Trace Fossils. A Synthesis of Principles, Problems, and Procedures in Ichnology*. Springer-Verlag, Berlin. https://doi.org/10.1007/978-3-642-65923-2_6

Owen, R. 1852: Description of the impressions and foot-prints of the Protichnites from the Postdam Sandstone of Canada. *Quarterly Journal of the Geological Society 8*, 214–225.

Pace, A., Bourillot, R., Bouton, A., Vennin, E., Braissant, O., Dupraz, C., Duteil, T., Bundeleva, I., Patrier, P., Galaup, S., Yokoyama, Y., Franceschi, M., Virgone, A. & Visscher, P. T. 2018: Formation of stromatolite lamina at the interface of oxygenic–anoxygenic photosynthesis. *Geobiology 16*, 378–398. https://doi.org/10.1111/gbi.12281

Pacześna, J. 1985: Skamieniałości śladowe górnego wendu i dolnego kambru południowej Lubelszczyzny. *Geological Quarterly 29*, 255–270.

Pacześna, J. 1986: Upper Vendian and lower Cambrian ichnocoenoses of Lublin region. *Biuletyn Instytutu Geologicznego 355*, 31–47.

Pacześna, J. 1996: The Vendian and Cambrian ichnocoenoses from the Polish part of the east-European platform. *Prace Pañstwowego Instytutu Geologicznego 152*, 1–77.

Pacześna, J. 2010: Ichnological record of the activity of Anthozoa in the early Cambrian succession of the upper Silesian Block (southern Poland). *Acta Geologica Polonica 60*, 93–103.

Palacios Medrano, T. 1989: Microfósiles de pared orgánica del Proterozoico superior (región central de la Península Ibérica). *Memorias del Museo Paleontologico de la Universidad de Zaragoza 3*, 1–91.

Palacios, T., Jensen, S., Barr, S. M., White, C. E. & Myrow, P. M. 2018: Organic-walled microfossils from the Ediacaran–Cambrian boundary stratotype section, Chapel Island and Random formations, Burin Peninsula, Newfoundland, Canada: global correlation and significance for the evolution of early complex ecosystems. *Geological Journal 53*, 1728–1742. https://doi.org/10.1002/gj.2998

Palij, V. M. 1974: Double traces (bilobites) in the deposits of the Baltic Series in the Dniester area. *Academy of Sciences of the Ukranian Socialist Republic, Series B 1*, 499–503.

Palij, V. M. 1976: Ostatki besskeletnoj fauny i sledy zhiznedeyatel'nosti iz otlozhenij verkhnego dokembriya i nizhnego kembriya Podolii. 63–77 *in*: *Paleontologiya i Stratigrafiya Verkhnego Dokembriya i Nizhnego Paleozoya Jugo-Zapadna Vostochno-Evropejskoj Platformy*. Naukova Dumka, Kiev.

Palij, V. M., Posti, E. & Fedonkin, M. A. 1979: Soft-bodied metazoa and trace fossils of Vendian and lower Cambrian. 49–82 *in* Keller, B. M. & Rozanov, A. Y. (eds): *Upper Precambrian and Cambrian palaeontology of east European platform*. Academy of Sciences, Moscow.

Palij, V. M., Posti, E. & Fedonkin, M. A. 1983: Soft-bodied metazoa and trace fossils of Vendian and early Cambrian. 56–94 *in* Urbanek, A. & Rozanov, A. Y. (eds): *Upper Precambrian and Cambrian palaeontology of east-European platform*. Publishing House Wydawnictwa Geologiczne, Warszawa.

Palma-Ramírez, A., Maldonado-Sarabia, R. C. & Stimson, M. R. 2019: Marginal marine trace fossils from the Cárdenas Formation (Maastrichtian), Rayón municipality, San Luis Potosí, Central Mexico. *Revista Brasileira de Paleontologia 22*, 89–96. https://doi.org/10.4072/rbp.2019.2.01

Pandey, D. K., Uchman, A., Kumar, V. & Shekhawat, R. S. 2014: Cambrian trace fossils of the *Cruziana* ichnofacies from the Bikaner-Nagaur Basin, north western Indian Craton. *Journal of Asian Earth Sciences 81*, 129–141. https://doi.org/10.1016/j.jseaes.2013.11.017

Parcha, S. K. & Singh, B. P. 2010: Stratigraphic significance of the Cambrian ichnofauna of the Zanskar region, Ladakh Himalaya, India. *Journal Geological Society of India 75*, 503–517. https://doi.org/10.1007/s12594-010-0040-x

Park, S.-C., Lee, H.-H., Han, H.-S., Lee, G.-H., Kim, D.-C. & Yoo, D.-G. 2000: Evolution of late Quaternary mud deposits and recent sediment budget in the southeastern Yellow Sea. *Marine Geology 170*, 271–288. https://doi.org/10.1016/S0025-3227(00)00099-2

Parkhaev, P. Y. & Karlova, G. A. 2011: Taxonomic revision and evolution of Cambrian mollusks of the genus *Aldanella* Vostokova, 1962 (Gastropoda: Archaeobranchia). *Paleontological Journal 45*, 1145–1205. https://doi.org/10.1134/S0031030111100030

Parry, L. A., Boggiani, P. C., Condon, D. J., Garwood, R. J., Leme, J. D. M., McIlroy, D., Brasier, M. D., Trindade, R., Campanha, G. A. C., Pacheco, M. L. A. F., Diniz, C. Q. C. & Liu, A. G. 2017: Ichnological evidence for meiofaunal bilaterians from the terminal Ediacaran and earliest Cambrian of Brazil. *Nature Ecology and Evolution 1*, 1455–1464. https://doi.org/10.1038/s41559-017-0301-9

Pattison, S. A. J. 2005: Storm-influenced prodelta turbidite complex in the lower Kenilworth Member at Hatch Mesa, Book Cliffs, Utah, USA: implications for shallow marine facies models. *Journal of Sedimentary Research 75*, 420–439. https://doi.org/10.2110/jsr.2005.033

Pattison, S. A. & Hoffman, T. A. 2008: Sedimentology, architecture, and origin of shelf turbidite bodies in the upper Cretaceous Kenilworth Member, Book Cliffs, Utah, USA. *SEPM Special Publication 90*, 391–420. https://doi.org/10.2110/pec.08.90.0391

Pattison, S. A., Ainsworth, R. B. & Hoffman, T. A. 2007: Evidence of across-shelf transport of fine-grained sediments: turbidite-filled shelf channels in the Campanian Aberdeen Member, Book Cliffs, Utah, USA. *Sedimentology 54*, 1033–1064. https://doi.org/10.1111/j.1365-3091.2007.00871.x

Paz, M., Ponce, J. J., Buatois, L. A., Mángano, M. G., Carmona, N. B., Pereira, E. & Desjardins, P. R. 2019: Bottomset and foreset sedimentary processes in the mixed carbonate-siliciclastic upper Jurassic-lower Cretaceous Vaca Muerta Formation, Picún Leufú Area, Argentina. *Sedimentary Geology 389*, 161–185. https://doi.org/10.1016/j.sedgeo.2019.06.007

Paz, M., Mángano, M. G., Buatois, L. A., Desjardins, P. R., Notta, R., Tomassini, F. G. & Carmona, N. B. 2022: Ichnology of muddy shallow-water contourites from the upper Jurassic–lower Cretaceous Vaca Muerta Formation, Argentina: implications for trace-fossil models. *Palaios 37*, 201–218. https://doi.org/10.2110/palo.2020.028

Pazos, P. J. & Gutiérrez, C. 2022: All post-Cambrian ichnospecies of *Psammichnites* Torell, 1870 belong to *Olivellites* Fenton and Fenton, 1937a. *Geological Society, London, Special Publications 522*, SP522-2021. https://doi.org/10.1144/SP522-2021-102

Pazos, P. J., Di Pasquo, M. & Amenabar, C. R. 2007: Trace fossils of the glacial to postglacial transition in the El Imperial Formation (upper Carboniferous), San Rafael basin, Argentina. 137–147 *in* Bromley, R. G., Buatois, L. A. Mángano, G., Genise, J. F. & Melchor, R .N. (eds): *Sediment-Organism Interactions: A Multifaceted Ichnology*. SEPM Special Publication No. 88. https://doi.org/10.2110/pec.07.88.0137

Peakall, J., Best, J., Baas, J. H., Hodgson, D. M., Clare, M. A., Talling, P. J., Dorrell, R. M. & Lee, D. R. 2020: An integrated process-based model of flutes and tool marks in deep-water environments: implications for palaeohydraulics, the Bouma sequence and hybrid event beds. *Sedimentology 67*, 1601–1666. https://doi.org/10.1111/sed.12727

Pearson, T. H. & Rosenberg, R. 1978: Macrobenthic succession in relation to organic enrichment and pollution of the marine environment. *Oceanography and Marine Biology Annual Review 16*, 229–311.

Pedernera, T. E., Ottone, E. G., Mancuso, A. C., Erra, G., Larriestra, F., Benavente, C. A., Pineda Alvarez, J. A., Campos, C., Bustos Escalona, E. L., Krapovickas, V. & Marsicano, C. A. 2021: Multiproxy analyses of the Triassic Agua de la Zorra Formation, Cuyana Basin, Argentina: palynofacies, geochemistry, and biotic record. *Journal of South American Earth Sciences 110*, 103374. https://doi.org/10.1016/j.jsames.2021.103374

Pemberton, S. G. & Frey, R. W. 1982: Trace fossil nomenclature and the *Planolites-Palaeophycus* dilemma. *Journal of Paleontology 56*, 843–881.

Pemberton, S. G. & Frey, R. W. 1984: Ichnology of storm-influenced shallow marine sequence: Cardium Formation (upper Cretaceous) at Seebe, Alberta. 281–304 *in* Stott, D. F. & Glass, D. J. (eds): *The Mesozoic of Middle North America*. Canadian Society of Petroleum Geologists, Memoir 9.

Pemberton, S. G. & Frey, R. W. 1985: The *Glossifungites* ichnofacies: modern examples from the Georgia coast, USA. 237–259 *in* Curran, H. A. (ed): *Biogenic structures: their use in interpreting depositional environments*. SEPM Special Publication, Vol. 35. https://doi.org/10.2110/pec.85.35.0237

Pemberton, S. G. & Frey, R. W. 1991: History of ichnology: J.W. Dawson and the interpretation of *Rusophycus*. *Ichnos 1*, 237–242. https://doi.org/10.1080/10420949109386356

Pemberton, S. G. & Magwood, J. P. 1990: A unique occurrence of *Bergaueria* in the lower Cambrian Gog Group near Lake Louise, Alberta. *Journal of Paleontology 64*, 436–440. https://doi.org/10.1017/S0022336000018667

Pemberton, S. G., Frey, R. W. & Bromley, R. G. 1988: The ichnotaxonomy of *Conostichus* and other plug-shaped ichnofossils. *Canadian Journal of Earth Sciences 25*, 866–892. https://doi.org/10.1139/e88-085

Pemberton, S. G., Van Wagoner, J. C. & Wach, G. D. 1992: Ichnofacies of a wave-dominated shoreline. 339–382 *in* Pemberton, S. G. (ed): *Applications of ichnology to petroleum exploration: A core workshop*. Society for Sedimentary Geology Core Workshop, Vol. 17. https://doi.org/10.2110/cor.92.01.0339

Pemberton, S. G., Spila, M., Pulham, A. J., Saunders, T., MacEachern, J. A., Robbins, D. & Sinclair, I. K. 2001: *Ichnology and Sedimentology of Shallow to Marginal Marine Systems*. Ben Nevis and Avalon Reservoirs, Jeanne d'Arc Basin, Geology Association of Canada Short Course Notes 15, 343 pp.

Peng, S. C. & Babcock, L. E. 2011: Continuing progress on chronostratigraphic subdivision of the Cambrian System. *Bulletin of Geosciences 86*, 391–396. https://doi.org/10.3140/bull.geosci.1273

Peng, S. C., Babcock, L. E. & Ahlberg, P. 2020: The Cambrian Period. 565–629 *in* Gradstein, F. M., Ogg, J. G., Schmitz, M. D. & Ogg, G. M. (eds): *Geologic Time Scale 2020*. Elsevier. https://doi.org/10.1016/B978-0-12-824360-2.00019-X

Peng, S. C., Babcock, L. E. & Cooper, R. A. 2012: The Cambrian Period. 437–488 *in* Gradstein, F.M., Ogg, J.G., Schmitz, M. & Ogg, G. (eds): *The Geologic Time Scale 2012*. Elsevier. https://doi.org/10.1016/B978-0-444-59425-9.00019-6

Pervesler, P. 2002: Crustaceenbauten aus dem Karpatium (Untermiozän) des Korneuburger Beckens (Niederösterreich). *Beiträge zur Paläontologie 27*, 333–337.

Pervesler, P., Uchman, A. & Hohenegger, J. 2008: New methods for ichnofabric analysis and correlation with orbital cycles exemplified by the Baden-Sooss section (middle Miocene, Vienna Basin). *Geologica Carpathica 59*, 395–409.

Peryt, T. M. 1981: Phanerozoic oncoids—an overview. *Facies 4*, 197–213. https://doi.org/10.1007/BF02536588

Pflüger, F. 1999: Matground structures and redox facies. *Palaios 14*, 25–39. https://doi.org/10.2307/3515359

Pickens, P. E. 1988: Systems that control the burrowing behaviour of a sea anemone. *Journal of experimental Biology 135*, 133–164. https://doi.org/10.1242/jeb.135.1.133

Pickerill, R. K. 1977: Trace fossils from the upper Ordovician (Caradoc) of the Berwyn Hills, central Wales. *Geological Journal 12*, 1–16. https://doi.org/10.1002/gj.3350120101

Pickerill, R. K. 1981: Trace fossils in a lower Palaeozoic submarine canyon sequence—the Siegas Formation of northwestern New Brunswick, Canada. *Atlantic Geology 17*, 37–58. https://doi.org/10.4138/1374

Pickerill, R. 1989: *Bergaueria perata* Prantl, 1945 from the Silurian of Cape George, Nova Scotia. *Atlantic Geology 25*, 191–197. https://doi.org/10.4138/1683

Pickerill, R. K. 1992: Carboniferous nonmarine invertebrate ichnocoenoses from southern New Brunswick, eastern Canada. *Ichnos 2*, 21–35. https://doi.org/10.1080/10420949209380072

Pickerill, R. K. 1995: Deep-water marine *Rusophycus* and *Cruziana* from the Ordovician Lotbiniere Formation of Quebec. *Atlantic Geology 31*, 103–108. https://doi.org/10.4138/2102

Pickerill, R. K. & Blissett, D. 1999: A predatory *Rusophycus* burrow from the Cambrian of southern New Brunswick, eastern Canada. *Atlantic Geology 35*, 179–185. https://doi.org/10.4138/2031

Pickerill, R. K. & Fillion, D. 1983: On the Tremadoc-Arenig and lower-upper Tremadoc boundries in the Bell Island Group, Conception Bay, eastern Newfoundland. *Maritime Sediments and Atlantic Geology 19*, 21–30. https://doi.org/10.4138/1561

Pickerill, R. K. & Forbes, W. H. 1979: Ichnology of the Trenton Group in the Quebec City area. *Canadian Journal of Earth Sciences 16*, 2022–2039. https://doi.org/10.1139/e79-188

Pickerill, R. & Fyffe, L. 1999: The stratigraphic significance of trace fossils from the lower Paleozoic Baskahegan Lake Formation near Woodstock, west-central New Brunswick. *Atlantic Geology 35*, 215–224. https://doi.org/10.4138/2035

Pickerill, R. K. & Keppie, J. D. 1981: Observations on the ichnology of the Meguma Group (? Cambro-Ordovician) of Nova Scotia. *Maritime Sediments and Atlantic Geology 17*, 130–138. https://doi.org/10.4138/1381

Pickerill, R. K. & Narbonne, G. M. 1995: Composite and compound ichnotaxa: a case example from the Ordovician of Quebec, eastern Canada. *Ichnos 4*, 53–69. https://doi.org/10.1080/10420949509380114

Pickerill, R. K. & Peel, J. S. 1990: Trace fossils from the lower Cambrian Bastion Formation of north-east Greenland. *Rapport Grønlands Geologiske Undersøgelse 147*, 5–43. https://doi.org/10.34194/rapggu.v147.8105

Pickerill, R. K. & Peel, J. S. 1991: *Gordia nodosa* isp. nov. and other trace fossils from the Cass Fjord Formation (Cambrian) of north Greenland. *Rapport Grønlands Geologiske Undersøgelse 150*, 15–28. https://doi.org/10.34194/rapggu.v150.8136

Pickerill, R. K., Fillion, D. & Harland, T. L. 1984a: Middle Ordovician trace fossils in carbonates of the Trenton Group between Montreal and Quebec City, St. Lawrence Lowland, eastern Canada. *Journal of Paleontology 58*, 416–439.

Pickerill, R. K., Romano, M. & Meléndez, B. 1984b: Arenig trace fossils from the Salamanca area, western Spain. *Geological Journal 19*, 249–269. https://doi.org/10.1002/gj.3350190305

Pickerill, R. K., Fyffe, L. R. & Forbes, W. H. 1987: Late Ordovician-early Silurian trace fossils from the Matapedia Group, Tobique River, western New Brunswick. *Atlantic Geology 23*, 77–88. https://doi.org/10.4138/1623

Pickerill, R. K., Fyffe, L. R. & Forbes, W. H. 1988: Late Ordovician-early Silurian trace fossils from the Matapedia Group, Tobique River, western New Brunswick, Canada. II. Additional discoveries with descriptions and comments. *Atlantic Geology 24*, 139–148. https://doi.org/10.4138/1646

Pickerill, R. K., Donovan, S. K., Dixon, H. L. & Doyle, E. N. 1993: *Bichordites monastiriensis* from the Pleistocene of southeast Jamaica. *Ichnos 2*, 225–230. https://doi.org/10.1080/10420949309380096

Pictet, F.-J. 1854: *Traité de Paléontologie ou Histoire Naturelle des Animaux Fossiles considérés dans leurs rapports Zoologiques et Géologiques. Seconde édition, tome deuxième*. J.-B. Baillière, Paris, 727 pp.

Plaziat, J.-C. & Mahmoudi, M. 1988: Trace fossils attributed to burrowing echinoids: a revision including new ichnogenus and ichnospecies. *Geobios 21*, 209–233. https://doi.org/10.1016/S0016-6995(88)80019-6

Plička, M. 1974: *Saerichnites beskidiensis* n. sp., a new trace fossil from the Carpathian Flysch of Czechoslovakia. *Vestník Ústredního ústavu geologického 49*, 75–82.

Plint, A. G. 1983: Liquefaction, fluidization and erosional structures associated with bituminous sands of the Bracklesham Formation (middle Eocene) of Dorset, England. *Sedimentology 30*, 525–535. https://doi.org/10.1111/j.1365-3091.1983.tb00690.x

Plint, A. G. 2010: Wave- and storm-dominated shoreline and shallow-marine systems. 167–200 *in* James, N. P. & Dalrymple, R. W. (eds): *Facies models 4*. The Geological Association of Canada, St John's.

Plint, A. G. 2014: Mud dispersal across a Cretaceous prodelta: storm-generated, wave-enhanced sediment gravity flows inferred from mudstone microtexture and microfacies. *Sedimentology 61*, 609–647. https://doi.org/10.1111/sed.12068

Plummer, P. S. & Gostin, V. A. 1981: Shrinkage cracks: desiccation or synaeresis? *Journal of Sedimentary Petrology 51*, 1147–1156. https://doi.org/10.1306/212F7E4B-2B24-11D7-8648000102C1865D

Poiré, D. G., del Valle, A. & Regalía, G. M. 1984: Trazas fósiles en cuarcitas de la Formación Sierras Bayas (Precámbrico) y su comparación con las de la Formación Balcarce (Cambro-Ordovícico), Sierras Septentrionales de la provincia de Buenos Aires. *Noveno Congreso Geológico Argentino, S.C. de Bariloche, Actas 4*, 249–266.

Pokorný, R., Krmíček, L. & Sudo, M. 2017: An endemic ichnoassemblage from a late Miocene paleolake in SE Iceland. *Palaeogeography, Palaeoclimatology, Palaeoecology 485*, 761–773. https://doi.org/10.1016/j.palaeo.2017.07.033

Pollard, J. E. 1981: A comparison between the Triassic trace fossils of Cheshire and south Germany. *Palaeontology 24*, 555–588.

Pollard, J. E. 1985: Evidence from trace fossils. *Philosophical Transactions of the Royal Society of London B 309*, 241–242. https://doi.org/10.1098/rstb.1985.0084

Pollard, J. E. & Walker, E. F. 1984: Reassessment of sediments and trace fossils from Old Red Sandstone (lower Devonian) of Dunure, Scotland, described by John Smith (1909). *Geobios 17*, 567–581. https://doi.org/10.1016/S0016-6995(84)80029-7

Pollock, J. C., Hibbard, J. P. & Sylvester, P. J. 2009: Early Ordovician rifting of Avalonia and birth of the Rheic Ocean: U–Pb detrital zircon constraints from Newfoundland. *Journal of the Geological Society, London 166*, 501–515. https://doi.org/10.1144/0016-76492008-088

Porada, H. & Bouougri, E. 2008: Neoproterozoic trace fossils vs. microbial mat structures: examples from the Tandilia Belt of Argentina. *Gondwana Research 13*, 480–487. https://doi.org/10.1016/j.gr.2007.05.007

Porada, H., Ghergut, J. & Bouougri, E. H. 2008: Kinneyia-type wrinkle structures—critical review and model of formation. *Palaios 23*, 65–77. https://doi.org/10.2110/palo.2006.p06-095r

Poschmann, M. 2015: The corkscrew-shaped trace fossil *Helicodromites* Berger, 1957, from Rhenish lower Devonian shallow-marine facies (upper Emsian; SW Germany). *Paläontologische Zeitschrift 89*, 635–643. https://doi.org/10.1007/s12542-014-0232-6

Poschmann, M. J., Knaust, D. & Schindler, T. 2023: New records of *Ctenopholeus* in the early Devonian Hunsrück Slate of Bundenbach, SW Germany. *Ichnos 30*, 150–156. https://doi.org/10.1080/10420940.2023.2258264

Potter, D. B. 1949: *Geology of the Fortune – Grand Bank area, Burin Peninsula, Newfoundland, Canada*. Unpublished Master Dissertation, Brown University, 48 pp.

Poulsen, C. 1967: Fossils from the lower Cambrian of Bornholm. *Det Kongelige Danske Videnskabernes Selskab, Matematisk-fysiske Meddelelser 36*, 1–48.

Powell, E. N. 1977: The relationship of the trace fossil *Gyrolithes* (= *Xenohelix*) to the family Capitellidae (Polychaeta). *Journal of Paleontology 51*, 552–556.

Prantl, F. 1945: Two new problematic trails from the Ordovician of Bohemia. *Académie Tchèque des Sciences, Bulletin International, Classe des Sciences Mathématiques Naturelles et de la Médecine 46*, 49–59.

Pratt, B. R. 1979: Early cementation and lithification in intertidal cryptalgal structures, Boca Jewfish, Bonaire, Netherlands Antilles. *Journal of Sedimentary Petrology 49*, 379–386. https://doi.org/10.1306/212F774D-2B24-11D7-8648000102C1865D

Pratt, B. R. 2002: Tepees in peritidal carbonates: origin via earthquake-induced deformation, with example from the middle

Cambrian of western Canada. *Sedimentary Geology 153*, 57–64. https://doi.org/10.1016/S0037-0738(02)00318-4

Pratt, B. R. 2010: Peritidal carbonates. 401–420 *in* James, N. P. & Dalrymple, R. W. (eds): *Facies models 4*. The Geological Association of Canada, St John's.

Pu, J. P., Bowring, S. A., Ramezani, J., Myrow, P., Raub, T. D., Landing, E., Mills, A., Hodgin, E. & Macdonald, F. A. 2016: Dodging snowballs: geochronology of the Gaskiers glaciation and the first appearance of the Ediacaran biota. *Geology 44*, 955–958. https://doi.org/10.1130/G38284.1

Qian, Y., Zhu, M.-Y., Li, G.-X., Jiang, Z.-W. & Van Iten, H. 2002: A supplemental Precambrian-Cambrian boundary global stratotype section in SW China. *Acta Palaeontologica Sinica 41*, 19–26.

Quiroz, L. I., Buatois, L. A., Mángano, M. G., Jaramillo, C. A. & Santiago, N. 2010: Is the trace fossil *Macaronichnus* an indicator of temperate to cold waters? Exploring the paradox of its occurrence in tropical coasts. *Geology 38*, 651–654. https://doi.org/10.1130/G30140.1

Rabu, D., Chauvel, J.-J., Alsac, C., Dabard, M.-P., Fletcher, T. P., Guerrot, C., Pillola, G. L., Tegyey, M. & Thieblemont, D. 1994: Le Protérozoïque terminal et la Paléozoïque de l'archipel de Saint-Pierre-et-Miquelon. *Géologie de la France 1*, 3–51.

Rabu, D., Chauvel, J.-J., Dabard, M.-P., Fletcher, T. P. & Pillola, G. L. 1993: Présence de Tommotien (Cambrien inférieur) à Saint-Pierre et Miquelon. *Comptes rendus de l'Académie des sciences, Série II, Mécanique, Physique, Chimie, Sciences de l'univers, Sciences de la Terre 317*, 379–386.

Radwański, A. & Roniewicz, P. 1963: Upper Cambrian trilobite ichnocoenosis from Wielka Wisniowka (Holy Cross Mountains, Poland). *Acta Palaeontologica Polonica 8*, 259–280.

Radwański, A. & Roniewicz, P. 1972: A long trilobite-trackway, *Cruziana semiplicata* Salter, from the upper Cambrian of the Holy Cross Mts. *Acta Geologica Polonica 22*, 439–448.

Rajkonwar, C., Tiwari, R. P. & Patel, S. J. 2013: *Arenicolites helixus* isp nov and associated ichnofossils from the Bhuban Formation, Surma Group (lower-middle Miocene) of Aizawl, Mizoram, India. *Himalayan Geology 34*, 18–37.

Rajkumar, H. S., Khaidem, K. S., Soibam, I. & Sanasam, S. 2012: Palaeoenvironment of the middle Bhuban, Surma Group of Mizoram, India: an ichnological approach. *Journal Indian Association of Sedimentologists 31*, 65–79.

Ranger, M. J. & Pemberton, S. G. 1988: Marine influence on the McMurray Formation in the Primerose area, Alberta. 439–450 *in* James, D. P. & Leckie, D. A. (eds): *Sequences, Stratigraphy, Sedimentology: Surface and Subsurface*. Canadian Society of Petroleum Geologists, Memoir 15.

Rasmussen, B. & Muhling, J. R. 2019: Syn-tectonic hematite growth in Paleoproterozoic Stirling Range "red beds", Albany-Fraser Orogen, Australia: evidence for oxidation during late-stage orogenic uplift. *Precambrian Research 321*, 54–63. https://doi.org/10.1016/j.precamres.2018.12.002

Ratcliffe, B. C. & Fagerstrom, J. A. 1980: Invertebrate lebensspuren of Holocene floodplains: their morphology, origin and paleoecological significance. *Journal of Paleontology 54*, 614–630.

Raup, D. M. & Seilacher, A. 1969: Fossil foraging behavior: computer simulation. *Science 166*, 994–995. https://doi.org/10.1126/science.166.3908.994

Raychaudhuri, I. & Pemberton, S. G. 1992: Ichnologic and sedimentologic characteristics of open marine to storm dominated restricted marine settings within the Viking/Bow Island formations, south-central Alberta. 119–139 *in* Pemberton, S. G. (ed): *Applications of ichnology to petroleum exploration: A core workshop*. Society for Sedimentary Geology Core Workshop, Vol. 17. https://doi.org/10.2110/cor.92.01.0119

Reif, D. M. & Slatt, R. M. 1979: Red bed members of the lower Triassic Moenkopi Formation, southern Nevada: sedimentology and paleogeography of a muddy tidal flat deposit. *Journal of Sedimentary Petrology 49*, 869–889. https://doi.org/10.1306/212F7865-2B24-11D7-8648000102C1865D

Reineck, H. E. & Singh, I. B. 1972: Genesis of laminated sand and graded rhythmites in storm-sand layers of shelf mud. *Sedimentology 18*, 123–128. https://doi.org/10.1111/j.1365-3091.1972.tb00007.x

Reineck, H.-E. & Wunderlich, F. 1968: Classification and origin of flaser and lenticular bedding. *Sedimentology 11*, 99–104. https://doi.org/10.1111/j.1365-3091.1968.tb00843.x

Reise, K. 1985: *Tidal Flat Ecology. An Experimental Approach to Species Interactions*. Springer-Verlag, Berlin, 191 pp.

Remane, J., Bassett, M. G., Cowie, J. W., Gohrbandt, K. H., Lane, H. R., Michelsen, O. & Naiwen, W. 1996: Revised guidelines for the establishment of global chronostratigraphic standards by the International Commission on Stratigraphy (ICS). *Episodes 19*, 77–81. https://doi.org/10.18814/epiiugs/1996/v19i3/007

Retallack, G. J. 2009: Cambrian–Ordovician non-marine fossils from south Australia. *Alcheringa 33*, 355–391. https://doi.org/10.1080/03115510903271066

Rhoads, D. C. & Boyer, L. F. 1982: The effects of marine benthos on physical properties of sediments: a successional perspective. 3–52 *in* McCall, P. L. & Tevesz, M. J. S. (eds): *Animal-Sediment Relations. The Biogenic Alteration of Sediments*. Topics in Geobiology, 100, Springer. https://doi.org/10.1007/978-1-4757-1317-6_1

Riahi, S., Uchman, A., Stow, D., Soussi, M. & Lattrache, K. B. I. 2014: Deep-sea trace fossils of the Oligocene–Miocene Numidian Formation, northern Tunisia. *Palaeogeography, Palaeoclimatology, Palaeoecology 414*, 155–177. https://doi.org/10.1016/j.palaeo.2014.08.010

Riaz, M., Zafar, T., Latif, K., Ghazi, S. & Xiao, E. 2020: Petrographic and rare earth elemental characteristics of Cambrian *Girvanella* oncoids exposed in the North China Platform: constraints on forming mechanism, REE sources, and paleoenvironments. *Arabian Journal of Geosciences 13*, 858. https://doi.org/10.1007/s12517-020-05750-8

Richter, R. 1850: Aus der Thüringischen Grauwacke. *Deutsche Geologische Gesellschaft, Zeitschrift 2*, 198–206.

Richter, R. 1924: Flachseebeobachtungen zur Geologie und Paläontologie. VII–XI. *Senckenbergiana 6*, 119–165.

Riemer, S., Turchyn, A.V., Pellerin, A. & Antler, G. 2023: Digging deeper: bioturbation increases the preserved sulfur isotope fractionation. *Frontiers in Marine Science 9*, 1039193. https://doi.org/10.3389/fmars.2022.1039193

Rindsberg, A. K. 1994: *Ichnology of the Upper Mississippian Hartselle Sandstone of Alabama, with notes on other Carboniferous formations*. Geological Survey of Alabama, Economic Geology Division, Bulletin 158, 107 pp.

Rindsberg, A. K. 2018: Ichnotaxonomy as a science. *Annales Societatis Geologorum Poloniae 88*, 91–110. https://doi.org/10.14241/asgp.2018.012

Rindsberg, A. K. & Gastaldo, R. A. 1990: New insight on ichnogenus *Rosselia* (Cretaceous and Holocene, Alabama). *Journal of the Alabama Academy of Science 61*, 154.

Rindsberg, A. K. & Kopaska-Merkel, D. C. 2005: *Treptichnus* and *Arenicolites* from the Steven C. Minkin Paleozoic footprint site (Langsettian, Alabama, USA). 121–141 *in* Butta, R. J., Rindsberg, A. K. & Kopaska-Merkel, D. C. (eds): *Pennsylvanian Footprints in the Black Warrior Basin of Alabama*. Alabama Paleontological Society Monograph No. 1.

Rode, H. & Staar, G. 1961: Die photographische darstellung der kriechspuren (ichnogramme) von nematoden und ihre bedeutung. *Nematologica 6*, 266–271. https://doi.org/10.1163/187529261X00126

Rodríguez-Tovar, F. J. & Uchman, A. 2006: Ichnological analysis of the Cretaceous–Palaeogene boundary interval at the Caravaca section, SE Spain. *Palaeogeography, Palaeoclimatology, Palaeoecology 242*, 313–325. https://doi.org/10.1016/j.palaeo.2006.06.006

Rodríguez-Tovar, F. J., Pérez-Valera, F. & Pérez-López, A. 2007: Ichnological analysis in high-resolution sequence stratigraphy: the *Glossifungites* ichnofacies in Triassic successions from the Betic Cordillera (southern Spain). *Sedimentary Geology 198*, 293–307. https://doi.org/10.1016/j.sedgeo.2007.01.016

Rodríguez-Tovar, F. J., Stachacz, M., Uchman, A. & Reolid, M. 2014: Lower/middle Ordovician (Arenigian) shallow-marine trace fossils of the Pochico Formation, southern Spain: palaeoenvironmental and palaeogeographic implications at the Gondwanan and peri-Gondwanan realm. *Journal of Iberian Geology 40*, 539–555. https://doi.org/10.5209/rev_JIGE.2014.v40.n3.44308

Rodríguez-Tovar, F. J., Mayoral, E., Santos, A., Dorador, J. & Wetzel, A. 2019: Crowded tubular tidalites in Miocene shelf sandstones of southern Iberia. *Palaeogeography, Palaeoclimatology, Palaeoecology 521*, 1–9. https://doi.org/10.1016/j.palaeo.2019.02.012

Rogov, V. I., Karlova, G. A., Marusin, V. V., Kochnev, B. B., Nagovitsin, K. E. & Grazhdankin, D.V. 2015: Duration of the first biozone in the Siberian hypostratotype of the Vendian. *Russian Geology and Geophysics 56*, 573–583. https://doi.org/10.1016/j.rgg.2015.03.016

Rohde, A. 2009: Hardeberga-Sandstein mit dem Spurenfossil *Psammichnites gigas* aus dem Geschiebe. *Der Geschiebesammler 42*, 51–58.

Romano, M. & Meléndez, B. 1979: An arthropod (Merostome) ichnocoenosis from the Carboniferous of northwest Spain. *Compte Rendu du Neuvième Congrès International de Stratigraphie et de Géologie du Carbonifère 5*, 317–325.

Romero-Wetzel, M. B. 1987: Sipunculans as inhabitants of very deep, narrow burrows in deep-sea sediments. *Marine Biology 96*, 87–91. https://doi.org/10.1007/BF00394841

Ronchi, A. & Santi, G. 2003: Non-marine biota from the lower Permian of the central Southern Alps (Orobic and Collio basins, N Italy): a key to the paleoenvironment. *Geobios 36*, 749–760. https://doi.org/10.1016/j.geobios.2003.01.004

Rouault, M. 1850: Note préliminaire sur une nouvelle formation découverte dans le terrain silurien inférieur de la Bretagne. *Bulletin de la Société Géologique de France 7*, 724–744.

Rozanov, A. Y. 1967: The Cambrian lower boundary problem. *Geological Magazine 104*, 415–434. https://doi.org/10.1017/S0016756800049165

Rozanov, A. Y. 1984: The Precambrian-Cambrian boundary in Siberia. *Episodes 7*, 20–24. https://doi.org/10.18814/epiiugs/1984/v7i4/004

Runkel, A. C. 1994: Deposition of the uppermost Cambrian (Croixan) Jordan Sandstone, and the nature of the Cambrian-Ordovician boundary in the upper Mississippi Valley. *Geological Society of America Bulletin 106*, 492–506. https://doi.org/10.1130/0016-7606(1994)106<0492:DOTUCC>2.3.CO;2

Runnegar, B. N. 1992: Proterozoic metazoan trace fossils. 1009–1015 *in* Schopf, J. W. & Klein, C. (eds): *The Proterozoic Biosphere*. Cambridge University Press.

Sadlok, G. 2010: Trace fossil *Cruziana tenella* from the Furongian (upper Cambrian) deposits of Poland. *Acta Geologica Polonica 60*, 349–355.

Sadlok, G. 2014: New data on the trace fossil, *Cruziana semiplicata* (Furongian, Wiśniówka Sandstone Formation, Poland): origin, ethology and producer. *Annales Societatis Geologorum Poloniae 84*, 35–50.

Saleh, F., Qi, C., Buatois, L. A., Mángano, M. G., Paz, M., Vaucher, R., Zheng, Q., Hou, X.-G., Gabbott, S. E. & Ma, X. 2022: The Chengjiang Biota inhabited a deltaic environment. *Nature Communications 13*, 1569. https://doi.org/10.1038/s41467-022-29246-z

Salter, J. W. 1856: On fossil remains in the Cambrian rocks of the Longmynd and north Wales. *Quarterly Journal of the Geological Society 12*, 246–251. https://doi.org/10.1144/GSL.JGS.1856.012.01-02.31

Salter, J. W. 1857: On annelide-burrows and surface-markings from the Cambrian rocks of the Longmynd. No. 2. *Quarterly Journal of the Geological Society 13*, 199–206. https://doi.org/10.1144/GSL.JGS.1857.013.01-02.29

Sandstedt, R., Sullivan, T. & Schuster, M. L. 1961: Nematode tracks in the study of movement of *Meloidogyne incognita incognita*. *Nematologica 6*, 261–265. https://doi.org/10.1163/187529261X00117

Savrda, C. 2003: Equilibrium responses reflected in a large *Conichnus* (upper Cretaceous Eutaw Formation, Alabama, USA). *Ichnos 9*, 33–40. https://doi.org/10.1080/10420940190034058

Savrda, C. E. 2007: Trace fossils and marine benthic oxygenation. *In* Miller III, W. (ed): *Trace Fossils. Concepts, Problems, Prospects*, 149–158. Elsevier. https://doi.org/10.1016/B978-044452949-7/50135-2

Savrda, C. E. & Ozalas, K. 1993: Preservation of mixed-layer ichnofabrics in oxygenation-event beds. *Palaios 8*, 609–613. https://doi.org/10.2307/3515036

Savrda, C. E., Bottjer, D. J. & Gorsline, D. S. 1984: Development of a comprehensive oxygen-deficient marine biofacies model: evidence from Santa Monica, San Pedro, and Santa Barbara Basins, California Continental Borderland. *AAPG Bulletin 68*, 1179–1192. https://doi.org/10.1306/AD4616F1-16F7-11D7-8645000102C1865D

Savrda, C. E., Bottjer, D. J. & Seilacher, A. 1991: Redox-related benthic events. 524–541 *in* Einsele, G., Ricken, W. & Seilacher, A. (eds): *Cycles and Events in Stratigraphy*. Springer-Verlag, Berlin.

Savrda, C. E., Locklair, R. E., Hall, J. K., Sadler, M. T., Smith, M. W. & Warren, J. D. 1998: Ichnofabrics, ichnocoenoses, and ichnofacies implications of an upper Cretaceous tidal-inlet sequence (Eutaw Formation, central Alabama). *Ichnos 6*, 53–74. https://doi.org/10.1080/10420949809386439

Schaefer, M. O., Gutzmer, J. & Beukes, N. J. 2001: Late Paleoproterozoic Mn-rich oncoids: earliest evidence for microbially mediated Mn precipitation. *Geology 29*, 835–838. https://doi.org/10.1130/0091-7613(2001)029<0835:LPMROE>2.0.CO;2

Schäfer, W. 1972: *Ecology and Palaeoecology of Marine Environments*. University of Chicago Press, Chicago, IL, 568 pp.

Schatz, E. R., Mángano, M. G., Buatois, L. A. & Limarino, C. O. 2011: Life in the late Paleozoic Ice Age: trace fossils from glacially influenced deposits in a late Carboniferous fjord of western Argentina. *Journal of Paleontology 85*, 502–518. https://doi.org/10.1666/10-046.1

Schatz, E. R., Mángano, M. G., Aitken, A. E. & Buatois, L. A. 2013: Response of benthos to stress factors in Holocene Arctic fjord settings: Maktak, Coronation, and North Pangnirtung Fjords, Baffin Island, Canada. *Palaeogeography, Palaeoclimatology, Palaeoecology 386*, 652–668. https://doi.org/10.1016/j.palaeo.2013.06.030

Schieber, J. 2011: Reverse engineering mother nature—shale sedimentology from an experimental perspective. *Sedimentary Geology 238*, 1–22. https://doi.org/10.1016/j.sedgeo.2011.04.002

Schieber, J. 2016: Mud re-distribution in epicontinental basins–exploring likely processes. *Marine and Petroleum Geology 71*, 119–133. https://doi.org/10.1016/j.marpetgeo.2015.12.014

Schieber, J. & Wilson, R.D. 2021: Burrows without a trace—how meioturbation affects rock fabrics and leaves a record of meiobenthos activity in shales and mudstones. *PalZ 95*, 767–791. https://doi.org/10.1007/s12542-021-00590-7

Schieber, J., Southard, J. & Thaisen, K. 2007: Accretion of mudstone beds from migrating floccule ripples. *Science 318*, 1760–1763. https://doi.org/10.1126/science.1147001

Schimper, W. P. 1890: *Handbuch der Palaeontologie. II. Abtheilung Palaeophytologie*. Druck und Verlag von R. Oldenbourg, München und Leipzig, 958 pp.

Schindewolf, O. H. 1921: Studien aus dem Marburger Buntsandstein I, II. *Seckenbergiana 3*, 33–49.

Schindewolf, O. H. 1928: Studien aus dem Marburger Buntsandstein III-VI. *Senckenbergiana 10*, 16–54.

Schlirf, M. 2000: Upper Jurassic trace fossils from the Boulonnais (northern France). *Geologica et Palaeontologica 34*, 145–213.

Schlirf, M. 2006: *Trusheimichnus* new ichnogenus from the middle Triassic of the Germanic Basin, Southern Germany. *Ichnos 13*, 249–254. https://doi.org/10.1080/10420940600843690

Schlirf, M. 2011: A new classification concept for U-shaped spreite trace fossils. *Neues Jahrbuch für Geologie und*

Paläontologie Abhandlungen 260, 33–54. https://doi.org/10.1127/0077-7749/2011/0127
Schlirf, M. & Bromley, R. G. 2007: *Teichichnus duplex* n. isp., new trace fossil from the Cambrian and the Triassic. *Beringeria 37*, 133–141.
Schlirf, M. & Uchman, A. 2005: Revision of the Ichnogenus *Sabellarifex* Richter, 1921 and its relationship to *Skolithos* Haldeman, 1840 and *Polykladichnus* Fürsich, 1981. *Journal of Systematic Palaeontology 3*, 115–131. https://doi.org/10.1017/S1477201905001550
Schlirf, M., Uchman, A. & Kümmel, M. 2001: Upper Triassic (Keuper) non-marine trace fossils from the Haßberge area (Franconia, south-eastern Germany). *Paläontologische Zeitschrift 75*, 71–96. https://doi.org/10.1007/BF03022599
Schlirf, M., Nara, M. & Uchman, A. 2002: Invertebraten-Spurenfossilien aus dem Taunusquarzit (Siegen, Unterdevon) von der "Rossel" nahe Rudesheim. *Jahrbücher des Nassauischen Vereins für Naturkunde 123*, 43–63.
Schmitz, M. D. 2012: Radiometric ages used in GTS 2012. 1045–1077 *in* Gradstein, F. M., Ogg, J. G, Schmitz, M. & Ogg, G. (eds): *The Geologic Time Scale 2012*. Elsevier, vol. 2. https://doi.org/10.1016/B978-0-444-59425-9.15002-4
Schmitz, M. D. 2020. Radioisotopic ages used in GTS 2020. 1285–1341 *in* Gradstein, F. M., Ogg, J. G, Schmitz, M. & Ogg, G. (eds): *Geologic Time Scale 2020*. Elsevier, vol. 2. https://doi.org/10.1016/B978-0-12-824360-2.00046-2
Schneer, C. J. 1978: The great Taconic controversy. *Isis 69*, 173–191. https://doi.org/10.1086/352002
Schneid, T. 1938: Über eine interessante fossile Lebensspur aus dem Mittleren Malm Frankens (*Xenohelix suprajurassica* n. sp.). *Zentralblatt für Mineralogie, Geologie und Paläontologie 8*, 312–315.
Scott, J. J., Buatois, L. A. & Mangano, M. G. 2012: Lacustrine environments. *Developments in Sedimentology 64*, 379–417. https://doi.org/10.1016/B978-0-444-53813-0.00013-7
Scott, J. J., Renaut, R. W., Buatois, L. A. & Owen, R. B. 2009: Biogenic structures in exhumed surfaces around saline lakes: an example from Lake Bogoria, Kenya Rift Valley. *Palaeogeography, Palaeoclimatology, Palaeoecology 272*, 176–198. https://doi.org/10.1016/j.palaeo.2008.12.002
Sedorko, D., Netto, R. G. & Bosetti, E. P. 2013: Paleoicnologia do Siluro-Devoniano do estado do Paraná e a obra de John Mason Clarke. *Terr@ Plural 7*, 59–74. https://doi.org/10.5212/TerraPlural.v.7iEspecial.0005
Seike, K., Nara, M., Takagawa, T. & Sato, S. 2015: Paleoecology of a marine endobenthic organism in response to beach morphodynamics: trace fossil *Macaronichnus segregatis* in Holocene and Pleistocene sandy beach deposits. *Regional Studies in Marine Science 2*, 5–11. https://doi.org/10.1016/j.rsma.2015.09.006
Seilacher, A. 1953: Studien zur Palichnologie. I. Über die Methoden der Palichnologie. *Neues Jahrbuch fur Geologie und Palaontologie Abhandlungen 96*, 421–452.
Seilacher, A. 1955a: Spuren und Lebensweise der Trilobiten. 346–372 *in* Schindewolf, O. H. & Seilacher, A. (eds): *Beiträge zur Kenntnis des Kambriums in der Salt Range (Pakistan)*. Akademie Wissenschaften und der Literatur zu Mainz, Mathematisch-Naturwissenschaftliche Klasse, Abhandlungen. vol. 10.
Seilacher, A. 1955b: Spuren und Fazies im Unterkambrium. 373–399 *in* Schindewolf, O. H. & Seilacher, A. (eds): *Beiträge zur Kenntnis des Kambriums in der Salt Range (Pakistan)*. Akademie Wissenschaften und der Literatur zu Mainz, Mathematisch-Naturwissenschaftliche Klasse, Abhandlungen. vol. 10.
Seilacher, A. 1956: Der beginn des Kambriums als biologische Wende. *Neues Jahrbuch für Geologie und Paläontologie Abhandlungen 103*, 155–180.
Seilacher, A. 1960: Lebensspuren als Leitfossilien. *Geologische Rundschau 49*, 41–50. https://doi.org/10.1007/BF01802391
Seilacher, A. 1964: Biogenic sedimentary structures. 296–316 *in* Imbrie, J. & Newell, N. (eds): *Approaches to Paleoecology*. John Wiley and Sons, New York.
Seilacher, A. 1967a: Bathymetry of trace fossils. *Marine Geology 5*, 413–428. https://doi.org/10.1016/0025-3227(67)90051-5
Seilacher, A. 1967b: Fossil behavior. *Scientific American 217*, 72–83. https://doi.org/10.1038/scientificamerican0867-72
Seilacher, A. 1969: Sedimentary rhythms and trace fossils in Paleozoic sandstones of Libya. 117–123 *in* Kanes, W. H. (ed): *Geology, Archaeology and Prehistory of the Southwestern Fezzan, Libya*. Petroleum Exploration Society of Libya, 11th annual field conference.
Seilacher, A. 1970: *Cruziana* stratigraphy of "non-fossiliferous" Palaeozoic sandstones. 447–476 *in* Crimes, T. P. & Harper, J. C. (eds): *Trace Fossils*. Seel House Press, Liverpool.
Seilacher, A. 1977: Pattern analysis of *Paleodictyon* and related trace fossils. 289–334 *in* Crimes, T. P. & Harper, J. C. (eds): *Trace Fossils 2*. Seel House Press, Liverpool.
Seilacher, A. 1982: Distinctive features of sandy tempestites. 333–349 *in* Einsele, G. & Seilacher, A. (eds): *Cyclic and Event Stratification*. Springer. https://doi.org/10.1007/978-3-642-75829-4_24
Seilacher, A. 1983: Paleozoic sandstones in southern Jordan: trace fossils, depositional environments and biogeography. 209–222 *in* Abed, A. M. & Khaled, H. D. (eds): *Geology of Jordan*. Proceedings of the first Jordanian Geology Conference, Jordan Geologists Association.
Seilacher, A. 1985: Trilobite palaeobiology and substrate relationships. *Transactions of the Royal Society of Edinburgh: Earth Sciences 76*, 231–237. https://doi.org/10.1017/S0263593300010464
Seilacher, A. 1990a: Paleozoic trace fossils. 649–670 *in* Said, R. (ed): *The Geology of Egypt*. A.A. Balkema, Rotterdam.
Seilacher, A. 1990b: Aberrations in bivalve evolution related to photo-and chemosymbiosis. *Historical Biology 3*, 289–311. https://doi.org/10.1080/08912969009386528
Seilacher, A. 1992: An updated *Cruziana* stratigraphy of Gondwanan Palaeozoic sandstones. 1565–1581 *in* Salem, M. J. & Busrewil, M. T. (eds): *The Geology of Libya*. Elsevier.
Seilacher, A. 1993: Problems of correlation in the Nubian Sandstone facies. 329–333 *in* Schandelmeier, H. & Thorweihe, U. (eds): *Geoscientific Research in Northeast Africa*. CRC Press.
Seilacher, A. 1994: How valid is Cruziana stratigraphy? *Geologische Rundschau 83*, 752–758. https://doi.org/10.1007/BF00251073
Seilacher, A. 1996: Evolution of burrowing behaviour in Silurian trilobites: ichnosubspecies of *Cruziana acacensis*. 523–530 *in* Salem, M. J. (ed): *The Geology of Sirt Basin*. Elsevier.
Seilacher, A. 1997a: *Fossil Art*. Geologisches Institut, Tuebingen University, 63 pp.
Seilacher, A. 1997b: The meaning of the Cambrian Explosion. *Bulletin of National Museum of Natural Science 10*, 1–9.
Seilacher, A. 1999: Biomat-related lifestyles in the Precambrian. *Palaios 14*, 86–93. https://doi.org/10.2307/3515363
Seilacher, A. 2007: *Trace Fossil Analysis*. Springer-Verlag, Heidelberg, 226 pp.
Seilacher, A. & Gamez-Vintaned, J. A. 1995: *Psammichnites gigas*: ichnological expression of the Cambrian Explosion. 151–152 *in* Cherchi, A. (ed): *Proceedings 6th Paleobenthos International Symposium*. Dipartimento di Scieze della Terra, Cagliari. https://doi.org/10.13140/RG.2.1.2116.3284/1
Seilacher, A. & Hagadorn, J. W. 2010: Early molluscan evolution: evidence from the trace fossil record. *Palaios 25*, 565–575. https://doi.org/10.2110/palo.2009.p09-079r
Seilacher, A. & Hemleben, C. 1966: Spurenfauna und Bildungstiefe der Hunsrückschiefer (Unterdevon). *Notizblatt des hessischen Landesamtes für Bodenforschung 94*, 40–53.
Seilacher, A. & Mrinjek, E. 2011: Benkovac Stone (Eocene, Croatia): a deep-sea Plattenkalk? *Swiss Journal of Geosciences 104*, 159–166. https://doi.org/10.1007/s00015-011-0051-7
Seilacher, A. & Pflüger, F. 1994: From biomats to benthic agriculture: a biohistoric revolution. 97–105 *in* Krumbein, W. E., Paterson, D. M. & Stal, L. J. (eds): *Biostabilization of Sediments*. Bibliotheks- und Informationsystem der Universität Oldenburg.

Seilacher, A. & Seilacher, E. 1994: Bivalvian trace fossils: a lesson from actuopaleontology. *Courier Forschungs-Institute Senckenberg 169*, 5–15.

Seilacher, A., Grazhdankin, D. & Legouta, A. 2003: Ediacaran biota: the dawn of animal life in the shadow of giant protists. *Paleontological Research 7*, 43–54. https://doi.org/10.2517/prpsj.7.43

Seilacher, A., Buatois, L. A. & Mángano, M. G. 2005: Trace fossils in the Ediacaran–Cambrian transition: behavioral diversification, ecological turnover and environmental shift. *Palaeogeography, Palaeoclimatology, Palaeoecology 227*, 323–356. https://doi.org/10.1016/j.palaeo.2005.06.003

Seilacher-Drexler, E. & Seilacher, A. 1999: Undertraces of Sea Pens and Moon Snails and possible fossil counterparts. *Neues Jahrbuch für Geologie und Paläontologie-Abhandlungen 214*, 195–210. https://doi.org/10.1127/njgpa/214/1999/195

Sepkoski Jr., J. J. & Knoll, A. H. 1983: Precambrian-Cambrian boundary: the spike is driven and the monolith crumbles. *Paleobiology 9*, 199–206. https://doi.org/10.1017/S0094837300007624

Severin, K. P., Culver, S. J. & Blanpied, C. 1982: Burrows and trails produced by *Quinqueloculina impressa* Reuss, a benthic foraminifer, in fine-grained sediment. *Sedimentology 29*, 897–901. https://doi.org/10.1111/j.1365-3091.1982.tb00093.x

Shah, S. K. & Sudan, C. S. 1983: Trace fossils from the Cambrian of Kashmir and their stratigraphic significance. *Journal Geological Society of India 24*, 194–202. https://doi.org/10.17491/jgsi/1983/240403

Shahkarami, S., Mángano, M. G. & Buatois, L. A. 2017a: Ichnostratigraphy of the Ediacaran-Cambrian boundary: new insights on lower Cambrian biozonations from the Soltanieh Formation of northern Iran. *Journal of Paleontology 91*, 1178–1198. https://doi.org/10.1017/jpa.2017.72

Shahkarami, S., Mángano, M. G. & Buatois, L. A. 2017b: Discriminating ecological and evolutionary controls during the Ediacaran–Cambrian transition: trace fossils from the Soltanieh Formation of northern Iran. *Palaeogeography, Palaeoclimatology, Palaeoecology 476*, 15–27. https://doi.org/10.1016/j.palaeo.2017.03.012

Shahkarami, S., Buatois, L. A., Mángano, M. G., Hagadorn, J. W. & Almond, J. 2020: The Ediacaran–Cambrian boundary: evaluating stratigraphic completeness and the Great Unconformity. *Precambrian Research 345*, 105721. https://doi.org/10.1016/j.precamres.2020.105721

Shanmugam, G. 2016: The seismite problem. *Journal of Palaeogeography 5*, 318–362. https://doi.org/10.1016/j.jop.2016.06.002

Sharma, M. & Shukla, Y. 2009: Taxonomy and affinity of early Mesoproterozoic megascopic helically coiled and related fossils from the Rohtas Formation, the Vindhyan Supergroup, India. *Precambrian Research 173*, 105–122. https://doi.org/10.1016/j.precamres.2009.05.002

Sharma, M., Pandey, S. K., Ahmad, S., Kumar, K. & Ansari, A. H. 2018a: Observations on the ichnospecies *Monomorphichnus multilineatus* from the Nagaur Sandstone (Cambrian Series 2-Stage 4), Marwar Supergroup, India. *Journal of Earth System Science 127*, 75. https://doi.org/10.1007/s12040-018-0973-9

Sharma, M., Ahmad, S., Pandey, S. K. & Kumar, K. 2018b: On the ichnofossil *Treptichnus pedum*: inferences from the Nagaur Sandstone, Marwar Supergroup, India. *Bulletin of Geosciences 93*, 305–325. https://doi.org/10.3140/bull.geosci.1666

Shchepetkina, A., Gingras, M. K. & Pemberton, S. G. 2018: Modern observations of floccule ripples: Petitcodiac River estuary, New Brunswick, Canada. *Sedimentology 65*, 582–596. https://doi.org/10.1111/sed.12393

Sheehan, P. M. & Schiefelbein, D. J. 1984: The trace fossil *Thalassinoides* from the upper Ordovician of the eastern Great Basin: deep burrowing in the early Paleozoic. *Journal of Paleontology 58*, 440-447.

Sheldon, N. D. 2005: Do red beds indicate paleoclimatic conditions?: a Permian case study. *Palaeogeography, Palaeoclimatology, Palaeoecology 228*, 305–319. https://doi.org/10.1016/j.palaeo.2005.06.009

Shen, Z., Zeng, Y., Mei, M. & Shen, J. 1990: The trace fossil associations of early Ordovician in the eastern side of Kangdian oldland and their facies-indication significance. *Acta Sedimentologica Sinica 8*, 110–119.

Shi, G. R. & Chen, Z. Q. 2006: Lower Permian oncolites from South China: implications for equatorial sea-level responses to late Palaeozoic Gondwanan glaciation. *Journal of Asian Earth Sciences 26*, 424–436. https://doi.org/10.1016/j.jseaes.2005.10.009

Shillito, A. P. & Davies, N. S. 2020: The Tumblagooda Sandstone revisited: exceptionally abundant trace fossils and geological outcrop provide a window onto Palaeozoic littoral habitats before invertebrate terrestrialization. *Geological Magazine 157*, 1939–1970. https://doi.org/10.1017/S0016756820000199

Shillito, A. P. & Davies, N. S. 2021: The Silurian inception of inland desert ecosystems: trace fossil evidence from the Mereenie Sandstone, Northern Territory, Australia. *Journal of the Geological Society 178*, 1–17. https://doi.org/10.1144/jgs2020-243

Shillito, A. P. & Gougeon, R. 2023: Identifying and accounting for outcrop constraints on observations in field-based ichnological studies. *Ichnos 30*, 269–282. https://doi.org/10.1080/10420940.2024.2330417

Shinn, E. A. 1968: Burrowing in recent lime sediments of Florida and the Bahamas. *Journal of Paleontology 42*, 879–894.

Shitole, A. D., Patel, S. J., Joseph, J. K. & Darngawn, J. L. 2019: Ethological and environmental significance of *Bergaueria hemispherica* from the late Cretaceous of the Bagh Group, Western India. *Comptes Rendus Palevol 18*, 287–297. https://doi.org/10.1016/j.crpv.2019.01.002

Shone, R. W. 1978: Giant *Cruziana* from the Beaufort group. *South African Journal of Geology 81*, 327–329.

Shone, R. W. 1979: Giant *Cruziana* from the Beaufort Group. Author's reply to discussion. *South African Journal of Geology 82*, 373–375.

Signor, P. W. 1994: Proterozoic–Cambrian boundary trace fossils: biostratigraphic significance of *Harlaniella* in the lower Cambrian Wood Canyon Formation, Death Valley, California. *New York State Museum Bulletin 481*, 317–322.

Simón, J. 2017: Trace fossils and dubiofossils from the Ediacaran and Cambrian of the Alcudia Anticline, Spain. *Estudios Geológicos 73*, e068. https://doi.org/10.3989/egeol.42724.442

Simón López-Villalta, J. 2019: Fossils from the Azorejo Formation (lower Cambrian, Central Iberian Zone) in the Guadiana River section at Picón, *Boletín de la Real Sociedad Española de Historia Natural (Sección Biológica) 113*, 1–22. https://doi.org/10.29077/bol/113/ce06_simon

Simpson, E. L. & Eriksson, K. A. 1990: Early Cambrian progradational and transgressive sedimentation patterns in Virginia: an example of the early history of a passive margin. *Journal of Sedimentary Petrology 60*, 84–100. https://doi.org/10.1306/212F911A-2B24-11D7-8648000102C1865D

Simpson, E. L., Dilliard, K. A., Rowell, B. F. & Higgins, D. 2002: The fluvial-to-marine transition within the post-rift lower Cambrian Hardyston Formation, Eastern Pennsylvania, USA. *Sedimentary Geology 147*, 127–142. https://doi.org/10.1016/S0037-0738(01)00193-2

Singh, I. B. & Rai, V. 1983: Fauna and biogenic structures in Krol-Tal succession (Vendian-early Cambrian), Lesser Himalaya: their biostratigraphic and palaeoecological significance. *Journal of the Palaeontological Society of India 28*, 67–90. https://doi.org/10.1177/0971102319830109

Singh, M. C., Kundal, P. & Kushwaha, R. A. S. 2010: Ichnology of Bhuban and Boka Bil formations, Oligocene-Miocene deposits of Manipur Western Hill, northeast India. *Journal Geological Society of India 76*, 573–586. https://doi.org/10.1007/s12594-010-0118-5

Singh, B. P., Bhargava, O. N., Mikuláš, R., Prasad, S. K., Morrison, S., Chaubey, R. S. & Kishore, N. 2019: Discovery of traces of *Cruziana semiplicata* and *C. rugosa* groups (Cambro-Ordovician) from the Lesser Himalaya, India and their stratigraphic, tectonic and palaeobiogeographic implications. *Journal of the Palaeontological Society of India 64*, 283–303. https://doi.org/10.1177/0971102320190209

Singh, B. P., Bhargava, O. N., Mikuláš, R., Prasad, S. K., Verma, V., Morrison, S., Chaubey, R. S., Negi, R. S. & Singla, G. 2024a: Plug-shaped burrow *Bergaueria* Prantl, 1945 from the Lower Cambrian of Nigalidhar Syncline, Himachal Pradesh, Lesser Himalaya and its biostratigraphic significance in Himalayan Cambrian sections. *Neues Jahrbuch für Geologie und Paläontologie Abhandlungen 312*, 281–297. https://doi.org/10.1127/njgpa/2024/1214

Singh, B. P., Bhargava, O. N., Chaubey, R. S., Prasad, S. K. & Verma, V. 2024b: Cambrian trace fossils from the Kunzam La Formation, Baralacha La syncline, Lahaul valley, Himachal Himalaya and their biostratigraphic significance. *Himalayan Geology 45*, 199–209.

Skipton, D. R., Dunning, G. R. & Sparkes, G. W. 2013: Late Neoproterozoic arc-related magmatism in the Horse Cove complex, eastern Avalon zone, Newfoundland. *Canadian Journal of Earth Sciences 50*, 462–482. https://doi.org/10.1139/cjes-2012-0090

Skwarko, S. K. & Seilacher, A. 1993: Trace fossils and problematica. 390–403 *in* Skwarko, S. K. (ed): *Palaeontology of the Permian of western Australia*. Geological Survey of western Australia, Bulletin 136.

Sleveland, A. R., Midtkandal, I., Galland, O. & Leanza, H. A. 2020: Sedimentary architecture of storm-influenced tidal flat deposits of the upper Mulichinco Formation, Neuquén Basin, Argentina. *Frontiers in Earth Science 8*, 219. https://doi.org/10.3389/feart.2020.00219

Smith, A. B. & Crimes, T. P. 1983: Trace fossils formed by heart urchins – a study of *Scolicia* and related traces. *Lethaia 16*, 79–92. https://doi.org/10.1111/j.1502-3931.1983.tb02001.x

Smith, A. M. & Mason, T. R. 1991: Pleistocene, multiple-growth, lacustrine oncoids from the Poacher's Point Formation, Etosha Pan, northern Namibia. *Sedimentology 38*, 591–599. https://doi.org/10.1111/j.1365-3091.1991.tb01010.x

Smith, C. R. 1992: Factors controlling bioturbation in deep-sea sediments and their relation to models of carbon diagenesis. 375–393 *in* Rowe, G. T. & Pariente, V. (eds): *Deep-Sea Food Chains and the Global Carbon Cycle*. Kluwer Academic Publishers. https://doi.org/10.1007/978-94-011-2452-2_23

Smith, C. R. & Rabouille, C. 2002: What controls the mixed-layer depth in deep-sea sediments? The importance of POC flux. *Limnology and Oceanography 47*, 418–426. https://doi.org/10.4319/lo.2002.47.2.0418

Smith, E. F., Macdonald, F. A., Petach, T. A., Bold, U. & Schrag, D. P. 2016a: Integrated stratigraphic, geochemical, and paleontological late Ediacaran to early Cambrian records from southwestern Mongolia. *Geological Society of America Bulletin 128*, 442–468. https://doi.org/10.1130/B31248.1

Smith, E. F., Nelson, L. L., Strange, M. A., Eyster, A. E., Rowland, S. M., Schrag, D. P. & Macdonald, F. A. 2016b: The end of the Ediacaran: two new exceptionally preserved body fossil assemblages from Mount Dunfee, Nevada, USA. *Geology 44*, 911–914. https://doi.org/10.1130/G38157.1

Smith, E. F., Macdonald, F. A., Petach, T. A. & Bold, U. 2017: Integrated stratigraphic, geochemical, and paleontological late Ediacaran to early Cambrian records from southwestern Mongolia: reply. *Geological Society of America Bulletin 129*, 1016–1018. https://doi.org/10.1130/B31763.1

Smith, J. 1893: Peculiar U-shaped tubes in sand- stone near Crawfurdland Castle and in Gowkha Quarry, near Killwinning. *Transactions of the Geological Society of Glasgow 9*, 289–292.

Smith, J. 1909: *Upland Fauna of the Old Red Sandstone Formation of Carrick, Ayrshire*. A.W. Cross, Kilwinning, 43 pp.

Smith, M. G. & Bustin, R. M. 1995: Sedimentology of the late Devonian and early Mississippian Bakken Formation, Williston Basin. 103–114 *in* Hunter, L. D. V. & Schalla, R. A. (eds): *Seventh International Williston Basin Symposium*. Montana Geological Survey Special Publication.

Smith, M. R., Harvey, T. H. & Butterfield, N. J. 2015: The macro- and microfossil record of the Cambrian priapulid *Ottoia*. *Palaeontology 58*, 705–721. https://doi.org/10.1111/pala.12168

Smith, S. A. & Hiscott, R. N. 1984: Latest Precambrian to early Cambrian basin evolution, Fortune Bay, Newfoundland: fault-bounded basin to platform. *Canadian Journal of Earth Sciences 21*, 1379–1392. https://doi.org/10.1139/e84-143

Sokolov, B. S. 1972: Vendian stage in the earth history. 114–125 *in* Sokolov, B. S., Hecker, R. F., Krimhoiz, G. Y., Merklin, R. L., Oleynikov, A. N. & Stepanov D. L. (eds): *International Geological Congress, XXIV Session, Reports of Soviet Geologists, Problem 7, Paleontology*. Nauka, Moscow.

Sokolov, B. S. 1973: Vendian of Northern Eurasia. 204–218 *in* Pitcher, M. G. (ed): *Artic geology*. American Association of Petroleum Geologists, Memoir 19. https://doi.org/10.1306/M19375C20

Sokolov, B. S. & Fedonkin, M. A. 1984: The Vendian as the terminal system of the Precambrian. *Episodes 7*, 12–19. https://doi.org/10.18814/epiiugs/1984/v7i1/004

Solan, M. & Wigham, B. D. 2005: Biogenic particle reworking and bacterial–invertebrate interactions in marine sediments. 105–124 *in* Kristensen, E., Haese, R. R. & Kostka, J. E. (eds): *Interactions Between Macro- and Microorganisms in Marine Sediments*. American Geophysical Union. https://doi.org/10.1029/CE060p0105

Solan, M., Ward, E. R., White, E. L., Hibberd, E. E., Cassidy, C., Schuster, J. M., Hale, R. & Godbold, J. A. 2019: Worldwide measurements of bioturbation intensity, ventilation rate, and the mixing depth of marine sediments. *Scientific Data 6*, 58. https://doi.org/10.1038/s41597-019-0069-7

Solan, M., Cardinale, B. J., Downing, A. L., Engelhardt, K. A., Ruesink, J. L. & Srivastava, D. S. 2004: Extinction and ecosystem function in the marine benthos. *Science 306*, 1177–1180. https://doi.org/10.1126/science.1103960

Song, S., Santos, I. R., Yu, H., Wang, F., Burnett, W. C., Bianchi, T. S., Dong, J., Lian, E., Zhao, B., Mayer, L., Yao, Q., Yu, Z. & Xu, B. 2022: A global assessment of the mixed layer in coastal sediments and implications for carbon storage. *Nature Communications 13*, 4903. https://doi.org/10.1038/s41467-022-32650-0

Sour-Tovar, F., Hagadorn, J. W. & Huitrón-Rubio, T. 2007: Ediacaran and Cambrian index fossils from Sonora, Mexico. *Palaeontology 50*, 169–175. https://doi.org/10.1111/j.1475-4983.2006.00619.x

Sowerby, J. 1829: *The mineral conchology of Great Britain; or coloured figures and descriptions of those remains of testaceous animals of shells, which have been preserved at various times and depths in the Earth*. R. Taylor, Red Lion Court, Fleet Street, Vol. 6, 230 pp.

Sparkes, G. W. & Dunning, G. R. 2014: Late Neoproterozoic epithermal alteration and mineralization in the western Avalon Zone: a summary of mineralogical investigations and new U/Pb geochronological results. *Current Research, Newfoundland and Labrador Department of Natural Resources Geological Survey 14-1*, 99–128.

Stachacz, M. 2012: Ichnology of Czarna Shale Formation (Cambrian, Holy Cross Mountains, Poland). *Annales Societatis Geologorum Poloniae 82*, 105–120.

Stachacz, M. 2016: Ichnology of the Cambrian Ociesęki Sandstone Formation (Holy Cross Mountains, Poland). *Annales Societatis Geologorum Poloniae 86*, 291–328. https://doi.org/10.14241/asgp.2016.007

Stachacz, M., Rodríguez-Tovar, F. J., Uchman, A. & Reolid, M. 2015: Deep endichnial *Cruziana* from the lower-middle Ordovician of Spain—a unique trace fossil record of trilobitomorph deep burrowing behavior. *Ichnos 22*, 12–18. https://doi.org/10.1080/10420940.2014.985671

Stanistreet, I. G., Le Blanc Smith, G. & Cadle, A. B. 1980: Trace fossils as sedimentological and palaeoenvironmental indices

in the Ecca Group (lower Permian) of the Transvaal. *South African Journal of Geology 83*, 333–344.

Stanley, D. C. A. & Pickerill, R. K. 1998: *Systematic ichnology of the Late Ordovician Georgian Bay Formation of southern Ontario, eastern Canada*. Royal Ontario Museum, Life Sciences Contributions 162, 55 pp.

Stanley, S. M. 1976: Fossil data and the Precambrian-Cambrian evolutionary transition. *American Journal of Science 276*, 56–76. https://doi.org/10.2475/ajs.276.1.56

Stanley, T. M. & Feldmann, R. M. 1998: Significance of nearshore trace-fossil assemblages of the Cambro-Ordovician Deadwood Formation and Aladdin Sandstone, south Dakota. *Annals of Carnegie Museum 67*, 1–51.

Stanton Jr., R. J. & Dodd, J. R. 1984: *Teichichnus pescaderoensis* – new ichnospecies in the Neogene shelf and slope sediments, California. *Facies 11*, 219–228. https://doi.org/10.1007/BF02536911

Starek, D., Šimo, V., Antolíková, S. & Fuksi, T. 2019: Turbidite sedimentology, biostratigraphy and paleoecology: a case study from the Oligocene Zuberec Fm. (Liptov Basin, central Western Carpathians). *Geologica Carpathica 70*, 279–297. https://doi.org/10.2478/geoca-2019-0016

Steiner, M., Yang, B., Hohl, S., Zhang, L. & Chang, S. 2020: Cambrian small skeletal fossil and carbon isotope records of the southern Huangling Anticline, Hubei (China) and implications for chemostratigraphy of the Yangtze Platform. *Palaeogeography, Palaeoclimatology, Palaeoecology 554*, 109817. https://doi.org/10.1016/j.palaeo.2020.109817

Strausfeld, N. J., Ma, X. & Edgecombe, G. D. 2016: Fossils and the evolution of the arthropod brain. *Current Biology 26*, R989–R1000. https://doi.org/10.1016/j.cub.2016.09.012

Strauss, H., Bengtson, S., Myrow, P. M. & Vidal, G. 1992: Stable isotope geochemistry and palynology of the late Precambrian to early Cambrian sequence in Newfoundland. *Canadian Journal of Earth Sciences 29*, 1662–1673. https://doi.org/10.1139/e92-131

Strong, D. F., O'Brien, S., Taylor, S. W., Strong, P. G. & Wilton, D. H. 1978: Aborted Proterozoic rifting in eastern Newfoundland. *Canadian Journal of Earth Sciences 15*, 117–131. https://doi.org/10.1139/e78-010

Such, P., Buatois, L. A. & Mángano, M. G. 2007: Stratigraphy, depositional environments and ichnology of the lower Paleozoic in the Azul Pampa area—Jujuy Province. *Revista de la Asociación Geológica Argentina 62*, 331–344.

Sun, W. G. 1985: *Contributions to palaeontology and stratigraphic correlation of the late Precambrian in China and Australia*. Unpublished Doctoral Dissertation, University of Adelaide, 291 pp.

Sutcliffe, O. E., Briggs, D. E. G. & Bartels, C. 1999: Ichnological evidence for the environmental setting of the Fossil-Lagerstatten in the Devonian Hunsruck Slate, Germany. *Geology 27*, 275–278. https://doi.org/10.1130/0091-7613(1999)027<0275:IEFTES>2.3.CO;2

Swift, D. J. P., Figueiredo Jr., A. G., Freeland, G. L. & Oertel, G. F. 1983: Hummocky cross-stratification and megaripples: a geological double standard? *Journal of Sedimentary Petrology 53*, 1295–1317. https://doi.org/10.1306/212F8369-2B24-11D7-8648000102C1865D

Swift, D. J. P., Hudelson, P. M., Brenner, R. L. & Thompson, P. 1987: Shelf construction in a foreland basin: storm beds, shelf sandbodies, and shelf-slope depositional sequences in the upper Cretaceous Mesaverde Group, Book Cliffs, Utah. *Sedimentology 34*, 423–457. https://doi.org/10.1111/j.1365-3091.1987.tb00578.x

Swinbanks, D. D. & Murray, J. W. 1981: Biosedimentological zonation of Boundary Bay tidal flats, Fraser River Delta, British Columbia. *Sedimentology 28*, 201–237. https://doi.org/10.1111/j.1365-3091.1981.tb01677.x

Systra, Y. J. & Jensen, S. 2006: Trace fossils from the Dividalen Group of northern Finland with remarks on early Cambrian trace fossil provincialism. *GFF 128*, 321–325. https://doi.org/10.1080/11035890601284321

Tanner, L. H., Smith, D. L. & Lucas, S. G. 2006: Trace fossils in eolian facies of the upper Triassic-lower Jurassic Dinosaur Canyon Member, Moenave Formation, northern Arizona. *Ichnos 13*, 21–29. https://doi.org/10.1080/10420940500511520

Tanner, W. F. 1958: An occurrence of flat-topped ripple marks. *Journal of Sedimentary Petrology 28*, 95–96. https://doi.org/10.1306/74D7076D-2B21-11D7-8648000102C1865D

Tarhan, L. G. 2018: The early Paleozoic development of bioturbation—evolutionary and geobiological consequences. *Earth-Science Reviews 178*, 177–207. https://doi.org/10.1016/j.earscirev.2018.01.011

Tarhan, L. G. & Droser, M .L. 2014: Widespread delayed mixing in early to middle Cambrian marine shelfal settings. *Palaeogeography, Palaeoclimatology, Palaeoecology 399*, 310–322. https://doi.org/10.1016/j.palaeo.2014.01.024

Tarhan, L. G., Droser, M. L. & Hughes, N. C. 2014: Exceptional trace fossil preservation and mixed layer development in Cambro-Ordovician siliciclastic strata. *Memoirs of the Association of Australasian Palaeontologists 45*, 71–88.

Tarhan, L. G., Droser, M. L., Planavsky, N. J. & Johnston, D. T. 2015: Protracted development of bioturbation through the early Palaeozoic Era. *Nature Geosciences 8*, 865–869. https://doi.org/10.1038/ngeo2537

Tarhan, L. G., Myrow, P. M., Smith, E. F., Nelson, L. L. & Sadler, P. M. 2020: Infaunal augurs of the Cambrian Explosion: an Ediacaran trace fossil assemblage from Nevada, USA. *Geobiology 18*, 486–496. https://doi.org/10.1111/gbi.12387

Tasch, P. 1968: A Permian trace fossil from the Antarctic Ohio Range. *Transactions of the Kansas Academy of Science 71*, 33–37. https://doi.org/10.2307/3627396

Taylor, A. M. & Goldring, R. 1993: Description and analysis of bioturbation and ichnofabric. *Journal of the Geological Society 150*, 141–148. https://doi.org/10.1144/gsjgs.150.1.0141

Taylor, M. E. 1981: *Short Papers for the Second International Symposium on the Cambrian System, 1981*. US Department of the Interior, Geological Survey, Open-File Report 81-743. https://doi.org/10.3133/ofr81743

Tchoumatchenco, P. & Uchman, A. 1999: Lower and middle Jurassic flysch trace fossils from the eastern Stara Planina Mountains, Bulgaria: a contribution to the evolution of Mesozoic ichnodiversity. *Neues Jahrbuch für Geologie und Paläontologie Abhandlungen 213*, 169–199. https://doi.org/10.1127/njgpa/213/1999/169

Tchoumatchenco, P. & Uchman, A. 2001: The oldest deep-sea *Ophiomorpha* and *Scolicia* and associated trace fossils from the upper Jurassic–lower Cretaceous deep-water turbidite deposits of SW Bulgaria. *Palaeogeography, Palaeoclimatology, Palaeoecology 169*, 85–99. https://doi.org/10.1016/S0031-0182(01)00218-8

Teal, L. R., Bulling, M. T., Parker, E. R. & Solan, M. 2008: Global patterns of bioturbation intensity and mixed depth of marine soft sediments. *Aquatic Biology 2*, 207–218. https://doi.org/10.3354/ab00052

Teal, L. R., Parker, E. R. & Solan, M. 2010: Sediment mixed layer as a proxy for benthic ecosystem process and function. *Marine Ecology Progress Series 414*, 27–40. https://doi.org/10.3354/meps08736

Tessier, B., Archer, A. W., Lanier, W. P. & Feldman, H. R. 1995: Comparison of ancient tidal rhythmites (Carboniferous of Kansas and Indiana, USA) with modern analogues (the Bay of Mont-Saint-Michel, France). *Special Publications of the International Association of Sedimentologists 28*, 259–271. https://doi.org/10.1002/9781444304138.ch17

Thayer, C. W. 1979: Biological bulldozers and the evolution of marine benthic communities. *Science 203*, 458–461. https://doi.org/10.1126/science.203.4379.458

Thayer, C. W. 1983: Sediment-mediated biological disturbance and the evolution of marine benthos. 479–625 *in* Tevesz, M. J. S. & McCall, P. L. (eds): *Biotic Interactions in Recent and Fossil*

Benthic Communities. Topics in Geobiology, Springer. https://doi.org/10.1007/978-1-4757-0740-3_11

Thompson, M. D., Grunow, A. M. & Ramezani, J. 2007: Late Neoproterozoic paleogeography of the southeastern New England Avalon zone: insights from U-Pb geochronology and paleomagnetism. *Geological Society of America Bulletin 119*, 681–696. https://doi.org/10.1130/B26014.1

Thomsen, E. & Vorren, T. O. 1984: Pyritization of tubes and burrows from late Pleistocene continental shelf sediments off north Norway. *Sedimentology 31*, 481–492. https://doi.org/10.1111/j.1365-3091.1984.tb01814.x

Thomson, J. & Wilson, T. R. S. 1980: Burrow-like structures at depth in a Cape Basin red clay core. *Deep Sea Research 27*, 197–202. https://doi.org/10.1016/0198-0149(80)90097-7

Tiwari, R. P. & Jauhri, A. K. 2014: Miocene palaeobiology of Mizoram: present status and future prospect. *Special Publication of the Palaeontology Society of India 5*, 189–205.

Tiwari, R. P., Rajkonwar, C., Lalchawimawii, Malsawma, P. L. J., Ralte, V. Z. & Patel, S. J. 2011: Trace fossils from Bhuban Formation, Surma Group (lower to middle Miocene) of Mizoram India and their palaeoenvironmental significance. *Journal of Earth System Science 120*, 1127–1143. https://doi.org/10.1007/s12040-011-0131-0

Topper, T., Betts, M. J., Dorjnamjaa, D., Li, G., Li, L., Altanshagai, G., Enkhbaatar, B. & Skovsted, C.B. 2022: Locating the BACE of the Cambrian: Bayan Gol in southwestern Mongolia and global correlation of the Ediacaran-Cambrian boundary. *Earth-Science Reviews 229*, 104017. https://doi.org/10.1016/j.earscirev.2022.104017

Torell, O. 1868: Bidrag till Sparagmitens geognosi och paleontologi. *Lunds Universitets Årsskrift 4*, 1–40.

Torell, O. 1869: Første Sammenkomst. Lørdag den 4de Juli. *Forhandlinger ved de Skandinaviske Naturforskeres Möde 10*, LXVI–LXVII.

Torell, O. 1870: Petrificata Suecana Formationis Cambricae. *Lunds Universitets Årsskrift 6*, 1–14.

Trauth, M. H., Sarnthein, M. & Arnold, M. 1997: Bioturbational mixing depth and carbon flux at the seafloor. *Paleoceanography 12*, 517–526. https://doi.org/10.1029/97PA00722

Trewin, N. H. 1976: *Isopodichnus* in a trace fossil assemblage from the Old Red Sandstone. *Lethaia 9*, 29–37. https://doi.org/10.1111/j.1502-3931.1976.tb00947.x

Trewin, N. H. 1994: A draft system for the identification and description of arthropod trackways. *Palaeontology 37*, 811–823.

Trewin, N. H. & McNamara, K. J. 1995: Arthropods invade the land: trace fossils and palaeoenvironments of the Tumblagooda Sandstone (? late Silurian) of Kalbarri, western Australia. *Transactions of The Royal Society of Edinburgh: Earth Sciences 85*, 177–210. https://doi.org/10.1017/S026359330000359X

Trusheim, F. 1934: Ein neuer Leithorizont im Hauptmuschelkalk von Unterfranken. *Neues Jahrbuch für Mineralogie, Geologie und Paläontologie Beilagenband 71*, 407–421.

Tunis, G. & Uchman, A. 1996a: Ichnology of Eocene flysch deposits of the Istria Peninsula, Croatia and Slovenia. *Ichnos 5*, 1–22. https://doi.org/10.1080/10420949609386403

Tunis, G., & Uchman, A. 1996b: Trace fossils and facies changes in Cretaceous-Eocene flysch deposits of the Julian Prealps (Italy and Slovenia): consequences of regional and world-wide changes. *Ichnos 4*, 169–190. https://doi.org/10.1080/10420949609380125

Turk, K. A., Wehrmann, A., Laflamme, M. & Darroch, S. A. F. 2024a: Priapulid neoichnology, ecosystem engineering, and the Ediacaran–Cambrian transition. *Palaeontology 67*, e12721. https://doi.org/10.1111/pala.12721

Turk, K. A., Pulsipher, M. A., Bergh, E., Laflamme, M. & Darroch, S. A. F. 2024b: *Archaeichnium haughtoni*: a robust burrow lining from the Ediacaran–Cambrian transition of Namibia. *Papers in Palaeontology 10*, e1546. https://doi.org/10.1002/spp2.1546

Uchman, A. 1995: Taxonomy and palaeoecology of flysch trace fossils: the Marnoso-arenacea Formation and associated facies (Miocene, northern Apennines, Italy). *Beringeria 15*, 3–115.

Uchman, A. 1998: Taxonomy and ethology of flysch trace fossils: revision of the Marian Ksiazkiewicz collection and studies of complementary material. *Annales Societatis Geologorum Poloniae 68*, 105–218.

Uchman, A. 1999: Ichnology of the Rhenodanubian flysch (lower Cretaceous-Eocene) in Austria and Germany. *Beringeria 25*, 67–173.

Uchman, A. 2001: Eocene flysch trace fossils from the Hecho Group of the Pyrenees, northern Spain. *Beringeria 28*, 3–41.

Uchman, A. 2004: Deep-sea trace fossils controlled by palaeo-oxygenation and deposition: an example from the lower Cretaceous dark flysch deposits of the Silesian Unit, Carpathians, Poland. *Fossils and Strata 51*, 39–57. https://doi.org/10.18261/9781405169851-2004-03

Uchman, A. 2005: *Treptichnus*-like traces made by insect larvae (Diptera: Chironomidae, Tipulidae). 143–146 *in* Buta, R. J., Rindsberg, A. K. & Kopaska-Merkel, D. C. (eds): *Pennsylvanian Footprints in the Black Warrior Basin of Alabama*. Alabama Paleontological Society Monograph No. 1.

Uchman, A. 2007: Trace fossils of the Pagliaro Formation (Paleocene) in the north Apennines, Italy. *Beringeria 37*, 217–237.

Uchman, A. & Geyer, G. 2020: *Segmentichnus mohri* igen. et isp. nov., a giant new trace fossil from the Culm facies (lower Carboniferous) of the Franconian Forest (Saxothuringian Belt, Germany). *Ichnos 28*, 12–23. https://doi.org/10.1080/10420940.2020.1840372

Uchman, A. & Hanken, N.-M. 2013: The new trace fossil *Gyrolithes lorcaensis* isp. n. from the Miocene of SE Spain and a critical review of the *Gyrolithes* ichnospecies. *Stratigraphy and Geological Correlation 21*, 312–322. https://doi.org/10.1134/S0869593813030088

Uchman, A. & Krenmayr, H. G. 1995: Trace fossils from lower Miocene (Ottnangian) molasse deposits of upper Austria. *Paläontologische Zeitschrift 69*, 503–524. https://doi.org/10.1007/BF02987810

Uchman, A., Bromley, R. G. & Leszczyński, S. 1998: Ichnogenus *Treptichnus* in Eocene flysch, Carpathians, Poland: taxonomy and preservation. *Ichnos 5*, 269–275. https://doi.org/10.1080/10420949809386425

Uchman, A., Drygant, D., Paszkowski, M., Porębski, S. J. & Turnau, E. 2004b: Early Devonian trace fossils in marine to non-marine redbeds in Podolia, Ukraine: palaeoenvironmental implications. *Palaeogeography, Palaeoclimatology, Palaeoecology 214*, 67–83. https://doi.org/10.1016/j.palaeo.2004.07.022

Uchman, A., Hanken, N. M. & Binns, R. 2005: Ordovician bathyal trace fossils from metasiliciclastics in central Norway and their sedimentological and paleogeographical implications. *Ichnos 12*, 105–133. https://doi.org/10.1080/10420940590914534

Uchman, A. & Krenmayr, H. G. 2004: Trace fossils, ichnofabrics and sedimentary facies in the shallow marine lower Miocene Molasse of upper Austria. *Jahrbuch der Geologischen Bundesanstalt 144*, 233–251.

Uchman, A. & Martyshyn, A. 2020: Taxis behaviour of burrowing organisms recorded in an Ediacaran trace fossil from Ukraine. *Palaeogeography, Palaeoclimatology, Palaeoecology 538*, 109441. https://doi.org/10.1016/j.palaeo.2019.109441

Uchman, A. & Pervesler, P. 2006: Surface lebensspuren produced by amphipods and isopods (crustaceans) from the Isonzo delta tidal flat, Italy. *Palaios 21*, 384–390. https://doi.org/10.2110/palo.2005.P05-63e

Uchman, A. & Rattazzi, B. 2011: The new complex helical trace fossil *Avetoichnus luisae* igen. n. et isp. n. from the Cainozoic deep-sea sediments of the Alpine realm: a non-graphoglyptid mid-tier agrichnion. *Neues Jahrbuch für Geologie und Paläontologie Abhandlungen 260*, 319–330. https://doi.org/10.1127/0077-7749/2011/0140

Uchman, A. & Rattazzi, B. 2019: The trace fossil *Circulichnis* as a record of feeding exploration: new data from deep-sea

Oligocene–Miocene deposits of northern Italy. *Comptes Rendus Palevol 18*, 1–12. https://doi.org/10.1016/j.crpv.2018.05.002

Uchman, A., Pika-Biolzi, M. & Hochuli, P. A. 2004a: Oligocene trace fossils from temporary fluvial plain ponds: an example from the Freshwater Molasse of Switzerland. *Eclogae Geologicae Helvetiae 97*, 133–148. https://doi.org/10.1007/s00015-004-1111-z

Uchman, A., Kazakauskas, V. & Gaigalas, A. 2009: Trace fossils from late Pleistocene varved lacustrine sediments in eastern Lithuania. *Palaeogeography, Palaeoclimatology, Palaeoecology 272*, 199–211. https://doi.org/10.1016/j.palaeo.2008.08.003

Uchman, A., Mikuláš, R. & Rindsberg, A. K. 2011: Mollusc trace fossils *Ptychoplasma* Fenton and Fenton, 1937 and *Oravaichnium* Plička and Uhrová, 1990: their type material and ichnospecies. *Geobios 44*, 387–397. https://doi.org/10.1016/j.geobios.2010.08.001

Umbgrove, J. H. F. 1925: Eenige problematische fossielen uit het Limburgsche Krijt. *Natuurhistorisch Maanblad 14,* 99–100.

Valentine, J. W. 1994: Late Precambrian bilaterians: grades and clades. *Proceedings of the National Academy of Sciences 91*, 6751–6757. https://doi.org/10.1073/pnas.91.15.6751

Valentine, J. W. 1995: Why no new phyla after the Cambrian? Genome and ecospace hypotheses revisited. *Palaios 10*, 190–194. https://doi.org/10.2307/3515182

van de Velde, S. & Meysman, F. J. 2016: The influence of bioturbation on iron and sulphur cycling in marine sediments: a model analysis. *Aquatic Geochemistry 22*, 469–504. https://doi.org/10.1007/s10498-016-9301-7

van der Horst, C. J. 1934: The burrow of an enteropneust. *Nature 134*, 852–852. https://doi.org/10.1038/134852a0

van Staal, C.R., Barr, S. M., McCausland, P. J. A., Thompson, M. D. & White, C. E. 2021: Tonian–Ediacaran tectonomagmatic evolution of West Avalonia and its Ediacaran–early Cambrian interactions with Ganderia: an example of complex terrane transfer due to arc–arc collision? *Geological Society, London, Special Publications 503*, 143–167. https://doi.org/10.1144/SP503-2020-23

Vannier, J. 2012: Gut contents as direct indicators for trophic relationships in the Cambrian marine ecosystem. *PLoS ONE 7*, 1–20. https://doi.org/10.1371/journal.pone.0052200

Vannier, J., Calandra, I., Gaillard, C. & Żylińska, A. 2010: Priapulid worms: pioneer horizontal burrowers at the Precambrian-Cambrian boundary. *Geology 38*, 711–714. https://doi.org/10.1130/G30829.1

Vassoevich, N. B. 1932: O nekotorykh priznakakh pozvolyayushchikh otlichť oprokinutoe polozhenie flishevykh obrazovaniy ot normalynogo. *Akademie Nauka SSSR Geologiduskiy Institut Trudy 2*, 47–64.

Vaucher, R., Pittet, B., Hormière, H., Martin, E. L. O. & Lefebvre, B. 2017: A wave-dominated, tide-modulated model for the lower Ordovician of the Anti-Atlas, Morocco. *Sedimentology 64*, 777–807. https://doi.org/10.1111/sed.12327

Vaucher, R., Vaccari, N. E., Balseiro, D., Muñoz, D. F., Dillinger, A., Waisfeld, B. G. & Buatois, L. A. 2020: Tectonic controls on late Cambrian-early Ordovician deposition in Cordillera Oriental (northwest Argentina). *International Journal of Earth Sciences 109*, 1897–1920. https://doi.org/10.1007/s00531-020-01879-9

Vaziri, S. H. & Fürsich, F. T. 2007: Middle to upper Triassic deep-water trace fossils from the Ashin Formation, Nakhlak area, Central Iran. *Journal of Sciences, Islamic Republic of Iran 18*, 253–268.

Védrine, S., Strasser, A. & Hug, W. 2007: Oncoid growth and distribution controlled by sea-level fluctuations and climate (late Oxfordian, Swiss Jura mountains). *Facies 53*, 535–552. https://doi.org/10.1007/s10347-007-0114-4

Vernhet, E. & Reijmer, J. J. 2010: Sedimentary evolution of the Ediacaran Yangtze platform shelf (Hubei and Hunan provinces, central China). *Sedimentary Geology 225*, 99–115. https://doi.org/10.1016/j.sedgeo.2010.01.005

Verrecchia, E. P., Freytet, P., Julien, J. & Baltzer, F. 1997: The unusual hydrodynamical behaviour of freshwater oncolites. *Sedimentary Geology 113*, 225–243. https://doi.org/10.1016/S0037-0738(97)00058-4

Vialov, O. S. 1969: Screw-like motion of Arthropoda from Cretaceous deposits of the Crimea. *Paleontologicheskiy Sbornik 6*, 105–109.

Vialov, O. S. 1979: New bioglyphs and problematics from Middle Asia. *Paleontologicheskiy Sbornik 16*, 80–89.

Vialov, O. S. 1971: The rare Mezosoic problematica from Pamir and the Caucasus. *Paleontologicheskiy Sbornik 7*, 85–93.

Vickers-Rich, P., Ivantsov, A., Kattan, F. H., Johnson, P. R., Al Qubsani, A., *et al.* 2013: *In search of the Kingdom's Ediacarans: The first genuine Metazoans (macroscopic body and trace fossils) from the Neoproterozoic Jibalah Group (Vendian/Ediacaran) on the Arabian Shield*. Saudi Geological Survey Technical Report SGS-TR-2013-5, 21 pp.

Vidal, G., Jensen, S. & Palacios, T. 1994a: Neoproterozoic (Vendian) ichnofossils from Lower Alcudian strata in central Spain. *Geological Magazine 131*, 169–179. https://doi.org/10.1017/S0016756800010700

Vidal, G., Palacios, T., Gámez-Vintaned, J. A., Díez Balda, M. A. & Grant, S. W. 1994b: Neoproterozoic—early Cambrian geology and palaeontology of Iberia. *Geological Magazine 131*, 729–765. https://doi.org/10.1017/S001675680001284X

Villegas-Martín, J. & Netto, R. G. 2019: Permian macroburrows as microhabitats for meiofauna organisms: an ancient behaviour common in extant organisms. *Lethaia 52*, 31–43. https://doi.org/10.1111/let.12288

Vilmova, E. S. 2012: The sequence of Etren Beds (the end of Devonian – the beginning of Carboniferous period) of Argaley Ridge in eastern Transbaikalia as an example of storm and interstorm precipitation of seaside paleoecosystems. 77–81 *in*: *Mineralogy and geochemistry of landscape of mountain-ore territories. Modern mineral formation*. Institute of Natural Resources, Ecology and Cryology SB RAS, Chita.

Vinn, O., Wilson, M. A. & Toom, U. 2015: Distribution of *Conichnus* and *Amphorichnus* in the lower Paleozoic of Estonia (Baltica). *Carnets de Géologie 15*, 269–278. https://doi.org/10.4267/2042/58180

Virtasalo, J. J., Kotilainen, A. T. & Gingras, M. K. 2006: Trace fossils as indicators of environmental change in Holocene sediments of the Archipelago Sea, northern Baltic Sea. *Palaeogeography, Palaeoclimatology, Palaeoecology 240*, 453–467. https://doi.org/10.1016/j.palaeo.2006.02.010

Virtasalo, J. J., Löwemark, L., Papunen, H., Kotilainen, A. T. & Whitehouse, M. J. 2010: Pyritic and baritic burrows and microbial filaments in postglacial lacustrine clays in the northern Baltic Sea. *Journal of the Geological Society, London 167*, 1185–1198. https://doi.org/10.1144/0016-76492010-017

von Ammon, L. 1900: Ueber das Vorkommen von "Steinschrauben" (Daemonhelix) in der oligocänen Molasse Oberbayerns. *Geognostische Jahreshefte 1900*, 55–69.

von Otto, E. 1854: *Additamente zur Flora des Quadergebirges in Sachsen. II. Heft*. G. Mayer, Leipzig, 53 pp.

Vossler, S. M., Magwood, J. P. & Pemberton, S. G. 1989: The youngest occurrence of the ichnogenus *Didymaulichnus* from the upper Cretaceous (Turonian) Cardium Formation. *Journal of Paleontology 63*, 384–386. https://doi.org/10.1017/S0022336000019569

Waggoner, B. 1999: Los comienzos de la historia evolutiva de los artrópodos: ¿qué nos pueden contar los fósiles? *Boletín de la S.E.A. 26*, 115–131.

Waggoner, B. & Hagadorn, J. W. 2002: New fossils from terminal Neoproterozoic strata of southern Nye County, Nevada. 87–93 *in* Corsetti, F .A. (ed): *Proterozoic-Cambrian of the Great Basin and beyond*. Field trip guidebook and volume prepared for the annual Pacific Section SEPM fall field trip, Shoshone, California, Book 93.

Walcott, C. D. 1899: Pre-Cambrian fossiliferous formations. *Bulletin of the Geological Society of America 10*, 199–244. https://doi.org/10.1130/GSAB-10-199

Walde, D. H. G., do Carmo, D. A., Guimarães, E. M., Vieira, L. C., Erdtmann, B.-D., Sanchez, E. A. M., Adorno, R. R. & Tobias, T. C. 2015: New aspects of Neoproterozoic-Cambrian transition in the Corumbá region (state of Mato Grosso do Sul, Brazil). *Annales de Paléontologie 101*, 213–224. https://doi.org/10.1016/j.annpal.2015.07.002

Walker, E. F. 1985: Arthropod ichnofauna of the Old Red sandstone at Dunure and Montrose, Scotland. *Transactions of The Royal Society of Edinburgh: Earth Sciences 76*, 287–297. https://doi.org/10.1017/S0263593300010506

Walker, R. G., Duke, W. L. & Leckie, D. A. 1983: Hummocky stratification: significance of its variable bedding sequences: discussion. *Geological Society of America Bulletin 94*, 1245–1249. https://doi.org/10.1130/0016-7606(1983)94<1245:HSSOIV>2.0.CO;2

Wallace, J. B. & Merritt, R. W. 1980: Filter-feeding ecology of aquatic insects. *Annual Review of Entomology 25*, 103–132. https://doi.org/10.1146/annurev.en.25.010180.000535

Walter, M. R., Oehler, J. H. & Oehler, D. Z. 1976: Megascopic algae 1300 million years old from the Belt Supergroup, Montana: a reinterpretation of Walcott's *Helminthoidichnites*. *Journal of Paleontology 50*, 872–881.

Walter, M. R., Elphinstone, R. & Heys, G.R. 1989: Proterozoic and early Cambrian trace fossils from the Amadeus and Georgina Basins, central Australia. *Alcheringa 13*, 209–256. https://doi.org/10.1080/03115518908527821

Walter, M. R., Du, R. & Horodyski, R. J. 1990: Coiled carbonaceous megafossils from the middle Proterozoic of Jixian (Tianjin) and Montana. *American Journal of Science 290*, 133–148.

Wang, Y. 1992: Trace fossils in Songjiaqiao Member of Dushan Formation of middle Devonian series in Guizhou and their environmental significance. *Geology of Guizhou 9*, 178–183.

Wang, Y. 2005: An ichnofossil, U-shaped burrow, in continental deposit from the lower Devonian Danlin Formation in Dushan County, Guizhou Province, China. *Acta Geologica Sinica 79*, 1–6.

Wang, Y. 2007: Arthropods tracks in Kaili ichnocoenosis from lower-middle Cambrian Kaili Formation in Jianhe County, Guizhou Province, China. *Geologial Review 53*, 539–555.

Wang, Y. & Wang, P. 2006: Ichnofossil *Treptichnus* from the Kaili Formation at Taijiang County, Guizhou Province. *Geological Review 52*, 1–10.

Wang, Y., Zhang, H.-J., Yang, X.-G., Li, S.-L. & Wang, Q.-S. 2006: Trace fossils from the middle Cambrian Jialao Formation at Nangao Town, Danzhai County, Guizhou Province, China. *Geological Bulletin of China 25*, 475–481. https://doi.org/10.12097/gbc.20060478

Wang, Y., Dong, H., Li, G., Zhang, W., Oguchi, T., Bao, M., Jiang, H. & Bishop, M. E. 2010: Magnetic properties of muddy sediments on the northeastern continental shelves of China: implication for provenance and transportation. *Marine Geology 274*, 107–119. https://doi.org/10.1016/j.margeo.2010.03.009

Wang, Y., Wang, X., Uchman, A., Hu, B. & Song, H. 2019: Burrows of the polychaete *Perinereis aibuhiutensis* on a tidal flat of the Yellow River Delta in China: implications for the ichnofossils Polykladichnus and Archaeonassa. *Palaios 34*, 271–279. https://doi.org/10.2110/palo.2018.105

Wang, Z., Davies, N. S., Liu, A. G., Minter, N. J. & Rahman, I. A. 2024: Identifying signatures of the earliest benthic bulldozers in emergent subaerial conditions during the colonization of land by animals. *Proceedings of the Royal Society B 291*, 20241629. https://doi.org/10.1098/rspb.2024.1629

Warren, L. V., Quaglio, F., Riccomini, C., Simões, M. G., Poiré, D. G., Strikis, N. M., Anelli, L. E. & Strikis, P. C. 2014: The puzzle assembled: Ediacaran guide fossil *Cloudina* reveals an old proto-Gondwana seaway. *Geology 42*, 391–394. https://doi.org/10.1130/G35304.1

Warren, L.V., Buatois, L. A., Mángano, M. G., Simões, M. G., Santos, M. G. M., Poiré, D. G., Riccomini, C. & Assine, M. L. 2020: Microbially induced pseudotraces from a Pantanal soda lake, Brazil: alternative interpretations for Ediacaran simple trails and their limits. *Geology 48*, 857–861. https://doi.org/10.1130/G47234.1

Weaver, P. P. E. & Schultheiss, P. J. 1983: Vertical open burrows in deep-sea sediments 2 m in length. *Nature 301*, 329–331. https://doi.org/10.1038/301329a0

Webby, B. D. 1970: Late Precambrian trace fossils from New South Wales. *Lethaia 3*, 79–109. https://doi.org/10.1111/j.1502-3931.1970.tb01265.x

Weber, B. & Braddy, S. J. 2004: A marginal marine ichnofauna from the Blaiklock Glacier Group (?lower Ordovician) of the Shackleton Range, Antarctica. *Transactions of The Royal Society of Edinburgh: Earth Sciences 94*, 1–20. https://doi.org/10.1017/S026359330000050X

Weber, B. & Zhu, M. 2003: Arthropod trace fossils from the Zhujiaqing Formation (Meishucunian, Yunnan) and their palaeobiological implications. *Progress in Natural Science 13*, 795–800. https://doi.org/10.1080/10020070312331344450

Weber, B., Steiner, M. & Zhu, M.-Y. 2007: Precambrian–Cambrian trace fossils from the Yangtze Platform (South China) and the early evolution of bilaterian lifestyles. *Palaeogeography, Palaeoclimatology, Palaeoecology 254*, 328–349. https://doi.org/10.1016/j.palaeo.2007.03.021

Weber, B., Hu, S., Steiner, M. & Zhao, F. 2012: A diverse ichnofauna from the Cambrian Stage 4 Wulongqing Formation near Kunming (Yunnan Province, South China). *Bulletin of Geosciences 87*, 71–92. https://doi.org/10.3140/bull.geosci.1239

Weber, B., Steiner, M., Evseev, S. & Yergaliev, G. 2013: First report of a Meishucun-type early Cambrian (Stage 2) ichnofauna from the Malyi Karatau area (SE Kazakhstan): palaeoichnological, palaeoecological and palaeogeographical implications. *Palaeogeography, Palaeoclimatology, Palaeoecology 392*, 209–231. https://doi.org/10.1016/j.palaeo.2013.08.021

Weidner, T., Geyer, G., Ebbestad, J. O. R. & von Seckendorff, V. 2015: Glacial erratic boulders from Jutland, Denmark, feature an uppermost lower Cambrian fauna of the Lingulid Sandstone Member of Västergötland, Sweden. *Bulletin of the Geological Society of Denmark 63*, 59–86. https://doi.org/10.37570/bgsd-2015-63-06

Weiss, E. 1884: Vorlegung des *Dictyophytum liebeanum* Gein. aus der Gegend von Gera. *Gesellschaft Naturforschender Freunde zu Berlin, Sitzungsberichte 1884*, 17.

Weissbrod, T. & Barthel, W. K. 1998: An early Aptian ichnofossil assemblage zone in southern Israel, Sinai and southwestern Egypt. *Journal of African Earth Sciences 26*, 151–165. https://doi.org/10.1016/S0899-5362(98)00003-7

Went, D. J. & McMahon, W. J. 2018: Fluvial products and processes before the evolution of land plants: evidence from the lower Cambrian Series Rouge, English Channel region. *Sedimentology 65*, 2559–2594. https://doi.org/10.1111/sed.12478

Wentworth, C. K. 1922: A scale of grade and class terms for clastic sediments. *The Journal of Geology 30*, 377–392. https://doi.org/10.1086/622910

Werner, F. & Wetzel, A. 1982: Interpretation of biogenic structures in oceanic sediments. *Bulletin de l'Institut de Géologie du Bassin d'Aquitaine 31*, 275–288.

Wescott, W. A. & Utgaard, J. E. 1987: An upper Mississippian trace-fossil assemblage from the Tar Springs Sandstone, southern Illinois. *Journal of Paleontology 61*, 231–241. https://doi.org/10.1017/S0022336000028432

Wesolowski, L. J. N., Buatois, L. A., Mángano, M. G., Ponce, J. J. & Carmona, N. B. 2018: Trace fossils, sedimentary facies and parasequence architecture from the lower Cretaceous Mulichinco Formation of Argentina: the role of fair-weather waves in shoreface deposits. *Sedimentary Geology 367*, 146–163. https://doi.org/10.1016/j.sedgeo.2018.02.007

Westergård, A. H. 1931: *Diplocraterion*, *Monocraterion* and *Scolithus*. *Sveriges Geologiska Undersökning C 372*, 1–25.

Westrop, S. R. & Landing, E. 2011: Lower Cambrian (Branchian) eodiscoid trilobites from the lower Brigus Formation, Avalon Peninsula, Newfoundland, Canada. *Memoirs of the Association of Australasian Palaeontologists 42*, 209–262.

Wetzel, A. 1981: Ökologische und stratigraphische Bedeutung biogener Gefüge in quartären Sedimenten am NW-afrikanischen Kontinentalrand. *"Meteor"-Forschungs-Ergebnisse 34*, 1–47.

Wetzel, A. 1983: Biogenic structures in modern slope to deep-sea sediments in the Sulu Sea Basin (Philippines). *Palaeogeography, Palaeoclimatology, Palaeoecology 42*, 285–304. https://doi.org/10.1016/0031-0182(83)90027-5

Wetzel, A. 1984: Bioturbation in deep-sea fine-grained sediments: influence of sediment texture, turbidite frequency and rates of environmental change. *Geological Society, London, Special Publications 15*, 595–608. https://doi.org/10.1144/GSL.SP.1984.015.01.37

Wetzel, A. 1991: Ecologic interpretation of deep-sea trace fossil communities. *Palaeogeography, Palaeoclimatology, Palaeoecology 85*, 47–69. https://doi.org/10.1016/0031-0182(91)90025-M

Wetzel, A. 2008: Recent bioturbation in the deep South China Sea: a uniformitarian ichnologic approach. *Palaios 23*, 601–615. https://doi.org/10.2110/palo.2007.p07-096r

Wetzel, A. & Blouet, J. P. 2023: The trace fossil *Tisoa siphonalis* in its type area—characteristics and environmental significance. *Palaios 38*, 76–97. https://doi.org/10.2110/palo.2022.036

Wetzel, A. & Bromley, R. G. 1996: Re-evaluation of the ichnogenus *Helminthopsis* - a new look at the type material. *Palaeontology 39*, 1–19.

Wetzel, A. & Uchman, A. 1997: Ichnology of deep-sea fan overbank deposits of the Ganei slates (Eocene, Switzerland)—a classical flysch trace fossil locality studied first by Oswald Heer. *Ichnos 5*, 139–162. https://doi.org/10.1080/10420949709386413

Wetzel, A. & Uchman, A. 2018: The former presence of organic matter caused its later absence: burn-down of organic matter in oceanic red beds enhanced by bioturbation (Eocene Variegated Shale, Carpathians). *Sedimentology 65*, 1504–1519. https://doi.org/10.1111/sed.12436

Wetzel, A., Blechschmidt, I., Uchman, A. & Matter, A. 2007: A highly diverse ichnofauna in late Triassic deep-sea fan deposits of Oman. *Palaios 22*, 567–576. https://doi.org/10.2110/palo.2006.p06-098r

Wetzel, A., Uchman, A., Blechschmidt, I. & Matter, A. 2009: *Omanichnus* and *Vitichnus*—two new graphoglyptid ichnogenera from upper Triassic deep-sea fan deposits in Oman. *Ichnos 16*, 179–185. https://doi.org/10.1080/10420940802686004

Wetzel, A., Tjallingii, R. & Stattegger, K. 2010: *Gyrolithes* in Holocene estuarine incised-valley fill deposits, offshore southern Vietnam. *Palaios 25*, 239–246. https://doi.org/10.2110/palo.2009.p09-131r

Wetzel, A., Carmona, N. & Ponce, J. 2014: Tidal signature recorded in burrow fill. *Sedimentology 61*, 1198–1210. https://doi.org/10.1111/sed.12097

Wetzel, A., Carmona, N. B. & Ponce, J. J. 2020: *Gyrochorte* "highways" and their environmental significance in shallow-marine sediments. *Acta Palaeontologica Polonica 65*, 209–218. https://doi.org/10.4202/app.00655.2019

Wheeler, H.E. 1947: Base of the Cambrian system. *The Journal of Geology 55*, 153–159. https://doi.org/10.1086/625425

Whitfield, R.P. 1882: Paleontology. 161–364 *in* Chamberlin, T. C. (ed): *Geology of Wisconsin. Survey of 1873-1879*. Vol. 4, D. Atwood, Madison.

Whitfield, R. P. 1904: Note on some worm (?) burrows in rocks of the Chemung Group of New York. *Bulletin American Museum of Natural History 20*, 473–474.

Widmer, K. 1950: *The geology of the Hermitage Bay Area, Newfoundland*. Unpublished Doctoral Dissertation, Princetown University, New Jersey, 459 pp.

Wignall, P. B. & Hallam, A. 1991: Biofacies, stratigraphic distribution and depositional models of British onshore Jurassic black shales. *Geological Society Special Publications, London 58*, 291–309. https://doi.org/10.1144/GSL.SP.1991.058.01.19

Wignall, P. B. & Myers, K. J. 1988: Interpreting benthic oxygen levels in mudrocks: a new approach. *Geology 16*, 452–455. https://doi.org/10.1130/0091-7613(1988)016<0452:IBOLIM>2.3.CO;2

Williams, H. 1971: *Geology of Belleoram map-area, Newfoundland*. Geological Survey of Canada, Department of Energy, Mines and Resources, Paper 70-65, 39 pp. https://doi.org/10.4095/125072

Williams, H. 1979: Appalachian orogen in Canada. *Canadian Journal of Earth Sciences 16*, 792–807. https://doi.org/10.1139/e79-070

Wilson, A. E. 1948: Miscellaneous classes of fossils, Ottawa Formation, Ottawa-St. Lawrence Valley. *Geological Survey Bulletin 11*, 1–116. https://doi.org/10.4095/101512

Wilson, J. P., Grotzinger, J. P., Fischer, W. W., Hand, K. P., Jensen, S., Knoll, A. H., Abelson, J., Metz, J. M., McLoughlin, N., Cohen, P. A. & Tice, M. M. 2012: Deep-water incised valley deposits at the Ediacaran-Cambrian boundary in southern Namibia contain abundant *Treptichnus pedum*. *Palaios 27*, 252–273. https://doi.org/10.2110/palo.2011.p11-036r

Wilson, R. D. & Schieber, J. 2015: Sedimentary facies and depositional environment of the middle Devonian Geneseo Formation of New York, USA. *Journal of Sedimentary Research 85*, 1393–1415. https://doi.org/10.2110/jsr.2015.88

Wolfe, J. M., Daley, A. C., Legg, D. A. & Edgecombe, G. D. 2016: Fossil calibrations for the arthropod Tree of Life. *Earth-Science Reviews 160*, 43–110. https://doi.org/10.1016/j.earscirev.2016.06.008

Won, S. & Kong, D.-Y. 2023: Application of RTI to improve image clarity of a trace fossil *Cochlichnus* found from the Jinju and Haman formations. *Korea Economic and Environmental Geology 56*, 397–408. https://doi.org/10.9719/EEG.2023.56.4.397

Wright, L. D. & Friedrichs, C.T. 2006: Gravity-driven sediment transport on continental shelves: a status report. *Continental Shelf Research 26*, 2092–2107. https://doi.org/10.1016/j.csr.2006.07.008

Wycisk, P., Klitzsch, E., Jas, C. & Reynolds, O. 1990: Intracratonal sequence development and structural control of Phanerozoic strata in Sudan. *Berliner Geowissenschaftliche Abhandlungen (A) 120*, 45–86.

Xiao, S. & Laflamme, M. 2009: On the eve of animal radiation: phylogeny, ecology and evolution of the Ediacara biota. *Trends in Ecology and Evolution 24*, 31–40. https://doi.org/10.1016/j.tree.2008.07.015

Xiao, S. H. & Narbonne, G. M. 2020: The Ediacaran Period. 521–561 *in* Gradstein, F. M., Ogg, J. G., Schmitz, M. D. & Ogg, G. M. (eds): *Geologic Time Scale 2020*. Elsevier. https://doi.org/10.1016/B978-0-12-824360-2.00018-8

Yamaguchi, N. & Sekiguchi, H. 2010: Effects of settling and preferential deposition of sediment on ripple roundness under shoaling waves. *Journal of Sedimentary Research 80*, 781–790. https://doi.org/10.2110/jsr.2010.072

Yan, Y. & Liu, Z. 1998: Does *Sangshuania* represent eukaryotic algae or trace fossils. *Acta Micropalaeontologica Sinica 15*, 101–11.

Yang, B. C. & Chun, S. S. 2001: A seasonal model of surface sedimentation on the Baeksu open-coast intertidal flat, southwestern coast of Korea. *Geosciences Journal 5*, 251–262. https://doi.org/10.1007/BF02910308

Yang, B., Steiner, M., Li, G. & Keupp, H. 2014: Terreneuvian small shelly faunas of east Yunnan (South China) and their biostratigraphic implications. *Palaeogeography, Palaeoclimatology, Palaeoecology 398*, 28–58. https://doi.org/10.1016/j.palaeo.2013.07.003

Yang, B. C. & Steiner, M. 2021: Terreneuvian bio- and chemostratigraphy of the south Sichuan Region (South China). *Journal of the Geological Society 178*, jgs2020-167. https://doi.org/10.1144/jgs2020-167

Yang, B. C., Dalrymple, R. W. & Chun, S. S. 2005: Sedimentation on a wave-dominated, open-coast tidal flat, south-western Korea: summer tidal flat–winter shoreface. *Sedimentology 52*, 235–252. https://doi.org/10.1111/j.1365-3091.2004.00692.x

Yang, B. C., Dalrymple, R. W. & Chun, S. 2006: The significance of hummocky cross-stratification (HCS) wavelengths: evidence from an open-coast tidal flat, South Korea. *Journal*

of Sedimentary Research 76, 2–8. https://doi.org/10.2110/jsr.2006.01

Yang, B. C., Gingras, M. K., Pemberton, S. G. & Dalrymple, R. W. 2008: Wave-generated tidal bundles as an indicator of wave-dominated tidal flats. *Geology 36*, 39–42. https://doi.org/10.1130/G24178A.1

Yang, B. C., Chang, T.S. & Dalrymple, R. W. 2021: Sedimentological and ichnological characteristics on macrotidal Baeksu tidal shoreface, southwestern coast of Korea. *Marine Geology 440*, 106607. https://doi.org/10.1016/j.margeo.2021.106607

Yang, S. 1983: Early Devonian trace fossils from Liujing, Hengxing, Guangxi, and their paleoecological significance. *Regional Geology of China 5*, 11–19. https://doi.org/10.12097/gbc.ZQYD198303001

Yang, S.-P. 1984: Silurian trace fossils from the Yangzi Gorges and their significance to depositional environments. *Acta Palaeontologica Sinica 23*, 705–715.

Yang, S. & Fu, S. 1985: Lower Ordovician trace fossil community *Cruziana* from Wuding, Yunnan and its stratigraphical and geographical distribution. *Chinese Journal of Geology 20*, 43–52.

Yang, S. & Sun, Y. 1982: Trace fossils of Guanling Formation and its sedimentary environment. *Oil and Gas Geology 3*, 369–378. https://doi.org/10.11743/ogg19820418

Yang, S.-P. & Wang, X.-C. 1991: Middle Cambrian Hsuchuangian trace fossils from southern North China Platform and their sedimentological significance. *Acta Palaeontologica Sinica 30*, 74–89.

Yang, S., Hu, C. & Sun, Y. 1987: Discovery of late Devonian trace fossils from Guodingshan district, Hanyang, China and its significance. *Earth Science Journal of the Wuhan College of Geology 12*, 1–8.

Yang, S., Zhang, J. & Yang, M. 2004: *Trace fossils of China*. Beijing, China, 353 pp.

Yang, Z., Yin, J. & He, T. 1982: Early Cambrian trace fossils from the Emei-Ganluo region, Sichuan, and other localities. *Geological Review 28*, 291–298.

Yin, J., Li, D. & He, T. 1993: Discovery of trace fossils from the Sinian–Cambrian boundary beds in eastern Yunnan and their significance for global correlation. *Acta Geologica Sinica 6*, 429–442. https://doi.org/10.1111/j.1755-6724.1993.mp6004005.x

Yochelson, E. L. & Fedonkin, M. A. 1997: The type specimens (middle Cambrian) of the trace fossil *Archaeonossa* Fenton and Fenton. *Canadian Journal of Earth Sciences 34*, 1210–1219. https://doi.org/10.1139/e17-097

Yochelson, E. L. & Schindel, D. E. 1978: A reexamination of the Pennsylvanian trace fossil *Olivellites*. *Journal of Research U.S. Geological Survey 6*, 789–796.

Yokokawa, M. 1995: Combined-flow ripples: genetic experiments and applications for geologic records. *Memoirs from the Faculty of Science, Kyushu University, Series D, Earth and Planetary Sciences 29*, 1–38. https://doi.org/10.5109/1543655

Young, D. K., Jahn, W. H., Richardson, M. D. & Lohanick, A. W. 1985: Photographs of deep-sea lebensspuren: a comparison of sedimentary provinces in the Venezuela Basin, Caribbean Sea. *Marine Geology 68*, 269–301. https://doi.org/10.1016/0025-3227(85)90016-7

Young, F. G. 1972: Early Cambrian and older trace fossils from the southern Cordillera of Canada. *Canadian Journal of Earth Sciences 9*, 1–17. https://doi.org/10.1139/e72-001

Zachos, L. G. & Platt, B. F. 2019: Actuopaleoichnology of a modern Bay of Fundy macro-tidal flat: analogy with a Mississippian tidal flat deposit (Hartselle Sandstone) from Alabama. *PeerJ 7*, e6975. https://doi.org/10.7717/peerj.6975

Zaitlin, B. A., Dalrymple, R. W. & Boyd, R. 1994: The stratigraphic organization of incised-valley systems associated with relative sea-level change. 45–60 *in* Dalrymple, R. W., Boyd, R. & Zaitlin, B. A. (eds): *Incised-Valley Systems: Origin and Sedimentary Sequences*. SEPM Special Publication, Vol. 51. https://doi.org/10.2110/pec.94.12.0045

Zavala, C. & Arcuri, M. 2016: Intrabasinal and extrabasinal turbidites: origin and distinctive characteristics. *Sedimentary Geology 337*, 36–54. https://doi.org/10.1016/j.sedgeo.2016.03.008

Zavala, C., Arcuri, M., Di Meglio, M., Zorzano, A., Otharán, G., Irastorza, A. & Torresi, A. 2021: Deltas: a new classification expanding Bates's concepts. *Journal of Palaeogeography 10*, 1–15. https://doi.org/10.1186/s42501-021-00098-w

Zavala, C., Arcuri, M., Zorzano, A., Trobbiani, V., Torresi, A. & Irastorza, A. 2024: Deltas: new paradigms. *The Depositional Record 10,* 600–636. https://doi.org/10.1002/dep2.266

Zenker, J. C. 1836: *Historisch-topographisches Taschenbuch von Jena und seiner Umgebung*. F. Frommann, Jena, 338 pp.

Zessin, W. 2008: Neue Spurenfossilien aus norddeutschen Geschieben des unterkambrischen Eophyton-Sandsteins. *Mitteilungen der Naturforschenden Gesellschaft West-Mecklenburg 8*, 29–41.

Zessin, W. 2009: Neue Spurenfossilien (*Bergaueria lagingi* n. ichnosp., *Cochlichnus karlae* n. ichnosp., *Dimorphichnus juchemi* und *Psammichnites pittermanni* n. ichnosp.) aus unterkambrischen Geschieben. *Mitteilungen der NGM 9*, 55–64.

Zhang, F., Zhou, Y.-X., Ge, R.-Q., Hu, X.-F., Xiong, C. & Yi, W.-C. 2018: A new type of lacustrine ichnofossils from the lower Jurassic Ziliujing Formation in Wanzhou of Chongqing and its paleoenvironmental significances. *Acta Palaeontologica Sinica 57*, 228–236.

Zhang, L. 1986: A discovery and preliminary study of the late stage of late Gaojiashan Biota from Sinian in Ningqiang county, Shaanxi. *Bulletin of the Xi'an Institute of Geology and Mineral Ressources, the Chinese Academy of Sciences 13*, 67–88.

Zhang, L.-J., Buatois, L. A., Mángano, M. G., Qi, Y.-A. & Tai, C. 2017a: Middle Cambrian *Diplocraterion parallelum* from North China: ethologic significance and facies controls. *Bollettino della Società Paleontologica Italiana 56*, 117–125. https://doi.org/10.4435/BSPI.2017.14

Zhang, L.-J., Buatois, L. A., Mángano, M. G., Qi, Y.-A., Zhang, X., Sun, S. & Tai, C. 2017b: Early Triassic estuarine depauperate *Cruziana* Ichnofacies from the Sichuan area of South China and its implications for the biotic recovery in brackish-water settings after the end-Permian mass extinction. *Palaeogeography, Palaeoclimatology, Palaeoecology 485*, 351–360. https://doi.org/10.1016/j.palaeo.2017.06.025

Zhang, L.-J., Buatois, L. A. & Mángano, M. G. 2022: Potential and problems in evaluating secular changes in the diversity of animal-substrate interactions at ichnospecies rank. *Terra Nova 34*, 433–440. https://doi.org/10.1111/ter.12596

Zhang, L.-J., Buatois, L. A., Mángano, M. G., Yang, Q., Zhang, S., Wei, F., Fan, R.-Y., Zhao, Z., Wang, Z., Ma, X.-Y. & Tang, F. 2025: Trace fossils from the Meishucun section of South China: revisiting ichnotaxonomy, behavioural diversification and ecosystem engineering from a key Ediacaran–Cambrian succession. *Papers in Palaeontology 11,* e70009. https://doi.org/10.1002/spp2.70009

Zhang, S., Solan, M. & Tarhan, L. 2024: Global distribution and environmental correlates of marine bioturbation. *Current Biology 34*, P2580-2593.E4. https://doi.org/10.1016/j.cub.2024.04.065

Zhang, X., Zhang, C. & Wang, D. 1986: The trace fossils of the Silurian and Devonian systems of the northwestern region, Hunan Province. *Hunan Geology 5*, 49–61.

Zhang, X. 1991: Trace fossils from Tiaomajian Formation of middle Devonian in Xinhua, Xiantan and other areas. *Hunan Geology 10*, 97–104.

Zhang, X.-P. & Wang, D.-R. 1996: A restudy on Silurian-Devonian ichnofossils from northwestern Hunan area. *Acta Palaeontologica Sinica 35*, 475–489.

Zhao, X., Tong, J., Yao, H., Niu, Z., Luo, M., Huang, Y. & Song, H. 2015: Early Triassic trace fossils from the Three Gorges area of South China: implications for the recovery of benthic ecosystems following the Permian–Triassic extinction. *Palaeogeography, Palaeoclimatology, Palaeoecology 429*, 100–116. https://doi.org/10.1016/j.palaeo.2015.04.008

Zhu, M. 1997: Precambrian–Cambrian trace fossils from eastern Yunnan, China: implications for Cambrian Explosion. *Bulletin of National Museum of Natural Science 10*, 275–312.

Zhu, M.-Y., Babcock, L. E. & Peng, S.-C. 2006: Advances in Cambrian stratigraphy and paleontology: integrating correlation techniques, paleobiology, taphonomy and paleoenvironmental reconstruction. *Palaeoworld 15*, 217–222. https://doi.org/10.1016/j.palwor.2006.10.016

Zhu, M., Yang, A., Yuan, J., Li, G., Zhang, J., Zhao, F., Ahn, S.-Y. & Miao, L. 2019: Cambrian integrative stratigraphy and timescale of China. *Science China Earth Sciences 62*, 25–60. https://doi.org/10.1007/s11430-017-9291-0

Zonneveld, J.-P. & Gingras, M. K. 2013: The ichnotaxonomy of vertically oriented, bivalve-generated equilibrichnia. *Journal of Paleontology 87*, 243–253. https://doi.org/10.1666/11-064R1.1

Zonneveld, J.-P., Pemberton, S. G., Saunders, T. D. A. & Pickerill, R. K. 2002: Large, robust *Cruziana* from the middle Triassic of northeastern British Columbia: ethologic, biostratigraphic, and paleobiologic significance. *Palaios 17*, 435–448. https://doi.org/10.1669/0883-1351(2002)017<0435:LRCFTM>2.0.CO;2

Zonneveld, J.-P., Zaim, Y., Rizal, Y., Ciochon, R. L., Bettis III, E. A. & Gunnell, G. F. 2012: Ichnological constraints on the depositional environment of the Sawahlunto Formation, Kandi, northwest Ombilin Basin, west Sumatra, Indonesia. *Journal of Asian Earth Sciences 45*, 106–113. https://doi.org/10.1016/j.jseaes.2011.06.017

FOSSILS AND STRATA

Number 72 • December 2025

ISSN print: 0300-9491 ISSN online: 2637-6032

Scandinavian University Press

Printed edition (print on demand): ISBN 978-82-94-16711-1